frontiers | Research Topics

The neuroscience of advancing age

Edited by
George M. Opie, Mitchell Ryan Goldsworthy, John Semmler, Rachael D. Seidler and Ann-Maree Vallence

Published in
Frontiers in Aging Neuroscience
Frontiers in Human Neuroscience

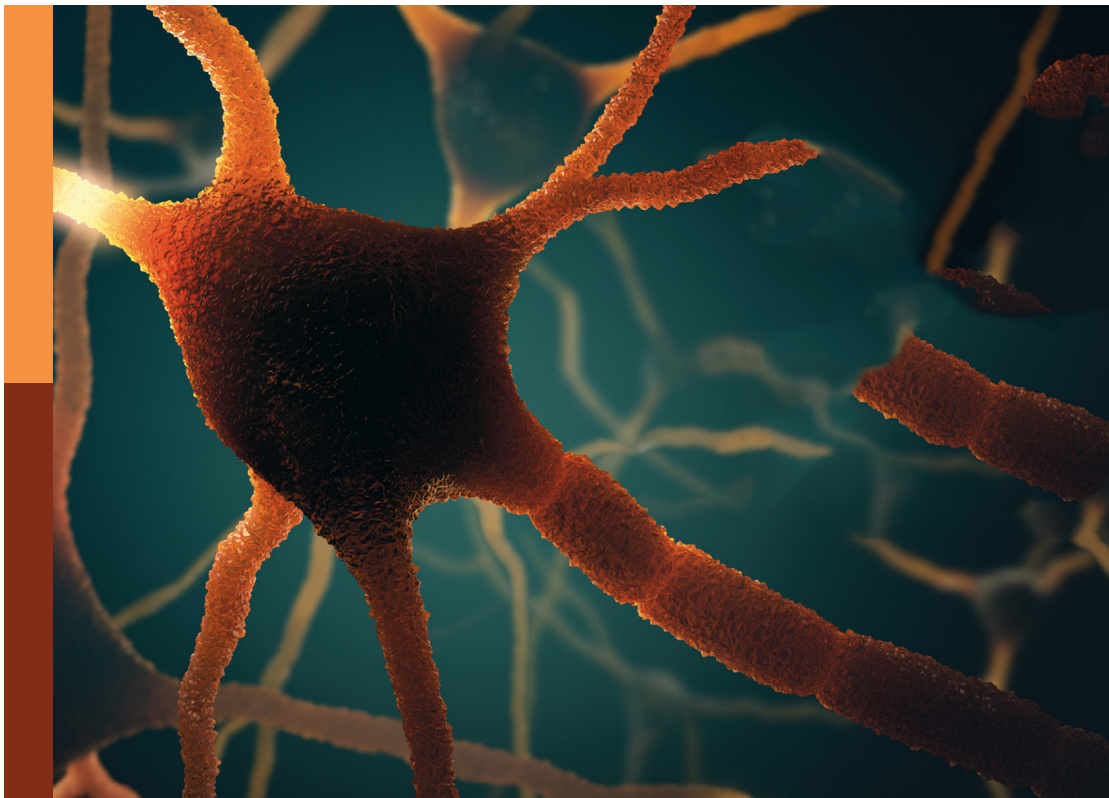

ISSN 1664-8714
ISBN 978-2-8325-2292-9
DOI 10.3389/978-2-8325-2292-9

About Frontiers

Frontiers is more than just an open access publisher of scholarly articles: it is a pioneering approach to the world of academia, radically improving the way scholarly research is managed. The grand vision of Frontiers is a world where all people have an equal opportunity to seek, share and generate knowledge. Frontiers provides immediate and permanent online open access to all its publications, but this alone is not enough to realize our grand goals.

Frontiers journal series

The Frontiers journal series is a multi-tier and interdisciplinary set of open-access, online journals, promising a paradigm shift from the current review, selection and dissemination processes in academic publishing. All Frontiers journals are driven by researchers for researchers; therefore, they constitute a service to the scholarly community. At the same time, the *Frontiers journal series* operates on a revolutionary invention, the tiered publishing system, initially addressing specific communities of scholars, and gradually climbing up to broader public understanding, thus serving the interests of the lay society, too.

Dedication to quality

Each Frontiers article is a landmark of the highest quality, thanks to genuinely collaborative interactions between authors and review editors, who include some of the world's best academicians. Research must be certified by peers before entering a stream of knowledge that may eventually reach the public - and shape society; therefore, Frontiers only applies the most rigorous and unbiased reviews. Frontiers revolutionizes research publishing by freely delivering the most outstanding research, evaluated with no bias from both the academic and social point of view. By applying the most advanced information technologies, Frontiers is catapulting scholarly publishing into a new generation.

What are Frontiers Research Topics?

Frontiers Research Topics are very popular trademarks of the *Frontiers journals series*: they are collections of at least ten articles, all centered on a particular subject. With their unique mix of varied contributions from Original Research to Review Articles, Frontiers Research Topics unify the most influential researchers, the latest key findings and historical advances in a hot research area.

Find out more on how to host your own Frontiers Research Topic or contribute to one as an author by contacting the Frontiers editorial office: frontiersin.org/about/contact

The neuroscience of advancing age

Topic editors

George M. Opie — University of Adelaide, Australia
Mitchell Ryan Goldsworthy — University of Adelaide, Australia
John Semmler — University of Adelaide, Australia
Rachael D. Seidler — University of Florida, United States
Ann-Maree Vallence — Murdoch University, Australia

Citation

Opie, G. M., Goldsworthy, M. R., Semmler, J., Seidler, R. D., Vallence, A.-M., eds. (2023). *The neuroscience of advancing age*. Lausanne: Frontiers Media SA. doi: 10.3389/978-2-8325-2292-9

Table of contents

frontiers | Frontiers in Aging Neuroscience

TYPE Editorial
PUBLISHED 14 April 2023
DOI 10.3389/fnagi.2023.1195785

OPEN ACCESS

EDITED AND REVIEWED BY
Kristy A. Nielson,
Marquette University, United States

*CORRESPONDENCE
George M. Opie
george.opie@adelaide.edu.au

RECEIVED 28 March 2023
ACCEPTED 03 April 2023
PUBLISHED 14 April 2023

CITATION
Vallence AM, Seidler RD, Goldsworthy MR, Semmler JG and Opie GM (2023) Editorial: The neuroscience of advancing age.
Front. Aging Neurosci. 15:1195785.
doi: 10.3389/fnagi.2023.1195785

Editorial: The neuroscience of advancing age

Ann-Maree Vallence[1,2], Rachael D. Seidler[3], Mitchell Ryan Goldsworthy[4,5], John G. Semmler[4] and George M. Opie[4]*

[1]School of Psychology, College of Health and Education, Murdoch University, Murdoch, WA, Australia, [2]Centre for Healthy Ageing, Health Futures Institute, Murdoch University, Murdoch, WA, Australia, [3]Department of Applied Physiology and Kinesiology, University of Florida, Gainesville, FL, United States, [4]Discipline of Physiology, School of Biomedicine, The University of Adelaide, Adelaide, SA, Australia, [5]Hopwood Centre for Neurobiology, Lifelong Health Theme, South Australian Health and Medical Research Institute (SAHMRI), Adelaide, SA, Australia

KEYWORDS

NIBS, healthy aging, pathological aging, neuroimaging, neuromodulation

Editorial on the Research Topic
The neuroscience of advancing age

While some older adults retain physical and mental capabilities comparable to individuals that are decades younger, others may be incapable of self-care. Understanding the factors that determine where an individual will find themselves on this spectrum, particularly those that may be modifiable, is therefore critical. In pursuit of this goal, the current Research Topic focussed specifically on how changes within the brain contribute to both healthy and pathological aging.

Changes in brain structure and network function

Changes to brain structure are a hallmark of aging that strongly influences how we age; reductions in white matter (WM) integrity are one example that has been suggested to underpin many age-related functional deficits (for example, [Madden et al., 2004; Van Petten et al., 2004; Kerchner et al., 2012]). To further investigate this, Yan et al. assessed how age-related changes in WM contribute to the ability of older adults to perceive global motion. This study used diffusion tensor imaging (DTI) to identify several specific white matter tracts where age-related reductions in integrity predicted reduced global motion perception. This was suggested to support the "disconnection hypothesis" of cognitive aging. Using a slightly different approach, Du et al. instead leveraged magnetic resonance histology (Johnson et al., 2022) to study genetic and age effects on brain volume within auditory areas. The volume of twelve auditory regions was quantified in 104 young and older animals from the BXD family of recombinant inbred mice. Interestingly, genotype was found to influence volume of auditory areas, and this effect differed in older animals. This important work provides a platform for better understanding age effects on auditory function, degradation of which is associated with many negative outcomes.

While local changes in specific brain structures are clearly important, considering how alterations to multiple structural elements interact to drive brain aging is also critical. To incorporate this, Hupfeld et al. recorded several indices of brain structure (including volumetric, surface and WM integrity) to report a number of deficits having

a complex relationship with reduced performance in a dual-task walking paradigm. In contrast, Vaughan et al. instead utilized machine-learning to quantify how an individual's chronological age differed from their brain-predicted age (as an indicator of accelerated or decelerated brain aging). They then demonstrated that accelerated brain aging moderated the relationship between leg strength and mobility.

One important factor often overlooked in studies of brain aging is the large differences in hormones between females and males across the lifespan. To assess the potential influence this may have on brain imaging studies, Hicks et al. examined associations between sex steroid hormones and age-network relationships in both males and females, focusing on network segregation. Although network segregation was not associated with hormone levels in females, network segregation in the cerebellar-basal ganglia and salience networks showed a complex relationship with age. Given their role in cognition and balance, it is important to understand how age-related changes in segregation within these networks drive behavior.

Modulating and testing function in older adults

Modulation of brain activity represents a promising avenue for improving how we age, and one approach to achieving this is to use non-invasive brain stimulation (NIBS). For example, Greeley et al. investigated how anodal transcranial direct current stimulation (atDCS) over prefrontal cortex influenced sequence learning in older adults. While increased performance was expected, atDCS instead reduced learning, possibly due to the timing of the intervention. These findings add to a growing body of literature demonstrating the need for optimized NIBS interventions in older adults.

As an alternative example of approaches to brain modulation, acupuncture has shown an ability to modify aberrant activity in patients with mild cognitive impairment (MCI), although the outcomes have been variable. Consequently, the meta-analysis by Ma and colleagues compiled the evidence examining the influence of acupuncture on functional MRI measures in MCI patients. Across studies, acupuncture was found to increase activity within several brain areas, with changes in thalamic areas associated with cognitive function. While supporting the potential utility of acupuncture in MCI, the authors also recognize confirmation is needed from more rigorous RCT studies. However, the outcomes of this study nonetheless demonstrate the potential utility of alternative approaches for influencing the aging brain. The study by Ma et al. further demonstrates this within the context of AD. This study investigated the therapeutic mechanisms of Cordycepin, a nucleoside adenosine analog derived from traditional Chinese medication that has shown anti-AD properties. Using network pharmacology and molecular docking methods, five genes (AKT1, MAPK8, BCL2L1, FOXO3, and CTNNB1) potentially serving as targets of Cordyceptin were identified. These in-silico findings provide novel insights for developing optimal treatments for AD.

While modulating function represents a core aim of many studies in aging neuroscience, assessing function remains a fundamental necessity. However, existing approaches are often time consuming or require specialist clinicians. To address this, Cattaneo et al. validated the "Guttman Cognitest" – a self-administered digital cognitive assessment requiring ~20 minutes – against conventional paper-and-pencil tests in a middle-aged cohort. Principal component analysis revealed three factors consistent between test types (memory, executive function, and visuomotor / visuospatial function), although there was some variance in how specific subtests loaded onto each factor. Furthermore, performance showed the expected negative association with age and positive association with years of education. The authors concluded that this digital assessment is appropriate for measuring cognitive function in large samples of middle-aged adults.

The role of systemic factors in brain aging

Consideration of the neuroanatomical and neurophysiological effects of age is often restricted to the context of the central nervous system (CNS). In contrast, interactions with the systemic environment may also contribute to age-related changes within the brain. For example, inflammation is increased in older adults, which may contribute to age-related cognitive deficits (Sartori et al., 2012). While this inflammatory state (and associated cognitive deficits) is often considered to develop with age, Ni and colleagues instead investigated if early-life events are also important. Specifically, a mouse model was used to show that maternal immune activation increases inflammation and exacerbates age-related cognitive deficits in offspring. Importantly, the same study also demonstrated that the influence of the prenatal environment could be mitigated by life-long environmental enrichment, demonstrating the importance of lifestyle on how we age. While interesting, the role played by inflammation during aging, particularly with respect to pathological aging, remains unclear. To clarify this, Leonardo and Fregni performed a systematic review and meta-analysis examining the relation between inflammatory cytokines and cognitive impairment from 79 studies in people with MCI or AD. Their findings suggested higher levels of several inflammatory cytokines in MCI and AD, in addition to greater risk of cognitive decline with high interleukin-6 (IL-6) levels. These outcomes indicate that increased cytokine levels within the CNS may be a potential therapeutic target for AD.

Hypertension represents another systemic condition prevalent in older adults. While its relationship with cognitive function in age has been demonstrated, Chen et al. instead assessed how hypertension may contribute to increased rates of depression and sleep disturbance in the elderly. Relative to normotensive older adults, those with hypertension showed poorer cognitive function and sleep quality, in addition to higher depression. Furthermore, mediation analysis suggested sleep quality and depression partially mediate the influence of hypertension on cognitive function. Consequently, sleep quality and depression represent potential targets in a multifaceted approach to improving cognitive function in older adults.

Conclusion

In conclusion, this Research Topic reports novel findings from 12 articles (involving >80 authors) covering a broad range of topics within the neuroscience of advancing age. This includes important new information about brain imaging, brain modulation, functional assessment, and the interaction between systemic and central factors. On the one hand, the breadth of this collection demonstrates the enormity of the challenge faced by the field. However, on the other hand, it's constellation of insightful approaches demonstrates that this challenge will be faced with enthusiasm.

Author contributions

GO drafted the manuscript. All authors critically revised and approved the manuscript.

Conflict of interest

The authors declare that the research was conducted in the absence of any commercial or financial relationships that could be construed as a potential conflict of interest.

Publisher's note

References

Johnson, G. A., Tian, Y., Cofer, G. P., Cook, J. C., Gee, J. C., Hall, A., et al. (2022). HiDiver: a suite of methods to merge magnetic resonance histology, light sheet microscopy, and complete brain delineations. *BioRxiv* 10, 479607. doi: 10.1101/2022.02.10.479607

Kerchner, G. A., Racine, C. A., Hale, S., Wilheim, R., Laluz, V., Miller, B. L., et al. (2012). Cognitive processing speed in older adults: relationship with white matter integrity. *PloS One* 7, e50425. doi: 10.1371/journal.pone.0050425

Madden, D. J., Whiting, W. L., Huettel, S. A., White, L. E., MacFall, J. R., Provenzale, J. M., et al. (2004). Diffusion tensor imaging of adult age differences in cerebral white matter: relation to response time. *Neuroimage* 21, 1174–1181. doi: 10.1016/j.neuroimage.2003.11.004

Sartori, A. C., Vance, D. E., Slater, L. Z., and Crowe, M. (2012). The impact of inflammation on cognitive function in older adults: implications for health care practice and research. *J. Neurosci. Nursing* 44, 206. doi: 10.1097/JNN.0b013e3182527690

Van Petten, C., Plante, E., Davidson, P. S., Kuo, T. Y., Bajuscak, L., Glisky, E. L., et al. (2004). Memory and executive function in older adults: relationships with temporal and prefrontal gray matter volumes and white matter hyperintensities. *Neuropsychologia* 42, 1313–1335. doi: 10.1016/j.neuropsychologia.2004.02.009

frontiers in Aging Neuroscience

ORIGINAL RESEARCH
published: 31 January 2022
doi: 10.3389/fnagi.2022.808022

Brain-Predicted Age Difference Moderates the Association Between Muscle Strength and Mobility

Brooke A. Vaughan[1,2], Janet E. Simon[1,3], Dustin R. Grooms[1,2,3], Leatha A. Clark[1,4,5], Nathan P. Wages[1,4] and Brian C. Clark[1,4]*

[1] Ohio Musculoskeletal and Neurological Institute (OMNI), Ohio University, Athens, OH, United States, [2] School of Rehabilitation and Communication Sciences, Ohio University, Athens, OH, United States, [3] School of Applied Health Sciences and Wellness, Ohio University, Athens, OH, United States, [4] Department of Biomedical Sciences, Ohio University, Athens, OH, United States, [5] Department of Family Medicine, Ohio University, Athens, OH, United States

Background: Approximately 35% of individuals over age 70 report difficulty with mobility. Muscle weakness has been demonstrated to be one contributor to mobility limitations in older adults. The purpose of this study was to examine the moderating effect of brain-predicted age difference (an index of biological brain age/health derived from structural neuroimaging) on the relationship between leg strength and mobility.

Methods: In community dwelling older adults (N = 57, 74.7 ± 6.93 years; 68% women), we assessed the relationship between isokinetic leg extensor strength and a composite measure of mobility [mobility battery assessment (MBA)] using partial Pearson correlations and multifactorial regression modeling. Brain predicted age (BPA) was calculated from T1 MR-images using a validated machine learning Gaussian Process regression model to explore the moderating effect of BPA difference (BPAD; BPA minus chronological age).

Results: Leg strength was significantly correlated with BPAD (r = −0.317, $p < 0.05$) and MBA score (r = 0.541, $p < 0.001$). Chronological age, sex, leg strength, and BPAD explained 63% of the variance in MBA performance ($p < 0.001$). BPAD was a significant moderator of the relationship between strength and MBA, accounting for 7.0% of MBA score variance [$\triangle R^2$ = 0.044, $F(1,51)$ = 6.83, p = 0.01]. Conditional moderation effects of BPAD indicate strength was a stronger predictor of mobility in those with a great BPAD.

Conclusion: The relationship between strength and mobility appears to be influenced by brain aging, with strength serving as a possible compensation for decline in neural integrity.

Keywords: weakness, physical function, sarcopenia, brain aging, dynapenia

OPEN ACCESS

Edited by:
George M. Opie, University of Adelaide, Australia

Reviewed by:
James H. Cole, University College London, United Kingdom
Chun Liang Hsu, University of British Columbia, Canada

****Correspondence:***
Brooke A. Vaughan
vaughanb@ohio.edu

Specialty section:
This article was submitted to Parkinson's Disease and Aging-related Movement Disorders, a section of the journal Frontiers in Aging Neuroscience

Received: *02 November 2021*
Accepted: *10 January 2022*
Published: *31 January 2022*

Citation:
Vaughan BA, Simon JE, Grooms DR, Clark LA, Wages NP and Clark BC (2022) Brain-Predicted Age Difference Moderates the Association Between Muscle Strength and Mobility. Front. Aging Neurosci. 14:808022. doi: 10.3389/fnagi.2022.808022

INTRODUCTION

The population of individuals over age 65 in the United States is expected to nearly double from 43.1 to 83.7 million by the year 2050 (Ortman et al., 2014). This shifting age demographic carries significant health, economic, and social implications and highlights the need to develop preventative and restorative interventions to facilitate healthy aging. Unfortunately, decline in

functional mobility [i.e., a person's ability to move independently and safely in a variety of environmental contexts to accomplish functional tasks (Bouça-Machado et al., 2018)] is a common consequence of aging, with as many as 35% of individuals over 70 and most individuals over 85 reporting difficulty with ambulation or activities of daily living (Cummings et al., 2014; Musich et al., 2018). Functional mobility deficits have been linked to increased fall risk, poorer psychosocial health, and greater health expenditure (Musich et al., 2018). In addition, mobility limitations are predictive of disability and mortality (Newman et al., 2006b).

The determinants of mobility are multi-factorial. Muscle weakness is one factor repeatedly shown to be associated with reduced functional mobility and future functional declines and mortality in older individuals (Visser et al., 2000; Newman et al., 2006a; Manini et al., 2007). Scientists and clinicians have long posited that age-related loss of lean mass is the primary mediator between weakness and mobility impairment in older adults. However, emerging evidence has highlighted the importance of central neural processes in muscle strength capacity (Clark et al., 2014; Carson, 2018; Clark and Carson, 2021). Age-related decreases in overall brain volume (Storsve et al., 2014), cortical thinning (Thambisetty et al., 2010; Storsve et al., 2014), and microvascular irregularities (Maniega et al., 2015) have been linked to frailty (Lu et al., 2020) and impaired functional mobility (de Laat et al., 2012; Pinter et al., 2018; Lockhart et al., 2021). Thus, we postulate that indices of brain pathology and aging may serve to moderate the well-known association between muscle strength/weakness and mobility in older adults.

Magnetic resonance imaging (MRI)-derived estimates have recently garnered attention as one approach to reliably quantify brain age (Franke et al., 2010; Cole and Franke, 2017; Cole et al., 2017, 2019). Here, "brain-predicted age" (BPA) is derived from T1-weighted neuroimages using machine learning approaches that have previously been employed to quantify the relationship between structural MRI data and chronological age (**Figure 1**). Subtracting chronological age from the estimated BPA results in a BPA difference (BPAD) score, which effectively quantifies how an individual's brain health differs from what would be expected for their chronological age (Franke et al., 2010; Cole and Franke, 2017; Cole et al., 2017). To date, researchers have linked accelerated brain aging to various pathological conditions including Alzheimer's disease (Franke et al., 2010), diabetes (Franke et al., 2013), and obesity (Ronan et al., 2016). Longitudinal studies have even demonstrated that individuals with older BPAD display early signs of cognitive decline from childhood to midlife (Elliott et al., 2019) and are more likely to receive a subsequent dementia diagnosis (Biondo et al., 2021). Thus, BPAD has been proposed as a biomarker of age-related deterioration of the brain (Cole and Franke, 2017; Cole et al., 2017).

Despite the promising application of neuroimaging to estimate biological brain age to disease populations, only one study has investigated the influence of biological brain age on physical function measures in a community-dwelling individuals. Here, Cole et al. (2018) reported an association between positive BPAD (i.e., an "older" brain relative to ones years) and decreased walking speed, poorer lung function, and weaker grip strength in a large, longitudinal study cohort. These findings offer support to the evolving perspective of the role of brain aging in relation to mobility. However, no study has investigated the influence of BPAD as a moderator of the well-established relationship between muscle strength and mobility. Accordingly, the primary purpose of this study was to examine the relationship between isokinetic leg extensor strength and mobility with BPAD as a potential moderator of this relationship in a community-dwelling older population.

MATERIALS AND METHODS

Overview of Study Design

Data presented in this report are derived from a larger study/dataset (UNCODE Study; NCT02505529). To be included in the original study, participants had to be $\geq$60 years of age, living independently and free from overt musculoskeletal and neurologic disease (see **Table 1** for a complete description of UNCODE inclusion and exclusion criteria). The Ohio University Institutional Review Board approved this study, and all participants provided written informed consent in accordance with the Declaration of Helsinki.

To characterize the study participants, we measured body composition (including estimates of appendicular and thigh lean mass) using DEXA (Hangartner et al., 2013; Tavoian et al., 2019) and moderate-to-vigorous intensity physical activity *via* accelerometry (Corbett et al., 2016). We quantified isokinetic (60°/s) leg extension strength and determined biological brain age estimates using T1 structural images and a previously validated machine-learning model (Cole et al., 2017). To capture the multi-dimensional nature of mobility, we measured functional performance using the mobility battery assessment (MBA) score, a multi-component evaluation of mobility that has been shown to be a more robust measure of self-reported lower extremity function and a more sensitive discriminator of mobility capacity in older individuals than single functional assessments (Riwniak et al., 2020). The specific methodological details related to our primary variables of interest have been outlined in previously published work (Clark et al., 2019, 2021; Wages et al., 2020), but a brief description is provided below.

Muscle Strength

Isokinetic leg extension strength was assessed using a Biodex System 4 Dynamometer (Biodex Medical Systems Inc., Shirley, NY, United States). Specific operational procedures follow those used in the Health ABC study (Manini et al., 2007). In brief, subjects performed six isokinetic trials measured at 60°/s with a 30 s rest period between each trial. Average isokinetic strength of the highest three trials was calculated using the peak isokinetic torque output from 90° to 30° of leg flexion. Isokinetic strength was normalized to body weight for all subsequent analyses as this measure has been shown to be predictive of the subsequent development of severe mobility limitations (Manini et al., 2007).

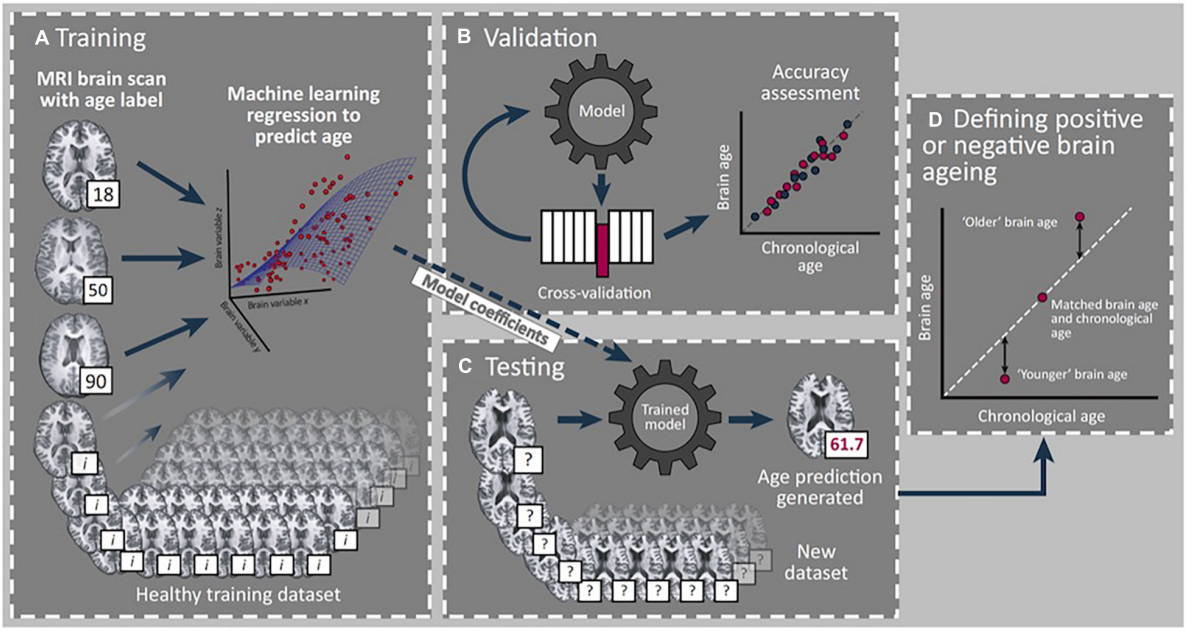

FIGURE 1 | Summary of brain age prediction using a supervised machine learning process. **(A)** Structural T-1 MRI scans labeled with chronological age from a training set of healthy individuals are loaded into a machine learning regression model. **(B)** Validation of model accuracy is conducted using cross-validation methods from a portion of the original dataset excluded from the model. Model generated predicted age values are compared with actual age values to determine model accuracy. **(C)** Model coefficients from the trained model are applied to a new test dataset to determine individual brain age prediction (61.7 years in this example). **(D)** A standardized metric for statistical comparison is created (brain-predicted age difference) by subtracting chronological age from predicted age to reflect rate of brain aging, with positive and negative values indicating older and younger brains, respectively. *Reprint permission from Elsevier from Trends in Neuroscience, 40 (12), Cole J. H. and Franke K., Predicting age using neuroimaging: innovative brain ageing biomarkers, 681–90, 2017.

Brain Predicted Age

T1 structural images were acquired on a 3.0 T Philips Achieva scanner with a 16-channel head coil with whole-brain axial gradient-echo MPRAGE 3-D T1-weighted images [*TE*/*TR* = 3.4/7.4 ms, flip angle = 8, slice thickness = 1 mm (contiguous slices), Field of View (FOV) = 250 × 250 × 200 mm,1 mm^3 resolution]. Participants were instructed to close their eyes during the scans. Scanner precision was assessed using repeat scans from a separate cohort of healthy, young adults who were scanned on two separate occasions ($n = 7$; age 25.43 ± 6.78 years).

Brain-predicted age was calculated using a previously validated Gaussian Process regression model published in other work (Cole et al., 2017). In brief, the brainageR model was trained on 3,377 healthy individuals (mean age = 40.6 years, *SD* = 21.4, range 18–92) from several large publicly available datasets. Model testing was subsequently performed on independent data representing 611 subjects, demonstrating a correlation with chronological age of 0.947 and a mean absolute error of 4.90 years (Cole et al., 2017). With respect to our data, we followed the procedure and employed the brainageR algorithm as previously established by Cole et al., 2015, 2017, 2019.[1] Raw T1-weighted MRI scans for each participant underwent segmentation and normalization procedures using SPM12 and a customized version of FSL *slicesdir* was used to create PNG and index.html files for quality control. Normalized image files were then loaded into R using the RNfiti package to separate and mask gray and white matter and cerebrospinal fluid. To calculate BPA for each participant in the current dataset, a rotation matrix with 435 components from the brainageR model was applied using kernlab (**Figure 1**). BPA was then converted to the variable of interest, BPAD, by subtracting participants' chronological age from their brain-predicted age estimate with positive and negative BPAD reflecting older and younger biological brains, respectively.

Mobility Battery Assessment

The MBA includes both locomotor (6-min walk gait speed, time to complete the four-square step test and stair climb power) and non-locomotor (5× chair rise time and time to complete a complex functional task) functional measures. The overall MBA score is calculated using principal component analysis and reflects performance on all five tasks. MBA scores have a distribution of a mean of 0 and a standard deviation of 1.0 (Riwniak et al., 2020). Below we describe the testing involved in the individual components of the MBA score.

Six-Minute Walk Test

Participants were asked to walk as far as possible in 6 min by repeating a 60-m course that included a 30-m straight walkway and two 180° turns to the left. Participants were informed of the time remaining after each 60m lap and were provided with verbal

[1]https://github.com/james-cole/brainageR

TABLE 1 | UNCODE inclusion and exclusion criteria.

INCLUSION
Age 60+ years (older adults) with no significant health issues or conditions that, in the investigator's opinion, would limit the subject's ability to complete the study per protocol or that would impact the capability to get an accurate measurement of study endpoints.
Body mass index between 18 and 40 kg/m^2.
Willingness to undergo all testing procedures.
Able to read, understand, and complete study-related questionnaires.
Able to read and understand, and willing to sign the informed consent form (ICF).
EXCLUSION
Failure to provide informed consent.
Known neuromuscular or neurological conditions affecting somatosensory or motor function or control (e.g., hemiplegia, multiple sclerosis, peripheral neuropathy, Parkinson's disease, Myasthenia Gravis, Ataxia, Apraxia, mitochondrial myopathy, etc.).
Unable to communicate because of severe hearing loss or speech disorder.
Severe visual impairment, which would preclude completion of the assessments.
Cancer requiring treatment currently or in the past 2 years (except primary non-melanoma skin cancer or *in situ* cervical cancer).
Any ADL disability.
Recent unexplained weight loss (>10 pounds in past month).
Hospitalization (medical confinement for 24 h), or immobilization, or major surgical procedure requiring general anesthesia within 12 weeks prior to screening, or any planned surgical procedures during the study period.
Chronic or relapsing/remitting gastrointestinal disorders such as inflammatory bowel disease and irritable bowel syndrome.
Known history of human immunodeficiency virus (HIV) antibody at screening.
Use of systemic glucocorticoids.
Severe pulmonary disease, requiring either steroid pills or injections or the use of supplemental oxygen.
Severe cardiac disease, including NYHA Class III or IV congestive heart failure, clinically significant aortic stenosis, recent history of cardiac arrest (within 6-months), use of a cardiac defibrillator, or uncontrolled angina.
Renal failure on hemodialysis.
Psychiatric conditions that warrant acute or chronic therapeutic intervention (e.g., major depressive disorder, bipolar disorder, panic disorder, schizophrenia) that in the investigator's opinion interfered with the conduct of study procedures.
Unable to undergo Magnetic Resonance Imaging (MRI), Transcranial Magnetic Stimulation (TMS), or DEXA (e. g. body containing any metallic medical devices or equipment, including heart pacemakers, metal prostheses, implants or surgical clips, any prior injury from shrapnel or grinding metal, exposure to metallic dusts, metallic shavings or having tattoos containing metallic dyes, body dimensions exceeding capacity of MRI or DEXA). Note: This manuscript is an analysis from a larger study and the MRI and brain stimulation exclusion criteria, which are not presented here, were part of this larger study.
Unable to reliably undergo exercise or strength tests described for this study.
Participation in any clinical trial within 12 weeks prior to screening.
Limb amputation (except for toes) and/or any fracture within 24 weeks of study screening.
Conditions (such as myasthenia gravis, myositis, muscular dystrophy, or myopathy, including drug-induced myopathy) leading to muscle loss, muscle weakness, muscle cramps, or myalgia.
Acute viral or bacterial upper or lower respiratory infection at screening.
Abnormal or uncontrolled blood pressure at the screening visit defined as BP > 170/100 mmHg. If taking anti-hypertensive medication, had to have been on stable doses of medication for more than 3 months.

encouragement. Gait speed for each participant was calculated by dividing the distance traveled during the task by 360 s.

Four Square Step Test

Participants were instructed to step over four pieces of tape placed on the floor in a plus sign (i.e., +) configuration in a predetermined sequence as quickly as possible. Trials were not considered successful if the participant touched the tape, did not follow the instructed stepping sequence or was unable to maintain balance. Time to complete the task was measured with a stopwatch to the nearest 0.01 s and performance scores reflect the mean of three successful trials.

Stair Climb Power

Participants were instructed to ascend a flight of eight stairs (∼18 cm rise) as quickly as possible without the use of upper extremity handrail support unless needed for safety. Time to complete the stair climb was measured using switch mats (Lafayette Instruments Model 54,060) interfaced with a digital timer to the nearest 0.01 s. Participants performed the task twice and results were averaged from both trials. Stair climb power was then calculated as: Power = [(body weight in kg) × (9.8 m/s^2) × (stair height in meters)]/time in seconds where stair height was the sum height of all eight stairs.

5× Chair Rise

From an erect sitting position, participants were instructed to fold their arms across their chest and stand and sit from a chair (∼46 cm high) five times consecutively. The time to complete the task was measured using a stopwatch to the nearest 0.01 s and participants performed only one trial.

Complex Functional Task

For this assessment, participants were asked to complete a composite skill previously described in other work (Wages et al., 2020). Briefly, subjects began the task seated on the floor and were asked to stand, lift a 4.5 kg weighted laundry basket, walk 1.5 m, and place the basket on a surface 0.75 m high. Time to complete the task was measured using a stopwatch to the nearest 0.01 s for two trials, with scores representing the mean of both trials. If a participant was unable to complete the task, or it took >30 s, a value of 30 s was assigned to that participant. If a participant was only able to complete the task once, the time on that trial represented their performance.

Statistical Analysis

All statistical analyses were conducted using Statistical Package for Social Sciences (SPSS) version 25 (SPSS Inc., Chicago, IL, United States) with a significance level of 5% (two-tailed). All data was expressed as the mean ± SD for the descriptive statistics.

The first level analysis was to explore the relationship between chronological age, lower extremity strength, BPAD, and the overall MBA score and components of the MBA using bivariate Pearson correlation tests. Partial Pearson correlation coefficients were also used to examine the relationship between average isokinetic lower extremity extensor strength normalized to body weight, the MBA, and individual functional performance measures (i.e., 5× chair rise, etc.) with sex and chronological age included as covariates. In a separate analysis, BPAD was included as an additional covariate to reflect the hypothesized neural contributions to mobility in older individuals. Since the brainageR model does not automatically correct brain age estimates for the statistical influence of chronological age, both chronological age and BPAD were included in this analysis to capture the differential impact of biological brain and chronological age discrepancies across the lifespan (Le et al., 2018). Finally, partial Pearson correlation coefficients were used to investigate any potential relationship between BPAD and functional performance measures with sex and chronological age as covariates. The same analyses were also performed using lower extremity extensor strength normalized to body weight as an additional covariate.

In a second level of analysis, a hierarchical multiple regression was conducted to investigate the predictive value of lower extremity extensor strength and BPAD for MBA performance. MBA was selected as the variable of interest for this level of analysis as it represents a composition of multiple aspects of functional mobility. Chronological age and sex were included in regression Model 1 to isolate the effects of the covariates. Model 2 included lower extremity isokinetic extensor strength and BPAD in addition to the covariates in Model 1. Independent contributions of each predictor variable were calculated using the semi-partial r^2 ($_{sp}r^2$) and the variance inflation factor (VIF) was used to evaluate collinearity of the predictors.

Lastly, to understand whether the relationship between strength and mobility depends on BPAD (i.e., presence of an interaction effect between isokinetic leg extensor strength and BPAD), a moderation analysis was conducted for isokinetic leg extensor strength and the MBA. To explore the impact of task difficulty with respect to our dataset, we performed additional moderation analyses on two subcomponents of the MBA, the four-square step test and gait speed during the six-minute walk test. Chronological age and sex were used as covariates for all analyses. Moderation effects were estimated using the PROCESS macro for SPSS as described by Hayes and Matthes (2009) and Hayes (2018), using 5,000 bootstrap samples with 95% confidence intervals. Following the moderation analysis the Johnson–Neyman technique was used to probe for the interaction and to identify ranges of values of the moderator for which the interaction effect is significant (Johnson and Neyman, 1936; Hayes and Matthes, 2009). Due to the exploratory nature of the analyses, correction for multiple comparisons was not performed for any correlations.

RESULTS

Participants were only included in the present analysis if they had complete data for all variables of interest. Three additional participants were excluded due to poor T1 image quality (e.g., excessive artifact), resulting in data from fifty-seven participants (68% women) available for statistical analyses. Scanner reliability was considered good-excellent with an ICC = 0.973 (CI 0.699–0.996). Statistical assumptions for correlation and linear regression analyses were satisfied. Detailed demographic information and average performance on functional measures are provided in **Table 2**. In our sample, average BPAD was positive, reflecting advanced brain aging and as expected, there was a significant amount of heterogeneity in BPAD between study participants (**Figure 2**). There were no significant differences in BPAD with respect to sex ($p = 0.504$).

Bivariate correlations revealed moderate to strong relationships between MBA composite, most functional subtests, normalized leg extensor strength and chronological age.

TABLE 2 | Participant demographics and functional performance.

Chronological age (yrs)	74.70 ± 6.93
Brain-predicted age difference (yrs)	0.801 ± 6.29
Height (cm)	164.07 ± 10.26
Weight (kg)	72.06 ± 15.66
Body mass index (kg/cm^2)	26.71 ± 5.14
Body fat (%)	35.04 ± 8.09
Appendicular lean mass/height^2 (kg/cm^2)	6.70 ± 1.19
Relative leg extensor strength (N-m/kg body weight)	86.16 ± 32.54
Accelerometry min/wk of moderate–vigorous activity	84.41 ± 56.23
Overall mobility battery assessment score	0.045 ± 0.972
6-minute walk test (m/sec)	1.34 ± 0.31
Four square step test (sec)	9.80 ± 3.87
Stair climb power (watts)	291.49 ± 106.51
5× chair rise (sec)	10.85 ± 3.62
Complex functional task (sec)	10.01 ± 8.65

yrs, years; cm, centimeters; kg, kilograms; N, Newtons; m, meters; wk, week; sec, seconds.

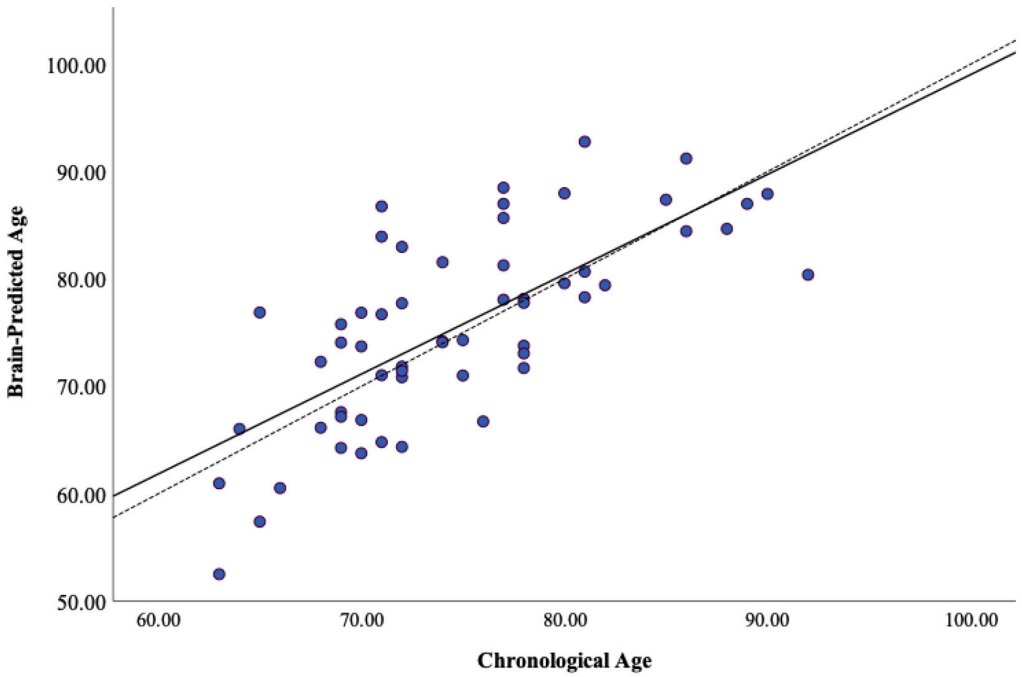

FIGURE 2 | Heterogeneity of brain-predicted age. Brain-predicted age from brainageR regression model. Scatterplot depicting chronological age (x-axis) by brain-predicted age (y-axis). Dashed line is the line of identity and solid black line is the regression line of chronological age on brain-predicted age.

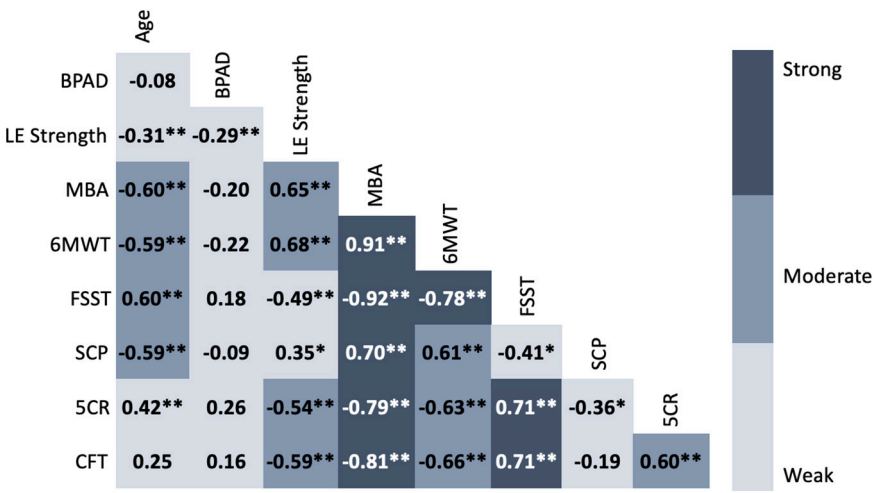

FIGURE 3 | Correlation matrix of chronological age, brain-predicted age difference, normalized leg strength and functional performance. Values represent Pearson's *r* for each bivariate correlation. *Weak* = 0.00–0.49, *Moderate* = 0.50–0.69, *Strong* = 0.70–1.0 (Jurs et al., 1998). BPAD, brain-predicted age difference; LE, lower extremity; MBA, mobility battery assessment; 6MWT, six-minute walk test; FSST, four square step test; SCP, stair climb power; 5CR, five times chair rise; CFT, complex functional task.

In contrast, BPAD was weakly correlated with the other variables of interest (**Figure 3**). When controlling for both chronological age and sex, isokinetic leg extensor strength normalized to body weight was significantly correlated with BPAD, composite MBA score, 6-min walk test gait speed, four square step test, 5× chair rise time, and time to complete a complex functional task The addition of BPAD as a covariate appeared to weaken the relationship between isokinetic leg extensor strength, composite MBA score, 6-min walk test gait speed, 5×-chair rise time, four square step test and time to complete a complex functional task. However, *r* to Z transformation analyses did not reveal any significant correlational differences when adding BPAD as a covariate. Isokinetic leg extensor strength was not significantly related to stair climb power in either scenario (**Table 3**).

Brain predicted age difference was also significantly correlated with overall MBA score, four square step test, and 5× chair rise time when controlling for both chronological age and sex. However, after including normalized leg extensor strength as a covariate, BPAD was no longer significantly correlated with any functional measure (**Table 4**).

Both Model 1 (chronological age and sex covariates) and Model 2 (covariates with normalized lower extremity extensor strength and BPAD) were found to be statistically significant predictors of composite MBA score. Model 1 accounted for 46% of the variance of the MBA score ($p < 0.001$), and both chronological age and sex were statistically significant independent predictors, accounting for a unique contribution in the explained variance in Model 1 of 61% ($p = 0.003$) and 31% ($p < 0.001$), respectively. Model 2 explained 63% of the total variance of composite MBA score ($p < 0.001$), but only normalized leg extensor strength and chronological age were significantly individually predictive of composite MBA score with normalized leg strength explaining 35% ($p < 0.001$) and chronological age 44% ($p < 0.001$) of the variability in composite MBA performance. Variance inflation factor values for both models are within a range that is not concerning for collinearity as all values are less than 2 (Hair et al., 2014). Details of the regression analyses are outlined in **Table 5**.

Brain predicted age difference was a significant moderator of the relationship between normalized leg extensor strength and composite MBA score and this interaction accounted for 7.0% of the variance in MBA score [$\triangle R^2 = 0.044$. $F(1,51) = 6.83$, $p = 0.01$]. Conditionally, normalized leg extensor strength was significantly predictive of composite MBA score when considering mean BPAD and BPAD at the 16th and 84th percentiles. However, the strength of the relationship between normalized leg extensor strength and MBA score varied according to brain age—biologically younger brains (i.e., 16th percentile) attenuated the relationship whereas older brains (i.e., 84th percentile) strengthened the relationship. In addition, the Johnson–Neyman technique revealed a conditional effect of BPAD for very young biological brains (**Figure 4**). While the relationship between normalized leg extensor strength and MBA was significant within the range of −7.02 to 15.76 years of BPAD, strength was not a significant predictor of functional performance in a small subset of very young brains (i.e., BPAD < −7.02).

Interestingly, BPAD was also a significant moderator of the relationship between normalized leg extensor strength and FSST time [$\triangle R^2 = 0.0808$. $F(1,51) = 9.45$, $p = 0.003$], but was not a moderator of the relationship between normalized leg extensor strength and gait speed [$\triangle R^2 = 0.0061$. $F(1,51) = 0.900$, $p = 0.347$]. Conditional moderation effects were also observed with respect to the four-square step test. Specifically, normalized leg extensor strength was only a significant predictor for "average" age brains (i.e., 50th percentile BPAD = −0.32) and "older" brains (i.e., 84th percentile BPAD = 7.8624) but not for four square step test performance in those with relatively "younger" brains (i.e., 14th percentile BPAD = −5.3188).

TABLE 3 | Correlations between lower extremity strength and functional performance measures.

Covariates	Chronological age Sex	Chronological age Sex BPAD	
BPAD	−0.317*	N/A	*Z* Value
Overall MBA Score	0.541**	0.493**	0.34 ($p = 0.734$)
6MWT	0.585**	0.537**	0.36 ($p = 0.72$)
FSST	−0.367*	−0.306*	−0.36 ($p = 0.72$)
SCP	0.130	0.122	N/A
5CR	−0.491**	−0.434**	−0.38 ($p = 0.70$)
CFT	−0.489**	−0.467**	−0.15 ($p = 0.88$)

*BPAD, brain-predicted age difference; MBA, mobility battery assessment; 6MWT, six-minute walk test; FSST, four square step test; SCP, stair climb power; 5CR, five times chair rise; CFT, complex functional task. *Statistical significance ($p < 0.05$). **Statistical significance ($p < 0.001$).*

TABLE 4 | Correlations between brain-predicted age difference and functional performance measures.

Covariates	Chronological age Sex	Chronological age Sex Average leg extensor strength
Average leg extensor strength	−0.317*	N/A
Overall MBA Score	−0.302*	−0.163
6MWT	−0.326	−0.183
FSST	0.278*	0.183
SCP	−0.046	−0.005
5CR	0.316*	0.159
CFT	0.162	0.009

*MBA, mobility battery assessment; 6MWT, six-minute walk test; FSST, four square step test; SCP, stair climb power; 5CR, five times chair rise; CFT, complex functional task. *Statistical significance ($p < 0.05$). **Statistical significance ($p < 0.001$).*

DISCUSSION

The primary purpose of this study was to examine the relationship between leg extensor strength and mobility

TABLE 5 | Regression model summary for the mobility battery assessment (MBA) score.

	Model characteristics		
	s-p r^2	VIF	*p*-value
Model 1			
$R^2 = 0.46$; p-value ≤ 0.001*			
Sex	−0.307	1.001	0.003*
Age	−0.611	1.001	<0.001*
Model 2			
$R^2 = 0.63$; p-value ≤ 0.001*			
Sex	−0.118	1.215	0.168
Age	−0.449	1.173	<0.001*
Isokinetic strength/BW	0.345	1.484	<0.001*
BPAD	−0.101	1.128	0.238

BW, Body weight.

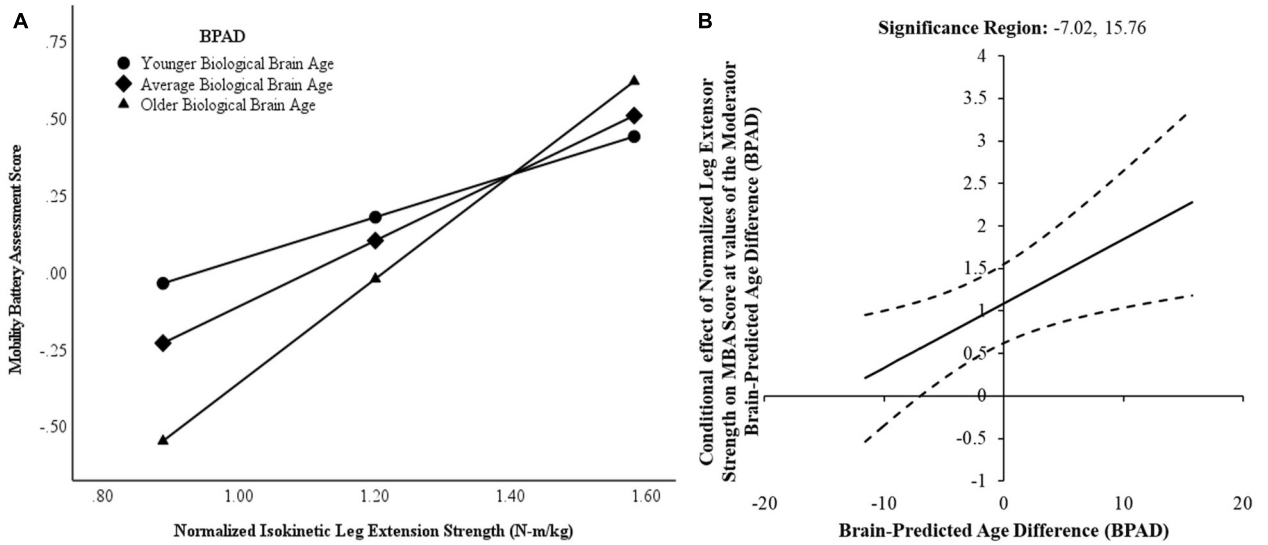

FIGURE 4 | Conditional effects of brain-predicted age difference (BPAD) on the strength-function relationship. **(A)** Normalized leg extensor strength and composite mobility battery assessment (MBA) score demonstrate a weaker relationship for low (younger) brain age (16th percentile). In contrast, normalized leg extensor strength is a stronger predictor of MBA score for average and high (older) brain age (84th percentile). **(B)** Johnson–Neyman plot indicating conditional effects of brain-predicted age difference (BPAD) on the relationship between leg extensor strength and mobility battery assessment (MBA) score performance with a 95% confidence interval (dashed line). Note the vertical boundary lines indicate the range of BPAD where normalized leg extensor strength is a significant predictor of MBA score.

with BPAD as a potential moderator of this relationship in a community-dwelling older population. Our findings indicated that normalized leg extensor strength and BPAD were significantly correlated, and BPAD weakened the association between normalized leg extensor strength and mobility. Interestingly, BPAD was also a significant moderator of the predictive value of normalized leg extensor strength for composite MBA score with an observed conditional effect.

Our current findings replicate the results of prior work, identifying muscle strength as a strong predictor of mobility (Visser et al., 2000; Newman et al., 2006a; Hicks et al., 2012). For example, Davis et al. (1998) reported a positive association between isometric quadriceps strength and functional mobility measures including the five times chair rise test and usual and fast walking speed in a sample of 705 women of Japanese ancestry between the ages of 55 and 93 years old. Similarly, Hairi et al. (2010) examined the relationship between appendicular measures of strength, low lean muscle mass and muscle quality and subjective and objective measures of mobility in a group of 1,705 men older than 75 years of age. Of the predictor variables, muscle strength demonstrated the strongest association with functional mobility (Hairi et al., 2010). Leg strength has also been identified as a potential preclinical marker of mobility decline in older adults. Manini et al. (2007) assessed isokinetic leg extensor strength and functional mobility in the Health, Aging and Body Composition cohort, identifying sex-specific low and high cut-points predictive of future development of severe mobility limitations. For our cohort, both men (1.45 ± 0.49 Nm/kg) and women (1.11 ± 0.33 Nm/kg), on average, demonstrated moderate risk for future mobility limitation based on these cut-points.

Despite the association between muscle strength and mobility, an individual's ability to generate maximal voluntary force is far from the sole determinant of physical function, leading researchers to call for investigation of additional mechanisms of mobility (Sorond et al., 2015). DiSalvio et al. (2020) identified a relationship between gray matter volume in vestibular, somatosensory and perceptual regions and functional performance as measured by gait speed, balance, and the four square step test, with higher cortical volumes associated with better physical performance. Lu et al. (2020) in a prospective study also reported an association with global gray matter volume and development of frailty—individuals with reduced gray matter volume were more likely to develop frailty than those with higher volumes. In addition, falling as a consequence of impaired mobility has been linked to decreased gray matter, subcortical and lower white matter volume (Hsu et al., 2016).

Given that brain aging encompasses more than one singular aspect of structural integrity (i.e., cortical thickness, white matter volume, etc.), we contend that BPAD may be considered a singular aggregate measure for global brain health and structural integrity to evaluate relative to functional mobility. In line with this approach, Cole et al. (2018) identified a relationship between BPAD and multiple domains of function as well as early mortality. Specifically, a greater BPAD (i.e., relatively "older" brains) was significantly associated with decreased fluid cognition, poorer lung function, weaker grip strength and slower walking speed (Cole et al., 2018). Similarly, our results also suggest a neural influence on function—BPAD was significantly correlated with MBA score and some of the functional subcomponents. However, this relationship was no longer significant when covarying for

normalized leg extensor strength, suggesting a more nuanced relationship between BPAD, strength, and function. Indeed, our findings do suggest a more complex interplay between BPAD and muscle strength whereby an interaction between brain age and normalized lower extremity strength resulted in a change in the strength of the relationship between normalized leg extensor strength and MBA composite scores.

Our results also indicate that BPAD has a conditional effect on the predictive value of leg strength for mobility. For individuals with very young brains relative to their chronological age, leg strength was not related to mobility performance. We interpret these findings to suggest that neural processes such as cognition and motor planning may minimize the importance of leg strength for functional performance in young brains. Dual task paradigms are often used to investigate the role of attentional and executive function processes in functional mobility and highlight performance differences in younger versus older adults. Differences in dual task performance across the lifespan may reflect decreased structural integrity of the dorsolateral prefrontal cortex and the orbitofrontal cortex, cognitive brain regions that are particularly sensitive to age-related changes (Raz et al., 2005). For example, in a study comparing young, middle and older aged adults, dual task cost on motor performance in the 10-meter walk test, the Timed Up and Go and the Four Square Step Test increased with age and older adults demonstrated the worst cognitive and motor performance (Brustio et al., 2017).

Anticipatory motor planning also demonstrates age-related decline as measured by end-state comfort effect paradigms. For motor tasks, adults have been shown to plan motor actions in such a manner that initial movement phases result in awkward postures to ensure that later movements lead to a comfortable end posture (Stöckel et al., 2017). However, this anticipatory planning capacity declines with age beginning in the seventh decade of life. In a bar-transport-task, older adults exhibited decreased end-state comfort sensitivity compared to younger adults, an observation exacerbated with increasing task complexity. While the mechanisms underlying this behavior are not entirely clear, older adults' inability to plan motor actions to increase end state comfort is theorized to reflect a decline in executive and/or motor function. Collectively, age-related decline in dual task and end state effect motor tasks suggests that in younger brains, neural processes (i.e., cognition, motor planning, etc.) may be the preferred mechanism of adequate motor performance.

Alternatively, leg strength may be a compensatory mechanism to maintain physical functioning in the context of advancing brain age. This interpretation of compensation to maintain function is consistent with theories of aging and cognition. For example, the Compensation-Related Utilization of Neural Circuits Hypothesis (CRUNCH) posits that frontal region overactivation in older compared to younger adults is compensatory for age-related changes (i.e., decreased gray matter volume, compromised sensory input) and serves to maintain cognitive task performance (Reuter-Lorenz and Cappell, 2008). CRUNCH also suggests with increasing task difficulty, frontal overactivation reaches a maximal "crunch point," resulting in insufficient compensatory reserves and impaired performance. The Scaffolding Theory of Aging and Cognition-Revised (STAC-r) takes a broader view of aging, compensation and cognitive performance (Reuter-Lorenz and Park, 2014). Specifically, aging is viewed as a neural insult resulting in structural and functional connectivity changes that necessitate the utilization of scaffolds to maintain cognitive function. In this context, scaffolds can represent variable compensatory mechanisms including increased frontal recruitment (Reuter-Lorenz and Cappell, 2008), recruitment of homologous contralateral regions (Cabeza, 2002) and neurogenesis (Fuchs and Flügge, 2014). Our data demonstrate a similar compensatory pathway for physical function and mobility, whereby increased strength can sustain mobility despite age-related neural structural decline.

Evidence highlighting a "common cause" of neural decline in cognitive, sensory and motor systems (Christensen et al., 2001) as well as observed overactivity in frontal and parietal regions in older individuals during motor tasks (Mattay et al., 2002) supports the adaptation of these theories to our current findings. Thus, we suggest greater BPAD derived from structural neuroimaging inherently reflects accelerated decline in structural brain integrity, resulting in the need for compensatory mechanisms to maintain physical function. At some point in brain aging, neural compensatory mechanisms likely reach maximum utility (i.e., crunch point). Based on our data we postulate that the crunch point of central mechanisms results in the need for additional *peripheral* scaffolding, namely, leg extensor strength, to maintain MBA performance. While not observed on our sample, a peripheral crunch point could theoretically also be reached whereby strength can no longer compensate for advancing neural insufficiency, resulting in a decline in functional mobility. Alternatively, individuals with muscle weakness may lack additional peripheral scaffolding, accelerating the loss of physical function in the context of neural decline.

These views are supported in part by observations in individuals with Alzheimer's and Parkinson's disease, two forms of central nervous system pathology shown to have advanced brain-predicted age (Franke et al., 2010; Beheshti et al., 2020). Recently, Sampaio et al. (2020) reported an interesting relationship between lower extremity strength, cognition and functional capacity. In their sample of institutionalized adults with dementia, lower extremity strength was not associated with cognition but was significantly associated with level of independence in activities of daily living (Sampaio et al., 2020). Similarly, progressive resistance and functional training in a cohort of 62 individuals with dementia resulted in significant improvements in both lower extremity strength and performance on a modified Short Physical Performance Battery and cognitive status was not a predictor of the training response (Hauer et al., 2012). In a group of 40 individuals with mild-moderate Parkinson's disease, low muscle power was significantly associated with walking speed even when controlling for Unified Parkinson's Disease Rating Scale motor scores (Allen et al., 2010).

Theories of cognitive aging also consider the influence of task difficulty in compensatory activation of alternative neural scaffolds during cognitive tasks. According to CRUNCH, increased neural recruitment in response to increased task

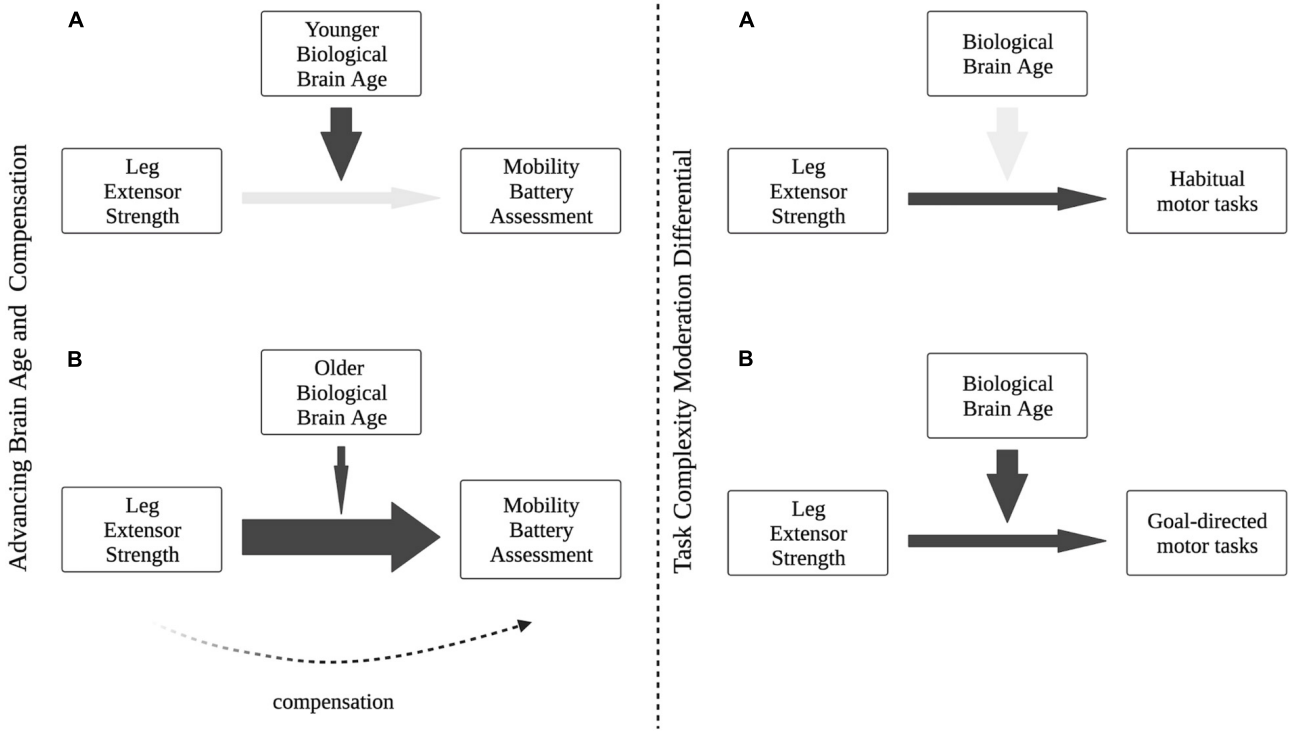

FIGURE 5 | Conceptual framework of our proposed Motoric Aging and Compensation Hypothesis (MACH). **(Left panel A)** In the context of relatively "younger" brains and adequate neural mechanisms of mobility, strength is not needed as a functional compensation. **(Left panel B)** With accelerated brain age and decline in neural integrity, strength becomes a stronger predictor of functional performance and maintains functional capacity. **(Right panel A)** Brain age difference does not moderate the predictive relationship between strength and habitual motor tasks (e.g., gait), indicating neural processing may not be as integral during simpler, more automatic mobility tasks. **(Right panel B)** Increased task complexity of goal-directed motor tasks necessitates greater neural contribution to functional performance, with brain age moderating the relationship between strength and mobility.

complexity is normal—both younger and older adults demonstrate frontal overactivation in response to increase task difficulty to maintain cognitive performance. However, older adults utilize compensatory resources earlier than younger counterparts for the same task. Our results suggest a similar influence of task difficulty on compensation in motor function—BPAD was not a significant moderator of the relationship between leg extensor strength and gait speed, a task that represents a less complex form of functional mobility (i.e., a "habitual" or "automatic" motor task). However, BPAD was a significant moderator when considering the relationship between leg extensor strength and the four-square step test, a task that incorporates additional elements of mobility complexity including change of direction and increased postural stability demands (i.e., a "goal-directed" task). While the results of these exploratory analyses should be interpreted with caution, they may reflect a nuanced compensatory task differential with regard to the relationship between BPAD and leg strength. While more work is certainly needed to identify specific mechanisms of neural and muscular motor compensation with age, a conceptual framework for brain aging, mobility performance and task complexity is presented in **Figure 5**.

There are several limitations inherent to our study that should be recognized. First, our sample size was relatively small and predominantly female, limiting the generalizability of our findings. Additionally, all subjects in this study were community-dwelling older individuals and as such these results may not be generalizable to all older adults. The cross-sectional nature of this study design also prevents any interpretation of causality or application of these findings to changes over time. Finally, the specific machine learning algorithm used in this study prevents any definitive interpretation of which structural parameters (i.e., gray matter volume, ventricle size, etc.) are most influential in calculating BPA.

CONCLUSION

We sought to investigate the moderation effects of brain age on the relationship between leg extensor strength and mobility tasks in older adults. Based on our findings, the previously highlighted relationship between lower extremity strength and physical function appears to be influenced by accelerated brain aging, with lower extremity strength serving as a possible compensation for a decline in neural integrity under more complex conditions. Collectively, these findings underscore the need to explore the nuances of the brain-muscle-function relationship in order to adequately address mobility decline associated with aging.

DATA AVAILABILITY STATEMENT

The raw data supporting the conclusions of this article will be made available by the authors, without undue reservation.

ETHICS STATEMENT

The studies involving human participants were reviewed and approved by Ohio University Institutional Review Board. The patients/participants provided their written informed consent to participate in this study.

AUTHOR CONTRIBUTIONS

BV, JS, DG, and BC: conception and design of the study and drafting a significant portion of the manuscript or figures. All authors: acquisition and analysis of data.

FUNDING

This work was supported, in part, by grants from the National Institutes of Health (NIA R01AG044424 and NIA R01AG067758).

REFERENCES

Allen, N. E., Sherrington, C., Canning, C., and Fung, V. (2010). Reduced muscle power is associated with slower walking velocity and falls in people with Parkinson's disease. *Parkins. Related Dis.* 16, 261–264. doi: 10.1016/j.parkreldis.2009.12.011

Beheshti, I., Mishra, S., Sone, D., Khanna, P., and Matsuda, H. (2020). T1-weighted MRI-driven brain age estimation in Alzheimer's disease and Parkinson's disease. *Aging Dis.* 11, 618–628. doi: 10.14336/AD.2019.0617

Biondo, F., Jewell, A., Pritchard, M., Aarsland, D., Steves, C. J., Mueller, C., et al. (2021). Brain-age predicts subsequent dementia in memory clinic patients. *medRxiv* [Preprint]. doi: 10.1101/2021.04.03.21254781

Bouça-Machado, R., Maetzler, W., and Ferreira, J. J. (2018). What is functional mobility applied to Parkinson's disease? *J. Parkinson's Dis.* 8, 121–130. doi: 10.3233/JPD-171233

Brustio, P. R., Magistro, D., Zecca, M., Rabaglietti, E., and Liubicich, M. E. (2017). Age-related decrements in dual-task performance: comparison of different mobility and cognitive tasks. a cross sectional study. *PLoS One* 12:e0181698. doi: 10.1371/journal.pone.0181698

Cabeza, R. (2002). Hemispheric asymmetry reduction in older adults: the harold model. *Psychol. Aging* 17:85. doi: 10.1037//0882-7974.17.1.85

Carson, R. G. (2018). Get a grip: individual variations in grip strength are a marker of brain health. *Neurobiol. Aging* 71, 189–222. doi: 10.1016/j.neurobiolaging.2018.07.023

Christensen, H., Mackinnon, A. J., Korten, A., and Jorm, A. F. (2001). The" common cause hypothesis" of cognitive aging: evidence for not only a common factor but also specific associations of age with vision and grip strength in a cross-sectional analysis. *Psychol. Aging* 16:588. doi: 10.1037//0882-7974.16.4.588

Clark, B. C., and Carson, R. G. (2021). Sarcopenia and neuroscience: learning to communicate. *J. Gerontol. A Biol. Sci. Med. Sci.* 76, 1882–1890. doi: 10.1093/gerona/glab098

Clark, B. C., Mahato, N. K., Nakazawa, M., Law, T. D., and Thomas, J. S. (2014). The power of the mind: the cortex as a critical determinant of muscle strength/weakness. *J. Neurophysiol.* 112, 3219–3226. doi: 10.1152/jn.00386.2014

Clark, B. C., Manini, T. M., Wages, N. P., Simon, J. E., and Clark, L. A. (2019). Voluntary vs electrically stimulated activation in age-related muscle weakness. *JAMA Network Open* 2:e1912052. doi: 10.1001/jamanetworkopen.2019.12052

Clark, L. A., Manini, T. M., Wages, N. P., Simon, J. E., Russ, D. W., and Clark, B. C. (2021). Reduced neural excitability and activation contribute to clinically meaningful weakness in older adults. *J. Gerontol. Ser. A* 76, 692–702. doi: 10.1093/gerona/glaa157

Cole, J. H., and Franke, K. (2017). Predicting age using neuroimaging: innovative brain ageing biomarkers. *Trends Neurosci.* 40, 681–690. doi: 10.1016/j.tins.2017.10.001

Cole, J. H., Leech, R., Sharp, D. J., and Alzheimer's Disease Neuroimaging Initiative. (2015). Prediction of brain age suggests accelerated atrophy after traumatic brain injury. *Ann. Neurol.* 77, 571–581. doi: 10.1002/ana.24367

Cole, J. H., Marioni, R. E., Harris, S. E., and Deary, I. J. (2019). Brain age and other bodily 'ages': implications for neuropsychiatry. *Mol. Psychiatry* 24, 266–281. doi: 10.1038/s41380-018-0098-1

Cole, J. H., Poudel, R. P., Tsagkrasoulis, D., Caan, M. W., Steves, C., Spector, T. D., et al. (2017). Predicting brain age with deep learning from raw imaging data results in a reliable and heritable biomarker. *NeuroImage* 163, 115–124. doi: 10.1016/j.neuroimage.2017.07.059

Cole, J. H., Ritchie, S. J., Bastin, M. E., Hernández, M. V., Maniega, S. M., Royle, N., et al. (2018). Brain age predicts mortality. *Mol. Psychiatry* 23, 1385–1392. doi: 10.1038/mp.2017.62

Corbett, D. B., Valiani, V., Knaggs, J. D., and Manini, T. M. (2016). Evaluating walking intensity with hip-worn accelerometers in elders. *Med. Sci. Sports Exerc.* 48:2216. doi: 10.1249/MSS.0000000000001018

Cummings, S. R., Studenski, S., and Ferrucci, L. (2014). A diagnosis of dismobility—giving mobility clinical visibility: a mobility working group recommendation. *JAMA* 311, 2061–2062. doi: 10.1001/jama.2014.3033

Davis, J. W., Ross, P. D., Preston, S. D., Nevitt, M. C., and Wasnich, R. D. (1998). Strength, physical activity, and body mass index: relationship to performance-based measures and activities of daily living among older Japanese women in Hawaii. *J. Am. Geriatr. Soc.* 46, 274–279. doi: 10.1111/j.1532-5415.1998.tb01037.x

de Laat, K. F., Reid, A. T., Grim, D. C., Evans, A. C., Kötter, R., van Norden, A. G., et al. (2012). Cortical thickness is associated with gait disturbances in cerebral small vessel disease. *Neuroimage* 59, 1478–1484. doi: 10.1016/j.neuroimage.2011.08.005

DiSalvio, N. L., Rosano, C., Aizenstein, H. J., Redfern, M. S., Furman, J. M., Jennings, J. R., et al. (2020). Gray matter regions associated with functional mobility in community-dwelling older adults. *J. Am. Geriatr. Soc.* 68, 1023–1028. doi: 10.1111/jgs.16309

Elliott, M. L., Belsky, D. W., Knodt, A. R., Ireland, D., Melzer, T. R., Poulton, R., et al. (2019). Brain-age in midlife is associated with accelerated biological aging and cognitive decline in a longitudinal birth cohort. *Mol. Psychiatry* 26, 3829–3838. doi: 10.1038/s41380-019-0626-7

Franke, K., Gaser, C., Manor, B., and Novak, V. (2013). Advanced brainage in older adults with type 2 diabetes mellitus. *Front. Aging Neurosci.* 5:90. doi: 10.3389/fnagi.2013.00090

Franke, K., Ziegler, G., Klöppel, S., Gaser, C., and Alzheimer's Disease Neuroimaging Initiative. (2010). Estimating the age of healthy subjects from T1-weighted MRI scans using kernel methods: exploring the influence of various parameters. *Neuroimage* 50, 883–892. doi: 10.1016/j.neuroimage.2010.01.005

Fuchs, E., and Flügge, G. (2014). Adult neuroplasticity: more than 40 years of research. *Neural. Plasticity* 2014:541870. doi: 10.1155/2014/541870

Hair, J., Black, W., Babin, B., and Anderson, R. (2014). *Multivariate Data Analysis*, 7th Edn. Harlow, England: Pearson.

Hairi, N. N., Cumming, R. G., Naganathan, V., Handelsman, D. J., Le Couteur, D. G., Creasey, H., et al. (2010). Loss of muscle strength, mass (sarcopenia), and quality (specific force) and its relationship with functional limitation and physical disability: the concord health and ageing in men project. *J. Am. Geriatr. Soc.* 58, 2055–2062. doi: 10.1111/j.1532-5415.2010.03145.x

Hangartner, T. N., Warner, S., Braillon, P., Jankowski, L., and Shepherd, J. (2013). The official positions of the international society for clinical densitometry: acquisition of dual-energy X-ray absorptiometry body composition and considerations regarding analysis and repeatability of measures. *J. Clin. Densitometry* 16, 520–536. doi: 10.1016/j.jocd.2013.08.007

Hauer, K., Schwenk, M., Zieschang, T., Essig, M., Becker, C., and Oster, P. (2012). Physical training improves motor performance in people with dementia: a randomized controlled trial. *J. Am. Geriatr. Soc.* 60, 8–15. doi: 10.1111/j.1532-5415.2011.03778.x

Hayes, A. F. (2018). *Introduction to Mediation, Moderation and Conditional Process Analysis*, 2nd Edn. New York: Guilford Press.

Hayes, A. F., and Matthes, J. (2009). Computational procedures for probing interactions in OLS and logistic regression: SPSS and SAS implementations. *Behav. Res. Methods* 41, 924–936. doi: 10.3758/BRM.41.3.924

Hicks, G. E., Shardell, M., Alley, D. E., Miller, R. R., Bandinelli, S., Guralnik, J., et al. (2012). Absolute strength and loss of strength as predictors of mobility decline in older adults: the InCHIANTI study. *J. Gerontol. Ser. A Biomed. Sci. Med. Sci.* 67, 66–73. doi: 10.1093/gerona/glr055

Hsu, C. L., Best, J. R., Chiu, B. K., Nagamatsu, L. S., Voss, M. W., Handy, T. C., et al. (2016). Structural neural correlates of impaired mobility and subsequent decline in executive functions: a 12-month prospective study. *Exp. Gerontol.* 80, 27–35. doi: 10.1016/j.exger.2016.04.001

Johnson, P. O., and Neyman, J. (1936). Tests of certain linear hypotheses and their application to some educational problems. *Stat. Res. Memoirs* 1, 57–93.

Jurs, H. W., Hinkle, D., and Wiersma, W. (1998). *Applied Statistics for the Behavioral Sciences*. Boston, MA: Houghton MIfflin.

Le, T. T., Kuplicki, R. T., McKinney, B. A., Yeh, H.-W., Thompson, W. K., Paulus, M. P., et al. (2018). A nonlinear simulation framework supports adjusting for age when analyzing brainage. *Front. Aging Neurosci.* 10:317. doi: 10.3389/fnagi.2018.00317

Lockhart, S., Haq, I., Hughes, T., Okonmah-Obazee, S., Bateman, J., Sachs, B., et al. (2021). Temporoparietal cortical thickness is related to cognitive and physical function in the absence of amyloid pathology (2103). *Neurology* 96(Suppl. 15).

Lu, W.-H., de Souto Barreto, P., Rolland, Y., Rodríguez-Mañas, L., Bouyahia, A., Fischer, C., et al. (2020). Cross-sectional and prospective associations between cerebral cortical thickness and frailty in older adults. *Exp. Gerontol.* 139:111018. doi: 10.1016/j.exger.2020.111018

Maniega, S. M., Hernández, M. C. V., Clayden, J. D., Royle, N. A., Murray, C., Morris, Z., et al. (2015). White matter hyperintensities and normal-appearing white matter integrity in the aging brain. *Neurobiol. Aging* 36, 909–918. doi: 10.1016/j.neurobiolaging.2014.07.048

Manini, T. M., Visser, M., Won-Park, S., Patel, K. V., Strotmeyer, E. S., Chen, H., et al. (2007). Knee extension strength cutpoints for maintaining mobility. *J. Am. Geriatr. Soc.* 55, 451–457. doi: 10.1111/j.1532-5415.2007.01087.x

Mattay, V. S., Fera, F., Tessitore, A., Hariri, A., Das, S., Callicott, J., et al. (2002). Neurophysiological correlates of age-related changes in human motor function. *Neurology* 58, 630–635. doi: 10.1212/wnl.58.4.630

Musich, S., Wang, S. S., Ruiz, J., Hawkins, K., and Wicker, E. (2018). The impact of mobility limitations on health outcomes among older adults. *Geriatr. Nursing* 39, 162–169. doi: 10.1016/j.gerinurse.2017.08.002

Newman, A. B., Simonsick, E. M., Naydeck, B. L., Boudreau, R. M., Kritchevsky, S. B., Nevitt, M. C., et al. (2006b). Association of long-distance corridor walk performance with mortality, cardiovascular disease, mobility limitation, and disability. *JAMA* 295, 2018–2026. doi: 10.1001/jama.295.17.2018

Newman, A. B., Kupelian, V., Visser, M., Simonsick, E. M., Goodpaster, B. H., Kritchevsky, S. B., et al. (2006a). Strength, but not muscle mass, is associated with mortality in the health, aging and body composition study cohort. *J. Gerontol. Ser. A Biol. Sci. Med. Sci.* 61, 72–77. doi: 10.1093/gerona/61.1.72

Ortman, J. M., Velkoff, V. A., and Hogan, H. (2014). *An Aging Nation: the Older Population in the United States*. Washington, DC: U.S. Census Bureau.

Pinter, D., Ritchie, S. J., Gattringer, T., Bastin, M. E., Hernández, M. D. C. V., Corley, J., et al. (2018). Predictors of gait speed and its change over three years in community-dwelling older people. *Aging* 10:144. doi: 10.18632/aging.101365

Raz, N., Lindenberger, U., Rodrigue, K. M., Kennedy, K. M., Head, D., Williamson, A., et al. (2005). Regional brain changes in aging healthy adults: general trends, individual differences and modifiers. *Cerebral. cortex* 15, 1676–1689. doi: 10.1093/cercor/bhi044

Reuter-Lorenz, P. A., and Cappell, K. A. (2008). Neurocognitive aging and the compensation hypothesis. *Curr. Direct. Psychol. Sci.* 17, 177–182. doi: 10.1111/j.1467-8721.2008.00570.x

Reuter-Lorenz, P. A., and Park, D. C. (2014). How does it STAC up? Revisiting the scaffolding theory of aging and cognition. *Neuropsychol. Rev.* 24, 355–370. doi: 10.1007/s11065-014-9270-9

Riwniak, C., Simon, J., Wages, N., Clark, L., Manini, T., Russ, D., et al. (2020). Comparison of a multi-component physical function battery to usual walking speed for assessing lower extremity function and mobility limitation in older adults. *J. Nutr. Health Aging* 24, 906–913. doi: 10.1007/s12603-020-1432-2

Ronan, L., Alexander-Bloch, A. F., Wagstyl, K., Farooqi, S., Brayne, C., Tyler, L. K., et al. (2016). Obesity associated with increased brain age from midlife. *Neurobiol. Aging* 47, 63–70. doi: 10.1016/j.neurobiolaging.2016.07.010

Sampaio, A., Marques-Aleixo, I., Seabra, A., Mota, J., Marques, E., and Carvalho, J. (2020). Physical fitness in institutionalized older adults with dementia: association with cognition, functional capacity and quality of life. *Aging Clin. Exp. Res.* 32, 2329–2338. doi: 10.1007/s40520-019-01445-7

Sorond, F. A., Cruz-Almeida, Y., Clark, D. J., Viswanathan, A., Scherzer, C. R., De Jager, P., et al. (2015). Aging, the central nervous system, and mobility in older adults: neural mechanisms of mobility impairment. *J. Gerontol. Ser. A Biomed. Sci. Med. Sci.* 70, 1526–1532. doi: 10.1093/gerona/glv130

Stöckel, T., Wunsch, K., and Hughes, C. M. L. (2017). Age-related decline in anticipatory motor planning and its relation to cognitive and motor skill proficiency. *Front. Aging Neurosci.* 9:283. doi: 10.3389/fnagi.2017.00283

Storsve, A. B., Fjell, A. M., Tamnes, C. K., Westlye, L. T., Overbye, K., Aasland, H. W., et al. (2014). Differential longitudinal changes in cortical thickness, surface area and volume across the adult life span: regions of accelerating and decelerating change. *J. Neurosci.* 34, 8488–8498. doi: 10.1523/JNEUROSCI.0391-14.2014

Tavoian, D., Ampomah, K., Amano, S., Law, T. D., and Clark, B. C. (2019). Changes in DXA-derived lean mass and MRI-derived cross-sectional area of the thigh are modestly associated. *Sci. Rep.* 9:10028. doi: 10.1038/s41598-019-46428-w

Thambisetty, M., Wan, J., Carass, A., An, Y., Prince, J. L., and Resnick, S. M. (2010). Longitudinal changes in cortical thickness associated with normal aging. *Neuroimage* 52, 1215–1223. doi: 10.1016/j.neuroimage.2010.04.258

Visser, M., Deeg, D. J., Lips, P., Harris, T. B., and Bouter, L. M. (2000). Skeletal muscle mass and muscle strength in relation to lower-extremity performance in older men and women. *J. Am. Geriatr. Soc.* 48, 381–386. doi: 10.1111/j.1532-5415.2000.tb04694.x

Wages, N. P., Simon, J. E., Clark, L. A., Amano, S., Russ, D. W., Manini, T. M., et al. (2020). Relative contribution of muscle strength, lean mass, and lower extremity motor function in explaining between-person variance in mobility in older adults. *BMC Geriatr.* 20:1–11. doi: 10.1186/s12877-020-01656-y

Conflict of Interest: In the past 5-years, BC has received research funding from NMD Pharma, Regeneron Pharmaceuticals, Astellas Pharma Global Development, Inc., and RTI Health Solutions for contracted studies that involved aging and neuromuscular related research. In the past 5-years, BC has received consulting fees from Regeneron Pharmaceuticals, Zev industries, and the Gerson Lehrman Group for consultation specific to age-related neuromuscular weakness. BC is a co-founder with equity of OsteoDx Inc.

The remaining authors declare that the research was conducted in the absence of any commercial or financial relationships that could be construed as a potential conflict of interest.

Publisher's Note: All claims expressed in this article are solely those of the authors and do not necessarily represent those of their affiliated organizations, or those of the publisher, the editors and the reviewers. Any product that may be evaluated in this article, or claim that may be made by its manufacturer, is not guaranteed or endorsed by the publisher.

frontiers in Human Neuroscience

ORIGINAL RESEARCH
published: 24 February 2022
doi: 10.3389/fnhum.2022.814204

Anodal Transcranial Direct Current Stimulation Over Prefrontal Cortex Slows Sequence Learning in Older Adults

*Brian Greeley[1], Jonathan S. Barnhoorn[2], Willem B. Verwey[2] and Rachael D. Seidler[3]**

[1] Department of Physical Therapy, University of British Columbia, Vancouver, BC, Canada, [2] Department of Learning, Data-Analytics and Technology, University of Twente, Enschede, Netherlands, [3] Department of Applied Physiology and Kinesiology, University of Florida, Gainesville, FL, United States

Aging is associated with declines in sensorimotor function. Several studies have demonstrated that transcranial direct current stimulation (tDCS), a form of non-invasive brain stimulation, can be combined with training to mitigate age-related cognitive and motor declines. However, in some cases, the application of tDCS disrupts performance and learning. Here, we applied anodal tDCS either over the left prefrontal cortex (PFC), right PFC, supplementary motor complex (SMC), the left M1, or in a sham condition while older adults (n = 63) practiced a Discrete Sequence Production (DSP), an explicit motor sequence, task across 3 days. We hypothesized that stimulation to either the right or left PFC would enhance motor learning for older adults, based on the extensive literature showing increased prefrontal cortical activity during motor task performance in older adults. Contrary to our predictions, stimulation to the right and left PFC resulted in slowed motor learning, as evidenced by a slower reduction rate of reduction of reaction time and the number of sequence chunks across trials relative to sham in session one and session two, respectively. These findings suggest an integral role of the right PFC early in sequence learning and a role of the left PFC in chunking in older adults, and contribute to mounting evidence of the difficultly of using tDCS in an aging population.

Keywords: tDCS, older adults, prefrontal cortex, motor sequence learning, reaction time, chunking, explicit learning, learning impairment

OPEN ACCESS

Edited by:
Filippo Brighina, University of Palermo, Italy

Reviewed by:
Jorge Leite, Portucalense University, Portugal
Claire Joy Hanley, Swansea University, United Kingdom
Maximilian Achim Friehs, University College Dublin, Ireland

***Correspondence:**
Rachael D. Seidler
rachaelseidler@ufl.edu

Specialty section:
This article was submitted to Brain Imaging and Stimulation, a section of the journal Frontiers in Human Neuroscience

Received: *12 November 2021*
Accepted: *25 January 2022*
Published: *24 February 2022*

Citation:
Greeley B, Barnhoorn JS, Verwey WB and Seidler RD (2022) Anodal Transcranial Direct Current Stimulation Over Prefrontal Cortex Slows Sequence Learning in Older Adults. Front. Hum. Neurosci. 16:814204. doi: 10.3389/fnhum.2022.814204

INTRODUCTION

Aging is associated with declines in sensorimotor function (Raz, 2000; Seidler, 2006). Given that sensorimotor function plays a role in activities of daily living, declines can translate into a loss of independence. Physical rehabilitation approaches to mitigate these declines largely rely upon motor learning based interventions. While these interventions result in some improvements, the addition of non-invasive brain stimulation has been shown to make them more effective (Patel et al., 2019). Transcranial direct current stimulation (tDCS) has emerged to be especially promising because of its low cost, safety, portability, and its ability to be successfully used at home with clinical (Charvet et al., 2015; Kasschau et al., 2016) and older adult (Ahn et al., 2019) populations.

Older adults typically learn new motor skills at a slower rate than young adults. Verwey (2010) found that when practicing a sequence of finger presses to a repeated sequence of targets, older adults exhibited poorer performance for the repeated sequence, as indicated by slower reaction time. Similarly, Brown et al. (2009) found that while older adults displayed motor sequence learning during a single session (online gains), when participants were re-tested 24 h later, young adults exhibited a beneficial, between-session consolidation effect (offline gains) while older adults did not. These findings are consistent with the idea that neural plasticity and consolidation may be reduced with advancing age (Wilhelm et al., 2008, 2012). Thus, previous research shows that despite age-related declines in the sensorimotor system, older adults can learn new motor tasks, albeit not as well as young adults.

The use of tDCS paired with motor practice in older adult populations shows promise for ameliorating age-related motor declines. In a five session study during which older adults practiced a serial reaction time task paired with anodal (typically excitatory) tDCS, researchers found that those who received M1 anodal tDCS exhibited greater sequence specific learning relative to those who received sham stimulation (Dumel et al., 2016). In another study, young and older adult participants received stimulation over M1 while learning a sequence of finger movements (Zimerman et al., 2013). Without stimulation, older adults demonstrated poorer motor performance relative to young adults. However, the older adult participants who received stimulation during practice no longer had a motor performance deficit. While the findings from these studies suggest that tDCS may improve motor learning for older adults, other studies show either no benefit or even poorer performance when tDCS is paired with task practice (Mooney et al., 2019; Muffel et al., 2019; Habich et al., 2020; Chow et al., 2021). For example, one study found no benefit of a single session of anodal M1 tDCS as older and young adult participants learned a sequential isometric force task using their non-dominant hand during practice (Mooney et al., 2019).

For tDCS to be considered a viable therapeutic option for older adults, the optimization of tDCS parameters such as intensity, timing, number of sessions, etc., is necessary. For example, a recent study used a computational model to show that older adults required a slightly higher stimulation intensity (i.e., ∼2.3 mA) to achieve the same current density as in young adults with 2 mA of tDCS over the left primary motor cortex (Indahlastari et al., 2020). Alternatively, the timing of the application of tDCS relative to task practice, the task specificity of tDCS, or a combination may explain the inconsistencies frequently observed in older adult populations. In a cognitive naming task, older adults that received anodal tDCS over the left prefrontal cortex (PFC) during task execution displayed significant improvements relative to sham, whereas older adults that received tDCS before the task showed no differences compared to sham; in contrast, young adults that received stimulation before or during task practice showed task improvements (Fertonani et al., 2014). In another study, older adults that received anodal tDCS over M1 immediately following training of a motor sequence task, but not an hour or 2 h after, showed enhanced consolidation (Rumpf et al., 2017). The number of active tDCS sessions also likely impacts the effectiveness of tDCS, with multi-session protocols appearing to be more effective than a single session of tDCS (Hashemirad et al., 2016; Talsma et al., 2017; Shekhawat and Vanneste, 2018; Song et al., 2019). Overall, these studies suggest that tDCS in older adult populations has potential for reducing motor and cognitive declines, but the benefits may be task dependent (Saucedo Marquez et al., 2013; Kimura et al., 2021), and require tDCS parameter optimization such as intensity (Indahlastari et al., 2020) or timing (Fertonani et al., 2014; Rumpf et al., 2017) relative to task practice. However, little is known about how anodal tDCS over other brain regions outside of M1 affects motor learning in older adults.

Non-invasive brain stimulation studies have uncovered a complex role of the prefrontal cortices (PFC) in motor sequence learning. Janacsek et al. (2015) observed enhanced consolidation (offline gains) after a single session of anodal right PFC tDCS but no benefit of acquisition (online gains) during implicit sequence learning in young healthy adults. Using a similar implicit learning task, Greeley and Seidler (2019) found that anodal stimulation to left PFC, but not right PFC, facilitated motor learning in young adults, but only when participants remained unaware of the sequence. More recently using the Discrete Sequence Production (DSP) task, an explicit sequence learning paradigm, we observed that either anodal tDCS over the left or right PFC, and cathodal tDCS over the left PFC during practice impaired sequence learning over the course of 3 days in young adults (Greeley et al., 2020). In contrast to using anodal (excitatory) stimulation over the PFC, two studies have observed learning benefits when the PFC is *inhibited* in young adults. Using rTMS, Galea et al. (2010) found enhanced retention after either the left or right dorsolateral PFC was disrupted immediately after learning. Similarly, the application of cathodal (inhibitory) tDCS over the left PFC resulted in increased golf putting performance relative to the sham group (Zhu et al., 2015). The results from Galea et al. (2010) and Zhu et al. (2015) suggest that engaging the prefrontal cortices during or after motor learning may impair learning for young adults. However, older adults consistently recruit frontal regions when performing a range of motor learning tasks (Wu and Hallett, 2005; Lin et al., 2012; Michely et al., 2018). This greater recruitment of prefrontal brain regions during motor task performance has been suggested to serve a compensatory role for older adults (cf. Seidler et al., 2010). Specifically, inhibitory non-invasive brain stimulation applied over brain regions thought to be involved in compensatory processes disrupts performance for older but not young adults (Rossi et al., 2004; Zimerman et al., 2014). Therefore, it may be that excitatory PFC stimulation aids motor learning in older adults. Thus, we sought to understand how using anodal tDCS over left or right PFC would affect learning and retention of a motor sequence in older adults.

We evaluate motor learning here using indices of reaction time and sequence chunking. Chunking, or the ability to "chunk" together individual actions, is thought to facilitate motor learning by reducing memory loads. It is evidenced by a significant difference between inter-response times of key presses (Verwey and Eikelboom, 2003; Kennerley et al., 2004; Bo et al., 2009).

Age-related declines in motor learning may stem from declines in working memory, which limits motor chunking. For example, working memory capacity was positively correlated with motor sequence chunk length in both young and older adults (Bo and Seidler, 2009). Older adults showed significantly reduced working memory capacities and sequence chunk lengths relative to young adults. In addition, 22% of older adults showed no evidence of chunking; this was the case for only 7% of young adults. The link between the prefrontal cortices and working memory is well established (Kane and Engle, 2002; Funahashi, 2017) and it is known that older adults show significant reductions in prefrontal gray matter volume relative to young adults (Scahill et al., 2003; Esiri, 2007). Two fMRI studies have reported that young adults recruit the left dorsolateral PFC and right supplementary motor area (SMA) (Pammi et al., 2012) and the mid-left dorsolateral PFC (Wymbs et al., 2012) during sequence chunking. Moreover, Verwey et al. (2019) showed that unfamiliar sequences activated the PFC whereas familiar sequences did not; they instead elicited SMA activation. Thus, it is possible that targeting prefrontal regions (which have been associated with chunking) with anodal tDCS may facilitate motor sequence learning in older adults.

In the current study, we sought to understand the contributions of the left and right prefrontal cortices to motor sequence learning and chunking in healthy older adults; participants received stimulation for 2 days and performance was assessed over 3 days. We tested four different anodal tDCS groups in which either the left PFC, the right PFC, the left M1, or the SMA were stimulated in two separate sessions and compared with a sham group to understand how excitatory stimulation affects motor performance and learning (using the right hand) over the course of three separate sessions. Specifically, we sought to understand whether anodal tDCS to the right or left PFC would enhance or interfere with sequence learning as assessed by reaction times and chunking in a *DSP* task as assessed by the correlation between key presses (Acuna et al., 2014), in older adults. We hypothesized that regardless of the hemisphere of stimulation, older adults would display motor learning benefits in both reaction time and chunking across sequence learning with prefrontal tDCS. Similar to previous tDCS results (Zimerman et al., 2013; Dumel et al., 2016; Greeley et al., 2020), we hypothesized that regardless of age, the M1 tDCS groups would display faster learning as measured by reaction time and number of chunks and given its role in chunking, we hypothesized that the SMA tDCS older adult group would display faster learning as measured by the number of chunks; we also expected that older adults would show greater benefits due to having more room for improvement.

MATERIALS AND METHODS

Participants

We recruited sixty-three older adult participants (age range 64–84, mean age = 70.7, ± 5.76 years; 29 male) and sixty-four young adult participants (age range 18–30, mean age = 20.5, ± 2.4 years, 26 male) from the University of Michigan campus and greater Ann Arbor area. It should be noted that the young adult data has been previously published (Greeley et al., 2020), and the main focus of the current paper is on older adults. We include the young adult data in some of the analyses here to allow for age group comparisons when appropriate. All participants were right handed as measured by the Edinburg handedness inventory (Oldfield, 1971), and reported no history of mental health events, drug abuse, neurological, or psychiatric disorders. During the first session, all participants signed a consent form approved by the University of Michigan Institutional Review Board, verbally answered an alcohol and drug abuse screening questionnaire, completed the Beck Depression inventory (Beck et al., 1988), a custom tDCS screening form, and the Montreal Cognitive Assessment (Nasreddine et al., 2005). Participants were excluded if they scored <23 on the MOCA (Lee et al., 2008; Carson et al., 2018), had a self-reported history of alcohol or drug abuse, and scored >13 on the Beck Depression Inventory. Additionally, participants were not taking medications that could interact with the central nervous system. Participants were compensated for their time at an hourly rate of $15 per hour.

Discrete Sequence Production Task

The study design implemented in the current paper was identical to that used in our recent publication (Greeley et al., 2020). See **Figure 1** for an abbreviated overview. Participants practiced a variant of the *DSP* task (Ruitenberg et al., 2014) programmed and presented in E-Prime (version 2.0) over the course of three sessions, two of which participants received either real or sham tDCS, while using their dominant, right hand to practice the sequence task. Participants were assigned two, six-element sequences for the duration of the study. One of the sequences had a repeated, simple structure (e.g., NCBNCB) whereas the other sequence did not have a structure and was thus considered complex (e.g., BCVNVC). Participants could practice each sequence up to a total of 224 times throughout the three sessions of practice (16 times per block across 14 blocks). To simplify data presentation and to be consistent with our previously published results (Greeley et al., 2020), we limited our analysis to the complex sequences. During sequence practice, participants placed their index, middle, ring, and pinky fingers of their dominant, right hand on the C, V, B, and N keys of a keyboard, respectively. Four, horizontally aligned white squares with black trim were presented in the middle of a monitor with a white background. During practice, one of the squares was filled in by a light green color for up to 2,000 ms, which cued participants to press the spatially corresponding key as quickly and accurately as possible. If the participant pressed the correct key, the green square returned to white and the next square in the sequence would immediately turn green. If participants made an incorrect key press, the message "mistake, again" was displayed on the screen in red for 1,000 ms. If participants did not respond to a stimulus within 2,000 ms of the message, "no response, again" was displayed at the bottom of the screen for 1,000 ms. Participants practiced their sequences across 3 days, with six blocks of practice during session one, another six blocks of practice during session two, and two blocks of practice in session three. Participants practiced each of their two sequences

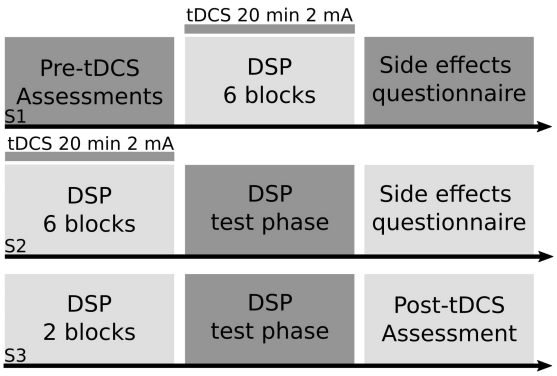

FIGURE 1 | Study design. Using a between-subjects design, right-handed older adult participants practiced a motor sequence task paired with transcranial direct current stimulation (tDCS). Participants were randomly assigned into one of four anodal tDCS groups (right prefrontal cortex, left prefrontal cortex, left primary motor cortex, supplementary motor complex) or sham for the entirety of the study. In session one (S1) older adult participants completed a battery of cognitive and motor tasks (pre-tDCS assessments), followed by six blocks of the discrete sequence production (DSP) task paired with either real or sham tDCS for a maximum of 20 min at 2 mA, followed by a tDCS side effects questionnaire. In session two (S2), participants practiced another six blocks of the DSP task paired with either real or sham tDCS, followed by a test portion of the DSP task, where participant's explicit knowledge of the sequence was tested, followed by a tDCS side effects questionnaire. In session three (S3), participants completed two blocks of the DSP task without tDCS, then completed the test portion of the DSP task, followed by the same battery of cognitive and motor tasks (post-tDCS assessment) that participants completed at the start of S1.

eight times during each block of practice. During sessions one and two when participants received tDCS, participants practiced their assigned sequences a total of 96 times.

Participants also received feedback halfway through a block of practice (after 8 of the 16 trials). The feedback screen was shown for 10 sec and displayed each participant's error percentage and mean reaction time. After 10 sec had passed, participants immediately started on the second half of the block. After completing an entire block of practice, another feedback screen was shown for 50 sec. This feedback screen had the same information as the mid-block feedback screen, however, at the bottom of the screen there was text which read, "After this, practice block x will start." Before each block (excluding block 1) on practice sessions one and two, the screen displayed, "As you have noticed, there are 2 fixed sequences. Please learn them! We will continue with the same task."

In sessions two and three immediately after the *DSP* awareness questionnaire (see below), participants completed an additional test phase of the *DSP* task, which consisted of four conditions. Each condition comprised 48 trials (24 of each sequence) and followed the same structure as practice. In the *familiar* condition, the stimuli were presented in the same way as during practice. In the *single-stimulus* condition, only the first stimulus of the sequence was presented as a green square. Once the correct key was pressed, the rest of the sequence was to be completed by the participants without the help of the squares turning green. In the *mixed-familiar* condition, 75% of the trials had modifications to the sequences. The modifications were that two of the six stimuli were changed. In the *unfamiliar* condition, participants were exposed to two sequences that they had not previously experienced.

Transcranial Direct Current Stimulation Set-Up

Participants were randomly assigned into one of five tDCS groups. tDCS was only applied during sessions one and two. All electrode placements were according to the 10–20 EEG system. If participants were randomized into the right or left prefrontal tDCS groups, the anode was placed over the scalp location F4 or F3, respectively and the reference/cathode electrode was placed over the contralateral orbit. For the left M1 stimulation group, the anode was placed over the C3 location and the cathode was placed over the contralateral orbit. For the placement of the anode electrode in the SMA region (henceforth referred to as the supplementary motor complex (SMC) group), we placed the anode 8.7% of the measured distance between the nasion and inion anterior to Cz (approximately 3 cm anterior to Cz) with the cathode over Fpz. The sham tDCS group received the same montage as the real, M1 tDCS group (anode over C3, cathode over contralateral orbit; **Figure 2**). Stimulation was always 2 mA based on safety recommendations (Iyer et al., 2005; Bikson et al., 2009), previous reports inducing plasticity in young (Monte-Silva et al., 2013; Waters-Metenier et al., 2014; Seidler et al., 2017; Waters et al., 2017; Greeley and Seidler, 2019; Greeley et al., 2020) and older adults (Dumel et al., 2016; Nomura and Kirimoto, 2018; Farnad et al., 2021), and recent evidence suggesting 2 mA is necessary to achieve a physiologically meaningful effect on the cortex (Huang et al., 2017; Filmer et al., 2020). We applied stimulation using a conventional tDCS device (Soterix Medical Inc., New York, NY, United States) for a maximum of 20 min *via* two rubber electrodes placed inside saline soaked sponges. Electrode size was always 5 × 5 cm, except for the SMC montage in which case the anode was 5 × 5 cm and the cathode was 5 × 7 cm (Vollmann et al., 2013); it is unlikely that this larger cathodal electrode comprises tDCS-induced corticospinal excitability changes (Nitsche et al., 2007). Setup for tDCS was the same for sessions one and two. tDCS was not administered during session three.

Realistic Volumetric-Approach-Based Simulator for Transcranial Electrical Stimulation Model

We used realistic volumetric-approach-based simulator for transcranial electrical stimulation (ROAST) (version 3.0), or Realistic vOlumetric-Approach to Simulate Transcranial electric stimulation, an open source tool (Huang et al., 2019). The output from the ROAST model was used as a qualitative means to aid in the interpretations of the electric field distributions of our electrode montages. We ran the ROAST model a total of 4 times for each tDCS electrode montage, electrode locations used in the model are in parentheses. The output of the model can be observed for the left PFC anode (F3), right orbitofrontal cortex cathode montage (Fp2; **Figure 2A**), the right PFC anode (F4),

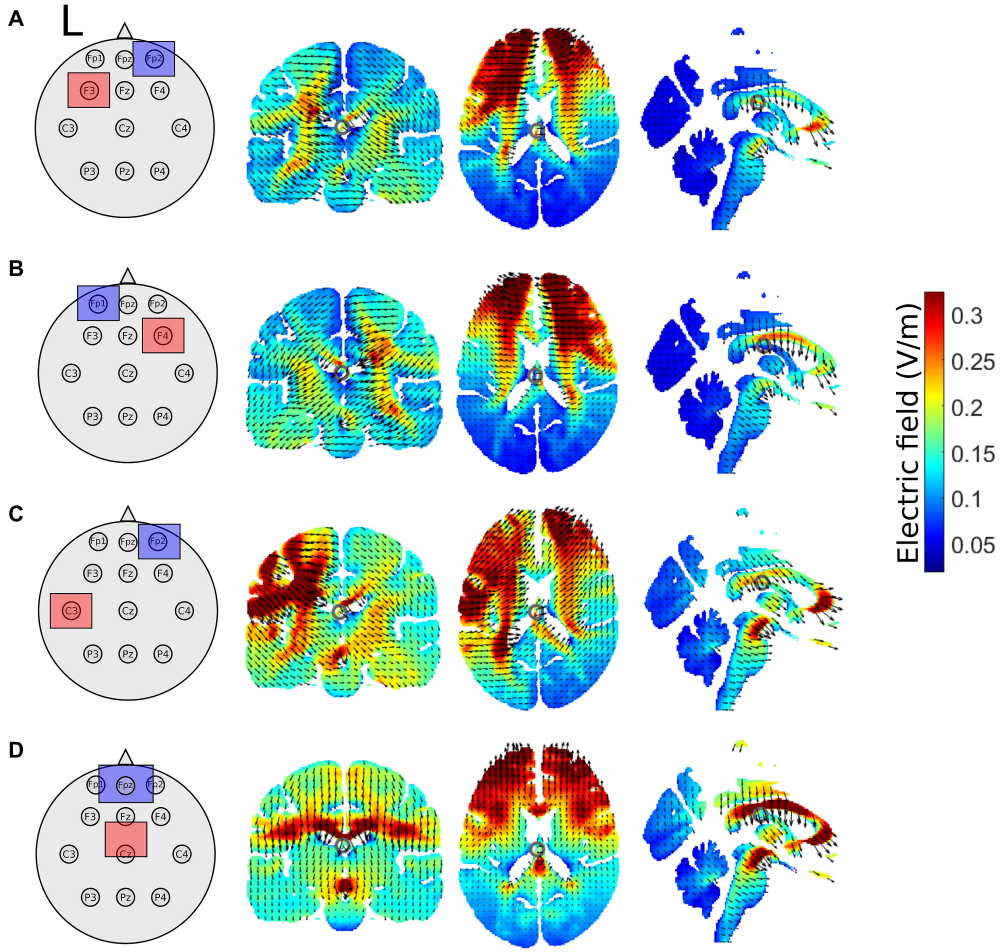

FIGURE 2 | Schematic of tDCS electrode montage and electric field magnitude distribution with current arrows in the coronal, axial, and sagittal slices for the **(A)** left prefrontal montage, **(B)** right prefrontal montage, **(C)** the left M1 montage, and **(D)** for the supplementary motor complex montage produced by the ROAST model. All images are in $x = -1$, $y = -17$, and $z = 17$ MNI space. The left hemisphere is denoted by L. Red squares represent the anode, whereas blue squares represent the cathode.

left orbitofrontal cortex cathode montage (Fp1; **Figure 2B**), the left M1 anode (C3), right orbitofrontal cortex cathode montage (Fp2; **Figure 2C**), and the SMA complex anode (FCz), orbit cathode montage (Fpz; **Figure 2D**). Simulations were run using the MNI152 averaged head. We specified pad electrodes as the electrode type with a height of 3 mm.

PROCEDURE

During session one, as part of the pre-tDCS assessments, participants completed Thurstone's card rotation task (Ekstrom et al., 1979), a custom computerized version of the visual search task, the digit symbol substitution task (Wechsler, 1958), a modified version of the visual array change working memory assessment (Luck and Vogel, 1997), three trials of the Purdue pegboard task (Tiffin and Asher, 1948) and a grip strength assessment before *DSP* practice. After this neuropsychological assessments, participants took a mandatory 3–5 min break before tDCS setup and *DSP* practice. After setup, we turned stimulation up to 1 mA (pre-stimulation tickle) for 15 s to ensure satisfactory contact quality of the electrodes on the scalp. After 15 s of stimulation, participants completed a shortened 10-item Positive and Negative Affect Schedule (PANAS) mood inventory. Then the participants were instructed on the *DSP* task. After the instructions, the experimenter would start the stimulation and the tDCS unit would ramp up over a period of 30 sec to full intensity (always 2 mA) and then remain active up to 20 min in duration. After the 6 blocks of practice, tDCS was turned off (for active tDCS) only if participants completed practice under 20 min ($n = 7$). For reference, participants took 23.3 min (± 3 min) to complete practice in session one. The right PFC group took 23.9 min (± 2.3), the left PFC group took 23.2 min (± 3.6), the left M1 group took 22.2 min (± 2.8), the SMC group took 23.6 min (± 3.5) and the sham group took 23.7 min (± 3.3). There were no group differences in terms of the amount of time it took to complete the task in session one. For the sham tDCS group, the tDCS would stay on for 30 sec then ramp back

down to 0 mA. If the task was not completed by the 20 min timer built into the tDCS unit, stimulation was automatically stopped by the device. Immediately following the 6 blocks of *DSP* practice, we administered a second version of the digit symbol coding task, the PANAS mood survey, and a custom tDCS side effects questionnaire. After the participant completed the tDCS side effects questionnaire, we removed the electrodes and sent the participants home with physical exercise and handedness questionnaires (Oldfield, 1971) to complete and return at their next visit (exercise data not included here).

Session two took place following at least one night's sleep but no longer than 72 h after session one. All but nine participants came to session two within 24 h of session one, whereas one participant came to session two within 72 h and eight participants came to session two within 48 h of session one (M = 1.2 days). In session two, participants completed the card rotation task followed by the digit symbol substitution task. tDCS was setup similar to session one, then pre-stimulation tickle was administered to ensure satisfactory contact quality. After the pre-stimulation tickle, we administered the mood survey and summarized the instructions of the *DSP* task. If participants had no questions, we turned on the tDCS, let the unit ramp up to full intensity, and started the *DSP* task (blocks 7–12, totaling 96 trials per sequence after session 2 at this point). For sham, the stimulation would again stay on 30 sec then ramp back down to 0 mA. Immediately following practice, the *DSP* awareness questionnaire was administered (tDCS stimulation was off at this point). The questionnaire was followed by instructions of the test portion of the *DSP* task. After the test portion of the task, participants completed the digit symbol substitution coding task and the mood survey again, and finally the tDCS side effects questionnaire.

The third session commenced at least one night's sleep but no longer than 72 h after session two. All but nine participants came into session three within 48 h of session two (M = 1.2 days). The main purpose of session three was to measure the impact of stimulation on the sequences (i.e., testing conditions) in the absence of stimulation. In session three, participants completed two blocks of practice (blocks 13–14, totaling 112 practice trials per sequence), the *DSP* awareness questionnaire, then the test portion of the *DSP* task. Participants were offered a break, then completed the battery of post-tDCS intervention assessments including the card rotation test, the visual search task, the digit symbol substitution coding task, and the visual array change task. Lastly, participants completed an exit survey to probe for strategies used during practice.

Discrete Sequence Production Awareness Questionnaire

Immediately following practice on sessions two and three, participants were asked about their awareness of the sequences. The first two questions probed the participants' knowledge of the questions by asking them to write down the two sequences they had practiced. The second two questions asked participants to verbally tell the experimenter what the sequences were from memory. The third question required participants to choose two sequences from a list of eighteen possible sequences. The *DSP* awareness questionnaire took approximately 5 min to complete.

Data Analyses

Data are presented as mean ± standard deviation (SD) unless otherwise noted. To study motor learning, our primary outcomes were reaction time, number of (motor) chunks, and number of errors for the complex sequences across the 3 days of practice. Prior to statistical analysis, data were checked to determine whether they were normally distributed. We opted to use a linear mixed model to investigate the effect of stimulation on the *rate* of learning across practice trials given the reaction time data for the older adults were partially skewed and linear mixed models can handle this data well (Arnau et al., 2012; Lo and Andrews, 2015; Schielzeth et al., 2020). Additionally, linear mixed models can handle missing data; every participant had a different number of removed trials due to errors. We also implemented separate ANOVAs to investigate the effect of stimulation on the testing conditions.

Using the software Stata (version 13.0), two linear mixed models were implemented using reaction time and number of chunks as dependent variables limited to the older adult group. Trials were used as a continuous factor, whereas Stimulation Group and Session were used as blocked factors. Random intercepts and fixed slopes were used for each participant. If a significant main effect or interaction emerged within the older adult group, follow-up pairwise comparisons were used to determine which pairs of the factor levels are significantly different from each other, always comparing each real stimulation group to sham if applicable. Additionally, if a significant difference between any active tDCS (right PFC, left PFC, left M1, SMC) and sham tDCS group emerged within the older adult group, we then included the young healthy adults receiving the same electrode montages in a follow-up analysis to understand whether tDCS differentially affected the age groups. P-values and confidence intervals were adjusted within Stata using Scheffé's method for pairwise comparisons. Prior to statistical analyses, data were checked to satisfy normality. To calculate an effect size for each pairwise comparison, we used the esize function in Stata, using number of observations, mean, and standard deviation to obtain Cohen's d (d). A computational model developed by Acuna et al. (2014) was used to determine the number of chunks, which uses reaction times as well as the covariation across key presses to detect chunk boundaries. In contrast to the linear mixed model which allowed us to understand how stimulation may affect the *rate* in learning, one-way ANOVAs were used to test whether there were any overall benefits of real tDCS relative to sham within the older adult group in terms of performance (magnitude). Independent t-tests were used to test for baseline demographic differences between the two age groups in terms of the Purdue Pegboard, visual array capacity, and MoCA. We also completed a series of independent t-tests and Mann-Whitney U tests to check for baseline demographic differences between the real tDCS and sham groups within older adults. For the number of errors, we first used a Kruskal–Wallis test to compare young and older adults, then a series of Mann–Whitney tests comparing each active tDCS group to sham within each session limited to the

older adult group (critical a' = 0.004). We also ran an additional 2 (Age group: young, old) by 5 (tDCS group: right PFC, left PFC, M1, SMC, sham) by 2 (Session: 2, 3) by 4 (Testing Condition: familiar, mixed familiar, mixed unfamiliar, and single stimulus) repeated measures ANOVA on the reaction time of the testing phase of the *DSP* task (see *DSP* description above).

RESULTS

Two older adults were unable to return after session one and three older adult participants were unable to return after session two. An additional two older adult participants were removed from analysis due to exessive errors (>3 SD). The breakdown of final sample sizes by stimulation group were the following: the right PFC (n = 13), left PFC (n = 12), left M1 (n = 12), SMC (n = 12), and sham (n = 12).

Demographics

Independent t-tests revealed demographic differences between the old and young adult groups. Young adults displayed higher MOCA scores [$t(121) = 4.04$, $p < 0.001$] and better manual function for the left [$t(115) = 8.10$, $p < 0.001$] and right [$t(115) = 9.65$, $p < 0.001$] hand as indicated by the number of pegs completed in the Purdue Pegboard test. Visuospatial working memory was also statistically different in that older adults showed an overall lower capacity [$t(121) = 8.69$, $p < 0.001$]. See **Table 1** for group averages. There were no demographic differences between any of the real tDCS and sham groups (p's > 0.37). See **Table 2** for older adult group demographic averages. Additionally, no older adults reported having experienced adverse effects (**Supplementary Table 1**).

Reaction Time

The linear mixed model revealed a main effect of Session [$\chi^2(2, N = 61) = 441.68$, $p < 0.001$]. Reaction time in the second session decreased at a lower rate compared to the first session ($\beta = 0.60$, SE = 0.03, $p < 0.001$, $d = -0.61$), whereas reaction time decreased at a faster rate in session three relative to session two ($\beta = -0.37$, SE = 0.11, $p = 0.005$, $d = -0.07$). There was no main effect of Stimulation Group ($\chi^2(4, N = 61) = 8.76$, $p = 0.067$).

There was a Stimulation Group by Session interaction [$\chi^2(8, N = 61) = 65.71$, $p < 0.001$]. To understand the interaction, follow-up pairwise contrasts were performed, with Scheffé correction. Older adults in the right PFC ($\beta = 0.39$, SE = 0.06, $p = 0.024$, $d = 0.33$) and SMC ($\beta = 0.43$, SE = 0.07, $p = 0.003$, $d = 0.23$) tDCS groups decreased their reaction times at a slower rate relative to older adults in the sham group during session one (**Figures 3**, **4** and **Tables 3**, **4**). No other comparisons reached significance.

To understand whether tDCS had differential effects between the young and older adults, we included two additional tests: one limited to young and older adults in the right PFC and sham tDCS groups within session one and another limited to young and older adults in the SMC and sham tDCS groups within session one. For the right PFC and sham tDCS groups, we observed a Stimulation by Age Group interaction [$\chi^2(1, N = 27) = 29.02$, $p < 0.001$]. Pairwise comparisons revealed that older adults in the right PFC reduced reaction time at a significantly slower rate relative to young adults in the right PFC tDCS group ($\beta = 0.24$, SE = 0.06, $p = 0.002$, $d = 1.67$) (**Table 4**). Importantly, while older adults in the sham group reduced reaction times at a significantly faster rate compared to older adults in the right PFC tDCS group, there was no difference between the sham and PFC tDCS groups for young adults ($p = 0.704$). Similarly, we observed a Stimulation by Age Group interaction [$\chi^2(1, N = 25) = 24.34$, $p < 0.001$] for the SMC and sham tDCS groups. Pairwise comparisons revealed that older adults in the SMC group reduced reaction time at a significantly slower rate relative to young adults ($\beta = 0.19$, SE = 0.06, $p = 0.021$, $d = 1.56$) (**Table 4**). While older adults in the sham group reduced their reaction times at a faster rate compared to older adults in the SMC group, there was no difference between the sham and SMC tDCS groups for young adults ($p = 0.989$).

To understand the overall impact of tDCS within older adults a series of one-way ANOVA contrasts comparing each active tDCS group to sham within each session. No contrasts were significant ($p > 0.4$; **Figures 3**, **4**).

Number of Chunks

The linear mixed model revealed significant main effects of Stimulation Group [$\chi^2(4, N = 60) = 20.79$, $p < 0.001$] and Session [$X^2(2, N = 60) = 279.33$, $p < 0.001$] for older adults.

TABLE 1 | Mean (SD) age group scores for the MoCA, Purdue Pegboard, and spatial working memory capacity (visual array capacity).

	YA group	OA group
	(*N* = 64)	(*N* = 63)
MoCA	28.42 (1.51)	27.16 (1.92)*
VAC capacity	4.67 (1.0)	3.00 (1.1)*
Purdue right	16.11 (1.73)	13.0 (1.76)*
Purdue left	14.84 (1.62)	12.37 (1.67)*

*MoCA, Montreal cognitive assessment; OA, older adults; VAC, visual array capacity; YA, young adults. *p < 0.05.*

TABLE 2 | Mean (SD) transcranial direct current stimulation (tDCS) group scores of age, MoCA, sex, Purdue Pegboard, and spatial working memory capacity (visual array capacity) for older adults.

	OA tDCS group				
	Right PFC (*n* = 13)	Left PFC (*n* = 12)	Left M1 (*n* = 12)	SMC (*n* = 12)	Sham (*n* = 12)
Age	69.2 (5.1)	70.8 (4.7)	72.8 (6.9)	71.0 (6.1)	68.5 (4.5)
MoCA	26.7 (2.3)	26.7 (1.3)	27.6 (0.9)	27.2 (2.4)	27.5 (2.0)
Sex	7 F/6 M	7 F/5 M	6 F/6 M	6 F/6 M	7 F/5 M
VAC capacity	2.9 (1.1)	3.2 (1.1)	2.7 (1.2)	3.2 (1.3)	3.1 (0.7)
Purdue right	13.2 (1.6)	13.1 (1.3)	12.5 (1.9)	13.2 (2.1)	13.1 (2.0)
Purdue left	12.6 (2.0)	12.8 (1.4)	11.8 (1.6)	11.8 (1.7)	12.8 (1.7)

There were no group differences between any of the real tDCS groups and sham for any of the demographic data (p's > 0.36). MoCA, Montreal cognitive assessment; OA, older adults; VAC, visual array capacity.

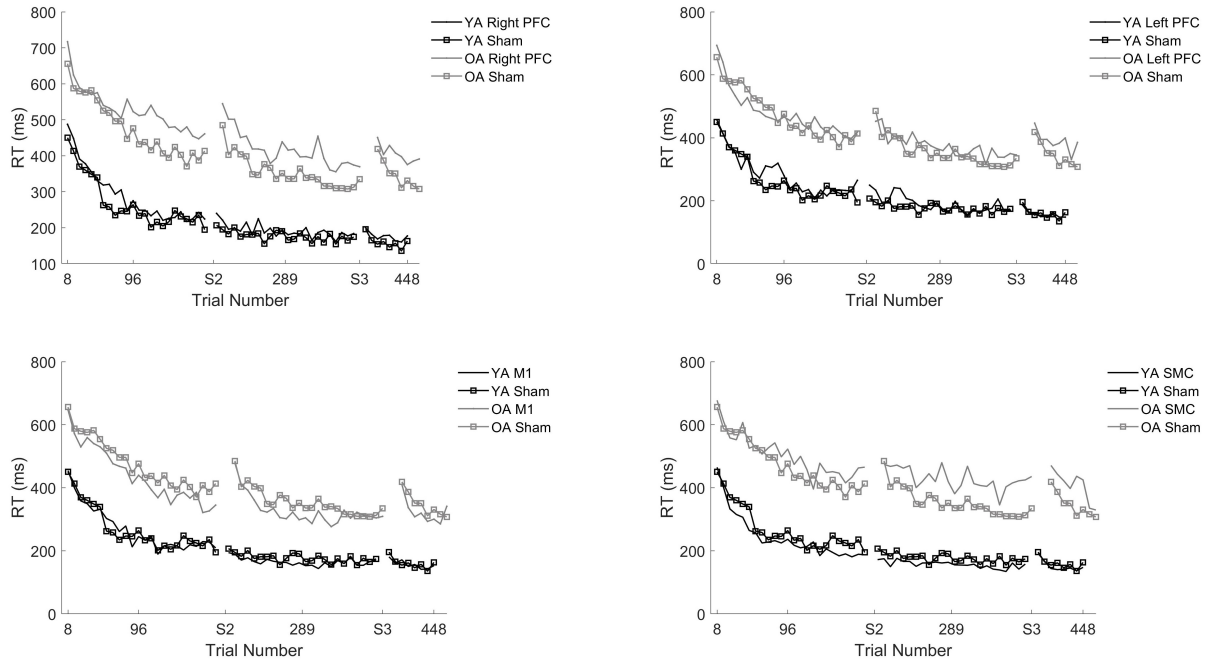

FIGURE 3 | Reaction time (RT) for young and older adults as a function of trial number. RT was binned across every eight trials. Each panel represents a tDCS stimulation location and sham group for reference. **(Top left)** Young (black) and older (gray) adults in the right prefrontal cortex (PFC) tDCS groups as well as young (black with squares) and older (gray with squares) sham groups. **(Top right)** Young (black) and older (gray) adults in the left PFC tDCS groups as well as sham (squares). **(Bottom left)** Young (black) and older (gray) adults primary motor cortex (M1) tDCS groups. **(Bottom right)** Young (black) and older (gray) adults in the supplementary motor complex (SMC) tDCS groups.

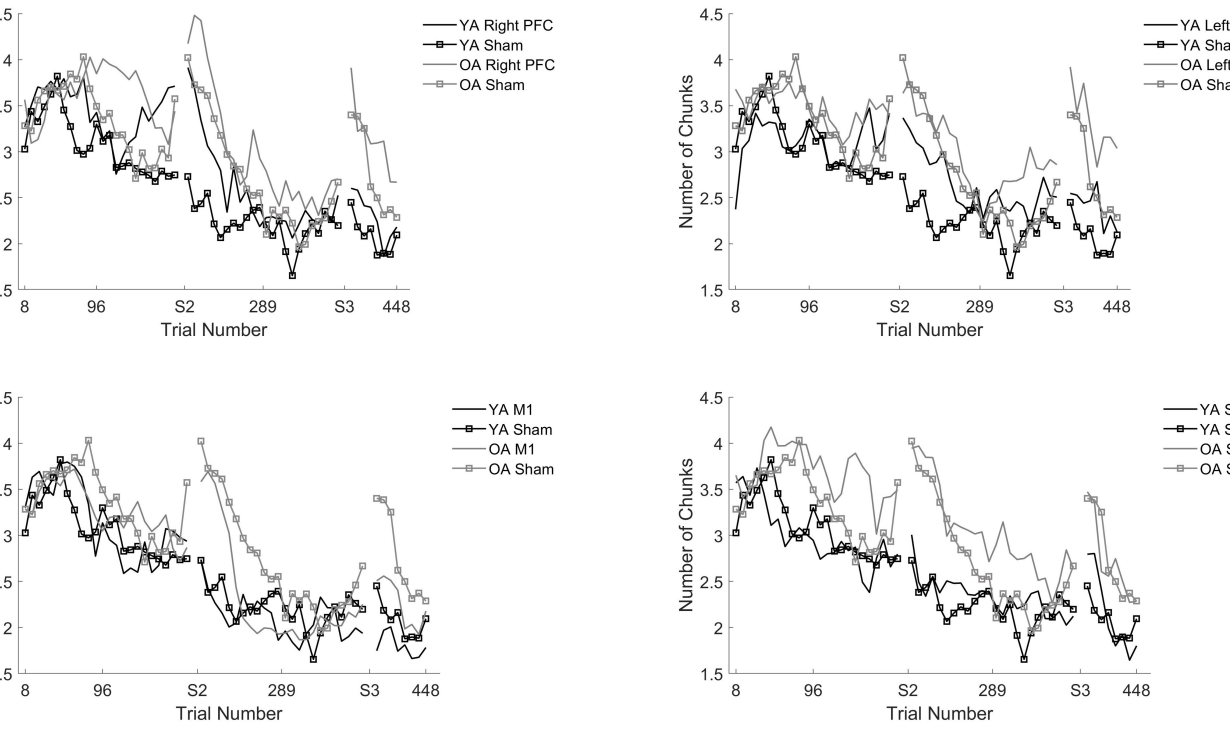

FIGURE 4 | Averaged reaction time for young (black) and older adults (gray) for each tDCS group within each practice session. Each panel represents one session. Error bars represent standard deviation.

TABLE 3 | Results from linear mixed model using reaction time as the dependent variable.

				Adjusted			
Reaction time	**β**	**Std Err.**	**Z**	***p*-value**	**95% conf. interval**		**Cohen's d**
Session							
Session 2 vs. Session 1	0.597	0.030	20.160	**<0.001**	0.524	0.669	−0.607
Session 3 vs. Session 2	−0.968	0.114	−8.500	**<0.001**	−1.25	−0.689	−0.050
Stimulation by session							
Sham vs. R PFC, session 1	−0.388	0.065	−5.980	**0.001**	−0.705	−0.072	−0.333
Sham vs. L PFC, session 1	−0.296	0.066	−4.460	0.133	−0.619	0.027	
Sham vs. M1, session 1	0.188	0.067	2.830	0.888	−0.135	0.512	
Sham vs. SMC, session 1	−0.431	0.066	−6.490	**<0.001**	−0.755	−0.108	−0.704
Sham vs. R PFC, session 2	0.033	0.067	0.490	1.000	−0.292	0.358	
Sham vs. L PFC, session 2	−0.095	0.066	−1.440	1.000	−0.416	0.227	
Sham vs. M1, session 2	−0.078	0.065	−1.190	1.000	−0.395	0.239	
Sham vs. SMC, session 2	−0.205	0.065	−3.160	0.765	−0.521	0.111	
Sham vs. R PFC, session 3	−0.473	0.354	−1.340	1.000	−2.198	1.251	
Sham vs. L PFC, session 3	−0.409	0.347	−1.180	1.000	−2.100	1.282	
Sham vs. M1, session 3	−0.468	0.351	−1.330	1.000	−2.178	1.242	
Sham vs. SMC, session 3	−0.212	0.344	−0.610	1.000	−1.886	1.463	

All p-values and confidence intervals have been Scheff adjusted. β, beta; conf., confidence. Std Err., standard error. Significant p-values are in bold.

We performed follow-up pairwise comparisons to understand each main effect. We observed a significantly faster rate in the reduction in the number of chunks in session two relative to session one ($\beta = -0.01$, SE = 0.00, $p < 0.001$, $d = -0.61$) and a significantly faster rate in the reduction in the number of chunks in session three relative to session two ($\beta = -0.01$, SE = 0.00, $p < 0.001$, $d = 0.03$). Across all sessions, the left prefrontal ($\beta = 0.01$, SE = 0.00, $p = 0.002$, $d = 0.19$) and the M1 ($\beta = 0.01$, SE = 0.00, $p = 0.023$, $d = -0.23$) tDCS groups reduced the number of chunks at a significantly slower rate relative to the sham tDCS group (**Figure 5** and **Table 5**). No other pairwise comparisons reached significance.

The model also revealed a Stimulation Group by Session interaction [$\chi^2(8, N = 60) = 53.93$, $p < 0.001$]. Pairwise comparisons revealed that older adults in the right prefrontal tDCS group ($\beta = 0.00$, SE = 0.00, $p = 0.011$, $d = 0.22$) reduced the number of chunks at a slower rate across trials compared to sham in session one. Similarly, older adults in the left prefrontal tDCS group ($\beta = 0.00$, SE = 0.00, $p = 0.010$, $d = 0.20$) reduced the number of chunks at a slower rate across trials than sham in session two. No other pairwise comparisons reached significance.

To understand whether the impairment of right or left prefrontal anodal tDCS on the rate of reduction in the number of chunks was different across age groups, we ran two additional tests. The first test included both young and older adults limited to the right prefrontal and sham tDCS groups within session one. We observed that there was no Stimulation by Age Group interaction [$X^2(1, N = 26) = 1.34$, $p = 0.247$]. The second test included both young and older adults in the left prefrontal and sham tDCS groups within session two. We observed there was a significant Stimulation by Age Group interaction [$X^2(1, N = 26) = 54.65$, $p < 0.001$]. The difference between the left prefrontal and sham tDCS groups was larger for the young than the older adults. That is, in session two left prefrontal stimulation was associated with more chunks for the young than the older adults, relative to sham (**Figure 5** and **Table 4**).

To understand the overall impact of tDCS within OA we completed three, one-way ANOVA contrasts comparing each active tDCS group to sham within each session. There was a significant main effect limited to Session [$F(4, 58) = 2.648$,

TABLE 4 | Means (SD) of reaction time and number of chunks for each stimulation group, age group, and session.

	Reaction time		**Number of chunks**	
Session 1	**YA**	**OA**	**YA**	**OA**
Right PFC	290.20 (77.77)	532.60 (135.65)	3.47 (0.69)	3.62 (0.49)
Left PFC	282.66 (111.75)	477.99 (140.47)	3.10 (0.61)	3.48 (0.64)
M1	269.08 (87.04)	447.38 (152.53)	3.17 (0.40)	3.27 (0.50)
SMC	249.61 (95.72)	513.33 (199.43)	3.05 (0.78)	3.27 (0.50)
Sham	271.92 (117.35)	477.71 (116.69)	3.08 (0.56)	3.41 (0.63)
Session 2				
Right PFC	191.28 (60.19)	421.68 (133.84)	2.58 (0.57)	3.02 (0.84)
Left PFC	187.99 (85.12)	375.23 (126.90)	2.65 (0.80)	2.94 (0.75)
M1	166.93 (56.36)	332.96 (173.74)	2.12 (0.66)	2.33 (0.46)
SMC	159.53 (56.87)	437.43 (219.75)	2.33 (0.68)	2.33 (0.46)
Sham	177.12 (97.24)	357.27 (114.34)	2.25 (0.77)	2.73 (0.83)
Session 3				
Right PFC	176.10 (53.85)	404.05 (156.47)	2.31 (0.99)	3.11 (0.98)
Left PFC	156.17 (53.30)	393.93 (155.65)	2.38 (0.86)	3.18 (1.52)
M1	154.74 (48.08)	331.46 (186.53)	1.80 (0.62)	2.25 (0.76)
SMC	151.39 (42.43)	413.74 (213.31)	2.14 (0.83)	2.25 (0.76)
Sham	162.54 (90.45)	345.48 (119.28)	2.13 (0.88)	2.84 (1.11)

M1, primary motor cortex; OA, older adults; PFC, prefrontal cortex; SMC, supplementary motor complex; YA, young adults.

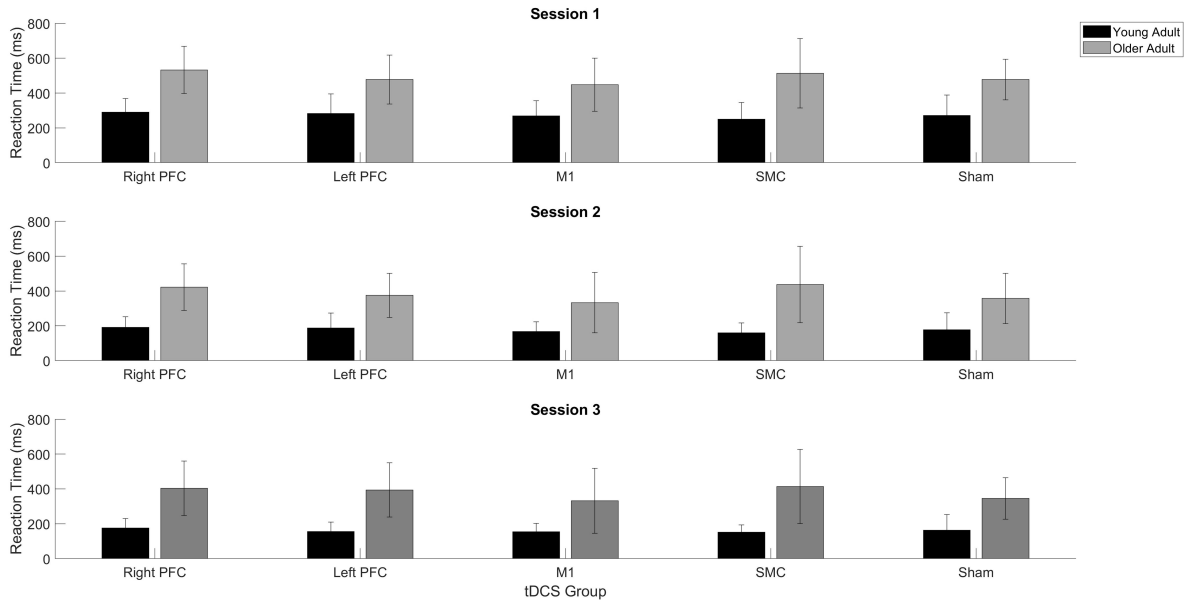

FIGURE 5 | Number of chunks for young and older adults as a function of trial number. Number of chunks were binned across every eight trials. Each panel represents a tDCS stimulation location and sham group for reference. Top left panel depicts young (black) and older (gray) adults in the right prefrontal cortex (PFC) tDCS groups as well as young (black with squares) and older (gray with squares) sham groups. Top right panel depicts young (black) and older (gray) adults in the left PFC tDCS groups as well as sham (squares). Bottom left panel depicts young (black) and older (gray) adults primary motor cortex (M1) tDCS groups. Bottom right panel depicts young (black) and older (gray) adults in the supplementary motor complex (SMC) tDCS groups.

$p = 0.043$]. Planned contrasts showed no differences between the active tDCS groups and sham ($p > 0.1$) (**Table 4**).

Errors

Within the older adult group, there were no differences in error commissions between any of the real and sham tDCS groups. Therefore, we performed three separate Mann–Whitney *U* tests to determine whether there was an age group effect for the number of errors committed in each session. There was no age group difference in the number of committed errors in session one ($Z = -1.726$, $p = 0.084$), two ($Z = -1.362$, $p = 0.173$), or three ($Z = -0.317$, $p = 0.751$). Within the older adult group, a Wilcoxon Signed Ranks test revealed that older adults reduced the number of errors made between sessions one ($M = 7.41$, SD ± 6.06) and two ($M = 6.15$, SD ± 4.33) ($Z = -2.63$, $p = 0.009$), and between sessions two and session three ($M = 1.86$, SD ± 1.60) ($Z = -6.214$, $p < 0.001$).

In summary, older adult individuals who received tDCS over either the right PFC or SMC showed slowed reaction time. This impairment was greater for older adults than young adults. For the number of chunks, older adults who received either left or right prefrontal tDCS displayed slower chunking. However, both older and young adults were impaired to the same extent.

TEST CONDITIONS

A 2 (Age group: young, old) by 5 (tDCS group: right PFC, left PFC, M1, SMC, sham) by 2 (Session: 2, 3) by 4 (Testing Condition: familiar, mixed familiar, mixed unfamiliar, and single stimulus) repeated measures ANOVA revealed a main effect of Session [$F(1,86) = 43.9$, $p < 0.001$], a main effect of Test Condition [$F(3,258) = 1717.212$, $p < 0.001$], a main effect of Age Group [$F(1,86) = 90.319$, $p < 0.001$], and a main effect of Stimulation Group [$F(1,86) = 2.985$, $p = 0.023$]. Pairwise comparisons revealed that reaction time was significantly slower in session two ($M = 359$ ms, SE ± 6.8 ms) relative to session three ($M = 342$ ms, SE ± 6.7 ms; $p < 0.001$). Reaction time in the familiar test condition ($M = 222$ ms, SE ± 7.8 ms) was shorter compared to the single stimulus ($M = 236$ ms, SE ± 8.6 ms; $p < 0.001$), the mixed ($M = 468$ ms, SE ± 6 ms; $p < 0.001$) and the mixed unfamiliar ($M = 477$ ms, SE ± 6 ms; $p < 0.001$) testing conditions. Older adults had overall longer reaction times ($M = 414$ ms, SE ± 11 ms) relative to the young group ($M = 287$ ms, SE ± 8 ms; $p < 0.001$). There were no significant differences between any real tDCS group and sham.

There was one significant interaction between Test Condition and Age Group [$F(3,86) = 2.985$, $p = 0.023$]. No other interactions were statistically significant ($p > 0.20$). To understand the significant Testing Condition and Age Group interaction, we performed four independent samples *t*-tests, comparing the reaction time within each testing condition between the two age groups. Young adults had shorter reaction times in the familiar condition ($M = 168$ ms, ± SD = 61 ms) relative to the older adults ($M = 364$ ms, ± SD = 160 ms; $t(240) = -12.762$, $p < 0.001$). Young adults also had shorter reaction times in the mixed condition ($M = 398$ ms, ± SD = 55 ms) relative to the older adults ($M = 560$ ms ± SD = 88 ms; $t(241) = -17.316$,

TABLE 5 | Results from linear mixed model using number of chunks as the dependent variable for older adults.

				Adjusted			
Chunking	**β**	**Std Err.**	**Z**	***p*-value**	**95% conf. interval**		**Cohen's d**
Session							
Session 2 vs. Session 1	−0.005	<0.001	−14.06	**<0.001**	−0.006	−0.004	−0.613
Session 3 vs. Session 2	−0.010	0.001	−7.11	**<0.001**	−0.014	−0.007	0.029
Stimulation							
Right PFC vs. Sham	0.004	0.001	2.60	0.150	−0.001	0.001	
Left PFC vs. Sham	0.006	0.002	4.17	**0.002**	0.002	0.012	0.190
M1 vs. Sham	0.005	0.001	−3.37	**0.023**	−0.010	<−0.001	−0.232
SMC vs. Sham	0.003	0.002	1.75	0.546	−0.002	0.007	
Stimulation by session							
Right PFC vs. Sham, session 1	0.004	0.001	5.36	**0.011**	<0.001	0.008	0.222
Left PFC vs. Sham, session 1	0.002	0.001	2.84	0.885	−0.002	0.007	
M1 vs. Sham, session 1	<0.001	0.001	0.56	1.000	−0.004	0.004	
SMC vs. Sham, session 1	0.002	0.001	2.14	0.991	−0.002	0.006	
Right PFC vs. Sham, session 2	−0.001	0.001	−0.95	1.000	−0.005	0.003	
Left PFC vs. Sham, session 2	0.005	0.001	5.39	**0.010**	<0.001	0.009	0.201
M1 vs. Sham, session 2	0.002	0.001	2.38	0.975	−0.006	0.002	
SMC vs. Sham, session 2	0.001	0.001	0.78	1.000	−0.003	0.005	
Right PFC vs. Sham, session 3	0.008	0.004	1.85	0.998	−0.013	0.028	
Left PFC vs. Sham, session 3	0.012	0.004	2.74	0.912	−0.009	0.033	
M1 vs. Sham, session 3	0.013	0.004	−2.94	0.853	−0.034	0.008	
SMC vs. Sham, session 3	−0.005	0.004	1.25	1.000	−0.016	0.027	

All p-values and confidence intervals have been Scheffé adjusted. β, beta; conf., confidence. Std Err., standard error. Significant p-values are in bold.

$p < 0.001$), faster reaction times in the mixed unfamiliar condition (M = 413 ms, ± SD = 52 ms) compared to the older adults (M = 568 ms ± SD = 93 ms; $t(242) = -16.027$, $p < 0.001$), and faster reaction times in the single stimulus condition (M = 181 ms ± SD = 78 ms) relative to the older adults (M = 312 ms ± SD = 126 ms; $t(208) = -9.285$, $p < 0.001$).

DISCUSSION

In contrast to our hypotheses, multi-session tDCS did not improve motor learning for older adults. Unexpectedly, anodal right prefrontal and SMC stimulation impaired learning for older adults as evidenced by longer reaction times across trials in session one. Similarly, anodal tDCS over either the right or left PFC impaired learning as assessed by the slowed reduction in the number of chunks in sessions one and two, respectively. In contrast to previously reported findings, older adults that received two separate sessions of stimulation to M1 showed no advantage or impairment in learning relative to sham.

Multiple sessions of stimulation over the prefrontal cortices did not enhance motor learning for older adults. In contrast, stimulation to the right PFC impaired learning as evidenced by a slowing of reaction time as well as a slowing in the reduction in the number of chunks for older adults limited to session one and a slowing in the reduction of the number of chunks limited to the left PFC tDCS group within session two. This replicates our previously reported results where we observed that young adults who received anodal (excitatory) tDCS either over the right or left PFC displayed impaired learning in the same motor learning task (Greeley et al., 2020). Based on the consistent impairment of motor sequence learning in young and older adults who received anodal tDCS over the prefrontal cortices, it is possible that using inhibitory stimulation may produce the opposite behavioral results and may be beneficial to motor learning. As such, there are two previous reported examples of non-invasive brain stimulation studies that demonstrate inhibiting the prefrontal cortices may facilitate sequence learning (Galea et al., 2010; Zhu et al., 2015). The findings from these studies suggest that suppressing the declarative memory system promotes the automatization of sequence learning regardless of age.

Counterintuitively, our findings also suggest that inhibiting prefrontal regions in older adults may also promote motor learning. We observed that right prefrontal anodal tDCS impaired learning as measured by both reaction time and the number of chunks limited to session one. Using the same design, we previously reported that anodal tDCS over the right PFC also impaired learning for young adults in session one (Greeley et al., 2020), indicating that the right PFC is involved for both age groups. However, it is of importance to note that when compared to young adults, right prefrontal stimulation was especially harmful to early learning (session one) to older adults as indexed by slowed reaction time. This suggests an integral role of the right PFC in this task and potentially to early motor sequence learning in general, because if the right PFC was not involved in this task stimulating this brain region, in theory, should *not* affect behavior. Our results support the model of hemispheric asymmetry reduction in older adults, or HAROLD (Cabeza, 2002; Przybyla et al., 2011), which suggests that during aging there is an increase in bilateral activity relative to young adults which is thought to be compensatory. While we observed impaired learning in the right prefrontal tDCS group, we found

no evidence for an early motor learning impairment for the left prefrontal tDCS older adult group. Thus, it is likely that older adults recruit both the left and right prefrontal cortices during learning and while right prefrontal anodal tDCS is especially harmful to explicit motor sequence learning, the left PFC is able to compensate and contribute to the task while the right hemisphere is affected with the anodal tDCS in the older adult group, whereas young adults display a far greater deficit (Greeley et al., 2020). Taken together, this suggests that regardless of age, tDCS over the right prefrontal cortices impairs learning, however, older adults are able to compensate due to bilateral compensatory mechanisms that are often observed in aging.

Stimulation to the prefrontal cortices in the older adult group also impaired chunking. In the current study we used a computational model that uses the covariation across key presses in order to detect chunk boundaries (Acuna et al., 2014). Using the number of chunks as identified by the Acuna et al. (2014) model, we observed a slower rate of chunking in the right prefrontal group limited to session one and slowed chunking in the left prefrontal group limited to session two. Unlike reaction time, however, we observed that this impairment was no different between the two age groups. Impaired chunking in the left and right PFC tDCS groups in older adults is surprising considering the involvement of the prefrontal cortices during chunking (Pammi et al., 2012; Wymbs et al., 2012), the positive relationship between working memory and chunking in older adults (Bo et al., 2009), and our previously reported findings demonstrating that prefrontal tDCS impaired chunking in young adults (Greeley et al., 2020). It remains an open question, however, whether using inhibitory stimulation (cathodal) over the prefrontal cortices would enhance chunking and whether it would affect older and young adults similarly. Future studies are needed to test these specific hypotheses but seem promising given the current results.

Our results also provide additional insight regarding the differential roles and specific time courses the prefrontal cortices play in motor learning. It is well established that the prefrontal cortices play an integral role early in motor sequence learning (Doyon and Benali, 2005; Floyer-Lea and Matthews, 2005). Our results replicate and extend these finding as we observed that stimulation to the right PFC impaired motor learning as evidenced by both a slower reduction in reaction time and the number of chunks limited to session one. However, we also observed that stimulation to the left, but not the right, PFC impaired chunking in session two. Two neuroimaging studies have also reported a specific role of the left PFC in chunking (Pammi et al., 2012; Wymbs et al., 2012). Taken together, our results suggest that the right PFC is involved early in sequence learning, whereas there is a specific role of the left PFC later in sequence learning related to chunking.

A limitation of the preceding discussion is that it assumes that anodal stimulation has excitatory effects on the underlying cortex. This has been shown in the motor cortex, where anodal stimulation over M1 leads to enhanced motor evoked potentials. However, tDCS electrode montages that do not include M1 have elicited unexpected effects. For instance, placing the anode over F3 and the cathode over F4 results in bilateral cortical excitation, based on functional connectivity changes (Nissim et al., 2019). The results of the current stimulation modeled in ROAST based on our prefrontal electrode montages also suggest a complex pattern of current distribution. The resulting current distribution is similar between our left and right prefrontal stimulation montages, making it less surprising that the two groups would show similar behavioral effects. In our prior work with young adults, we found that both anodal and cathodal stimulation applied to the left PFC resulted in slower sequence learning (Greeley et al., 2020), further supporting the complex effects arising with prefrontal stimulation. Regardless, it is important to know for the future design of potential therapies combining brain stimulation with training that both young and older adults exhibit sequence learning impairments with prefrontal tDCS.

Older adults that received stimulation to the left M1 showed no advantage in motor learning. This finding is in contrast to our previously reported findings in young adults, where we observed a benefit of left M1 stimulation in both reaction time and number of chunks in the same task (Greeley et al., 2020). Several other studies also report that anodal M1 tDCS facilitates learning across a variety of motor sequence tasks in both young (Reis et al., 2009; Stagg et al., 2011; Saucedo Marquez et al., 2013) and older adults (Zimerman et al., 2013; Dumel et al., 2016). Unexpected age-related responses to tDCS such as priming or preconditioning may account for the attenuated and null results observed in the older adults here. For example, older adult participants that received anodal tDCS to M1 immediately, but not an hour or 2 h following training on a motor sequence task, showed enhanced consolidation during a retest 24 h later (Rumpf et al., 2017). Another example comes from Fujiyama et al. (2017) who found enhanced force control and increased corticospinal excitability following a preconditioning period where cathodal (inhibitory) stimulation was applied prior to learning, followed by anodal stimulation during learning. The findings of Rumpf et al. (2017) and Fujiyama et al. (2017) conflict with Stagg et al. (2011), who found that the optimal timing of stimulation in young adults was during, but not before or after, a motor sequence task (Stagg et al., 2011). Thus, the lack of anodal M1 tDCS on motor sequence learning in older adults in the current study may be due to the timing of stimulation administration. Specifically, it may be that stimulating the prefrontal cortices during sequence learning was not an ideal protocol for older adults and instead tDCS should have been performed immediately before or after learning. Future studies should consider exploring how various tDCS timing protocols affect excitability and learning in older adults, as most previous permutations has been exclusively studied in young adults.

The present study is not without limitations. The sample size for each tDCS group is modest; however, the study design required a substantial time commitment from participants. Future studies should consider recruiting larger sample sizes to understand whether the negative impact of anodal PFC tDCS on motor learning can be replicated. Another potential limitation is the task specific effects of tDCS (Saucedo Marquez et al., 2013; Kimura et al., 2021). It is possible that the motor sequencing task employed here is not appropriate to pair with anodal prefrontal stimulation. Not collecting baseline reaction times can

also be a potential limitation. However, the inclusion of a sham group similar in age, sex, MoCA, handedness, and time between sessions to the other real stimulation groups helped control for this limitation. While we took several measures to ensure participants were engaged throughout the task such as stretch and water breaks, performance feedback, a relatively short amount of task practice time each session (∼20 min), and monetary compensation, it is possible that participants could have been bored during task performance. Future studies should consider the use of gamified motor learning tasks to increase motivation (Alexandrovsky et al., 2019; Friehs et al., 2020). Our study design also assumed that anodal stimulation would result in cortical excitation, which may not be the case as described above. Finally, the size and placement of the electrodes used in the present study likely affected the spread of the current to other brain regions outside the targeted area (see ROAST output). However, the tDCS protocol used here was standard.

CONCLUSION

Similar to what we reported with young adults (Greeley et al., 2020), we observed impaired sequence learning after the application of anodal tDCS over the left or right PFC for older adults. In combination, these two studies suggest a role for the bilateral prefrontal cortices in the early stages of sequence learning, regardless of age. Additionally, there was no instance where the application of anodal tDCS either over the right or left PFC, left M1, or SMC improved explicit motor sequence learning for older adults. These findings contribute to mounting evidence of the difficultly of using tDCS in an aging population and reveal a need for the field to adopt an individualized approach to non-invasive brain stimulation, especially in older adults. Recent work by Albizu et al. (2020) suggests that machine learning algorithms can use current density models to predict tDCS responsivity in older adults; such approaches will lead to better optimization of training interventions coupled with brain stimulation in the future.

DATA AVAILABILITY STATEMENT

The raw data supporting the conclusions of this article will be made available by the authors, without undue reservation.

ETHICS STATEMENT

The studies involving human participants were reviewed and approved by IRB Ethics Board at the University of Michigan. The patients/participants provided their written informed consent to participate in this study.

AUTHOR CONTRIBUTIONS

BG was responsible for design, data collection, analysis, interpretation of results, and writing and preparation of the manuscript. JB was responsible for design, assistance with the chunking analysis and editing of the manuscript. WV and RS were jointly responsible for conceptualization (ideas, substance, and design) and manuscript edits. All authors contributed to the article and approved the submitted version.

FUNDING

This project was supported by NSF ORA-PLUS 1420042 and an NIA Training Grant AG000114.

ACKNOWLEDGMENTS

We thank Brittany Gluskin for assistance with data collection.

SUPPLEMENTARY MATERIAL

The Supplementary Material for this article can be found online at: https://www.frontiersin.org/articles/10.3389/fnhum.2022.814204/full#supplementary-material

REFERENCES

Acuna, D. E., Wymbs, N. F., Reynolds, C. A., Picard, N., Turner, R. S., Strick, P. L., et al. (2014). Multifaceted aspects of chunking enable robust algorithms. *J. Neurophysiol.* 112, 1849–1856. doi: 10.1152/jn.00028.2014

Ahn, H., Zhong, C., Miao, H., Chaoul, A., Park, L., Yen, I. H., et al. (2019). Efficacy of combining home-based transcranial direct current stimulation with mindfulness-based meditation for pain in older adults with knee osteoarthritis: a randomized controlled pilot study. *J. Clin. Neurosci.* 70, 140–145. doi: 10.1016/j.jocn.2019.08.047

Albizu, A., Fang, R., Indahlastari, A., O'Shea, A., Stolte, S. E., See, K. B., et al. (2020). Machine learning and individual variability in electric field characteristics predict tDCS treatment response. *Brain Stimul.* 13, 1753–1764. doi: 10.1016/j.brs.2020.10.001

Alexandrovsky, D., Friehs, M. A., Birk, M. V., Yates, R. K., and Mandryk, R. L. (2019). "Game dynamics that support snacking, not feasting," in *Proceedings of the Annual Symposium on Computer-Human Interaction in Play*, Barcelona, 573–588.

Arnau, J., Bono, R., Blanca, M. J., and Bendayan, R. (2012). Using the linear mixed model to analyze nonnormal data distributions in longitudinal designs. *Behav. Res. Methods* 44, 1224–1238. doi: 10.3758/s13428-012-0196-y

Beck, A. T., Steer, R. A., and Carbin, M. G. (1988). Psychometric properties of the beck depression inventory: twenty-five years of evaluation. *Clin. Psychol. Rev.* 8, 77–100. doi: 10.1016/0272-7358(88)90050-5

Bikson, M., Datta, A., and Elwassif, M. (2009). Establishing safety limits for transcranial direct current stimulation. *Clin. Neurophysiol.* 120:1033. doi: 10.1016/j.clinph.2009.03.018

Bo, J., and Seidler, R. D. (2009). Visuospatial working memory capacity predicts the organization of acquired explicit motor sequences. *J. Neurophysiol.* 101, 3116–3125. doi: 10.1152/jn.00006.2009

Bo, J., Borza, V., and Seidler, R. D. (2009). Age-related declines in visuospatial working memory correlate with deficits in explicit motor sequence learning. *J. Neurophysiol.* 102, 2744–2754. doi: 10.1152/jn.00393.2009

Brown, R. M., Robertson, E. M., and Press, D. Z. (2009). Sequence skill acquisition and off-line learning in normal aging. *PLoS One* 4:e6683. doi: 10.1371/journal.pone.0006683

Cabeza, R. (2002). Hemispheric asymmetry reduction in older adults: the HAROLD model. *Psychol. Aging* 17:85.

Carson, N., Leach, L., and Murphy, K. J. (2018). A re-examination of Montreal cognitive assessment (MoCA) cutoff scores. *Int. J. Geriatr. Psychiatry* 33, 379–388. doi: 10.1002/gps.4756

Charvet, L. E., Kasschau, M., Datta, A., Knotkova, H., Stevens, M. C., Alonzo, A., et al. (2015). Remotely-supervised transcranial direct current stimulation (tDCS) for clinical trials: guidelines for technology and protocols. *Front. Syst. Neurosci.* 9:26. doi: 10.3389/fnsys.2015.00026

Chow, R., Noly-Gandon, A., Moussard, A., Ryan, J. D., and Alain, C. (2021). Effects of transcranial direct current stimulation combined with listening to preferred music on memory in older adults. *Sci. Rep.* 11:12638. doi: 10.1038/s41598-021-91977-8

Doyon, J., and Benali, H. (2005). Reorganization and plasticity in the adult brain during learning of motor skills. *Curr. Opin. Neurobiol.* 15, 161–167. doi: 10.1016/j.conb.2005.03.004

Dumel, G., Bourassa, M. E., Desjardins, M., Voarino, N., Charlebois-Plante, C., Doyon, J., et al. (2016). Multisession anodal tDCS protocol improves motor system function in an aging population. *Neural Plast.*2016:5961362. doi: 10.1155/2016/5961362

Ekstrom, R. B., French, J. W., and Harman, H. H. (1979). Cognitive factors: their identification and replication. *Multivariate Behav. Res. Monogr.* 79:84.

Esiri, M. M. (2007). Ageing and the brain. *J. Pathol.* 211, 181–187.

Farnad, L., Ghasemian-Shirvan, E., Mosayebi-Samani, M., Kuo, M. F., and Nitsche, M. A. (2021). Exploring and optimizing the neuroplastic effects of anodal transcranial direct current stimulation over the primary motor cortex of older humans. *Brain Stimul.* 14, 622–634. doi: 10.1016/j.brs.2021.03.013

Fertonani, A., Brambilla, M., Cotelli, M., and Miniussi, C. (2014). The timing of cognitive plasticity in physiological aging: a tDCS study of naming. *Front. Aging Neurosci.* 6:131. doi: 10.3389/fnagi.2014.00131

Filmer, H. L., Mattingley, J. B., and Dux, P. E. (2020). Modulating brain activity and behaviour with tDCS: rumours of its death have been greatly exaggerated. *Cortex* 123, 141–151. doi: 10.1016/j.cortex.2019.10.006

Floyer-Lea, A., and Matthews, P. M. (2005). Distinguishable brain activation networks for short-and long-term motor skill learning. *J. Neurophysiol.* 94, 512–518. doi: 10.1152/jn.00717.2004

Friehs, M. A., Dechant, M., Vedress, S., Frings, C., and Mandryk, R. L. (2020). Effective gamification of the stop-signal task: two controlled laboratory experiments. *JMIR Serious Games* 8:e17810. doi: 10.2196/17810

Fujiyama, H., Hinder, M. R., Barzideh, A., Van de Vijver, C., Badache, A. C., Manrique-C, M. N., et al. (2017). Preconditioning tDCS facilitates subsequent tDCS effect on skill acquisition in older adults. *Neurobiol. Aging* 51, 31–42.

Funahashi, S. (2017). Working memory in the prefrontal cortex. *Brain Sci.* 7:49.

Galea, J. M., Albert, N. B., Ditye, T., and Miall, R. C. (2010). Disruption of the dorsolateral prefrontal cortex facilitates the consolidation of procedural skills. *J. Cogn. Neurosci.* 22, 1158–1164. doi: 10.1162/jocn.2009.21259

Greeley, B., and Seidler, R. D. (2019). Differential effects of left and right prefrontal cortex anodal transcranial direct current stimulation during probabilistic sequence learning. *J. Neurophysiol.* 121, 1906–1916. doi: 10.1152/jn.00795.2018

Greeley, B., Barnhoorn, J. S., Verwey, W. B., and Seidler, R. D. (2020). Multi-session transcranial direct current stimulation over primary motor cortex facilitates sequence learning, chunking, and one year retention. *Front. Hum. Neurosci.* 14:75. doi: 10.3389/fnhum.2020.00075

Habich, A., Slotboom, J., Peter, J., Wiest, R., and Klöppel, S. (2020). No effect of anodal tDCS on verbal episodic memory performance and neurotransmitter levels in young and elderly participants. *Neural Plast.* 2020:8896791. doi: 10.1155/2020/8896791

Hashemirad, F., Zoghi, M., Fitzgerald, P. B., and Jaberzadeh, S. (2016). The effect of anodal transcranial direct current stimulation on motor sequence learning in healthy individuals: a systematic review and meta-analysis. *Brain Cogn.* 102, 1–12. doi: 10.1016/j.bandc.2015.11.005

Huang, Y., Datta, A., Bikson, M., and Parra, L. C. (2019). Realistic volumetric-approach to simulate transcranial electric stimulation—ROAST—a fully automated open-source pipeline. *J. Neural Eng.* 16:056006. doi: 10.1088/1741-2552/ab208d

Huang, Y., Liu, A. A., Lafon, B., Friedman, D., Dayan, M., Wang, X., et al. (2017). Measurements and models of electric fields in the in vivo human brain during transcranial electric stimulation. *elife* 6:e18834.

Indahlastari, A., Albizu, A., O'Shea, A., Forbes, M. A., Nissim, N. R., Kraft, J. N., et al. (2020). Modeling transcranial electrical stimulation in the aging brain. *Brain Stimul.* 13, 664–674. doi: 10.1016/j.brs.2020.02.007

Iyer, M. B., Mattu, U., Grafman, J., Lomarev, M., Sato, S., and Wassermann, E. M. (2005). Safety and cognitive effect of frontal DC brain polarization in healthy individuals. *Neurology* 64, 872–875. doi: 10.1212/01.WNL.0000152986.07469.E9

Janacsek, K., Ambrus, G. G., Paulus, W., Antal, A., and Nemeth, D. (2015). Right hemisphere advantage in statistical learning: evidence from a probabilistic sequence learning task. *Brain Stimul.* 8, 277–282. doi: 10.1016/j.brs.2014.11.008

Kane, M. J., and Engle, R. W. (2002). The role of prefrontal cortex in working-memory capacity, executive attention, and general fluid intelligence: an individual-differences perspective. *Psychonom. Bull. Rev.* 9, 637–671. doi: 10.3758/bf03196323

Kasschau, M., Reisner, J., Sherman, K., Bikson, M., Datta, A., and Charvet, L. E. (2016). Transcranial direct current stimulation is feasible for remotely supervised home delivery in multiple sclerosis. *Neuromodulation* 19, 824–831. doi: 10.1111/ner.12430

Kennerley, S. W., Sakai, K., and Rushworth, M. F. S. (2004). Organization of action sequences and the role of the pre-SMA. *J. Neurophysiol.* 91, 978–993. doi: 10.1152/jn.00651.2003

Kimura, T., Kaneko, F., and Nagamine, T. (2021). The effects of transcranial direct current stimulation on dual-task interference depend on the dual-task content. *Front. Hum. Neurosci.* 15:653713. doi: 10.3389/fnhum.2021.653713

Lee, J. Y., Lee, D. W., Cho, S. J., Na, D. L., Jeon, H. J., Kim, S. K., et al. (2008). Brief screening for mild cognitive impairment in elderly outpatient clinic: validation of the Korean version of the Montreal Cognitive Assessment. *J. Geriatr. Psychiatry Neurol.* 21, 104–110. doi: 10.1177/0891988708316855

Lin, C. H. J., Chiang, M. C., Wu, A. D., Iacoboni, M., Udompholkul, P., Yazdanshenas, O., et al. (2012). Age related differences in the neural substrates of motor sequence learning after interleaved and repetitive practice. *Neuroimage* 62, 2007–2020. doi: 10.1016/j.neuroimage.2012.05.015

Lo, S., and Andrews, S. (2015). To transform or not to transform: using generalized linear mixed models to analyse reaction time data. *Front. Psychol.* 6:1171. doi: 10.3389/fpsyg.2015.01171

Luck, S. J., and Vogel, E. K. (1997). The capacity of visual working memory for features and conjunctions. *Nature* 390, 279–281.

Michely, J., Volz, L. J., Hoffstaedter, F., Tittgemeyer, M., Eickhoff, S. B., Fink, G. R., et al. (2018). Network connectivity of motor control in the ageing brain. *NeuroImage Clin.* 18, 443–455. doi: 10.1016/j.nicl.2018.02.001

Monte-Silva, K., Kuo, M. F., Hessenthaler, S., Fresnoza, S., Liebetanz, D., Paulus, W., et al. (2013). Induction of late LTP-like plasticity in the human motor cortex by repeated non-invasive brain stimulation. *Brain Stimul.* 6, 424–432. doi: 10.1016/j.brs.2012.04.011

Mooney, R. A., Cirillo, J., and Byblow, W. D. (2019). Neurophysiological mechanisms underlying motor skill learning in young and older adults. *Exp. Brain Res.* 237, 2331–2344. doi: 10.1007/s00221-019-05599-8

Muffel, T., Kirsch, F., Shih, P. C., Kalloch, B., Schaumberg, S., Villringer, A., et al. (2019). Anodal transcranial direct current stimulation over S1 differentially modulates proprioceptive accuracy in young and old adults. *Front. Aging Neurosci.* 11:264. doi: 10.3389/fnagi.2019.00264

Nasreddine, Z. S., Phillips, N. A., Bédirian, V., Charbonneau, S., Whitehead, V., Collin, I., et al. (2005). The montreal cognitive assessment, MoCA: a brief screening tool for mild cognitive impairment. *J. Am. Geriatr Soc.* 53, 695–699. doi: 10.1111/j.1532-5415.2005.53221.x

Nissim, N. R., O'Shea, A., Indahlastari, A., Telles, R., Richards, L., Porges, E., et al. (2019). Effects of in-scanner bilateral frontal tDCS on functional connectivity of the working memory network in older adults. *Front. Aging Neurosci.* 11:51. doi: 10.3389/fnagi.2019.00051

Nitsche, M. A., Doemkes, S., Karakose, T., Antal, A., Liebetanz, D., Lang, N., et al. (2007). Shaping the effects of transcranial direct current stimulation of the human motor cortex. *J. Neurophysiol.* 97, 3109–3117. doi: 10.1152/jn.01312.2006

Nomura, T., and Kirimoto, H. (2018). Anodal transcranial direct current stimulation over the supplementary motor area improves anticipatory postural adjustments in older adults. *Front. Hum. Neurosci.* 12:317. doi: 10.3389/fnhum.2018.00317

Oldfield, R. C. (1971). The assessment and analysis of handedness: the Edinburgh inventory. *Neuropsychologia* 9, 97–113. doi: 10.1016/0028-3932(71)90067-4

Pammi, V. C., Miyapuram, K. P., Samejima, K., Bapi, R. S., and Doya, K. (2012). Changing the structure of complex visuo-motor sequences selectively activates the fronto-parietal network. *Neuroimage* 59, 1180–1189. doi: 10.1016/j.neuroimage.2011.08.006

Patel, R., Ashcroft, J., Patel, A., Ashrafian, H., Woods, A. J., Singh, H., et al. (2019). The impact of transcranial direct current stimulation on upper-limb motor performance in healthy adults: a systematic review and meta-analysis. *Front. Neurosci.* 13:1213. doi: 10.3389/fnins.2019.01213

Przybyla, A., Haaland, K. Y., Bagesteiro, L. B., and Sainburg, R. L. (2011). Motor asymmetry reduction in older adults. *Neurosci. Lett.* 489, 99–104.

Raz, N. (2000). "Aging of the brain and its impact on cognitive performance: integration of structural and functional findings," in *The Handbook of Aging and Cognition*, eds F. I. M. Craik and T. A. Salthouse (Mahwah, NJ: Lawrence Erlbaum Associates Publishers), 1–90.

Reis, J., Schambra, H. M., Cohen, L. G., Buch, E. R., Fritsch, B., Zarahn, E., et al. (2009). Noninvasive cortical stimulation enhances motor skill acquisition over multiple days through an effect on consolidation. *Proc. Natl. Acad. Sci. U.S.A.* 106, 1590–1595. doi: 10.1073/pnas.0805413106

Rossi, S., Miniussi, C., Pasqualetti, P., Babiloni, C., Rossini, P. M., and Cappa, S. F. (2004). Age-related functional changes of prefrontal cortex in long-term memory: a repetitive transcranial magnetic stimulation study. *J. Neurosci.* 24, 7939–7944. doi: 10.1523/JNEUROSCI.0703-04.2004

Ruitenberg, M. F., Verwey, W. B., Schutter, D. J., and Abrahamse, E. L. (2014). Cognitive and neural foundations of discrete sequence skill: a TMS study. *Neuropsychologia* 56, 229–238. doi: 10.1016/j.neuropsychologia.2014.01.014

Rumpf, J. J., Wegscheider, M., Hinselmann, K., Fricke, C., King, B. R., Weise, D., et al. (2017). Enhancement of motor consolidation by post-training transcranial direct current stimulation in older people. *Neurobiol. Aging* 49, 1–8. doi: 10.1016/j.neurobiolaging.2016.09.003

Saucedo Marquez, C. M., Zhang, X., Swinnen, S. P., Meesen, R., and Wenderoth, N. (2013). Task-specific effect of transcranial direct current stimulation on motor learning. *Front. Hum. Neurosci.* 7:333. doi: 10.3389/fnhum.2013.00333

Scahill, R. I., Frost, C., Jenkins, R., Whitwell, J. L., Rossor, M. N., and Fox, N. C. (2003). A longitudinal study of brain volume changes in normal aging using serial registered magnetic resonance imaging. *Arch. Neurol.* 60, 989–994. doi: 10.1001/archneur.60.7.989

Schielzeth, H., Dingemanse, N. J., Nakagawa, S., Westneat, D. F., Allegue, H., Teplitsky, C., et al. (2020). Robustness of linear mixed-effects models to violations of distributional assumptions. *Methods Ecol. Evol.* 11, 1141–1152.

Seidler, R. D. (2006). Differential effects of age on sequence learning and sensorimotor adaptation. *Brain Res. Bull.* 70, 337–346. doi: 10.1016/j.brainresbull.2006.06.008

Seidler, R. D., Bernard, J. A., Burutolu, T. B., Fling, B. W., Gordon, M. T., Gwin, J. T., et al. (2010). Motor control and aging: links to age-related brain structural, functional, and biochemical effects. *Neurosci. Biobehav. Rev.* 34, 721–733. doi: 10.1016/j.neubiorev.2009.10.005

Seidler, R. D., Gluskin, B. S., and Greeley, B. (2017). Right prefrontal cortex transcranial direct current stimulation enhances multi-day savings in sensorimotor adaptation. *J. Neurophysiol.* 117, 429–435. doi: 10.1152/jn.00563.2016

Shekhawat, G. S., and Vanneste, S. (2018). Optimization of transcranial direct current stimulation of dorsolateral prefrontal cortex for tinnitus: a non-linear dose-response effect. *Sci. Rep.* 8:8311. doi: 10.1038/s41598-018-26665-1

Song, S., Zilverstand, A., Gui, W., Li, H. J., and Zhou, X. (2019). Effects of single-session versus multi-session non-invasive brain stimulation on craving and consumption in individuals with drug addiction, eating disorders or obesity: a meta-analysis. *Brain Stimul.* 12, 606–618. doi: 10.1016/j.brs.2018.12.975

Stagg, C. J., Jayaram, G., Pastor, D., Kincses, Z. T., Matthews, P. M., and Johansen-Berg, H. (2011). Polarity and timing-dependent effects of transcranial direct current stimulation in explicit motor learning. *Neuropsychologia* 49, 800–804. doi: 10.1016/j.neuropsychologia.2011.02.009

Talsma, L. J., Kroese, H. A., and Slagter, H. A. (2017). Boosting cognition: effects of multiple-session transcranial direct current stimulation on working memory. *J. Cogn. Neurosci.* 29, 755–768. doi: 10.1162/jocn_a_01077

Tiffin, J., and Asher, E. J. (1948). The Purdue pegboard: norms and studies of reliability and validity. *J. Appl. Psychol.* 32:234. doi: 10.1037/h0061266

Verwey, W. B. (2010). Diminished motor skill development in elderly: indications for limited motor chunk use. *Acta Psychol.* 134, 206–214. doi: 10.1016/j.actpsy.2010.02.001

Verwey, W. B., and Eikelboom, T. (2003). Evidence for lasting sequence segmentation in the discrete sequence-production task. *J. Motor Behav.* 35, 171–181. doi: 10.1080/00222890309602131

Verwey, W. B., Jouen, A. L., Dominey, P. F., and Ventre-Dominey, J. (2019). Explaining the neural activity distribution associated with discrete movement sequences: evidence for parallel functional systems. *Cogn. Affect. Behav. Neurosci.* 19, 138–153. doi: 10.3758/s13415-018-00651-6

Vollmann, H., Conde, V., Sewerin, S., Taubert, M., Sehm, B., Witte, O. W., et al. (2013). Anodal transcranial direct current stimulation (tDCS) over supplementary motor area (SMA) but not pre-SMA promotes short-term visuomotor learning. *Brain Stimul.* 6, 101–107. doi: 10.1016/j.brs.2012.03.018

Waters, S., Wiestler, T., and Diedrichsen, J. (2017). Cooperation not competition: bihemispheric tDCS and fMRI show role for ipsilateral hemisphere in motor learning. *J. Neurosci.* 37, 7500–7512.

Waters-Metenier, S., Husain, M., Wiestler, T., and Diedrichsen, J. (2014). Bihemispheric transcranial direct current stimulation enhances effector-independent representations of motor synergy and sequence learning. *J. Neurosci.* 34, 1037–1050. doi: 10.1523/JNEUROSCI.2282-13.2014

Wechsler, D. (1958). *The Measurement and Appraisal of Adult Intelligence*, 4th Edn. Philadelphia, PA: Williams & Wilkins Co.

Wilhelm, I., Diekelmann, S., and Born, J. (2008). Sleep in children improves memory performance on declarative but not procedural tasks. *Learn. Mem.* 15, 373–377. doi: 10.1101/lm.803708

Wilhelm, I., Prehn-Kristensen, A., and Born, J. (2012). Sleep-dependent memory consolidation–what can be learnt from children? *Neurosci. Biobehav. Rev.* 36, 1718–1728. doi: 10.1016/j.neubiorev.2012.03.002

Wu, T., and Hallett, M. (2005). The influence of normal human ageing on automatic movements. *J. Physiol.* 562, 605–615. doi: 10.1113/jphysiol.2004.076042

Wymbs, N. F., Bassett, D. S., Mucha, P. J., Porter, M. A., and Grafton, S. T. (2012). Differential recruitment of the sensorimotor putamen and frontoparietal cortex during motor chunking in humans. *Neuron* 74, 936–946. doi: 10.1016/j.neuron.2012.03.038

Zhu, F. F., Yeung, A. Y., Poolton, J. M., Lee, T. M., Leung, G. K., and Masters, R. S. (2015). Cathodal transcranial direct current stimulation over left dorsolateral prefrontal cortex area promotes implicit motor learning in a golf putting task. *Brain Stimul.* 8, 784–786. doi: 10.1016/j.brs.2015.02.005

Zimerman, M., Heise, K. F., Gerloff, C., Cohen, L. G., and Hummel, F. C. (2014). Disrupting the ipsilateral motor cortex interferes with training of a complex motor task in older adults. *Cereb. Cortex* 24, 1030–1036. doi: 10.1093/cercor/bhs385

Zimerman, M., Nitsch, M., Giraux, P., Gerloff, C., Cohen, L. G., and Hummel, F. C. (2013). Neuroenhancement of the aging brain: restoring skill acquisition in old subjects. *Ann. Neurol.* 73:10. doi: 10.1002/ana.23761

Conflict of Interest: The authors declare that the research was conducted in the absence of any commercial or financial relationships that could be construed as a potential conflict of interest.

Publisher's Note: All claims expressed in this article are solely those of the authors and do not necessarily represent those of their affiliated organizations, or those of the publisher, the editors and the reviewers. Any product that may be evaluated in this article, or claim that may be made by its manufacturer, is not guaranteed or endorsed by the publisher.

frontiers in Aging Neuroscience

ORIGINAL RESEARCH
published: 11 March 2022
doi: 10.3389/fnagi.2022.809281

Differential Relationships Between Brain Structure and Dual Task Walking in Young and Older Adults

*Kathleen E. Hupfeld[1], Justin M. Geraghty[1†], Heather R. McGregor[1], C. J. Hass[1], Ofer Pasternak[2] and Rachael D. Seidler[1,3]**

[1] Department of Applied Physiology and Kinesiology, University of Florida, Gainesville, FL, United States, [2] Departments of Psychiatry and Radiology, Brigham and Women's Hospital, Harvard Medical School, Boston, MA, United States, [3] University of Florida Norman Fixel Institute for Neurological Diseases, Gainesville, FL, United States

OPEN ACCESS

Edited by:
Hakuei Fujiyama, Murdoch University, Australia

Reviewed by:
Emad Al-Yahya, University of Nottingham, United Kingdom
Woei-Nan Bair, University of the Sciences, United States

***Correspondence:**
Rachael D. Seidler
rachaelseidler@ufl.edu

†Present address:
Justin M. Geraghty, School of Medicine, University of Central Florida, Orlando, FL, United States

Specialty section:
This article was submitted to Neurocognitive Aging and Behavior, a section of the journal Frontiers in Aging Neuroscience

Received: *04 November 2021*
Accepted: *31 January 2022*
Published: *11 March 2022*

Citation:
Hupfeld KE, Geraghty JM, McGregor HR, Hass CJ, Pasternak O and Seidler RD (2022) Differential Relationships Between Brain Structure and Dual Task Walking in Young and Older Adults. Front. Aging Neurosci. 14:809281. doi: 10.3389/fnagi.2022.809281

Almost 25% of all older adults experience difficulty walking. Mobility difficulties for older adults are more pronounced when they perform a simultaneous cognitive task while walking (i.e., dual task walking). Although it is known that aging results in widespread brain atrophy, few studies have integrated across more than one neuroimaging modality to comprehensively examine the structural neural correlates that may underlie dual task walking in older age. We collected spatiotemporal gait data during single and dual task walking for 37 young (18–34 years) and 23 older adults (66–86 years). We also collected T_1-weighted and diffusion-weighted MRI scans to determine how brain structure differs in older age and relates to dual task walking. We addressed two aims: (1) to characterize age differences in brain structure across a range of metrics including volumetric, surface, and white matter microstructure; and (2) to test for age group differences in the relationship between brain structure and the dual task cost (DTcost) of gait speed and variability. Key findings included widespread brain atrophy for the older adults, with the most pronounced age differences in brain regions related to sensorimotor processing. We also found multiple associations between regional brain atrophy and greater DTcost of gait speed and variability for the older adults. The older adults showed a relationship of both thinner temporal cortex and shallower sulcal depth in the frontal, sensorimotor, and parietal cortices with greater DTcost of gait. Additionally, the older adults showed a relationship of ventricular volume and superior longitudinal fasciculus free-water corrected axial and radial diffusivity with greater DTcost of gait. These relationships were not present for the young adults. Stepwise multiple regression found sulcal depth in the left precentral gyrus, axial diffusivity in the superior longitudinal fasciculus, and sex to best predict DTcost of gait speed, and cortical thickness in the superior temporal gyrus to best predict DTcost of gait variability for older adults. These results contribute to scientific understanding of how individual variations in brain structure are associated with mobility function in aging. This has implications for uncovering mechanisms of brain aging and for identifying target regions for mobility interventions for aging populations.

Keywords: aging, dual task walking, dual task cost (DTcost), gray matter volume, cortical thickness, sulcal depth, ventricular volume, free water

1. INTRODUCTION

Nearly 25 percent of older adults report serious mobility problems such as difficulty walking or climbing stairs (Kraus, 2016). Older adults tend to encounter even greater difficulty with performing a secondary cognitive task while walking, i.e., dual task walking (e.g., Springer et al., 2006; Hollman et al., 2007; Malcolm et al., 2015; Smith et al., 2016). A common measure of dual task walking performance is dual task cost (DTcost), or the magnitude of performance decline when conducting two tasks at once as opposed to individually (Yogev-Seligmann et al., 2008; Bayot et al., 2020). Older adults typically exhibit greater DTcosts compared with young adults, such as greater slowing of gait speed from dual to single task conditions (for review, see Al-Yahya et al., 2011; Beurskens and Bock, 2012). Examining DTcost is considered more useful than assessing single or dual condition performance in isolation, as cost metrics incorporate individual differences in baseline performance (Verhaeghen et al., 2003).

Poorer dual task walking abilities have been related to increased fall risk (e.g., Lundin-Olsson et al., 1997; Montero-Odasso et al., 2012; Bridenbaugh and Kressig, 2015), cognitive decline (Montero-Odasso et al., 2017), frailty, disability, and mortality (Verghese et al., 2012). Importantly, dual task walking performance is more predictive of falls in aging than single task walking performance (Ayers et al., 2014; Johansson et al., 2016; Verghese et al., 2017; Halliday et al., 2018; Gillain et al., 2019). This could be because dual task walking provides a better analog for real-world scenarios. Indeed, a recent study reported that in-lab dual task walking attributes were more similar to real-world gait, as compared with normal walking in the lab with no dual tasking requirements (Hillel et al., 2019). Thus, given the link between dual task walking performance and falls, and its greater ecological validity, we selected to analyze dual instead of single task walking.

There are clear cortical contributions to the control of walking (Miyai et al., 2001; Petersen et al., 2012; Allali et al., 2014; Koenraadt et al., 2014; Takakusaki, 2017). Thus, poorer dual task walking performance in older age has been attributed, at least in part, to age-related brain atrophy (Allali et al., 2019; Lucas et al., 2019; Ross et al., 2021). A large body of literature suggests that age-related structural brain atrophy occurs in an anterior-to-posterior pattern, with the frontal cortices atrophying earlier and faster than other regions of the brain (e.g., Salat et al., 2004; Fjell et al., 2009a; Thambisetty et al., 2010; Lemaitre et al., 2012). Given this, it is not surprising that previous work has linked lower prefrontal cortex gray matter volume with poorer dual task walking abilities in older adults (Tripathi et al., 2019; Wagshul et al., 2019). Aging is hypothesized to increase reliance on alternative (i.e., non-motor) neural resources, such as the frontal cortex (Mirelman et al., 2017), to compensate for brain atrophy in sensorimotor regions and maintain performance (Cabeza et al., 2002; Steffener and Stern, 2012; Fettrow et al., 2021b). Interestingly, recent work in a large sample of middle- to older-aged adults ($n = 966$) has reported disproportionately steep age differences (i.e., atrophy, demyelination, and iron reduction) in the sensorimotor cortices rather than in more anterior prefrontal regions (Taubert et al., 2020). Thus, structural changes in the sensorimotor cortices with aging may also contribute to age-related mobility declines.

Many previous studies have reported relationships between age differences in regional brain structure and worse gait for older adults during single task walking (for review, see Tian et al., 2017; Wilson et al., 2019). However, compared to the extensive literature examining single task walking, only limited work examining brain structure has focused on dual task walking in aging. A majority of the studies examining correlates of dual task walking in aging have instead focused on brain function, using functional near-infrared spectroscopy (fNIRS). These studies have largely found increases in prefrontal cortex oxygenation levels from single to dual task walking for older adults, suggesting that dual compared with single task walking demands more prefrontal neural resources (e.g., Doi et al., 2013; Beurskens et al., 2014; Holtzer et al., 2015). As dual task walking is more cognitively demanding than normal walking, it is logical that functional contributions from the prefrontal cortex increase during dual task walking (Holtzer et al., 2015); thus, markers of prefrontal cortex structure might also relate to dual task walking performance in older age. Overall, while these functional studies provide important insight into the vasodynamic response to dual task walking, further work is needed to understand how markers of brain structure relate to dual task walking in aging.

The small body of work that has investigated relationships between brain structure and dual task walking in older adults suggests an important link between "maintenance" of brain structure and maintenance of dual task walking abilities. Two previous studies found associations between greater gait slowing during dual task walking in older adults and lower gray matter volume in the middle frontal gyrus (Allali et al., 2019), medial prefrontal and cingulate cortices, and thalamus (Tripathi et al., 2019). Further, several studies found that older adults who showed a greater increase in prefrontal cortex oxygenation from single to dual task walking also had lower white matter fractional anisotropy (averaged across the whole white matter mask; Lucas et al., 2019), lower gray matter volume within the frontal lobe (Wagshul et al., 2019), and reduced thickness across the cortex (Ross et al., 2021). These imaging metrics were not related to faster dual task walking, though, suggesting that the observed increases in prefrontal cortex activity represented compensation to maintain walking performance, despite atrophying brain structure.

The prior work described above examining the brain structural correlates of dual task walking tested only one imaging modality in isolation. Here we combined across multiple structural imaging modalities to provide more comprehensive information about age differences in brain structure and how these relate to dual task walking. We assessed volumetric measures of atrophy, i.e., gray matter, cerebellum, hippocampus, and ventricular volume. In addition to widespread declines in gray matter volume (paired with ventricular enlargement) with aging (Raz et al., 2010; Lemaitre et al., 2012), prior work has also reported widespread cerebellar atrophy with aging, particularly in the anterior and superior-posterior lobes of the cerebellum (Koppelmans et al., 2017). We also examined surface metrics, including cortical thickness (Dahnke et al., 2013),

sulcal depth (Yun et al., 2013), cortical complexity (i.e., folding complexity of the cortex; Yotter et al., 2011b), and gyrification index (i.e., mean curvature of the cortex; Luders et al., 2006). Surface-based morphometry metrics have several advantages over volume-based metrics (Hutton et al., 2009; Winkler et al., 2010; Lemaitre et al., 2012), including more accurate spatial registration (Desai et al., 2005), sensitivity to surface folding, and independence from head size (Gaser and Kurth, 2017). Despite these potential benefits, compared to volumetric measures, less work has examined how surface measures relate to dual task walking in aging.

We also examined white matter microstructure metrics derived from diffusion MRI, including free-water (FW) corrected fractional anisotropy (FAt, "t" refers to the tissue compartment remaining after FW correction), axial diffusivity (ADt), and radial diffusivity (RDt), and the fractional volume of FW (Pasternak et al., 2009). FW correction is particularly important for analyses of older adult brains because age-related white matter degeneration can lead to enlarged interstitial spaces (Meier-Ruge et al., 1992) and thereby increased partial volume effects between white matter fibers and extracellular water (Chad et al., 2018). Recent work found that FW correction results in less pronounced age differences in white matter microstructure than previously reported (Chad et al., 2018), suggesting that prior age difference results are at least partially driven by fluid effects. Thus, to increase interpretability of white matter microstructural effects, it is important to correct for FW when examining white matter in aging. Moreover, higher FW has been related to poorer cognition in aging (Maillard et al., 2019; Gullett et al., 2020) and poorer function (e.g., bradykinesia) in Parkinson's disease (Ofori et al., 2015).

In the present work, we addressed several aims: (1) To characterize age differences in brain structure; we predicted the most pronounced age differences in the prefrontal cortex. (2) To identify regions of age differences in the relationship between brain structure and DTcost of gait speed and variability; given the fNIRS literature reporting increased prefrontal cortex activation during dual task walking (Doi et al., 2013; Beurskens et al., 2014; Holtzer et al., 2015), we predicted that greater prefrontal atrophy would correlate with greater DTcost of gait speed and variability for older but not younger adults. (3) To determine the strongest predictors(s) of DTcost of gait in older adults using a stepwise regression approach. This was an exploratory aim, and thus we did not define an *a priori* hypothesis.

2. MATERIALS AND METHODS

The University of Florida's Institutional Review Board provided ethical approval for the study. All individuals provided their written informed consent.

2.1. Participants

37 young and 25 older adults from the Gainesville, FL community participated in this study. Participants were in generally good health, with no reported neurologic or psychiatric problems. Two older adults were excluded from analyses of the T_1-weighted images. Thus, $n = 23$ older adults for all analyses involving the T_1-weighted images. A diffusion MRI was not collected for one young and two older adults; thus, $n = 36$ young and $n = 21$ older adults for all diffusion MRI analyses. See **Supplementary Section 1** for further details regarding participant selection and exclusion criteria. Of note, we reported on a different subset of behavioral and brain metrics from this same cohort in two recent publications (Fettrow et al., 2021a; Hupfeld et al., 2021a).

2.2. Testing Sessions

Before the first session, we collected self-reported participant information on: demographics (e.g., age, sex, and years of education), medical history, handedness, footedness, exercise, and sleep. We also collected anthropometric information (e.g., height and weight). Participants then completed mobility testing, followed by an MRI scan approximately 5 days later (**Figure 1**). For 24 h prior to each session, participants were requested to not consume alcohol, nicotine, or any drugs other than the medications they disclosed to us.

2.3. Session 1: Mobility Testing

Participants completed three walking tasks while instrumented with six Opal inertial measurement units (IMUs; v2; APDM Wearable Technologies Inc., Portland, OR, USA). IMUs were placed on the feet, wrists, around the waist at the level of the lumbar spine, and across the torso at the level of the sternal angle (**Figure 1**). First, participants walked back and forth across a 9.75 m room for 4 min at whichever pace they considered to be their "normal" walking speed (NW). Participants were instructed to refrain from talking, to keep their arms swinging freely at their sides, and to keep their head up and gaze straight ahead. Each time they reached the end of the room, they completed a 180-degree turn and walked the length of the room again.

Next, participants completed two trials of walking while talking (WWT-1 and WWT-2) and one trial of talking only. The WWT and talking only trials lasted for 2 min each. During the WWT trials, participants walked at their normal speed while counting backwards by 7s (Li et al., 2014), starting at number 299, 298, or 296. The WWT instructions were identical to those provided for the 4-min walk, except that participants were additionally instructed to "try and pay equal attention to walking and talking" (Verghese et al., 2007). For the talking only trial, participants sat in a chair and counted backwards by 7s for 2 min. We counterbalanced the order of the WWT-1, WWT-2, and talking only trials and the starting number across all participants.

2.4. Spatiotemporal Variable Calculation

During the walking tasks, we recorded inertial data using MobilityLab software (v2; APDM Wearable Technologies Inc., Portland, OR, USA). After each trial, MobilityLab calculated 14 spatiotemporal gait variables based on the straight-ahead (non-turning) portions of each walking trial. The algorithm for calculating these metrics has been validated through comparison to force plate and motion capture data (see internal validation by MobilityLab: https://support.apdm.com/hc/en-us/articles/360000177066-How-are-Mobility-Lab-s-algorithms-validated- and Washabaugh et al., 2017). To condense the gait variables into

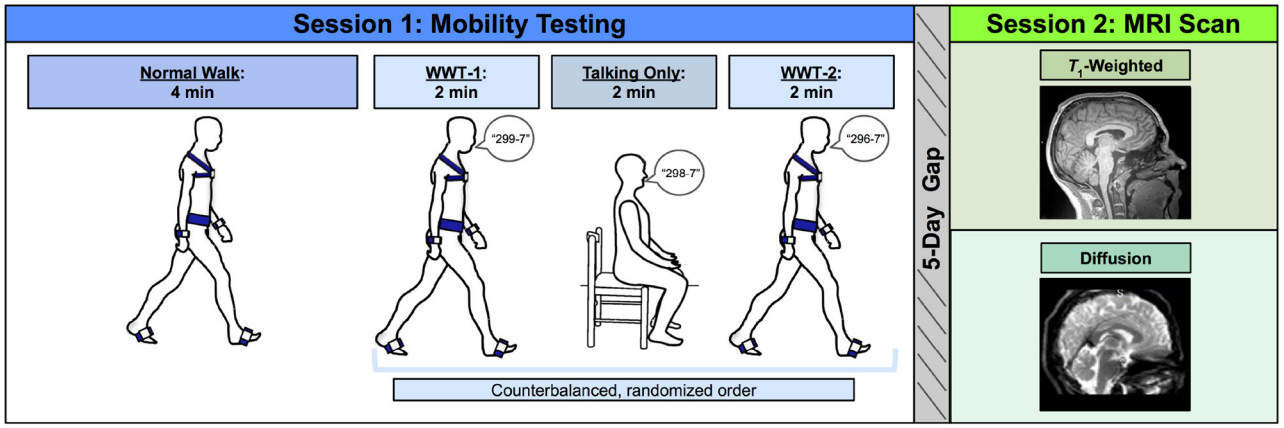

FIGURE 1 | Methods overview. Left: During Session 1, participants first completed a normal (single task) overground walk (NW) at a comfortable self-selected speed. Next, participants completed three trials in a counterbalanced order: two walking while talking trials (WWT-1 and WWT-2) in which participants counted backwards by 7s while walking, and one talking only trial in which participants stayed seated while counting backwards by 7s. Right: Approximately 5 days later, during Session 2, participants completed an MRI protocol, which included a T_1-weighted anatomical scan and a diffusion-weighted scan.

several summary metrics, for each trial, we extracted one variable from each of the four gait domains described by Hollman et al. (2011a): gait rhythm [cadence (steps/min)], gait phase [stance (% gait cycle)], gait pace [speed (m/s)], and gait variability [step time variability (standard deviation)]. Each of these variables was reported to have high validity when compared to the same metrics calculated using force plate data (Washabaugh et al., 2017). We then calculated the average of each of these four variables for the NW and WWT-1 and WWT-2 trials to produce one variable for each of the four gait domains for NW and WWT.

2.5. Cognitive Outcome Variable Calculation

We also measured cognitive performance during the seated compared to WWT conditions. We examined both speed (i.e., total number of subtraction problems attempted) and accuracy (i.e., % correct) during both the seated and WWT conditions.

2.6. DTcost Calculation

To characterize differences in these gait and cognitive performance summary metrics between single and dual task conditions, similar to a large body of previous work (e.g., Kelly et al., 2010; Van Impe et al., 2011; Patel et al., 2014), we calculated the DTcost of each variable as follows:

$$DTcost = \left(\frac{WWT\ measure - ST\ measure}{WWT\ measure}\right) * 100 \qquad (1)$$

We then calculated a correlation matrix for the four resulting DTcost of gait measures across the whole sample. This revealed that DTcost of gait speed was highly correlated with the DTcost of cadence ($r = 0.90$, $p < 0.001$) and DTcost of stance time ($r = -0.85$, $p < 0.001$). Thus, we opted to analyze only two variables as primary outcome metrics in our final statistical analyses: (1) DTcost of gait speed; and (2) DTcost of step time variability. Both slower gait speed and increased step time variability have been related to higher fall risk for older adults (Espy et al., 2010; Callisaya et al., 2011; Quach et al., 2011).

2.7. Session 2: MRI Scan

We acquired an MRI scan for each participant using a Siemens MAGNETOM Prisma 3 T scanner (Siemens Healthcare, Erlangen, Germany) with a 64-channel head coil. We collected a 3D T_1-weighted anatomical image using a magnetization-prepared rapid gradient-echo (MPRAGE) sequence. The parameters for this anatomical image were as follows: repetition time (TR) = 2,000 ms, echo time (TE) = 3.06 ms, flip angle = 8°, field of view = 256 × 256 mm^2, slice thickness = 0.8 mm, 208 slices, voxel size = 0.8 mm^3. We also collected a diffusion-weighted spin-echo prepared echo-planar imaging sequence with the following parameters: 5 b_0 scans (without diffusion weighting), 64 gradient directions with diffusion weighting 1,000 s/mm^2, TR = 6,400 ms, TE = 58 ms, isotropic resolution = 2 x 2 x 2 mm, FOV = 256 x 256 mm^2, 69 slices, phase encoding direction = Anterior to Posterior. Immediately prior to this acquisition, we collected 5 b_0 scans (without diffusion weighting) in the opposite phase encoding direction (Posterior to Anterior) for later use in distortion correction.

2.8. T_1-Weighted Image Processing for Voxelwise Analyses

For further details regarding T_1-weighted image preprocessing, see **Supplementary Section 2**.

2.8.1. Gray Matter Volume

We processed the T_1-weighted scans using the Computational Anatomy Toolbox toolbox (version r1725; Gaser and Dahnke, 2016; Gaser and Kurth, 2017) in MATLAB (R2019b). We implemented default CAT12 preprocessing steps, which ultimately produces whole-brain modulated, normalized gray matter maps for each participant. To increase signal-to-noise ratio, we smoothed these modulated, normalized gray matter segments using Statistical Parametric Mapping 12 (SPM12, v7771; Ashburner et al., 2014) with an 8 mm full width at half maximum kernel. We entered these preprocessed gray

matter volume maps into the group-level voxelwise statistical models described in Section 2.11.2. We used CAT12 to calculate total intracranial volume for each participant for later use as a covariate in these group-level statistical analyses.

2.8.2. Cortical Surface Metrics

The CAT12 pipeline also extracts surface-based morphometry metrics (Yotter et al., 2011a; Dahnke et al., 2013). We used CAT12 to extract four surface metrics: (1) cortical thickness: the thickness of the cortical gray matter between the outer surface (i.e., the gray matter-cerebrospinal fluid boundary) and the inner surface (i.e., the gray matter-white matter boundary) (Dahnke et al., 2013); (2) cortical complexity: fractal dimension, a metric of folding complexity of the cortex (Yotter et al., 2011b); (3) sulcal depth: the Euclidean distance between the central surface and its convex hull (Yun et al., 2013); and (4) gyrification index: a metric based on the absolute mean curvature, which quantifies the amount of cortex buried within the sulcal folds as opposed to the amount of cortex on the "outer" visible surface (Luders et al., 2006). We resampled and smoothed the surfaces at 15 mm for cortical thickness and 20 mm for the three other metrics (Gaser and Kurth, 2017). We entered these resampled and smoothed surface files into the group-level voxelwise statistical models described in Section 2.11.2.

2.8.3. Cerebellar Volume

To improve the normalization of the cerebellum (Diedrichsen, 2006; Diedrichsen et al., 2009), similar to our past work (Salazar et al., 2020, 2021; Hupfeld et al., 2021b), we applied specialized preprocessing steps to the cerebellum to produce cerebellar volume maps. First, we entered each participant's whole-brain T_1-weighted image into the CEREbellum Segmentation (CERES) pipeline (Romero et al., 2017). We then used the Advanced Normalization Tools package (ANTs; v1.9.17; Avants et al., 2010, 2011) to warp (in a single step) each participant's extracted subject space cerebellum to the Spatially Unbiased Infratentorial Template (SUIT) template (Diedrichsen, 2006; Diedrichsen et al., 2009). The flowfields that were applied to warp these cerebellar segments to SUIT space were additionally used to calculate the Jacobian determinant image, using ANTs' *CreateJacobianDeterminantImage.sh* function. We multiplied each normalized cerebellar segment by its corresponding Jacobian determinant to produce modulated cerebellar images in standard space for each participant. Lastly, to increase signal-to-noise ratio, we smoothed the modulated, normalized cerebellar images using a kernel of 2 mm full width at half maximum and entered the resulting cerebellar volume maps into the group-level voxelwise statistical models described in Section 2.11.2. Of note, we examined cerebellar total volumes in our statistical analyses instead of segmenting the cerebellum by tissue type, in order to avoid any inaccuracy due to low contrast differences between cerebellar gray and white matter.

2.9. Diffusion-Weighted Image Processing for Voxelwise Analyses

See **Supplementary Section 3** for further details regarding preprocessing of the diffusion-weighted data.

2.9.1. Diffusion Preprocessing

We then corrected images for signal drift (Vos et al., 2017) using the ExploreDTI graphical toolbox (v4.8.6; www.exploredti.com; Leemans et al., 2009) in MATLAB (R2019b). Next, we used the FMRIB Software Library (FSL; v6.0.1; Smith et al., 2004; Jenkinson et al., 2012) processing tool *topup* to estimate the susceptibility-induced off-resonance field (Andersson et al., 2003). This procedure yielded a single corrected field map for use in eddy current correction. We used FSL's *eddy_cuda* to simultaneously correct the data for eddy current-induced distortions and both inter- and intra-volume head movement (Andersson and Sotiropoulos, 2016).

2.9.2. FW Correction and Tensor Fitting

We implemented a custom FW imaging algorithm (Pasternak et al., 2009) in MATLAB. This algorithm estimates FW fractional volume and FW-corrected diffusivities by fitting a two-compartment model at each voxel (Pasternak et al., 2009). The two-compartment model consists of: (1) a tissue compartment modeling water molecules within or in the vicinity of white matter tissue, quantified by diffusivity (FAt, RDt, and ADt); and (2) a FW compartment, reflecting the proportion of water molecules with unrestricted diffusion, and quantified by the fractional volume of this compartment. FW ranges from 0 to 1; FW = 1 indicates that a voxel is filled with freely diffusing water molecules (e.g., as in the ventricles). These metrics (FAt, RDt, ADt, FW) are provided as maps for each voxel in the brain.

2.9.3. Tract-Based Spatial Statistics

We applied FSL's tract-based spatial statistics (TBSS) processing steps to prepare the data for voxelwise analyses across participants (Smith et al., 2006). We used the TBSS pipeline as provided in FSL, which first includes eroding the FA images slightly and zeroing the end slices. Next, each participant's FA data is brought into a common space (i.e., the FMRIB58_FA 1 mm isotropic template) using the nonlinear registration tool FNIRT (Andersson et al., 2007a,b). A mean FA image is then calculated and thinned to create a mean FA skeleton. Then, each participant's aligned FA data is projected onto the group mean skeleton. Lastly, we applied the same nonlinear registration to the FW, FAt, RDt, and ADt maps to project these data onto the original mean FA skeleton. Ultimately, these TBSS procedures resulted in skeletonized FW, FAt, ADt, and RDt maps in standard space for each participant. These were the maps that we entered in the group-level voxelwise statistical models described in Section 2.11.2.

2.10. Image Processing for Region of Interest Analyses

See **Supplementary Section 4** for further details regarding extraction of the regions of interest (ROIs).

2.10.1. Ventricle and Gray Matter Volume ROIs

CAT12 automatically calculates the inverse warp, from standard space to subject space, for several volume-based atlases. We isolated multiple ROIs from these atlases in subject space: the lateral ventricles and pre- and postcentral gyri

from the Neuromorphometrics (http://Neuromorphometrics.com) volume-based atlas, and the thalamus, striatum, and globus pallidus from the CoBra Subcortical atlas (Tullo et al., 2018; **Supplementary Figure S1**). We then calculated ROI volume in mL as: (number of voxels in the ROI mask)*(mean intensity of the tissue segment within the ROI mask)*(volume/voxel). In subsequent statistical analyses, we used the average of the left and right side structures for each ROI, and we entered these ROI volumes as a percentage of total intracranial volume (to account for differences in head size).

2.10.2. FW ROIs

We also extracted FW values from the diffusion MRI maps for the same ROIs for which we calculated gray matter volume. We rigidly registered the subject space T_1-weighted image to the subject space FW image. We then used ANTs to apply the inverse of that transformation to the subject T_1-space atlases described in Section 2.10.1. This resulted in volumetric atlases for each participant in their native diffusion space. We then isolated masks for the same ROIs described in Section 2.10.1. Finally, we used *fslstats* to extract mean image intensity in the FW map within each ROI mask. Here we used mean intensity as our outcome metric (rather than volume in mL as above) to estimate the fractional volume of FW within the ROI and obtain a metric more representative of microstructural FW, rather than the size of the ROI which represents macrostructural atrophy. We calculated the average mean intensity for the left and right side for each structure and used this average value in subsequent statistical analyses.

2.10.3. Hippocampal ROIs

We implemented the Automatic Segmentation of Hippocampal Subfields (ASHS)-T1 (Yushkevich et al., 2015) pipeline within ITK-SNAP (Yushkevich et al., 2015) to segment and extract the volume in mL of three hippocampal structures: anterior hippocampus, posterior hippocampus, and parahippocampal cortex. Though this pipeline is currently validated for use on only older adults (defined as those 55+ years old; Yushkevich et al., 2015), for completeness, here we also implemented the pipeline on my younger adult participants. For statistical analyses, we used the average of the left and right side structures, and we entered these volumes as a percentage of total intracranial volume (to account for differences in head size).

2.11. Statistical Analyses

2.11.1. Participant Characteristics and Behavioral Data

We conducted all statistical analyses on the demographic and behavioral data using using R (v4.0.0; R Core Team, 2013). For each set of analyses, we applied the Benjamini-Hochberg false discovery rate (FDR) correction to the *p*-values for the age group predictor (Benjamini and Hochberg, 1995).

First, we compared demographic, physical characteristics, and testing timeline variables between the age groups. We tested the parametric *t*-test assumptions: normality within each group (Shapiro test, $p > 0.05$) and homogeneity of variances between groups (Levene's test, $p > 0.05$). The majority of variables did not meet parametric assumptions, so we conducted nonparametric two-sided Wilcoxon rank-sum tests for age group differences. We report the group medians and interquartile ranges for each of these variables. We also report nonparametric effect sizes (Rosenthal et al., 1994; Field et al., 2012). To test for differences in the sex distribution within each age group, we conducted a Pearson chi-square test.

To examine whether gait and subtraction performance differed between the single and dual task conditions and/or between the age groups, we used a linear mixed model approach (*lme*; Pinheiro et al., 2007). We entered age group, condition (i.e., single or dual task), and the age group*condition interaction as predictors, and included a random intercept for each subject. In the case of outliers (i.e., ±3 SD from the whole-group mean), we reran the linear mixed model excluding outlier data points. In all of these instances, the statistical significance of each predictor did not change with the exclusion of outliers.

2.11.2. Voxelwise Statistical Models

We tested the same voxelwise models for each of the imaging modalities. In each case, we defined the model using SPM12 and then re-estimated each model using the Threshold-Free Cluster Enhancement toolbox (TFCE; http://dbm.neuro.uni-jena.de/tfce) with 5,000 permutations. This toolbox provides non-parametric estimation using TFCE for models previously estimated using SPM parametric designs. Non-parametric estimation avoids parametric (e.g., random field theory) distribution assumptions. TFCE produces results in which voxelwise values represent the amount of cluster-like local spatial support. TFCE is favorable as it does not require an arbitrary cluster-forming threshold, and it is more sensitive compared with other thresholding methods (Smith and Nichols, 2009). Statistical significance was determined at $p < 0.05$, family-wise error (FWE) corrected for multiple comparisons.

2.11.2.1. Age Differences in Brain Structure

First, we conducted two-sample *t*-tests to test for age differences in brain structure. In each of these models, we set the imaging modality (e.g., normalized, modulated gray matter volume segments) as the outcome variable and controlled for sex (as there are reported sex differences in brain structure across the lifespan Ruigrok et al., 2014, including greater between-subject variability in brain structure for males compared to females Wierenga et al., 2020). In the gray matter and cerebellar volume models, we also controlled for head size (i.e., total intracranial volume). Also in the gray matter volume models only, we set the absolute masking threshold to 0.1 (Gaser and Kurth, 2017) and used an explicit gray matter mask that excluded the cerebellum (because we analyzed cerebellar volume separately from "whole brain" gray matter volume; Section 2.8.3).

2.11.2.2. Age Differences in Brain Structure - DTcost of Gait Relationships

Our primary analysis of interest then tested for regions in which the relationship between brain structure and the DTcost of gait differed between young and older adults. We ran two-group

t-test models and included the DTcost of gait speed or step time variability for young and older adults as covariates of interest. We tested for regions in which the correlation between brain structure and DTcost was greater for the young compared with the older adults, and where the correlation between brain structure and DTcost was lower for the young compared with the older adults. As above, we controlled for sex in all models, and we controlled for head size in the gray matter and cerebellar volume models.

2.11.3. ROI Statistical Models

We conducted ROI analyses in R. For each set of analyses, we applied the Benjamini-Hochberg FDR correction to the *p*-values for the predictor(s) of interest (Benjamini and Hochberg, 1995).

2.11.3.1. Age Differences in Brain Structure

Similar to the above voxelwise models, we first ran linear models to test for age group differences in ROI volume or mean intensity, controlling for sex. We applied the FDR correction to the *p*-values for the age group predictor (i.e., the primary analysis of interest). *Post hoc*, we also FDR-corrected the *p*-values for the sex predictor, to better interpret several statistically significant sex difference results.

2.11.3.2. Age Differences in Brain Structure - DTcost of Gait Relationships

Also similar to above, we ran linear models testing for an interaction of age group with the DTcost of gait speed or step time variability, controlling for sex. We FDR-corrected the *p*-values for the interaction term.

2.11.4. Multiple Regression to Identify the Best Predictors of DTcost of Gait in Older Adults

We used two stepwise multivariate linear regressions to directly compare the neural correlates of the DTcost of gait identified by the voxelwise and ROI analyses described above. We ran one model for the DTcost of gait speed, and one model for the DTcost of step time variability. We included only the older adults in these models because the older adults showed stronger relationships between brain structure and the DTcost of gait (whereas the young adults tended to show either a weak relationship or no clear relationship between brain structure and the DTcost of gait).

In each of the two full models, we included sex and values from the peak result coordinate for each voxelwise model that indicated a statistically significant age difference in the relationship between brain structure and the DTcost of gait as predictors. We also included ROI values as predictors in any cases where the linear model yielded a significant age group by DTcost interaction term. We used *stepAIC* (Venables and Ripley, 1999) to produce a final model that retained only the best predictor variables; *stepAIC* selects a maximal model based on the combination of predictors that produces the smallest Akaike information criterion (AIC). Overall, this stepwise regression approach allowed us to fit the best models using brain structure to predict the DTcost of gait for the older adults.

3. RESULTS

3.1. Comparison of Participant Characteristics and Testing Timeline

There were no statistically significant differences between the age groups in sex, handedness, footedness, alcohol use, or hours of sleep prior to each testing session. Both groups reported a strong preference for using their right hand and right foot for motor tasks (Oldfield, 1971; Elias et al., 1998), and both groups reported "low-risk" consumption of alcohol (Saunders et al., 1993). In addition, there were no age group differences in the number of days elapsed between the testing sessions or in the difference in start time for the sessions. Older adults did report higher body mass indices (BMIs); the group median young adult BMI (22.71 kg/m^2) fell into the "normal" range, while the group median older adult BMI (25.86 kg/m^2) fell into the "overweight" range. Older adults also self-reported less physical activity than the young adults, though both groups reported sufficient physical activity to be classified as "active" (Godin and Shephard, 1985). Compared to the young adults, the older adults reported lower balance confidence and greater fear of falling, though the older adults did not report a clinically significant fear of falling (i.e., scores >70; Tinetti et al., 1990). See **Table 1** for complete demographic information.

3.2. Age and Condition Differences in Performance

Across both age groups, gait speed slowed and gait variability increased during WWT compared to NW (**Table 2** and **Supplementary Figure S2**). There was not a statistically significant difference in serial subtraction accuracy between the seated and WWT conditions (**Table 2**), though both young and older adults attempted fewer subtraction problems during the WWT conditions compared to the seated condition (**Table 2** and **Supplementary Figure S2**). Thus, across both age groups, subtraction speed decreased from single to dual task, but accuracy did not change.

Across both conditions, the young adults performed with higher accuracy compared with the older adults (**Table 2**). However, there were no statistically significant age group differences in the DTcost of walking or subtraction performance (i.e., there were no significant age group by condition interactions; **Figure 2** and **Supplementary Figure S2**). That is, the magnitude of single to dual task decrements in gait speed and number of subtraction problems attempted, as well as the magnitude of the increase in gait variability, was similar for young and older adults.

3.3. Comparison of Brain Structure Between Age Groups

3.3.1. T_1-Weighted MRI Metrics

Across the whole brain, older adults had significantly lower gray matter volume compared with young adults (**Figure 3**). The greatest differences between young and older adults occurred in the bilateral pre- and postcentral gyri, temporal lobe, insula, and inferior portion of the frontal cortex. Cerebellar volume was lower for older compared with younger adults across most of

TABLE 1 | Participant characteristics and testing timeline.

Variables	Young adult median (IQR)	Older adult median (IQR)	W or χ^2	FDR corr. *p*	Effect size[a]
Demographics					
Sample size	37	23			
Age (years)	21.78 (2.45)	72.82 (9.94)			
Sex	19 F; 18 M	12 F; 11 M	0.004	0.951	
Physical characteristics and fitness					
Handedness laterality score[b]	85.71 (25.00)	100.00 (22.43)	351.00	0.373	–0.15
Footedness laterality score[b]	100.00 (22.22)	100.00 (133.93)	479.00	0.522	–0.12
Body mass index (kg/m^2)	22.71 (5.57)	25.86 (3.72)	200.50	**0.009****	–0.44
Leisure-time physical activity[c]	46.00 (38.00)	26.00 (22.00)	578.50	**0.020***	–0.35
Balance and fear of falling					
Balance confidence[d]	97.81 (3.75)	94.38 (4.85)	624.50	**0.014****	–0.39
Fear of falling[d]	17.00 (3.00)	19.00 (2.00)	233.00	**0.014***	–0.38
Education and cognition					
Years of education	15.00 (3.00)	16.00 (4.00)	243.00	**0.018****	–0.36
MoCA score	28.00 (3.00)	27.00 (2.50)	563.50	0.079	–0.27
Alcohol use					
AUDIT score[e]	2.00 (3.00)	1.00 (4.00)	509.50	0.347	–0.17
Hours of sleep					
Behavioral session	7.00 (1.50)	7.50 (1.38)	365.00	0.647	–0.09
MRI session	7.00 (2.00)	7.00 (1.25)	339.00	0.347	–0.17
Testing timeline[f]					
Behav. vs. MRI (days)	4.00 (7.00)	5.00 (4.50)	392.00	0.716	–0.07
Behav. vs. MRI start (hours)	1.33 (1.45)	1.25 (1.01)	432.50	0.951	–0.01

*In the second and third columns, we report the median ± interquartile range (IQR) for each age group in all cases except for sex. For sex, we report the number of males and females in each age group. In the fourth and fifth columns, for all variables except sex, we report the result of a nonparametric two-sample, two-sided Wilcoxon rank-sum test. For sex, we report the result of a Pearson's chi-square test for differences in the sex distribution within each age group. All participants with T_1-weighted scans are included in the comparisons in this table. However, we excluded several individuals from the diffusion-weighted image analyses (see Section 2.1). P values were FDR-corrected (Benjamini and Hochberg, 1995) across all models included in this table. *$p_{FDR-corr} < 0.05$, **$p_{FDR-corr} < 0.01$. Significant p values are bolded.*

[a]In the sixth column, we report the nonparametric effect size as described by (Rosenthal et al., 1994; Field et al., 2012).

[b]We calculated handedness and footedness laterality scores using two self-report surveys: the Edinburgh Handedness Inventory (Oldfield, 1971) and the Waterloo Footedness Questionnaire (Elias et al., 1998). Higher positive scores indicate stronger preference for using the right hand and foot, respectively.

[c]We assessed self-reported physical activity using the Godin Leisure-Time Exercise Questionnaire (Godin and Shephard, 1985). Higher scores indicate more frequent self-reported physical activity.

[d]Participants self-reported Activities-Specific Balance Confidence scores (Powell and Myers, 1995) and fear of falling using the Falls Efficacy Scale (Tinetti et al., 1990). Higher scores indicate greater confidence in one's ability to maintain balance in various scenarios, and greater fear of falling, respectively.

[e]Participants self-reported alcohol use on the Alcohol Use Disorders Identification Test (AUDIT) (Piccinelli, 1998). Higher scores indicate more alcohol use.

[f]Here we report the days between the testing sessions and the hours between the start time of the testing sessions.

the cerebellum, though there were no age differences in some regions, including the vermis and bilateral crus I (**Figure 3**). Across the entire cortical surface, older adults had lower cortical thickness compared with young adults (**Figure 4**). The largest age differences in cortical thickness occurred in the bilateral pre- and postcentral gyri and portions of the superior frontal cortex. Gyrification index was lower for older adults in the bilateral insula only. Cortical complexity was lower for older adults across portions of the bilateral insula, left middle frontal cortex, and posterior cingulate gyrus. Sulcal depth was reduced for older adults across the bilateral temporal lobes and insula, within the lateral fissure of the brain. Sulcal depth was higher for older compared with young adults across the superior frontal cortex, along the midline (**Figure 4**).

3.3.2. Diffusion MRI Metrics

Compared with young adults, older adults showed lower FAt, lower ADt, higher RDt, and higher FW across almost the entire white matter skeleton (**Figure 5**). There were some exceptions to this pattern, however, in portions of the superior corona radiata, corpus callosum (e.g., splenium), internal capsule, and thalamic radiations in which older adults showed higher FAt, higher ADt, and lower RDt compared with young adults.

3.3.3. ROIs

Lateral ventricular volume was higher for older compared with younger adults (**Supplementary Figure S3** and **Supplementary Table S1**). Older adults exhibited lower gray matter volume in all ROIs except for the globus pallidus and higher FW in all ROIs except for postcentral gyrus (**Supplementary Figure S4** and **Supplementary Table S1**). Older adults had lower hippocampal volume across each of the three hippocampal ROIs (**Supplementary Figure S5** and **Supplementary Table S1**). In several regions, pooling across both age groups, females had higher gray matter volume (thalamus) and FW (pre- and postcentral gyri and thalamus) compared with males.

3.4. Age Differences in the Relationship of Brain Structure With the DTcost of Gait Speed

There were no statistically significant age group by DTcost of gait speed interactions for gray matter or cerebellar volume. However, for the older adults, shallower sulcal depth across the sensorimotor, supramarginal, and superior frontal and parietal cortices was associated with greater DTcost of gait speed (**Figure 6** and **Table 3**). That is, those older adults who showed the largest decreases in gait speed from single to dual task also had the shallowest sulcal depth across these regions. Young adults did not exhibit a clear relationship between sulcal depth in these regions and the DTcost of gait speed. There were no statistically significant age group differences in the correlation of cortical thickness, cortical complexity, or gyrification index with the DTcost of gait speed.

There were age differences in the relationship between DTcost of gait speed and both ADt and RDt in portions of the left

TABLE 2 | Age and condition differences in gait and subtraction performance.

Mean (SD)		Predictors	Estimates (SE)	CI	t	FDR corr. *p*	R^2
Gait speed (m/s)							
Young: 1.02 (0.17)	Old: 0.97 (0.20)	Fixed effects					
Single: 1.06 (0.16)	Dual: 0.95 (0.19)	*(Intercept)*	1.08 (0.03)	1.02–1.14	37.90		
		Age group *(Old)*	–0.05 (0.05)	–0.14-0.04	–1.12	0.358	
		Condition *(Dual)*	–0.12 (0.02)	–0.15–(–0.09)	-7.41	**<0.001*** **	
		Age group *(Old)** Condition *(Dual)*	0.01 (0.03)	–0.05–0.06	0.24	0.810	
		Random effects					
		σ^2	0.00				
		$\tau_{00Participant}$	0.03				
							0.12
Step time variability (SD)							
Young: 0.02 (0.01)	Old: 0.02 (0.01)	Fixed effects					
Single: 0.02 (0.01)	Dual: 0.02 (0.01)	*(Intercept)*	0.02 (0.002)	0.01–0.02	9.91		
		Age group *(Old)*	0.0004 (0.003)	0.00–0.01	0.16	0.870	
		Condition *(Dual)*	0.01 (0.002)	0.00–0.01	3.23	**0.004****	
		Age group *(Old)** Condition *(Dual)*	0.003 (0.003)	0.00–0.01	1.15	0.787	
		Random effects					
		σ^2	0.00				
		$\tau_{00Participant}$	0.03				
							0.11
Subtraction accuracy (% correct)							
Young: 93.53 (8.34)	Old: 85.87 (11.15)	Fixed effects					
Single: 89.72 (91.63)	Dual: 91.63 (9.11)	*(Intercept)*	92.93 (1.56)	89.80–96.06	59.50		
		Age group *(Old)*	–8.62 (2.56)	–13.75–(–3.50)	-3.37	**0.005****	
		Condition *(Dual)*	1.20 (1.36)	–1.53–3.93	0.88	0.381	
		Age group *(Old)** Condition *(Dual)*	1.92 (2.23)	–2.55–6.39	0.86	0.787	
		Random effects					
		σ^2	34.34				
		$\tau_{00Participant}$	55.92				
							0.30
Total # of subtractions attempted							
Young: 33.97 (16.52)	Old: 28.14 (15.08)	Fixed effects					
Single: 33.36 (17.82)	Dual: 30.24 (14.34)	*(Intercept)*	35.62 (2.64)	30.33–40.91	13.49		
		Age group *(Old)*	–6.08 (4.32)	–14.74-2.58	–1.41	0.331	
		Condition *(Dual)*	–3.30 (1.19)	–5.69–(–0.91)	-2.76	**0.010***	
		Age group *(Old)** Condition *(Dual)*	0.48 (1.95)	-3.43-4.39	0.25	0.810	
		Random effects					
		σ^2	26.33				
		$\tau_{00Participant}$	231.65				
							0.29

On the left, we report the mean (standard deviation) for each outcome variable, split by age group and by condition (i.e., single or dual). On the right, we report the results of a linear mixed effects model testing for age group, condition, and interaction effects for each variable. P values were FDR-corrected based on each predictor of interest (e.g., age group; Benjamini and Hochberg, 1995). We report marginal R^2 values, which consider only the variance of the fixed effects. SD, standard deviation; SE, standard error; CI, 95% confidence interval. $^*p_{FDR-corr} < 0.05$, $^{**}p_{FDR-corr} < 0.01$, $^{***}p_{FDR-corr} < 0.001$. Significant p values are bolded.

superior corona radiata involving the superior longitudinal fasciculus and corticospinal tract (**Figure 7** and **Table 4**). For the older adults only, higher ADt and lower RDt in these regions was associated with greater slowing of gait speed from single to dual task conditions. Young adults showed no relationship between ADt or RDt in these regions and DTcost of gait speed. There were

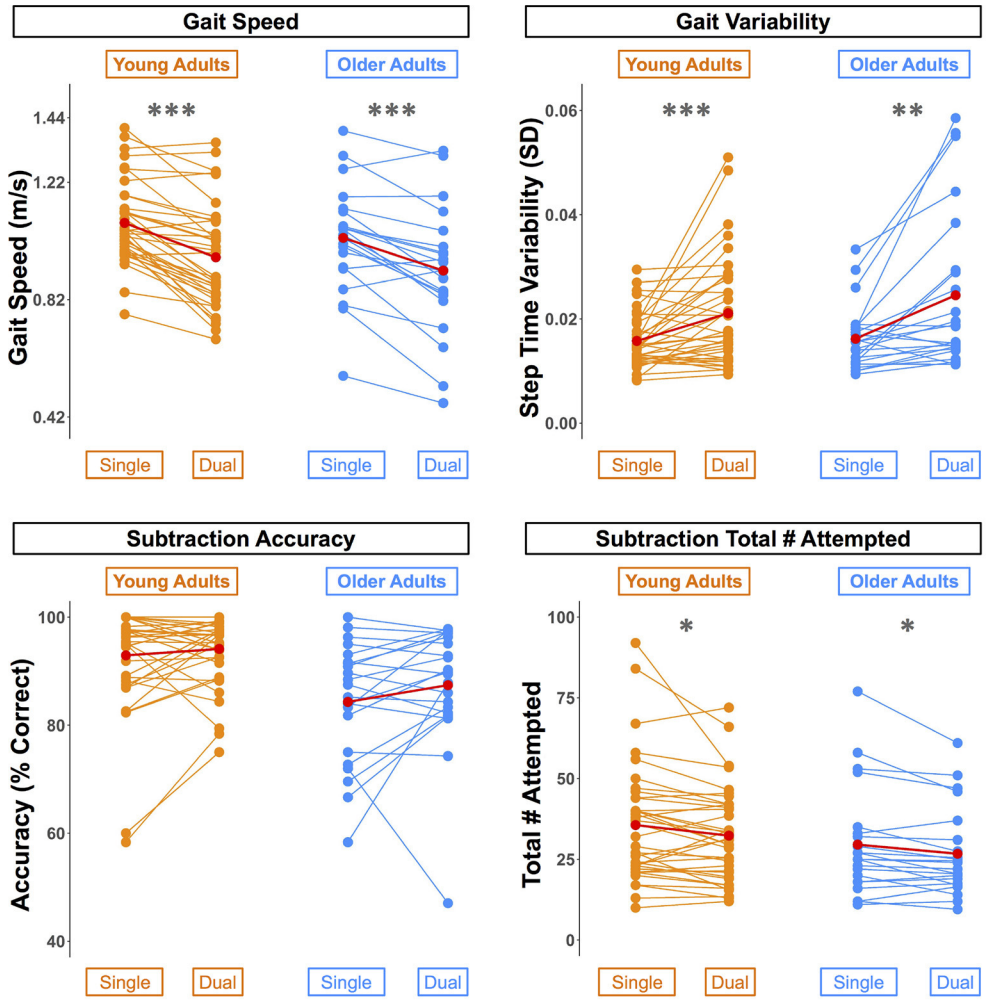

FIGURE 2 | Differences in walking and subtraction performance during single vs. dual task conditions. Gait and serial subtraction performance are depicted for each young (orange) and older (blue) adult. Each line represents one participant. Group means are shown in red. Across both age groups, gait speed slowed, gait variability increased, and number of subtraction problems attempted decreased from single to dual task conditions. $^{*}p_{FDR-corr} < 0.05$, $^{**}p_{FDR-corr} < 0.01$, $^{***}p_{FDR-corr} < 0.001$.

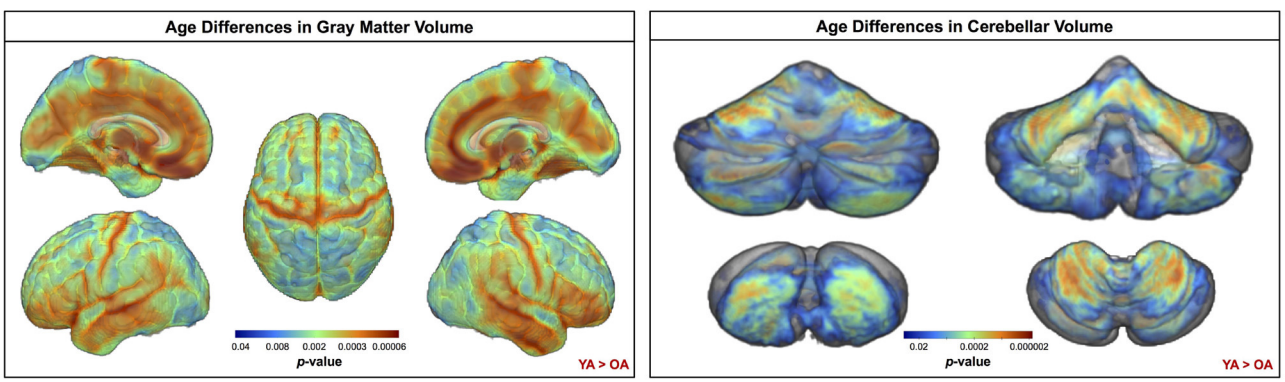

FIGURE 3 | Age differences in gray matter and cerebellar volume. Increasingly warm colors indicate regions where young adult volumes were greater than older adult volumes. Results are overlaid onto a whole brain MNI-space template (left) and onto the SUIT cerebellar template (right). $p_{FWE-corr} < 0.05$.

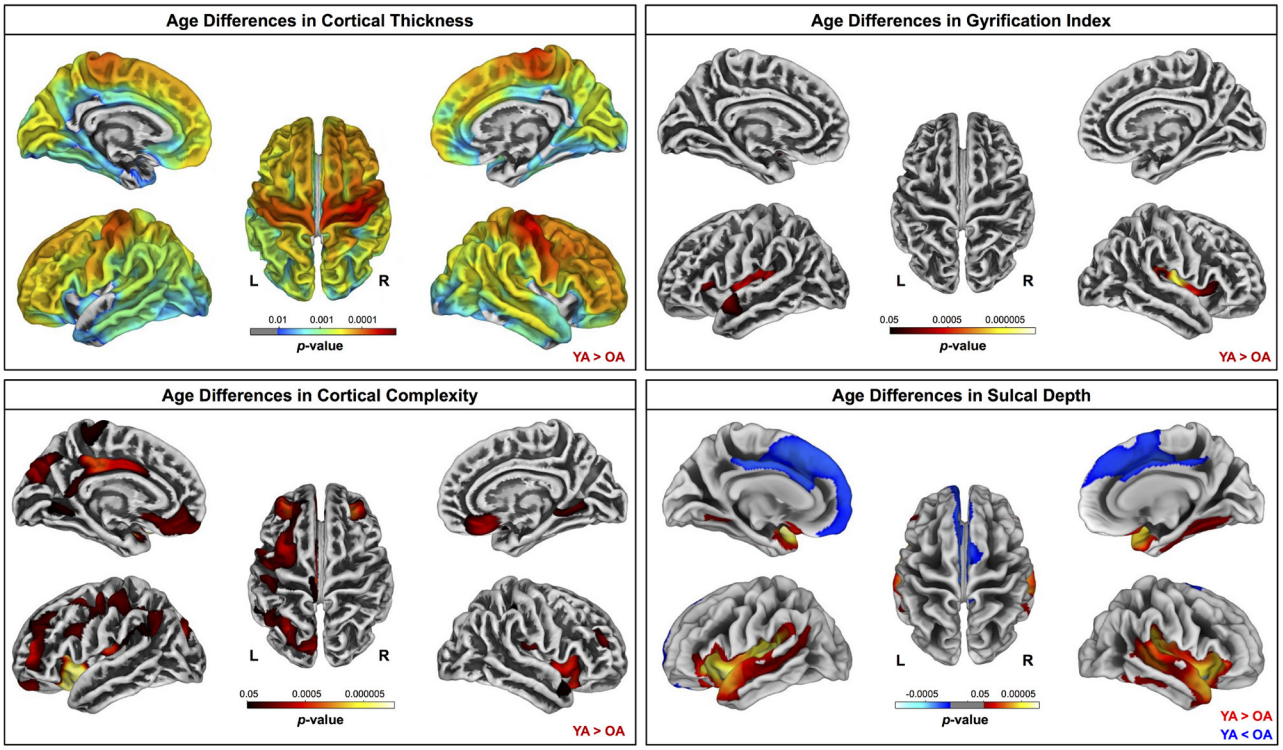

FIGURE 4 | Age differences in surface measures. Warm colors indicate regions where young adult values were greater than older adult values. Cool colors indicate regions where young adult values were lower than older adult values. Results are overlaid onto CAT12 standard space templates. L, left; R, right. $p_{FWE-corr} < 0.05$.

no statistically significant age group differences in the correlation of FAt or FW with the DTcost of gait speed.

For older adults only, larger lateral ventricular volume was associated with greater decreases in gait speed from single to dual task walking (**Figure 8** and **Table 5**). There was no relationship between lateral ventricular volume and DTcost of gait speed for young adults. Older adult relationships between DTcost of gait speed with several other ROIs [i.e., thalamus gray matter volume ($p = 0.025$; $p_{FDR-corr} = 0.172$) and parahippocampal cortex volume ($p = 0.045$; $p_{FDR-corr} = 0.208$)] did not survive FDR correction. There were no other statistically significant interactions between age group and DTcost of gait speed for the remaining ROIs.

3.5. Age Differences in the Relationship of Brain Structure With the DTcost of Step Time Variability

There were no statistically significant age group by DTcost of step time variability interactions for gray matter or cerebellar volume. For older adults, thinner temporal lobe cortex was associated with greater DTcost of step time variability (**Figure 6** and **Table 6**). That is, those older adults with the thinnest temporal cortex also showed the greatest increase in step time variability from single to dual task. Young adults showed a weak opposite relationship between temporal cortex thickness and the DTcost of step time variability. In addition, those older adults with shallower sulcal depth across the sensorimotor, supramarginal, insular, and superior frontal and parietal cortices also showed a greater DTcost of step time variability (**Figure 6** and **Table 3**). Young adults showed a weak opposite relationship between sulcal depth in these regions and the DTcost of step time variability. There were no statistically significant age differences in the relationship of cortical complexity or gyrification index with the DTcost of step time variability.

There were no statistically significant age differences in the relationship between the DTcost of step time variability and FW-corrected white matter microstructure. Greater DTcost of step time variability was associated with lower parahippocampal cortex volume for the older adults, though this relationship did not survive FDR correction ($p = 0.039$; $p_{FDR-corr} = 0.433$). There were no statistically significant interactions between age group and the DTcost of step time variability for the remaining ROIs (**Supplementary Table S2**).

3.6. Multiple Regression to Identify the Best Predictors of DTcost of Gait in Older Adults

For the DTcost of gait speed full model, we entered each participant's left precentral gyrus sulcal depth and superior longitudinal fasciculus ADt and RDt (extracted from the peak region resulting from each voxelwise model). We also entered lateral ventricular volume (expressed as a percentage of total intracranial volume) and sex. The stepwise regression returned a

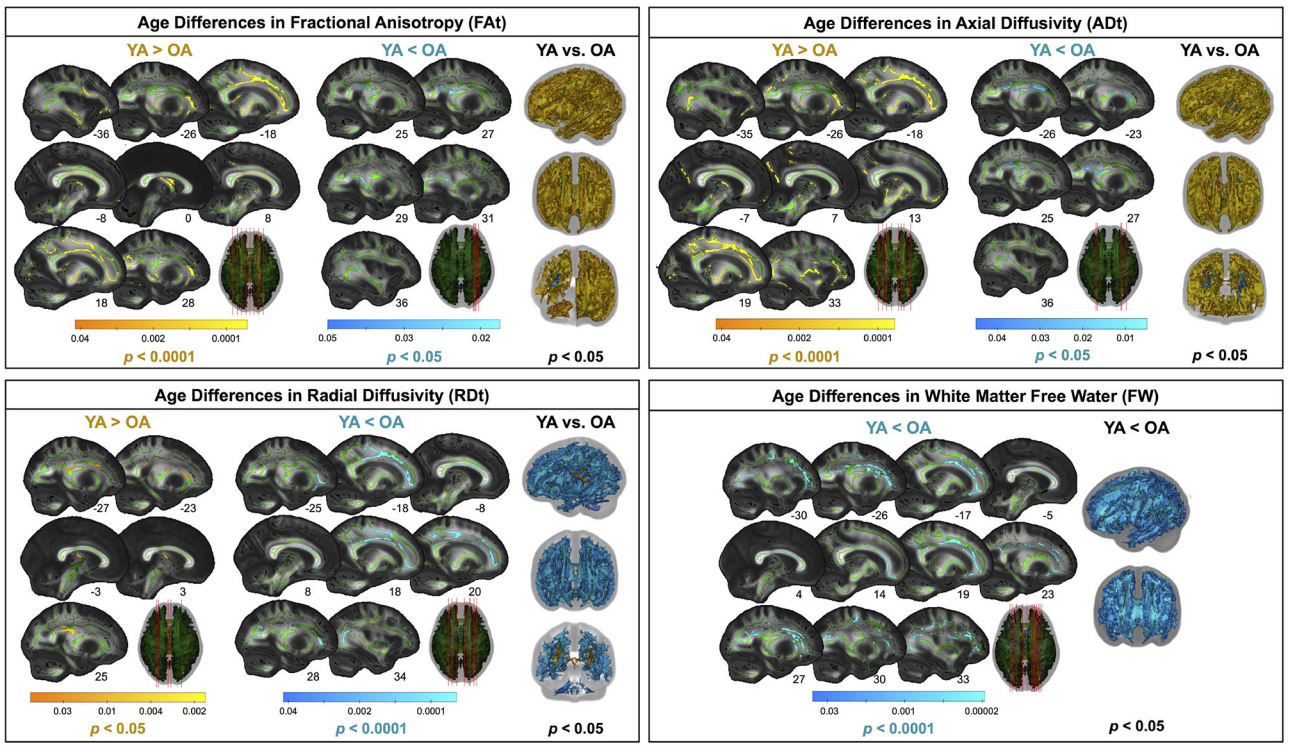

FIGURE 5 | Age differences in FW-corrected white matter microstructure. Warm colors indicate regions where young adult values were greater than older adult values. Cool colors indicate regions where young adult values were lower than older adult values. Results are shown on the FMRIB58 FA template with the group mean white matter skeleton (green) overlaid. Age differences at $p_{FWE-corr} < 0.05$ covered almost the entire white matter skeleton; these results are depicted in the rightmost column of each panel. The left portion of each panel depicts more conservative statistical thresholding (noted under each colorbar) to better illustrate which regions showed the most pronounced age differences.

model containing only sulcal depth, ADt, and sex, indicating that the combination of these three variables best predicts the DTcost of gait speed for older adults (**Table 7**).

For the DTcost of step time variability full model, we entered each participant's right superior temporal gyrus cortical thickness and left precentral gyrus sulcal depth, as well as sex. The stepwise regression returned a model containing only cortical thickness, indicating that this surface metric best predicts the DTcost of step time variability for older adults (**Table 7**).

4. DISCUSSION

We examined a comprehensive set of structural MRI metrics in relation to dual task walking in older adults. We identified widespread brain atrophy for older adults; across imaging modalities, we found the most prominent age-related atrophy in brain regions related to sensorimotor processing. Moreover, though the DTcost of gait speed and variability did not differ by age group, we identified multiple age differences in the relationship between brain structure and DTcost of gait. These age differences occurred both in regional metrics such as the temporal cortices and white matter tracts involved in motor control, and also for more general markers of brain atrophy, such as the lateral ventricles. We selected dual task walking performance as our outcome metric, as it is more predictive of falls in aging than single task walking (Ayers et al., 2014; Johansson et al., 2016; Verghese et al., 2017; Halliday et al., 2018; Gillain et al., 2019) and more related to real-world mobility (Hillel et al., 2019). Together, these results provide greater scientific understanding of the structural correlates of dual task walking in aging and highlight potential targets for future mobility interventions.

4.1. No Age Differences in the DTcost of Gait

Gait speed slowed, gait variability increased, and total number of subtraction problems attempted decreased between the single and dual task conditions. However, there were no age differences in the DTcost of gait speed, step time variability, or serial subtraction performance. That is, older adults did not exhibit a disproportionately larger decrease in gait speed or increase in gait variability between the NW and WWT conditions. Older adults also did not exhibit a disproportionately larger decrease in the total number of subtraction problems attempted between the seated and WWT conditions. While previous literature has mostly reported larger DTcosts to gait in older adults (e.g., for review see Al-Yahya et al., 2011; Beurskens and Bock, 2012), other previous work (which used a similar linear mixed model

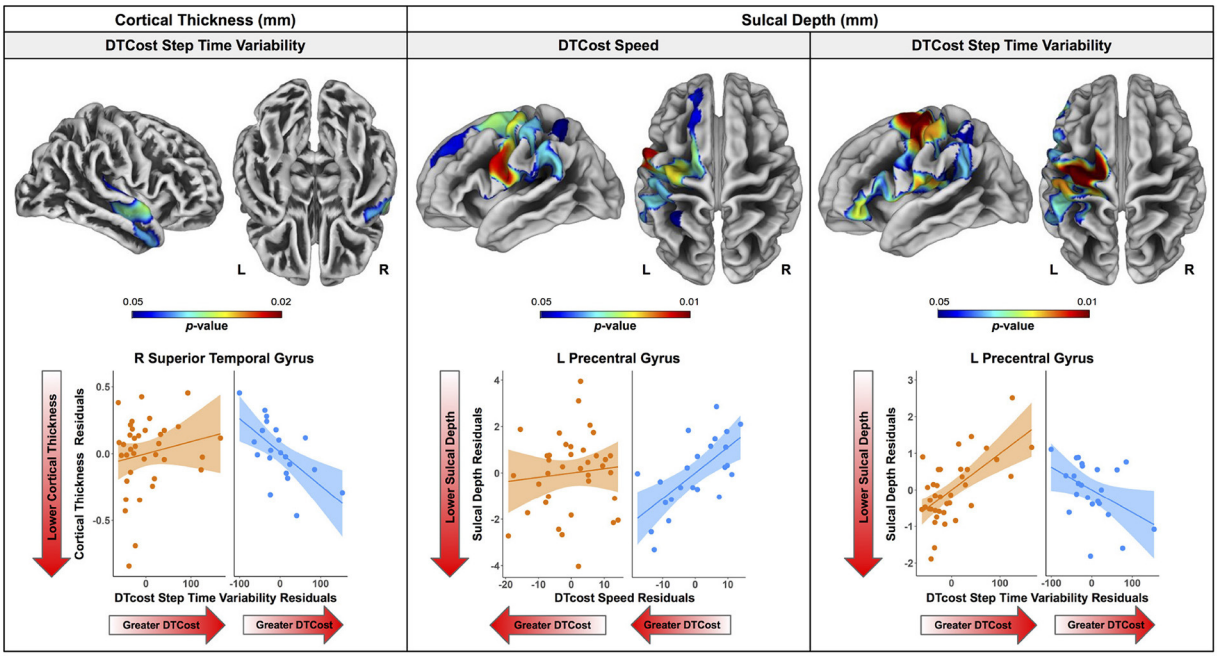

FIGURE 6 | Age differences in the relationship of surface metrics with the DTcost of gait. Top. Regions showing statistically significant ($p_{FWE-corr}$ < 0.05) age group differences in the relationship of cortical thickness (left) and sulcal depth (middle, right) with the DTcost of gait speed and step time variability. Warmer colors indicate regions of greater age differences in brain-behavior correlations. Results are overlaid onto CAT12 standard space templates. L = left; R = right. Bottom. Surface values for the peak result coordinate for each model are plotted against DTcost of gait to illustrate examples of the relationships identified by the voxelwise statistical tests. The fit line and confidence interval shading are included only to aid visualization of these relationships. We plotted the residuals instead of the raw values here to adjust for the effects of the sex covariate included in each model.

TABLE 3 | Regions of age difference in the relationship of sulcal depth with the DTcost of gait speed and step time variability.

Region	Overlap of atlas region (%)	TFCE Level	
		Extent (k_E)	$p_{FWE-corr}$
DTcost of gait speed			
L precentral gyrus	31	3,573	**0.012***
L postcentral gyrus	25	–	–
L supramarginal gyrus	19	–	–
L superior frontal gyrus	15	–	–
L superior parietal lobule	100	196	**0.048***
DTcost of step time variability			
L precentral gyrus	25	5,720	**0.008****
L postcentral gyrus	20	–	–
L supramarginal gyrus	17	–	–
L insula	8	–	–
L pars opercularis	7	–	–
L pars triangularis	6	–	–
L superior parietal lobule	5	–	–
L superior frontal gyrus	5	–	–

*Here we list all atlas regions from the Desikan-Killiany DK40 atlas (Desikan et al., 2006) that overlapped by 5% or more with each resulting cluster. The clusters were sorted by $p_{FWE-corr}$ value (from smallest to largest), then by cluster size (from largest to smallest). We do not list volumetric (e.g., MNI space) coordinates in this table because volumetric coordinates cannot be mapped directly onto cortical surfaces. L, left. *$p_{FWE-corr}$ < 0.05, **$p_{FWE-corr}$ < 0.01. Significant p values are bolded.*

approach to our study) has found no age differences in the DTcost of gait speed (Holtzer et al., 2011). Moreover, much of this prior work has focused on comparisons of aging with pathologies such as cognitive impairment (Pettersson et al., 2007; Montero-Odasso et al., 2012), rather than comparisons of young and older adults. In our sample of relatively high-functioning older adults, the lack of group differences in the DTcost of gait and subtraction performance is perhaps unsurprising. Of note, we do believe that our cognitive task (serial 7s) was sufficiently difficult to divide attention between walking and talking for both age groups, as our task was more difficult than other common paradigms, such as reciting alternate letters of the alphabet (Verghese et al., 2007; Ayers et al., 2014; Tripathi et al., 2019). This lack of group differences in behavioral performance then frames our brain structure analyses to probe the neural correlates of preservation of function in aging. Thus, we can explore the neural correlates that might underlie compensation for normal brain aging and permit successful maintenance of dual task walking abilities into older age.

4.2. Age Differences in Brain Structure

4.2.1. Gray Matter Volume, Cerebellar Volume, and Cortical Thickness

Overall, we found evidence of widespread brain atrophy for older compared with young adults. This observation is well in line with previous literature, which has similarly identified

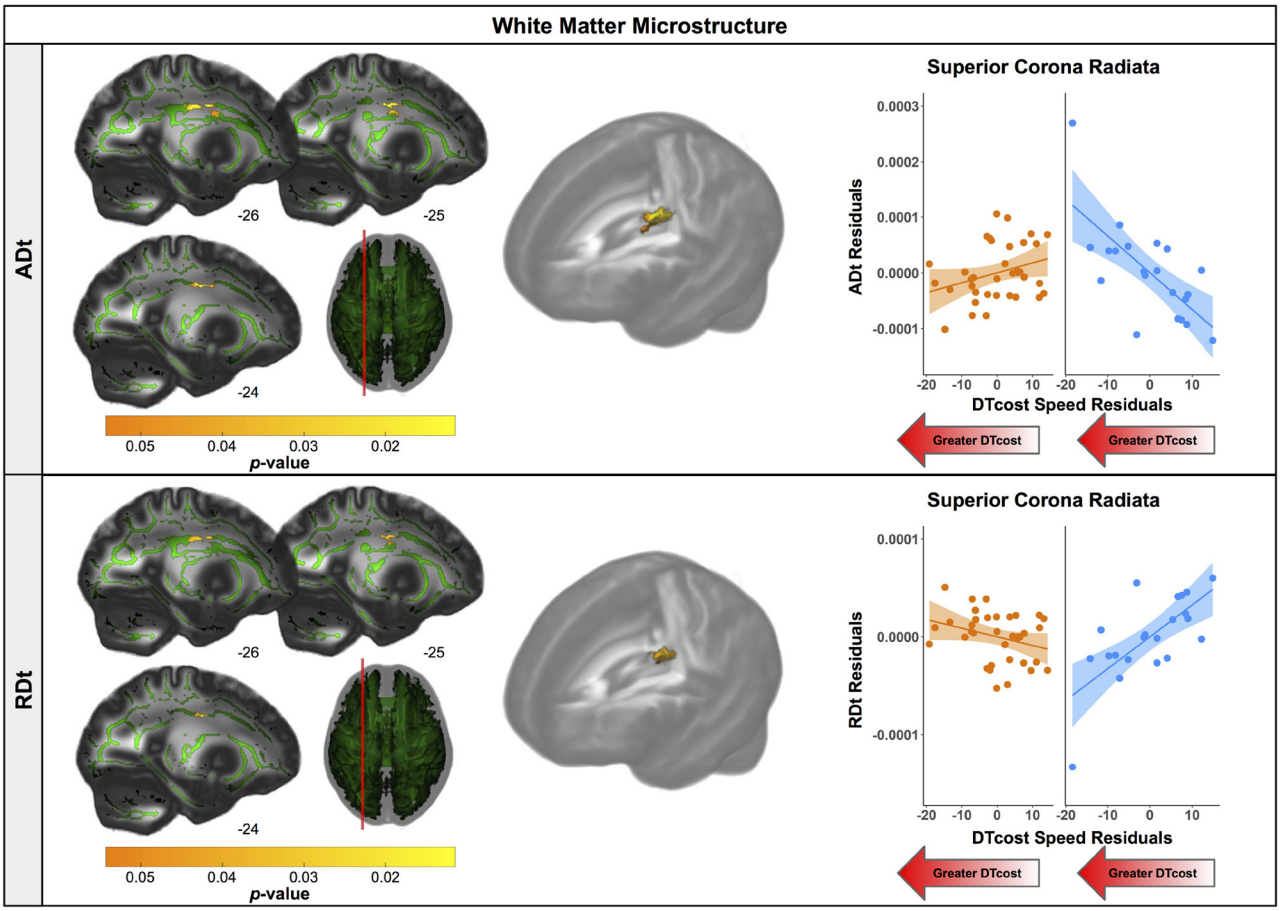

FIGURE 7 | Age differences in the relationship of FW-corrected white matter microstructure with the DTcost of gait speed. Left. Regions showing statistically significant ($p_{FWE-corr} < 0.05$) age group differences in the relationship of ADt (top) and RDt (bottom) with the DTcost of gait speed. Warmer colors indicate regions of greater age differences. Results are shown on the FMRIB58 FA template with the group mean white matter skeleton (green) overlaid. Right. ADt and RDt values for the peak result coordinate for each model are plotted against the DTcost of gait speed to illustrate examples of the relationships identified by the voxelwise statistical tests. The fit line and confidence interval shading are included only to aid visualization of these relationships. We plotted the residuals instead of the raw values here to adjust for the effects of the sex covariate included in each model.

widespread age differences in brain gray matter volume (e.g., Raz et al., 2010; Lemaitre et al., 2012; Storsve et al., 2014), cerebellar volume (e.g., Raz et al., 2010; Bernard et al., 2015; Koppelmans et al., 2017; Han et al., 2020), and cortical thickness (e.g., Salat et al., 2004; Fjell et al., 2009b; Thambisetty et al., 2010; Lemaitre et al., 2012; van Velsen et al., 2013; Storsve et al., 2014). Many reports suggest that age-related atrophy occurs disproportionately in the frontal cortices (e.g., Salat et al., 2004; Fjell et al., 2009a; Thambisetty et al., 2010; Lemaitre et al., 2012). However, our finding of the most prominent age differences in gray matter volume and thickness of the sensorimotor cortices (and comparatively less age difference in the frontal cortices) fits with recent work which identified the greatest age differences (gray and white matter atrophy, demyelination, FW, and iron reduction) within the sensorimotor cortices in a large ($n = 966$) sample of middle- to older-aged adults (Taubert et al., 2020). Taubert et al. suggested that the particular age differences in sensorimotor cortex structure could be either a cause or an effect of age-related impairments to motor control (Papegaaij et al., 2014; Taubert et al., 2020).

4.2.2. Additional Surface Metrics

While previous reports indicate that patterns of cortical thinning with aging largely mirror age-related changes in gray matter volume, the effects of aging on the other surface metrics studied here (i.e., sulcal depth, cortical complexity, and gyrification index) are not as well characterized. A couple of prior reports have indicated that, with aging, sulci become wider and shallower (Rettmann et al., 2006; Jin et al., 2018), and the cortex becomes less complex (Madan and Kensinger, 2016), with lower gyrification indices (Hogstrom et al., 2013; Cao et al., 2017; Madan and Kensinger, 2018; Lamballais et al., 2020; Madan, 2021). Our findings fit with these patterns, although across each of these metrics, we found the most prominent age differences within the lateral sulcus, whereas some previous work identified the largest age differences in other regions

TABLE 4 | Regions of age difference in the relationship of FW-corrected white matter microstructure with the DTcost of gait speed.

Region	TFCE Level		MNI Coordinates (mm)		
	Extent (k_E)	$p_{FWE-corr}$	X	Y	Z
ADt					
L corona radiata (superior)/ superior long. fasciculus	204	**0.026***	–24	–7	34
L corona radiata (superior)/ corticospinal tract	–	**0.027***	–26	–15	31
L corona radiata (superior)/ superior long. fasciculus	–	**0.045***	–26	1	27
RDt					
L corona radiata (superior)/ superior long. fasciculus	126	**0.034***	–24	–7	34
L corona radiata (superior)/ corticospinal tract	–	**0.035***	–26	–15	30

*Here we list up to three local maxima separated by more than 8 mm per cluster for all clusters with size k > 10 voxels. The clusters were labeled using two atlases: the Johns Hopkins University (JHU) ICBM-DTI-82 White Matter Labels (listed first, to the left side of the slash), and the JHU White Matter Tractography atlas within FSL (listed second, to the right side of the slash) (Wakana et al., 2007; Hua et al., 2008). The clusters were sorted by $p_{FWE-corr}$ value (from smallest to largest), then by cluster size (from largest to smallest). L, left; Long, longitudinal. *$p_{FWE-corr}$ < 0.05. Significant p values are bolded.*

such as the central sulcus (cortical thickness; Rettmann et al., 2006), parietal lobe (sulcal depth; Jin et al., 2018), and frontal lobe (cortical complexity; Madan and Kensinger, 2016; and gyrification index; Lamballais et al., 2020). Differences in subject characteristics across studies might explain these differences; for instance, Jin et al. (2018) reported sulcal depth differences in middle vs. older aged adults, rather than young compared with older adults.

4.2.3. FW-Corrected White Matter Microstructure

Only one previous study has directly compared FW-corrected white matter microstructure between healthy young and older adults (Chad et al., 2018), despite that FW-corrected diffusion metrics have significantly higher test-retest reliability than conventional diffusion-weighted metrics (Albi et al., 2017), and that FW correction allows for separation of atrophy effects (i.e., increased extracellular fluid) from changes to the structure of the remaining white matter. Our findings here of age differences in FW-corrected white matter microstructure largely mirror those of Chad et al. (2018). As anticipated, we found lower FAt and ADt, paired with higher RDt and FW across almost the entire white matter skeleton. This pattern fits with previous literature examining FW-uncorrected white matter as well: prominent declines in FA, typically interpreted as decreased white matter microstructural organization and integrity (Bennett et al., 2010; Sexton et al., 2014) although also reflective of crossing fiber integrity (Chad et al., 2018), decreases in AD, interpreted as accumulation of debris or metabolic damage with

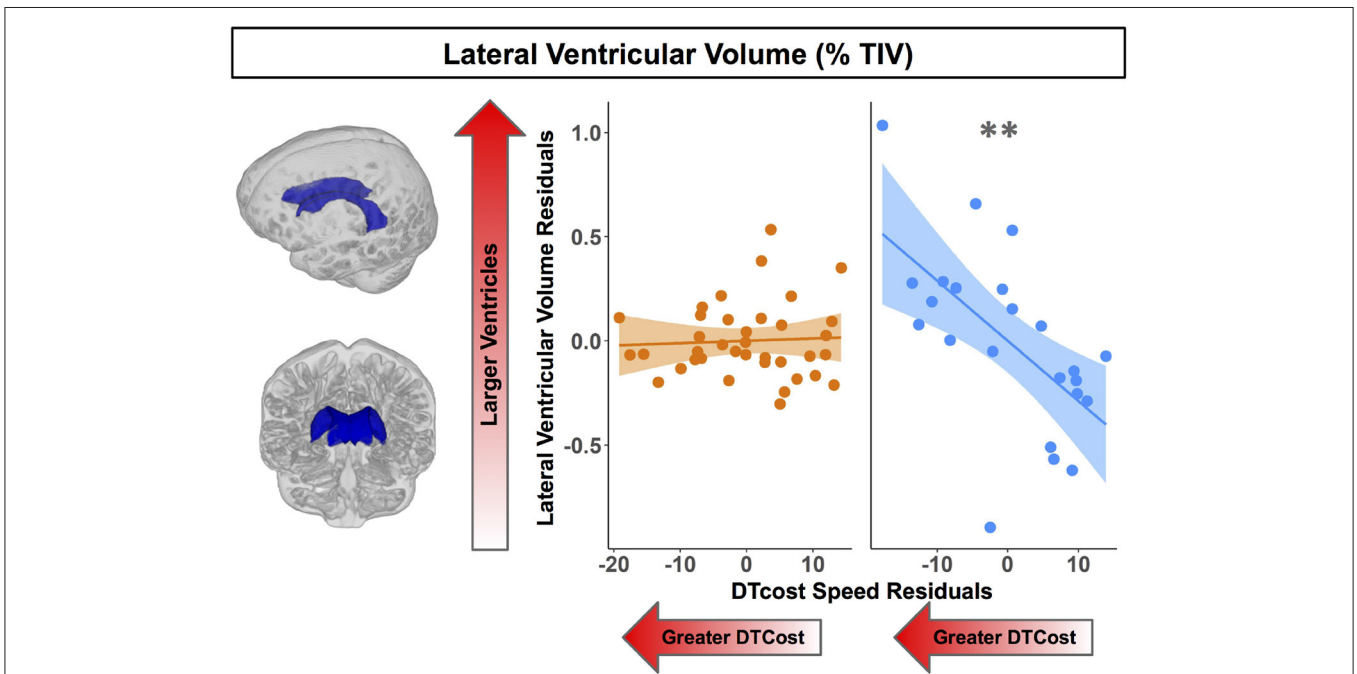

FIGURE 8 | Age differences in the relationship of lateral ventricular volume with the DTcost of gait speed. Left. Here we depict the lateral ventricular volume mask for a single exemplar participant overlaid onto that participant's native space cerebrospinal fluid segment. Right. Lateral ventricular volume residuals (expressed as a percentage of total intracranial volume) are plotted against the DTcost of gait speed. We plotted the residuals instead of the raw values here to adjust for the effects of the sex covariate included in the model. **$p_{FDR-corr}$ < 0.01.

TABLE 5 | Regions of age difference in the relationship of structural ROIs with the DTcost of gait speed.

	Predictors	Estimates (SE)	*t*	FDR corr. *p*
Ventricular volume (% TIV)				
Lateral ventricle	DTcost speed*age group	–0.03 (0.01)	–3.23	**0.030***
GM volume (% TIV)				
Precentral gyrus	DTcost speed*age group	0.001 (0.002)	0.46	0.782
Postcentral gyrus	DTcost speed*age group	0.002 (0.002)	0.96	0.782
Thalamus	DTcost speed*age group	0.002 (0.001)	2.31	0.172
Striatum	DTcost speed*age group	–0.002 (0.001)	–1.16	0.782
Globus pallidus	DTcost speed*age group	–0.0001 (0.0002)	–0.57	0.782
FW (mean intensity)				
Precentral gyrus	DTcost speed*age group	0.0003 (0.0004)	0.76	0.782
Postcentral gyrus	DTcost speed*age group	0.0002 (0.0003)	0.82	0.782
Thalamus	DTcost speed*age group	0.0001 (0.0004)	0.23	0.820
Striatum	DTcost speed*age group	–0.0002 (0.0005)	–0.43	0.782
Globus pallidus	DTcost speed*age group	0.0002 (0.001)	0.28	0.820
Hippocampal volume (% TIV)				
Ant. hippocampus	DTcost speed*age group	0.001 (0.001)	0.98	0.782
Post. hippocampus	DTcost speed*age group	0.0004 (0.001)	0.60	0.782
Parahippo. cortex	DTcost speed*age group	0.001 (0.001)	2.06	0.208

Here we report the results of linear models testing for age differences in the DTcost of gait speed, controlling for sex. For conciseness, we report only the estimates (standard error, SE), t, and p *values for the statistical test of interest: the interaction of age group with the DTcost of gait speed.* P *values for the interaction term were FDR-corrected (Benjamini and Hochberg, 1995). TIV, total intracranial volume; Ant, anterior; Post, posterior; Parahippo, parahippocampal. *$p_{FDR-corr}$ < 0.05. Significant p values are bolded.*

TABLE 6 | Regions of age difference in the correlation of cortical thickness with the DTcost of step time variability.

Region	Overlap of atlas region (%)	TFCE Level	
		Extent (k_E)	$p_{FWE-corr}$
DTcost of step time variability			
R superior temporal gyrus	68	790	**0.032***
R middle temporal gyrus	22	–	–
R transverse temporal gyrus	8	–	–

*Here we list all atlas regions from the Desikan-Killiany DK40 atlas (Desikan et al., 2006) that overlapped by 5% or more with the resulting cluster. We do not list volumetric (e.g., MNI space) coordinates in this table because volumetric coordinates cannot be mapped directly onto cortical surfaces. R, right. *$p_{FWE-corr}$ < 0.05. Significant p values are bolded.*

TABLE 7 | Stepwise multiple regression results for the best models of DTcost of gait in older adults.

Predictors	Estimates (SE)	*t*	*p*	R^2
DTcost of gait speed				
Intercept	7.47 (22.01)	0.34	0.738	
L precentral gyrus sulcal depth	2.65 (0.86)	3.09	**0.007****	
L superior longitudinal fasciculus ADt	–57084.67 (15931.84)	–3.58	**0.002****	
Sex	–4.29 (1.24)	–3.46	**0.003****	0.73
DTcost of step time variability				
Intercept	406.64 (97.23)	4.18	**0.001****	
R superior temporal gyrus cortical thickness	–134.61 (36.17)	–3.72	**0.001****	0.42

Here we report the results of the stepwise multiple linear regressions testing for the best models of the DTcost of gait speed and step time variability, for the older adults only. In each full model, we included as predictors sex, as well as the top result coordinate for any significant voxelwise analyses, and values for any ROI models which returned a significant age group by DTcost of gait interaction. As diffusion-weighted results were included in these models, n = *21 older adults, as this was the number of older adults who completed a diffusion-weighted scan. L, left; R, right. **p < 0.01. Significant p values are bolded.*

age (Pierpaoli et al., 2001; Song et al., 2003; Madden et al., 2012), and increases in RD, interpreted as decreased myelin integrity or demyelination (Song et al., 2002, 2005; Madden et al., 2012).

After applying the FW correction to our data, we found several areas of opposite age differences, quite similar to the results described by Chad et al. (2018). Specifically, we observed a seemingly paradoxical finding in portions of the superior corona radiata, corpus callosum (e.g., splenium), internal capsule, and thalamic radiations, in which FAt and ADt were higher and RDt was lower for the older compared with the young adults. In addition to the report by Chad et al. (2018), several large datasets of normal aging (examining FW-uncorrected white matter) also corroborate this finding (Sexton et al., 2014; de Groot et al., 2016; Miller et al., 2016). Previous interpretations of this increased FA include selective degeneration of non-dominant tracts paired with a relative sparing of the primary bundle at fiber crossings (Chad et al., 2018). In particular, in this region, the corona radiata, internal capsule, and corpus callosum all cross the corticospinal tract (Tuch et al., 2003). The diffusion tensors in these regions indicate that the corticospinal tract is the principal fiber (Chad et al., 2018); *bedpostx* tractography analyses by Chad et al. (2018) suggest that the superior longitudinal fasciculus crosses the corona radiata in this region, and that the thalamic radiations also cross the corticospinal tract in this region of the internal capsule. Thus, as the superior longitudinal fasciculus and thalamic radiations are thought to degenerate substantially with age (Cox et al., 2016), while the corticospinal tract is thought to be relatively spared in aging (Jang and Seo, 2015), it is likely

that the selective degeneration of non-dominant fibers in these locations is driving this seemingly paradoxical finding in the older adults.

4.2.4. Structural ROIs

We selected the ROIs used in this study because of their purported roles in mobility function (i.e., the sensorimotor cortices, basal ganglia, and hippocampus; Callisaya et al., 2013; Beauchet et al., 2015, 2019). We also examined the lateral ventricles as a more general metric of subcortical atrophy. As anticipated, almost all of these ROIs showed significant age differences (i.e., reduced gray matter volume, increased FW, and increased ventricular volume). This fits with the existing literature reporting ventricular expansion in older age (Carmichael et al., 2009; Fjell et al., 2009a). However, it is interesting to note that FW fractional volumes showed less pronounced age differences compared to gray matter volumes. This could indicate that microstructural FW does not change as markedly with normal aging, in comparison to macrostructural gray matter tissue. Comparison of FW fractional volumes to prior aging work is difficult, as most previous papers report increased subcortical (e.g., substantia nigra) FW in pathological aging (e.g., Parkinson's disease) compared with controls (Guttuso et al., 2018; Yang et al., 2019), as opposed to reporting comparisons of healthy young and older adults.

4.3. Interaction of Age Group With the DTcost of Gait

4.3.1. Gray Matter and Cerebellar Volumes

We did not identify any statistically significant age group differences in the relationship between the DTcost of gait speed or variability and regional gray matter volume. While extensive previous literature has examined relationships of single task overground walking with gray matter and cerebellar volume (e.g., Rosano et al., 2007; Dumurgier et al., 2012; Callisaya et al., 2013; Beauchet et al., 2015; Demnitz et al., 2017), comparatively less work has examined such relationships with dual task walking (Allali et al., 2019; Lucas et al., 2019; Tripathi et al., 2019; Wagshul et al., 2019; Ross et al., 2021). Further, these studies had methodological differences from our work (e.g., they used an alphabet task instead of serial 7s as the cognitive task). Moreover, it could be that we did not identify gray matter volume associations with the DTcost of gait because other measures (e.g., surface-based morphometry metrics) may provide a more sensitive correlate of behavior as compared with volume metrics. Surface-based metrics have been found to have several advantages over volume-based metrics (Hutton et al., 2009; Winkler et al., 2010; Lemaitre et al., 2012), including more accurate spatial registration (Desai et al., 2005), sensitivity to surface folding, and independence from head size (Gaser and Kurth, 2017).

4.3.2. Surface Metrics

We identified several age differences in brain-behavior relationships for two surface metrics: cortical thickness and sulcal depth. Only a few previous studies have examined relationships between cortical thickness and dual task walking in aging (Maidan et al., 2021; Ross et al., 2021), and, to our knowledge, no prior literature has examined sulcal depth in relation to dual task walking in aging. In the present work, we identified a relationship between thinner temporal cortex and greater increases in step time variability from single to dual task walking for older adults. Interestingly, the superior, middle, and transverse temporal gyri where we identified this result have functions in visual perception (Miyashita, 1993; Ishai et al., 1999), multimodal sensory integration (Mesulam, 1998; Downar et al., 2000), and spatial navigation (Howard et al., 2005). Given these functional roles, it is plausible that these regions of the temporal cortex would play a role in gait control.

Moreover, this region of temporal cortex is not one in which we found prominent age-related cortical thinning. Thus, it is possible that this temporal region plays a compensatory role in aging, to compensate for the substantial cortical thinning with aging that we identified in classical sensorimotor brain regions, such as the pre- and postcentral gyri. This notion fits with the hypothesis of neural inefficiency in aging (Zahodne and Reuter-Lorenz, 2019; Fettrow et al., 2021b), which suggests that, when neural resources become limited (as with age-related atrophy of the sensorimotor cortices), different neural resources (e.g., in this case, the temporal cortices) are used to compensate and maintain performance (e.g., as seen in the lack of age differences in the DTcost of gait). This also results in a stronger relationship between temporal lobe structure and dual task walking, which only emerges in older age when these neural resources start to become limited. This interpretation fits with a recent report of an association between lower cortical thickness and greater increases in prefrontal oxygenation from single to dual task walking, with no effect on performance (Ross et al., 2021). The study authors suggested that older adults with the poorest neural resources (i.e., the thinnest cortex) also required the most compensation from alternative brain regions (i.e., the greatest increases in prefrontal oxygenation) to maintain performance. One caveat to this interpretation, however, is that hypotheses of neural compensation with aging were largely developed in relation to functional, not structural, MRI data—though our data appear to follow a similar pattern.

We also identified two relationships between sulcal depth in aging and greater DTcost of gait speed and variability for older adults. Similar to cortical thickness, these brain-behavior relationships did not fall within the prominent regions of age difference in sulcal depth (i.e., the bilateral temporal lobes and insula), and instead spanned the sensorimotor, supramarginal, superior frontal and parietal cortices. Thus, these sulcal depth findings could similarly represent an age-related compensation. That is, in compensation for shallowing of other cortical regions in aging, those who retained deeper sulci into older age were also able to maintain the best functional walking performance.

Of note, while young adults did not show a clear relationship between cortical thickness or sulcal depth and DTcost of gait speed, young adults did exhibit a relationship between greater sulcal depth and lower DTcost of step time variability (which is in the opposite direction of what we might expect). Greater step time variability is clearly related to negative outcomes for older adults, such as higher fall risk (Callisaya et al., 2011). However,

the case is less clear for young adults (Beauchet et al., 2009; Moe-Nilssen et al., 2010). For instance, higher gait variability for younger adults can indicate more stable gait (Beauchet et al., 2009). Additionally, it could be that young adults were using a different strategy to complete the task.

4.3.3. FW-Corrected White Matter Microstructure

Several prior studies have linked lower white matter diffusivity metrics to poorer overground walking (e.g., Bruijn et al., 2014; Tian et al., 2016; Verlinden et al., 2016) and dual task walking in older adults (e.g., Ghanavati et al., 2018). However, though one prior study identified relationships between FW-corrected white matter microstructure and cognition in normal aging (Gullett et al., 2020), to our knowledge, no previous work has examined how FW-corrected white matter microstructure relates to mobility in older adults.

We identified two relationships in which higher ADt and lower RDt were associated with worse dual task performance, i.e., greater slowing of gait speed from single to dual task conditions. This is perhaps the opposite pattern from what one might expect, as lower ADt is often associated with accumulation of debris or metabolic damage (Pierpaoli et al., 2001; Song et al., 2003; Madden et al., 2012), and higher RDt is interpreted as decreased myelin integrity or demyelination (Song et al., 2002, 2005; Madden et al., 2012). However, this result occurred in the superior corona radiata, where older adults had higher ADt and lower RDt than young adults (see Section 4.2.3). It could be that, in these white matter regions, the poorest performing older adults also have the greatest degeneration of crossing fibers, such as the superior longitudinal fasciculus crossing the corticospinal tract. As the superior longitudinal fasciculus is implicated in functions such as motor control, proprioception, and visuospatial attention and awareness (Spena et al., 2006; Shinoura et al., 2009; Rodríguez-Herreros et al., 2015; Amemiya and Naito, 2016), it is logical that deterioration of this pathway could negatively impact dual task walking in aging.

4.3.4. Structural ROIs

We identified a relationship between larger lateral ventricular volume and greater DTcost of gait speed for older but not younger adults. This fits with some previous work that has linked larger ventricular volume with higher gait variability (Annweiler et al., 2014) and slower gait speed (Camicioli et al., 1999) in older adults. However, it is surprising that we did not identify relationships between DTcost of gait and the remaining structural ROIs, as previous work has linked sensorimotor (Rosano et al., 2007), basal ganglia (Dumurgier et al., 2012), and hippocampal (Beauchet et al., 2015) volumes to gait in aging. Our results thus suggest that generalized atrophy of subcortical structures, as opposed to atrophy of a single subcortical structure, is a better correlate of dual task locomotor function in aging.

4.4. Best Models of DTcost of Gait in Aging

Across the multimodal neuroimaging markers examined, left precentral gyrus sulcal depth, left superior longitudinal fasciculus ADt, and sex were the best predictors of DTcost of gait speed for older adults, and right superior temporal gyrus cortical thickness represented the best predictor of DTcost of step time variability. Given the purported benefits of surface metrics over volumetric measures (Desai et al., 2005; Hutton et al., 2009; Winkler et al., 2010; Lemaitre et al., 2012), the inclusion of sulcal depth and cortical thickness in these final models is perhaps unsurprising. Further, by minimizing partial volume effects resulting from white matter atrophy with aging, FW-corrected measures should provide greater sensitivity than traditional diffusion metrics for detecting true microstructural effects in aging cohorts. Thus, it is also perhaps unsurprising that ADt in a region (superior longitudinal fasciculus) particularly affected by aging (Cox et al., 2016) was also a good predictor of DTcost of gait in aging. Females showed larger DTcosts of gait speed; previous literature has only infrequently reported sex differences in dual task walking in older adults (e.g., Yogev-Seligmann et al., 2010; Hollman et al., 2011b; MacAulay et al., 2014), and findings have been conflicting.

We would like to note that these surface and white matter metrics are complicated measures and that, although these produced the best models of DTcost of gait, it is worth mentioning that lateral ventricular volume also represented a good predictor of DTcost of gait speed in aging. Ventricular volume can be extracted easily by applying automated algorithms to common T_1-weighted MRI sequences, and provides a useful general metric of subcortical atrophy, which our data suggest contributes functionally to gait speed slowing in aging.

4.5. Limitations

Our cross-sectional approach precluded us from tracking concurrent changes in brain structure and mobility over time. Additionally, our statistical models focused on the interaction of age group with the DTcost of gait, in order to identify regions where the relationship between brain structure and DTcost of gait differed for young vs. older adults. We did not test for regions where brain structure related to DTcost of gait in the same manner for each age group. Such models may have uncovered more brain-behavior relationships in classical motor control regions, such as pre- and postcentral gyrus and the cerebellum. However, this was not a focus of the present work. Instead, our primary goal was to understand what brain regions contributed differently to maintenance of dual task walking in older age, to probe age-related shifts in the cortical control of gait and potential compensatory processes. In addition, we did not test for relationships between brain structure and subtraction performance. Subtraction accuracy did not differ between single and dual task conditions (i.e., most DTcost scores were close to 0) and thus it would not have made sense to assess brain-behavior relationships in this case. The total number of subtraction problems attempted was lower for both age groups during single compared to dual task, though this difference was less pronounced compared to the gait metrics. Future work could test whether there are different brain structure-behavior relationships for the DTcost of serial subtraction speed compared to the DTcost of gait metrics. Finally, though instructions affect self-selected gait speed (Brinkerhoff et al., 2019) and we provided identical instructions to all participants, we cannot

be sure that participants all similarly interpreted and followed our instructions to "try and pay equal attention to walking and talking."

4.6. Conclusions

In this multimodal neuroimaging study, we found widespread age-related atrophy across cortical, subcortical, and cerebellar regions, but particularly in regions related to sensorimotor processing (e.g., the pre- and postcentral gyri). We then identified potential compensatory relationships between better maintenance of brain structure in regions not classically associated with motor control (e.g., the temporal cortices) and preserved dual task walking abilities in older adults. This suggests a role for the temporal cortices in maintaining behavioral function in aging, particularly when other brain regions responsible for locomotor control (e.g., the sensorimotor cortex, basal ganglia, and cerebellum) may be largely atrophied. Additionally, we identified one relationship between less specific subcortical atrophy (i.e., larger lateral ventricles) and greater slowing during dual task walking in aging. As the global population quickly ages, and emerging evidence continues to relate mobility problems with pathologies such as cognitive decline (Dodge et al., 2012; Knapstad et al., 2019), it is becoming increasingly critical to understand the structural neural correlates of locomotor function in aging. Identifying such brain markers could help identify those at the greatest risk of mobility declines, as well as identify targets for future interventions to preserve mobility and prevent disability among older adults.

DATA AVAILABILITY STATEMENT

The raw data supporting the conclusions of this article will be made available by the authors, without undue reservation.

ETHICS STATEMENT

The studies involving human participants were reviewed and approved by University of Florida Institutional Review Board. The patients/participants provided their written informed consent to participate in this study.

AUTHOR CONTRIBUTIONS

KH led the initial study design, collected and preprocessed all of the neuroimaging and gait data, conducted all statistical analyses, created the figures and tables, and wrote the first draft of the manuscript. JG assisted with data collection, data processing, and manuscript preparation. OP and HM consulted on DWI preprocessing and contributed to manuscript preparation. CH consulted on the design and analysis of the gait assessments. RS oversaw project design and led the interpretation and discussion of the results. All authors participated in revision of the manuscript.

FUNDING

During completion of this work, KH was supported by a National Science Foundation Graduate Research Fellowship under grant nos. DGE-1315138 and DGE-1842473, National Institute of Neurological Disorders and Stroke training grant no. T32-NS082128, and National Institute on Aging fellowship 1F99AG068440. HM was supported by a Natural Sciences and Engineering Research Council of Canada postdoctoral fellowship and a NASA Human Research Program augmentation grant. RS was supported by a grant from the National Institute on Aging U01AG061389. A portion of this work was performed in the McKnight Brain Institute at the National High Magnetic Field Laboratory's Advanced Magnetic Resonance Imaging and Spectroscopy (AMRIS) Facility, which is supported by National Science Foundation Cooperative Agreement No. DMR-1644779 and the State of Florida.

ACKNOWLEDGMENTS

The authors wish to thank Aakash Anandjiwala, Pilar Alvarez Jerez, and Alexis Jennings-Coulibaly for their assistance in subject recruitment and data collection, as well as Sutton Richmond for his help in applying the signal drift correction to the diffusion-weighted data. The authors also wish to thank all of the participants who volunteered their time, as well as the McKnight Brain Institute MRI technologists, without whom this project would not have been possible.

SUPPLEMENTARY MATERIAL

The Supplementary Material for this article can be found online at: https://www.frontiersin.org/articles/10.3389/fnagi.2022.809281/full#supplementary-material

REFERENCES

Albi, A., Pasternak, O., Minati, L., Marizzoni, M., Bartrés-Faz, D., Bargallo, N., et al. (2017). Free water elimination improves test-retest reproducibility of diffusion tensor imaging indices in the brain: a longitudinal multisite study of healthy elderly subjects. *Hum. Brain Mapp*. 38, 12–26. doi: 10.1002/hbm.23350

Allali, G., Montembeault, M., Brambati, S. M., Bherer, L., Blumen, H. M., Launay, C. P., et al. (2019). Brain structure covariance associated with gait control in aging. *J. Gerontol. A Biol. Sci. Med. Sci*. 74, 705–713. doi: 10.1093/gerona/gly123

Allali, G., Van Der Meulen, M., Beauchet, O., Rieger, S. W., Vuilleumier, P., and Assal, F. (2014). The neural basis of age-related changes in motor imagery of gait: an fMRI study. *J. Gerontol. A Biol. Sci. Med. Sci*. 69, 1389–1398. doi: 10.1093/gerona/glt207

Al-Yahya, E., Dawes, H., Smith, L., Dennis, A., Howells, K., and Cockburn, J. (2011). Cognitive motor interference while walking: a systematic review and meta-analysis. *Neurosci. Biobehav. Rev*. 35, 715–728. doi: 10.1016/j.neubiorev.2010.08.008

Amemiya, K., and Naito, E. (2016). Importance of human right inferior frontoparietal network connected by inferior branch of superior longitudinal

fasciculus tract in corporeal awareness of kinesthetic illusory movement. *Cortex* 78, 15–30. doi: 10.1016/j.cortex.2016.01.017

Andersson, J. L., Jenkinson, M., Smith, S., et al. (2007b). *Non-linear Registration, Aka Spatial Normalisation. FMRIB technical report tr07ja2*. FMRIB Analysis Group of the University of Oxford.

Andersson, J. L., Jenkinson, M., Smith, S., and Andersson, J. (2007a). *Non-linear optimisation*. FMRIB technical report tr07ja1. FMRIB Analysis Group of the University of Oxford.

Andersson, J. L., Skare, S., and Ashburner, J. (2003). How to correct susceptibility distortions in spin-echo echo-planar images: application to diffusion tensor imaging. *Neuroimage* 20, 870–888. doi: 10.1016/S1053-8119(03)00336-7

Andersson, J. L., and Sotiropoulos, S. N. (2016). An integrated approach to correction for off-resonance effects and subject movement in diffusion MR imaging. *Neuroimage* 125, 1063–1078. doi: 10.1016/j.neuroimage.2015.10.019

Annweiler, C., Montero-Odasso, M., Bartha, R., Drozd, J., Hachinski, V., and Beauchet, O. (2014). Association between gait variability and brain ventricle attributes: a brain mapping study. *Exp. Gerontol.* 57, 256–263. doi: 10.1016/j.exger.2014.06.015

Ashburner, J., Barnes, G., Chen, C.-C., Daunizeau, J., Flandin, G., Friston, K., et al. (2014). *SPM12 Manual*. London, UK: Wellcome Trust Centre for Neuroimaging.

Avants, B. B., Tustison, N. J., Song, G., Cook, P. A., Klein, A., and Gee, J. C. (2011). A reproducible evaluation of ANTs similarity metric performance in brain image registration. *Neuroimage* 54, 2033–2044. doi: 10.1016/j.neuroimage.2010.09.025

Avants, B. B., Yushkevich, P., Pluta, J., Minkoff, D., Korczykowski, M., Detre, J., et al. (2010). The optimal template effect in hippocampus studies of diseased populations. *Neuroimage* 49, 2457–2466. doi: 10.1016/j.neuroimage.2009.09.062

Ayers, E. I., Tow, A. C., Holtzer, R., and Verghese, J. (2014). Walking while talking and falls in aging. *Gerontology* 60, 108–113. doi: 10.1159/000355119

Bayot, M., Dujardin, K., Dissaux, L., Tard, C., Defebvre, L., Bonnet, C. T., et al. (2020). Can dual-task paradigms predict falls better than single task?-a systematic literature review. *Neurophysiol. Clin.* 50, 401–440. doi: 10.1016/j.neucli.2020.10.008

Beauchet, O., Allali, G., Annweiler, C., Bridenbaugh, S., Assal, F., Kressig, R. W., et al. (2009). Gait variability among healthy adults: low and high stride-to-stride variability are both a reflection of gait stability. *Gerontology* 55, 702–706. doi: 10.1159/000235905

Beauchet, O., Launay, C. P., Annweiler, C., and Allali, G. (2015). Hippocampal volume, early cognitive decline and gait variability: which association? *Exp. Gerontol.* 61, 98–104. doi: 10.1016/j.exger.2014.11.002

Beauchet, O., Launay, C. P., Sekhon, H., Montembeault, M., and Allali, G. (2019). Association of hippocampal volume with gait variability in pre-dementia and dementia stages of alzheimer disease: results from a cross-sectional study. *Exp. Gerontol.* 115, 55–61. doi: 10.1016/j.exger.2018.11.010

Benjamini, Y., and Hochberg, Y. (1995). Controlling the false discovery rate: a practical and powerful approach to multiple testing. *J. R. Stat. Soc. Series B Stat. Methodol.* 57, 289–300. doi: 10.1111/j.2517-6161.1995.tb02031.x

Bennett, I. J., Madden, D. J., Vaidya, C. J., Howard, D. V., and Howard, J. H. (2010). Age-related differences in multiple measures of white matter integrity: a diffusion tensor imaging study of healthy aging. *Hum. Brain Mapp.* 31, 378–390. doi: 10.1002/hbm.20872

Bernard, J. A., Leopold, D. R., Calhoun, V. D., and Mittal, V. A. (2015). Regional cerebellar volume and cognitive function from adolescence to late middle age. *Hum. Brain Mapp.* 36, 1102–1120. doi: 10.1002/hbm.22690

Beurskens, R., and Bock, O. (2012). Age-related deficits of dual-task walking: a review. *Neural Plast.* 2012, 131608. doi: 10.1155/2012/131608

Beurskens, R., Helmich, I., Rein, R., and Bock, O. (2014). Age-related changes in prefrontal activity during walking in dual-task situations: a fNIRS study. *Int. J. Psychophysiol.* 92, 122–128. doi: 10.1016/j.ijpsycho.2014.03.005

Bridenbaugh, S. A., and Kressig, R. W. (2015). Motor cognitive dual tasking: early detection of gait impairment, fall risk and cognitive decline. *Zeitschrift für Gerontologie und Geriatrie* 48, 15–21. doi: 10.1007/s00391-014-0845-0

Brinkerhoff, S. A., Murrah, W. M., Hutchison, Z., Miller, M., and Roper, J. A. (2019). Words matter: instructions dictate "self-selected" walking speed in young adults. *Gait Posture*. 93. doi: 10.1016/j.gaitpost.2019.07.379

Bruijn, S. M., Van Impe, A., Duysens, J., and Swinnen, S. P. (2014). White matter microstructural organization and gait stability in older adults. *Front. Aging Neurosci.* 6, 104. doi: 10.3389/fnagi.2014.00104

Cabeza, R., Anderson, N. D., Locantore, J. K., and McIntosh, A. R. (2002). Aging gracefully: compensatory brain activity in high-performing older adults. *Neuroimage* 17, 1394–1402. doi: 10.1006/nimg.2002.1280

Callisaya, M. L., Beare, R., Phan, T. G., Blizzard, L., Thrift, A. G., Chen, J., et al. (2013). Brain structural change and gait decline: a longitudinal population-based study. *J. Am. Geriatr. Soc.* 61, 1074–1079. doi: 10.1111/jgs.12331

Callisaya, M. L., Blizzard, L., Schmidt, M. D., Martin, K. L., McGinley, J. L., Sanders, L. M., et al. (2011). Gait, gait variability and the risk of multiple incident falls in older people: a population-based study. *Age Ageing* 40, 481–487. doi: 10.1093/ageing/afr055

Camicioli, R., Moore, M., Sexton, G., Howieson, D., and Kaye, J. A. (1999). Age-related brain changes associated with motor function in healthy older people. *J. Am. Geriatr. Soc.* 47, 330–334. doi: 10.1111/j.1532-5415.1999.tb02997.x

Cao, B., Mwangi, B., Passos, I. C., Wu, M.-J., Keser, Z., Zunta-Soares, G. B., et al. (2017). Lifespan gyrification trajectories of human brain in healthy individuals and patients with major psychiatric disorders. *Sci. Rep.* 7, 1–8. doi: 10.1038/s41598-017-00582-1

Carmichael, O. T., Lopez, O., Becker, J. T., and Kuller, L. (2009). Trajectories of brain loss in aging and the development of cognitive impairment. *Neurology* 72, 771–772. doi: 10.1212/01.wnl.0000339386.26096.93

Chad, J. A., Pasternak, O., Salat, D. H., and Chen, J. J. (2018). Re-examining age-related differences in white matter microstructure with free-water corrected diffusion tensor imaging. *Neurobiol. Aging* 71, 161–170. doi: 10.1016/j.neurobiolaging.2018.07.018

Cox, S. R., Ritchie, S. J., Tucker-Drob, E. M., Liewald, D. C., Hagenaars, S. P., Davies, G., et al. (2016). Ageing and brain white matter structure in 3,513 UK biobank participants. *Nat. Commun.* 7, 1–13. doi: 10.1038/ncomms13629

Dahnke, R., Yotter, R. A., and Gaser, C. (2013). Cortical thickness and central surface estimation. *Neuroimage* 65, 336–348. doi: 10.1016/j.neuroimage.2012.09.050

de Groot, M., Cremers, L. G., Ikram, M. A., Hofman, A., Krestin, G. P., van der Lugt, A., et al. (2016). White matter degeneration with aging: longitudinal diffusion MR imaging analysis. *Radiology* 279, 532–541. doi: 10.1148/radiol.2015150103

Demnitz, N., Zsoldos, E., Mahmood, A., Mackay, C. E., Kivimäki, M., Singh-Manoux, A., et al. (2017). Associations between mobility, cognition, and brain structure in healthy older adults. *Front. Aging Neurosci.* 9, 155. doi: 10.3389/fnagi.2017.00155

Desai, R., Liebenthal, E., Possing, E. T., Waldron, E., and Binder, J. R. (2005). Volumetric vs. surface-based alignment for localization of auditory cortex activation. *NeuroImage* 26, 1019–1029. doi: 10.1016/j.neuroimage.2005.03.024

Desikan, R. S., Ségonne, F., Fischl, B., Quinn, B. T., Dickerson, B. C., Blacker, D., et al. (2006). An automated labeling system for subdividing the human cerebral cortex on MRI scans into gyral based regions of interest. *Neuroimage* 31, 968–980. doi: 10.1016/j.neuroimage.2006.01.021

Diedrichsen, J. (2006). A spatially unbiased atlas template of the human cerebellum. *Neuroimage* 33, 127–138. doi: 10.1016/j.neuroimage.2006.05.056

Diedrichsen, J., Balsters, J. H., Flavell, J., Cussans, E., and Ramnani, N. (2009). A probabilistic MR atlas of the human cerebellum. *Neuroimage* 46, 39–46. doi: 10.1016/j.neuroimage.2009.01.045

Dodge, H., Mattek, N., Austin, D., Hayes, T., and Kaye, J. (2012). In-home walking speeds and variability trajectories associated with mild cognitive impairment. *Neurology* 78, 1946–1952. doi: 10.1212/WNL.0b013e318259e1de

Doi, T., Makizako, H., Shimada, H., Park, H., Tsutsumimoto, K., Uemura, K., et al. (2013). Brain activation during dual-task walking and executive function among older adults with mild cognitive impairment: a fNIRS study. *Aging Clin. Exp. Res.* 25, 539–544. doi: 10.1007/s40520-013-0119-5

Downar, J., Crawley, A. P., Mikulis, D. J., and Davis, K. D. (2000). A multimodal cortical network for the detection of changes in the sensory environment. *Nat. Neurosci.* 3, 277–283. doi: 10.1038/72991

Dumurgier, J., Crivello, F., Mazoyer, B., Ahmed, I., Tavernier, B., Grabli, D., et al. (2012). MRI atrophy of the caudate nucleus and slower walking speed in the elderly. *Neuroimage* 60, 871–878. doi: 10.1016/j.neuroimage.2012.01.102

Elias, L. J., Bryden, M. P., and Bulman-Fleming, M. B. (1998). Footedness is a better predictor than is handedness of emotional lateralization. *Neuropsychologia* 36, 37–43. doi: 10.1016/S0028-3932(97)00107-3

Espy, D. D., Yang, F., Bhatt, T., and Pai, Y.-C. (2010). Independent influence of gait speed and step length on stability and fall risk. *Gait Posture* 32, 378–382. doi: 10.1016/j.gaitpost.2010.06.013

Fettrow, T., Hupfeld, K., Reimann, H., Choi, J., Hass, C., and Seidler, R. (2021a). Age differences in adaptation of medial-lateral gait parameters during split-belt treadmill walking. *Res. Square*. 11, 1–17. doi: 10.21203/rs.3.rs-777512/v1

Fettrow, T., Hupfeld, K., Tays, G., Clark, D. J., Reuter-Lorenz, P. A., and Seidler, R. D. (2021b). Brain activity during walking in older adults: Implications for compensatory versus dysfunctional accounts. *Neurobiol. Aging* 105, 349–364. doi: 10.1016/j.neurobiolaging.2021.05.015

Field, A., Miles, J., and Field, Z. (2012). *Discovering Statistics Using R*. London: Sage Publications.

Fjell, A. M., Walhovd, K. B., Fennema-Notestine, C., McEvoy, L. K., Hagler, D. J., Holland, D., et al. (2009a). One-year brain atrophy evident in healthy aging. *J. Neurosci.* 29, 15223–15231. doi: 10.1523/JNEUROSCI.3252-09.2009

Fjell, A. M., Westlye, L. T., Amlien, I., Espeseth, T., Reinvang, I., Raz, N., et al. (2009b). High consistency of regional cortical thinning in aging across multiple samples. *Cereb. Cortex* 19, 2001–2012. doi: 10.1093/cercor/bhn232

Gaser, C., and Dahnke, R. (2016). CAT-a computational anatomy toolbox for the analysis of structural MRI data. *Hum. Brain Mapp*. 2016, 336–348. Available online at: https://www.neuro.uni-jena.de/hbm2016/GaserHBM2016.pdf

Gaser, C., and Kurth, F. (2017). *Manual Computational Anatomy Toolbox-CAT12*. Structural Brain Mapping Group at the Departments of Psychiatry and Neurology, University of Jena.

Ghanavati, T., Smitt, M. S., Lord, S. R., Sachdev, P., Wen, W., Kochan, N. A., et al. (2018). Deep white matter hyperintensities, microstructural integrity and dual task walking in older people. *Brain Imaging Behav*. 12, 1488–1496. doi: 10.1007/s11682-017-9787-7

Gillain, S., Boutaayamou, M., Schwartz, C., Brüls, O., Bruyère, O., Croisier, J.-L., et al. (2019). Using supervised learning machine algorithm to identify future fallers based on gait patterns: a two-year longitudinal study. *Exp. Gerontol*. 127, 110730. doi: 10.1016/j.exger.2019.110730

Godin, G., and Shephard, R. (1985). A simple method to assess exercise behavior in the community. *Can. J. Appl. Sport Sci*. 10, 141–146.

Gullett, J. M., O'Shea, A., Lamb, D. G., Porges, E. C., O'Shea, D. M., Pasternak, O., et al. (2020). The association of white matter free water with cognition in older adults. *Neuroimage* 219, 117040. doi: 10.1016/j.neuroimage.2020.117040

Guttuso, T., Bergsland, N., Hagemeier, J., Lichter, D. G., Pasternak, O., and Zivadinov, R. (2018). Substantia nigra free water increases longitudinally in Parkinson disease. *Am. J. Neuroradiol.* 39, 479–484. doi: 10.3174/ajnr.A5545

Halliday, D. W., Hundza, S. R., Garcia-Barrera, M. A., Klimstra, M., Commandeur, D., Lukyn, T. V., et al. (2018). Comparing executive function, evoked hemodynamic response, and gait as predictors of variations in mobility for older adults. *J. Clin. Exp. Neuropsychol.* 40, 151–160. doi: 10.1080/13803395.2017.1325453

Han, S., An, Y., Carass, A., Prince, J. L., and Resnick, S. M. (2020). Longitudinal analysis of regional cerebellum volumes during normal aging. *Neuroimage* 220, 117062. doi: 10.1016/j.neuroimage.2020.117062

Hillel, I., Gazit, E., Nieuwboer, A., Avanzino, L., Rochester, L., Cereatti, A., et al. (2019). Is every-day walking in older adults more analogous to dual-task walking or to usual walking? elucidating the gaps between gait performance in the lab and during 24/7 monitoring. *Eur. Rev. Aging Phys. Act*. 16, 1–12. doi: 10.1186/s11556-019-0214-5

Hogstrom, L. J., Westlye, L. T., Walhovd, K. B., and Fjell, A. M. (2013). The structure of the cerebral cortex across adult life: age-related patterns of surface area, thickness, and gyrification. *Cereb. Cortex* 23, 2521–2530. doi: 10.1093/cercor/bhs231

Hollman, J. H., Kovash, F. M., Kubik, J. J., and Linbo, R. A. (2007). Age-related differences in spatiotemporal markers of gait stability during dual task walking. *Gait Posture* 26, 113–119. doi: 10.1016/j.gaitpost.2006.08.005

Hollman, J. H., McDade, E. M., and Petersen, R. C. (2011a). Normative spatiotemporal gait parameters in older adults. *Gait Posture* 34, 111–118. doi: 10.1016/j.gaitpost.2011.03.024

Hollman, J. H., Youdas, J. W., and Lanzino, D. J. (2011b). Gender differences in dual task gait performance in older adults. *Am. J. Men Health* 5, 11–17. doi: 10.1177/1557988309357232

Holtzer, R., Mahoney, J. R., Izzetoglu, M., Izzetoglu, K., Onaral, B., and Verghese, J. (2011). fNIRS study of walking and walking while talking in young and old individuals. *J. Gerontol. A Biol. Sci. Med. Sci.* 66, 879–887. doi: 10.1093/gerona/glr068

Holtzer, R., Mahoney, J. R., Izzetoglu, M., Wang, C., England, S., and Verghese, J. (2015). Online fronto-cortical control of simple and attention-demanding locomotion in humans. *Neuroimage* 112, 152–159. doi: 10.1016/j.neuroimage.2015.03.002

Howard, M. W., Fotedar, M. S., Datey, A. V., and Hasselmo, M. E. (2005). The temporal context model in spatial navigation and relational learning: toward a common explanation of medial temporal lobe function across domains. *Psychol. Rev*. 112, 75. doi: 10.1037/0033-295X.112.1.75

Hua, K., Zhang, J., Wakana, S., Jiang, H., Li, X., Reich, D. S., et al. (2008). Tract probability maps in stereotaxic spaces: analyses of white matter anatomy and tract-specific quantification. *Neuroimage* 39, 336–347. doi: 10.1016/j.neuroimage.2007.07.053

Hupfeld, K. E., Hyatt, H. W., Alvarez Jerez, P., Mikkelsen, M., Hass, C. J., Edden, R. A., et al. (2021a). *In vivo* brain glutathione is higher in older age and correlates with mobility. *Cereb. Cortex* 31, 4576–4594. doi: 10.1093/cercor/bhab107

Hupfeld, K. E., McGregor, H., Koppelmans, V., Beltran, N., Kofman, I., De Dios, Y., et al. (2021b). Brain and behavioral evidence for reweighting of vestibular inputs with long-duration spaceflight. *Cereb. Cortex* 239, bhab239. doi: 10.1093/cercor/bhab239

Hutton, C., Draganski, B., Ashburner, J., and Weiskopf, N. (2009). A comparison between voxel-based cortical thickness and voxel-based morphometry in normal aging. *Neuroimage* 48, 371–380. doi: 10.1016/j.neuroimage.2009.06.043

Ishai, A., Ungerleider, L. G., Martin, A., Schouten, J. L., and Haxby, J. V. (1999). Distributed representation of objects in the human ventral visual pathway. *Proc. Natl. Acad. Sci. U.S.A.* 96, 9379–9384. doi: 10.1073/pnas.96.16.9379

Jang, S. H., and Seo, J. P. (2015). Aging of corticospinal tract fibers according to the cerebral origin in the human brain: a diffusion tensor imaging study. *Neurosci. Lett.* 585, 77–81. doi: 10.1016/j.neulet.2014.11.030

Jenkinson, M., Beckmann, C. F., Behrens, T. E., Woolrich, M. W., and Smith, S. M. (2012). FSL. *Neuroimage* 62, 782–790. doi: 10.1016/j.neuroimage.2011.09.015

Jin, K., Zhang, T., Shaw, M., Sachdev, P., and Cherbuin, N. (2018). Relationship between sulcal characteristics and brain aging. *Front. Aging Neurosci.* 10, 339. doi: 10.3389/fnagi.2018.00339

Johansson, J., Nordström, A., and Nordström, P. (2016). Greater fall risk in elderly women than in men is associated with increased gait variability during multitasking. *J. Am. Med. Dir. Assoc*. 17, 535–540. doi: 10.1016/j.jamda.2016.02.009

Kelly, V. E., Janke, A. A., and Shumway-Cook, A. (2010). Effects of instructed focus and task difficulty on concurrent walking and cognitive task performance in healthy young adults. *Exp. Brain Res*. 207, 65–73. doi: 10.1007/s00221-010-2429-6

Knapstad, M. K., Steihaug, O. M., Aaslund, M. K., Nakling, A., Naterstad, I. F., Fladby, T., et al. (2019). Reduced walking speed in subjective and mild cognitive impairment: a cross-sectional study. *J. Geriatr. Phys. Ther.* 42, E122–E128. doi: 10.1519/JPT.0000000000000157

Koenraadt, K. L., Roelofsen, E. G., Duysens, J., and Keijsers, N. L. (2014). Cortical control of normal gait and precision stepping: an fNIRS study. *Neuroimage* 85, 415–422. doi: 10.1016/j.neuroimage.2013.04.070

Koppelmans, V., Hoogendam, Y. Y., Hirsiger, S., Mérillat, S., Jäncke, L., and Seidler, R. D. (2017). Regional cerebellar volumetric correlates of manual motor and cognitive function. *Brain Struct. Funct*. 222, 1929–1944. doi: 10.1007/s00429-016-1317-7

Kraus, L. (2016). *2015 disability statistics annual report. a publication of the rehabilitation research and training center on disability statistics and demographics*. Institute on Disability, University of New Hampshire.

Lamballais, S., Vinke, E. J., Vernooij, M. W., Ikram, M. A., and Muetzel, R. L. (2020). Cortical gyrification in relation to age and cognition in older adults. *Neuroimage* 212, 116637. doi: 10.1016/j.neuroimage.2020.116637

Leemans, A., Jeurissen, B., Sijbers, J., and Jones, D. (2009). ExploreDTI: a graphical toolbox for processing, analyzing, and visualizing diffusion MR data. *Proc. Int. Soc. Magn. Reson. Med. Sci*. 17:3537.

Lemaitre, H., Goldman, A. L., Sambataro, F., Verchinski, B. A., Meyer-Lindenberg, A., Weinberger, D. R., et al. (2012). Normal age-related brain morphometric changes: nonuniformity across cortical thickness, surface area and gray matter volume? *Neurobiol. Aging* 33, 617–e1. doi: 10.1016/j.neurobiolaging.2010.07.013

Li, C., Verghese, J., and Holtzer, R. (2014). A comparison of two walking while talking paradigms in aging. *Gait Posture* 40, 415–419. doi: 10.1016/j.gaitpost.2014.05.062

Lucas, M., Wagshul, M. E., Izzetoglu, M., and Holtzer, R. (2019). Moderating effect of white matter integrity on brain activation during dual-task walking in older adults. *J. Gerontol. A Biol. Sci. Med. Sci.* 74, 435–441. doi: 10.1093/gerona/gly131

Luders, E., Thompson, P. M., Narr, K., Toga, A. W., Jancke, L., and Gaser, C. (2006). A curvature-based approach to estimate local gyrification on the cortical surface. *Neuroimage* 29, 1224–1230. doi: 10.1016/j.neuroimage.2005.08.049

Lundin-Olsson, L., Nyberg, L., and Gustafson, Y. (1997). Stops walking when talking as a predictor of falls in elderly people. *Lancet* 349, 617. doi: 10.1016/S0140-6736(97)24009-2

MacAulay, R. K., Brouillette, R. M., Foil, H. C., Bruce-Keller, A. J., and Keller, J. N. (2014). A longitudinal study on dual-tasking effects on gait: cognitive change predicts gait variance in the elderly. *PLoS ONE* 9, e99436. doi: 10.1371/journal.pone.0099436

Madan, C. R. (2021). Age-related decrements in cortical gyrification: Evidence from an accelerated longitudinal dataset. *European J. Neurosci.* 53, 1661–1671. doi: 10.1111/ejn.15039

Madan, C. R., and Kensinger, E. A. (2016). Cortical complexity as a measure of age-related brain atrophy. *Neuroimage* 134, 617–629. doi: 10.1016/j.neuroimage.2016.04.029

Madan, C. R., and Kensinger, E. A. (2018). Predicting age from cortical structure across the lifespan. *European J. Neurosci.* 47, 399–416. doi: 10.1111/ejn.13835

Madden, D. J., Bennett, I. J., Burzynska, A., Potter, G. G., Chen, N.-K., and Song, A. W. (2012). Diffusion tensor imaging of cerebral white matter integrity in cognitive aging. *Biochim. Biophys. Acta Mol. Basis Dis.* 1822, 386–400. doi: 10.1016/j.bbadis.2011.08.003

Maidan, I., Mirelman, A., Hausdorff, J. M., Stern, Y., and Habeck, C. G. (2021). Distinct cortical thickness patterns link disparate cerebral cortex regions to select mobility domains. *Sci. Rep.* 11, 1–11. doi: 10.1038/s41598-021-85058-z

Maillard, P., Fletcher, E., Singh, B., Martinez, O., Johnson, D. K., Olichney, J. M., et al. (2019). Cerebral white matter free water: a sensitive biomarker of cognition and function. *Neurology* 92, e2221–e2231. doi: 10.1212/WNL.0000000000007449

Malcolm, B. R., Foxe, J. J., Butler, J. S., and De Sanctis, P. (2015). The aging brain shows less flexible reallocation of cognitive resources during dual-task walking: a mobile brain/body imaging (MoBI) study. *Neuroimage* 117, 230–242. doi: 10.1016/j.neuroimage.2015.05.028

Meier-Ruge, W., Ulrich, J., Brühlmann, M., and Meier, E. (1992). Age-related white matter atrophy in the human brain. *Ann. N. Y. Acad Sci.* 673, 260–269. doi: 10.1111/j.1749-6632.1992.tb27462.x

Mesulam, M. (1998). From sensation to perception. *Brain* 121, 1013–1052. doi: 10.1093/brain/121.6.1013

Miller, K. L., Alfaro-Almagro, F., Bangerter, N. K., Thomas, D. L., Yacoub, E., Xu, J., et al. (2016). Multimodal population brain imaging in the UK Biobank prospective epidemiological study. *Nat. Neurosci.* 19, 1523–1536. doi: 10.1038/nn.4393

Mirelman, A., Maidan, I., Bernad-Elazari, H., Shustack, S., Giladi, N., and Hausdorff, J. M. (2017). Effects of aging on prefrontal brain activation during challenging walking conditions. *Brain Cogn.* 115, 41–46. doi: 10.1016/j.bandc.2017.04.002

Miyai, I., Tanabe, H. C., Sase, I., Eda, H., Oda, I., Konishi, I., et al. (2001). Cortical mapping of gait in humans: a near-infrared spectroscopic topography study. *Neuroimage* 14, 1186–1192. doi: 10.1006/nimg.2001.0905

Miyashita, Y. (1993). Inferior temporal cortex: where visual perception meets memory. *Annu. Rev. Neurosci.* 16, 245–263. doi: 10.1146/annurev.ne.16.030193.001333

Moe-Nilssen, R., Aaslund, M. K., Hodt-Billington, C., and Helbostad, J. L. (2010). Gait variability measures may represent different constructs. *Gait Posture* 32, 98–101. doi: 10.1016/j.gaitpost.2010.03.019

Montero-Odasso, M., Verghese, J., Beauchet, O., and Hausdorff, J. M. (2012). Gait and cognition: a complementary approach to understanding brain function and the risk of falling. *J. Am. Geriatr. Soc.* 60, 2127–2136. doi: 10.1111/j.1532-5415.2012.04209.x

Montero-Odasso, M. M., Sarquis-Adamson, Y., Speechley, M., Borrie, M. J., Hachinski, V. C., Wells, J., et al. (2017). Association of dual-task gait with incident dementia in mild cognitive impairment: results from the gait and brain study. *JAMA Neurol.* 74, 857–865. doi: 10.1001/jamaneurol.2017.0643

Ofori, E., Pasternak, O., Planetta, P. J., Li, H., Burciu, R. G., Snyder, A. F., et al. (2015). Longitudinal changes in free-water within the substantia nigra of Parkinson's disease. *Brain* 138, 2322–2331. doi: 10.1093/brain/awv136

Oldfield, R. C. (1971). The assessment and analysis of handedness: the Edinburgh inventory. *Neuropsychologia* 9, 97–113. doi: 10.1016/0028-3932(71)90067-4

Papegaaij, S., Taube, W., Baudry, S., Otten, E., and Hortobágyi, T. (2014). Aging causes a reorganization of cortical and spinal control of posture. *Front. Aging Neurosci.* 6, 28. doi: 10.3389/fnagi.2014.00028

Pasternak, O., Sochen, N., Gur, Y., Intrator, N., and Assaf, Y. (2009). Free water elimination and mapping from diffusion MRI. *Magn. Reson. Imaging* 62, 717–730. doi: 10.1002/mrm.22055

Patel, P., Lamar, M., and Bhatt, T. (2014). Effect of type of cognitive task and walking speed on cognitive-motor interference during dual-task walking. *Neuroscience* 260, 140–148. doi: 10.1016/j.neuroscience.2013.12.016

Petersen, T. H., Willerslev-Olsen, M., Conway, B. A., and Nielsen, J. B. (2012). The motor cortex drives the muscles during walking in human subjects. *J. Physiol.* 590, 2443–2452. doi: 10.1113/jphysiol.2012.227397

Pettersson, A. F., Olsson, E., and Wahlund, L.-O. (2007). Effect of divided attention on gait in subjects with and without cognitive impairment. *J. Geriatr. Psychiatry Neurol.* 20, 58–62. doi: 10.1177/0891988706293528

Piccinelli, M. (1998). Alcohol use disorders identification test (AUDIT). *Epidemiol. Psychiatr. Sci.* 7, 70–73. doi: 10.1017/S1121189X00007144

Pierpaoli, C., Barnett, A., Pajevic, S., Chen, R., Penix, L., Virta, A., et al. (2001). Water diffusion changes in wallerian degeneration and their dependence on white matter architecture. *Neuroimage* 13, 1174–1185. doi: 10.1006/nimg.2001.0765

Pinheiro, J., Bates, D., DebRoy, S., Sarkar, D., and Team, R. C. (2007). Linear and nonlinear mixed effects models. *R* 3, 1–89.

Powell, L. E., and Myers, A. M. (1995). The activities-specific balance confidence (ABC) scale. *J. Gerontol. A Biol. Sci. Med. Sci.* 50, M28–M34. doi: 10.1093/gerona/50A.1.M28

Quach, L., Galica, A. M., Jones, R. N., Procter-Gray, E., Manor, B., Hannan, M. T., et al. (2011). The nonlinear relationship between gait speed and falls: the maintenance of balance, independent living, intellect, and zest in the elderly of boston study. *J. Am. Geriatr. Soc.* 59, 1069–1073. doi: 10.1111/j.1532-5415.2011.03408.x,

R Core Team, X. (2013). *R: A Language and Environment for Statistical Computing*. Vienna: R Core Team.

Raz, N., Ghisletta, P., Rodrigue, K. M., Kennedy, K. M., and Lindenberger, U. (2010). Trajectories of brain aging in middle-aged and older adults: regional and individual differences. *Neuroimage* 51, 501–511. doi: 10.1016/j.neuroimage.2010.03.020

Rettmann, M. E., Kraut, M. A., Prince, J. L., and Resnick, S. M. (2006). Cross-sectional and longitudinal analyses of anatomical sulcal changes associated with aging. *Cereb. Cortex* 16, 1584–1594. doi: 10.1093/cercor/bhj095

Rodríguez-Herreros, B., Amengual, J. L., Gurtubay-Antolín, A., Richter, L., Jauer, P., Erdmann, C., et al. (2015). Microstructure of the superior longitudinal fasciculus predicts stimulation-induced interference with on-line motor control. *Neuroimage* 120, 254–265. doi: 10.1016/j.neuroimage.2015.06.070

Romero, J. E., Coupé, P., Giraud, R., Ta, V.-T., Fonov, V., Park, M. T. M., et al. (2017). CERES: a new cerebellum lobule segmentation method. *Neuroimage* 147, 916–924. doi: 10.1016/j.neuroimage.2016.11.003

Rosano, C., Aizenstein, H. J., Studenski, S., and Newman, A. B. (2007). A regions-of-interest volumetric analysis of mobility limitations in community-dwelling older adults. *J. Gerontol. A Biol. Sci. Med. Sci.* 62, 1048–1055. doi: 10.1093/gerona/62.9.1048

Rosenthal, R., Cooper, H., and Hedges, L. (1994). Parametric measures of effect size. *Handbook Res. Synth.* 621, 231–244.

Ross, D., Wagshul, M. E., Izzetoglu, M., and Holtzer, R. (2021). Prefrontal cortex activation during dual-task walking in older adults is moderated

by thickness of several cortical regions. *Geroscience* 43, 1959–1974. doi: 10.1007/s11357-021-00379-1

Ruigrok, A. N., Salimi-Khorshidi, G., Lai, M.-C., Baron-Cohen, S., Lombardo, M. V., Tait, R. J., et al. (2014). A meta-analysis of sex differences in human brain structure. *Neurosci. Biobehav. Rev*. 39, 34–50. doi: 10.1016/j.neubiorev.2013.12.004

Salat, D. H., Buckner, R. L., Snyder, A. Z., Greve, D. N., Desikan, R. S., Busa, E., et al. (2004). Thinning of the cerebral cortex in aging. *Cereb. Cortex* 14, 721–730. doi: 10.1093/cercor/bhh032

Salazar, A. P., Hupfeld, K. E., Lee, J. K., Banker, L. A., Tays, G. D., Beltran, N. E., et al. (2021). Visuomotor adaptation brain changes during a spaceflight analog with elevated carbon dioxide (co_2): a pilot study. *Front. Neural Circ*. 15, 51. doi: 10.3389/fncir.2021.659557

Salazar, A. P., Hupfeld, K. E., Lee, J. K., Beltran, N. E., Kofman, I. S., De Dios, Y. E., et al. (2020). Neural working memory changes during a spaceflight analog with elevated carbon dioxide: a pilot study. *Front. Syst. Neurosci*. 14, 48. doi: 10.3389/fnsys.2020.00048

Saunders, J. B., Aasland, O. G., Babor, T. F., De la Fuente, J. R., and Grant, M. (1993). Development of the alcohol use disorders identification test (audit): who collaborative project on early detection of persons with harmful alcohol consumption-ii. *Addiction* 88, 791–804. doi: 10.1111/j.1360-0443.1993.tb02093.x

Sexton, C. E., Walhovd, K. B., Storsve, A. B., Tamnes, C. K., Westlye, L. T., Johansen-Berg, H., et al. (2014). Accelerated changes in white matter microstructure during aging: a longitudinal diffusion tensor imaging study. *J. Neurosci*. 34, 15425–15436. doi: 10.1523/JNEUROSCI.0203-14.2014

Shinoura, N., Suzuki, Y., Yamada, R., Tabei, Y., Saito, K., and Yagi, K. (2009). Damage to the right superior longitudinal fasciculus in the inferior parietal lobe plays a role in spatial neglect. *Neuropsychologia* 47, 2600–2603. doi: 10.1016/j.neuropsychologia.2009.05.010

Smith, E., Cusack, T., and Blake, C. (2016). The effect of a dual task on gait speed in community dwelling older adults: a systematic review and meta-analysis. *Gait Posture* 44, 250–258. doi: 10.1016/j.gaitpost.2015.12.017

Smith, S. M., Jenkinson, M., Johansen-Berg, H., Rueckert, D., Nichols, T. E., Mackay, C. E., et al. (2006). Tract-based spatial statistics: voxelwise analysis of multi-subject diffusion data. *Neuroimage* 31, 1487–1505. doi: 10.1016/j.neuroimage.2006.02.024

Smith, S. M., Jenkinson, M., Woolrich, M. W., Beckmann, C. F., Behrens, T. E., Johansen-Berg, H., et al. (2004). Advances in functional and structural MR image analysis and implementation as FSL. *Neuroimage* 23:S208–S219. doi: 10.1016/j.neuroimage.2004.07.051

Smith, S. M., and Nichols, T. E. (2009). Threshold-free cluster enhancement: addressing problems of smoothing, threshold dependence and localisation in cluster inference. *Neuroimage* 44, 83–98. doi: 10.1016/j.neuroimage.2008.03.061

Song, S.-K., Sun, S.-W., Ju, W.-K., Lin, S.-J., Cross, A. H., and Neufeld, A. H. (2003). Diffusion tensor imaging detects and differentiates axon and myelin degeneration in mouse optic nerve after retinal ischemia. *Neuroimage* 20, 1714–1722. doi: 10.1016/j.neuroimage.2003.07.005

Song, S.-K., Sun, S.-W., Ramsbottom, M. J., Chang, C., Russell, J., and Cross, A. H. (2002). Dysmyelination revealed through MRI as increased radial (but unchanged axial) diffusion of water. *Neuroimage* 17, 1429–1436. doi: 10.1006/nimg.2002.1267

Song, S.-K., Yoshino, J., Le, T. Q., Lin, S.-J., Sun, S.-W., Cross, A. H., et al. (2005). Demyelination increases radial diffusivity in corpus callosum of mouse brain. *Neuroimage* 26, 132–140. doi: 10.1016/j.neuroimage.2005.01.028

Spena, G., Gatignol, P., Capelle, L., and Duffau, H. (2006). Superior longitudinal fasciculus subserves vestibular network in humans. *Neuroreport*. 17, 1403–1406. doi: 10.1097/01.wnr.0000223385.49919.61

Springer, S., Giladi, N., Peretz, C., Yogev, G., Simon, E. S., and Hausdorff, J. M. (2006). Dual-tasking effects on gait variability: The role of aging, falls, and executive function. *Mov. Disord*., 21, 950–957. doi: 10.1002/mds.20848

Steffener, J., and Stern, Y. (2012). Exploring the neural basis of cognitive reserve in aging. *Biochim. Biophys. Acta Mol. Basis Dis*. 1822, 467–473. doi: 10.1016/j.bbadis.2011.09.012

Storsve, A. B., Fjell, A. M., Tamnes, C. K., Westlye, L. T., Overbye, K., Aasland, H. W., et al. (2014). Differential longitudinal changes in cortical thickness, surface area and volume across the adult life span: regions of accelerating and decelerating change. *J. Neurosci*. 34, 8488–8498. doi: 10.1523/JNEUROSCI.0391-14.2014

Takakusaki, K. (2017). Functional neuroanatomy for posture and gait control. *J. Mov. Disord*. 10, 1. doi: 10.14802/jmd.16062

Taubert, M., Roggenhofer, E., Melie-Garcia, L., Muller, S., Lehmann, N., Preisig, M., et al. (2020). Converging patterns of aging-associated brain volume loss and tissue microstructure differences. *Neurobiol. Aging* 88, 108–118. doi: 10.1016/j.neurobiolaging.2020.01.006

Thambisetty, M., Wan, J., Carass, A., An, Y., Prince, J. L., and Resnick, S. M. (2010). Longitudinal changes in cortical thickness associated with normal aging. *Neuroimage* 52, 1215–1223. doi: 10.1016/j.neuroimage.2010.04.258

Tian, Q., Chastan, N., Bair, W.-N., Resnick, S. M., Ferrucci, L., and Studenski, S. A. (2017). The brain map of gait variability in aging, cognitive impairment and dementia–a systematic review. *Neurosci. Biobehav. Rev*. 74, 149–162. doi: 10.1016/j.neubiorev.2017.01.020

Tian, Q., Ferrucci, L., Resnick, S. M., Simonsick, E. M., Shardell, M. D., Landman, B. A., et al. (2016). The effect of age and microstructural white matter integrity on lap time variation and fast-paced walking speed. *Brain Imaging Behav*. 10, 697–706. doi: 10.1007/s11682-015-9449-6

Tinetti, M. E., Richman, D., and Powell, L. (1990). Falls efficacy as a measure of fear of falling. *J. Gerontol*. 45, P239–P243. doi: 10.1093/geronj/45.6.P239

Tripathi, S., Verghese, J., and Blumen, H. M. (2019). Gray matter volume covariance networks associated with dual-task cost during walking-while-talking. *Hum. Brain Mapp*. 40, 2229–2240. doi: 10.1002/hbm.24520

Tuch, D. S., Reese, T. G., Wiegell, M. R., and Wedeen, V. J. (2003). Diffusion MRI of complex neural architecture. *Neuron* 40, 885–895. doi: 10.1016/S0896-6273(03)00758-X

Tullo, S., Devenyi, G. A., Patel, R., Park, M. T. M., Collins, D. L., and Chakravarty, M. M. (2018). Warping an atlas derived from serial histology to 5 high-resolution MRIs. *Sci. Data* 5, 1–10. doi: 10.1038/sdata.2018.107

Van Impe, A., Coxon, J. P., Goble, D. J., Wenderoth, N., and Swinnen, S. P. (2011). Age-related changes in brain activation underlying single-and dual-task performance: visuomanual drawing and mental arithmetic. *Neuropsychologia* 49, 2400–2409. doi: 10.1016/j.neuropsychologia.2011.04.016

van Velsen, E. F., Vernooij, M. W., Vrooman, H. A., van der Lugt, A., Breteler, M. M., Hofman, A., et al. (2013). Brain cortical thickness in the general elderly population: the Rotterdam Scan Study. *Neurosci. Lett*. 550, 189–194. doi: 10.1016/j.neulet.2013.06.063

Venables, W. N., and Ripley, B. D. (1999). *Modern Applied Statistics With s-Plus*. New York, NY: Springer-Verlag.

Verghese, J., Holtzer, R., Lipton, R. B., and Wang, C. (2012). Mobility stress test approach to predicting frailty, disability, and mortality in high-functioning older adults. *J. Am. Geriatr. Soc*. 60, 1901–1905. doi: 10.1111/j.1532-5415.2012.04145.x

Verghese, J., Kuslansky, G., Holtzer, R., Katz, M., Xue, X., Buschke, H., et al. (2007). Walking while talking: effect of task prioritization in the elderly. *Arch. Phys. Med. Rehabil*. 88, 50–53. doi: 10.1016/j.apmr.2006.10.007

Verghese, J., Wang, C., Ayers, E., Izzetoglu, M., and Holtzer, R. (2017). Brain activation in high-functioning older adults and falls: prospective cohort study. *Neurology* 88, 191–197. doi: 10.1212/WNL.0000000000003421

Verhaeghen, P., Steitz, D. W., Sliwinski, M. J., and Cerella, J. (2003). Aging and dual-task performance: a meta-analysis. *Psychol. Aging* 18, 443. doi: 10.1037/0882-7974.18.3.443

Verlinden, V. J., De Groot, M., Cremers, L. G., van der Geest, J. N., Hofman, A., Niessen, W. J., et al. (2016). Tract-specific white matter microstructure and gait in humans. *Neurobiol. Aging* 43, 164–173. doi: 10.1016/j.neurobiolaging.2016.04.005

Vos, S. B., Tax, C. M., Luijten, P. R., Ourselin, S., Leemans, A., and Froeling, M. (2017). The importance of correcting for signal drift in diffusion MRI. *Magn. Reson. Imaging* 77, 285–299. doi: 10.1002/mrm.26124

Wagshul, M. E., Lucas, M., Ye, K., Izzetoglu, M., and Holtzer, R. (2019). Multi-modal neuroimaging of dual-task walking: Structural MRI and fNIRS analysis reveals prefrontal grey matter volume moderation of brain activation in older adults. *Neuroimage* 189, 745–754. doi: 10.1016/j.neuroimage.2019.01.045

Wakana, S., Caprihan, A., Panzenboeck, M. M., Fallon, J. H., Perry, M., Gollub, R. L., et al. (2007). Reproducibility of quantitative tractography methods applied to cerebral white matter. *Neuroimage* 36, 630–644. doi: 10.1016/j.neuroimage.2007.02.049

Washabaugh, E. P., Kalyanaraman, T., Adamczyk, P. G., Claflin, E. S., and Krishnan, C. (2017). Validity and repeatability of inertial measurement units for measuring gait parameters. *Gait Posture* 55, 87–93. doi: 10.1016/j.gaitpost.2017.04.013

Wierenga, L. M., Doucet, G. E., Dima, D., Agartz, I., Aghajani, M., Akudjedu, T. N., et al. (2020). Greater male than female variability in regional brain structure across the lifespan. *Hum Brain Mapp*. 43, 470–499. doi: 10.1101/2020.02.17.952010

Wilson, J., Allcock, L., Mc Ardle, R., Taylor, J.-P., and Rochester, L. (2019). The neural correlates of discrete gait characteristics in ageing: a structured review. *Neurosci. Biobehav. Rev*. 100, 344–369. doi: 10.1016/j.neubiorev.2018.12.017

Winkler, A. M., Kochunov, P., Blangero, J., Almasy, L., Zilles, K., Fox, P. T., et al. (2010). Cortical thickness or grey matter volume? the importance of selecting the phenotype for imaging genetics studies. *Neuroimage* 53, 1135–1146. doi: 10.1016/j.neuroimage.2009.12.028

Yang, J., Archer, D. B., Burciu, R. G., Müller, M. L., Roy, A., Ofori, E., et al. (2019). Multimodal dopaminergic and free-water imaging in Parkinson's disease. *Parkinsonism Related Dis*. 62, 10–15. doi: 10.1016/j.parkreldis.2019.01.007

Yogev-Seligmann, G., Hausdorff, J. M., and Giladi, N. (2008). The role of executive function and attention in gait. *Mov. Disord*. 23, 329–342. doi: 10.1002/mds.21720

Yogev-Seligmann, G., Rotem-Galili, Y., Mirelman, A., Dickstein, R., Giladi, N., and Hausdorff, J. M. (2010). How does explicit prioritization alter walking during dual-task performance? effects of age and sex on gait speed and variability. *Phys. Ther*. 90, 177–186. doi: 10.2522/ptj.20090043

Yotter, R. A., Dahnke, R., Thompson, P. M., and Gaser, C. (2011a). Topological correction of brain surface meshes using spherical harmonics. *Hum. Brain Mapp*. 32, 1109–1124. doi: 10.1002/hbm.21095

Yotter, R. A., Nenadic, I., Ziegler, G., Thompson, P. M., and Gaser, C. (2011b). Local cortical surface complexity maps from spherical harmonic reconstructions. *Neuroimage* 56, 961–973. doi: 10.1016/j.neuroimage.2011.02.007

Yun, H. J., Im, K., Yang, J.-J., Yoon, U., and Lee, J.-M. (2013). Automated sulcal depth measurement on cortical surface reflecting geometrical properties of sulci. *PLoS ONE* 8, e55977. doi: 10.1371/journal.pone.0055977

Yushkevich, P. A., Pluta, J. B., Wang, H., Xie, L., Ding, S.-L., Gertje, E. C., et al. (2015). Automated volumetry and regional thickness analysis of hippocampal subfields and medial temporal cortical structures in mild cognitive impairment. *Hum. Brain Mapp*. 36, 258–287. doi: 10.1002/hbm.22627

Zahodne, L. B., and Reuter-Lorenz, P. A. (2019). "Compensation and brain aging: a review and analysis of evidence," in *The Aging Brain: Functional Adaptation Across Adulthood*, ed G. R. Samanez-Larkin (Washington, DC: American Psychological Association), 185–216.

Conflict of Interest: The authors declare that the research was conducted in the absence of any commercial or financial relationships that could be construed as a potential conflict of interest.

Publisher's Note: All claims expressed in this article are solely those of the authors and do not necessarily represent those of their affiliated organizations, or those of the publisher, the editors and the reviewers. Any product that may be evaluated in this article, or claim that may be made by its manufacturer, is not guaranteed or endorsed by the publisher.

frontiers | Frontiers in Aging Neuroscience

TYPE Systematic Review
PUBLISHED 23 September 2022
DOI 10.3389/fnagi.2022.914049

OPEN ACCESS

EDITED BY
George M. Opie,
University of Adelaide, Australia

REVIEWED BY
Haiqing Song,
Xuanwu Hospital, Capital Medical University, China
Carolyn Berryman,
University of South Australia, Australia

*CORRESPONDENCE
Hongfeng Wang
ccwhf@126.com

†These authors have contributed equally to this work

SPECIALTY SECTION
This article was submitted to Alzheimer's Disease and Related Dementias,
a section of the journal
Frontiers in Aging Neuroscience

RECEIVED 20 April 2022
ACCEPTED 31 August 2022
PUBLISHED 23 September 2022

CITATION
Ma S, Huang H, Zhong Z, Zheng H, Li M, Yao L, Yu B and Wang H (2022) Effect of acupuncture on brain regions modulation of mild cognitive impairment: A meta-analysis of functional magnetic resonance imaging studies.
Front. Aging Neurosci. 14:914049.
doi: 10.3389/fnagi.2022.914049

Effect of acupuncture on brain regions modulation of mild cognitive impairment: A meta-analysis of functional magnetic resonance imaging studies

Shiqi Ma[1†], Haipeng Huang[2†], Zhen Zhong[1], Haizhu Zheng[1], Mengyuan Li[1], Lin Yao[1], Bin Yu[3] and Hongfeng Wang[2*]

[1]College of Acupuncture and Massage, Changchun University of Chinese Medicine, Changchun, China, [2]Northeast Asian Institute of Traditional Chinese Medicine, Changchun University of Chinese Medicine, Changchun, China, [3]College of Traditional Chinese Medicine, Changchun University of Chinese Medicine, Changchun, China

Background: As a non-pharmacological therapy, acupuncture has significant efficacy in treating Mild Cognitive Impairment (MCI) compared to pharmacological therapies. In recent years, advances in neuroimaging techniques have provided new perspectives to elucidate the central mechanisms of acupuncture for MCI. Many acupuncture brain imaging studies have found significant improvements in brain function after acupuncture treatment of MCI, but the underlying mechanisms of brain regions modulation are unclear.

Objective: A meta-analysis of functional magnetic resonance imaging studies of MCI patients treated with acupuncture was conducted to summarize the effects of acupuncture on the modulation of MCI brain regions from a neuroimaging perspective.

Methods: Using acupuncture, neuroimaging, magnetic resonance, and Mild Cognitive Impairment as search terms, PubMed, EMBASE, Web of Science, Cochrane Library, Cochrane Database of Systematic Reviews, Cochrane Database of Abstracts of Reviews of Effects (DARE), Google Scholar, China National Knowledge Infrastructure (CNKI), China Biology Medicine disk (CBM disk), Wanfang and Chinese Scientific Journal Database (VIP) for brain imaging studies on acupuncture on MCI published up to April 2022. Voxel-based neuroimaging meta-analysis of fMRI data was performed using voxel-based d Mapping with Permutation of Subject Images (SDM-PSI), allowing for Family-Wise Error Rate (FWER) correction correction for correction multiple comparisons of results. Subgroup analysis was used to compare the differences in brain regions between the acupuncture treatment group and other control groups. Meta-regression was used to explore demographic information and altered cognitive function effects on brain imaging outcomes. Linear models were drawn using MATLAB 2017a, and visual graphs for quality evaluation were produced using R software and RStudio software.

Results: A total of seven studies met the inclusion criteria, with 94 patients in the treatment group and 112 patients in the control group. All studies were analyzed using the regional homogeneity (ReHo) method. The experimental design of fMRI included six task state studies and one resting-state study. The meta-analysis showed that MCI patients had enhanced activity in the right insula, left anterior cingulate/paracingulate gyri, right thalamus, right middle frontal gyrus, right median cingulate/paracingulate gyri, and right middle temporal gyrus brain regions after acupuncture treatment. Further analysis of RCT and longitudinal studies showed that Reho values were significantly elevated in two brain regions, the left anterior cingulate/paracingulate gyrus and the right insula, after acupuncture. The MCI group showed stronger activity in the right supramarginal gyrus after acupuncture treatment compared to healthy controls. Meta-regression analysis showed that the right anterior thalamic projection ReHo index was significantly correlated with the MMSE score after acupuncture treatment in all MCI patients.

Conclusions: Acupuncture therapy has a modulating effect on the brain regions of MCI patients. However, due to the inadequate experimental design of neuroimaging studies, multi-center neuroimaging studies with large samples are needed better to understand the potential neuroimaging mechanisms of acupuncture for MCI. In addition, machine learning algorithm-based predictive models for evaluating the efficacy of acupuncture for MCI may become a focus of future research.

Systematic review registration: https://www.crd.york.ac.uk/prospero/display_record.php?ID=CRD42022287826, identifier: CRD 42022287826.

KEYWORDS

mild cognitive impairment, acupuncture, meta-analysis, brain regions modulation, functional magnetic resonance imaging

Introduction

Mild cognitive impairment (MCI) is a neurodegenerative disorder between normal aging and dementia that is most prominently characterized by the presence of mild isolated cognitive decline without significant impairment in activities of daily living. MCI is considered a pre-dementia state associated with a 10-fold increased risk of progression to dementia, severely affecting the patient's quality of life (Petersen, 2011). The first clinical feature of mild cognitive impairment is memory impairment, which can involve other specific changes in motor function, executive function, language, and visuospatial structural skills, depending on the cause or the site of brain damage (Marshall et al., 2011; Montero-Odasso et al., 2017). The current global prevalence of MCI is 6.7%, with an estimated overall prevalence of 15.5% among adults aged 60 years and older in China (Petersen et al., 2018; Jia et al., 2020). MCI has become an important issue in public health and has attracted the attention of a growing number of researchers, policy makers and healthcare providers.

The main pathological mechanisms of MCI are related to amyloid pathology, neurofibrillary tangle pathology, neuronal deficits, and damage to synaptic plasticity in the hippocampal region (Kordower et al., 2001). Among these, brain amyloid-beta (Aβ) plaques are a hallmark lesion of people with a clinical diagnosis of MCI (Mufson et al., 2012). As neuroimaging methods have proliferated in recent years, more researchers have focused on alterations in brain structure and function in amnestic mild cognitive impairment (aMCI), particularly in identifying relevant neural markers. A meta-analysis reported resting-state abnormalities in the posterior cingulate, angular gyrus, parahippocampal gyrus, fusiform gyrus, superior limbic gyrus, and middle temporal gyrus in participants with MCI (Lau et al., 2016). There are no FDA-approved drugs for the treatment of MCI, and neither cholinesterase inhibitors nor memantine is recommended for the treatment of MCI (Langa and Levine, 2014). Therefore, exploring the potential of non-pharmacological interventions to prevent MCI has received increasing attention.

As a suitable alternative medical treatment, acupuncture has been used empirically for thousands of years while gaining worldwide attention and recognition (Kim et al., 2019). Numerous previous clinical and animal studies have shown that acupuncture may be an effective adjunctive treatment for neurological disorders, such as cognitive impairment, Alzheimer's disease, and dementia, and can effectively improve cognitive and memory function (Du et al., 2018; Ding et al., 2019; Ji et al., 2021; Su et al., 2021; Zhi et al., 2021). The therapeutic mechanism may be related to downregulation of Aβ accumulation and tau protein phosphorylation, reduction of neuroinflammation, reduction of neuronal apoptosis, improvement of mitochondrial activity, enhancement of synaptic plasticity, and restoration of the blood-brain barrier (Yin et al., 2021). However, there is a lack of research to explore the therapeutic mechanisms of acupuncture for MCI from the perspective of brain region modulation. Therefore, it is necessary to explore the mechanism of action from the perspective of brain structure and function.

Numerous studies have proven that neuroimaging techniques can accurately record changes in brain regions for neurological diseases and treatment effects (Jiang et al., 2015; Dan, 2019; Risacher and Saykin, 2021). Neuroimaging methods have become a critical tool for performing research to develop a better understanding of brain circuit alterations associated with etiology, pathophysiology, and treatment response (Kalin, 2021). The spatial variability properties of the brain were evaluated by analyzing changes in regional homogeneity (ReHo) and amplitude of low-frequency fluctuations (ALFFs). An increasing number of studies have applied fMRI techniques to evaluate the clinical effects of acupuncture for MCI (Wang et al., 2012; Liu et al., 2014; Shan et al., 2018). However, the small sample size between the different clinical designs led to variability in the experimental results.

Therefore, to elucidate the modulatory effects of brain regions in acupuncture for MCI, this paper uses a coordinate-based meta-analysis (CBMA) to integrate the imaging findings from clinical studies quantitatively. The CBMA is a widely used method to solve the discrepancies of regional alterations among various neuroimaging studies (Jiang et al., 2017). The Seed-based d Mapping with Permutation of Subject Images (SDM-PSI) is an advanced statistical technique for CBMA on different neuroimaging techniques such as structural MRI, fMRI, DTI, or PET (Albajes-Eizagirre et al., 2019a). The SDM-PSI approach allows reported peak coordinates combined with statistical parametric maps, thus ensuring more exhaustive and accurate meta-analyses (Albajes-Eizagirre et al., 2019c). By analyzing the effect of acupuncture on the modulation of MCI brain regions, the therapeutic effect of acupuncture was elucidated from a neuroimaging perspective, providing new ideas for treating neurological diseases with acupuncture.

Materials and methods

All procedures for this meta-analysis were performed following the Preferred Reporting Items for Systematic Reviews and Meta-Analyses guidelines (PRISMA guidelines) (PRISMA). This study was registered on the International Prospective Register of Systematic Reviews (PROSPERO: CRD 42022287826) (Liberati et al., 2009; Moher et al., 2009; Page et al., 2021).

Literature search

We searched the following electronic databases from the establishment of the databases to April 2022: PubMed, EMBASE, Web of Science, Cochrane Library, Cochrane Database of Systematic Reviews, Cochrane Database of Abstracts of Reviews of Effects (DARE), Google Scholar, China National Knowledge Infrastructure (CNKI), China Biology Medicine disk (CBM disk), Wan Fang, and Chinese Scientific Journal Database (VIP). The search process was carried out independently by two researchers. The search terms included: (mild cognitive impairment OR cognitive impairment OR cognitive decline OR cognitive deficit OR cognitive dysfunction OR cognitive disorders OR cognitive dissonance OR amnestic OR MCI) AND (acupuncture OR meridian OR acupuncture therapy OR acupuncture treatment OR acupoint OR electroacupuncture OR electro-acupuncture OR ear acupuncture OR auriculotherapy OR scalp acupuncture) AND (RCT OR randomized controlled trial OR controlled clinical trial OR randomized OR clinical trial OR randomly OR trial OR "random∗" OR "alloc∗"OR "assign∗) AND (fMRI OR functional MRI OR functional magnetic resonance imaging OR neuroimaging OR voxel-based morphometry OR VBM OR resting state). In addition, professional journals, reference lists of relevant articles, and conference abstracts related to MCI and acupuncture were hand-searched in the library to ensure a comprehensive literature search. Among them, four Chinese journals and two English journals related to acupuncture were manually searched in the library:Acupuncture Research (from 1976), Chinese Acupuncture and Moxibustion (from 1981), Journal of Clinical Acupuncture and Moxibustion (from 1985), Shanghai Journal of Acupuncture and Moxibustion (from 1982), Acupuncture in Medicine (from 1982), and Medical Acupuncture (from 2007) through March 2017. The language during the search process is restricted to articles published in English or Chinese. Boolean logic operations are used to develop search formulas for different search libraries.

Inclusion and exclusion criteria

All studies were screened for title, abstract and full text and were conducted independently by two researchers (ML and ZZ). In case of disagreement, the two researchers reached an agreed result through discussion. The following inclusion criteria were based on PICO standards:

Participants: Clinical trials with clear diagnostic criteria for MCI, with no restrictions on participant age or gender.

(1) Interventions: The treatment group used various acupuncture therapies (e.g., pure acupuncture, body acupuncture, electroacupuncture, ear acupuncture) or acupuncture combined with other medications. We did not set limitations for intensity, frequency, or course of treatment.
(2) Comparison Groups: The comparison group can be treated with any non-acupuncture method but should be consistent with the baseline information of the intervention group (e.g., age, gender, etc.).
(3) Outcomes: Functional magnetic resonance imaging (fMRI) and subjective scale outputs. It mainly involves whole-brain functional imaging (ReHo or ALFFs) at rest or in the task state. Peak coordinates (x, y, z) and effect sizes (t-value, or z-value or P-value) reported in Talairach or Montreal Neurological Institute (MNI) standard stereotactic space. All samples were included if one study involved two or more comparable datasets. Secondary outcomes were used to assess clinical efficacy, measured using the Clinical Dementia Rating (CDR) and the Brief Mental State Examination (MMSE).

We excluded the following types of articles: articles using ROI or seed voxel-based analyses, missing significant information on results [e.g., coordinates significant clusters ($P < 0.05$)], methodological studies, conference summaries, and preliminary trials with complete overlap.

Study selection

Two independent evaluators (ZZ and HZ) screened the literature based on inclusion criteria. Titles and abstracts of all studies retrieved through the search strategy were first screened using EndNote and duplicates were removed. The second screening was performed mainly by further review of the full text of the literature. In case of disagreement during the screening process, the document was submitted to a third evaluator for consultation and eventual agreement.

Data extraction

We extracted the full text of the literature based on a pretest post data extraction form. Data extraction was performed independently by two assessors (LY and YL) based on inclusion and exclusion criteria, followed by cross-checking. Data were validated by a third assessor (HH). If data were missing, authors were contacted by email for further information. Data were extracted from the included studies with the following standardization: (1) publication data (author, year); (2) basic information about the trial design study (Study trial type, Comparison, Sample size, Scanning instrument, clinical outcome measures, neuroimaging techniques, task-based/resting-state study design, episodic/interval conditions, image acquisition timing, analysis methods); (3) acupuncture manipulation (primary acupoints, acupuncture modality, frequency, duration, duration of treatment); (4) participants (gender, age, education, Symptom severity); (5) neuroimaging results.

Quality assessment

Quality assessment was based on the Cochrane Risk of Bias tool and was conducted independently by two researchers. All reports were assessed according to the following seven criteria: random sequence generation, allocation concealment, blinding of participants and personnel, blinding of outcome assessment, incomplete outcome data, selective reporting, and other sources of bias. For each criterion, studies were judged to be at low, high, or unclear risk of bias. Visual graph production for quality evaluation using R software version 4.1.3 and R Studio version 2022.02.0.

SDM-PSI meta-analysis

Voxel-based meta-analyses of regional brain differences were performed using Seed-based d Mapping with Permutation of Subject Images (SDM-PSI) (version 6.21, https://www.sdmproject.com/). This software package uses reported peak coordinates extracted from databases with statistical parametric maps. It reconstructed the original maps of regional differences in the brain, thus revealing the neural substrates of many brain functions and neuropsychiatric disorders (Radua et al., 2012; Albajes-Eizagirre and Radua, 2018). The procedures included collecting the data, creating SDM table, pre-processing, mean analysis, heterogeneity, publication bias, and grading.

In the data collection step, a text file is created for each study, containing the peak coordinates and t-values, and the name of the text file must be "XXX.spm_mni.txt." If the study had no peaks, its text file was recorded as having no content with the extension ".no_peaks.txt". In the Create SDM Table

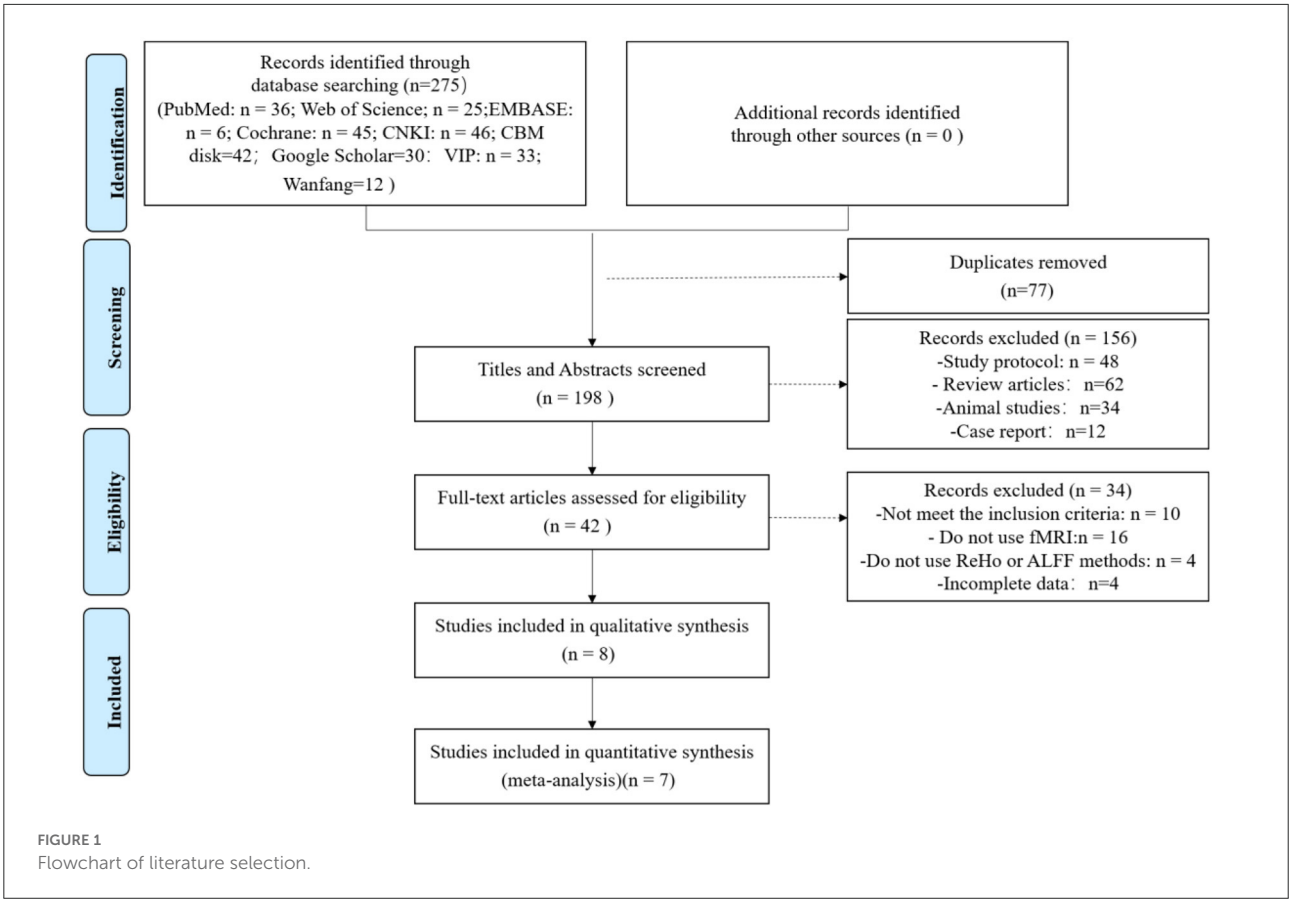

FIGURE 1
Flowchart of literature selection.

step, enter general information about the studies in the SDM Table Editor, including their identification (column "study"), their sample sizes, the *t*-value that they used as statistical thresholds (column "t_thr"), and other potential variables to conduct subgroup analyses or meta-regressions. Of particular note is the presence of specified thresholds in each study, applying the same statistical thresholds to estimate the maps more accurately. In the preprocessing step, SDM-PSI estimates the lower limit of the size of the possible effect size images (i.e., the lowest potential effect size for each voxel) and their upper limit (i.e., the maximum potential effect size for each voxel) of the images from the peak coordinates and effect sizes collected for each study, respectively, to compare the peak coordinates and effect sizes between the treatment and control groups. SDM-PSI performed a meta-analysis of NSUE (MetaNSUE) based on maximum likelihood estimation and multiple imputation algorithms (Radua et al., 2012; Albajes-Eizagirre et al., 2019b). MetaNSUE was used to estimate the most likely effect sizes and their standard errors, thus creating several imputations. In the mean analysis, the weighted mean difference of the regional gray matter of the sample size of this study is expressed. This includes calculating the random-effects mean of the ReHo values, with the mean weighted by the sample size and variance of each study. Secondly, a meta-analysis was performed for each dataset using a standard random-effects model, and then the coefficients of these datasets and their covariances and heterogeneity statistics I and Q were combined using Rubin's rule. Finally, corrections were made by clustering-based thresholds, using uncorrected $p < 0.001$ as the threshold for cluster formation at the cluster level, along with Family-Wise Error Rate (FWER) correction ($p < 0.05$ and voxel extent ≥ 10) and the use of threshold-free clustering enhancement (TFCE) in statistical thresholds at the cluster level. To set the null distribution, 1000 replacement trials were performed. The details of these procedures are extensively described in the SDM-PSI reference manual (https://www.sdmproject.com/manual/).

Heterogeneity and publication bias

The MNI peak coordinates were extracted and analyzed for heterogeneity to obtain the standard heterogeneity statistic I^2. $I^2 < 50\%$ indicates low heterogeneity. Funnel plots were not performed because the amount of included studies ($n = 7$) was <10, but the Egger test was used to assess the publication bias.

Meta-regression analysis

The potential effects of clinical variables such as gender, age, years of education, duration of illness, and severity of clinical symptoms ($p < 0.00005$, uncorrected, and voxels > 10 indicate statistical differences) were explored by simple linear regression analysis. Linear models were drawn using MATLAB 2017a.

Results

Characteristics of included studies

Our search identified seven studies that met the inclusion criteria (Hou et al., 2010; Jiang et al., 2012; Wang et al., 2012, 2020; Liu et al., 2014; Jia et al., 2015; Shan et al., 2018). Based on the search strategy, the database search identified 275 articles and 77 articles were deleted due to duplication. After screening by title and abstract, 156 articles were further excluded. Of the 42 eligible relevant studies, 34 studies were excluded after the full-text screening. Of these 34 studies, 10 articles did not meet the inclusion criteria, 16 did not use fMRI, four did not use ReHo or ALFF methods, and four had incomplete data. A total of seven studies were included in the final analyses. Figure 1 represents the PRISMA flow diagram of the article search.

All trials that met the inclusion criteria were published between 2010 and 2020. All clinical studies recruited one hundred and eighty patients (112 MCI patients and 68 healthy controls). There were no significant differences in demographic baseline characteristics (including age, gender, and years of education) between the two groups. Baseline characteristics of clinical symptoms were assessed using subjective scales (including MMSE, CDR, and auditory verbal learning test), and all met the inclusion criteria. Most studies used a new non-repeated event-related (NRER) fMRI design model to explore the ongoing effects of acupuncture on MCI. Only 1 study used a conventional acupuncture modality with a 4-week duration of treatment (Wang et al., 2020). The Main acupoints included Tai Chong (LR3), Tai Xi (KI3), Bai Hui (DU20) and He Gu (LI4). The acupuncture method was mainly carried out in the balanced "tonifying and reducing" technique, while the positioning and operation of acupuncture points were based on international standards (Hui et al., 2000). All studies reported fMRI coordinate data using the ReHo variable to analyze the brain region activation effect before and after acupuncture treatment and the difference in its comparison with sham acupuncture and healthy control group. The details and features of the studies are shown in Tables 1, 2. Anatomical localization of the acupoints mentioned in the included studies are shown in Supplementary material 2.

Quality assessment

The quality assessment was performed using the Cochrane Risk of Bias tool, and the evaluation criteria were divided into seven entries. Of the seven studies, only one reported on the method of random sequence generation (Shan et al., 2018). No studies mentioned allocation concealment and blinding, and the risk of bias was unclear. Evaluation of incomplete outcome data depended on whether the clear descriptions of baseline data were shown. Based on this evaluation criterion, all studies reported outcome data in full and were judged to be low risk. Although none of the studies had a study protocol, all expected outcome indicators were reported, including those that were predetermined and therefore judged to be low risk. In addition, we did not find any other sources of bias. In general, the quality of these studies was not high, mainly in terms of study design. Figure 2 illustrates the quality assessment of the included studies.

Results of meta-analysis

Acupuncture for the modulation of brain regions in MCI patients

In a pooled meta-analysis, brain region coordinates based on Family-Wise Error Rate (FWER) correction ($p < 0.05$) thresholds were analyzed for PRE and POST acupuncture treatment for MCI patients in the group. The results showed that acupuncture treatment showed significant increases in Reho values in six brain regions, mainly including the right insula ($p < 0.05$, $z = 3.362$), left anterior cingulate/paracingulate gyri ($p < 0.05$, $z = 3.482$), right thalamus ($p < 0.05$, $z = 3.967$), right middle frontal gyrus ($p < 0.05$, $z = 2.544$), right median cingulate/paracingulate gyri ($p < 0.05$, $z = 2.185$) and right middle temporal gyrus ($p < 0.05$, $z = 2.332$), indicating hyperactivation of these brain regions after acupuncture treatment. The differences in regional activity in the gray matter of the brain PRE and POST acupuncture treatment in MCI patients based on coordinate analysis are shown in Table 3 and Figure 3. Further analysis of the RCTs and longitudinal studies (Jiang et al., 2012; Wang et al., 2020) revealed significantly higher Reho values in two brain regions after acupuncture, including the left anterior cingulate/paracingulate gyrus ($p < 0.05$, $z = 3.482$) and the right insula ($p < 0.05$, $z = 3.362$) (see Table 4).

Differences in brain region modulation by acupuncture in MCI patients and healthy subjects

A pooled meta-analysis analyzed differences in brain areas between the MCI and healthy control groups after acupuncture treatment and included four cross-sectional studies Hou et al., 2010; Wang et al., 2012; Liu et al., 2014; Jia et al., 2015;

TABLE 1 Demographic and clinical characteristics of included studies.

References	Study design	Groups (*n*, male/female)	Treatments (*n*)	Age (years)	Education (years)	Symptom severity (baseline)	Main acupoints (placement, number)	Experimental design (parameters, session duration, total period)
Wang et al. (2020)	Longitudinal study	MCI (36, 16/20)	MA (36)	MA: 64.96 ± 3.22	/	MMSE: 24.61 ± 1.73; MoCA: 22.79 ± 1.79	Head: DU20 (1), BG13 (2), GB20 (2);Foot: LR3 (2), SP3 (2), KI3 (2);Abdomen: RN4;Hand: HT7 (2); Leg: ST40 (2), BL58 (2)	MA: uniform reinforcing-reducing method; 40 min/time, 6 times/w, for 4 weeks.
Shan et al. (2018)	Cross sectional	MCI (14, 6/8); HC(14, 6/8)	RA: MCI(8), HC(14); SA: MCI (6)	RA: 66.38 ± 10.97; SA: 67.83 ± 6.01; HC: 66.07 ± 5.78	RA: 10.63 ± 3.54; SA: 11.00 ± 3.16; HC: 11.00 ± 4.52	MMSE: RA: 25.38 ± 1.30, SA: 25.67 ± 2.34; HC: 28.00 ± 1.41 CDR: RA: 0.5, SA: 0.5, HC: 0 AVLT (immediate): RA: 14.13 ± 3.52, SA: 22.50 ± 3.02, HC: 26.86 ± 5.25 AVLT (delayed): RA: 4.38 ± 1.60, SA: 7.83 ± 3.92, HC: 11.07 ± 2.76 AVLT (recognition): RA: 7.38 ± 3.11, SA: 9.17 ± 3.19, HC: 12.71 ± 2.09	Foot: LR3 (2); Hand: LI4 (2)	MA: needles are 0.3 mm in diameter, 25 mm long and 2 cm deep;rotated continuously (±180°, 60 times/min); 3 min; SA: 10 mm next to LR3 and Hegu; SA and HC needle specifications and treatment time are the same as MA.
Jia et al. (2015)	Cross sectional	MCI (8, 2/6); HC (15, 8/7)	RA: MCI (8); SA: MCI (8); HC (15)	MCI: 74.1 ± 7.8; HC: 70.2 ± 7.1	MCI: 12.5 ± 3; HC: 11.4 ± 4.2	MMSE: MCI: 27.0 ± 2.3; HC: 29.2 ± 1.3 ADAS-cog: MCI: 6.7 ± 2.9; HC: 2.5 ± 1.7	Foot: KI3 (2)	RA: needles are 0.25 mm in diameter, 40 mm long and 2 cm deep 1 min, continuous rotation, right then left, at a frequency of 2 Hz for 60 s; SA: 25 mm directly above KI3 as a sham control, and the rest was the same as RA.
Liu et al. (2014)	Cross sectional	MCI (12, 1/11); HC(12, 4/8)	MA: MCI (12), HC (12)	MCI: 59.3 ± 3.3; HC: 60.6 ± 5.8	MCI: 10.5 ± 1.8; HC: 10.6 ± 2.06	MMSE: MCI: 26.4 ± 0.9, HC: 29.8 ± 0.4 CDR: MCI: 0.5, HC: 0	Foot: KI3 (2)	MA: needle is 0.2 mm in diameter, 40 mm long and 1-2 cm deep; rotated continuously (±180°, 60 times/ min), 3 min; HC and MA operate in the same way.
Wang et al. (2012)	Cross sectional	MCI (8, 3/5); HC (14, 6/8)	MA: MCI (8); HC (14)	MCI: 66.37 ± 10.9; HC: 66.07 ± 5.78	/	MMSE; MCI: 25.37 ± 1.30, HC: 28.00 ± 1.41 AVLT (immediate): MCI: 14.13 ± 3.52, HC: 26.86 ± 5.24 AVLT (delayed): MCI: 4.37 ± 1.59, HC: 11.07 ± 2.76 AVLT (recognition): MCI: 7.38 ± 3.11;HC: 12.71 ± 2.09 CDR: MCI: 0.5, HC: 0	Foot: LR3 (2); Hand: LI4 (2)	MA: 3 min; HC: None

(Continued)

10.3389/fnagi.2022.914049

TABLE 1 (Continued)

References	Study design	Groups (*n*, male/female)	Treatments (*n*)	Age (years)	Education (years)	Symptom severity (baseline)	Main acupoints (placement, number)	Experimental design (parameters, session duration, total period)
Jiang et al. (2012)	RCT	MCI (24, 12/12)	RA: MCI (12); SA: MCI (12)	MA: 63.83 ± 4.90; SA: 67.08 ± 5.26	/	CDR: 0.5, MMSE ≥ 24	Foot: LR3 (2)	MA: Needle diameter of 0.35 mm, 25 mm long, 1.5 cm deep; uniform lifting and inserting twisting row needle method, lifting and inserting amplitude in the upper and lower 2–3 mm, 30 min; SA: The midpoint of the line between the right KI3 point and the Achilles tendon.
Hou et al. (2010)	Cross sectional	MCI (10); HC (13)	EA: MCI (10); HC: 13	50–80	/	MMSE ≥ 24, MoCA < 26	Head: DU20 (1), EX-HN1 (4), BG13 (2); Leg: ST36 (2), ST40 (2), SP6 (2)	EA: Needle diameter of 0.30 mm, 40 mm long, 1.5 cm deep; rotated continuously (±180°, 120 times/min), Sparse and dense waves, 2 min

EA, electroacupuncture; MA, manual acupuncture; RA, real acupuncture; MMSE, Mini-mental State Examination; MoCA, Montreal Cognitive Assessment; AVLT, auditory verbal learning test; CDR, Clinical Dementia Rating; SA, sham acupuncture; HC, healthy controls; RCT, randomized controlled trial; Min, minutes; DU20, Baihui; KI3, Taixi; GV20, Baihui; RN4, Guanyuan; LR3, Taichong; LI4, Hegu; SP6, Sanyinjiao; GB20, Fengchi; EX-HN1, Sishecong; SP3,Taibai; ST40, Fenglong; BL58, Feiyang; HT7, Shenmen; BG13, Benshen; ST36, Zusanli.

Shan et al., 2018. The results showed a significant difference in the right supramarginal gyrus after acupuncture treatment in the MCI group compared to the healthy control group. At the same time, the right supramarginal gyrus extended to the right postcentral gyrus and right superior longitudinal fasciculus III. The differences in the regulation of brain regions between MCI patients and healthy individuals by acupuncture are shown in Table 5 and Figure 4.

Heterogeneity analysis and publication bias

Heterogeneity analysis showed variability among the different studies included. In addition, we used Egger's test to assess potential publication bias in the meta-analysis. There was low heterogeneity in the peak coordinate effect size differences in the right insula, left anterior cingulate/paracingulate gyrus, right thalamus, right middle frontal gyrus, right cingulate/paracingulate gyrus, and right middle temporal gyrus (I^2 = 0.64–17.23). The heterogeneity results are shown in Table 2. The Egger test differences were not statistically significant (p = 0.432), and the study had no significant publication bias.

Meta regression analysis

Meta-regression was used to find potential correlations between acupuncture treatment MCI subjective scale scores, baseline information and brain regions. Whole-brain meta-regression analysis found that MMSE scores in MCI patients were negatively correlated with regional activity in the right corticospinal projection (peak coordinates: $x = 10$, $y = -18$, $z = -2$, voxel = 22, $r = 0.73$, $p = 0.003354549$). However, there were two discrete values in the regression plots. No significant correlation was found between any regional functional change and mean age, gender percentage, education, or CDR score. The meta-regression analysis of brain regions significantly associated with MMSE scores is shown in Table 6 and Figure 5.

Discussion

In this study, we used the SDM-PSI method to summarize the effect of acupuncture on the modulation of MCI brain regions from the neuroimaging perspective through a meta-analysis of brain imaging studies of MCI patients treated with acupuncture. The within-group comparison results confirmed the effect of acupuncture on regional brain region modulation in MCI patients, with enhanced activity in the right insula, left anterior cingulate/paracingulate gyri, right thalamus, right middle frontal gyrus, right cingulate/central

TABLE 2 Scanning methods and major brain region alterations in the included studies.

References	Scanning instrument/ experimental design	Seed regions	Analysis of fMRI	Statistical threshold	Number of coordinates	Main conclusions
Wang et al. (2020)	Achieva 3.0 T; RS	Whole brain	Reho	$P = 0.001$, uncorrected	MNI, 7	Acu vs. HC: right parahippocampal gyrus, left thalamus, right insula, and left anterior cingulate gyrus↑; left posterior cerebellar lobe, left inferior temporal gyrus, right inferior temporal gyrus, left inferior frontal gyrus, left middle temporal gyrus, left inferior occipital gyrus, and left superior parietal lobule↓
Shan et al. (2018)	Siemens3.0T; NRER	Whole brain	Reho	$P < 0.05$, AlphaSim corrected	MNI, 11	Acu vs. Sham: left supramarginal gyrus, left superior temporal gyrus, left rolandic operculum, left cerebellum, right middle frontal gyrus, and right inferior frontal gyrus (pars opercularis) ↑; left inferior parietal gyrus↓ Acu vs. HC: right superior temporal gyrus, right superior temporal gyrus, right superior parietal gyrus, right supramarginal gyrus, right postcentral gyrus, right precentral gyrus, right cerebellum, left inferior parietal gyrus, left middle occipital gyrus, and left inferior occipital gyrus↑
Jia et al. (2015)	Tesla Signa (GE) MR 1.5 T;NRER	Whole brain	Reho	$P < 0.01$, AlphaSim corrected	MNI, 3	Acu vs. Sham: right superior temporal gyrus↑; middle prefrontal gyrus ↓
Liu et al. (2014)	Tesla Signa (GE) MR 3.0T; NRER	Whole brain	Reho	$P < 0.01$, AlphaSim corrected	MNI, 13	Acu vs. HC: MTG, superior parietal lobule (SPL), middle frontal gyrus (MFG), superior marginal gyrus (SMG), and PCG↑
Wang et al. (2012)	Siemens3.0T; NRER	Whole brain	Reho	$P < 0.001$, uncorrected	MNI, 44	AS vs. RS(First): bilateral cerebellum posterior lobe, temporal lobe, frontal lobe, parietal lobe and occipital lobe↑; bilateral CPL, temporal lobe, frontal lobe, parietal lobe right lingual gyrus and limbic regions↓ AS vs. RS(Second):bilateral CPL, temporal lobe, frontal lobe, right lentiform nucleus, left extra nuclear and right thalamus↑; bilateral CPL, temporal lobe, frontal lobe, parietal lobe and occipital lobe↓
Jiang et al. (2012)	Achieva 3.0T; NRER	Whole brain	Reho	$P < 0.001$, uncorrected	MNI,5	Acu vs. Sham: right cingulate gyrus, bilateral medial frontal gyrus and left postcentral gyrus↑
Hou et al. (2010)	Achieva 1.5T; NRER	Whole brain	Reho	$P < 0.001$, uncorrected	MNI, 6	Acu vs. HC: superior temporal gyrus in the posterior temporal lobe, orbitofrontal and frontopolar regions of the frontal lobe, and temporal cortex↑

RS, resting state; AS, acupuncture stste; NRER, non-repeated event-related; ReHo: regional homogeneity; MNI: Montreal Neurological Institute.

parabrachial gyrus and right middle temporal gyrus brain regions after acupuncture treatment. Further analysis of RCT and longitudinal studies showed that Reho values were significantly elevated in two brain regions, the left anterior cingulate/paracingulate gyrus and the right insula, after acupuncture. Also, the results of intergroup comparison showed significant differences in brain activation regions in the MCI group compared with the healthy control

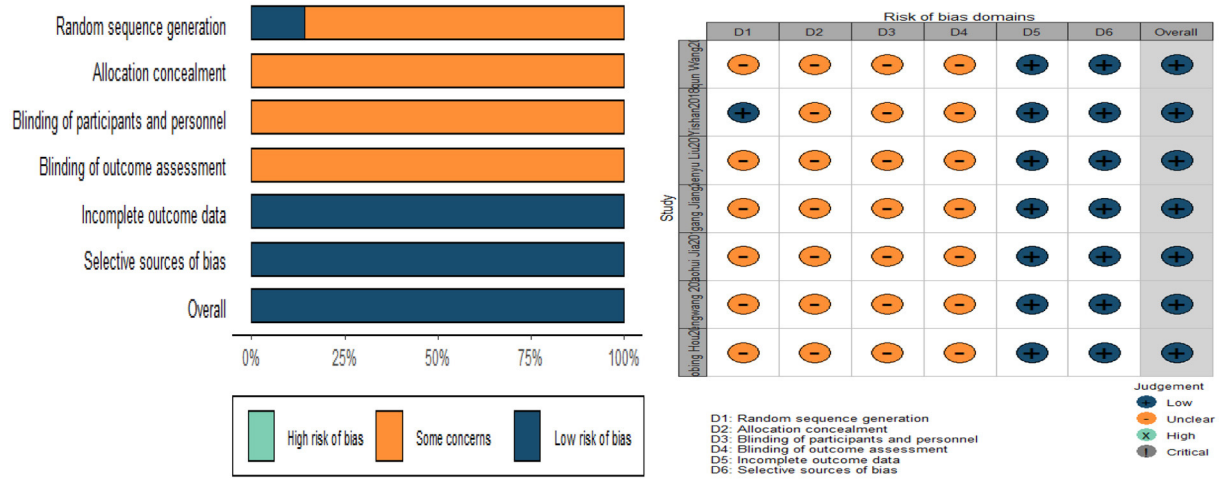

FIGURE 2
Quality assessment of included studies.

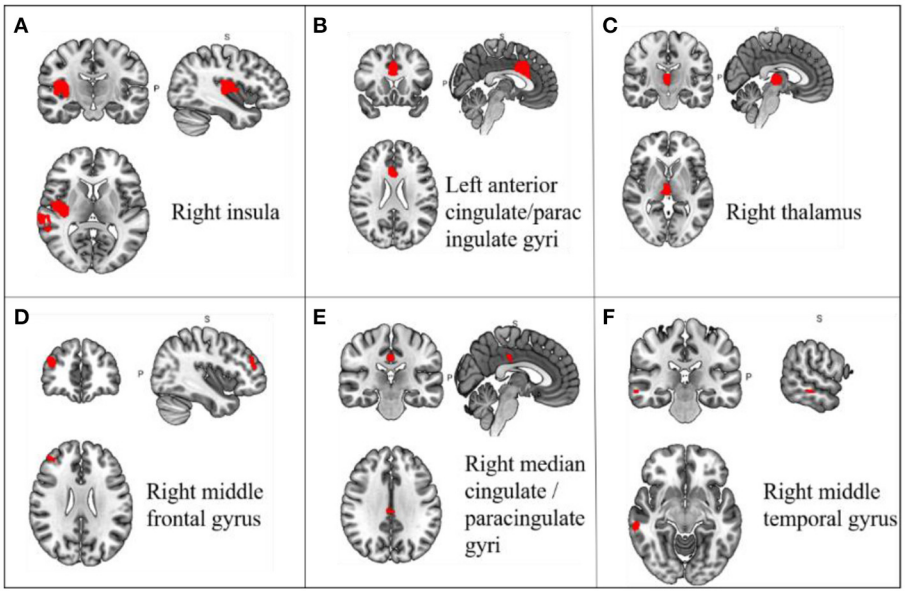

FIGURE 3
Changes in gray matter regions PRE and POST acupuncture treatment in MCI patients. **(A)** Right insula; **(B)** Left anterior cingulate/paracingulate gyri; **(C)** Right thalamus; **(D)** Right middle frontal gyrus; **(E)** Right median cingulate/paracingulate gyri; **(F)** Right middle temporal gyrus. Important clusters are presented with MRIcron templates.

group after acupuncture treatment, mainly in the right supramarginal gyrus. In addition, the right anterior thalamic projection ReHo index was significantly correlated with MMSE scores. Functional characterization showed that these regions were mainly involved in cognitive, emotional, and decision-making regions, which may provide a possible central mechanism for acupuncture treatment of MCI from a neuroimaging perspective.

Modulatory effects of acupuncture on brain regions of MCI

The results showed that MCI patients had increased Reho values and enhanced brain region activity in the right insula, left cingulate/paracentral gyrus, right thalamus, right middle frontal gyrus, right median cingulate/paracingulate gyri, and right middle temporal gyrus after acupuncture treatment. In

TABLE 3 Regional differences in brain gray matter volume activity PRE and POST acupuncture treatment in the coordinate-based meta-analysis.

Brain regions	MNI coordinates			SDM Value	*p*-value	Voxels	Cluster breakdown (number of voxels)	I^2
	x	*y*	*z*					
Right insula, BA 48	40	−18	8	3.362	0.000386775	1,342	Right insula, BA 48 (315); Right superior temporal gyrus, BA 21, 22, 42, 48 (360); Right rolandic operculum, BA 48 (148) Corpus callosum (119) Right heschl gyrus, BA 48 (106) Right middle temporal gyrus, BA 21, 22 (130) Right lenticular nucleus, putamen, BA 48 (50) Right fronto-insular tract 5 (23) Right supramarginal gyrus, BA 48 (13)	1.01%
Left anterior cingulate/paracingulate gyri	0	14	26	3.482	0.000248611	748	Left median cingulate/paracingulate gyri, BA 24 (164) Right median cingulate/paracingulate gyri, BA 24, 32 (179) Right median network, cingulum (121) Right anterior cingulate/paracingulate gyri, BA 24 (141) Left anterior cingulate/paracingulate gyri(64) Corpus callosum (53) Left superior frontal gyrus, medial, BA 32 (18)	0.95%
Right thalamus	4	−18	4	3.967	0.000036418	349	Right thalamus (130) Left thalamus (60) Right anterior thalamic projections (27)	0.64%
Right middle frontal gyrus, BA 46	42	48	18	2.544	0.005474687	138	Right middle frontal gyrus, BA 46 (78) Right middle frontal gyrus, BA 45 (51)	17.23%
Right median cingulate/paracingulate gyri, BA 23	4	−24	34	2.185	0.014458418	83	Right median cingulate/paracingulate gyri, BA 23 (42) Left median cingulate/paracingulate gyri, BA 23 (32)	1.34%
Right middle temporal gyrus, BA 21	64	−26	−12	2.332	0.009853780	45	Right middle temporal gyrus, BA 21 (31) Right middle temporal gyrus, BA 20 (12)	5.90%

Peak height threshold: $z > 1$. Voxel probability threshold: $P < 0.005$ uncorrected and remained after correcting threshold (TFCE) of $P < 0.05$. Cluster extent threshold: number ≥ 10 voxels. BA, Brodmann area; I^2, heterogeneity I^2; MNI, Montreal Neurological Institute; R, right; ReHo, regional homogeneity; SDM, signed differential mapping.

particular, activity was significantly increased in the left anterior cingulate/paracingulate gyrus and the right insula. The above brain regions were mainly involved in cognitive, emotional, and decision-making regions, which confirmed to some extent the modulatory effect of acupuncture on brain regions in MCI. Regional homogeneity (ReHo), a measure of local resting functional connectivity, has been shown to be a promising biomarker in a variety of psychiatric disorders (Liu et al., 2008; Chen et al., 2013; Jiang and Zuo, 2016). ReHo is a voxel-based measure of brain activity that assesses the time series of a given voxel in relation to its similarity or synchrony between the time series of a particular voxel (Liu et al., 2008).

A brain imaging study of Parkinson's disease with mild cognitive impairment (PD-MCI) showed reduced ReHo values and reduced spontaneous synchronization in the left insula and that ReHo values were significantly correlated with the Montreal Cognitive Assessment Scale (Li et al., 2020). The association between regional ReHo values and the clinical severity index of cognitive impairment (i.e., MoCA) may laterally validate the potential correlation between the insula and cognitive function. The insula is associated with sensory, motor, visual perceptual, memory, and executive impairments (Chang et al., 2016; Namkung et al., 2018). A functional neuroimaging study of the insula showed that activation of the anterior insula cortex

TABLE 4 Regional differences in brain gray matter volume activity before and after acupuncture treatment in cross-sectional and longitudinal studies.

Brain regions	MNI coordinates			SDM Value	*p*-value	Voxels	Cluster breakdown (number of voxels)	I^2
	x	*y*	*z*					
Left anterior cingulate/paracingulate gyri	0	14	26	3.482	0.029999971	51	Right anterior cingulate/paracingulate gyri, BA 24 (24) Left anterior cingulate/paracingulate gyri, BA 24 (14) Right median cingulate/paracingulate gyri, BA 24 (7) Right median network, cingulum (6) Right heschl gyrus, BA 48 (106) Right middle temporal gyrus, BA 21, 22 (130) Right lenticular nucleus, putamen, BA 48 (50) Right fronto-insular tract 5 (23) Right supramarginal gyrus, BA 48 (13)	0.72%
Right insula, BA 48	40	−18	8	3.362	0.029999971	41	Right insula, BA 48 (29) Right heschl gyrus, BA 48 (11) Corpus callosum (1)	3.75%

Peak height threshold: $z > 1$. Voxel probability threshold: $P < 0.005$ uncorrected and remained after correcting threshold (TFCE) of $P < 0.05$. Cluster extent threshold: number ≥ 10 voxels. BA, Brodmann area; I^2, heterogeneity I^2; MNI, Montreal Neurological Institute; R, right; ReHo, regional homogeneity; SDM, signed differential mapping.

TABLE 5 Regional differences in gray matter volume after acupuncture treatment in MCI patients vs. healthy controls in a coordinate-based meta-analysis.

Brain regions	MNI coordinates			SDM Value	P-value	Voxels	Cluster breakdown (number of voxels)	I^2
	x	*y*	*z*					
Right supramarginal gyrus, BA 2	56	−26	38	3.525	0.000999987	180	Right supramarginal gyrus, BA 2 (67); Right supramarginal gyrus, BA 40 (50); Right superior longitudinal fasciculus III (32); Right supramarginal gyrus, BA 48 (18); Right supramarginal gyrus, BA 3 (8); Right postcentral gyrus, BA 3 (3); Right postcentral gyrus, BA 2 (2)	1.92%

Peak height threshold: $z > 1$. Voxel probability threshold: $P < 0.005$ uncorrected and remained after correcting threshold (TFCE) of $P < 0{:}05$. Cluster extent threshold: number ≥ 10 voxels. BA, Brodmann area; I^2, heterogeneity I^2; MNI, Montreal Neurological Institute; R, right; ReHo, regional homogeneity; SDM, signed differential mapping.

and anterior cingulate cortex was the most common focus of cognitive tasks, including detection processes of perception and consciousness (Sterzer et al., 2007). This study showed that acupuncture therapy was also associated with hyperactivation of the insula and could activate the insula to exert therapeutic effects, which is consistent with previous studies.

The anterior cingulate gyrus (ACC) is a critical limbic system component. Previous studies have shown that ACC is primarily involved in affective motivation and cognitive attention (Bush et al., 2000; Apps et al., 2016). A neuroimaging meta-analysis on MCI showed reduced anterior cingulate ReHo values in amnestic MCI, which could serve as a potential imaging biomarker for MCI and also as a new target for appropriate intervention to delay progression (Song et al., 2021). Previous studies have shown that acupuncture activates brain regions in the anterior cingulate gyrus, primarily in MCI, ischemic stroke, and migraine (Tan et al., 2017; Wu et al., 2018; Chang et al., 2021). Our meta-analysis found that acupuncture increased ReHo in the Left anterior cingulate/paracingulate gyri, which is consistent with the previous findings. Therefore, the increased ReHo of left anterior cingulate/paracingulate gyri may be a potential mechanism for acupuncture in the treatment of MCI.

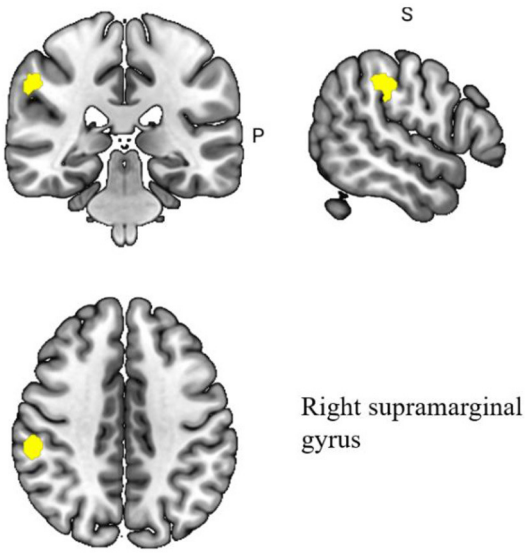

FIGURE 4
Regional differences in gray matter between MCI patients and healthy controls after acupuncture treatment.

TABLE 6 Meta-regression analysis of MMSE scores in treatment group.

Region	MNI coordinate			SDM *z*-score[a]	*p*-value[b]	Number of voxels[c]
	x	*y*	*z*			
Right anterior thalamic projections	8	−18	0	2.622	0.001930118	130

[a]Peak height threshold: $z > 1$.
[b]Voxel probability threshold: $p < 0.005$.
[c]Cluster extent threshold: number ≥ 10 voxels.
SDM, signed differential mapping.

The thalamus, as a diverse hub, is involved in a wide range of behavioral cognitions, such as arousal regulation, attentional selection, and working memory (Saalmann et al., 2012; Crossley et al., 2013; De Bourbon-Teles et al., 2014; Hwang et al., 2017). The thalamus has been shown to interact with different cortical regions convergently and be involved in various cognitive functions, and memory may be the first cognitive function formally associated with the thalamus (Wolff and Vann, 2019). A clinical study on functional magnetic resonance imaging (fMRI) techniques for aMCI showed reduced right thalamic ReHo values in patients with aMCI compared to normal older adults (Min et al., 2019). In a clinical trial of acupuncture in relation to MCI, patients with MCI showed significant changes in functional connectivity in brain regions such as the hippocampus, thalamus and syrinx gyrus after acupuncture to K13 compared to HC (Feng et al., 2012). The thalamus, ACC, and insula constitute significant central autonomic networks, and they are also commonly activated in tasks related to emotion, memory, and mutual sensation (Cauda et al., 2012; Lee et al., 2020). Thus, acupuncture's modulation of brain regions in MCI may be related to homogeneous regional activation of the thalamus, insula and ACC, but the presence of structural-functional connections remains to be further investigated.

The middle frontal gyrus (MFG) is involved in attention, working memory, and language related processing (Briggs et al., 2021). Several functional magnetic resonance imaging studies have shown that the middle frontal gyrus (MFG) plays a role in working memory (Klingberg et al., 1997; Vartanian et al., 2013; Yin et al., 2016). In a study examining the different responses to acupuncture in MCI patients and age-matched healthy individuals as reflected by the regional homogeneity (ReHo) index, the elevated ReHo values in MCI patients were mainly distributed in the middle temporal gyrus (MTG), superior parietal lobe (SPL), middle frontal gyrus (MFG), and superior marginal gyrus (SMG) in the resting state after acupuncture (Liu et al., 2014). Numerous studies have shown that right median cingulate/paracingulate gyri (DCG) is associated with cognitive function, possibly as part of the default network connection (Feng et al., 2019; Cui et al., 2021). A study showed that the integration and dissociation of dynamic functional connectivity states tended to decrease as MCI worsened, and in some states, such as IPL.L-MTG.R and DCG.R-SMG.L, functional brain connectivity was significantly enhanced (Jiao et al., 2021). Reduced glucose metabolism in the right middle temporal gyrus (RMTG) is a powerful biomarker of subjective cognitive decline (Dong et al., 2021). According to previous reports, the MTG region has close functional connectivity with the hippocampus, is primarily involved in verbal or semantic cognition, and is also associated with oral memory (Vandenberghe et al., 1996; Beason-Held et al., 2021). In previous studies, changes in MTG after acupuncture treatment were mainly in Parkinson's Disease (Chae et al., 2009; Yeo et al., 2018). An fMRI study on acupuncture for Parkinson's disease showed increased connectivity between the left MTG and the pre-central gyrus (PCG) in the acupuncture group (Yu et al., 2019). And as a result of dopamine insensitivity, patients with Parkinson's disease have some degree of cognitive deficits (Robbins and Cools, 2014). Also, several studies have shown that there is a co-morbid mechanism between Parkinson's disease and cognitive impairment in neuroimaging, which also provides a reference for future research on the mechanism of acupuncture on cognitive impairment (Delgado-Alvarado et al., 2016; Jozwiak et al., 2017; Baiano et al., 2020).

In addition, the results of the group comparison showed that there was a significant difference between the MCI group in the right supramarginal gyrus after acupuncture treatment compared to the healthy control group. This may imply a specific brain region modulatory effect of acupuncture in the MCI population compared to healthy individuals. In a

brain imaging study exploring region-specific neurovascular uncoupling associated with cognitive decline in patients with Parkinson's disease, it was shown that local regulatory abnormalities in the PD-MCI group were specific and restricted to brain regions such as the right supramarginal gyrus and right angular gyrus, which is consistent with the findings of the present study (Shang et al., 2021). Notably, there was a high degree of overlap between the activated brain regions involved in the acupuncture treatment of MCI in the current study and the brain regions where the pain occurred (Henderson et al., 2007; Christidi et al., 2020; Smith et al., 2021). Previous studies have demonstrated that pain processing disorders are often present in patients with cognitive impairment and that various forms and degrees of dementia can affect pain processing (Cole et al., 2006; Kunz et al., 2007, 2009; Jensen-Dahm et al., 2014; Defrin et al., 2015; Beach et al., 2016). A study on pain processing in MCI and its relationship to executive function and memory showed a strong association between pain response and executive function in MCI patients, meaning that poorer executive function was associated with pain onset and escalation (Lautenbacher et al., 2021). This also demonstrates to some extent that the modulatory effect of acupuncture on the brain regions of MCI may also have a modulatory effect on the brain regions of pain, providing a good idea for the multi-target disease treatment of acupuncture.

Basic characteristics of research on acupuncture for MCI

Of the seven studies included, all were from China, which may be because acupuncture is more popular and widely accepted in Chinese society but can cause language bias. The small sample size of between 22–64 cases per study may be due to the limitations of MRI trials on sample size. Because many functional MRI studies are small and performed at a single site, meta-analyses are thought to help improve the accuracy of results and generalize conclusions from individual studies (Cohn and Decker, 2003). Although the field has studied the optimal sample size needed to detect or evaluate experimental factors, the number of subjects is often limited by practical constraints such as scanning time and cost (Desmond and Glover, 2002; Murphy and Garavan, 2004; Mumford and Nichols, 2008). However, too small a sample size may lead to excessive random errors and make the study results more heterogeneous. Estimates of effect sizes, between-and within-subject variance, and temporal autocorrelation matrices should be added to reduce subject bias's adverse effects on study results (Guo et al., 2014).

Regarding the choice of specific acupuncture modalities, manual acupuncture (MA) and electroacupuncture (EA) are the most common methods used to treat MCI. According to the theory of acupuncture, the stimulation of MA comes from specific finger manipulation that drives the translation, rotation, or tremor of the needle (Dilts et al., 2021). Electroacupuncture works by setting up electrical stimulation at specific points on the body, thereby activating these neural networks and regulating the function of certain organs (Ulloa, 2021). With these two modalities, specific neural network modulation of brain regions can be achieved in MCI patients. LR3 is located between the first and second metatarsal bones on the dorsal side of the foot, in the anterior depression of the metatarsal union, and is part of the Jueyin Liver Meridian of Foot. The K13 point is located on the medial side of the foot, in the depression between the back of the inner ankle and the tendon of the heel bone, and is part of the Shaoyin Kidney Meridian of Foot. Recent studies have shown that acupuncture LR3 and K13 play a positive activating role in social behavior and decision-making in MCI (Chen et al., 2014b). Among the single duration and duration of acupuncture treatment, only one study mentioned that the duration of acupuncture treatment should be 40 min, and most of the studies used a block design to observe the immediate effects of acupuncture. Acupuncture of LR3 and K13 specifically regulates blood flow and activates brain regions associated with emotion, decision making, semantic processing, memory, attention, and sensation. Three studies used only one acupuncture point for treatment, while others combined multiple acupuncture points for MCI. Studies suggest that the combination of acupuncture points may produce novel central effects. Comparison of LR3 plus KI3 acupuncture vs. LR3 alone revealed that ALFF alterations were concentrated in BA6, BA10, BA24, BA32, the posterior cerebellum lobe, and inferior semilunar lobule regions of the brain (Zhang et al., 2016). Studying the combined LR3 and KI3 acupuncture patterns with the relationship between LR3 and KI3 acupoint patterns and regional activation in the brain will be important in the future.

Study design

The rigorous and scientific clinical trial design is essential to observe the efficacy and effectiveness of interventions. A rigorous and scientific clinical trial design is essential to observe the efficacy and effectiveness of an intervention. In this study, three clinical trial designs including randomized controlled trials (RCTs), cross-sectional studies, and longitudinal studies were included, and the results of the meta-analysis of brain images between different study designs were also presented. RCTs are considered the highest level of evidence to establish causal associations in clinical research (Zabor et al., 2020). Limitations in the case-control study design used in most clinical fMRI studies tend to raise questions as to how samples are drawn and matched to potentially confounding variables (Carter et al., 2008). In contrast, only one of the original studies we included was an RCT, and most were cross-sectional studies. Currently,

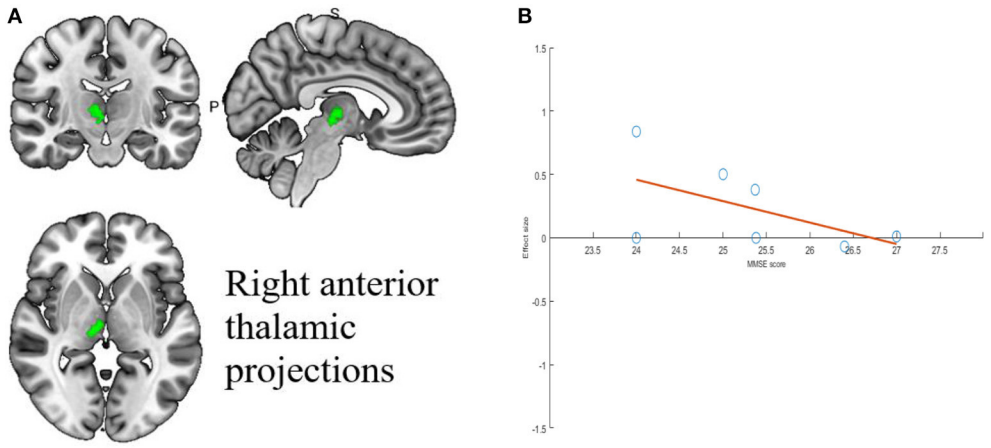

FIGURE 5
Results of Meta-regression linear model analysis. **(A)** MMSE scores of MCI patients are negatively correlated with regional activity in Right anterior thalamic projections. **(B)** The effect sizes needed to create this plot were extracted from the peak voxels of the maximum slope difference. All studies are indicated by the empty blue circles. Regression lines (Meta-regression SDM slopes) are shown as straight lines.

the application of MRI modalities has shown promising results in cross-sectional studies of neurodegenerative diseases (Argiris et al., 2021). However, in studies related to cognitive function, cross-sectional showed differences in outcomes between cross-sectional and longitudinal, as aptly demonstrated by the results of the meta-analysis in this study (Salthouse, 2019).

In most of our studies, the control group was healthy individuals, and only three studies used the placebo group as a control group. Randomized controlled trials with placebo control groups have high internal validity and are considered a reliable method for assessing treatment effects (Gøtzsche, 1994; Walach and Loef, 2015). The long time required for MRI acquisition resulted in the inability to set up a placebo control group due to the non-participation of many potential subjects, ultimately creating a potential bias (Carter et al., 2008). In this study, a placebo control group was set up for sham acupuncture. Sham acupuncture (SA), also known as a placebo, may be considered a sham intervention because it is based on non-acupuncture points. "Sham acupuncture" controls, in which needles are inserted at wrong points or non-points, which deliberately violate traditional acupuncture theories of point locations or indications and are therefore predicted to be incapable of achieving the outcomes intended by true acupuncture (Moffet, 2009). In clinical trials, the placebo control group should be consistent with the treatment group at baseline, except for physiological inertia (Chae, 2017). Currently, relevant validation focuses only on the blinding and credibility of the interventions, and few studies have validated the physiological inertia of these sham interventions. Sham acupuncture has a non-inert character, which can cause the public to question its actual effectiveness. In addition, in acupuncture trials, the key to distinguishing between acupuncture and sham acupuncture is the presence or absence of the sensory stimulus of "getting qi". Data from imaging studies also suggest that expectation, learning, and contextual factors play an important role in the placebo effect (Enck et al., 2008; Wager and Atlas, 2015; Geuter et al., 2017).

Experimental designs of MRI

The rs-fMRI and the task-state fMRI are the two primary paradigms for functional MRI studies. In the experimental design of MRI on acupuncture, rs-fMRI is the closest to the response of brain activity in the actual state, while task-state fMRI reflects the persistent effect of acupuncture. In the present study, a non-repeated event-related block design was mainly used, in which the inserted needles were continuously stimulated for 30 s to 2 min before the scan to observe the immediate effects of acupuncture. According to TCM theory, acupuncture produces a sustained effect, even after 30 min of retention, with corresponding neural responses, so NRER is more consistent with the MRI experimental design of acupuncture (Cho et al., 1998; Bai et al., 2009, 2010). They also can reduce interference from the persistent effect of acupuncture that occurs when a single, prolonged acupuncture stimulation is given during the scanning process (Liu et al., 2009). However, this type of experiment usually selects single acupuncture point, which has the limitation of single stimulation to some extent, and the clinical treatment for MCI usually uses multiple acupuncture points.

In recent years, rs-fMRI has provided new research perspectives on the central mechanisms of acupuncture treatment. By observing the changes in ReHo/ALFF after

acupuncture, the changes in brain function after acupuncture treatment are analyzed, and such changes are more reflected as long-term cumulative effects. In addition, in recent years, rs-fMRI imaging has been increasingly used to explore the central mechanisms of acupuncture treatment, such as pain, migraine, and stroke (Lan et al., 2013; Chen et al., 2014a; Leung et al., 2014). Therefore, future studies should focus on the experimental design of rs-fMRI as a way to observe the long-lasting therapeutic effects of acupuncture on MCI in the real world.

Limitations

Although this review provides an SDM-PSI-based meta-analysis of current MRI studies of acupuncture for MCI, there are still some limitations. First, all of the literature that met the inclusion criteria was conducted in China in this study. The language of publication included only Chinese and English, which may lead to potential publication bias and reduce the applicability and readability of this study. Although our search strategy appears to be comprehensive, the possibility of relevant literature appearing in other databases cannot be excluded. The high level of the review emphasizes the need for multi-center studies that especially considering the apparent heterogeneity of social backgrounds between countries (Ewers et al., 2015). Future studies should consider the need for multicenter studies in which language, country, region, and other influencing factors are taken into account to expand treatment coverage. Second, due to the small sample size of the included studies, there is significant heterogeneity between studies in terms of acupuncture point selection, clinical protocol design, and analytical methods, which significantly reduces the credibility of the findings. Given the financial burden and additional limitations of neuroimaging studies, small samples are standard, which can lead to low statistical power and may obscure essential results that may be clinically significant (Moayedi et al., 2018). Therefore, more rigorous randomized controlled trials with large samples should be designed to avoid confounding factors and methodological bias in future clinical trials.

In order to make the findings more reproducible and accurate and to precisely elucidate the mechanisms of brain region regulation in acupuncture for MCI, larger sample sizes of RCTs are needed in the future. When designing and reporting MRI for acupuncture studies, investigators should follow the Standards for Reporting Interventions in Controlled Trials of Acupuncture (STRICTA) guidelines (MacPherson et al., 2010). Standardized clinical treatment protocols should be developed around six regions: the theoretical rationale for acupuncture, details of acupuncture measures, treatment protocols, ancillary interventions, acupuncturist credentials, and control interventions. Third, most of the studies did not specify the specific implementation of blinding and allocation concealment in the clinical trial design, which exposes the results to a certain degree of risk of methodological bias. In addition, most of the studies had healthy controls, making it difficult to exclude the placebo effect of acupuncture or other factors from interfering. Future studies should design rigorous scientific RCTs with sham acupuncture placebo controls to increase the reliability of MRI mechanism studies. In subsequent clinical designs, the design of sham acupuncture groups should be standardized, and more standard implementation guidelines should be adopted for appliance selection, baseline patient characteristics, and effect determination to maximize the actual therapeutic effect of acupuncture (Birch et al., 2022). Fourth, adverse events during acupuncture treatment and MRI acquisition were not reported in any studies. We suggest that in future studies and reporting on the primary outcome, clinical changes and adverse events during treatment should be monitored simultaneously to provide comprehensive standardized clinical guidelines for neuroimaging studies.

Future outlook of acupuncture for MCI

Early screening for MCI is generally performed through cognitive assessments, such as the Montreal Cognitive Assessment (MoCA), MMSE, etc (Gauthier et al., 2006). However, the accuracy of MCI diagnosis is compromised by the highly subjective nature of cognitive assessment and its low sensitivity to early identification of MCI and dementia. Some studies in which neuroimaging may help determine the etiology and prognosis of MCI suggest that structural magnetic resonance imaging (MRI), Fludeoxyglucose PET, and other neuroimaging may help identify people with MCI and those at high risk of progressing from MCI to dementia (Langa and Levine, 2014). Most recently, PET imaging of the extent of Aβ plaques in the brain has become more feasible with the radiopharmaceutical tracer florbetapir (Clark et al., 2011). Currently, amyloid A (Chen et al., 2021). Likewise, the efficacy and effectiveness of acupuncture can be evaluated similarly. In addition to the use of MRI to investigate the central mechanisms of acupuncture, quantitative analysis of efficacy can be performed using biomarkers based on PET technology. In addition, indicators of cognitive function, functional status, medications, neurological or psychiatric abnormalities, and laboratory tests are combined to distinguish MCI from normal aging or dementia and identify possible forms of mild cognitive impairment caused by other conditions. Older adults fear cognitive decline, and most patients prefer testing that would indicate future Alzheimer's disease risk (Wikler et al., 2013). Clinical prediction and management of MCI may become a hot topic in the future as diagnostic techniques change. Recently, Yang et al. developed a clinical prediction model for acupuncture treatment in patients recovering from stroke under different conditions by standardizing acupuncture treatment

in 1,410 patients recovering from a stroke, combined with CART decision tree analysis, to provide a tool for predicting the effect of acupuncture treatment (Burge et al., 2014). Regarding the prediction model of MCI, the current research directions are primarily focused on the conversion of mild cognitive impairment to Alzheimer's disease. For example, Huang et al., based on the Least Absolute contraction and Selection Operator (LASSO), which provides a personalized MCI to AD, found significant associations between neuropsychological scores, cortical features, Aβ levels, and underlying genetic pathways (Huang et al., 2020). The above study shows that the establishment of a neuroimaging-based prediction model can guide clinical diagnosis and provide an objective reference for the assessment of the efficacy of acupuncture in the treatment of MCI and contribute to the development of personalized treatment. In addition, the prediction of acupuncture response can reduce the medical costs for patients identified as likely non-responders. Future research can start from the prediction model of acupuncture for MCI and integrate machine learning algorithms better to explain the neuroimaging mechanism of acupuncture for MCI.

Conclusion

A ReHo-based meta-analysis showed that acupuncture has potential modulatory effects on MCI in brain regions, suggesting that the left anterior cingulate/paracingulate gyrus, right insula, right thalamus, right middle frontal gyrus, right median cingulate/paracingulate gyri, and right middle temporal gyrus may be the precise brain region response targets of acupuncture for MCI. In particular, activity was significantly increased in the left anterior cingulate/paracingulate gyrus and the right insula. The MCI group showed stronger activity in the right supramarginal gyrus after acupuncture treatment compared to healthy controls. The above study provides a new perspective to elucidate the role of brain region modulation in acupuncture for MCI. In the future, guidelines and procedures should be followed to conduct large-scale rigorous randomized controlled trials to ensure the validity of future clinical evidence.

Data availability statement

The original contributions presented in the study are included in the article/Supplementary material, further inquiries can be directed to the corresponding author/s.

Author contributions

SM and HH designed the entire study and wrote the manuscript. ZZ and HZ screened the study for inclusion in the study. ML and LY performed the data extraction. SM and BY were involved in the analysis of the data. HW made good suggestions for the article. All authors read and approved the final manuscript.

Funding

This work was supported by National Natural Science Foundation of China (Grant No. 82074548).

Acknowledgments

We thank Yunzhou Shi from Chengdu University of Traditional Chinese Medicine for his contribution to this article. We also thank Xiangrui Zeng of Yanshan University for his contribution to this paper.

Conflict of interest

The authors declare that the research was conducted in the absence of any commercial or financial relationships that could be construed as a potential conflict of interest.

Publisher's note

Supplementary material

The Supplementary Material for this article can be found online at: https://www.frontiersin.org/articles/10.3389/fnagi.2022.914049/full#supplementary-material

References

Albajes-Eizagirre, A., and Radua, J. (2018). What do results from coordinate-based meta-analyses tell us? *Neuroimage* 176, 550–553. doi: 10.1016/j.neuroimage.2018.04.065

Albajes-Eizagirre, A., Solanes, A., Fullana, M. A., Ioannidis, J. P. A., Fusar-Poli, P., Torrent, C., et al. (2019a). Meta-analysis of voxel-based neuroimaging studies using seed-based d mapping with permutation of subject images (Sdm-psi). *J. Vis. Exp.* 153. doi: 10.3791/59841

Albajes-Eizagirre, A., Solanes, A., and Radua, J. (2019b). Meta-analysis of non-statistically significant unreported effects. *Stat. Methods Med. Res.* 28, 3741–3754. doi: 10.1177/0962280218811349

Albajes-Eizagirre, A., Solanes, A., Vieta, E., and Radua, J. (2019c). Voxel-based meta-analysis via permutation of subject images (PSI): theory and implementation for SDM. *Neuroimage* 186, 174–184. doi: 10.1016/j.neuroimage.2018.10.077

Apps, M. A. J., Rushworth, M. F. S., and Chang, S. W. C. (2016). The anterior cingulate gyrus and social cognition: tracking the motivation of others. *Neuron* 90, 692–707. doi: 10.1016/j.neuron.2016.04.018

Argiris, G., Stern, Y., and Habeck, C. (2021). Quantifying age-related changes in brain and behavior: a longitudinal versus cross-sectional approach. *eNeuro* 8, ENEURO.0273-21.2021. doi: 10.1523/ENEURO.0273-21.2021

Bai, L., Qin, W., Tian, J., Liu, P., Li, L., Chen, P., et al. (2009). Time-varied characteristics of acupuncture effects in fMRI studies. *Hum. Brain Mapp.* 30, 3445–3460. doi: 10.1002/hbm.20769

Bai, L., Tian, J., Zhong, C., Xue, T., and you, Y., Liu, Z., et al. (2010). Acupuncture modulates temporal neural responses in wide brain networks: Evidence from fMRI study. *Mol. Pain*. 6, 73–73. doi: 10.1186/1744-8069-6-73

Baiano, C., Barone, P., Trojano, L., and Santangelo, G. (2020). Prevalence and clinical aspects of mild cognitive impairment in Parkinson's disease: a meta-analysis. *Mov. Disord.* 35, 45–54. doi: 10.1002/mds.27902

Beach, P. A., Huck, J. T., Miranda, M. M., Foley, K. T., and Bozoki, A. C. (2016). Effects of Alzheimer disease on the facial expression of pain. *Clin. J. Pain*. 32, 478–487. doi: 10.1097/AJP.0000000000000302

Beason-Held, L. L., Shafer, A. T., Goh, J. O., Landman, B. A., Davatzikos, C., Viscomi, B., et al. (2021). Hippocampal activation and connectivity in the aging brain. *Brain Imaging Behav.* 15, 711–726. doi: 10.1007/s11682-020-00279-6

Birch, S., Lee, M. S., Kim, T. H., and Alraek, T. (2022). Historical perspectives on using sham acupuncture in acupuncture clinical trials. *Integr. Med. Res.* 11, 100725. doi: 10.1016/j.imr.2021.100725

Briggs, R. G., Lin, Y. H., Dadario, N. B., Kim, S. J., Young, I. M., Bai, M. Y., et al. (2021). Anatomy and white matter connections of the middle frontal gyrus. *World Neurosurg.* 150, e520–e529. doi: 10.1016/j.wneu.2021.03.045

Burge, D. L., Boucherle, G., Sarbacker, S. R., Singleton, M., Goldberg, E., Waghorne, J. P., et al. (2014). *Yoga and Kabbalah as World Religions? A Comparative Perspective on Globalization of Religious Resources*. Beersheba: Ben Gurion University of the Negev Press, 233–250.

Bush, G., Luu, P., and Posner, M. I. (2000). Cognitive and emotional influences in anterior cingulate cortex. *Trends Cogn. Sci.* 4, 215–222. doi: 10.1016/S1364-6613(00)01483-2

Carter, C. S., Heckers, S., Nichols, T., Pine, D. S., and Strother, S. (2008). Optimizing the design and analysis of clinical functional magnetic resonance imaging research studies. *Biol. Psychiatry*. 64, 842–849. doi: 10.1016/j.biopsych.2008.06.014

Cauda, F., Torta, D. M. E., Sacco, K., Geda, E., D'Agata, F., Costa, T., et al. (2012). Shared "core" areas between the pain and other task-related networks. *PLoS ONE* 7, e41929. doi: 10.1371/journal.pone.0041929

Chae, Y. (2017). The dilemma of placebo needles in acupuncture research. *Acupunct. Med.* 35, 382–383. doi: 10.1136/acupmed-2017-011394

Chae, Y., Lee, H., Kim, H., Kim, C. H., Chang, D., Kim, K. M., et al. (2009). Parsing brain activity associated with acupuncture treatment in Parkinson's diseases. *Mov. Disord.* 24, 1794–1802. doi: 10.1002/mds.22673

Chang, A., Jones-hagata, L. B., Ortega, B. N., Galatzer-levy, I., Fox, P. T., and Etkin, A. (2016). Identification of a common neurobiological substrate for mental illness. *JAMA Psychiatry* 72, 305–315. doi: 10.1001/jamapsychiatry.2014.2206

Chang, C. M., Yang, C. P., Yang, C. C., Shih, P. H., and Wang, S. J. (2021). Evidence of potential mechanisms of acupuncture from functional MRI data for migraine prophylaxis. *Curr. Pain Headache Rep.* 25, 49. doi: 10.1007/s11916-021-00961-4

Chen, J., Wang, J., Huang, Y., Lai, X., Tang, C., Yang, J., et al. (2014a). Modulatory effect of acupuncture at Waiguan (TE5) on the functional connectivity of the central nervous system of patients with ischemic stroke in the left basal ganglia. *PLoS ONE* 9, e96777. doi: 10.1371/journal.pone.0096777

Chen, J., Xu, Y., Zhang, K., Liu, Z., Xu, C., Shen, Y., et al. (2013). Comparative study of regional homogeneity in schizophrenia and major depressive disorder. *Am. J. Med. Genet. Part B Neuropsychiatr. Genet.* 162B, 36–43. doi: 10.1002/ajmg.b.32116

Chen, S. J., Xu, M. S., Li, H., Liang, J. P., Yin, L., Liu, X., et al. (2014b). Acupuncture at the Taixi (KI3) acupoint activates cerebral neurons in elderly patients with mild cognitive impairment. *Neural Regen. Res.* 9, 1163–1168. doi: 10.4103/1673-5374.135319

Chen, Y. R., Liang, C. S., Chu, H., Voss, J., Kang, X. L., O'Connell, G., et al. (2021). Diagnostic accuracy of blood biomarkers for Alzheimer's disease and amnestic mild cognitive impairment: a meta-analysis. *Ageing Res. Rev.* 71, 101446. doi: 10.1016/j.arr.2021.101446

Cho, Z. H., Chung, S. C., Jones, J. P., Park, J. B., Park, H. J., Lee, H. J., et al. (1998). New findings of the correlation between acupoints and corresponding brain cortices using functional MRI. *Proc. Natl. Acad. Sci. U. S. A.* 95, 2670–2673. doi: 10.1073/pnas.95.5.2670

Christidi, F., Karavasilis, E., Michels, L., Riederer, F., Velonakis, G., Anagnostou, E., et al. (2020). Dimensions of pain catastrophising and specific structural and functional alterations in patients with chronic pain: evidence in medication-overuse headache. *World J. Biol. Psychiatry* 21, 726–738. doi: 10.1080/15622975.2019.1669822

Clark, C. M., Schneider, J. A., Bedell, B. J., Beach, T. G., Bilker, W. B., Mintun, M. A., et al. (2011). Use of florbetapir-PET for imaging [beta]-amyloid pathology. *J. Am. Med. Assoc.* 305, 275–283. doi: 10.1001/jama.2010.2008

Cohn, L. D., and Decker, B. J. (2003). How meta-analysis increases statistical power. *Psychol. Methods* 8, 243–253. doi: 10.1037/1082-989X.8.3.243

Cole, L. J., Farrell, M. J., Duff, E. P., Barber, J. B., Egan, G. F., and Gibson, S. J. (2006). Pain sensitivity and fMRI pain-related brain activity in Alzheimer's disease. *Brain* 129(Pt 11), 2957–2965. doi: 10.1093/brain/awl228

Crossley, N. A., Mechelli, A., Vértes, P. E., Winton-Brown, T. T., Patel, A. X., Ginestet, C. E., et al. (2013). Cognitive relevance of the community structure of the human brain functional coactivation network. *Proc. Natl. Acad. Sci. U. S. A.* 110, 11583–11588. doi: 10.1073/pnas.1220826110

Cui, L., Zhang, Z., Zac Lo, C. Y., and Guo, Q. (2021). Local functional MR change pattern and its association with cognitive function in objectively-defined subtle cognitive decline. *Front. Aging Neurosci.* 13, 684918. doi: 10.3389/fnagi.2021.684918

Dan, B. (2019). Neuroscience underlying rehabilitation: what is neuroplasticity? *Dev. Med. Child Neurol.* 61, 1240.doi: 10.1111/dmcn.14341

De Bourbon-Teles, J., Bentley, P., Koshino, S., Shah, K., Dutta, A., Malhotra, P., et al. (2014). Thalamic control of human attention driven by memory and learning. *Curr. Biol.* 24, 993–999. doi: 10.1016/j.cub.2014.03.024

Defrin, R., Amanzio, M., De Tommaso, M., Dimova, V., Filipovic, S., Finn, D. P., et al. (2015). Experimental pain processing in individuals with cognitive impairment: current state of the science. *Pain* 156, 1396–1408. doi: 10.1097/j.pain.0000000000000195

Delgado-Alvarado, M., Gago, B., Navalpotro-Gomez, I., Jiménez-Urbieta, H., and Rodriguez-Oroz, M. C. (2016). Biomarkers for dementia and mild cognitive impairment in Parkinson's disease. *Mov. Disord.* 31, 861–881. doi: 10.1002/mds.26662

Desmond, J. E., and Glover, G. H. (2002). Estimating sample size in functional MRI (fMRI) neuroimaging studies: statistical power analyses. *J. Neurosci. Methods*. 118, 115–128. doi: 10.1016/S0165-0270(02)00121-8

Dilts, J. J., Esparham, A., Boorigie, M., Connelly, M., and Bickel, J. (2021). Development and assessment of a basic acupuncture curriculum for pediatricians. *Acad. Pediatr.* 22, 160–165. doi: 10.1016/j.acap.2021.08.011

Ding, N., Jiang, J., Xu, A., Tang, Y., and Li, Z. (2019). Manual acupuncture regulates behavior and cerebral blood flow in the SAMP8 mouse model of Alzheimer's disease. *Front. Neurosci.* 13, 37. doi: 10.3389/fnins.2019.00037

Dong, Q. Y., Li, T. R., Jiang, X. Y., Wang, X. N., Han, Y., and Jiang, J. H. (2021). Glucose metabolism in the right middle temporal gyrus could be a potential biomarker for subjective cognitive decline: a study of a Han population. *Alzheimers Res. Ther.* 13, 74. doi: 10.1186/s13195-021-00811-w

Du, S. Q., Wang, X. R., Zhu, W., Ye, Y., Yang, J. W., Ma, S. M., et al. (2018). Acupuncture inhibits TXNIP-associated oxidative stress and inflammation to attenuate cognitive impairment in vascular dementia rats. *CNS Neurosci. Ther.* 24, 39–46. doi: 10.1111/cns.12773

Enck, P., Benedetti, F., and Schedlowski, M. (2008). New insights into the placebo and nocebo responses. *Neuron* 59, 195–206. doi: 10.1016/j.neuron.2008.06.030

Ewers, M., Mattsson, N., Minthon, L., Molinuevo, J. L., Antonell, A., Popp, J., et al. (2015). CSF biomarkers for the differential diagnosis of Alzheimer's disease: a large-scale international multicenter study. *Alzheimers Dement.* 11, 1306–1315. doi: 10.1016/j.jalz.2014.12.006

Feng, Q., Wang, M., Song, Q., Wu, Z., Jiang, H., Pang, P., et al. (2019). Correlation between hippocampus MRI radiomic features and resting-state intrahippocampal functional connectivity in Alzheimer's disease. *Front. Neurosci.* 13, 435. doi: 10.3389/fnins.2019.00435

Feng, Y., Bai, L., Ren, Y., Chen, S., Wang, H., Zhang, W., et al. (2012). FMRI connectivity analysis of acupuncture effects on the whole brain network in mild cognitive impairment patients. *Magn. Reson. Imaging.* 30, 672–682. doi: 10.1016/j.mri.2012.01.003

Gauthier, S., Reisberg, B., Zaudig, M., Petersen, R. C., Ritchie, K., Broich, K., et al. (2006). Mild cognitive impairment. *Lancet* 367, 1262–1270. doi: 10.1016/S0140-6736(06)68542-5

Geuter, S., Koban, L., and Wager, T. D. (2017). The cognitive neuroscience of placebo effects: concepts, predictions, and physiology. *Annu. Rev. Neurosci.* 40, 167–188. doi: 10.1146/annurev-neuro-072116-031132

Gøtzsche, P. C. (1994). Is there logic in the placebo? *Lancet* 344, 925–926. doi: 10.1016/S0140-6736(94)92273-X

Guo, Q., Thabane, L., Hall, G., McKinnon, M., Goeree, R., and Pullenayegum, E. (2014). A systematic review of the reporting of sample size calculations and corresponding data components in observational functional magnetic resonance imaging studies. *Neuroimage* 86, 172–181. doi: 10.1016/j.neuroimage.2013.08.012

Henderson, L. A., Gandevia, S. C., and Macefield, V. G. (2007). Somatotopic organization of the processing of muscle and cutaneous pain in the left and right insula cortex: a single-trial fMRI study. *Pain* 128, 20–30. doi: 10.1016/j.pain.2006.08.013

Hou, X., Zhang, Y., Liu, M., and Zhou, L.(2010). Effect of acupuncture on functional magnetic resonance of mild cognitive impairment in cerebral white matter osteoporosis. *World J. Integr. Med.* 2, 122–125. doi: 10.13935/j.cnki.sjzx.2010.02.009

Huang, K., Lin, Y., Yang, L., Wang, Y., Cai, S., Pang, L., et al. (2020). A multipredictor model to predict the conversion of mild cognitive impairment to Alzheimer's disease by using a predictive nomogram. *Neuropsychopharmacology* 45, 358–366. doi: 10.1038/s41386-019-0551-0

Hui, K. K. S., Liu, J., Makris, N., Gollub, R. L., Chen, A. J. W., Moore, C. I., et al. (2000). Acupuncture modulates the limbic system and subcortical gray structures of the human brain: evidence from fMRI studies in normal subjects. *Hum. Brain Mapp.* 9, 13–25. doi: 10.1002/(SICI)1097-0193(2000)9:1<13::AID-HBM2>3.0.CO;2-F

Hwang, K., Bertolero, M. A., Liu, W. B., and D'Esposito, M. (2017). The human thalamus is an integrative hub for functional brain networks. *J. Neurosci.* 37, 5594–5607. doi: 10.1523/JNEUROSCI.0067-17.2017

Jensen-Dahm, C., Werner, M. U., Dahl, J. B., Jensen, T. S., Ballegaard, M., Hejl, A. M., et al. (2014). Quantitative sensory testing and pain tolerance in patients with mild to moderate Alzheimer disease compared to healthy control subjects. *Pain* 155, 1439–1445. doi: 10.1016/j.pain.2013.12.031

Ji, S., Zhang, H., Qin, W., Liu, M., Zheng, W., Han, Y., et al. (2021). Effect of acupuncture stimulation of Hegu (LI4) and Taichong (LR3) on the resting-state networks in Alzheimer's Disease: beyond the default mode network. *Neural Plast.* 2021, 8876873. doi: 10.1155/2021/8876873

Jia, B., Liu, Z., Min, B., Wang, Z., Zhou, A., Li, Y., et al. (2015). The effects of acupuncture at real or sham acupoints on the intrinsic brain activity in mild cognitive impairment patients. *Evid Based Comp. Altern. Med.* 2015, 529675. doi: 10.1155/2015/529675

Jia, L., Du, Y., Chu, L., Zhang, Z., Li, F., Lyu, D., et al. (2020). Prevalence, risk factors, and management of dementia and mild cognitive impairment in adults aged 60 years or older in China: a cross-sectional study. *Lancet Public Health* 5, e661–e671. doi: 10.1016/S2468-2667(20)30185-7

Jiang, C., Cui, S., Nie, B., Tang, C., and Zhang, J. (2012). Effect of needling taixi (KI3) acupoint and sham point on functional magnetic resonance imaging in mild cognitive impairment patients. *J. New Chin. Med.* 1, 93–95. doi: 10.13457/j.cnki.jncm.2012.01.033

Jiang, G., Yin, X., Li, C., Li, L., Zhao, L., Evans, A. C., et al. (2015). The plasticity of brain gray matter and white matter following lower limb amputation. *Neural Plast.* 2015, 823185. doi: 10.1155/2015/823185

Jiang, J., Zhao, Y. J., Hu, X. Y., Du, M. Y., Chen, Z. Q., Wu, M., et al. (2017). Microstructural brain abnormalities in medication-free patients with major depressive disorder: a systematic review and meta-analysis of diffusion tensor imaging. *J. Psychiatry Neurosci.* 42, 150–163. doi: 10.1503/jpn.150341

Jiang, L., and Zuo, X. N. (2016). Regional homogeneity: a multimodal, multiscale neuroimaging marker of the human connectome. *Neuroscientist* 22, 486–505. doi: 10.1177/1073858415595004

Jiao, Z., Gao, P., Ji, Y., and Shi, H. (2021). Integration and segregation of dynamic functional connectivity states for mild cognitive impairment revealed by graph theory indicators. *Contrast Media Mol. Imaging.* 2021, 6890024. doi: 10.1155/2021/6890024

Jozwiak, N., Postuma, R. B., Montplaisir, J., Latreille, V., Panisset, M., Chouinard, S., et al. (2017). Rem sleep behavior disorder and cognitive impairment in parkinson's disease. *Sleep* 40, zsx101. doi: 10.1093/sleep/zsx101

Kalin, N. H. (2021). Understanding the value and limitations of MRI neuroimaging in psychiatry. *Am. J. Psychiatry.* 178, 673–676. doi: 10.1176/appi.ajp.2021.21060616

Kim, H., Kim, H. K., Kim, S. Y., Kim, Y., Il, Y.oo, H. R., and Jung, I. C. (2019). Cognitive improvement effects of electro-acupuncture for the treatment of MCI compared with Western medications: a systematic review and meta-analysis 11 medical and health sciences 1103 clinical sciences. *BMC Compl. Altern. Med.* 19, 13. doi: 10.1186/s12906-018-2407-2

Klingberg, T., O'Sullivan, B. T., and Roland, P. E. (1997). Bilateral activation of fronto-parietal networks by incrementing demand in a working memory task. *Cereb. Cortex.* 7, 465–471. doi: 10.1093/cercor/7.5.465

Kordower, J. H., Chu, Y., Stebbins, G. T., Dekosky, S. T., Cochran, E. J., Bennett, D., et al. (2001). Loss and atrophy of layer II entorhinal cortex neurons in elderly people with mild cognitive impairment. *Ann. Neurol.* 49, 202–213. doi: 10.1002/1531-8249(20010201)49:2<202::AID-ANA40>3.0.CO;2-3

Kunz, M., Mylius, V., Scharmann, S., Schepelman, K., and Lautenbacher, S. (2009). Influence of dementia on multiple components of pain. *Eur. J. Pain* 13, 317–325. doi: 10.1016/j.ejpain.2008.05.001

Kunz, M., Scharmann, S., Hemmeter, U., Schepelmann, K., and Lautenbacher, S. (2007). The facial expression of pain in patients with dementia. *Pain* 133, 221–228. doi: 10.1016/j.pain.2007.09.007

Lan, L., Gao, Y. J., Zeng, F., Qin, W., Dong, M. K., Liu, M. L., et al. (2013). A central analgesic mechanism of acupuncture for migraine: An ongoing functional MRI study. *Neural Regen. Res.* 8, 2649–2655. doi: 10.3969/j.issn.1673-5374.2013.28.007

Langa, K. M., and Levine, D. A. (2014). The diagnosis and management of mild cognitive impairment: a clinical review. *J. Am. Med. Assoc.* 312, 2551–2561. doi: 10.1001/jama.2014.13806

Lau, W. K. W., Leung, M. K., Lee, T. M. C., and Law, A. C. K. (2016). Resting-state abnormalities in amnestic mild cognitive impairment: a meta-analysis. *Transl. Psychiatry* 6, e790. doi: 10.1038/tp.2016.55

Lautenbacher, S., Hoos, A., Hajak, G., Trapp, W., and Kunz, M. (2021). Pain processing in cognitive impairment and its association with executive function and memory: which neurocognitive factor takes the lead? *Brain Sci.* 11, 1319. doi: 10.3390/brainsci11101319

Lee, I. S., Necka, E. A., and Atlas, L. Y. (2020). Distinguishing pain from nociception, salience, and arousal: how autonomic nervous system activity can improve neuroimaging tests of specificity. *Neuroimage* 204, 116254. doi: 10.1016/j.neuroimage.2019.116254

Leung, A., Zhao, Y., and Shukla, S. (2014). The effect of acupuncture needle combination on central pain processing-an fMRI study. *Mol. Pain* 10, 23. doi: 10.1186/1744-8069-10-23

Li, M. G., Liu, T. F., Zhang, T. H., Chen, Z. Y., Nie, B. B., Lou, X., et al. (2020). Alterations of regional homogeneity in Parkinson's disease with mild cognitive impairment: a preliminary resting-state fMRI study. *Neuroradiology* 62, 327–334. doi: 10.1007/s00234-019-02333-7

Liberati, A., Altman, D. G., Tetzlaff, J., Mulrow, C., Gøtzsche, P. C., Ioannidis, J. P. A., et al. (2009). The PRISMA statement for reporting systematic reviews and meta-analyses of studies that evaluate healthcare interventions: explanation and elaboration. *BMJ* 339, b2700. doi: 10.1136/bmj.b2700

Liu, P., Qin, W., Zhang, Y., Tian, J., Bai, L., Zhou, G., et al. (2009). Combining spatial and temporal information to explore function-guide action of acupuncture using fMRI. *J. Magn. Reson. Imaging* 30, 41–46. doi: 10.1002/jmri.21805

Liu, Y., Wang, K., YU, C., He, Y., Zhou, Y., Liang, M., et al. (2008). Regional homogeneity, functional connectivity and imaging markers of Alzheimer's disease: a review of resting-state fMRI studies. *Neuropsychologia* 46, 1648–1656. doi: 10.1016/j.neuropsychologia.2008.01.027

Liu, Z., Wei, W., Bai, L., Dai, R., You, B., Chen, S., et al. (2014). Exploring the patterns of acupuncture on mild cognitive impairment patients using regional homogeneity. *PLoS ONE* 9, e99335. doi: 10.1371/journal.pone.0099335

MacPherson, H., Altman, D. G., Hammerschlag, R., Youping, L., Taixiang, W., White, A., et al. (2010). Revised STandards for Reporting Interventions in Clinical Trials of Acupuncture (STRICTA): extending the CONSORT statement. *J. Evid. Based Med.* 3, 140–155. doi: 10.1111/j.1756-5391.2010.01086.x

Marshall, G. A., Rentz, D. M., Frey, M. T., Locascio, J. J., Johnson, K. A., and Sperling, R. A. (2011). Executive function and instrumental activities of daily living in mild cognitive impairment and Alzheimer's disease. *Alzheimers Dement.* 7, 300–308. doi: 10.1016/j.jalz.2010.04.005

Min, J., Zhou, X. X., Zhou, F., Tan, Y., and Wang, W. D. (2019). A study on changes of the resting-state brain function network in patients with amnestic mild cognitive impairment. *Braz. J. Med. Biol. Res.* 52, e8244. doi: 10.1590/1414-431x20198244

Moayedi, M., Salomons, T. V., and Atlas, L. Y. (2018). Pain neuroimaging in humans: a primer for beginners and non-imagers. *J. Pain* 19, 961.e1–961.e21. doi: 10.1016/j.jpain.2018.03.011

Moffet, H. H. (2009). Sham acupuncture may be as efficacious as true acupuncture: a systematic review of clinical trials. *J. Altern. Comp. Med.* 15, 213–216. doi: 10.1089/acm.2008.0356

Moher, D., Liberati, A., Tetzlaff, J., Altman, D. G., Altman, D., Antes, G., et al. (2009). Preferred reporting items for systematic reviews and meta-analyses: the PRISMA statement. *PLoS Med.* 6, e1000097. doi: 10.1371/journal.pmed.1000097

Montero-Odasso, M. M., Sarquis-Adamson, Y., Speechley, M., Borrie, M. J., Hachinski, V. C., Wells, J., et al. (2017). Association of dual-task gait with incident dementia in mild cognitive impairment: Results from the gait and brain study. *JAMA Neurol.* 74, 857–865. doi: 10.1001/jamaneurol.2017.0643

Mufson, E. J., Binder, L., Counts, S. E., Dekosky, S. T., Detoledo-Morrell, L., Ginsberg, S. D., et al. (2012). Mild cognitive impairment: pathology and mechanisms. *Acta Neuropathol.* 123, 13–30. doi: 10.1007/s00401-011-0884-1

Mumford, J. A., and Nichols, T. E. (2008). Power calculation for group fMRI studies accounting for arbitrary design and temporal autocorrelation. *Neuroimage* 39, 261–268. doi: 10.1016/j.neuroimage.2007.07.061

Murphy, K., and Garavan, H. (2004). An empirical investigation into the number of subjects required for an event-related fMRI study. *Neuroimage* 22, 879–885. doi: 10.1016/j.neuroimage.2004.02.005

Namkung, H., Kim, S.-H., and Sawa, A. (2018). The insula: an underestimated brain area in clinical neuroscience, psychiatry, and neurology. *Trends Neurosci.* 40, 200–207. doi: 10.1016/j.tins.2017.02.002

Page, M. J., McKenzie, J. E., Bossuyt, P. M., Boutron, I., Hoffmann, T. C., Mulrow, C. D., et al. (2021). The PRISMA 2020 statement: an updated guideline for reporting systematic reviews. *J. Clin. Epidemiol.* 134, 178–189. doi: 10.1016/j.jclinepi.2021.03.001

Petersen, R. C. (2011). Clinical practice mild cognitive impairment. *N. Engl. J. Med.* 364, 2227–2234. doi: 10.1056/NEJMcp0910237

Petersen, R. C., Lopez, O., Armstrong, M. J., Getchius, T. S. D., Ganguli, M., Gloss, D., et al. (2018). Author response: practice guideline update summary: Mild cognitive impairment: Report of the Guideline Development, Dissemination, and Implementation Subcommittee of the American Academy of Neurology. *Neurology* 91, 373–374. doi: 10.1212/WNL.0000000000006042

Radua, J., Mataix-Cols, D., Phillips, M. L., El-Hage, W., Kronhaus, D. M., Cardoner, N., et al. (2012). A new meta-analytic method for neuroimaging studies that combines reported peak coordinates and statistical parametric maps. *Eur. Psychiatry* 27, 605–611. doi: 10.1016/j.eurpsy.2011.04.001

Risacher, S. L., and Saykin, A. J. (2021). Neuroimaging advances in neurologic and neurodegenerative diseases. *Neurotherapeutics* 18, 659–660. doi: 10.1007/s13311-021-01105-7

Robbins, T. W., and Cools, R. (2014). Cognitive deficits in Parkinson's disease: a cognitive neuroscience perspective. *Mov. Disord.* 29, 597–607. doi: 10.1002/mds.25853

Saalmann, Y. B., Pinsk, M. A., Wang, L., Li, X., and Kastner, S. (2012). The pulvinar regulates information transmission between cortical areas based on attention demands. *Science* 337, 753–756. doi: 10.1126/science.1223082

Salthouse, T. A. (2019). Trajectories of normal cognitive aging. *Psychol. Aging* 34, 17–24. doi: 10.1037/pag0000288

Shan, Y., Wang, J. J., Wang, Z. Q., Zhao, Z. L., Zhang, M., Xu, J. Y., et al. (2018). Neuronal specificity of acupuncture in Alzheimer's Disease and mild cognitive impairment patients: a functional MRI study. *Evid Based Comp. Altern. Med.* 2018, 7619197. doi: 10.1155/2018/7619197

Shang, S., Zhang, H., Feng, Y., Wu, J., Dou, W., Chen, Y. C., et al. (2021). Region-specific neurovascular decoupling associated with cognitive decline in Parkinson's Disease. *Front. Aging Neurosci.* 13, 770528. doi: 10.3389/fnagi.2021.770528

Smith, M. L., Asada, N., and Malenka, R. C. (2021). Anterior cingulate inputs to nucleus accumbens control the social transfer of pain and analgesia. *Science* 371, 153–159. doi: 10.1126/science.abe3040

Song, Y., Xu, W., Chen, S., Hu, G., Ge, H., Xue, C., et al. (2021). Functional MRI-specific alterations in salience network in mild cognitive impairment: an ALE meta-analysis. *Front. Aging Neurosci.* 13, 695210. doi: 10.3389/fnagi.2021.695210

Sterzer, P., Stadler, C., Poustka, F., and Kleinschmidt, A. (2007). A structural neural deficit in adolescents with conduct disorder and its association with lack of empathy. *Neuroimage* 37, 335–342. doi: 10.1016/j.neuroimage.2007.04.043

Su, X. T., Sun, N., Zhang, N., Wang, L. Q., Zou, X., Li, J. L., et al. (2021). Effectiveness and safety of acupuncture for vascular cognitive impairment: a systematic review and meta-analysis. *Front. Aging Neurosci.* 13, 692508. doi: 10.3389/fnagi.2021.692508

Tan, T. T., Wang, D., Huang, J. K., Zhou, X. M., Yuan, X., Liang, J. P., et al. (2017). Modulatory effects of acupuncture on brain networks in mild cognitive impairment patients. *Neural Regen. Res.* 12, 250–258. doi: 10.4103/1673-5374.200808

Ulloa, L. (2021). Electroacupuncture activates neurons to switch off inflammation. *Nature*. 598, 573–574. doi: 10.1038/d41586-021-02714-0

Vandenberghe, R., Price, C., Wise, R., Josephs, O., and Frackowiak, R. S. J. (1996). Functional anatomy of a common semantic system for words and pictures. *Nature* 383, 254–256. doi: 10.1038/383254a0

Vartanian, O., Kwantes, P. J., Mandel, D. R., Bouak, F., Nakashima, A., Smith, I., et al. (2013). Right inferior frontal gyrus activation as a neural marker of successful lying. *Front. Hum. Neurosci.* 7, 616. doi: 10.3389/fnhum.2013.00616

Wager, T. D., and Atlas, L. Y. (2015). The neuroscience of placebo effects: connecting context, learning and health. *Nat. Rev. Neurosci.* 16, 403–418. doi: 10.1038/nrn3976

Walach, H., and Loef, M. (2015). Using a matrix-analytical approach to synthesizing evidence solved incompatibility problem in the hierarchy of evidence. *J. Clin. Epidemiol.* 68, 1251–1260. doi: 10.1016/j.jclinepi.2015.03.027

Wang, F., Wei, S., Li, X., Cao, D., Zhang, K., Liu, X., et al. (2020). Resting-state fMRI study of the brain in patients with mild cognitive impairment treated with acupuncture. *Magn. Resonan. Imag.* 2, 94–98.

Wang, Z., Nie, B., Li, D., Zhao, Z., Han, Y., Song, H., et al. (2012). Effect of acupuncture in mild cognitive impairment and Alzheimer disease: a functional MRI study. *PLoS ONE* 7, e42730. doi: 10.1371/journal.pone.0042730

Wikler, E. M., Blendon, R. J., and Benson, J. M. (2013). Would you want to know? Public attitudes on early diagnostic testing for Alzheimer's disease. *Alzheimers Res. Ther.* 5, 43. doi: 10.1186/alzrt206

Wolff, M., and Vann, S. D. (2019). The cognitive thalamus as a gateway to mental representations. *J. Neurosci.* 39, 3–14. doi: 10.1523/JNEUROSCI.0479-18.2018

Wu, P., Zhou, Y. M., Liao, C. X., Tang, Y. Z., Li, Y. X., Qiu, L. H., et al. (2018). Structural changes induced by acupuncture in the recovering brain after ischemic stroke. *Evid. Based Comp. Altern. Med.* 2018, 5179689. doi: 10.1155/2018/5179689

Yeo, S., Van Den Noort, M., Bosch, P., and Lim, S. (2018). A study of the effects of 8-week acupuncture treatment on patients with Parkinson's disease. *Medicine* 97, e13434. doi: 10.1097/MD.0000000000013434

Yin, L., Reuter, M., and Weber, B. (2016). Let the man choose what to do: Neural correlates of spontaneous lying and truth-telling. *Brain Cogn.* 102, 13–25. doi: 10.1016/j.bandc.2015.11.007

Yin, W., Lv, G., Li, C., and Sun, J. (2021). Acupuncture therapy for Alzheimer's disease: the effectiveness and potential mechanisms. *Anat. Rec.* 304, 2397–2411. doi: 10.1002/ar.24780

Yu, S. W., Lin, S. H., Tsai, C. C., Chaudhuri, K. R., Huang, Y. C., Chen, Y. S., et al. (2019). Acupuncture effect and mechanism for treating pain in patients with parkinson's disease. *Front. Neurol.* 10, 1114. doi: 10.3389/fneur.2019.01114

Zabor, E. C., Kaizer, A. M., and Hobbs, B. P. (2020). Randomized controlled trials. *Chest* 158, S79–S87. doi: 10.1016/j.chest.2020.03.013

Zhang, J., Zheng, Y., Wang, Y., Qu, S., Zhang, S., Wu, C., et al. (2016). Evidence of a synergistic effect of acupoint combination: a resting-state functional magnetic resonance imaging study. *J. Altern. Comp. Med.* 22, 800–809. doi: 10.1089/acm.2016.0016

Zhi, H., Wang, Y., Chang, S., Pan, P., Ling, Z., Zhang, Z., et al. (2021). Acupuncture can regulate the distribution of lymphocyte subsets and the levels of inflammatory cytokines in patients with mild to moderate vascular dementia. *Front. Aging Neurosci.* 13, 747673. doi: 10.3389/fnagi.2021.747673

frontiers | Frontiers in Aging Neuroscience

TYPE Original Research
PUBLISHED 03 November 2022
DOI 10.3389/fnagi.2022.987891

OPEN ACCESS

EDITED BY
Rachael D. Seidler,
University of Michigan, United States

REVIEWED BY
Joaquin Alberto Anguera,
University of California, San Francisco, United States
Alexandru Iordan,
University of Michigan, United States

*CORRESPONDENCE
Gabriele Cattaneo
gcattaneo@guttmann.com

SPECIALTY SECTION
This article was submitted to Neurocognitive Aging and Behavior, a section of the journal Frontiers in Aging Neuroscience

RECEIVED 18 July 2022
ACCEPTED 10 October 2022
PUBLISHED 03 November 2022

CITATION
Cattaneo G, Pachón-García C, Roca A, Alviarez-Schulze V, Opisso E, García-Molina A, Bartrés-Faz D, Pascual-Leone A, Tormos-Muñoz JM and Solana-Sánchez J (2022) "Guttmann Cognitest"®, preliminary validation of a digital solution to test cognitive performance. Front. Aging Neurosci. 14:987891. doi: 10.3389/fnagi.2022.987891

"Guttmann Cognitest"®, preliminary validation of a digital solution to test cognitive performance

Gabriele Cattaneo[1,2,3]*, Catherine Pachón-García[1,2,3], Alba Roca[1,3,4], Vanessa Alviarez-Schulze[4,5], Eloy Opisso[1,2,3], Alberto García-Molina[1,2,3], David Bartrés-Faz[1,4], Alvaro Pascual-Leone[1,6,7,8], Josep M. Tormos-Muñoz[1,2,3] and Javier Solana-Sánchez[1,2,3]

[1]Institut Guttmann, Institut Universitari de Neurorehabilitació adscrit a la UAB, Barcelona, Spain, [2]Departament de Medicina, Universitat Autònoma de Barcelona, Bellaterra, Spain, [3]Fundació Institut d'Investigació en Ciències de la Salut Germans Trias i Pujol, Barcelona, Spain, [4]Departament de Medicina, Facultat de Medicina i Ciències de la Salut, Universitat de Barcelona, Barcelona, Spain, [5]Departamento de Ciencias del Comportamiento, Escuela de Psicología, Universidad Metropolitana, Caracas, Venezuela, [6]Hinda and Arthur Marcus Institute for Aging Research, Hebrew SeniorLife, Boston, MA, United States, [7]Deanna and Sidney Wolk Center for Memory Health, Hebrew SeniorLife, Boston, MA, United States, [8]Department of Neurology, Harvard Medical School, Boston, MA, United States

Thanks to technological advances, the administration of cognitive assessments *via* digital solutions continues to increase, both in research and clinical practice. "Guttmann Cognitest"® is a digital solution for cognitive assessment which includes seven computerized tasks designed to assess main cognitive functions requiring approximately 20 min to be completed. The purpose of the present study was to validate it against standard and more extensive in-person neuropsychological assessments in the context of the Barcelona Brain Health Initiative (BBHI) cohort study. We studied 274 participants of the BBHI (126 women, mean age = 56.14, age range 44–69), who underwent an extensive in-person assessment, including a classical paper-and-pencil neuropsychological assessment and a cognitive assessment *via* the "Guttmann Cognitest"®. Principal component analysis indicated that "Guttmann Cognitest"® measures four main cognitive domains and convergent validity analysis demonstrated that cognitive performance was associated with gold standard paper and pencil tests. Results also showed an expected negative correlation with age, a relation with educational level as well as a gender effect. Regression-based norming equations for the sample tested are also reported. Performing a cognitive assessment with this digital solution is feasible and potentially useful to gather information about cognitive functioning in large samples and experimental settings.

KEYWORDS

aging, cognitive decline, cognitive functioning, computerized cognitive assessment, memory

Introduction

Age-related cognitive decline is one of the leading public health challenges worldwide (Minghui, 2019). In recent years, an increasing number of studies have tried to find effective strategies to prevent the development of cognitive impairment, dementia, and functional impairment due to Alzheimer's disease and other brain-related pathologies (Amariglio et al., 2015; Cattaneo et al., 2018; Kulmala et al., 2018). A key need towards this goal is the establishment of sensitive, efficient, and accessible cognitive assessments that allow the identification of preclinical stages of diseases and the detection of subtle cognitive changes over time. Alzheimer's disease and other neurodegenerative diseases are preceded by a long preclinical phase and the possibility to detect these cases quickly and accurately could potentially have important implications for quality of life and level of independence. For example, it will allow the implementation of preventive actions (Sternin et al., 2019) to promote resilience to pathological processes (Pascual-Leone and Bartres-Faz, 2021).

However, nowadays many of these cases remain undiagnosed, and the diagnosis of subtle symptoms in primary care is often difficult due to the lack of specially qualified personnel, resources, or optimal tools (Mortamais et al., 2017). In this scenario, mobile technologies may offer an effective solution.

Neuropsychological testing is a widely used and standardized procedure to obtain objective indicators of cognitive functioning, allowing the detection of preclinical stages of dementia (Rentz et al., 2013; Duke Han et al., 2017). Nevertheless, classical neuropsychological testing has specific limitations in terms of costs and time-consumption that make it not suitable for large-scale assessments.

The context of the COVID-19 pandemic, moreover, showed the need to find alternative ways to efficiently explore cognitive functioning, reducing people's mobility and physical contact between clinicians and patients.

As an alternative to in-person classical neuropsychological testing, computerized assessment tools have been developed for years, and the administration of cognitive assessment *via* digital solutions continues to increase both in research and clinical practice (Tierney and Lermer, 2010; De Rover et al., 2011; Koo and Vizer, 2019), with several systems now available (O'Connell et al., 2004; Junkkila et al., 2012; Assmann et al., 2016).

This kind of assessment has been shown to offer many advantages over traditional neuropsychological testing (Zygouris and Tsolaki, 2015; Soldan et al., 2016), including saving costs and time. Moreover these tools could provide an objective and accurate recording of responses, with enhanced overall sensitivity, less dependent on professional expertise or prone to human error, and with the possibility to automatically store and compare a person's performance between assessment sessions to, for example, trigger alerts (Dwolatzky et al., 2003; Wild et al., 2008).

However, for people not comfortable with the use of technology, computerized assessments can represent a challenge, with test interfaces appearing intimidating or counterintuitive (Zygouris and Tsolaki, 2015), making it essential to implement strategies (e.g., practice trials, clear instructions, etc.) that can reduce this bias, maximizing the possibility of a correct execution of the tests (Feenstra, 2018).

Another critical aspect is the need to validate these digital solutions in different contexts and with different populations of large enough sample sizes (Sternin et al., 2019).

This article aims to make a preliminary validation of the "Guttmann Cognitest"® to explore if it can represent a self-administered, useful, and efficient instrument to measure cognitive functioning in middle-aged healthy subjects for research purposes and large-scale assessments.

Materials and methods

Participants

Two-hundred and seventy four participants (126 women) from the Barcelona Brain Health Initiative (BBHI, Cattaneo et al., 2018) took part in this study (see **Table 1**).

Participants with a history or current diagnosis of neurological or psychiatric diseases, TBI with loss of consciousness, substance abuse/dependence, treatment with psychopharmacological drugs, or visual impairments were excluded from the study. Participants provided explicit informed consent, and the protocol was approved by the Ethics and Clinical Research Committee of the Catalan Hospitals Union (Comité d'Ètica I Investigació Clínica de la Unió Catalana hospitals, CEIC18/07).

Procedures

Participants took part in a paper-and-pencil classical neuropsychological testing session, and also a cognitive testing session *via* the digital solution "Guttmann Cognitest"®, in the context of the in-person assessments phase of the BBHI (Cattaneo et al., 2018).

TABLE 1 Demographic characteristics of participants.

Variable	Mean (SD)/range	Percentage (%)
Age	56.14 (6.95)/44–69	-
Sex	-	Female: 46.0
Education level	-	Primary: 5.1 Secondary: 27.7 Superiors: 67.2

These two cognitive assessments were completed in different sessions (mean delay in days = 4.60, SD = 28.20), and their order was counterbalanced across subjects.

The "Guttmann Cognitest"® testing session was implemented at the Institut Guttmann facilities, partially supervised by a technician who provided the smartphone to the participant, explained the purpose of the activity, and was available for any request during the assessment. This procedure was implemented to "control" the testing setting and reduce the presence of possible bias during the validation phase.

Paper and pencil classical neuropsychological assessment

Two expert clinical neuropsychologists conducted the paper and pencil assessments (Vanessa Alviarez-Schulze and Alba Roca), which lasted between 60 and 90 min, with tests being administered in the same order for all participants.

The test battery included well-established neuropsychological tests, exploring main cognitive functions: general/fluid intelligence (WAIS-IV Matrix Reasoning subtest, Weschler, 2008), visuospatial searching, selective attention, visual/motor and processing speed (Cancelation test WAIS-IV, Digit symbol substitution, and Trail making test A; Reitan and Wolfson, 1985; Weschler, 2008), cognitive flexibility and set-shifting (Trail making test B; Reitan and Wolfson, 1985), working memory (Digit backward, Digit forward, Letter-number sequencing, Corsi Tap Test; Weschler, 2008), episodic memory (RAVLT; Schmidt, 1996), and visuospatial abilities (Block design; Weschler, 2008).

"Guttmann Cognitest"® digital solution assessment

The "Guttmann Cognitest"® is a digital solution that includes seven computerized tasks designed to assess main cognitive functions from three main domains: memory, executive functions, and visuospatial abilities.

This solution is designed to be self-administered, to be potentially used for large-scale assessments and research purposes.

After logging in, the user is presented with a welcome screen containing a short description of the testing session and its main purpose. Then, instructions to focus and pay attention on the tasks, realize the session in a quiet location, and avoid interruptions, are given. The time needed to complete the full assessment is approximately 20 min.

All tasks follow the same logic. First, an initial screen with a brief description of the task is presented. Then, more detailed instructions, together with a video tutorial, are showed, explaining the objective and rationale of the task. This tutorial can be repeated as needed and the user can also move forward and backward along it (see Figure 1). After this, the user can start the task itself.

FIGURE 1
Screenshot of the video tutorial and text instructions explaining task's logic; the user can move forward (*Siguiente*) and backwards (*Anterior*) if needed.

When the user presses the start button, a countdown from 3 to 1 appears on the screen, aiming to get the user ready for the task. After this, a simple demo screen of the task comes as a practice, to ensure that the user have understood the objective, rationale, and expected responses for the task. Only once the practice is completed correctly (there are two attempts) the task begins. If the practice is not completed correctly the task is not administered, and the system moves directly to the next one, assuming that the person would not have been able to complete that task correctly. After a task is completed, a final screen displays the results obtained, and the user can continue to the next task.

Only the "Long-term memory" task (*Task 7*) does not follow this logic, as there is no tutorial nor practice screen, and the user is only informed that she/he will be required to remember the image-number associations seen in the previous "Short-term memory" task (*Task 2*).

After the seven tasks, a final questionnaire is presented to gather more information about the conditions of execution, interruptions, technical problems, or any other issues that could have affected the results of the tasks.

The seven tasks included in the solution are:

Task 1: visual span backward

This task, designed to assess working memory, is based on the visual span backward paradigm.

Participants are instructed to memorize a sequence of lights that appears sequentially, and then repeat this sequence in reverse order. Lights appear on a grid, for a presentation time of 1 s each, and the number of elements of the series increases by one after a correct answer (Figure 2). In case of a wrong response, another sequence of the same length is presented. After two consecutive errors, the task ends, with the final score being the number of elements of the longest sequence correctly repeated.

10.3389/fnagi.2022.987891

FIGURE 2
Screenshot of the visual span backward task.

Task 2: free and cued image and number associations

This associative memory task consists of memorizing six pairs of 2-digit numbers and images. The series of number-image pairs are displayed one by one, for 2 s each, in the middle of the screen. Once the presentation is finished, the images are again presented one by one, but in a different order, and participants are requested to write the number associated with each image (Figure 3).

Items that are not correctly remembered are presented again with a cue, consisting of two possible numbers associated with it, where the subject must select the correct one. The whole procedure is repeated three times.

Then, two scores are calculated for this task: one score represents the number of correct associations reported on the free recall mode, whilst the second score represents the number of correct answers on the cued mode.

Task 3: logic sequences

Twelve logic sequences were designed to evaluate fluent intelligence and logical reasoning. Each series is composed of a 3 × 3 matrix of elements, where the element at the bottom-right is missing. The task consists of selecting one out of four possibilities, presented on the right-hand side of the screen, to complete the sequence (see Figure 4). The maximum time available to solve each series is 90 s, with an alert message appearing on the screen when there are 10 s left.

The score for this task is the number of sequences completed correctly.

Task 4: cancelation

The symbol cancelation test was designed to assess visuo-spatial searching and selective attention. Participants are required to select, as fast as possible, a target of a specific shape and color among a matrix of different forms. Distractors come in the form of different shapes of the same color or the same shape of a different color. The task consists of seven consecutive screens.

In the first four screens, participants must select one colored shape (27 targets in total), while in the next three screens, they must choose two colored shapes (30 targets in total; see Figure 5).

There are two different ways of advancing to the next screen: either the subject selects all correct answers appearing on that screen, or the maximum 45 s threshold is reached.

The total score for this task is the sum of symbols correctly selected on all screens.

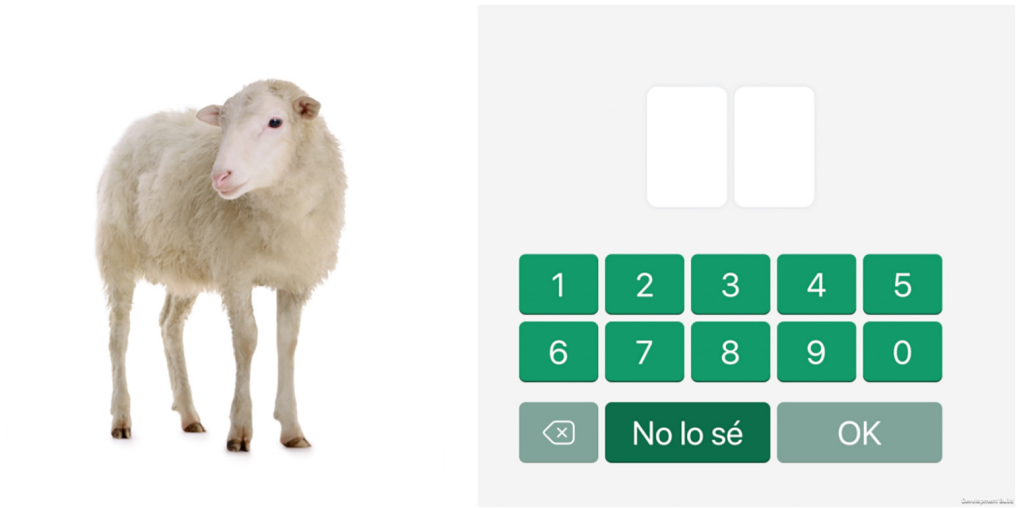

FIGURE 3
Screenshot of the free recall mode of the free and cued image and number associations task.

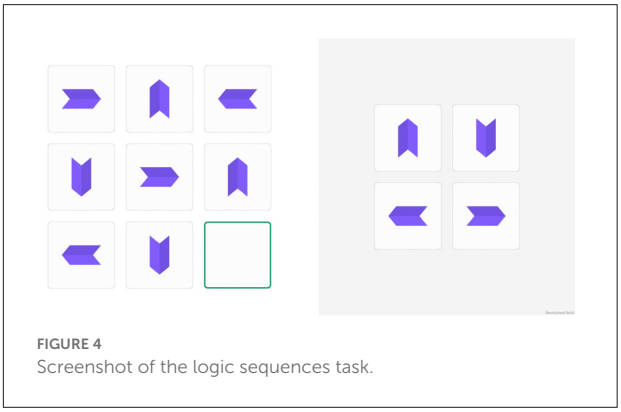

FIGURE 4
Screenshot of the logic sequences task.

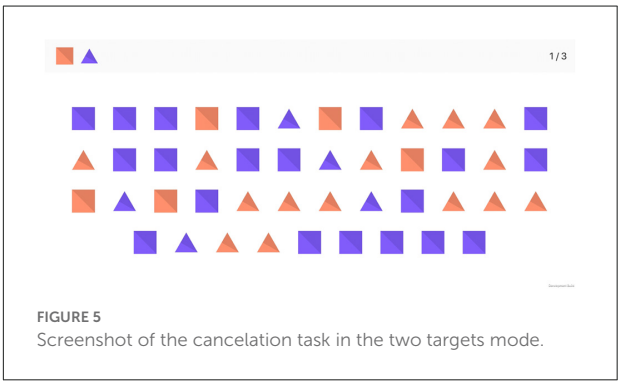

FIGURE 5
Screenshot of the cancelation task in the two targets mode.

Task 5: circle tapping

This task was designed to measure visuomotor speed and sustained attention.

This task shows six circles on the screen for 2 min. One by one, each of them appears either red or blue, with a presentation time of 1 s. The participant is instructed to only press the screen when the circles appear in red (as fast as possible; see **Figure 6**) and to not give any response when they appear in blue.

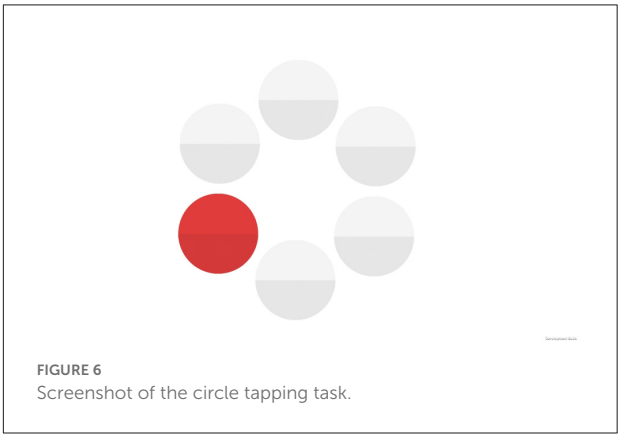

FIGURE 6
Screenshot of the circle tapping task.

The calculated score for this task is determined by the total number of correct answers and the average reaction time of those correct answers in seconds.

Task 6: mental rotation

This task, based on the mental rotation paradigm (Shepard and Metzler, 1971), was designed to evaluate visuospatial abilities. Participants are presented with pairs of 3D figures with different orientations, and they must indicate if they are identical or not, regardless of their orientation (see **Figure 7**), by pressing one of the two buttons shown at the bottom of the screen.

The task consists of 12 couple of 3D figures, and the timeout to respond is set to 10 s.

The total score of this task is the number of correct responses.

Task 7: long-term memory

To explore the subject's retention capacity over time, the final task consists of presenting the same six pictures previously shown in task 2. Pictures are presented one by one, and the user must write the number associated to each picture. Similarly to the short-term task, a free recall mode comes first, whilst a cued mode is presented if the participant gives a wrong answer.

The score for this task is the number of correctly remembered associations. The mean of delay between the immediate and delayed memory tasks (Task 2 and Task 7) was 13.48 min (SD = 4.12).

Data and statistical analysis

Following the same procedure reported in previous studies (e.g., España-Irla et al., 2021; Cattaneo et al., 2022; Redondo-Camós et al., 2022), we transformed raw scores obtained by classical gold-standard paper and pencil cognitive tests, and scores obtained in "Guttmann Cognitest"®, into z-scores. To create composite scores of different cognitive domains, we ran two exploratory principal component analyses (one for

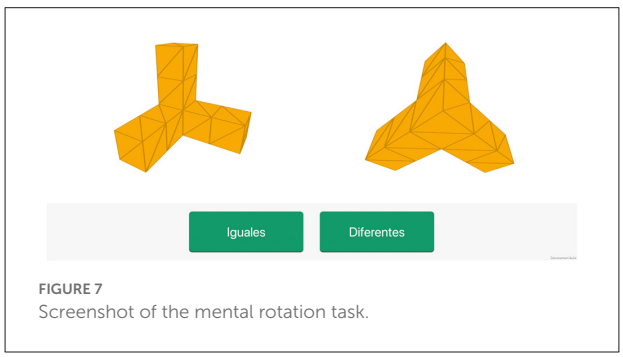

FIGURE 7
Screenshot of the mental rotation task.

classical cognitive testing and another one for "Guttmann Cognitest"®) using Oblimin rotation, fixing the acceptable level of factor loading to 0.30 (Hair et al., 1998). Based on the factorial structure obtained, we calculated composite scores of the different domains as the mean of the z-scores of each neuropsychological measure, multiplying it for the component loading value, to weigh its contribution to that component. Moreover, we calculated a global cognition composite score, as the mean of all the transformed z-scores, in line with previous studies (Kaffashian et al., 2013; Lampit et al., 2015; Cattaneo et al., 2022).

Following this, we explored the relationship between socio-demographic variables and cognitive results using Spearman correlations to examine the effects of age and education, and using one-way ANOVA's for biological sex.

Convergent validity was assessed using Spearman's rank correlations between gold standard neuropsychological tests and results of the tasks administered with the "Guttmann Cognitest"® in the different cognitive domains. To explore discriminant validity, we used Steiger's Z statistic (Hittner et al., 2003; Diedenhofen and Musch, 2015) to compare correlation coefficients.

Spearman's rank correlations were used considering the no normal distribution of almost all cognitive scores, the fact that we did not want to make any *a priori* hypothesis about the relationship between variables (linear or monotonic), and the ordinal nature of some of the variables included in the analysis.

Furthermore, we estimated demographically adjusted based-regression norms that provided the resulting z-scores metric. Equations were obtained by calculating the predicted raw scores adjusted for sociodemographic variables (age, sex, and years of education) that resulted in the regression model that is statistically significant (Bezdicek et al., 2014; Cavaco et al., 2015; Kormas et al., 2018; Lavoie et al., 2018).

Results

Cognitive composite score calculation and structure

First, the results of the composite score calculation for the gold-standard paper and pencil neuropsychological assessment are presented, followed by the results obtained with the same process for the "Guttmann Cognitest"® digital solution assessment.

Paper and pencil classical neuropsychological assessment

Neuropsychological raw data of the 274 participants were transformed into z-scores and used in the principal component analysis. Bartlett's test revealed a significant relationship between the factors ($p < 0.001$), and the Kaiser-Meyer-Olkin (KMO) test confirmed that the data was suitable for principal component analysis (KMO = 0.62). To select the number of components we used the eigenvalue-one Kaiser's criterion (Kaiser, 1960), controlling also the cumulative variance explained.

The analysis resulted in four components that explained 60.89% of the variance (see **Table 2**). The first component included the digit span backward (0.75), digit span forward (0.68), letter-number sequencing tests (0.68), Corsi Tap Test (0.37), and WAIS-IV logical Matrices (0.59), indicating an executive functions domain embracing working memory and reasoning abilities.

A second episodic memory domain was composed of all the measures of the Rey Auditory Verbal Learning Test (immediate recall = 0.83, delayed recall = 0.90, and recognition = 0.77).

A third visuospatial searching and attentional component comprised of the Trail Making Test A (0.72), the block design test (0.58), the digit-symbol substitution test (0.78), and the cancelation test (0.69).

Finally, set-shifting abilities were reflected in a fourth component, with the Trail Making Test Part B (0.81) and the Trail Making Test Part B-A (0.87). As mentioned above, based on this factorial structure we calculated composite scores of the four domains, and a global cognition score, as the mean of all tests.

"Guttmann Cognitest"® digital solution assessment

Bartlett's test revealed a significant relationship between the factors ($p < 0.001$), and the Kaiser-Meyer-Olkin (KMO) test confirmed that the data was acceptable for principal component analysis (KMO = 0.59). As in the previous analysis, the number of components was selected using Kaiser's rule (Kaiser, 1960), checking for the cumulative variance explained.

The analysis resulted in four components that explained 70.27% of the variance (see **Table 3**). A first domain was

TABLE 2 Results of formal neuropsychological testing of participants and principal components structure.

Cognitive domain	Neuropsychological test	*Mean (SD)*
Executive fcuntions	Digit span forward	6.20 (1.20)
	Digit span dackward	5.01 (1.22)
	Letter-number sequencing	5.72 (1.31)
	Corsi tap test	6.64 (1.21)
	WAIS-IV logical matrices	20.09 (3.56)
Episodic memory	RAVLT immediate recall	55.78 (9.34)
	RAVLT delayed recall	12.30 (2.56)
	RAVLT recognizing	14.55 (1.01)
Visuo spatial searching/attention	WAIS-IV block design	46.72 (10.25)
	Digit symbol substitution	77.20 (13.84)
	WAIS-IV cancelation	41.78 (8.82)
	TMT A	26.23 (7.70)
Set shifting	TMT B	79.44 (28.76)
	TMT B-A	53.20 (26.19)

TABLE 3 Principal components structure for the Cognitest app.

Cognitive domain	Cognitest task
Executive fcuntions and attention	Logic sequences
	Visual span backward
	Cancelation
Episodic memory	Free recall
	Cued recall
	Delayed recall
Visuomotor speed	Circle tapping accuracy
	Circle tapping reaction time
Visuospatial processing	Mental rotation

composed by logic sequences (0.71), cancelation (0.67), and visual span backward (0.65) tasks, possibly reflecting attention and executive functions (attention, reasoning, and working memory).

The second component included free recall (0.86), cued recall (0.84), and delayed recall (0.75) of images and numbers association tasks, indicating a potential memory component.

A third visuomotor speed component included the circle tapping accuracy (0.92) and reaction times (0.93).

The last component comprised only the mental rotation task (0.87).

Composite scores were calculated as the mean of the z-scores of each task, and a global score as the mean of all tasks results.

Age, sex, education, and cognition

Age correlated negatively with results of the "Guttmann Cognitest"® digital solution in memory ($rs = -0.20$, $p < 0.001$), executive functions and attention ($rs = -0.35$, $p < 0.001$), visuomotor speed ($rs = -0.30$, $p < 0.001$), and mental rotation ($rs = -0.14$, $p = 0.027$). Also, the global score in the "Guttmann Cognitest"® was negatively associated with age ($rs = -0.48$, $p < 0.001$).

We found a positive correlation between education and results obtained in memory ($rs = 0.28$, $p < 0.001$), executive functions and attention ($rs = -0.15$, $p = 0.009$), and the global cognitive score ($rs = 0.25$, $p < 0.001$).

Regarding biological sex differences, males outperformed women in executive functions and attention (0.19 and −0.22 respectively; $F = 8.457$, $p = 0.001$, $\eta^2 = 0.032$), visuomotor speed (0.14 and −0.17; $F = 3.883$, $p = 0.050$, $\eta^2 = 0.015$), mental rotation (0.17 and −0.20; $F = 8.041$, $p = 0.005$, $\eta^2 = 0.031$) and global cognition (0.11 and −0.12; $F = 8.496$, $p = 0.004$, $\eta^2 = 0.033$). On the other hand, women outperformed males in memory performance (0.98 and −0.08 respectively; $F = 4.150$, $p = 0.043$, $\eta^2 = 0.016$).

For gold-standard and classical neuropsychological tests, age correlated negatively with visuospatial searching and attention ($rs = -0.43$, $p < 0.001$), executive functions ($rs = -0.28$, $p < 0.001$), and global cognition ($rs = -0.29$, $p < 0.001$).

Regard education we found positive correlations with results in memory ($rs = 0.22$, $p < 0.001$), visuo-motor speed ($rs = 0.23$, $p < 0.001$), executive functions ($rs = 0.23$, $p < 0.001$), and global cognition ($rs = 0.30$, $p < 0.001$).

When we explored sex differences, similarly with what found previously, women outperformed males in memory (0.18 and −0.15 respectively; $F = 8.805$, $p = 0.003$, $\eta^2 = 0.032$), whereas men performed better than women in executive functions (0.28 and −0.33 respectively; $F = 26.787$, $p < 0.001$, $\eta^2 = 0.091$), set shifting (0.12 and −0.15 respectively; $F = 5.801$, $p = 0.017$, $\eta^2 = 0.021$), and global cognition (0.07 and −0.09 respectively; $F = 4.909$, $p = 0.028$, $\eta^2 = 0.018$).

Convergent validity

To explore convergent validity, cognitive domains calculated with the results of the "Guttmann Cognitest"® digital solution were correlated with those obtained by paper and pencil tests (see Table 4).

Memory measured by "Guttmann Cognitest"®

Memory correlated with results of the gold-standard paper and pencil assessment in memory ($rs = 0.27$, $p < 0.001$), visuospatial searching and attention ($rs = 0.18$, $p = 0.004$), set-shifting ($rs = 0.14$, $p = 0.021$), and global cognition ($rs = 0.19$, $p = 0.002$).

When we compared correlation magnitudes (Hittner et al., 2003), we found that the correlation between memory measured by "Guttmann Cognitest"® and the same domain measured by classical neuropsychological tests was higher compared with the correlation between memory measured by "Guttmann Cognitest"® and set-shifting ($z = 1.68$, $p = 0.046$). However, it was similar in magnitude compared to the correlation with visuo-spatial searching and attention, and global cognition measured with gold-standard tests.

Attention and executive functions measured by "Guttmann Cognitest"®

Attention and executive functions measured by "Guttmann Cognitest"® correlated with results of gold-standard paper and pencil neuropsychological tests in episodic memory ($rs = 0.13$, $p = 0.034$), visuospatial searching and attention ($rs = 0.24$, $p < 0.001$), executive functions ($rs = 0.37$, $p < 0.001$), and global cognition ($rs = 0.37$, $p < 0.001$). When we compared correlations magnitude (Hittner et al., 2003) we found that the correlation between executive functions measured by "Guttmann Cognitest"® and the same domain measured by classical gold-standard measures was greater than the correlation between executive functions measured by

TABLE 4 Correlations between results of the "Guttmann Cognitest"® digital solution and those obtained by classical paper and pencil neuropsychological testing.

		Gold-standard paper and pencil tests				
		Memory	*Executive functions*	*Visuo-spatial searching and attention*	*Set-shifting*	*Global cognition*
"Guttmann Cognitest"®	*Memory*	***rs* = 0.27****	*rs* = 0.11	***rs* = 0.18***	*rs* = 0.14*	***rs* = 0.19***
	Executive functions and attention	*rs* = 0.13*	***rs* = 0.37****	*rs* = 0.24**	*rs* = 0.03	***rs* = 0.37****
	Visuo-motor speed	*rs* = 0.04	*rs* = 0.09	***rs* = 0.26****	***rs* = −0.22****	*rs* = 0.06**
	Mental rotation	*rs* = −0.07	*rs* = 0.10	***rs* = 0.17***	*rs* = 0.03	*rs* = 0.09
	Global cognition	*rs* = 0.19*	***rs* = 0.37****	***rs* = 0.36****	*rs* = 0.14*	***rs* = 0.36****

Correlation coefficients in bold represents higher correlations, at a statistically significant level. *$p < 0.05$, **$p < 0.001$.

"Guttmann Cognitest"® and memory ($z = 2.91$, $p = 0.002$), and visuo-spatial searching ($z = 1.78$, $p = 0.038$). However, it produced similar results in terms of magnitude in relation to the correlation with global cognition.

Visuomotor speed measured by "Guttmann Cognitest"®

This component correlated with classical tests of visuospatial searching and attention ($rs = 0.25$, $p < 0.001$) and set-shifting abilities ($rs = 0.22$, $p < 0.001$), with similar magnitude.

Mental rotation measured by "Guttmann Cognitest"®

Mental rotation results correlated only with executive functions measured with classical neuropsychological tests ($rs = 0.17$, $p = 0.008$).

Global cognition measured by "Guttmann Cognitest"®

The Global "Cognitest" composite score correlated with gold-standard tests of episodic memory ($rs = 0.19$, $p = 0.003$), visuo-spatial searching and attention ($rs = 0.36$, $p < 0.001$), executive functions ($rs = 0.37$, $p < 0.001$), set shifting ($rs = 0.14$, $p = 0.025$), and global cognition ($rs = 0.36$, $p < 0.001$). In relation to the magnitude of the correlation between global composite scores, it resulted in higher than the correlation between the Global "Cognitest" composite score and classical tests of memory ($z = 2.84$, $p = 0.002$) and set-shifting ($z = 3.33$, $p < 0.001$).

Regression-based norming equations

We estimated regression-based norms that provided z-score metrics for each of the tasks included in the "Guttmann Cognitest"® digital solution. Equations included sociodemographic variables that were statistically significant in the regression model (for biological sex we created a dummy variable; see Table 5 for values used), multiplied for not standardized "B" coefficients, model constant (k), and the Root Mean Square Error (RMSE):

$$z = \frac{Raw\ Score - [k + (B_{age} * Age) + (B_{sex} * sex) + (B_{education} * Education)]}{RMSE}$$

Task 1: visual span backward

$$z = \frac{Raw\ Score - [7.623 + (-0.060 * Age) + (-0.404 * sex)]}{1.361}$$

Task 2: free and cued images and numbers associations

Free recall

$$z = \frac{Raw\ Score - [12.904 + (-0.136 * Age) + (1.076 * sex) + (1.398 * Education)]}{3.164}$$

Cued recall

$$z = \frac{Raw\ Score - [16.573 + (-0.035 * Age) + (0.628 * sex) + (0.587 * Education)]}{1.707}$$

TABLE 5 Variables included in the equations and values to be used in the regression-based norms formulae.

Variables		Values
Age		age in years
Sex	Male	0
	Female	1
Education level	Primary (≤8 years)	1
	Secondary (9–12 years)	2
	Superiors (≥13 years)	3

Task 3: logic sequences

$$z = \frac{Raw\ Score - [12.020 + (-0.103 * Age) + (-1.010 * sex) + (1.009 * Education)]}{2.642}$$

Task 4: cancelation

$$z = \frac{Raw\ Score - [67.884 + (-0.246 * Age) + (-0.163 * sex) + (-1.240 * Education)]}{11.604}$$

Task 5: circle tapping

Accuracy (%)

$$z = \frac{Raw\ Score - [93.934 + (-0.042 * Age)]}{1.288}$$

Reaction time (seconds)

$$z = \frac{Raw\ Score - [0.343 + (-0.006 * Age) + (0.032 * sex)]}{0.099}$$

Task 6: mental rotation

$$z = \frac{Raw\ Score - [12.062 + (-0.781 * sex)]}{2.457}$$

Task 7: long-term memory

$$z = \frac{Raw\ Score - [5.934 + (-0.018 * Age) + (0.237 * Education)]}{0.680}$$

Discussion

This study aimed to make a preliminary validation of the "Guttmann Cognitest"® digital solution as a tool for measuring cognitive functioning in a sample of healthy middle-aged adults. Results showed that it is a useful and suitable instrument for this population.

Principal component analysis on "Guttmann Cognitest"® tasks showed the presence of four main components: memory, executive functions and attention, visuomotor speed, and mental rotation. Moreover, it was possible to calculate a global score reflecting unspecific global cognitive functioning.

Similarly, also for classical neuropsychological tests, the analysis showed the presence of four main components, corresponding to the cognitive domains of memory, executive functions, visuospatial searching and attention, and set-shifting.

Beyond similarities, the components obtained by the two analyses did not include the same exact test, and consequently did not completely overlap in terms of cognitive processes involved.

For example, the domain of executive function for the classical neuropsychological tests includes principally working memory tests, together with a reasoning test, while the "correspondent" component in the "Guttmann Cognitest"® includes a working memory task, a reasoning task, but also a cancelation task.

A possible reason for this could be the greater involvement of working memory, and/or inhibition processing, in the cancelation task we designed. Indeed it has been proposed that working memory could be involved in visual selective attention (De Fockert et al., 2001) and strongly related to inhibition (McNab et al., 2008).

However, even considering these potential differences in terms of sub-processes involved in each task, we consider that, in terms of "broad" cognitive domains and functions, the overlapping between cognitive domains measured with "Guttmann Cognitest"® and classical neuropsychological tests should be considerable.

Crucially, convergent validity analysis indicated that these domains were associated with the correspondent and expected domains measured by gold-standard paper and pencil neuropsychological tests.

In order to interpret these correspondences we specifically considered the magnitude of the effect sizes obtained in the correlation analyses, following the criteria proposed by Cohen (1988); see also Hemphill (2003).

For memory tasks, we found small to medium correlations with all cognitive domains, except executive functions, with the strongest of these being episodic memory, visuo-spatial searching and attention, and global cognition.

Another component measured by "Guttmann Cognitest"®, reflecting attention and executive functions, showed medium correlations with classical tasks measuring similar attentional and executive components and the global cognition composite score, while showed only small correlations with visuo-spatial searching and memory classically measured.

The visuomotor speed component correlated with tests related to visuospatial searching and attention and set-shifting with coefficients small in magnitude.

Finally, the mental rotation component only showed a small correlation with the executive function component. This could be explained considering that this test measures mainly visual ability and visual imagery (Campos, 2012) that were not assessed in the neuropsychological testing, with only a low engagement of executive functions (Hyun and Luck, 2007). Future studies must include these

tests to evaluate the convergent validity of the mental rotation task.

These results are in line with previous validation studies of computerized neuropsychological testing (see Gualtieri and Johnson, 2006; Tsoy et al., 2021 for reviews) , showing great variability in convergent validity and concurrent validity, varying from small to large effect sizes (from 0.2 to 0.88 with an average of 0.40).

This variability makes it somehow difficult to make clear *a priori* expectation about desirable effect sizes for a useful solution, but from our point of view coefficients lower than 0.2, even if statistically significant, should be interpreted with caution.

Considering all the obtained results, beyond differences in magnitude between the different components, the "Guttmann Cognitest"® showed a satisfactory overall convergent validity with gold-standard correspondent neuropsychological tests.

Divergent validity analysis showed a certain overlap between components, and almost all cognitive domains measured by "Guttmann Cognitest"® correlated with visuospatial searching and attention measured by gold-standard paper and pencil tests. This finding indicates that this cognitive component represents a subjacent and common cognitive process involved in all tasks, in line with the involvement of specific cognitive processes (e.g., working memory) in tasks designed to mainly measure other cognitive functions (e.g., visual searching and attention; De Fockert et al., 2001).

However, the same patterns of results were found for classical paper and pencil tests, and the relationship and overlap between different cognitive processes involved in different tests is a widely debated issue, exhaustively explored in the past (Vanderploeg et al., 1994; Cunningham et al., 1997; Fossati et al., 1999; Tremont et al., 2000; Bryson et al., 2001).

In clinical populations, for example, a clear dissociation between deficits in different cognitive domains is not always detectable, a fact that can be explained due to different levels of overlapping depending on the tests used (Fossati et al., 1999; Tremont et al., 2000).

Trying to quantify this overlap, Duff et al. (2005) found a strong relationship between different cognitive domains that explained up to 59% of the shared variance.

For these reasons, it is sometimes appropriate to calculate a global cognitive score that could be fully informative of general cognitive functioning, and therefore, provide valuable information for population screening or in large sample studies.

Regarding the relation with socio-demographic variables, we found that age, as expected, correlated negatively with performance in all cognitive domains, indicating a sort of sensitivity of these tasks to cognitive changes due to age. On the other hand, education correlated positively with memory, executive functions, and global cognition.

Interestingly, males outperformed women in all cognitive domains apart from memory, where women performed better. One possible interpretation of these results could be related to the great involvement of visuospatial components in all the task of the "Guttmann Cognitest"® digital solution, but similar results were observed also for the classical neuropsychological tests. However, in both cases, the effect sizes were very small, and, in line with what was reported above, the observed differences must be interpreted with caution.

This is particularly important if we consider reviews and meta-analysis on this topic showing that beyond a consistently observed advantage for males in mental rotation (Hyde, 2014), differences in other cognitive domains are often very heterogeneous (Gaillard et al., 2021), trivial in effect size (Hyde, 2014), and not supported by differences in brain anatomy or brain functioning (Jäncke, 2018).

To conclude, our results showed that the "Guttmann Cognitest"® digital solution is a suitable instrument to measure cognitive functioning in different domains for research purposes and large samples assessments of middle-aged adults, supporting the potential relevance of these kinds of tools for large-scale assessment.

Digital solutions like this one indeed could serve as a reference point for further, more specialized, testing. Despite their limitations, they could provide a brief picture of cognitive functioning, helping to detect early impairments in specific domains in large-scale samples. In this context, these "screening" tests should focus on functions that deteriorate first in the preclinical stage of cognitive disorders (Payton et al., 2020). For this reason, we decided to include very sensitive tests previously related to the early detection of Alzheimer's Disease (AD), like the associative memory task, sensitive to the medial temporal lobe dysfunctions (O'Connell et al., 2004; De Rover et al., 2011; Junkkila et al., 2012; Soldan et al., 2016).

However, this study presents several limitations that should be considered. First, due to the difference between the set of tasks included in our digital solution and the classical neuropsychological tests used to validate it (e.g., associative memory task vs. word list), the cognitive component calculated may not totally overlap and reflect exactly the same subjacent cognitive processes. Second, even if we try to weigh the contribution to each test to a cognitive domain, each task could contribute differently to a single domain and the different domains could contribute differently to the global cognitive score calculated. Third, the neuropsychological tests included to validate "Guttmann Cognitest"® tasks did not include tests that mainly measure visuospatial abilities and visual imagery, making difficult a proper validation of the mental rotation task.

Further work is needed to examine the use of this kind of cognitive assessment in clinical populations of older

adults, alongside the validation of the test-retest reliability and learning effect of these tests. In this regard, two versions of each task with different stimuli have already been designed, and a specific validation study is already underway. We view this as a crucial aspect to allow us to efficiently implement cognitive assessments and follow-ups over time.

Data availability statement

The raw data supporting the conclusions of this article will be made available by the authors, without undue reservation.

Ethics statement

The studies involving human participants were reviewed and approved by Ethics and Clinical Research Committee of the Catalan Hospitals Union—Comité d'Ètica I Investigació Clínica de la Unió Catalana hospitals, CEIC18/07. The patients/participants provided their written informed consent to participate in this study.

Author contributions

GC, JS-S, AG-M, EO, and JT-M participated in the initial conception of the design of the "Guttmann Cognitest"® digital solution. GC, JS-S, VA-S, CP-G, and AR participated actively in the data collection and analysis. AG-M, EO, DB-F, AP-L, and JT-M contributed to the interpretation of the results. GC and CP-G drafted the article and all other authors made critical revisions, introducing important intellectual content. All authors contributed to the article and approved the submitted version.

Funding

DB-F was funded by the Spanish Ministry of Science, Innovation, Universities (RTI2018-095181-B-C21) and ICREA Academia 2019 award research grants. JT-M was partly supported by Fundació Joan Ribas Araquistain_Fjra, AGAUR, Agència de Gestió d'Ajuts Universitaris i de Recerca (2018 PROD 00172), Fundació La Marató De TV3 (201735.10), and the European Commission (Call H2020-SC1-2016-2017_RIA_777107).

Acknowledgments

We extend our gratitude to all participants, for their invaluable collaboration. No companies were involved in any step of the study, from design to data collection and analysis, data interpretation, the writing of the article or the decision to submit it for publication.

Conflict of interest

The authors declare that the research was conducted in the absence of any commercial or financial relationships that could be construed as a potential conflict of interest.

Publisher's note

All claims expressed in this article are solely those of the authors and do not necessarily represent those of their affiliated organizations, or those of the publisher, the editors and the reviewers. Any product that may be evaluated in this article, or claim that may be made by its manufacturer, is not guaranteed or endorsed by the publisher.

References

Amariglio, R. E., Donohue, M. C., Marshall, G. A., Rentz, D. M., Salmon, D. P., Ferris, S. H., et al. (2015). Tracking early decline in cognitive function in older individuals at risk for Alzheimer disease dementia. *JAMA Neurol.* 72, 446–454. doi: 10.1001/jamaneurol.2014.3375

Assmann, K. E., Bailet, M., Lecoffre, A. C., Galan, P., Hercberg, S., Amieva, H., et al. (2016). Comparison between a self-administered and supervised version of a web-based cognitive test battery: results from the nutri net-santé cohort study. *J. Med. Internet Res.* 18:e68. doi: 10.2196/jmir.4862

Bezdicek, O., Stepankova, H., Moták, L., Axelrod, B. N., Woodard, J. L., Preiss, M., et al. (2014). Czech version of Rey Auditory Verbal Learning test: normative data. *Neuropsychol. Dev. Cogn. B Aging Neuropsychol. Cogn.* 21, 693–721. doi: 10.1080/13825585.2013.865699

Bryson, G., Whelahan, H. A., and Bell, M. (2001). Memory and executive function impairments in deficit syndrome schizophrenia. *Psychiatry Res.* 102, 29–37. doi: 10.1016/s0165-1781(01)00245-1

Campos, A. (2012). Measure of the ability to rotate mental images. *Psicothema* 24, 431–434. doi: 10.1037/t14408-000

Cattaneo, G., Bartrés-faz, D., Morris, T. P., Sánchez, J. S., Macià, D., Tarrero, C., et al. (2018). The barcelona brain health initiative: a cohort study to define and promote determinants of brain health. *Front. Aging Neurosci.* 10:321. doi: 10.3389/fnagi.2018.00321

Cattaneo, G., Solana-Sánchez, J., Abellaneda-Pérez, K., Portellano-Ortiz, C., Delgado-Gallén, S., Alviarez Schulze, V., et al. (2022). Sense of coherence mediates the relationship between cognitive reserve and cognition in middle-aged adults. *Front. Psychol.* 13:835415. doi: 10.3389/fpsyg.2022.835415

Cavaco, S., Gonçalves, A., Pinto, C., Almeida, E., Gomes, F., Moreira, I., et al. (2015). Auditory verbal learning test in a large nonclinical portuguese population. *Appl. Neuropsychol. Adult* 22, 321–331. doi: 10.1080/23279095.2014.927767

Cohen, J. (1988). *Statistical Power Analysis for the Behavioral Sciences*, Second Edition. New York: Routledge. Available online at:

https://www.taylorfrancis.com/books/mono/10.4324/9780203771587/statistical-power-analysis-behavioral-sciences-jacob-cohen.

Cunningham, J. M., Pliskin, N. H., Cassisi, J. E., Tsang, B., and Rao, S. M. (1997). Relationship between confabulation and measures of memory and executive function. *J. Clin. Exp. Neuropsychol.* 19, 867–877. doi: 10.1080/01688639708403767

De Fockert, J. W., Rees, G., Frith, C. D., and Lavie, N. (2001). The role of working memory in visual selective attention. *Science* 291, 1803–1806. doi: 10.1126/science.1056496

De Rover, M., Pironti, V. A., McCabe, J. A., Acosta-Cabronero, J., Arana, F. S., Morein-Zamir, S., et al. (2011). Hippocampal dysfunction in patients with mild cognitive impairment: a functional neuroimaging study of a visuospatial paired associates learning task. *Neuropsychologia* 49, 2060–2070. doi: 10.1016/j.neuropsychologia.2011.03.037

Diedenhofen, B., and Musch, J. (2015). Cocor: a comprehensive solution for the statistical comparison of correlations. *PLoS One* 10:e0121945. doi: 10.1371/journal.pone.0121945

Duff, K., Schoenberg, M., Scott, J., and Adams, R. (2005). The relationship between executive functioning and verbal and visual learning and memory. *Arch. Clin. Neuropsychol.* 20, 111–122. doi: 10.1016/j.acn.2004.03.003

Duke Han, S., Nguyen, C. P., Stricker, N. H., and Nation, D. A. (2017). Detectable neuropsychological differences in early preclinical Alzheimer's disease: a meta-analysis. *Neuropsychol. Rev.* 27, 305–325. doi: 10.1007/s11065-017-9345-5

Dwolatzky, T., Whitehead, V., Doniger, G. M., Simon, E. S., Schweiger, A., Jaffe, D., et al. (2003). Validity of a novel computerized cognitive battery for mild cognitive impairment. *BMC Geriatr.* 3:4. doi: 10.1186/1471-2318-3-4

España-Irla, G., Gomes-Osman, J., Cattaneo, G., Albu, S., Cabello-Toscano, M., Solana-Sanchéz, J., et al. (2021). Associations between cardiorespiratory fitness, cardiovascular risk and cognition are mediated by structural brain health in midlife. *J. Am. Heart Assoc.* 10:e020688. doi: 10.1161/JAHA.120.020688

Feenstra, H. E. M. (2018). *The Development of an Online Neuropsychological Test Battery: The Amsterdam Cognition Scan.* Available online at: http://dare.uva.nl.

Fossati, P., Amar, G., Raoux, N., Ergis, A. M., and Allilaire, J. F. (1999). Executive functioning and verbal memory in young patients with unipolar depression and schizophrenia. *Psychiatry Res.* 89, 171–187. doi: 10.1016/s0165-1781(99)00110-9

Gaillard, A., Fehring, D. J., and Rossell, S. L. (2021). A systematic review and meta-analysis of behavioural sex differences in executive control. *Eur. J. Neurosci.* 53, 519–542. doi: 10.1111/ejn.14946

Gualtieri, C. T., and Johnson, L. G. (2006). Reliability and validity of a computerized neurocognitive test battery, CNS Vital Signs. *Arch. Clin. Neuropsychol.* 21, 623–643. doi: 10.1016/j.acn.2006.05.007

Hair, J. F., Black, W. C., Babin, B. J., Anderson, R. E., and Tatham, R. L. (1998). *Multivariate Data Analysis*, 5th Edition. Upper Saddle River, NJ: Prentice Hall.

Hemphill, J. F. (2003). Interpreting the magnitudes of correlation coefficients. *Am. Psychol.* 58, 78–79. doi: 10.1037/0003-066x.58.1.78

Hittner, J. B., May, K., and Silver, N. C. (2003). A Monte Carlo evaluation of tests for comparing dependent correlations. *J. Gen. Psychol.* 130, 149–168. doi: 10.1080/00221300309601282

Hyde, J. S. (2014). Gender similarities and differences. *Ann. Rev. Psychol.* 65, 373–398. doi: 10.1146/annurev-psych-010213-115057

Hyun, J. S., and Luck, S. J. (2007). Visual working memory as the substrate for mental rotation. *Psychon. Bull. Rev.* 14, 154–158. doi: 10.3758/bf03194043

Jäncke, L. (2018). Sex/gender differences in cognition, neurophysiology and neuroanatomy. *F1000Res.* 7:F1000 Faculty Rev-805. doi: 10.12688/f1000research.13917.1

Junkkila, J., Oja, S., Laine, M., and Karrasch, M. (2012). Applicability of the CANTAB-PAL computerized memory test in identifying amnestic mild cognitive impairment and Alzheimer's disease. *Dement. Geriatr. Cogn. Disord.* 34, 83–89. doi: 10.1159/000342116

Kaffashian, S., Dugravot, A., Elbaz, A., Shipley, M. J., Sabia, S., Kivimäki, M., et al. (2013). Predicting cognitive decline: a dementia risk score vs. the Framingham vascular risk scores. *Neurology* 80, 1300–1306. doi: 10.1212/WNL.0b013e31828ab370

Kaiser, H. F. (1960). The application of electronic computers to factor analysis. *Educ. Psychol. Meas.* 20, 141–151. doi: 10.1177/001316446002000116

Koo, B. M., and Vizer, L. M. (2019). Mobile technology for cognitive assessment of older adults: a scoping review. *Innov. Aging* 3:igy038. doi: 10.1093/geroni/igy038

Kormas, C., Megalokonomou, A., Zalonis, I., Evdokimidis, I., Kapaki, E., and Potagas, C. (2018). Development of the greek version of the face name associative memory exam (GR-FNAME12) in cognitively normal elderly individuals. *Clin. Neuropsychol.* 32, 152–163. doi: 10.1080/13854046.2018.1495270

Kulmala, J., Ngandu, T., and Kivipelto, M. (2018). Prevention matters: time for global action and effective implementation. *J. Alzheimers Dis.* 64, S191–S198. doi: 10.3233/JAD-179919

Lampit, A., Hallock, H., Suo, C., Naismith, S. L., and Valenzuela, M. (2015). Cognitive training-induced short-term functional and long-term structural plastic change is related to gains in global cognition in healthy older adults: a pilot study. *Front. Aging Neurosci.* 7:14. doi: 10.3389/fnagi.2015.00014

Lavoie, M., Bherer, L., Joubert, S., Gagnon, J. F., Blanchet, S., Rouleau, I., et al. (2018). Normative data for the rey auditory verbal learning test in the older french-quebec population. *Clin. Neuropsychol.* 32, 15–28. doi: 10.1080/13854046.2018.1429670

McNab, F., Leroux, G., Strand, F., Thorell, L., Bergman, S., and Klingberg, T. (2008). Common and unique components of inhibition and working memory: an fMRI, within-subjects investigation. *Neuropsychologia* 46, 2668–2682. doi: 10.1016/j.neuropsychologia.2008.04.023

Minghui, R. (2019). *Risk Reduction of Cognitive Decline and Dementia: WHO Guidelines*. Geneva: Word Health Organization.

Mortamais, M., Ash, J. A., Harrison, J., Kaye, J., Kramer, J., Randolph, C., et al. (2017). Detecting cognitive changes in preclinical Alzheimer's disease: a review of its feasibility. *Alzheimers Dement.* 13, 468–492. doi: 10.1016/j.jalz.2016.06.2365

O'Connell, H., Coen, R., Kidd, N., Warsi, M., Chin, A.-V., and Lawlor, B. A. (2004). Early detection of Alzheimer's disease (AD) using the CANTAB paired Associates Learning Test. *Int. J. Geriatr. Psychiatry* 19, 1207–1208. doi: 10.1002/gps.1180

Pascual-Leone, A., and Bartres-Faz, D. (2021). Human brain resilience: a call to action. *Ann. Neurol.* 90, 336–349. doi: 10.1002/ana.26157

Payton, N. M., Rizzuto, D., Fratiglioni, L., Kivipelto, M., Bäckman, L., and Laukka, E. J. (2020). Combining cognitive markers to identify individuals at increased dementia risk: influence of modifying factors and time to diagnosis. *J. Int. Neuropsychol. Soc.* 26, 785–797. doi: 10.1017/S1355617720000272

Redondo-Camós, M., Cattaneo, G., Perellón-Alfonso, R., Alviarez-Schulze, V., Morris, T. P., Solana-Sanchez, J., et al. (2022). Local prefrontal cortex TMS-induced reactivity is related to working memory and reasoning in middle-aged adults. *Front. Psychol.* 13:813444. doi: 10.3389/fpsyg.2022.813444

Reitan, R. M., and Wolfson, D. (1985). *The Halstead-Reitan Neuropsycholgical Test Battery: Therapy and Clinical Interpretation.* Tucson, AZ: Neuropsychological Press.

Rentz, D. M., Parra Rodriguez, M. A., Amariglio, R., Stern, Y., Sperling, R., and Ferris, S. (2013). Promising developments in neuropsychological approaches for the detection of preclinical Alzheimer's disease: a selective review. *Alzheimers Res. Ther.* 5:58. doi: 10.1186/alzrt222

Schmidt, M. (1996). *Rey Auditory and Verbal Learning Test: A Handbook*. Los Angeles, CA: Western Psychological Services.

Shepard, R. N., and Metzler, J. (1971). Mental rotation of three-dimensional objects. *Science* 171, 701–703. doi: 10.1126/science.171.3972.701

Soldan, A., Pettigrew, C., Moghekar, A., and Albert, M. (2016). Computerized cognitive tests are associated with biomarkers of Alzheimer's disease in cognitively normal individuals 10 years prior. *J. Int. Neuropsychol. Soc.* 22, 968–977. doi: 10.1017/S1355617716000722

Sternin, A., Burns, A., and Owen, A. M. (2019). Thirty-five years of computerized cognitive assessment of aging—where are we now? *Diagnostics (Basel)* 9:114. doi: 10.3390/diagnostics9030114

Tierney, M. C., and Lermer, M. A. (2010). Computerized cognitive assessment in primary care to identify patients with suspected cognitive impairment. *J. Alzheimers Dis.* 20, 823–832. doi: 10.3233/JAD-2010-091672

Tremont, G., Halpert, S., Javorsky, D. J., and Stern, R. A. (2000). Differential impact of executive dysfunction on verbal list learning and story recall. *Clin. Neuropsychol.* 14, 295–302. doi: 10.1076/1385-4046(200008)14:3;1-P;FT295

Tsoy, E., Zygouris, S., and Possin, K. L. (2021). Current state of self-administered brief computerized cognitive assessments for detection of cognitive disorders in older adults: a systematic review. *J. Prev. Alzheimers Dis.* 8, 267–276. doi: 10.14283/jpad.2021.11

Vanderploeg, R. D., Schinka, J. A., and Retzlaff, P. (1994). Relationships between measures of auditory verbal learning and executive functioning. *J. Clin. Exp. Neuropsychol.* 16, 243–252. doi: 10.1080/01688639408402635

Weschler, D. (2008). *Wechsler Adult Intelligence Scale - Fourth Edition.* San Antonio, TX: Pearson, Ed., NCS.

Wild, K., Howieson, D., Webbe, F., Seelye, A., and Kaye, J. (2008). The status of computerized cognitive testing in aging: a systematic review. *Alzheimers Dement.* 4, 428–437. doi: 10.1016/j.jalz.2008.07.003

Zygouris, S., and Tsolaki, M. (2015). Computerized cognitive testing for older adults: a review. *Am. J. Alzheimers Dis. Other Dement.* 30, 13–28. doi: 10.1177/1533317514522852

frontiers | Frontiers in Aging Neuroscience

TYPE Original Research
PUBLISHED 10 November 2022
DOI 10.3389/fnagi.2022.1034073

OPEN ACCESS

EDITED BY
Rachael D. Seidler,
University of Michigan, United States

REVIEWED BY
Ruili Xie,
The Ohio State University,
United States
Zahra Jafari,
University of Lethbridge, Canada

*CORRESPONDENCE
Rick A. Friedman
rafriedman@health.ucsd.edu
G. Allan Johnson
gjohnson@duke.edu

SPECIALTY SECTION
This article was submitted to Cellular and Molecular Mechanisms of Brain-aging, a section of the journal Frontiers in Aging Neuroscience

RECEIVED 01 September 2022
ACCEPTED 27 October 2022
PUBLISHED 10 November 2022

CITATION
Du EY, Ortega BK, Ninoyu Y, Williams RW, Cofer GP, Cook JJ, Hornburg KJ, Qi Y, Johnson GA and Friedman RA (2022) Volumetric analysis of the aging auditory pathway using high resolution magnetic resonance histology. *Front. Aging Neurosci.* 14:1034073. doi: 10.3389/fnagi.2022.1034073

Volumetric analysis of the aging auditory pathway using high resolution magnetic resonance histology

Eric Y. Du[1], Briana K. Ortega[1], Yuzuru Ninoyu[1], Robert W. Williams[2], Gary P. Cofer[3], James J. Cook[3], Kathryn J. Hornburg[3], Yi Qi[3], G. Allan Johnson[3]* and Rick A. Friedman[1]*

[1]Department of Otolaryngology—Head and Neck Surgery, University of California, San Diego, San Diego, CA, United States, [2]Department of Genetics, Genomics and Informatics, University of Tennessee Health Science Center (UTHSC), Memphis, TN, United States, [3]Department of Radiology, Center for *In Vivo* Microscopy, Duke University Medical Center, Durham, NC, United States

Numerous shown consequences of age-related hearing loss have been unveiled; however, the relationship of the cortical and subcortical structures of the auditory pathway with aging is not well known. Investigations into neural structure analysis remain sparse due to difficulties of doing so in animal models; however, recent technological advances have been able to achieve a resolution adequate to perform such studies even in the small mouse. We utilize 12 members of the BXD family of recombinant inbred mice and aged separate cohorts. Utilizing novel magnetic resonance histology imaging techniques, we imaged these mice and generated high spatial resolution three dimensional images which were then comprehensively labeled. We completed volumetric analysis of 12 separate regions of interest specific to the auditory pathway brainstem nuclei and cortical areas with focus on the effect of aging upon said structures. Our results showed significant interstrain variation in the age-related effect on structure volume supporting a genetic influence in this interaction. Through multivariable modeling, we observed heterogenous effects of aging between different structures. Six of the 12 regions of interests demonstrated a significant age-related effect. The auditory cortex and ventral cochlear nucleus were found to decrease in volume with age, while the medial division of the medial geniculate nucleus, lateral lemniscus and its nucleus, and the inferior colliculus increased in size with age. Additionally, no sex-based differences were noted, and we observed a negative relationship between auditory cortex volume and mouse weight. This study is one of the first to perform comprehensive magnetic resonance imaging and quantitative analysis in the mouse brain auditory pathway cytoarchitecture, offering both novel insights into the neuroanatomical basis

of age-related changes in hearing as well as evidence toward a genetic influence in this interaction. High resonance magnetic resonance imaging provides a promising efficacious avenue in future mouse model hearing loss investigations.

KEYWORDS

magnetic resonance imaging, aging, neuroanatomy, auditory pathway, neuroaging, volumetric 3D, hearing, BXD family

Introduction

Hearing loss is the most common human sensory deficit worldwide and age-related hearing loss has now been associated with cognitive decline and increased risk of incident dementia and depression (Loughrey et al., 2018; Choi et al., 2021). The relationships and implication of changes in auditory pathways and in the volumes of cortical and subcortical regions as a function of age is not yet well understood but is a growing nascent area of research. Recent studies using imaging-based quantitative analysis of brain structures have uncovered a connection between hearing loss and decreased volume of auditory regions as well as a biased decline in right temporal lobe volume (Lin et al., 2014). However, work in this area is difficult due to significant variation in both the environments and genetics of human populations. As a result, large numbers of participants are required to perform well powered investigations on the effect of aging on the human auditory system (Wright et al., 2002).

Generally well conserved genomics between humans and mice make the laboratory mouse an appropriate model in hearing research. We have used a family of genetically diverse strains of mice that mimic the diversity of humans but for which the environment can be controlled. The particular BXD family that we have utilized previously segregates for about 6 million common variants. Both the BXD family and the Hybrid Mouse Diversity Panel superset of strains have driven advances in systems genetics in many research disciplines (Ashbrook et al., 2019; Ohlemiller, 2019). Analysis of these isogenic but diverse cohorts allows control of both genetic and environmental factors and can be extended to multiple time points in development and aging; as such, it is possible to study gene-by-environment effects in manners that have high translational relevance to humans. While the mouse brain has less relative white matter than that of human, it contains a similar range of cell sizes and axonal diameters and likely provides an excellent translational model for imaging studies (Johnson et al., 2019).

Despite these advantages we currently do not known much about age-related changes in auditory system anatomy as a function of genotype. Conventional neuroanatomical methods rely on imaging of histological sections, and this poses difficulty in accurate estimation of the true volume and morphology of key components of the auditory system. Despite magnetic resonance imaging (MRI) of the human brain being a mainstay in clinical care and neuroscience research, technical difficulties of acquiring images in the mouse with sufficient resolution has limited research advances. Achieving sufficient power and precision for the quantitative analysis of structural variation to demonstrate relationships with behavior is difficult; however, it will ultimately be necessary to link neuroanatomical and molecular variation in brain to the key function and behavioral differences in audition.

In recent years, advances in technology have allowed systematic analysis of mouse central brain structures by structural and functional MRI (Wang et al., 2020). Johnson et al. (2022) have developed a process to efficiently generate magnetic resonance histology (MRH) images of the mouse brain with comprehensive 3D volumetric labeling (Johnson et al., 2022). Their results proved generalizable to different ages, sexes, and genotypes with spatial resolution more than 500,000 times that of comparable clinical protocols. This methodology generates 3 dimensional images without appreciable distortion and allows acquisition of hundreds of specimens a year. This is sufficiently high to target neurogenetic and genome-wide mapping studies and enable global analysis and genetic dissection of variation in CNS architecture with mice which require large numbers of specimens.

This process has been used in global brain analysis; however, analyzing an individual system utilizing this methodology has not been done (Wang et al., 2020). No three-dimensional mapping of the auditory pathway in mice is available. The objective of this study was to perform a volumetric analysis on the auditory pathway structures in mice and to evaluate possible influences of genetics and aging. We aim to do so by leveraging the MRH data set. Findings can potentially lay foundations for the neuroanatomical mechanistic basis in the findings observed in auditory research and provide novel avenues into future genetics research.

Materials and methods

Mice

Mouse experiments were completed in accordance with Duke University Institutional Animal Care and Use Committee. Here we have studied 12 members of the BXD family obtained from University of Tennessee Health Science Center: BXD24, BXD29, BXD34, BXD43, BXD44, BXD48a, BXD51, BXD60, BXD62, BXD65b, BXD89, and BXD101. Upon arrival, animals were housed for at least 10 days to allow adjustment to a new environment. Mice were housed in HEPA-filtered cages with standard, commercial lab bedding either individually or in pairs (Wang et al., 2018, Wang et al., 2020). They were fed a standard laboratory chow *ad libitum* diet and maintained a 12-h light/dark cycle and were subsequently aged. Two cohorts of mice were imaged. Mice of all 12 BXD strains were aged to either 3 months of age, categorized as young mice, or to fifteen months, categorized as old mice. Upon aging, the mice were sacrificed, and their brains fixed, imaged, and analyzed. Johnson et al. (2022) described the process of tissue preparation, imaging, analysis, and validation of accurately aligned multimodal 3D images of the mouse brain with the high-dimensional integrated volume with registration (HiDiver) suite of methods (Johnson et al., 2022). This is summarized in the following sections "Tissue preparation" and "Image acquisition and analysis." For each mouse undergoing the imaging protocol, sex, age in days, and body weight in grams were also obtained.

Tissue preparation

Animals were anesthetized with Nembutal (75 mg/kg) and a catheter was inserted into the left ventricle of the heart. A mixture of 0.9% saline and ProHance (10:1) followed by a mixture of 10% buffered formalin and ProHance (10:1) were perfused with a peristaltic pump. ProHance is a chelated gadolinium compound (Gd, a transition metal with unpaired electrons) commonly used in clinical MRI as a contrast agent and reduces the spin lattice relaxation time (T1) (Johnson et al., 2007; Wang et al., 2020). Following this, the skull was removed and placed in 10% buffered formalin at 4°C for 24 h and the mandible was removed to enable use of a smaller radiofrequency coil. Following fixation, the brain was kept in 1% Prohance/saline solution for at least 3 weeks to allow for adequate rehydration. This allowed for a reduction of T1 to ∼ 100 ms and T2 to ∼ 25 ms. Fixation reduced the apparent diffusion coefficient by ∼ 4X and so b values were increased relative to *in vivo* studies. Specimens were mounted in a 12-mm-diameter plastic cylinder filled with fomblin, an inert fluorocarbon that reduces susceptibility artifacts (Wang et al., 2020).

Image acquisition and analysis

Specimens were mounted in a 12 mm diameter radiofrequency (rf) coil constructed from a single sheet of silver foil which yields a low resistance. To tune the coil, necessary capacitance is added by placing a layer of dielectric material at the juncture of the coil ends. The resulting unloaded Q is > 500. MRH images were acquired on a 9.4T vertical bore Oxford magnet with Resonance Research gradients providing peak gradients of 2,000 mT/m. The scanner was controlled by an Agilent Direct Drive console with VnmrJ 4.0 software. Three-dimensional (3D) diffusion weighted images were acquired with a Stejskal Tanner rf refocused spin echo sequence with TR/TE of 100/12.7 ms and b values of 4,000 s/mm^2. Forty-six 3D volumes, each with a different gradient angle along with five baseline (b0) images distributed throughout the four-dimensional (4D) acquisition, were acquired. Sampling angles were uniformly distributed on the unit sphere. Compressed sensing was used with 8X acceleration to reduce the acquisition time to 11.7 h/specimen. This resulted in a 4D image array with isotropic spatial resolution of 45 μm (voxel volume of 91 pl) (Wang et al., 2020).

The 4D array (256 × 256 × 420 × 51) was created by first averaging the five b0 images. To correct for eddy current distortion, the diffusion-weighted 3D volumes were then registered to this template. The 4D array was processed with DSI Studio yielding the following scalar images: axial diffusivity (AD), radial diffusivity (RD), mean diffusivity (MD), fractional anisotropy (FA), and color fractional anisotropy (ClrFA) using the DTI model (Yeh et al., 2021). A Matlab script averaged the diffusion weighted images to yield a DWI volume.

A 3D label set consistent with the Allen Brain Atlas Common Coordinate Framework version 3 (CCFv3) was registered to all the scalar images (Johnson et al., 2022). The CCFv3 consists of 461 labels. A reduced but comprehensive subset of 180 ROIs (per hemisphere) that combine smaller adjacent sub-volumes was generated as many ROIs were too small to be reliably registered. A symmetric atlas was generated by reflecting the label set through the midline to minimize bias in lateral comparisons (Bowden et al., 2011). This label set of 180 total ROIs in each half of the brain was used to provide a full and isotropic parcellation of each brain (Johnson et al., 2010; Calabrese et al., 2015).

Auditory pathway region of interest selection

The central auditory system is comprised of a complex set of nuclei extending from the cochlear nuclei up to auditory cortical regions. The largest of these structures include, in ascending order, the cochlear nuclei, the superior olivary complex, tract and nuclei of the lateral lemniscus, the inferior colliculus,

and the medial geniculate nuclei. The spatial mapping which originally defined a set of 180 regions of interest (ROIs) per side was pared down to a subset of 11 well defined ROIs that are part of the auditory system. The three subdivisions of the medial geniculate nucleus were summed and combined as a separate summation ROI which was included in addition to its individual subdivisions, totaling 12 ROIs included in analyses. These are, with abbreviations, as follows (**Figure 1**):

1. Auditory cortex (AUD)
2. Medial geniculate nucleus (MGN)
3. Medial geniculate nucleus, dorsal part (MGd)
4. Medial geniculate nucleus, ventral part (MGv)
5. Medial geniculate nucleus, medial part (MGm)
6. Inferior colliculus (IC)
7. Inferior colliculus, central nucleus (Icc)
8. Lateral lemniscus (LL)
9. Lateral lemniscus, nucleus (NLL)
10. Superior olivary complex (SOC)
11. Dorsal cochlear nucleus (DCO)
12. Ventral cochlear nucleus (VCO)

Total brain volume (TBV) was also measured and used to determine the selective of effects on auditory ROIs.

Voxel-based volumetric analysis

Utilizing the 12 ROIs as described in section "Auditory pathway region of interest selection," a voxel-based volumetric analysis was completed with the primary aim of understanding relationships in auditory pathway structure volume. The imaging protocol provided a voxel volume of 9.1×10^{-5} mm^3 per voxel and, utilizing this factor, the voxel count of each ROI was converted to volume. The size of the two individual structures in each mouse brain from the left and right hemispheres was summed for an overall structure volume in the entire mouse brain. This volume was averaged in each age group and strain pairing for analysis of the aging and genetic basis in auditory structure size. We then calculated within-animal coefficient of variation for all structures to assess precision and segmentation repeatability of our measurements.

For quantitative analysis, we calculated percentage volumes relative to whole brain (or formally "whole brain volume minus ROI") to factor out global or non-selective changes in brain volume. We also used a linear regression model to determine age-related structural changes controlling for body weight, sex and total brain volume and potential confounding factors. This statistical approach was adapted from Williams (2000), in which the rationale behind statistical treatment of phenotypic data and linear regression methods phenotypic is explained in greater detail (Williams, 2000). We first confirmed data assumptions to conduct linear regression, including linearity and normality. In the model, we regressed individual structural volume on various mice characteristics including age in months, weight in grams, sex, and total brain volume. Akaike information criterion was used for parsimonious model criteria selection. In the end, sex was not included in the model because this variable was not a significant covariate for any auditory system ROI. Associations were considered significant if the confidence intervals at an alpha = 0.05 threshold did not overlap with 0.

Statistical analysis

All data processing and statistical analysis were performed with the R 4.1.1 statistical computing software (R Core Team, 2021). We utilized the tidyverse collection of packages: in particular dplyr 1.0.7, tidyr 1.1.3, tibble 3.1.3 for data manipulation, including calculation of means and standard errors, and analysis, including calculation one-way paired analysis of variance with corresponding p-values as well as creation of linear regression models; and ggplot2 3.3.5 for creation of figures (Wickham et al., 2019). Due to the greater number of old mice data, pair analyses matched unpaired old mice with an already paired isogenic young mice that were similar in sex and weight.

Results

104 mice were imaged with the protocol in sections "Tissue preparation"-"Image acquisition and analysis." Young mice (n = 45) had a median age of 98 days, ranging between 72 and 129 days, and a mean (SD) weight of 22.8 (4.7) grams. Old mice (n = 59) had a median age of 446 days, ranging between 341 and 687 days and a mean weight of 29.7 (6.1) grams. There was a slight female preponderance in sex distribution with 45 male mice and 59 female mice (43.3% male), within which there were 23 male and 27 female mice (46.0% male) in the young cohort and 22 male and 32 female mice (37.3% male) in the old cohort. Representative 3D volume rendering and magnetic resonance images of the structures in the auditory pathway are depicted in **Figure 1**. A summary of the mean volumes of all 12 ROIs as well as TBV is tabulated in **Table 1**. Raw data for all 104 mice is presented and available in **Supplementary material**.

Volumetric differences arise between strains

We first evaluated the absolute volume of the 12 auditory ROIs and the effect of age, sex, and strain. We compiled mean absolute volume in all 12 evaluated auditory structures by BXD strains and mouse age cohort (**Figure 2**). Although isogenic mice overall had little to no variation in individual

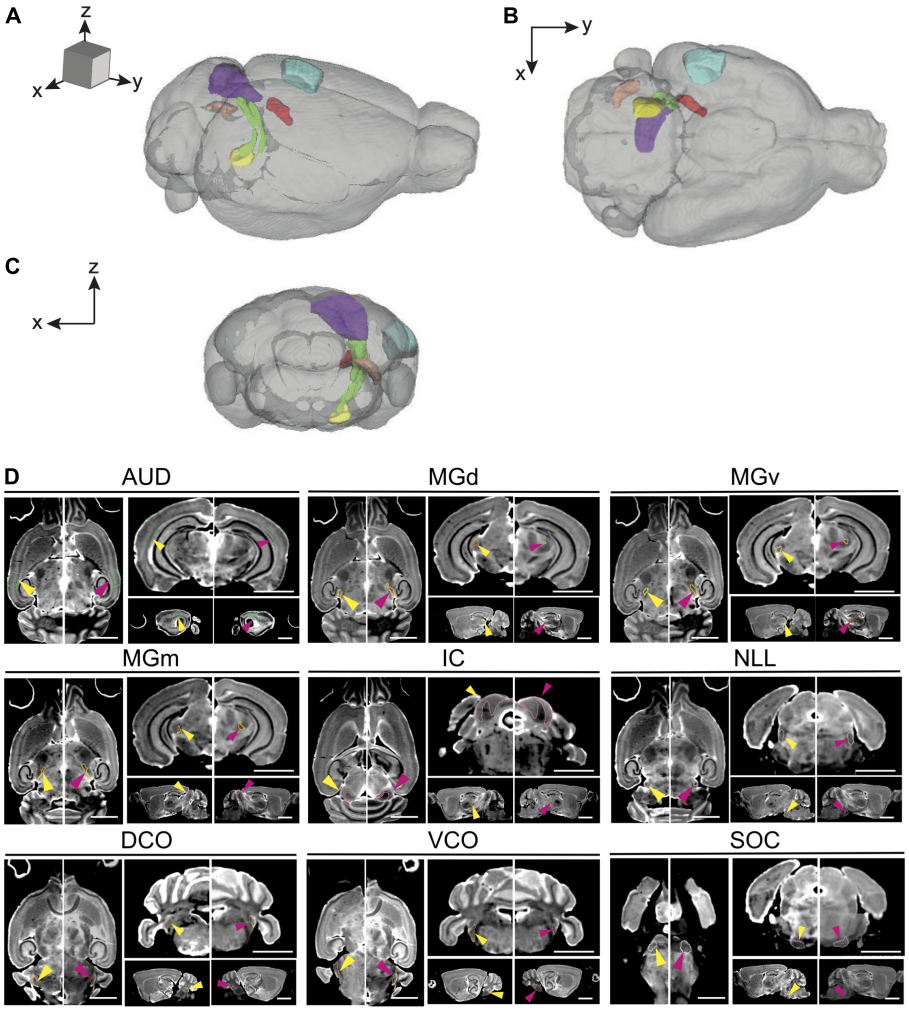

FIGURE 1
Magnetic resonance imaging of the auditory pathway. **(A–C)** 3D volume rendering of mouse auditory brain structures of the average old mouse structure size within the **(A)** sagittal, **(B)** axial, and **(C)** coronal planes. Colored structures represent specific central auditory structures: Blue; auditory cortex, Red; medial geniculate complex (dorsal, ventral and medial), Purple; inferior colliculus and its nucleus, Yellow; superior olivary complex, Orange; dorsal cochlear nucleus, Green; lateral lemniscus. **(D)** Representative axial, coronal, and sagittal plane magnetic resonance images of all structures in the auditory pathway of a young and an old BXD51 mouse. The images have an arrow aimed at the individual outlined structure. Within each image pair, the left image with a yellow arrow is the young mouse image and the right image with a pink arrow is the old mouse image. Scale bars in all planes is 2.5 mm. AUD, Auditory cortex; MGd, Medial geniculate nucleus, dorsal part; MGv, Medial geniculate nucleus, ventral part; MGm, Medial geniculate nucleus, medial part; IC, Inferior colliculus; LL, Lateral lemniscus; SOC, Superior olivary complex; DCO, Dorsal cochlear nucleus; VCO, Ventral cochlear nucleus.

structure volume, mean individual structure volumes differed markedly across strains; analysis of variance supported that there are significant variations between groups of mouse strains and auditory structures independent of aging ($p < 0.0001$ for all individual structures). Visualization of these mean values between young and old cohorts do show differences in the effect of aging on volume not only among all structures but also between the various strains evaluated, supporting a genetic influence on the age-related effect on structure volume in the auditory pathway. Interestingly, we observed no intersex differences in both univariate and multivariate analyses between the entire cohort. Coefficient of variation within-animal between hemispheres were low in all structures, ranging between a minimum 1.64% ± 0.01% SEM in the inferior colliculus and a maximum 4.04% ± 0.04% SEM in the dorsal cochlear nucleus, supporting reproducibility of our imaging and parcellation methodology.

Aging affects auditory pathway structure size heterogeneously

We then quantified the age- and strain-/genetic-based relationship and interaction with auditory structure volume.

TABLE 1 Summary volumes of region of interests.

Structure	Mean volume, mm^3 (SD)		
	Young (n = 45)	Old (n = 59)	P-value
TBV	416 (21)	433 (23)	< 0.001
AUD	4.67 (0.35)	4.43 (0.31)	< 0.001
MGd	0.142 (0.018)	0.148 (0.017)	0.003
MGv	0.247 (0.025)	0.253 (0.024)	0.002
MGm	0.211 (0.014)	0.226 (0.016)	< 0.001
MGN	0.600 (0.054)	0.627 (0.052)	< 0.001
IC	3.28 (0.28)	3.54 (0.33)	< 0.001
Icc	0.964 (0.077)	1.03 (0.21)	0.005
LL	0.724 (0.055)	0.782 (0.055)	< 0.001
NLL	0.669 (0.062)	0.744 (0.055)	< 0.001
SOC	0.654 (0.061)	0.699 (0.067)	< 0.001
DCO	0.482 (0.037)	0.507 (0.042)	< 0.001
VCO	0.737 (0.058)	0.755 (0.058)	0.004

Mean volume of all regions of interest in the auditory pathway investigated. A significant difference was noted between young and old mice in every structure analyzed through paired Student's t-test. The higher number of old mice were paired with a matched isogenic young mouse by sex. TBV, Total brian volume; AUD, Auditory cortex; MGd, Medial geniculate nucleus, dorsal part; MGv, Medial geniculate nucleus, ventral part; MGm, Medial geniculate nucleus, medial part; MGN, Medial geniculate nucleus; IC, Inferior colliculus; Icc, Medial geniculate nucleus, medial part; LL, Lateral lemniscus; NLL, Lateral lemniscus, nucleus; SOC, Superior olivary complex; DCO, Dorsal cochlear nucleus; VCO, Ventral cochlear nucleus.

Among all strains, a significant change in absolute structure volume was observed in all individual structures evaluated as well as total brain volume (Table 1). Utilizing percentage change in the proportion of total brain volume occupied for each structure between young and old mice of the same strain, we observe that 97/144 (67.4%) of structure-strain pairings in the auditory pathway demonstrated an increase in size after aging, to varying degrees (Figure 3). Of the minority of structure-strain pairings that decreased in size with age, the auditory cortex (AUD) brain volume proportion decreased with age in all strains, to varying degrees. The remainder of the 35 pairings that demonstrated a decrease in structure volume with aging were heterogeneously distributed between all remainder structures and strains, except for the medial portion of the medial geniculate nucleus which displayed an increased in brain volume proportion with age.

While these initial findings do support genetic variation's influence on structure volume, interpretation is limited as they do not account for possible confounders. We created a voxel-based multivariable linear regression model to control for such factors including total brain volume and mouse weight in the age and structure volume relationship (Figure 4). Six of the 12 ROIs evaluated in our multivariable analysis demonstrated a significant age-related effect independent of global brain volume or mouse weight changes. In ascending rate of volume change with age, these six structures were the auditory cortex [change in volume (95% confidence interval): −0.0274 (−0.0361, −0.0186) mm^3/month], ventral cochlear nucleus [−0.0019 (−0.0035, −0.0004) mm^3/month], medial division of the medial geniculate nucleus [0.0008 (0.0004, 0.0012) mm^3/month], lateral lemniscus [0.0018 (0.0004, 0.0031) mm^3/month], the nucleus of the lateral lemniscus [0.0031 (0.0016, 0.0046) mm^3/month], and the inferior colliculus [0.0106 (0.0025, 0.0188) mm^3/month].

To evaluate the model, adjusted R2 values were utilized to estimate corrected goodness-of-fit. The model only accounted for a low amount of the variation of structure volume in three of the 12 structures: dorsal division of the medial geniculate nucleus (24.8%), ventral division of the medial geniculate nucleus (23.8%), and central nucleus of the inferior colliculus (14.6%). However, it did account for a high amount of variation for the remaining ROIs, ranging from 36.1% in the whole medial geniculate nucleus to 63.5% in the lateral lemniscus. A significant portion of the remaining variation is likely accounted for by genetic differences, which our model does not account for due to a relatively low number of mice in each strain and age pairing.

Mouse weight is negatively associated with auditory cortex volume

While our analysis focused on the effect of age on auditory structure volume, we did observe notable findings in the other covariates in our model (Figure 4). We observed that the auditory cortex is the sole ROI that displays a significant relationship with mouse weight that is age and total brain volume independent. For every gram increase in mouse weight, a corresponding 0.0142 mm^3 decrease in auditory cortex volume is observed. Expectedly, all individual structure volumes evaluated do increase commensurately with increasing total brain volume (Figure 4). Unsurprisingly, the corresponding magnitude of the ratio between volume increases does align with the absolute size of the structure itself: for example, the large auditory cortex demonstrates a 0.0114 mm^3 increase in size per 1 mm^3 total brain volume, whereas the small dorsal cochlear nucleus, commensurate to its relatively smaller size, demonstrates a 0.0007 mm^3 increase per 1 mm^3 total brain volume.

Discussion

In this study, we leverage MRI data sets of a genetically diverse set of mouse strains in a comprehensive quantitative analysis of the mouse brain auditory pathway cytoarchitecture (Johnson et al., 2022). We observed strain-based volumetric differences in all individual structures of the auditory pathway

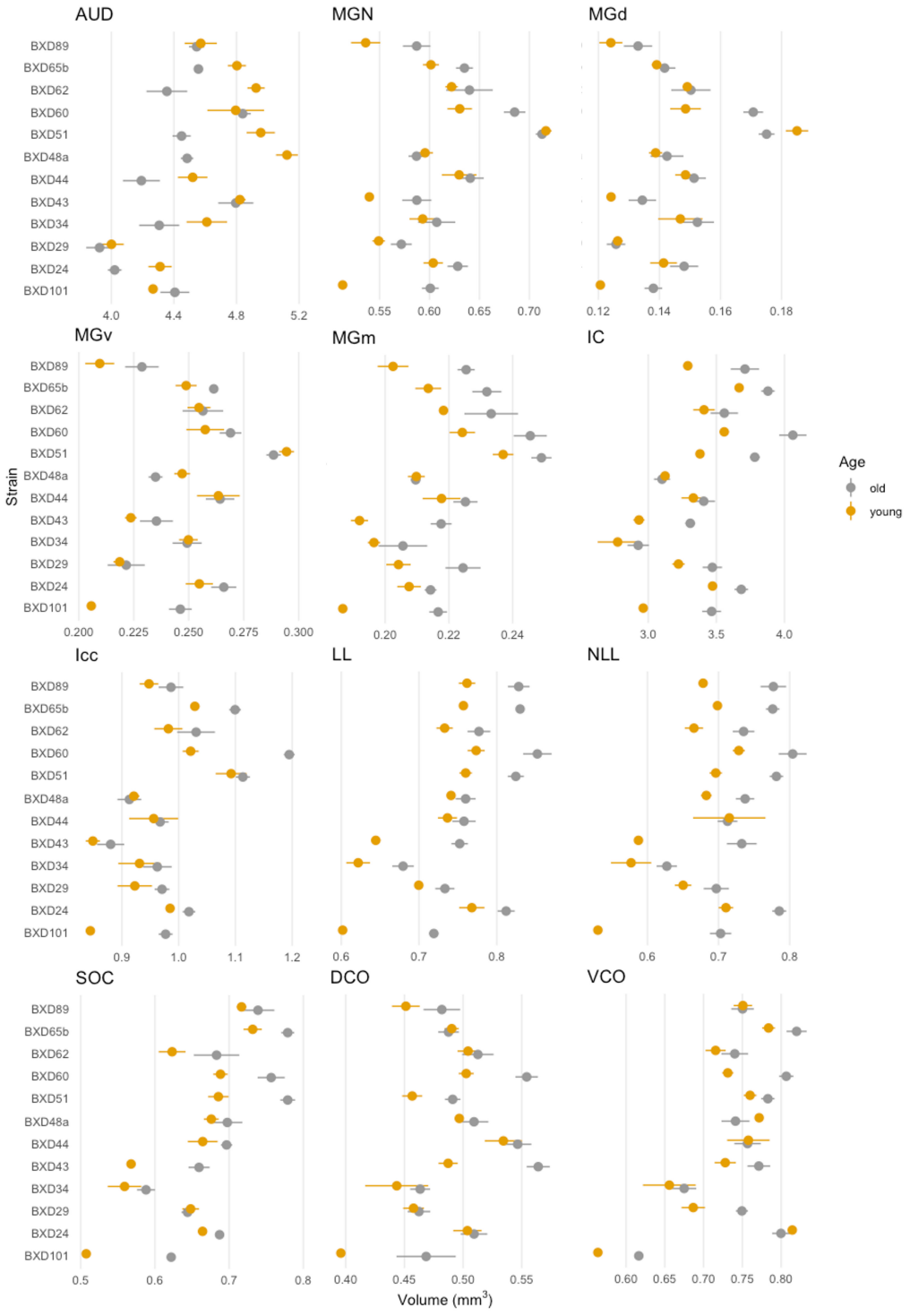

FIGURE 2
Summary of individual structure volumes by strain. Mean individual structure volume with horizontal lines indicating standard error in all strains. A variety of strain-based differences in both absolute volume and age-related change is observed in all structures. A range of 4–6 mice were in each age cohort and strain pairing with the exception of BXD101, in which only one mouse was imaged in the young group. AUD, Auditory cortex; MGd, Medial geniculate nucleus, dorsal part; MGv, Medial geniculate nucleus, ventral part; MGm, Medial geniculate nucleus, medial part; MGN, Medial geniculate nucleus; IC, Inferior colliculus; Icc, Inferior colliculus, central nucleus; LL, Lateral lemniscus; NLL, Lateral lemniscus, nucleus; SOC, Superior olivary complex; DCO, Dorsal cochlear nucleus; VCO, Ventral cochlear nucleus.

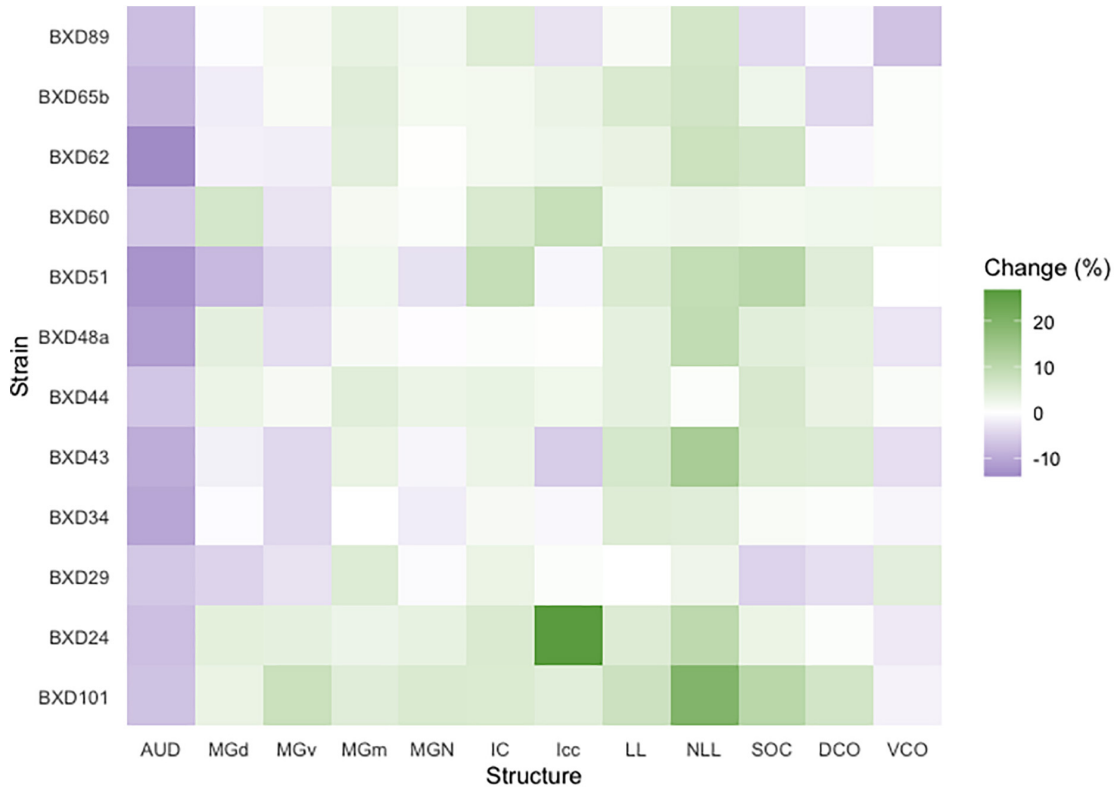

FIGURE 3
Brain proportion percentage change with aging. A heatmap matrix showing percentage change in individual structure brain proportion with age in every strain evaluated. Except for the auditory cortex in which there was an age-related decline in brain proportion, there were substantial strain-based variation in all structures with aging. A range of 4–6 mice were in each age cohort and strain pairing with the exception of BXD101, in which only one mouse was imaged in the young group. AUD, Auditory cortex; MGd, Medial geniculate nucleus, dorsal part; MGv, Medial geniculate nucleus, ventral part; MGm, Medial geniculate nucleus, medial part; MGN, Medial geniculate nucleus; IC, Inferior colliculus; Icc, Inferior colliculus, central nucleus; LL, Lateral lemniscus; NLL, Lateral lemniscus, nucleus; SOC, Superior olivary complex; DCO, Dorsal cochlear nucleus; VCO, Ventral cochlear nucleus.

as well as a heterogenous effect of aging in different strains upon structure size. Secondarily, we describe an independent negative effect of mice weight on auditory cortex volume. Our results support a genetic basis and influence in auditory structure volume and identify age-related volumetric changes in auditory structures. This study, to our knowledge, was the first attempt to utilize magnetic resonance histology for the volumetric analysis of a single functional pathway in the mouse model.

Imaging and parcellation of the auditory pathway

Current knowledge of the neuroanatomical basis of the auditory pathway is limited, and it is difficult to derive conclusive inferences from available work as with no single method is sufficient to provide a complete picture of the brain. The mouse brain is ∼ 3,000 times smaller than the human brain requiring a commensurate increase in spatial resolution for comparable anatomic measurement. Many advances in the molecular and neuroimaging techniques used in the study of fine structures have led to revelations in neurosciences research. Investigations into this area are becoming possible with technological advances and this field is becoming a nascent frontier for the future of research.

The high-resolution MRH and registration algorithm described in this study rely on extension of previous methods and merging of histological methods that allows collection and registration of key structures in whole individual brains in an efficient and systematic method. This process defines features accurately and without the registration issues that compromises many histological procedures. Utilizing this, we have successfully imaged, identified, and registered all individual structures of the auditory pathway. In addition, individual nuclei of the lateral lemniscus and inferior colliculus as well as the three subdivisions of the medial geniculate nucleus were able to be parcellated from the whole structure. The voxel volume at 9.1 × 10–5 mm^3 per voxel is more than 21,000

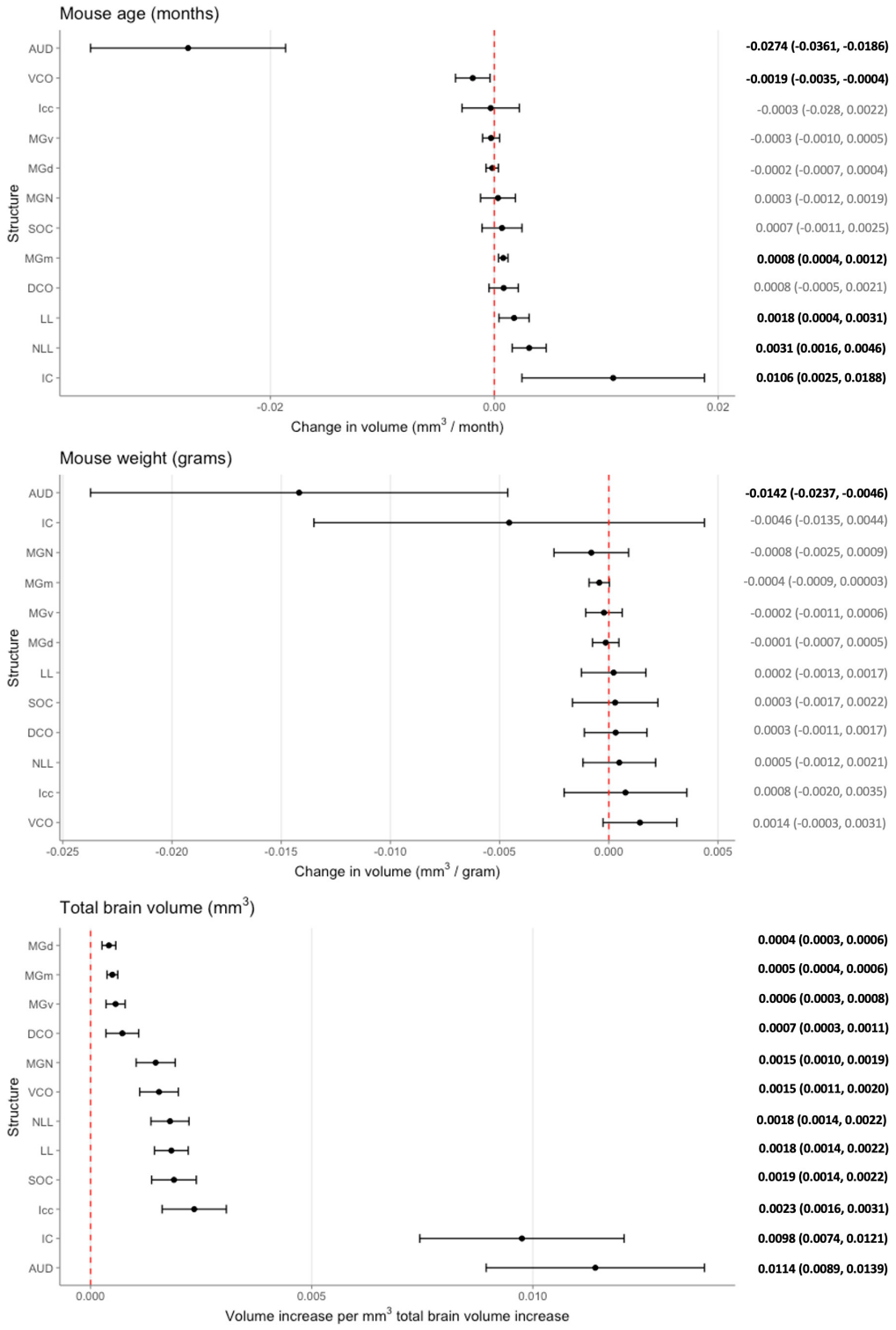

FIGURE 4
Multivariable analysis of the association of mouse age, weight, and total brain volume on auditory structure volume. Markers indicate degree of individual structure change per month mouse age **(top)**, gram mouse weight **(middle)**, and mm^3 total brain volume **(bottom)**, respectively. Horizontal lines indicate 95% confidence intervals. Raw coefficient values with their 95% confidence intervals were listed on the right with bolded values indicating significance. Structures were arranged from the lowest to greatest coefficient in each chart. AUD, Auditory cortex; MGd, Medial geniculate nucleus, dorsal part; MGv, Medial geniculate nucleus, ventral part; MGm; Medial geniculate nucleus, medial part; MGN, Medial geniculate nucleus; IC, Inferior colliculus; Icc, Inferior colliculus, central nucleus; LL, Lateral lemniscus; NLL, Lateral lemniscus, nucleus; SOC, Superior olivary complex; DCO, Dorsal cochlear nucleus; VCO, Ventral cochlear nucleus.

times smaller than the voxels of the Human Connectome Project and nearly 90,000 times smaller than routine clinical exams (Uğurbil et al., 2013; Van Essen et al., 2013). While much of the previous work in small animal imaging research has been focused on achieving greater spatial resolution, this more recent work has focused on increasing throughput. This high throughput fulfills large power requirements needed for quantitively genetic dissection investigations targeted at neurogenetic and genome-wide mapping. Imaging studies have shown evidence of homology between human and mice (Keifer et al., 2015). There is great translational potential in these novel approaches for understanding genetic variation and environmental influence that underlie differences in hearing behaviors across species. Further advances in this technique toward artificial intelligence-driven workflows and algorithms can allow complex modeling and elucidation of the genetic and environmental influences of possible causal relationships between cellular and subcellular structure and functional behavior (Johnson et al., 2022).

Strain-based volumetric differences

Advanced neuroimaging efforts combined with classical genetics and genome-wide association studies such as the Human Connectome Project represent the frontier for *in vivo* understanding of the neural connections of individuals (Van Essen et al., 2013). However, there is little conclusive evidence in the neuroanatomical basis in hearing. Not only is the variability of the absolute and relative size of the individual brain regions highly diverse within populations, there is also wide heterogeneity in the brain alterations found in hearing loss (Andrews et al., 1997; Kral et al., 2016; Tarabichi et al., 2018). Studies are also regularly limited by high degrees of measurement inconsistency. With the progress of small animal neuroimaging as described, there is enormous potential for utilization in genetics-based research as it avoids many of these issues by virtue of a controlled environment. In our analysis, we observed significant strain-based differences in all auditory structures analyzed in both age cohorts, supporting a genetic disposition to both structure volume and the aging effect within the mouse (**Table 1** and **Figure 1**). There is evidence currently supporting heritability in all imaging scalar metrics; however, mapping of the volumetric phenotypic trait requires the imaging data of significantly more strains than was analyzed in this study—approximately to the degree of 600 mice. The throughput of this imaging and processing methodology makes this a reality. Complex interactions between variants as well as complex environmental factors and confounders can very soon be evaluated and understood. More realistic and robust population models that incorporate levels of genetic variation comparable to human populations are now possible.

Mixed effects of aging on structure volume

Hearing is one of our main sensory senses and presbycusis is the most common sensory deficit in the elderly with severe social and health implications (Lin et al., 2011; Goman et al., 2017). Age-related hearing loss or presbycusis is the most prevalent sensory deficit in the elderly population (Huang and Tang, 2010). It is known that the aging process is associated with significant decrease in global and regional brain volumes, particularly in the temporal lobe and temporal gyri that comprise the human auditory cortex, and that hearing impairment is associated with acceleration of this brain volume decline (Scahill et al., 2003; Lin et al., 2014). These age-associated structural changes is a potential mechanism underlying the association between hearing impairment and cognitive decline and dementia and a better understanding of this process may help to elucidate expected age-related changes from neurodegenerative pathology (Lin and Albert, 2014). Our results are consistent with clinical findings in the auditory cortex and ventral cochlear nucleus, showing a decline in size with aging independent of global volume changes (Frisina and Walton, 2006). The most pronounced change with aging was observed in the auditory cortex, to a greater degree than that accounted for it being the largest structure in the pathway. The mechanistic basis for such findings has not been conclusive. In addition to gray matter loss and age-related atrophy of these areas, it has been proposed that a ventricle expansion effect contributes to changes in morphology (Eckert et al., 2019; Koops et al., 2020). The basis for the relationship between volume declines and behavior in hearing impairment is also not clear; hypotheses diverge as to whether auditory deprivation lead to declines in auditory area or if aging-caused changes in the peripheral and central auditory structures lead to subsequent hearing loss (Ren et al., 2018; Eckert et al., 2019).

In direct contrast, age-associated volume increases were observed in the medial division of the medial geniculate nucleus, the lateral lemniscus and its nucleus, and the inferior colliculus. While the age-associated changes reported in the cochlear nucleus and the auditory cortex have been a focus of research, these other structures in the auditory pathway are less studied (Tarabichi et al., 2018). A degree of increase in size is expected as the brains of some strains of mice grow in size as a function of age even in advanced age; however, our model does control for this factor (Peirce et al., 2003). While neurogenesis has been known in certain areas of the mouse brain even into late adulthood, such as the olfactory bulb via the rostral migratory stream, studies reflecting such a concept in the auditory system are few (Williams et al., 2001). Upregulation of parvalbumin expressing neurons in the inferior colliculus

and medial geniculate body has been reported and is likely related to changes in frequency processing (Ouda et al., 2008; Gray et al., 2013; Engle et al., 2014). There have also been findings of age-related compensatory changes in certain auditory neuronal populations to maintain information fidelity; similarly, projections to the auditory cortex from the medial geniculate nucleus that remain specific with age have been found and likely have a gain control function (Engle et al., 2014; Gray et al., 2014; Chen et al., 2019). These support the hypothesis of a compensatory increase in auditory structure volume as a response to auditory cortex decline. Alternatively, the increase in size of these structures may be a result of recruitment by other systems after auditory deprivation; such an effect has been observed in humans and hypothesized to support speech perception by the visual system after hearing impairment (Slade et al., 2020; Manno et al., 2021).

Mouse weight displays negative association with auditory cortex volume

Beyond age and strain-based changes, we also observed a significant independent negative relationship between mouse weight and the auditory cortex. To the best of our knowledge, this volumetric relationship has not been reported in literature. There is a hypothesized relationship between obesity and hyperlipidemia with hearing degeneration via an oxidative stress-based inflammatory response in the peripheral neurons (Hwang et al., 2013). Our study suggests that these same factors may have an influence in the cortical structures. Additionally, the vascular implications of obesity may also play a role as it is known to have a vasoconstrictive effect on the vascularly sensitive inner ear that may subsequently influence higher order structures (Dhanda and Taheri, 2017).

Limitations

There are several limitations of this study. While we aimed to age mice to certain time points considered young and old, there was a significant age range in both cohorts of the study which we attempted to control via continuous modeling. The low number of strains evaluated in this study limited potential evaluation of genetic differences and modeling was not able to incorporate strain-based differences. Imaging of an expanded set of strains is ongoing and examination of volumetric differences using complex trait analysis will soon be possible with the aim to localize genetic factors modulating structural variation. Despite these limitations, our study remains one of the few to attempt structural quantitative analysis in the mouse model of a specific functional pathway. The great majority of studies have focused on behavioral variants with a rationalistic basis anchoring on an underlying mechanism in the brain; however, a thorough understanding of the neuroanatomical structural relationships and underpinnings is ultimately necessary.

Conclusion

We present a novel approach for the volumetric analysis of the auditory pathway in the mouse utilizing magnetic resonance histology. Our results support a genetic basis and influence in auditory structure volume and identify novel age-related volumetric changes in auditory structures. An understanding of the structural differences in auditory structures is crucial in unwinding the genetic groundworks and links of hearing and is ultimately foundational knowledge in the pursuit of understanding hearing physiology and impairment. Robust structural analyses within individual functional systems will allow novel means of translation integral in our understanding of the inner workings in the complex brain.

Data availability statement

The original contributions presented in the study are included in the article/**Supplementary material**, further inquiries can be directed to the corresponding author/s.

Ethics statement

The animal study was reviewed and approved by the Duke University Institutional Animal Care and Use Committee.

Author contributions

ED, BO, YN, RW, GJ, and RF contributed to conception and design of the study. GC, JC, KH, YQ, and GJ contributed to novel technique development, data collection and curation, and database organization. ED and RW performed the statistical analysis and interpretation. ED and BO wrote the first draft of the manuscript. YN and GJ wrote sections of the manuscript. RF, RW, and GJ contributed to critical manuscript revision. RF contributed to funding acquisition and project supervision. All authors contributed read, and approved the submitted version.

Funding

This research was supported by the National Institute on Deafness and Other Communication Disorders (NIDCD) (grant R01 DC018566-02).

Conflict of interest

The authors declare that the research was conducted in the absence of any commercial or financial relationships that could be construed as a potential conflict of interest.

Publisher's note

All claims expressed in this article are solely those of the authors and do not necessarily represent those of their affiliated organizations, or those of the publisher, the editors and the reviewers. Any product that may be evaluated in this article, or claim that may be made by its manufacturer, is not guaranteed or endorsed by the publisher.

Supplementary material

The Supplementary Material for this article can be found online at: https://www.frontiersin.org/articles/10.3389/fnagi.2022.1034073/full#supplementary-material

SUPPLEMENTARY TABLE 1
Complete raw volumetric data using magnetic resonance imaging for 104 mice for 11 well defined regions of interests as well as total brain volume separated by hemisphere. Mice strain, sex, weight in grams, age in days, and age category (young/old) were included and the data set is currently sorted by strain and age category. Within analysis, the three subdivisions of the medial geniculate nucleus were summed and combined as a separate summation ROI not included in this raw data.

References

Andrews, T. J., Halpern, S. D., and Purves, D. (1997). Correlated size variations in human visual cortex, lateral geniculate nucleus, and optic tract. *J. Neurosci.* 17, 2859–2868. doi: 10.1523/JNEUROSCI.17-08-02859.1997

Ashbrook, D. G., Arends, D., Prins, P., Mulligan, M. K., Roy, S., Williams, E. G., et al. (2019). The expanded BXD family of mice: A cohort for experimental systems genetics and precision medicine. *bioRxiv* [Preprint]. doi: 10.1101/672097

Bowden, D. M., Johnson, G. A., Zaborsky, L., Green, W. D., Moore, E., Badea, A., et al. (2011). A symmetrical Waxholm canonical mouse brain for NeuroMaps. *J. Neurosci. Methods* 195, 170–175. doi: 10.1016/j.jneumeth.2010.11.028

Calabrese, E., Badea, A., Cofer, G., Qi, Y., and Johnson, G. A. (2015). A diffusion MRI tractography connectome of the mouse brain and comparison with neuronal tracer data. *Cereb. Cortex* 25, 4628–4637. doi: 10.1093/cercor/bhv121

Chen, L., Wang, X., Ge, S., and Xiong, Q. (2019). Medial geniculate body and primary auditory cortex differentially contribute to striatal sound representations. *Nat. Commun.* 10:418. doi: 10.1038/s41467-019-08350-7

Choi, J. Y., Lee, S., and Lee, W. (2021). The impact of hearing loss on clinical dementia and preclinical cognitive impairment in later life. *J. Alzheimers Dis.* 81, 963–972. doi: 10.3233/JAD-210074

Dhanda, N., and Taheri, S. (2017). A narrative review of obesity and hearing loss. *Int. J. Obes.* 41, 1066–1073. doi: 10.1038/ijo.2017.32

Eckert, M. A., Vaden, K. I. Jr., and Dubno, J. R. (2019). Age-related hearing loss associations with changes in brain morphology. *Trends Hear.* 23:2331216519857267. doi: 10.1177/2331216519857267

Engle, J. R., Gray, D. T., Turner, H., Udell, J. B., and Recanzone, G. H. (2014). Age-related neurochemical changes in the rhesus macaque inferior colliculus. *Front. Aging Neurosci.* 6:73. doi: 10.3389/fnagi.2014.00073

Frisina, R. D., and Walton, J. P. (2006). Age-related structural and functional changes in the cochlear nucleus. *Hear. Res.* 21, 216–223. doi: 10.1016/j.heares.2006.02.003

Goman, A. M., Reed, N. S., and Lin, F. R. (2017). Addressing estimated hearing loss in adults in 2060. *JAMA Otolaryngol. Head Neck Surg.* 143, 733–734. doi: 10.1001/jamaoto.2016.4642

Gray, D. T., Engle, J. R., and Recanzone, G. H. (2014). Age-related neurochemical changes in the rhesus macaque cochlear nucleus. *J. Comp. Neurol.* 522, 1527–1541. doi: 10.1002/cne.23479

Gray, D. T., Rudolph, M. L., Engle, J. R., and Recanzone, G. H. (2013). Parvalbumin increases in the medial and lateral geniculate nuclei of aged rhesus macaques. *Front. Aging Neurosci.* 5:69. doi: 10.3389/fnagi.2013.00069

Huang, Q., and Tang, J. (2010). Age-related hearing loss or presbycusis. *Eur. Arch. Otorhinolaryngol.* 267, 1179–1191. doi: 10.1007/s00405-010-1270-7

Hwang, J.-H., Hsu, C.-J., Yu, W.-H., Liu, T.-C., and Yang, W.-S. (2013). Diet-induced obesity exacerbates auditory degeneration via hypoxia, inflammation, and apoptosis signaling pathways in CD/1 mice. *PLoS One* 8:e60730. doi: 10.1371/journal.pone.0060730

Johnson, G. A., Ali-Sharief, A., Badea, A., Brandenburg, J., Cofer, G., Fubara, B., et al. (2007). High-throughput morphologic phenotyping of the mouse brain with magnetic resonance histology. *Neuroimage* 37, 82–89. doi: 10.1016/j.neuroimage.2007.05.013

Johnson, G. A., Badea, A., Brandenburg, J., Cofer, G., Fubara, B., Liu, S., et al. (2010). Waxholm space: An image-based reference for coordinating mouse brain research. *Neuroimage* 53, 365–372. doi: 10.1016/j.neuroimage.2010.06.067

Johnson, G. A., Tian, Y., Cofer, G. P., Cook, J. C., Gee, J. C., Hall, A., et al. (2022). HiDiver: A suite of methods to merge magnetic resonance histology, light sheet microscopy, and complete brain delineations. *bioRxiv* [Preprint]. doi: 10.1101/2022.02.10.479607

Johnson, G. A., Wang, N., Anderson, R. J., Chen, M., Cofer, G. P., Gee, J. C., et al. (2019). Whole mouse brain connectomics. *J. Comp. Neurol.* 527, 2146–2157. doi: 10.1002/cne.24560

Keifer, O. P. Jr., Gutman, D. A., Hecht, E. E., Keilholz, S. D., and Ressler, K. J. (2015). A comparative analysis of mouse and human medial geniculate nucleus connectivity: A DTI and anterograde tracing study. *Neuroimage* 105, 53–66. doi: 10.1016/j.neuroimage.2014.10.047

Koops, E. A., de Kleine, E., and van Dijk, P. (2020). Gray matter declines with age and hearing loss, but is partially maintained in tinnitus. *Sci. Rep.* 10:21801. doi: 10.1038/s41598-020-78571-0

Kral, A., Kronenberger, W. G., Pisoni, D. B., and O'Donoghue, G. M. (2016). Neurocognitive factors in sensory restoration of early deafness: A connectome model. *Lancet Neurol.* 15, 610–621. doi: 10.1016/S1474-4422(16)00034-X

Lin, F. R., and Albert, M. (2014). Hearing loss and dementia - Who is listening? *Aging Ment. Health* 18, 671–673. doi: 10.1080/13607863.2014.915924

Lin, F. R., Ferrucci, L., An, Y., Goh, J. O., Doshi, J., Metter, E. J., et al. (2014). Association of hearing impairment with brain volume changes in older adults. *Neuroimage* 90, 84–92. doi: 10.1016/j.neuroimage.2013.12.059

Lin, F. R., Niparko, J. K., and Ferrucci, L. (2011). Hearing loss prevalence in the United States. *Arch. Intern. Med.* 171, 1851–1852. doi: 10.1001/archinternmed.2011.506

Loughrey, D. G., Kelly, M. E., Kelley, G. A., Brennan, S., and Lawlor, B. A. (2018). Association of age-related hearing loss with cognitive function,

cognitive impairment, and dementia: A systematic review and meta-analysis. *JAMA Otolaryngol. Head Neck Surg.* 144, 115–126. doi: 10.1001/jamaoto.2017.2513

Manno, F. A. M., Rodríguez-Cruces, R., Kumar, R., Ratnanather, J. T., and Lau, C. (2021). Hearing loss impacts gray and white matter across the lifespan: Systematic review, meta-analysis and meta-regression. *Neuroimage* 231:117826. doi: 10.1016/j.neuroimage.2021.117826

Ohlemiller, K. K. (2019). Mouse methods and models for studies in hearing. *J. Acoust. Soc. Am.* 146:3668. doi: 10.1121/1.5132550

Ouda, L., Druga, R., and Syka, J. (2008). Changes in parvalbumin immunoreactivity with aging in the central auditory system of the rat. *Exp. Gerontol.* 43, 782–789. doi: 10.1016/j.exger.2008.04.001

Peirce, J. L., Chesler, E. J., Williams, R. W., and Lu, L. (2003). Genetic architecture of the mouse hippocampus: Identification of gene loci with selective regional effects. *Genes Brain Behav.* 2, 238–252. doi: 10.1034/j.1601-183X.2003.00030.x

R Core Team (2021). *R: A language and environment for statistical computing*. Vienna: R Foundation for Statistical Computing.

Ren, F., Ma, W., Li, M., Sun, H., Xin, Q., Zong, W., et al. (2018). Gray matter atrophy is associated with cognitive impairment in patients with presbycusis: A comprehensive morphometric study. *Front. Neurosci.* 12:744. doi: 10.3389/fnins.2018.00744

Scahill, R. I., Frost, C., Jenkins, R., Whitwell, J. L., Rossor, M. N., Fox, N. C., et al. (2003). A longitudinal study of brain volume changes in normal aging using serial registered magnetic resonance imaging. *Arch. Neurol.* 60, 989–994. doi: 10.1001/archneur.60.7.989

Slade, K., Plack, C. J., and Nuttall, H. E. (2020). The effects of age-related hearing loss on the brain and cognitive function. *Trends Neurosci.* 43, 810–821. doi: 10.1016/j.tins.2020.07.005

Tarabichi, O., Kozin, E. D., Kanumuri, V. V., Barber, S., Ghosh, S., Sitek, K. R., et al. (2018). Diffusion tensor imaging of central auditory pathways in patients with sensorineural hearing loss: A systematic review. *Otolaryngol. Head Neck Surg.* 158, 432–442. doi: 10.1177/0194599817739838

Uğurbil, K., Xu, J., Auerbach, E. J., Moeller, S., Vu, A. T., Duarte-Carvajalino, J. M., et al. (2013). Pushing spatial and temporal resolution for functional and diffusion MRI in the Human Connectome Project. *Neuroimage* 80, 80–104. doi: 10.1016/j.neuroimage.2013.05.012

Van Essen, D. C., Smith, S. M., Barch, D. M., Behrens, T. E., Yacoub, E., Ugurbil, K., et al. (2013). The WU-Minn human connectome project: An overview. *Neuroimage* 80, 62–79. doi: 10.1016/j.neuroimage.2013.05.041

Wang, N., Anderson, R. J., Badea, A., Cofer, G., Dibb, R., Qi, Y., et al. (2018). Whole mouse brain structural connectomics using magnetic resonance histology. *Brain Struct. Funct.* 223, 4323–4335. doi: 10.1007/s00429-018-1750-x

Wang, N., Anderson, R. J., Ashbrook, D. G., Gopalakrishnan, V., Park, Y., Priebe, C. E., et al. (2020). Variability and heritability of mouse brain structure: Microscopic MRI atlases and connectomes for diverse strains. *Neuroimage* 222:117274. doi: 10.1016/j.neuroimage.2020.117274

Wickham, H., Averick, M., Bryan, J., Chang, W., McGowan, L. D. A., François, R., et al. (2019). Welcome to the tidyverse. *J. Open Source Softw.* 4:1686. doi: 10.21105/joss.01686

Williams, R. W. (2000). Mapping genes that modulate mouse brain development: A quantitative genetic approach. *Results Probl. Cell Differ.* 30, 21–49. doi: 10.1007/978-3-540-48002-0_2

Williams, R. W., Airey, D. C., Kulkarni, A., Zhou, G., and Lu, L. (2001). Genetic dissection of the olfactory bulbs of mice: QTLs on four chromosomes modulate bulb size. *Behav. Genet.* 31, 61–77. doi: 10.1023/A:1010209925783

Wright, I. C., Sham, P., Murray, R. M., Weinberger, D. R., and Bullmore, E. T. (2002). Genetic contributions to regional variability in human brain structure: Methods and preliminary results. *Neuroimage* 17, 256–271. doi: 10.1006/nimg.2002.1163

Yeh, C.-H., Jones, D. K., Liang, X., Descoteaux, M., and Connelly, A. (2021). Mapping structural connectivity using diffusion MRI: Challenges and opportunities. *J. Magn. Reson. Imaging* 53, 1666–1682. doi: 10.1002/jmri.27188

frontiers | Frontiers in Aging Neuroscience

TYPE Original Research
PUBLISHED 21 November 2022
DOI 10.3389/fnagi.2022.1021237

OPEN ACCESS

EDITED BY
George M. Opie,
University of Adelaide,
Australia

REVIEWED BY
Shane Ohline,
University of Otago,
New Zealand
Fang Wang,
First Affiliated Hospital of Anhui Medical University, China
Christian Griñán-Ferré,
University of Barcelona,
Spain

*CORRESPONDENCE
Xue-Wei Li
lixuewei2003@163.com
Gui-Hai Chen
doctorcgh@163.com

†These authors have contributed equally to this work

SPECIALTY SECTION
This article was submitted to Neurocognitive Aging and Behavior, a section of the journal Frontiers in Aging Neuroscience

RECEIVED 17 August 2022
ACCEPTED 03 November 2022
PUBLISHED 21 November 2022

CITATION
Ni M-Z, Zhang Y-M, Li Y, Wu Q-T, Zhang Z-Z, Chen J, Luo B-L, Li X-W and Chen G-H (2022) Environmental enrichment improves declined cognition induced by prenatal inflammatory exposure in aged CD-1 mice: Role of NGPF2 and PSD-95.
Front. Aging Neurosci. 14:1021237.
doi: 10.3389/fnagi.2022.1021237

Environmental enrichment improves declined cognition induced by prenatal inflammatory exposure in aged CD-1 mice: Role of NGPF2 and PSD-95

Ming-Zhu Ni[1†], Yue-Ming Zhang[1†], Yun Li[1], Qi-Tao Wu[1], Zhe-Zhe Zhang[1], Jing Chen[1], Bao-Ling Luo[1], Xue-Wei Li[2*] and Gui-Hai Chen[1*]

[1]Department of Neurology (Sleep Disorders), The Affiliated Chaohu Hospital of Anhui Medical University, Hefei, China, [2]Department of Neurology, The First Affiliated Hospital, Hengyang Medical School, University of South China, Hengyang, China

Introduction: Research suggests that prenatal inflammatory exposure could accelerate age-related cognitive decline that may be resulted from neuroinflammation and synaptic dysfunction during aging. Environmental enrichment (EE) may mitigate the cognitive and synaptic deficits. Neurite growth-promoting factor 2 (NGPF2) and postsynaptic density protein 95 (PSD-95) play critical roles in neuroinflammation and synaptic function, respectively.

Methods: We examined whether this adversity and EE exposure can cause alterations in *Ngpf2* and *Psd-95* expression. In this study, CD-1 mice received intraperitoneal injection of lipopolysaccharide (50μg/kg) or normal saline from gestational days 15–17. After weaning, half of the male offspring under each treatment were exposed to EE. The Morris water maze was used to assess spatial learning and memory at 3 and 15months of age, whereas quantitative real-time polymerase chain reaction and Western blotting were used to measure hippocampal mRNA and protein levels of NGPF2 and PSD-95, respectively. Meanwhile, serum levels of IL-6, IL-1β, and TNF-α were determined by enzyme-linked immunosorbent assay.

Results: The results showed that aged mice exhibited poor spatial learning and memory ability, elevated NGPF2 mRNA and protein levels, and decreased PSD-95 mRNA and protein levels relative to their young counterparts during natural aging. Embryonic inflammatory exposure accelerated age-related changes in spatial cognition, and in *Ngpf2* and *Psd-95* expression. Additionally, the levels of *Ngpf2* and *Psd-95* products were significantly positively and negatively correlated with cognitive dysfunction, respectively, particularly in prenatal inflammation-exposed aged mice. Changes in serum levels of IL-6, IL-1β, and TNF-α reflective of systemic inflammation and their correlation with cognitive decline during accelerated aging were similar to those of hippocampal NGPF2. EE exposure could partially restore the accelerated decline in age-related cognitive function and in *Psd-95* expression, especially in aged mice.

Discussion: Overall, the aggravated cognitive disabilities in aged mice may be related to the alterations in *Ngpf2* and *Psd-95* expression and in systemic state of inflammation due to prenatal inflammatory exposure, and long-term EE exposure may ameliorate this cognitive impairment by upregulating *Psd-95* expression.

KEYWORDS

aging, inflammation, learning and memory, environmental enrichment, NGPF2, PSD-95

Introduction

The risk of developing many pathological conditions, especially cognitive decline, increases rapidly with age. It is estimated that 40% of the population, aged 60 years or more, is affected by age-related cognitive decline (Vanguilder and Freeman, 2011). Age-related cognitive decline hampers quality of life, and, consequently, the financial cost of providing long-term care for current and future sufferers of this condition is overwhelming. Thus, there is a need to understand the mechanisms that contribute to this loss of cognitive function with normal aging. However, the aforementioned mechanisms remain largely unclear, and effective approaches to alleviate brain aging are still lacking.

Current evidence demonstrates that exposure to maternal immune activation (MIA) *in utero* in rodents causes cognitive abnormalities, such as spatial learning and memory impairments, in adult offspring (Batinić et al., 2016; Simões et al., 2018). These abnormalities are similar to those reported in human studies (Ross-Munro et al., 2020; Veerasammy et al., 2020). Lipopolysaccharide (LPS), a component of the Gram-negative bacterial cell wall, activates the immune system (Domínguez-Rivas et al., 2021). Administration of LPS in rodents leads to inflammatory responses in astrocytes and microglial cells, which subsequently produce multiple pro-inflammatory mediators, such as interleukin (IL)-6, IL-1β, and tumor necrosis factor-alpha (TNF-α; Colonna and Butovsky, 2017; Liang et al., 2019; Domínguez-Rivas et al., 2021). Pro-inflammatory mediators cross the dysfunctional placental and blood–brain barriers to enter the fetal blood circulation and brain, thereby elevating concentrations of cytokines in fetuses during and after LPS-induced MIA (Simões et al., 2018; Cadaret et al., 2019). In addition, fetuses *in utero* trigger their own inflammatory response and promote the production of inflammatory cytokines after MIA (Elovitz et al., 2011; Henrique et al., 2021). These changes have the capacity to modulate fetal neurodevelopmental trajectories, thereby impairing cognitive performance in adult offspring (Henrique et al., 2021; Guma et al., 2022). However, only a limited number of studies have investigated the age-associated cognitive consequences of prenatal MIA exposure in these offspring, especially after midlife. Our previous studies indicated that exposure to LPS-induced MIA during late embryogenesis accelerated age-related learning and memory impairment in mouse offspring, particularly at midlife to senectitude (Li et al., 2016; Wang et al., 2020; Zhang et al., 2020).

The hippocampus, a brain region critical for learning and memory, is vulnerable to the aging process (Geinisman et al., 1995). Neuroinflammation is thought to contribute to aging and age-related cognitive impairment by damaging hippocampal synaptic function (Vanguilder and Freeman, 2011; Bettio et al., 2017; Juan and Adlard, 2019). The neurite growth-promoting factor 2 (NGPF2; also referred to as midkine) is not only a cytokine but also a neurotrophic factor (Ross-Munro et al., 2020; Zhou et al., 2021). It is principally expressed in the developing central nervous system (CNS; Zhou et al., 2021) and is usually reduced to negligible level in adulthood (Yoshida et al., 2014). However, mounting evidence indicates that NGPF2 is markedly upregulated in many pathological conditions that are characterized by inflammatory injury. For example, NGPF2 was highly expressed in the cerebral peri-infarct area (Yoshida et al., 1995) and in senile plaques in the brain of Alzheimer's disease (AD) patients (Yasuhara et al., 1993). Further investigations indicate that NGPF2 exhibits neuroprotective properties in the aforementioned diseases (Ishikawa et al., 2009; Herradón and Pérez-García, 2014), which may be beneficial for cognitive function. NGPF2 also exacerbates various pathological processes (Cai et al., 2020; Filippou et al., 2020; Ross-Munro et al., 2020). Interestingly, NGPF2 was found to specifically modulate neuroinflammation resulting from amphetamine injection and traumatic brain injury, thereby impairing cognitive and neurological consequences (Vicente-Rodríguez et al., 2016; Takada et al., 2020). Briefly, NGPF2 is also a regulator of cognitive impairment. Various research has revealed the "double-edged sword" effect of NGPF2, due to its ability to repair nerve damage or aggravate injury outcomes depending on different pathological factors, including age, brain region, disease state, and stimuli (such as amphetamine and LPS; Yoshida et al., 2014; Vicente-Rodríguez et al., 2016; Fernández-Calle et al., 2018). We hypothesized that the "double-edged sword" effect of NGPF2 may impair or protect cognition in specific conditions. Therefore, we aimed to investigate how inflammatory exposure during late embryogenesis changes *Ngpf2* gene expression in the brain at different ages, and whether NGPF2 is associated with age-related impairment in spatial learning and memory that is caused by embryonic MIA exposure.

Additionally, studies have demonstrated chronic and systemic immune activation in offspring following prenatal exposure to MIA (Hsiao et al., 2012; Rose et al., 2017). Human and animal studies suggest that systemic inflammation reflected by peripheral inflammatory cytokines may be linked to the exacerbation of neurodegenerative diseases such as AD and cognitive decline in older adults (Walker et al., 2019; Ashraf-Ganjouei et al., 2020). However, it is unknown whether MIA exposure *in utero* increases systemic inflammation in aged offspring.

The disruption of hippocampal synaptic function contributes to age-related cognitive decline (Petralia et al., 2014; Juan and Adlard, 2019). Indeed, synaptic deficits observed in the hippocampus may be partially explained by alterations in the level of postsynaptic density protein 95 (PSD-95; Bettio et al., 2017; Juan and Adlard, 2019). PSD-95 is a critical synaptic protein that regulates synaptic plasticity (Dore et al., 2021) and supports the stability of hippocampus-dependent memory (Fitzgerald et al., 2015). PSD-95 is reduced in the hippocampus of an AD mouse model (Shao et al., 2011; Xiao et al., 2021), as well as in aged rats with cognitive impairment when compared to aged cognitively unimpaired or young rats (Savioz et al., 2014). Neuroinflammation and other pathologies could reduce hippocampal *Psd-9* expression (Savioz et al., 2014). As mentioned, NGPF2 is induced after inflammatory injury and may also aggravate various pathologies. Although many studies have involved PSD-95, there are only limited reports on whether embryonic inflammatory exposure alters hippocampal *Psd-95* expression in aged mice.

In contrast, studies in rodents suggest that environmental enrichment (EE) may increase PSD-95 level in the brain (Savioz et al., 2014; Griñán-Ferré et al., 2018). It is well-known that rodents exposed to EE, either sensory or social, and physical exercises (i.e., larger group and larger cage equipped with additional running wheels, tunnels, ladders, and toys) have higher levels of brain-derived neurotrophic factor and improved inflammation and synaptic plasticity in the hippocampus (Griñan-Ferré et al., 2016a,b; Bettio et al., 2017). Thus, EE has been proposed as a non-invasive mean to ameliorate spatial learning and memory deficits (Wang et al., 2018; Kubo et al., 2021). However, it remains elusive whether EE is sufficient to mitigate the detrimental effects of prenatal inflammatory exposure and normal aging on age-related learning and memory decline, as well as the possible concomitant changes in *Psd*-95 and N*gpf2* expression, or systematic inflammation.

In this study, the effects of prenatal inflammatory exposure and EE treatment after weaning on spatial learning and memory were investigated in young and aged CD-1 mice. Additionally, whether mRNA and protein levels of NGPF2 and PSD-95 in the hippocampus and the levels of serum inflammatory cytokines differed among the different treatment groups, including both young and old mice, were examined. Finally, correlations between measured neurobiological indicators and cognitive performance were determined.

Materials and methods

Animals and experimental protocol

CD-1 mice (4–6 weeks old) were purchased from Beijing Vital River Laboratory Animal Technology Co. Ltd. The animals were housed in standard plastic mouse cages ($31.8 \times 20.2 \times 13.5\,cm^3$) and maintained under standard laboratory conditions, with a constant temperature of 22°C–25°C and 55 ± 5% humidity on a 12-h light–dark cycle (lights on at 07:00). Food and water were available *ad libitum*. After 2 weeks of adaptive feeding, female mice were paired with males at a 2:1 ratio. On the next morning, the emergence of a vaginal plug was considered as gestational day (GD) 0. From GDs 15–17, the pregnant mice received a daily intraperitoneal injection (i.p.) of LPS (50 μg/kg) or the same volume of normal saline, as previously described (Wang et al., 2020; Zhang et al., 2020). The offspring were raised by their mother until weaning at postnatal day 21. The male pups were assigned to one of four groups: (1) the control (CON) group—whose mother received i.p. saline; (2) the LPS group—whose mother received i.p. LPS; (3) control exposed to EE treatment group (CON-EE); and (4) LPS exposed to EE treatment group (LPS-EE). Specifically, half of the male pups in each litter whose mothers received LPS ip were randomly assigned to the LPS group and the other half were assigned to the LPS-EE group, and this assignment rule was also followed for male pups whose mothers received saline ip. CON and LPS groups were assigned to the same mouse cages (4–5 mice per cage) as their mothers. The other two groups exposed to the EE were housed in larger cages ($54.5 \times 39.5 \times 20\,cm^3$, 8–10 mice per cage) equipped with additional toys, including running wheels, tunnels, ladders, bridges, and log cabins, which were used to trigger cognitive and physical activities and social interactions (Ismail et al., 2021). Mice were exposed to novelty stimulation by renewing toys daily, and the program cycled weekly. EE exposure (short-term EE: from weaning to 3 months of age; long-term EE: from weaning to 15 months of age) continued until the end of the behavioral experiment. When the mice reached 3 and 15 months of age, 6 mice from each group were randomly selected for the experiment. The experimental schedule is shown in Figure 1. All experimental procedures complied with the guidelines established by the National Institutes of Health Guide for the Care and Use of Laboratory Animals, and were approved by the Experimental Animal Ethics Committee of Anhui Medical University (No. LLSC20160165).

Morris water maze

The Morris water maze (MWM) is a widely used task for evaluating hippocampus-dependent spatial learning and memory (Domínguez-Rivas et al., 2021). Our apparatus consisted of a circular tank (150 cm diameter, 30 cm height) with a black inside wall and an escape platform (10 cm diameter,

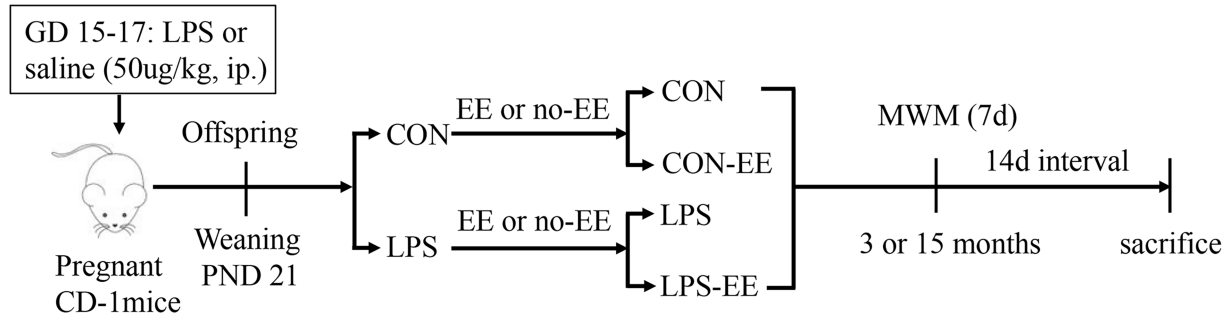

FIGURE 1
Timeline of experimental events. Pregnant mice were intraperitoneally injected with LPS or normal saline daily on days 15–17 of gestation (GD). All male offspring were weaned at postnatal day (PND) 21 and were divided into four groups (CON, CON-EE, LPS, and LPS-EE). Morris water maze tests were performed at 3 and 15months of age. Fourteen days after testing, mice were sacrificed for subsequent biochemical experiments. CON, untreated control group; LPS, lipopolysaccharide treatment group; EE, group of mice exposed to environmental enrichment; MWM, Morris water maze.

24 cm height). The tank was placed on a secure steel frame with a height of 30 cm and was filled with water (20°C–22°C, depth of 25 cm). The pool was divided into four quadrants, and the escape platform was placed 1 cm below the water's surface in the center of one of the quadrants. The periphery of the pool was surrounded by a white curtain, forming a cylindrical shape from the ceiling to the ground. Three clearly seen black geometric figures (circles, squares, and triangles) were equidistantly suspended inside the drapery, 150 cm above the ground, to serve as spatial cues. The mice to be tested were moved to the behavioral assessment room for acclimatization 3 days prior to testing. The day before the experiment, the mice were trained to find platforms placed in different positions, to assess mice for adequate vision and swimming ability. The platform had a flag and was 1 cm above the water's surface. During training or acquisition trials (learning phase), the mice were tested four times per day, with 15-min intervals between trials, for 7 days. On day 1, the mice were placed on the escape platform for 30 s before the first trial began. Subsequently, mice were randomly placed into the water from different quadrants (except the platform quadrant) facing the pool wall. Mice were allowed to spend 60 s to reach a hidden escape platform and rest on the platform for 30 s in each trial. If they failed to find the platform within 60 s, they were gently guided to the platform for 30 s. On the last day, the mice underwent probe trials (memory phase) with the platform removed. Two hours after the last learning trial, the mice were placed in the quadrant opposite the platform position and allowed to swim for 60 s. All the parameters of the swimming velocity, distance, and time were recorded using Any-maze software (Stoelting, United States). Experiments were conducted by fixed experimenters at the same time of day.

The time that mice take to reach an escape platform (escape latency) is the most widely used measure of learning ability. However, escape latency can be affected by the swimming speed of mice. Because the swimming distance can better reflect the learning ability of aged mice in the learning phase (Zhang et al., 2020), the swimming distance was preferentially used as an indicator of learning performance of mice in the present study, and the percentage of swimming distance and time in the target quadrant was recorded to evaluate the level of memory consolidation, as per previous studies (Wu et al., 2020; Zhuang et al., 2021).

Tissue and serum preparation

To avoid the possible effects of previous experimental manipulations on mRNA or protein level, the mice were sacrificed by cervical dislocation and decapitated 2 weeks after the behavioral tests. Retro-orbital blood samples were collected, and serum was subsequently separated by centrifuging samples at 4,000 rpm for 6 min. Serum was stored at −80°C. The hippocampus was isolated and immediately stored at −80°C for quantitative real-time polymerase chain reaction (qRT-PCR) and Western blotting.

Serum inflammatory cytokine measurement

Serum concentrations of IL-6, IL-1β, and TNF-α were determined by enzyme-linked immunosorbent assay using IL-6, IL-1β, and TNF-α kits, respectively (Wuhan ColorfulGene Biological Technology Co., Ltd., China).

qRT-PCR

qRT-PCR was conducted as previously reported (Zhuang et al., 2021). Total RNA was extracted from the hippocampus

using Trizol reagent according to the manufacturer's instructions. The purity and content of total RNA were determined using a spectrophotometer. The PrimeScript™ RT reagent Kit (Takara, RR047A) was used for reverse transcription of total RNA to complementary DNA (cDNA). Transcripts were amplified by qRT-PCR using Novostart SYBR qPCR SuperMix Plus in a 10 μl total reaction mixture (5 μl of 2× SYBR Green mixture, 1 μl of each primer (10 μM), 1 μl of cDNA template, and 2 μl of RNase-free water). qRT-PCR was performed under the following conditions: one cycle of 95°C for 1 min, 40 cycles of 95°C for 20 s, and 60°C for 1 min. mRNA levels were quantified using the $2^{\triangle\triangle Ct}$ method. Beta-actin was used as the endogenous control, and the primer sequences are listed in Table 1.

Western blotting

Hippocampal tissue was lysed in RIPA lysis buffer (Beyotime, China) and centrifuged at 12,000 rpm for 15 min at 4°C. The supernatant was extracted and mixed with 5× sodium dodecyl sulfate polyacrylamide gel electrophoresis (SDS-PAGE) protein loading buffer and boiled for 15 min. An equal amount of total protein from each sample was separated by 10% SDS-PAGE and transferred onto polyvinylidene fluoride immunoblotting membranes (Millipore, United States). Membranes were blocked with nonfat powdered milk in Tris-buffered saline with Tween-20 (TBST) for 2 h at 25°C, and then incubated overnight with primary antibodies to rabbit NGPF2 (1:1,000; ab52637, Abcam), rabbit PSD-95 (1:2,000; ab238135, Abcam), and mouse GAPDH (1:1,000; TA-08; Zsbio, China) at 4°C. After washing three times with TBST, the membranes were incubated with horseradish peroxidase-conjugated secondary antibodies (1:12,000; ZB2301, ZB-2305; Zsbio, China) for 1.2 h at room temperature. After rinsing again, the immunoreactive bands for the protein of interest were visualized using an enhanced chemiluminescence reagent (Thermo, United States). Immunoreactive bands revealed positive expression at 16 kDa (NGPF2), 80 kDa (PSD-95), or 36 kDa (GAPDH, internal standard). The quantification of band density was analyzed using ImageJ. Duplicate samples were averaged for each subject. All quantitative analyses were normalized to the corresponding GAPDH control.

TABLE 1 Primer sequences used for qRT-PCR.

Gene	Forward primer (5′ → 3′)	Reverse primer (5′ → 3′)
β-actin	AGTGTGACGTTGACATCCGT	TGCTAGGAGCCAGAGCAGTA
NGPF2	CTGAGACATCGGTTCCAAGT	ATCTTGTCCCACTTTCCAGG
PSD-95	CCCAGGATATGTGAACGGAA	CCTGAGTTACCCCTTTCCAA

Statistical analysis

All data with normal distribution are presented as the mean ± standard error of the mean (SEM). For data with normal distribution and equal variance, Student's *t*-test, one-way analysis of variance, or mixed-effects model with repeated measures and *post hoc* Tukey's tests for multiple comparison were used as appropriate. Specifically, data reflecting performance in the MWM learning task were analyzed using mixed-effects model with repeated measures. To determine the main effects of treatment, the other data were analyzed by one-way analysis of variance. The student's *t*-test was used to analyze the effect of age. Correlations between MWM performance and target mRNA or protein level in the hippocampus were analyzed using the Pearson's correlation coefficient test. All analyses were performed using GraphPad Prism 8 Software, and $p < 0.05$ was considered to be statistically significant.

Results

Performances in the Morris water maze

Age effects

Results of swimming velocity in the CON mice (Figure 2A) indicated that age did not significantly alter motor performance of aged mice. The distance swam (Figure 2B) and escape latency (Figure 2C) of the CON group gradually decreased with the increase in training days. Furthermore, age significantly affected learning and memory functions. Compared to the 3-month-old CON mice, the15-month-old CON mice had longer distance swam (Figure 2B) and latency (Figure 2C) during the training phase and lower percentage of distance (Figure 2D) and time (Figure 2E) swam in the target quadrant during the memory phase.

Treatment effects

During the acquisition phase

The effects of treatment were significant for the distance swam (Figures 3A,B) but not the latency (Figures 3C,D) or swimming velocity (Figures 3E,F) in the different treatment groups at both 3 and 15 months of age. At 3 months of age, the LPS group exhibited a significant spatial learning disability, with a greater distance swam, as compared with the CON group (Figure 3A). However, the short-term EE exposure did not significantly affect learning ability (CON vs. CON-EE; LPS vs. LPS-EE; Figure 3A). At 15 months of age, prenatal MIA exposure significantly impaired spatial learning function in the LPS mice compared to the CON ones, measured by the distance swam (Figure 3B). The long-term EE treatment improved the spatial learning performance in the LPS-EE group (LPS vs. LPS-EE; Figure 3B).

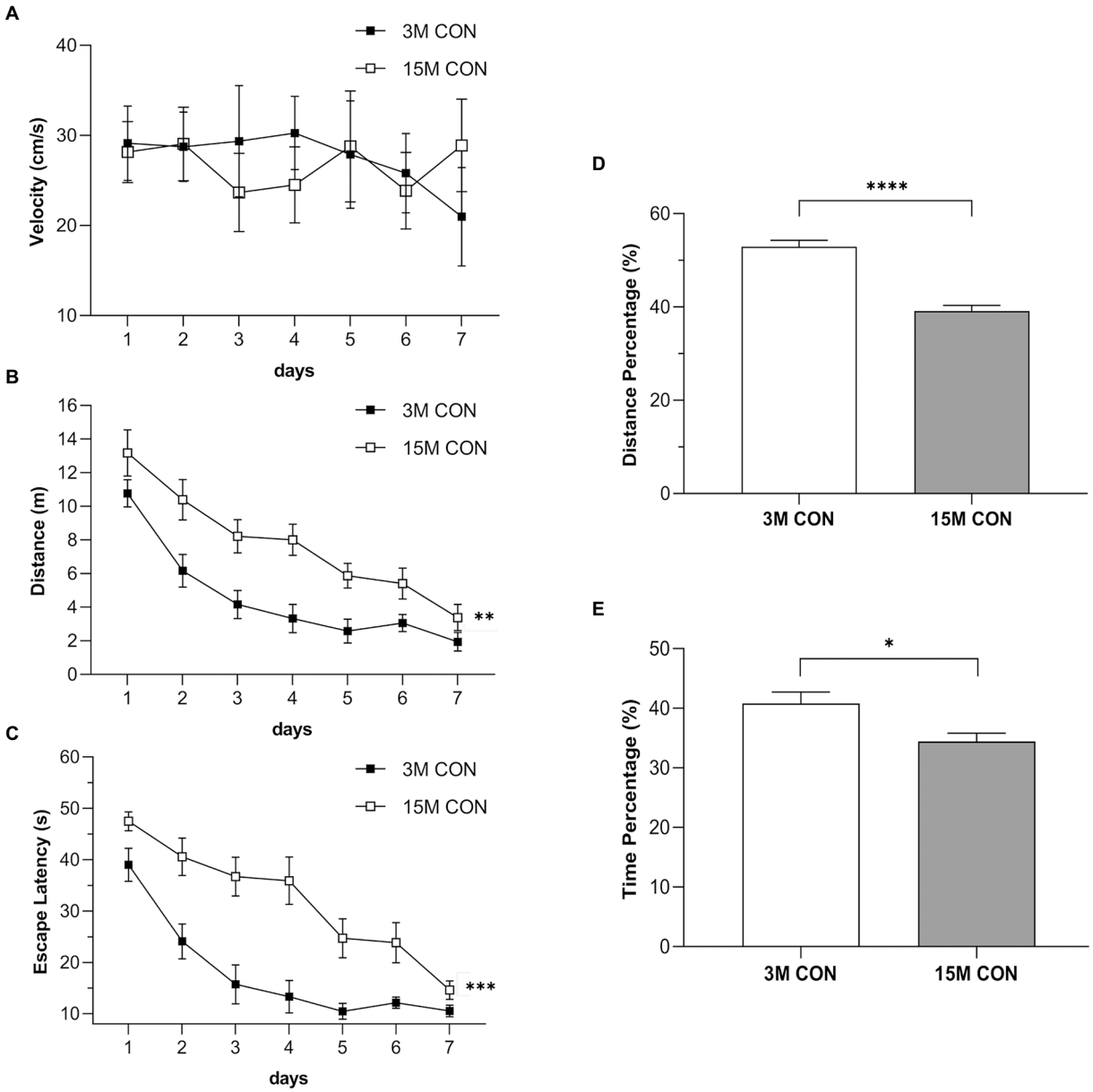

FIGURE 2
Performances illustrating the age effects in the Morris water maze test. Swimming velocity **(A)**, distance swam **(B)** and escape latency **(C)** during the training phase, and the percentage of distance **(D)** and time **(E)** swam in the target quadrant during the memory phase in the CON group at 3months (3M) and 15months (15M) of age. Data are presented as means±SEM (n=6 male mice/group). **p<0.01, ***p<0.001 compared with the CON group; CON, untreated control group.

In the memory phase

At 3 months of age, the percentage of distance (Figure 3G) and time (Figure 3H) swam in the LPS group was significantly decreased compared to the CON group, indicating that the spatial memory was declined in the LPS mice. Moreover, short-term EE intervention reversed the memory deficit (LPS vs. LPS-EE; Figure 3G). At 15 months of age, the LPS group showed a decrease in memory consolidation compared to the CON group, as assessed by the percentage of distance and time swam (Figures 3G,H). Meanwhile, the long-term EE exposure restored the memory decline in the LPS-EE group (LPS vs. LPS-EE, Figures 3G,H) and the CON-EE group (CON vs. CON-EE, Figure 3G).

Serum inflammatory cytokine levels

Results obtained in the CON mice showed that the serum levels of IL-6, IL-1β, and TNF-α increased with age (Figures 4A–C).

10.3389/fnagi.2022.1021237

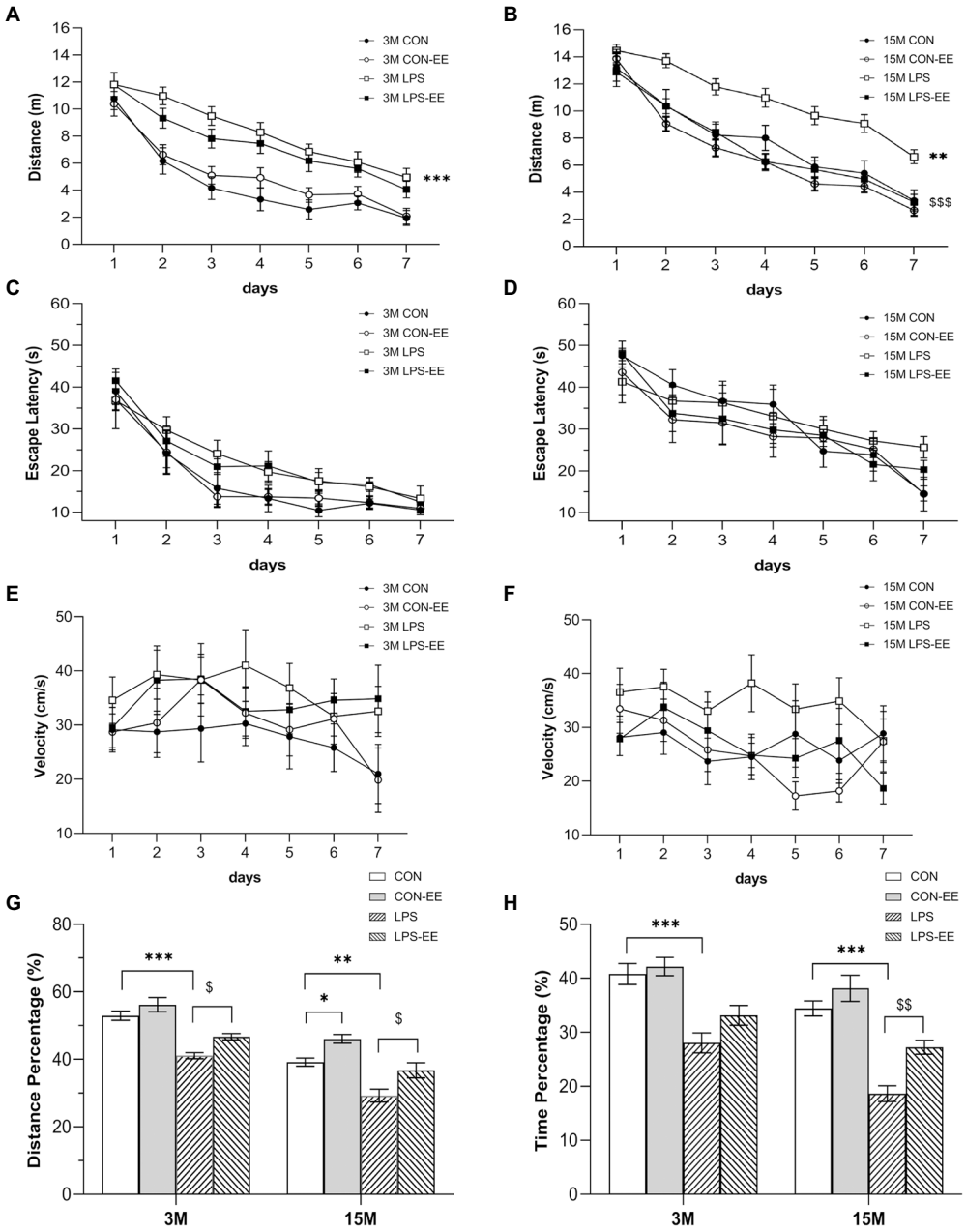

FIGURE 3
Performances in the Morris water maze test with different treatments. Distance swam **(A,B)**, escape latency **(C,D)**, and swimming velocity **(E,F)** during the learning phase, and percentage of distance **(G)** and time **(H)** swam in the target quadrant during the memory phase in the different treatment groups at 3months (3M) and 15months (15M) of age. All data are shown as means±SEM (n=6 male mice/group). *p<0.05, **p<0.01, ***p<0.001 compared with the CON group; $^{\$}p$<0.05, $^{\$\$}p$<0.01, $^{\$\$\$}p$<0.001 compared with the LPS group; CON, untreated control group; LPS, lipopolysaccharide treatment group; EE, group of mice exposed to environmental enrichment.

At 3 months of age, embryonic inflammatory exposure activated systemic immune responses accompanied by elevated serum inflammatory cytokine levels (Figures 4D–F). Exposure of mice to EE did not significantly alter serum cytokine concentrations (CON vs. CON-EE; LPS vs. LPS-EE; Figures 4D–F). At 15 months of age, the LPS mice showed a long-term increased inflammatory response compared to the CON ones (Figures 4G–I). Meanwhile, the long-term EE reduced IL-1β and TNF-α levels in the LPS-EE group (LPS vs. LPS-EE; Figures 4H,I).

Levels of NGPF2 and PSD-95 in the hippocampus

NGPF2 mRNA and protein levels

The levels of NGPF2 mRNA and protein were significantly increased in 15-month-old CON mice compared with 3-month-old mice with the same treatment (Figures 5A–C).

Besides, NGPF2 mRNA and protein levels in the LPS group were significantly higher than those in the CON group,

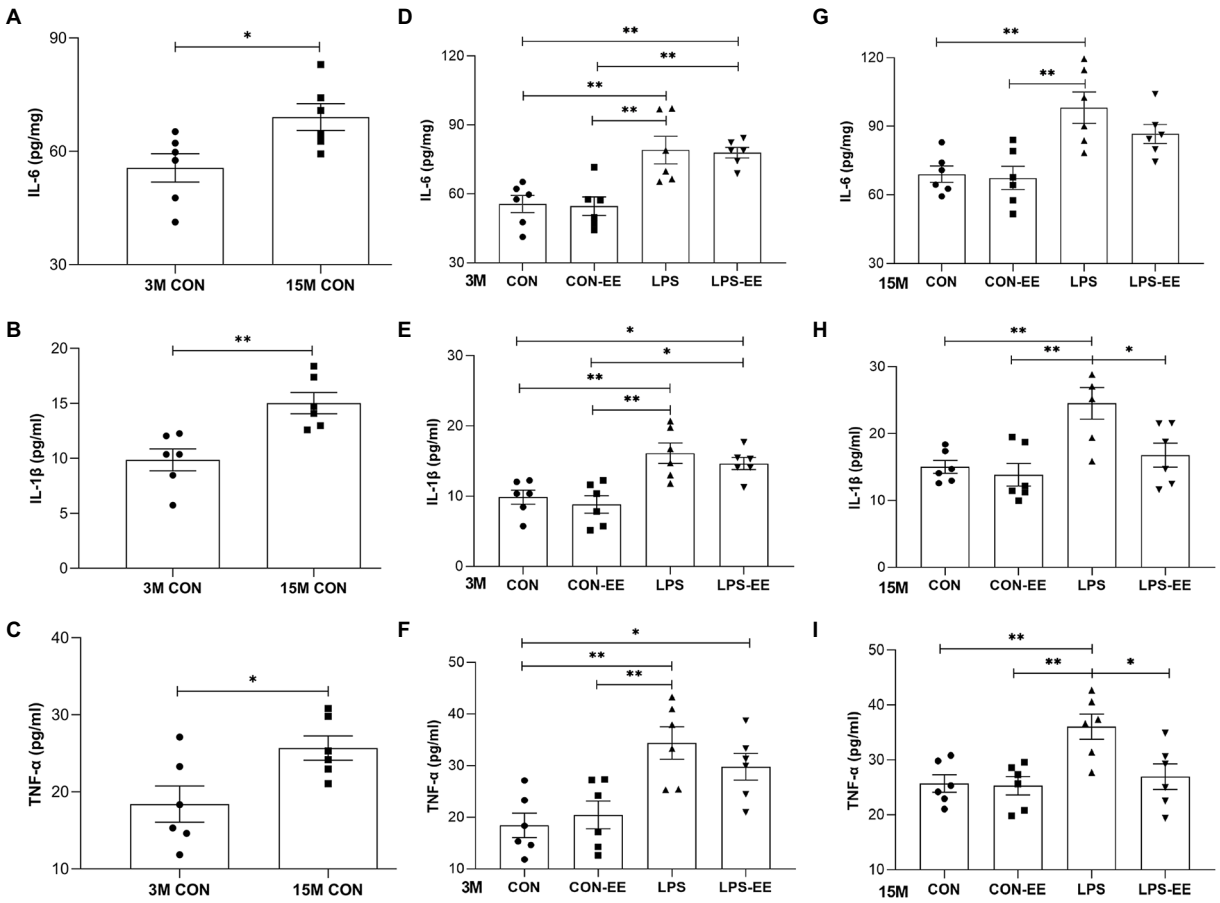

FIGURE 4
Serum levels of IL-6, IL-1β and TNF-α in mice. Serum levels of IL-6 **(A)**, IL-1β **(B)** and TNF-α **(C)** in the CON group at 3months (3M) and 15months (15M) of age depicted the effect of age on systematic inflammation. IL-6, IL-1β, and TNF-α levels in the different treatment groups at 3M **(D-F)** and 15M **(G-I)**. All data are shown as means±SEM (n=6 male mice/group). Significance is as follows: *p<0.05, **p<0.01. CON, untreated control group; LPS, lipopolysaccharide treatment group; EE, group of mice exposed to environmental enrichment.

regardless of age (Figures 5D,E). Meanwhile, no significant effects of short or long-term EE intervention were found on NGPF2 mRNA and protein levels (CON vs. CON-EE; LPS vs. LPS-EE).

PSD-95 mRNA and protein levels

In contrast to the mRNA and protein levels of NGPF in the CON group, the mRNA and protein levels of PSD-95 in 15-month-old mice were decreased (Figures 6A–C).

At both 3 and 15 months of age, PSD-95 mRNA and protein levels were downregulated in the LPS group relative to the CON group (Figures 6D,E). Meanwhile, both short- and long-term EE exposure upregulated the levels of PSD-95 mRNA and protein (LPS vs. LPS-EE). In addition, long-term EE alleviated the reduction of *Psd-95* mRNA expression in aged CON mice (CON vs. CON-EE; Figure 6D).

Correlations between cognitive performance and inflammatory cytokine, NGPF2, and PSD-95

Serum inflammatory cytokine

In 3-month-old mice, serum levels of IL-6, IL-1β, and TNF-α were positively correlated with the distance swam during the learning phase in the LPS and LPS-EE groups, and negatively correlated with the percentage of time swam in the target quadrant during the memory phase in the LPS group (Table 2).

In 15-month-old mice, IL-6, IL-1β, and TNF-α levels positively correlated with the learning distance swam in the LPS and LPS-EE groups and negatively correlated with the memory percentage of distance and time swam in the LPS group (Table 2). Additionally, IL-6 and IL-1β levels showed a negative correction with the memory percentage of distance swam in the LPS-EE group (Table 2).

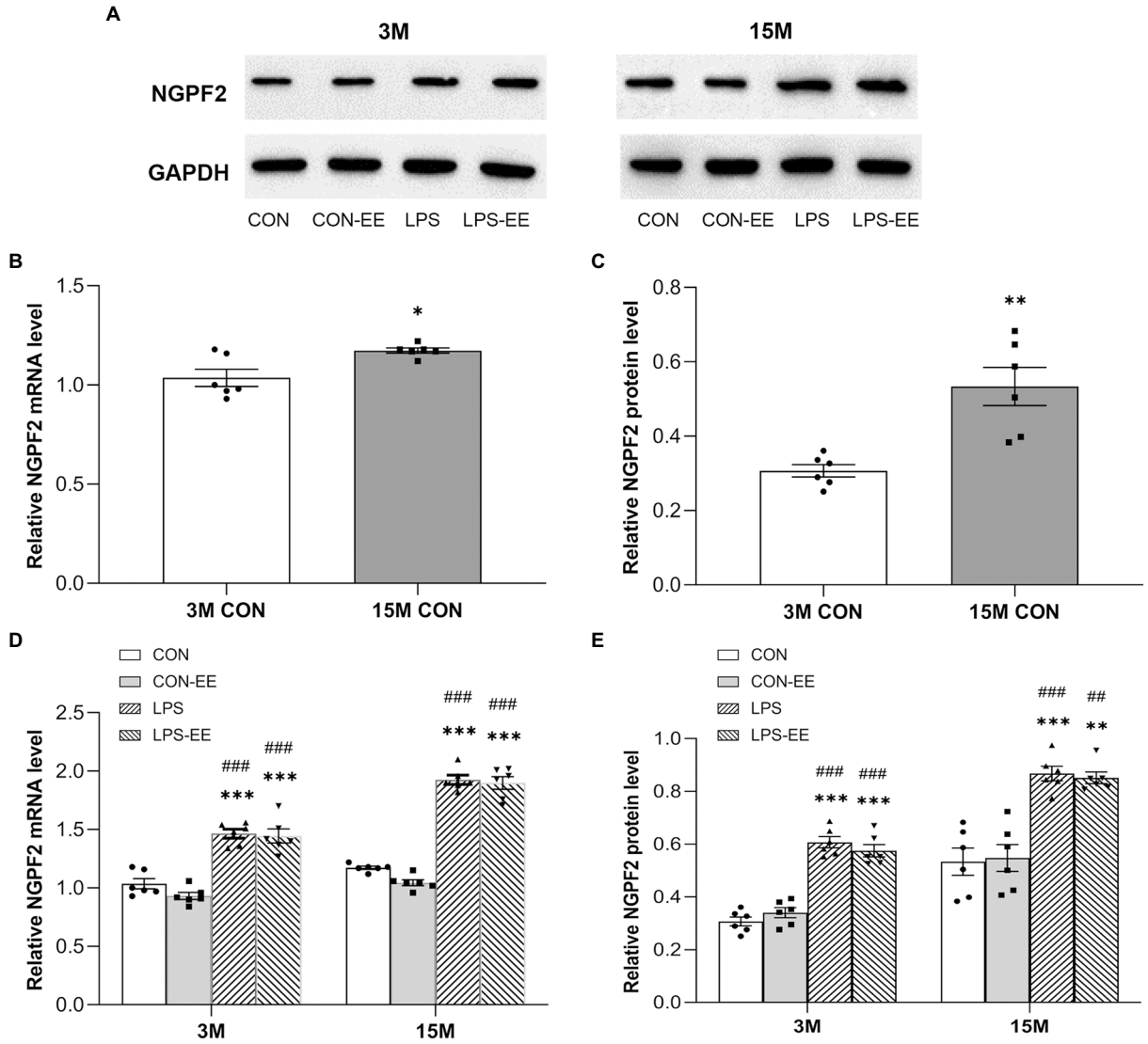

FIGURE 5
The hippocampal mRNA and protein levels of NGPF2 in CD-1 mice. **(A)** Representative immunoreactive bands for NGPF2 in the different treatment groups at 3months (3M) and 15months (15M) of age. NGPF2 mRNA and protein levels in the CON group **(B,C)**, and in the CON, CON-EE, LPS and LPS-EE groups **(D,E)** at 3M and 15M. All data are provided as mean±SEM (n=6 male mice/group). *p<0.05, **p<0.01, ***p<0.001 compared with the CON group; $^{\#\#}p$<0.01, $^{\#\#\#}p$<0.001 compared with the CON-EE group; CON, untreated control group; LPS, lipopolysaccharide treatment group; EE, group of mice exposed to environmental enrichment.

NGPF2

In 3-month-old mice, NGPF2 mRNA and protein levels showed a positive correlation with the learning distance swam in the LPS and LPS-EE groups and a negative correlation with the memory percentage of time swam in the LPS group (Table 3). Furthermore, NGPF2 protein level was negatively correlated with the memory percentage of time swam in the LPS-EE group.

In 15-month-old mice, NGPF2 mRNA and protein levels in the LPS and LPS-EE groups positively correlated with learning distance swam and negatively correlated with the memory percentage of distance swam (Table 3). Besides, the memory percentage of time swam was negatively correlated with *Ngpf2* mRNA in the LPS-EE group, as was NGPF2 protein in the LPS group.

PSD-95

In 3-month-old mice, PSD-95 mRNA and protein levels negatively correlated with the learning distance swam in the LPS and LPS-EE groups and positively correlated with the memory percentage of swimming time in the LPS group (Table 3). *Psd-95* mRNA level showed a positive correlation with the memory percentage of distance swam in the LPS-EE group, and PSD-95 protein level was positively correlated with the memory percentage of swimming time in the LPS-EE group.

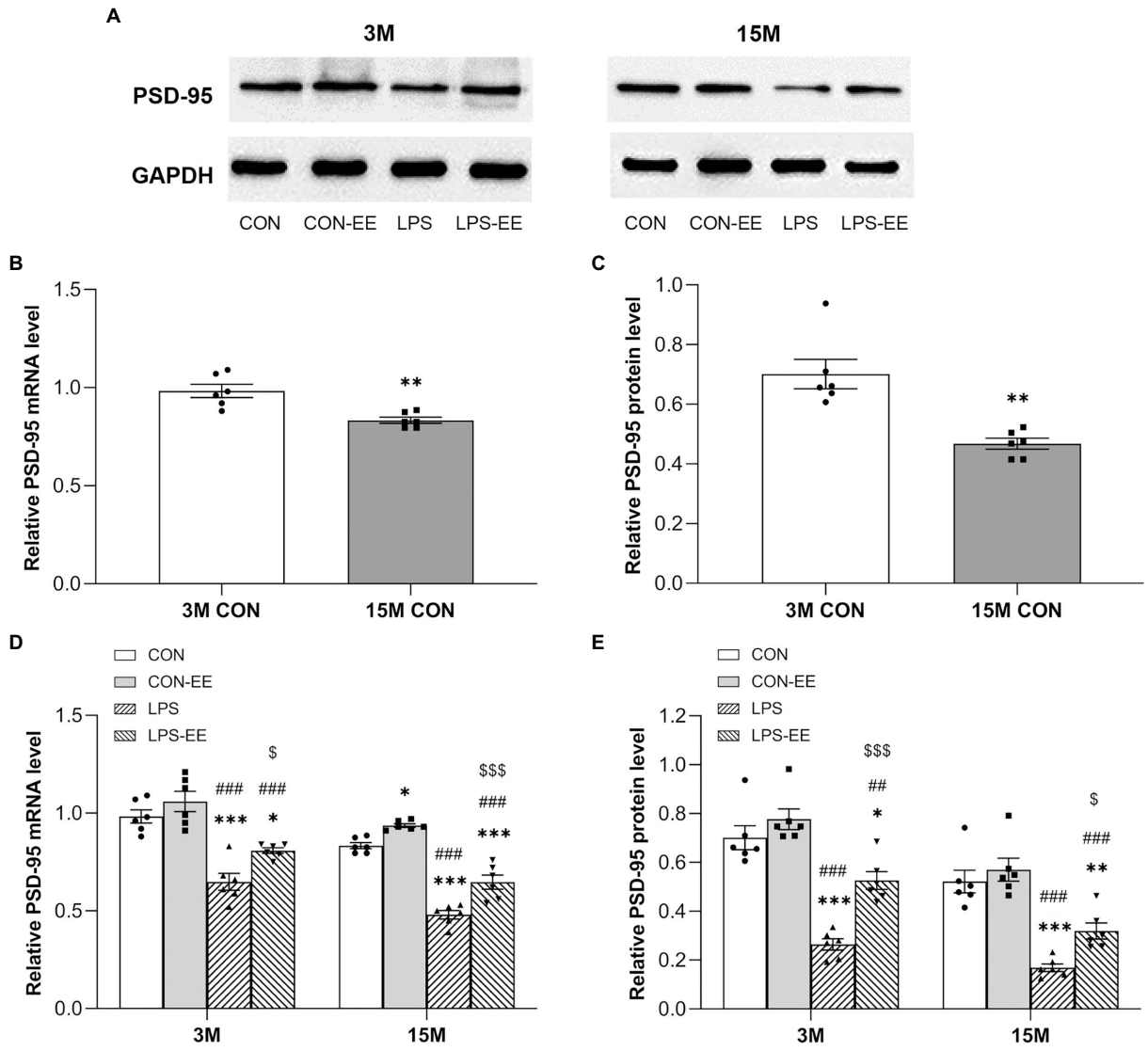

FIGURE 6
The hippocampal mRNA and protein levels of PSD-95 CD-1 mice. **(A)** Representative immunoblots of PSD-95 in the different groups at 3months (3M) and 15months (15M) of age. PSD-95 mRNA and protein levels in the CON group **(B,C)**, and in the CON, CON-EE, LPS, and LPS-EE groups **(D,E)** at different ages. All data are shown as mean±SEM (n=6 male mice/group), *p<0.05, **p<0.01, ***p<0.001 compared with the CON group; $^{\#\#}p$<0.01, $^{\#\#\#}p$<0.001 compared with the CON-EE group; $^{\$}p$<0.05, $^{\$\$\$}p$<0.001 compared with the LPS group; CON, untreated control group; LPS, lipopolysaccharide treatment group; EE, group of mice exposed to environmental enrichment.

In 15-month-old mice, PSD-95 mRNA and protein levels in the LPS and LPS-EE groups exhibited a negative correlation with the learning distance swam and a positive correlation with the memory percentage of distance swam (Table 3). Furthermore, the memory percentage of time spent swimming positively correlated with *Psd-95* mRNA expression in the LPS-EE group and with PSD-95 protein level in the LPS and LPS-EE groups.

Discussion

Pregnancy can be complicated by bacterial infections that lead to increases in immune responses in the offspring (Rose et al., 2017; Wang et al., 2020; Su et al., 2022), and bring the neural and behavioral sequelae throughout the lifespan of the offspring (Hambrick et al., 2019; Nelson and Gabard-Durnam, 2020; Van den Bergh et al., 2020). Several studies have shown that there is a gender-dependent effects of learning and memory during aging, while different research demonstrate conflicting results (Wang et al., 2010; Li et al., 2016). Our previous research showed that there were no significant sex differences in spatial learning and memory in normal mice or prenatal MIA-exposed mice at young and old ages (Xiong et al., 2018; Wu et al., 2019; Wang et al., 2020). So were hippocampal levels of inflammation, synaptic proteins, histones, and markers of AD pathology. In this study, we only selected male offspring for research. Here, the

TABLE 2 Correlations between performance in MWM trial and serum levels of inflammatory cytokines.

Cognitive phase	Age	Group	IL-6	IL-1β	TNF-α
			r (p)	*r (p)*	*r (p)*
Learning distance swam	3 months	CON	0.687 (0.132)	0.544 (0.265)	0.794 (0.060)
		CON-EE	0.566 (0.242)	0.799 (0.056)	0.808 (0.052)
		LPS	**0.862 (0.027)***	**0.846 (0.034)***	**0.818 (0.047)***
		LPS-EE	**0.887 (0.019)***	**0.849 (0.032)***	**0.824 (0.044)***
	15 months	CON	0.784 (0.065)	0.793 (0.060)	0.783 (0.065)
		CON-EE	0.803 (0.054)	0.687 (0.132)	0.789 (0.062)
		LPS	**0.876 (0.022)***	**0.868 (0.025)***	**0.826 (0.043)***
		LPS-EE	**0.891 (0.017)***	**0.8198 (0.046)***	**0.849 (0.032)***
Percentage of distance swam in the target quadrant	3 months	CON	−0.793 (0.060)	−0.508 (0.303)	−0.752 (0.085)
		CON-EE	−0.714 (0.111)	−0.698 (0.123)	−0.752 (0.085)
		LPS	−0.616 (0.193)	−0.752 (0.085)	−0.764 (0.077)
		LPS-EE	−0.775 (0.070)	−0.664 (0.150)	−0.655 (0.158)
	15 months	CON	−0.810 (0.051)	−0.657 (0.156)	−0.775 (0.071)
		CON-EE	−0.694 (0.126)	−0.754 (0.084)	−0.758 (0.081)
		LPS	**−0.831 (0.040)***	**−0.852 (0.031)***	**−0.864 (0.026)***
		LPS-EE	**−0.879 (0.021)***	**−0.824 (0.044)***	−0.6969 (0.124)
Percentage of time spent swimming in the target quadrant	3 months	CON	−0.750 (0.086)	−0.348 (0.499)	−0.675 (0.141)
		CON-EE	−0.274 (0.600)	−0.629 (0.181)	−0.463 (0.355)
		LPS	**−0.832 (0.040)***	**−0.821 (0.045)***	**−0.860 (0.028)***
		LPS-EE	−0.725 (0.103)	−0.603 (0.205)	−0.645 (0.167)
	15 months	CON	−0.664 (0.151)	−0.254 (0.628)	−0.808 (0.052)
		CON-EE	−0.331 (0.520)	−0.608 (0.200)	−0.472 (0.345)
		LPS	**−0.838 (0.037)***	**−0.867 (0.026)***	**−0.846 (0.034)***
		LPS-EE	−0.810 (0.051)	−0.810 (0.051)	−0.634 (0.176)

Denotes significant correlation coefficients ($p < 0.05$); Significant *p*-values are marked in bold. CON, untreated control group; LPS, lipopolysaccharide treatment group; EE, group of mice exposed to environmental enrichment.

results suggested that the LPS mice have elevated levels of systemic inflammation. Meanwhile, prenatal inflammatory exposure accelerated age-associated cognitive dysfunction and changes in *Ngpf2* and *Psd-95* expression in aged mice, whereas EE treatment counteracts some of these influences. Exploration of this potential causal relationship may, to some extent, provide new insights into the mechanisms underlying age-related cognitive impairment.

Environmental enrichment improved spatial cognitive decline aggravated by embryonic inflammatory exposure

Aging fosters cognitive disabilities (Juan and Adlard, 2019). As described in this study, aging is accompanied by spatial learning and memory decline. Consistent with our results, previous studies had shown age-related decreases in learning and memory starting at 12 months of age in mice (Li et al., 2016; Wang et al., 2020). Moreover, converging lines of evidence indicate that prenatal MIA exposure exacerbates age-related cognitive decline (Wu et al., 2020; Zhang et al., 2020). In the present study, embryonic MIA exposure impaired learning and memory in young mice and accelerated aged-related cognitive deficits in aged mice.

In contrast, multiple studies have demonstrated that EE conveys beneficial effects on cognitive function in mice (Ohline and Abraham, 2019; Crawford et al., 2020; Ismail et al., 2021). Moreover, some detrimental effects of early adverse events can be counteracted by housing mice in cages with more favorable environments (Aghighi Bidgoli et al., 2020; Cordier et al., 2021). Adolescence also represents a critical and sensitive stage in brain development, making it susceptible to environmental stimuli (Wu et al., 2020; Cordier et al., 2021), and therefore, the EE intervention in our study was initiated during adolescence. However, our findings showed that short-term EE (from weaning to 3 months of age) had little effect on cognitive impairment (CON vs. CON-EE; LPS vs. LPS-EE). Notably, long-term EE (from weaning to 15 months of age) exerted a significantly restorative effect on impaired cognition in aged LPS-EE mice (LPS vs. LPS-EE), but not in aged CON-EE ones (CON vs. CON-EE). Other studies have shown that 13 or 14 months of EE exposure improves cognitive deficits in 18-month-old mouse dams exposed to LPS during pregnancy

TABLE 3 Correlations between performance in the MWM trial and mRNA/protein levels of NGPF2 and PSD-95.

Cognitive phase	Age	Group	*Ngpf2* mRNA	NGPF2 protein	*Psd-95* mRNA	PSD-95 protein
			r (p)	*r (p)*	*r (p)*	*r (p)*
Learning distance swam	3 months	CON	0.268 (0.608)	0.189 (0.720)	−0.736 (0.095)	−0.669 (0.146)
		CON-EE	0.214 (0.683)	0.789 (0.062)	−0.519 (0.291)	−0.611 (0.194)
		LPS	**0.874 (0.023)***	**0.916 (0.010)***	**−0.874 (0.023)***	**−0.871 (0.024)***
		LPS-EE	**0.841 (0.036)***	**0.859 (0.028)***	**−0.900 (0.014)***	**−0.855 (0.030)***
	15 months	CON	0.101 (0.850)	0.785 (0.064)	−0.738 (0.094)	−0.567 (0.241)
		CON-EE	0.809 (0.051)	0.797 (0.058)	−0.560 (0.247)	−0.450 (0.370)
		LPS	**0.860 (0.028)***	**0.886 (0.019)***	**−0.834 (0.039)***	**−0.830 (0.041)***
		LPS-EE	**0.867 (0.025)***	**0.890 (0.018)***	**−0.885 (0.019)***	**−0.827 (0.042)***
Percentage of distance swam in the target quadrant	3 months	CON	−0.331 (0.522)	−0.636 (0.175)	0.706 (0.117)	0.441 (0.381)
		CON-EE	−0.772 (0.072)	−0.772 (0.072)	0.664 (0.150)	0.698 (0.123)
		LPS	−0.558 (0.250)	−0.557 (0.250)	0.773 (0.071)	0.236 (0.653)
		LPS-EE	−0.663 (0.152)	−0.396 (0.437)	**0.889 (0.018)***	0.543(0.260)
	15 months	CON	−0.734 (0.097)	−0.674 (0.143)	0.300 (0.563)	0.684(0.134)
		CON-EE	−0.617 (0.192)	−0.782 (0.066)	0.79e8 (0.057)	0.497 (0.316)
		LPS	**−0.840 (0.036)***	**−0.852 (0.031)***	**0.878 (0.021)***	**0.898 (0.015)***
		LPS-EE	**−0.828 (0.042)***	**−0.908 (0.012)***	**0.877 (0.022)***	**0.936 (0.006)****
Percentage of time spent swimming in the target quadrant	3 months	CON	−0.396 (0.437)	−0.273 (0.600)	0.542 (0.266)	0.645 (0.167)
		CON-EE	−0.293 (0.573)	−0.793 (0.060)	0.803(0.055)	0.652 (0.161)
		LPS	**−0.835 (0.038)***	**−0.885 (0.019)***	**0.833 (0.040)***	**0.870 (0.024)***
		LPS-EE	−0.702 (0.120)	**−0.824 (0.044)***	0.681(0.136)	**0.901 (0.014)***
	15 months	CON	−0.564 (0.244)	−0.800 (0.056)	0.761 (0.079)	0.653 (0.160)
		CON-EE	−0.561 (0.247)	−0.742 (0.092)	0.612 (0.197)	0.666 (0.149)
		LPS	−0.747 (0.088)	**−0.879 (0.021)***	0.766 (0.076)	**0.904 (0.013)***
		LPS-EE	**−0.864 (0.027)***	−0.636 (0.174)	**0.862 (0.027)***	**0.911 (0.012)***

Denotes significant correlation coefficients ($p < 0.05$, **$p < 0.01$); Significant p-values are marked in bold. CON, untreated control group; LPS, lipopolysaccharide treatment group; EE, group of mice exposed to environmental enrichment.

and in their 15-month-old offspring (Wu et al., 2020; Zhuang et al., 2021). These results are similar to ours. In short, our results suggested that long-term EE is necessary to alleviate age-related cognitive decline that is accelerated by embryonic inflammatory exposure.

Additionally, prenatal MIA exposure could also increase the risk of developing psychiatric disorders later in life, such as schizophrenia and autism spectrum disorder (Batinić et al., 2016; Simões et al., 2018). The development of these psychiatric disorders is often accompanied by memory loss during aging. (Roy et al., 2021), which may complicate the results of the measured memory. Our previous work showed that the LPS mice had similar anxieties compared to the same-aged controls at 1, 6, 9, and 14 months of age (Chen et al., 2011; Wang et al., 2020). At 18 months of age, MIA-exposed mice exhibited increased anxieties relative to the same-aged controls (Wang et al., 2020). Overall, these results suggest that prenatal MIA exposure induces an increase in anxiety in an age-dependent manner. In this study, the lack of evaluation of anxiety and depression that may affect memory in mice is a limitation.

The effects of environmental enrichment on changes in inflammatory cytokine, NGPF2, and PSD-95 accelerated by prenatal inflammatory exposure

Aging is a distinct pro-inflammatory fate (Baker and Petersen, 2018). As shown in this study, the serum inflammatory cytokine levels reflective of systemic inflammatory responses increased with age. In aged mice, the level of glial fibrillary acidic protein, an astrogliosis marker, was also significantly increased in the hippocampus (Rogers et al., 2017).

Several studies suggest that prenatal MIA exposure could alter the immune function in offspring (Hsiao et al., 2012; Rose et al., 2017; Wang et al., 2020). In a MIA model of rhesus monkeys, the offspring were followed until 4 years of age and exhibited increased levels of plasma inflammatory cytokines (Rose et al., 2017). However, little literature has reported whether exposure of embryos to LPS-induced MIA affects systemic immune responses in aged mice. Our data indicated that serum inflammatory cytokine levels were significantly elevated in the LPS group compared to the CON group at both young and old ages. MIA

exposure *in utero* also altered neuroimmune modulations in the offspring from embryonic to old age in the mouse hippocampus (Simões et al., 2018; Wang et al., 2020; Guma et al., 2022; Su et al., 2022). For example, previous work from our group has shown that aged LPS mice have increased levels of glial fibrillary acidic protein in the hippocampus relative to age-matched controls (Wang et al., 2020). Briefly, the findings of our group suggested that prenatal MIA exposure enhances age-related increases in inflammatory responses in aged offspring.

NGPF2 has important pathophysiological roles in the CNS (Yoshida et al., 2014). However, there are currently no studies on age-related changes of NGPF2 in the hippocampus. In this study, the results, for the first time, showed an increase in *Ngpf2* expression in the hippocampus of aged mice. Although NGPF2 is at a trivial level in healthy adult mice, it is often upregulated in neuroinflammatory conditions (Kadomatsu et al., 2013; Winkler and Yao, 2014; Ross-Munro et al., 2020). This age-related increase in NGPF2 may somewhat reflect changes in the hippocampal aging process.

The *Ngpf2* gene promoter region contains a binding site for the nuclear factor kappa-B response element, which could be activated by LPS and inflammatory cytokines, such as TNF-α and IL-1β (Cai et al., 2020; Ross-Munro et al., 2020; Domínguez-Rivas et al., 2021). Thus, *Ngpf2* expression is induced after inflammatory injury. For example, NGPF2 protein level was significantly increased after induction of experimental autoimmune encephalitis (Yoshida et al., 2014). Results of our group suggested that prenatal inflammatory exposure increased the inflammation in offspring. As expected, inflammatory exposure *in utero* significantly affected the hippocampal *Ngpf2* expression in this research, with an increase in the LPS mice relative to the CON mice at both young and old ages. Hence, this indicated that prenatal inflammation exposure accelerates age-related upregulation of NGPF2 in aged mice.

Although some studies suggest that EE exposure may improve immune system responses, this possibility has not been widely explored (Keymoradzadeh et al., 2020; Domínguez-Rivas et al., 2021). In this experiment, the effect of EE exposure on serum inflammatory cytokine levels and hippocampal *Ngpf2* expression was minimal (CON vs. CON-EE; LPS vs. LPS-EE).

PSD-95 is a major synaptic protein involved in aging (Savioz et al., 2014; Bustos et al., 2017). In this study, hippocampal *Psd-95* expression decreased with aging, which has been confirmed in other experiments (Rogers et al., 2017; Cały et al., 2021).

Numerous studies have shown that PSD-95 level is reduced in neurodegenerative diseases, like AD (Savioz et al., 2014; Zarate et al., 2021). In young rodents, hippocampal PSD-95 levels have been found to be affected by AD-like pathology or early life stress (Jung and Kim, 2017; Shen et al., 2019; Xiao et al., 2021). Currently, the effects of embryonic inflammatory exposure on hippocampal *Psd-95* expression in aged mice are rarely reported. Here, *Psd-95* expression was significantly decreased in the LPS mice compared to the same-aged controls, especially at old age. In other words, this suggested that prenatal inflammatory exposure enhances age-related downregulation of hippocampal PSD-95. Growing evidence suggests that EE could improve loss of synaptic proteins and impaired synaptic plasticity (Aghighi Bidgoli et al., 2020; Wei et al., 2020; Cordier et al., 2021). PSD-95 is the most abundant scaffolding protein in excitatory postsynaptic density and potently regulates synaptic plasticity (Bustos et al., 2017). Indeed, loss of PSD-95 could cause synaptic dysfunction (Zarate et al., 2021). Our findings showed that both short- and long-term EE treatment significantly restored the decrease in *Psd-95* expression in the mouse hippocampus (LPS vs. LPS-EE). Similarly, EE exposure significantly reversed chronic stress-induced reduction in PSD-95 in the hippocampus of young rats (Shen et al., 2019). Besides, reduced hippocampal PSD-95 was also restored by EE treatment in aged socially isolated mice (Wang et al., 2018). Interestingly, this therapeutic effect was virtually absent in CON-EE mice (CON vs. CON-EE). Thus, our results suggested that EE may serve as a potential intervention to improve impairments in *Psd-95* expression and synaptic function in prenatal MIA-exposed mice.

Alterations in inflammatory cytokine, NGPF2, and PSD-95 are associated with cognitive dysfunction in aged mice with accelerated aging

Chronic systemic inflammation increases the risk of cognitive impairment (Ashraf-Ganjouei et al., 2020). Specifically, systemic inflammation ultimately activates microglia and astrocytes *via* different pathways, contributing to AD pathology and age-related cognitive decline (Walker et al., 2019). In current study, elevated levels of IL-6, IL-1β, and TNF-α were positively associated with poorer cognition, especially in aged LPS and LPS-EE mice, demonstrating that increased systemic inflammation is closely related to cognitive decline during the accelerated aging. Other studies have shown that patients with AD and mild cognitive deficits tend to have higher levels of peripheral inflammatory cytokines, which are similar to ours.

However, to date, no studies have reported whether *Ngpf2* expression is associated with cognitive impairment in adult mice. Our results showed that cognitive performance was significantly associated with the hippocampal *Ngpf2* expression. Specifically, *Ngpf2* expression was positively correlated with spatial learning and memory impairment in MWM trials, particularly in aged LPS and LPS-EE mice. In traumatic brain injury mice, NGPF2 enhanced neuroinflammation in the brain lesions, leading to worse neurological consequences (Takada et al., 2020). Importantly, NGPF2 could specifically modulate neuroinflammation and influence cognitive changes (Vicente-Rodríguez et al., 2016; Fernández-Calle et al., 2018). In this study, the results demonstrated that an increase in hippocampal NGPF2 appears to be involved in spatial cognition impairment induced by embryonic MIA exposure, especially in aged mice.

As a member of the membrane-associated guanylate kinase family (Savioz et al., 2014), PSD-95 facilitates synaptic maturation by trafficking and anchoring ionotropic glutamate receptors to the postsynaptic membrane (Hambrick et al., 2019). Changes in the level of PSD-95 alter clustering and maintenance of glutamate receptors (Zarate et al., 2021). Thus, PSD-95 plays an essential role in regulating synaptic plasticity, which are fundamental mechanisms that contribute to hippocampal-dependent learning and memory (Savioz et al., 2014; Bustos et al., 2017; Zarate et al., 2021).

However, it is uncertain whether changes in hippocampal *Psd-95* expression are associated with cognitive decline in mice during accelerated aging. As opposed to NGPF2, here, *Psd-95* expression was negatively correlated with spatial learning and memory decline in the aged LPS and LPS-EE mice. Collectively, this suggests that reduced *Psd-95* expression in the hippocampus is associated with cognitive deficits in the mice with accelerated aging. In a young rat model of AD, hippocampal PSD-95 were found to be reduced, with concomitant declines in learning and memory (Xiao et al., 2021). These changes were similar to our 3-month-old LPS mice. A study of natural aging showed that aged mice exhibited reduced hippocampal PSD-95. Interestingly, deficits in long-term potentiation, spatial learning and memory were not observed until 6 months later. This suggested that changes in PSD-95 level do not completely parallel the decline in cognitive and synaptic function during normal aging. In our study, there was also no statistically significant correlation between PSD-95 and cognition in normal aging mice. But when prenatal inflammatory exposure accelerated the decrease in PSD-95, the association was significant, especially in aged mice.

Finally, this study found that long-term EE exposure significantly improved age-related cognitive deficits in the LPS-EE mice. However, the mechanism of this cognitive-improving effect of EE has not yet been elucidated. EE exposure was found to induce an increase in PSD-95 protein level and synaptic plasticity in rodent's hippocampus, with concomitant improvement in cognitive deficits (Jung and Kim, 2017; Shen et al., 2019). Moreover, *Psd-95* expression is downregulated in hippocampus with aging, AD, and other pathologies (Savioz et al., 2014; Rogers et al., 2017; Xiao et al., 2021). Thus, *Psd-95* expression may counteract aging or pathological processes (Savioz et al., 2014). Because the effects of EE intervention on *Ngpf2* expression and serum inflammatory cytokine levels were minimal, we speculate that EE exposure repaired cognitive impairment by increasing *Psd*-95 expression and thereby improving synaptic plasticity. Indeed, our results confirmed that EE exposure significantly restored the decrease in hippocampal *Psd-95* expression in the LPS-EE mice. Collectively, changes in hippocampal *Ngpf2* and *Psd-95* expression were associated with age-dependent cognitive decline in mice with accelerated aging, and long-term EE may ameliorate this cognitive decline by improving *Psd-95* expression.

In summary, prenatal MIA exposure accelerates age-related declines in spatial learning and memory and exacerbates age-related changes in hippocampal *Ngpf2* and *Psd-95* expression and peripheral inflammatory cytokine levels in offspring mice. These biochemical changes were closely correlated with impaired spatial cognition, particularly during "pathological" aging. Furthermore, long-term EE exposure attenuated these cognitive declines, possibly by enhancing *Psd-95* expression. Therefore, EE exposure and targeted modulation of neuroinflammation may represent a potential therapeutic strategy for age-related cognitive decline. Limitations in the present study include not investigating the level of hippocampal inflammation, treatment effects on *Ngpf2* and *Psd-95* expression in different subregions of the hippocampus, and sex differences. In the future, we will explore the effects of embryonic exposure to maternal inflammation on NGPF2-related signaling pathways, neuroinflammatory signaling pathways, and synaptic plasticity in mice.

Data availability statement

The raw data supporting the conclusions of this article will be made available by the authors, without undue reservation.

Ethics statement

The animal study was reviewed and approved by the Experimental Animal Ethics Committee of Anhui Medical University.

Author contributions

M-ZN and Y-MZ conceived and designed the study, performed the experiments, and drafted the manuscript. Q-TW and YL conducted the experiments. JC and B-LL conducted the behavioral tests and collected the data. Z-ZZ performed the statistical analyses. G-HC and X-WL revised the manuscript. All authors contributed to the article and approved the submitted version.

Funding

This work was financially supported by the National Natural Science Foundation of China (81370444 and 81671316), Scientific Research Fund Project of Hunan Provincial Health Commission (20200497), and Natural Science Foundation of Hunan Province of China (2021JJ70040).

Acknowledgments

Thanks to all my classmates and partners who gave me generous support and helpful advice in this research.

Conflict of interest

The authors declare that the research was conducted in the absence of any commercial or financial relationships that could be construed as a potential conflict of interest.

Publisher's note

All claims expressed in this article are solely those of the authors and do not necessarily represent those of their affiliated organizations, or those of the publisher, the editors and the reviewers. Any product that may be evaluated in this article, or claim that may be made by its manufacturer, is not guaranteed or endorsed by the publisher.

Supplementary material

The Supplementary material for this article can be found online at: https://www.frontiersin.org/articles/10.3389/fnagi.2022.1021237/full#supplementary-material

References

Aghighi Bidgoli, F., Salami, M., and Talaei, S. A. (2020). Environmental enrichment restores impaired spatial memory and synaptic plasticity in prenatally stress exposed rats: the role of GABAergic neurotransmission. *Int. J. Dev. Neurosci.* 80, 573–585. doi: 10.1002/jdn.10052

Ashraf-Ganjouei, A., Moradi, K., Bagheri, S., and Aarabi, M. H. (2020). The association between systemic inflammation and cognitive performance in healthy adults. *J. Neuroimmunol.* 345:577272. doi: 10.1016/j.jneuroim.2020.577272

Baker, D. J., and Petersen, R. C. (2018). Cellular senescence in brain aging and neurodegenerative diseases: evidence and perspectives. *J. Clin. Invest.* 128, 1208–1216. doi: 10.1172/JCI95145

Batinić, B., Santrač, A., Divović, B., Timić, T., Stanković, T., Obradović, A., et al. (2016). Lipopolysaccharide exposure during late embryogenesis results in diminished locomotor activity and amphetamine response in females and spatial cognition impairment in males in adult, but not adolescent rat offspring. *Behav. Brain Res.* 299, 72–80. doi: 10.1016/j.bbr.2015.11.025

Bettio, L., Rajendran, L., and Gil-Mohapel, J. (2017). The effects of aging in the hippocampus and cognitive decline. *Neurosci. Biobehav. Rev.* 79, 66–86. doi: 10.1016/j.neubiorev.2017.04.030

Bustos, F. J., Ampuero, E., Jury, N., Aguilar, R., Falahi, F., Toledo, J., et al. (2017). Epigenetic editing of the Dlg4/PSD95 gene improves cognition in aged and Alzheimer's disease mice. *Brain* 140, 3252–3268. doi: 10.1093/brain/awx272

Cadaret, C. N., Merrick, E. M., Barnes, T. L., Beede, K. A., Posont, R. J., Petersen, J. L., et al. (2019). Sustained maternal inflammation during the early third-trimester yields intrauterine growth restriction, impaired skeletal muscle glucose metabolism, and diminished β-cell function in fetal sheep1,2. *J. Anim. Sci.* 97, 4822–4833. doi: 10.1093/jas/skz321

Cai, Y. Q., Lv, Y., Mo, Z. C., Lei, J., Zhu, J. L., and Zhong, Q. Q. (2020). Multiple pathophysiological roles of midkine in human disease. *Cytokine* 135:155242. doi: 10.1016/j.cyto.2020.155242

Cały, A., Śliwińska, M. A., Ziółkowska, M., Łukasiewicz, K., Pagano, R., Dzik, J. M., et al. (2021). PSD-95 in CA1 area regulates spatial choice depending on age. *J. Neurosci.* 41, 2329–2343. doi: 10.1523/JNEUROSCI.1996-20.2020

Chen, G. H., Wang, H., Yang, Q. G., Tao, F., Wang, C., and Xu, D. X. (2011). Acceleration of age-related learning and memory decline in middle-aged CD-1 mice due to maternal exposure to lipopolysaccharide during late pregnancy. *Behav. Brain Res.* 218, 267–279. doi: 10.1016/j.bbr.2010.11.001

Colonna, M., and Butovsky, O. (2017). Microglia function in the central nervous system during health and Neurodegeneration. *Annu. Rev. Immunol.* 35, 441–468. doi: 10.1146/annurev-immunol-051116-052358

Cordier, J. M., Aguggia, J. P., Danelon, V., Mir, F. R., Rivarola, M. A., and Mascó, D. (2021). Postweaning enriched environment enhances cognitive function and brain-derived Neurotrophic factor signaling in the hippocampus in maternally separated rats. *Neuroscience* 453, 138–147. doi: 10.1016/j.neuroscience.2020.09.058

Crawford, L. E., Knouse, L. E., Kent, M., Vavra, D., Harding, O., LeServe, D., et al. (2020). Enriched environment exposure accelerates rodent driving skills. *Behav. Brain Res.* 378:112309. doi: 10.1016/j.bbr.2019.112309

Domínguez-Rivas, E., Ávila-Muñoz, E., Schwarzacher, S. W., and Zepeda, A. (2021). Adult hippocampal neurogenesis in the context of lipopolysaccharide-induced neuroinflammation: a molecular, cellular and behavioral review. *Brain Behav. Immun.* 97, 286–302. doi: 10.1016/j.bbi.2021.06.014

Dore, K., Carrico, Z., Alfonso, S., Marino, M., Koymans, K., Kessels, H. W., et al. (2021). PSD-95 protects synapses from β-amyloid. *Cell Rep.* 35:109194. doi: 10.1016/j.celrep.2021.109194

Elovitz, M. A., Brown, A. G., Breen, K., Anton, L., Maubert, M., and Burd, I. (2011). Intrauterine inflammation, insufficient to induce parturition, still evokes fetal and neonatal brain injury. *Int. J. Dev. Neurosci.* 29, 663–671. doi: 10.1016/j.ijdevneu.2011.02.011

Fernández-Calle, R., Vicente-Rodríguez, M., Gramage, E., de la Torre-Ortiz, C., Pérez-García, C., Ramos, M. P., et al. (2018). Endogenous pleiotrophin and midkine regulate LPS-induced glial responses. *Neurosci. Lett.* 662, 213–218. doi: 10.1016/j.neulet.2017.10.038

Filippou, P. S., Karagiannis, G. S., and Constantinidou, A. (2020). Midkine (MDK) growth factor: a key player in cancer progression and a promising therapeutic target. *Oncogene* 39, 2040–2054. doi: 10.1038/s41388-019-1124-8

Fitzgerald, P. J., Pinard, C. R., Camp, M. C., Feyder, M., Sah, A., Bergstrom, H. C., et al. (2015). Durable fear memories require PSD-95. *Mol. Psychiatry* 20, 901–912. doi: 10.1038/mp.2014.161

Geinisman, Y., Detoledo-Morrell, L., Morrell, F., and Heller, R. E. (1995). Hippocampal markers of age-related memory dysfunction: behavioral, electrophysiological and morphological perspectives. *Prog. Neurobiol.* 45, 223–252. doi: 10.1016/0301-0082(94)00047-l

Griñán-Ferré, C., Izquierdo, V., Otero, E., Puigoriol-Illamola, D., Corpas, R., Sanfeliu, C., et al. (2018). Environmental enrichment improves cognitive deficits, AD hallmarks and epigenetic alterations presented in 5xFAD mouse model. *Front. Cell. Neurosci.* 12:224. doi: 10.3389/fncel.2018.00224

Griñan-Ferré, C., Pérez-Cáceres, D., Gutiérrez-Zetina, S. M., Camins, A., Palomera-Avalos, V., Ortuño-Sahagún, D., et al. (2016a). Environmental enrichment improves behavior, cognition, and brain functional markers in young senescence-accelerated prone mice (SAMP8). *Mol. Neurobiol.* 53, 2435–2450. doi: 10.1007/s12035-015-9210-6

Griñan-Ferré, C., Puigoriol-Illamola, D., Palomera-Ávalos, V., Pérez-Cáceres, D., Companys-Alemany, J., Camins, A., et al. (2016b). Environmental enrichment modified epigenetic mechanisms in SAMP8 mouse hippocampus by reducing oxidative stress and Inflammaging and achieving Neuroprotection. *Front. Aging Neurosci.* 8:241. doi: 10.3389/fnagi.2016.00241

Guma, E., Bordeleau, M., González Ibáñez, F., Picard, K., Snook, E., Desrosiers-Grégoire, G., et al. (2022). Differential effects of early or late exposure to prenatal maternal immune activation on mouse embryonic neurodevelopment. *Proc. Natl. Acad. Sci. U. S. A.* 119:e2114545119. doi: 10.1073/pnas.2114545119

Hambrick, E. P., Brawner, T. W., and Perry, B. D. (2019). Timing of early-life stress and the development of brain-related capacities. *Front. Behav. Neurosci.* 13:183. doi: 10.3389/fnbeh.2019.00183

Henrique, F. L., Zanella, A. J., Bezerra, H., Polato, H. Z., Fernandes, A. C., Hooper, H. B., et al. (2021). Stress during first gestation of ewes impairs memory and learning of male offspring. *Vet. Res. Commun.* 45, 251–260. doi: 10.1007/s11259-021-09805-3

Herradón, G., and Pérez-García, C. (2014). Targeting midkine and pleiotrophin signalling pathways in addiction and neurodegenerative disorders: recent progress and perspectives. *Br. J. Pharmacol.* 171, 837–848. doi: 10.1111/bph.12312

Hsiao, E. Y., McBride, S. W., Chow, J., Mazmanian, S. K., and Patterson, P. H. (2012). Modeling an autism risk factor in mice leads to permanent immune dysregulation. *Proc. Natl. Acad. Sci. U. S. A.* 109, 12776–12781. doi: 10.1073/pnas.1202556109

Ishikawa, E., Ooboshi, H., Kumai, Y., Takada, J., Nakamura, K., Ago, T., et al. (2009). Midkine gene transfer protects against focal brain ischemia and augments neurogenesis. *J. Neurol. Sci.* 285, 78–84. doi: 10.1016/j.jns.2009.05.026

Ismail, T. R., Yap, C. G., Naidu, R., and Pamidi, N. (2021). Enrichment protocol for rat models. *Curr. Protoc.* 1:e152. doi: 10.1002/cpz1.152

Juan, S., and Adlard, P. A. (2019). Ageing and cognition. *Subcell. Biochem.* 91, 107–122. doi: 10.1007/978-981-13-3681-2_5

Jung, S. Y., and Kim, D. Y. (2017). Treadmill exercise improves motor and memory functions in cerebral palsy rats through activation of PI3K-Akt pathway. *J. Exerc. Rehabil.* 13, 136–142. doi: 10.12965/jer.1734964.482

Kadomatsu, K., Kishida, S., and Tsubota, S. (2013). The heparin-binding growth factor midkine: the biological activities and candidate receptors. *J. Biochem.* 153, 511–521. doi: 10.1093/jb/mvt035

Keymoradzadeh, A., Hedayati, C. M., Abedinzade, M., Gazor, R., Rostampour, M., and Taleghani, B. K. (2020). Enriched environment effect on lipopolysaccharide-induced spatial learning, memory impairment and hippocampal inflammatory cytokine levels in male rats. *Behav. Brain Res.* 394:112814. doi: 10.1016/j.bbr.2020.112814

Kubo, K. Y., Ogasawara, A., Tsugane, H., Iinuma, M., Takahashi, T., and Azuma, K. (2021). Environmental enrichment improves hypomyelination, synaptic alterations, and memory deficits caused by tooth loss in aged SAMP8 mice. *Arch. Oral.* 123:105039. doi: 10.1016/j.archoralbio.2021.105039

Li, X. W., Cao, L., Wang, F., Yang, Q. G., Tong, J. J., Li, X. Y., et al. (2016). Maternal inflammation linearly exacerbates offspring age-related changes of spatial learning and memory, and neurobiology until senectitude. *Behav. Brain Res.* 306, 178–196. doi: 10.1016/j.bbr.2016.03.011

Liang, M., Zhong, H., Rong, J., Li, Y., Zhu, C., Zhou, L., et al. (2019). Postnatal lipopolysaccharide exposure impairs adult neurogenesis and causes depression-like behaviors through astrocytes activation triggering GABAA receptor Downregulation. *Neuroscience* 422, 21–31. doi: 10.1016/j.neuroscience.2019.10.025

Nelson, C. A. 3rd, and Gabard-Durnam, L. J. (2020). Early adversity and critical periods: neurodevelopmental consequences of violating the expectable environment. *Trends Neurosci.* 43, 133–143. doi: 10.1016/j.tins.2020.01.002

Ohline, S. M., and Abraham, W. C. (2019). Environmental enrichment effects on synaptic and cellular physiology of hippocampal neurons. *Neuropharmacology* 145, 3–12. doi: 10.1016/j.neuropharm.2018.04.007

Petralia, R. S., Mattson, M. P., and Yao, P. J. (2014). Communication breakdown: the impact of ageing on synapse structure. *Ageing Res. Rev.* 14, 31–42. doi: 10.1016/j.arr.2014.01.003

Rogers, J. T., Liu, C. C., Zhao, N., Wang, J., Putzke, T., Yang, L., et al. (2017). Subacute ibuprofen treatment rescues the synaptic and cognitive deficits in advanced-aged mice. *Neurobiol. Aging* 53, 112–121. doi: 10.1016/j.neurobiolaging.2017.02.001

Rose, D. R., Careaga, M., Van de Water, J., McAllister, K., Bauman, M. D., and Ashwood, P. (2017). Long-term altered immune responses following fetal priming in a non-human primate model of maternal immune activation. *Brain Behav. Immun.* 63, 60–70. doi: 10.1016/j.bbi.2016.11.020

Ross-Munro, E., Kwa, F., Kreiner, J., Khore, M., Miller, S. L., Tolcos, M., et al. (2020). Midkine: the who, what, where, and when of a promising Neurotrophic therapy for perinatal brain injury. *Front. Neurol.* 11:568814. doi: 10.3389/fneur.2020.568814

Roy, D. S., Zhang, Y., Aida, T., Choi, S., Chen, Q., Hou, Y., et al. (2021). Anterior thalamic dysfunction underlies cognitive deficits in a subset of neuropsychiatric disease models. *Neuron* 109, 2590–2603.e13. doi: 10.1016/j.neuron.2021.06.005

Savioz, A., Leuba, G., and Vallet, P. G. (2014). A framework to understand the variations of PSD-95 expression in brain aging and in Alzheimer's disease. *Ageing Res. Rev.* 18, 86–94. doi: 10.1016/j.arr.2014.09.004

Shao, C. Y., Mirra, S. S., Sait, H. B., Sacktor, T. C., and Sigurdsson, E. M. (2011). Postsynaptic degeneration as revealed by PSD-95 reduction occurs after advanced Aβ and tau pathology in transgenic mouse models of Alzheimer's disease. *Acta Neuropathol.* 122, 285–292. doi: 10.1007/s00401-011-0843-x

Shen, J., Li, Y., Qu, C., Xu, L., Sun, H., and Zhang, J. (2019). The enriched environment ameliorates chronic unpredictable mild stress-induced depressive-like behaviors and cognitive impairment by activating the SIRT1/miR-134 signaling pathway in hippocampus. *J. Affect. Disord.* 248, 81–90. doi: 10.1016/j.jad.2019.01.031

Simões, L. R., Sangiogo, G., Tashiro, M. H., Generoso, J. S., Faller, C. J., Dominguini, D., et al. (2018). Maternal immune activation induced by lipopolysaccharide triggers immune response in pregnant mother and fetus, and induces behavioral impairment in adult rats. *J. Psychiatr. Res.* 100, 71–83. doi: 10.1016/j.jpsychires.2018.02.007

Su, Y., Lian, J., Hodgson, J., Zhang, W., and Deng, C. (2022). Prenatal poly I:C challenge affects behaviors and neurotransmission via elevated Neuroinflammation responses in female juvenile rats. *Int. J. Neuropsychopharmacol.* 25, 160–171. doi: 10.1093/ijnp/pyab087

Takada, S., Sakakima, H., Matsuyama, T., Otsuka, S., Nakanishi, K., Norimatsu, K., et al. (2020). Disruption of Midkine gene reduces traumatic brain injury through the modulation of neuroinflammation. *J. Neuroinflammation* 17:40. doi: 10.1186/s12974-020-1709-8

Van den Bergh, B., van den Heuvel, M. I., Lahti, M., Braeken, M., de Rooij, S. R., Entringer, S., et al. (2020). Prenatal developmental origins of behavior and mental health: the influence of maternal stress in pregnancy. *Neurosci. Biobehav. Rev.* 117, 26–64. doi: 10.1016/j.neubiorev.2017.07.003

Vanguilder, H. D., and Freeman, W. M. (2011). The hippocampal neuroproteome with aging and cognitive decline: past progress and future directions. *Front. Aging Neurosci.* 3:8. doi: 10.3389/fnagi.2011.00008

Veerasammy, S., Van Steenwinckel, J., Le Charpentier, T., Seo, J. H., Fleiss, B., Gressens, P., et al. (2020). Perinatal IL-1β-induced inflammation suppresses $Tbr2^{+}$ intermediate progenitor cell proliferation in the developing hippocampus accompanied by long-term behavioral deficits. *Brain Behav. Immun. Health.* 7:100106. doi: 10.1016/j.bbih.2020.100106

Vicente-Rodríguez, M., Fernández-Calle, R., Gramage, E., Pérez-García, C., Ramos, M. P., and Herradón, G. (2016). Midkine is a novel regulator of amphetamine-induced striatal gliosis and cognitive impairment: evidence for a stimulus-dependent regulation of Neuroinflammation by Midkine. *Mediat. Inflamm.* 2016, 9894504–9894511. doi: 10.1155/2016/9894504

Walker, K. A., Ficek, B. N., and Westbrook, R. (2019). Understanding the role of systemic inflammation in Alzheimer's disease. *ACS Chem. Neurosci.* 10, 3340–3342. doi: 10.1021/acschemneuro.9b00333

Wang, L., Cao, M., Pu, T., Huang, H., Marshall, C., and Xiao, M. (2018). Enriched physical environment attenuates spatial and social memory impairments of aged socially isolated mice. *Int. J. Neuropsychopharmacol.* 21, 1114–1127. doi: 10.1093/ijnp/pyy084

Wang, H., Meng, X. H., Ning, H., Zhao, X. F., Wang, Q., Liu, P., et al. (2010). Age- and gender-dependent impairments of neurobehaviors in mice whose mothers were exposed to lipopolysaccharide during pregnancy. *Toxicol. Lett.* 192, 245–251. doi: 10.1016/j.toxlet.2009.10.030

Wang, F., Zhang, Z. Z., Cao, L., Yang, Q. G., Lu, Q. F., and Chen, G. H. (2020). Lipopolysaccharide exposure during late embryogenesis triggers and drives Alzheimer-like behavioral and neuropathological changes in CD-1 mice. *Brain Behav.* 10:e01546. doi: 10.1002/brb3.1546

Wei, Z., Meng, X., El Fatimy, R., Sun, B., Mai, D., Zhang, J., et al. (2020). Environmental enrichment prevents Aβ oligomer-induced synaptic dysfunction through mirna-132 and hdac3 signaling pathways. *Neurobiol. Dis.* 134:104617. doi: 10.1016/j.nbd.2019.104617

Winkler, C., and Yao, S. (2014). The midkine family of growth factors: diverse roles in nervous system formation and maintenance. *Br. J. Pharmacol.* 171, 905–912. doi: 10.1111/bph.12462

Wu, Z. X., Cao, L., Li, X. W., Jiang, W., Li, X. Y., Xu, J., et al. (2019). Accelerated deficits of spatial learning and memory resulting from prenatal inflammatory insult are correlated with abnormal phosphorylation and methylation of histone 3 in CD-1 mice. *Front. Aging Neurosci.* 11:114. doi: 10.3389/fnagi.2019.00114

Wu, Y. F., Zhang, Y. M., Ge, H. H., Ren, C. Y., Zhang, Z. Z., Cao, L., et al. (2020). Effects of embryonic inflammation and adolescent psychosocial environment on cognition and hippocampal Staufen in middle-aged mice. *Front. Aging Neurosci.* 12:578719. doi: 10.3389/fnagi.2020.578719

Xiao, Y., Wang, X., Wang, S., Li, J., Xu, X., Wang, M., et al. (2021). Celastrol attenuates learning and memory deficits in an Alzheimer's disease rat model. *Biomed. Res. Int.* 2021:5574207. doi: 10.1155/2021/5574207

Xiong, X. D., Xiong, W. D., Xiong, S. S., and Chen, G. H. (2018). Age-and gender-based differences in Nest-building behavior and learning and memory performance measured using a radial six-armed Water maze in C57BL/6 mice. *Behav. Neurol.* 2018:8728415. doi: 10.1155/2018/8728415

Yasuhara, O., Muramatsu, H., Kim, S. U., Muramatsu, T., Maruta, H., and McGeer, P. L. (1993). Midkine, a novel neurotrophic factor, is present in senile plaques of Alzheimer disease. *Biochem. Biophys. Res. Commun.* 192, 246–251. doi: 10.1006/bbrc.1993.1406

Yoshida, Y., Goto, M., Tsutsui, J., Ozawa, M., Sato, E., Osame, M., et al. (1995). Midkine is present in the early stage of cerebral infarct. *Brain Res. Dev. Brain Res.* 85, 25–30. doi: 10.1016/0165-3806(94)00183-z

Yoshida, Y., Sakakima, H., Matsuda, F., and Ikutomo, M. (2014). Midkine in repair of the injured nervous system. *Br. J. Pharmacol.* 171, 924–930. doi: 10.1111/bph.12497

Zarate, N., Intihar, T. A., Yu, D., Sawyer, J., Tsai, W., Syed, M., et al. (2021). Heat shock factor 1 directly regulates postsynaptic scaffolding PSD-95 in aging and Huntington's disease and influences striatal synaptic density. *Int. J. Mol. Sci.* 22:13113. doi: 10.3390/ijms222313113

Zhang, Z. Z., Zhuang, Z. Q., Sun, S. Y., Ge, H. H., Wu, Y. F., Cao, L., et al. (2020). Effects of prenatal exposure to inflammation coupled with stress exposure during adolescence on cognition and synaptic protein levels in aged CD-1 mice. *Front. Aging Neurosci.* 12:157. doi: 10.3389/fnagi.2020.00157

Zhou, Z., He, G., Zhang, X., Lv, X., Zhang, X., Liu, A., et al. (2021). NGPF2 triggers synaptic scaling up through ALK-LIMK-cofilin-mediated mechanisms. *Cell Rep.* 36:109515. doi: 10.1016/j.celrep.2021.109515

Zhuang, Z. Q., Zhang, Z. Z., Zhang, Y. M., Ge, H. H., Sun, S. Y., Zhang, P., et al. (2021). A long-term enriched environment ameliorates the accelerated age-related memory impairment induced by gestational Administration of Lipopolysaccharide: role of plastic mitochondrial quality control. *Front. Cell. Neurosci.* 14:559182. doi: 10.3389/fncel.2020.5591

frontiers | Frontiers in Aging Neuroscience

TYPE Original Research
PUBLISHED 23 December 2022
DOI 10.3389/fnagi.2022.1058780

OPEN ACCESS

EDITED BY
Mitchell Ryan Goldsworthy,
University of Adelaide,
Australia

REVIEWED BY
Suren Tatulian,
University of Central Florida, United States
Anil Kumar Sharma,
Maharishi Markandeshwar University,
India

*CORRESPONDENCE
Jun Xiao
xiaojun20002@163.com

SPECIALTY SECTION
This article was submitted to Alzheimer's Disease and Related Dementias, a section of the journal Frontiers in Aging Neuroscience

RECEIVED 30 September 2022
ACCEPTED 21 November 2022
PUBLISHED 23 December 2022

CITATION
Ma X, Zhao Y, Yang T, Gong N, Chen X, Liu G and Xiao J (2022) Integration of network pharmacology and molecular docking to explore the molecular mechanism of Cordycepin in the treatment of Alzheimer's disease.
Front. Aging Neurosci. 14:1058780.
doi: 10.3389/fnagi.2022.1058780

Integration of network pharmacology and molecular docking to explore the molecular mechanism of Cordycepin in the treatment of Alzheimer's disease

Xiaoying Ma, Ying Zhao, Tao Yang, Na Gong, Xun Chen, Guoli Liu and Jun Xiao*

The Institute of Edible Fungi, Liaoning Academy of Agricultural Sciences, Shenyang, China

Background: Cordycepin is a nucleoside adenosine analog and an active ingredient isolated from the liquid fermentation of *Cordyceps*. This study sought to explore the mechanism underlying the therapeutic effect of Cordycepin against Alzheimer's disease using network pharmacology and molecular docking technology.

Methods: TCMSP, SYMMAP, CTD, Super-pred, SEA, GeneCards, DisGeNET database, and STRING platform were used to screen and construct the target and protein interaction network of Cordycepin for Alzheimer's disease. The results of Gene Ontology annotation and KEGG pathway enrichment analysis were obtained based on the DAVID database. The Omicshare database was also applied in GO and KEGG pathway enrichment analysis of the key targets. The protein–protein interaction network was constructed using the STRING database, and the potential effective targets for AD were screened based on the degree values. The correlation between the potential targets of Cordycepin in the treatment of AD and APP, MAPT, and PSEN2 was analyzed using (GEPIA) databases. We obtained potential targets related to aging using the Aging Altas database. Molecular docking analysis was performed by AutoDock Vina and Pymol software. Finally, we validated the significant therapeutic targets in the Gene Expression Omnibus (GEO) database.

Results: A total of 74 potential targets of Cordycepin for treating Alzheimer's disease were identified. The potential targets of Cordycepin for the treatment of AD mainly focused on Lipid and atherosclerosis (hsa05417), Platinum drug resistance (hsa01524), Apoptosis (hsa04210), and Pathways in cancer (hsa05200). Our findings suggest that the therapeutic effect of Cordycepin on AD is primarily associated with these biologicalprocesses. We obtained 12 potential therapeutic targets for AD using the degree value in Cytoscape. Interestingly, AKT1, MAPK8, BCL2L1, FOXO3, and CTNNB1 were not only significantly associated with pathogenic genes (APP, MAPT, and PSEN2) but also with longevity in Alzheimer's Disease. Thus we speculated that the five target genes were potential core targets mediating the therapeutic effect of Cordycepin against AD. Moreover, molecular docking results analysis showed good binding affinity between Cordycepin and the five core targets. Overall,

MAPK8, FOXO3 and CTNNB1 may have significant clinical and treatment implications.

Conclusion: Network pharmacology demonstrated that Cordycepin exerts a therapeutic effect against Alzheimer's disease *via* multiple targets and signaling pathways and has huge prospects for application in treating neurodegenerative diseases.

KEYWORDS

network pharmacology, molecular docking, Cordycepin, Alzheimer's disease, target

Introduction

In recent years, the prevalence of geriatic diseases has significantly increased in China due to population aging. According to the latest Alzheimer's disease (AD) International (ADI) data documented in the World Alzheimer's Report 2021, there are about 55 million dementia patients in the world, and it is expected that by 2030, this number will reach 78 million (McGill University Alzheimer's disease international, World Alzheimer Report 2021, Journey through the diagnosis of dementia, 2021).

Alzheimer's disease is a progressive neurodegenerative disease related to aging (Holtzman and Ulrich, 2019). It is widely acknowledged that clinical characteristics of Alzheimer's disease, including cognitive decline, memory disorders, aphasia, apraxia, and agnosia, severely affect patient lives (Zhang and Zheng, 2019). AD is a complex neurodegenerative disorder with various pathological factors. Although the past decade has witnessed unprecedented progress in understanding AD, more basic research is warranted. So far, there are still no related effective drugs to cure AD patients. Notwithstanding that many drugs have been developed for treating central nervous system diseases, they have significant limitations, including severe side effects and complications (Govindula et al., 2021). Currently available treatments, based on early findings of cholinergic deficit, have only provided limited improvement in cognitive functions in AD. It is widely thought that previous studies have been largely ineffective given that they only targeted a single aspect or mechanism of the disease, which is often caused by the interplay of different factors (Ju and Tam, 2020, 2021). Therefore, considering the complexity of AD pathogenesis, designing multifunctional drugs exhibiting multitarget potential may lead to better results in developing AD treatments (Ju and Tam, 2020).

Cordycepin is a nucleoside adenosine analog and an active ingredient isolated from the liquid fermentation of *Cordyceps* (a precious medicinal mushroom). Cordycepin exhibits a wide range of biological activities and has an enormous impact in many therapeutic research areas (Yang et al., 2019). *Cordyceps Sinensis* is one of the most widely used medicinal fungi and has various positive pharmacological effects (Elkhateeb et al., 2019). It exerts a protective effect against senescence, inhibits fatigue, and exerts antioxidant, anti-inflammatory, anticancer, antihepatotoxic, anti-fibrotic and neuroprotective effects (Qin et al., 2019). It has been reported that Cordycepin can treat neurodegenerative diseases by inhibiting the expression of iNOS, Akt, MAPKs, NF-κB, and COX-2 in microglial cells (Jeong et al., 2010). Besides, it has been found that Cordycepin can restore Lipopolysaccharide (LPS)-induced decrease of primary hippocampal neurons and enhance cell viability and neuronal differentiation (Peng et al., 2015). Indeed, it is challenging to study the anti-Alzheimer's effect of Cordycepin based on traditional Chinese medicine pharmacology; however, studying pharmacological mechanisms using network pharmacology makes it feasible (Zhai et al., 2018). Importantly, network pharmacology analysis can elucidate the mechanism of drugs and provides an effective method for developing traditional Chinese medicine through the nodes and edges in the biological network. In this regard, network pharmacology can screen active ingredients and potential therapy targets, elucidate the complex mechanisms by which drugs and prescriptions treat diseases, and reveal medicinal properties. The combination of TCM database and computer software analysis not only expands TCM knowledge, but also greatly promotes the internationalization of TCM. In this study, the anti-Alzheimer disease targets of Cordycepin were retrieved by network pharmacology (Figure 1). PPI, gene ontology, and KEGG pathway analyses were carried out, the correlation between the potential target and disease-related genes was analyzed, and screening of potential targets related to aging was conducted using Aging Altas. Molecular docking verification of the core target was carried out, and the clinical significance of the core target was evaluated in the GEO database to elucidate the mechanisms underlying the therapeutic effect of Cordycepin against Alzheimer's disease.

Materials and methods

Screening of Cordycepin targets

The biological targets of cordycepin were obtained from TCMSP,[1] Pubmed,[2] SYMMAP,[3] CTD,[4] Super-pred (prediction. Charite.de) (probability >80%), and SEA (https://sea.bkslab.org/;

1 http://tcmspw.com/tcmsp.php
2 https://www.ncbi.nlm.nih.gov/gene
3 http://www.symmap.org/
4 http://ctdbase.org/

z score > 30). Cordycepin target information was generated by entering "Cordycepin" in these databases, searching for cordycepin targets, and selecting its default option in parameter settings. We merged the results of the six databases and removed duplicate targets to obtain targets of Cordycepin.

Determination of the targets of Cordycepin in Alzheimer's disease

The targets of Alzheimer's disease were obtained from Genecards,[5] DisGeNT,[6] and CTD[7] databases. Similarly, we translated the AD target proteins ID into the corresponding gene symbol by UniProt ID mapping tools. Then, we obtained the intersection of gene targets of Cordycepin and Alzheimer's disease using Venny[8] online tools. The intersected targets were further analyzed to obtain candidate targets for AD treatment. The study was conducted in accordance with the tenets of the Declaration of Helsinki (as revised in 2013).

Enrichment analysis of the intersected genes

To better understand the functions of the intersected targets, gene ontology (GO) and KEGG enrichment analysis were carried out using the DAVID.[9] For GO enrichment analysis and KEGG analysis, GO terms and KEGG pathways with p-values <0.05 were considered significantly enriched. The results of pathway enrichment analysis were plotted using the bioinformatics[10] online platform.

Construction of the drug-ingredient-target network (including protein–protein interactions) and pathways

STRING[11] is an online biological database that can predict protein–protein interaction (PPI) networks. We used common targets Cordycepin against Alzheimer's disease as inputs to a STRING database, obtaining complete PPI networks and related data. To describe the mechanisms of Cordycepin against Alzheimer's disease, a network of components-disease-targets-pathways was constructed using Cytoscape software (3.9.1) based on the active constituents, corresponding targets, and pathway information. Components, targets, pathways, and diseases are represented as nodes, and connections between proteins are represented as edges.

Correlation analysis between key targets and key genes of AD

To confirm the relationship between key genes and major causative gene amyloidprecursor protein (APP) or microtubule-associated protein tau (MAPT) and presenilin2 (PSEN2), gene correlation analysis was conducted using GEPIA. Key genes and APP, MAPT and PSEN2 were input into the search words in turn, and all brain tissues were selected from GTEx tissues for correlation analysis.AgingAtlas is a bioinformatics tool used for assessing the genetic correlation between Ageing and Longevity (Liu et al., 2020). It is well-established that AD is an aging-related disease. The aging-associated genes in this study were obtained from the Aging Altas. We selected genes that were not only aging-related but also significantly associated with AD.

Molecular docking

The screened key genes served as the key targets for receptors, and the information on receptor structures was obtained from PDB[12] and the Uniprot database. The 2D structures of Cordycepin were obtained from TSCMP databases, and optimized ligands were used as starting points for docking. The protein-ligand molecular docking and docking calculations study was performed with AutoDock Vina. We obtained the conformation and the lowest binding energy of ligand-receptor interactions after the docking search was completed. Finally, the receptor-ligand binding image was visualized using Pymol software.

Clinical characteristics and tissue enrichment of key targets

To obtain clinical implications of potential key targets, we searched transcriptome data for normal control and AD patient brain tissues in the GEO database (http://www.ncbi.nlm.nih.gov/geo/). Differentially expression analysis of AD-related genes was conducted between control and AD patients using the GEO2R tool. Graphs were generated using GraphPad Prism 8. Then, the expression distribution of key targets in neural typical was analyzed using the Human eFP Browser (http://bar.utoronto.ca/efp_human/; Patel et al., 2016), and the distribution of key genes in the whole body was obtained. The distribution of key gene expression was researched in the whole body of mice using the mouse EFP browser.[13]

5 https://www.genecards.org/
6 https://www.disgenet.org/
7 http://ctdbase.org/
8 https://bioinfogp.cnb.csic.es/tools/venny/
9 https://david.ncifcrf.gov/
10 http://www.bioinformatics.com.cn
11 http://string-db.org
12 https://www.rcsb.org/
13 http://bar.utoronto.ca/mouse_efp/cgi-bin/efpWeb.cgi

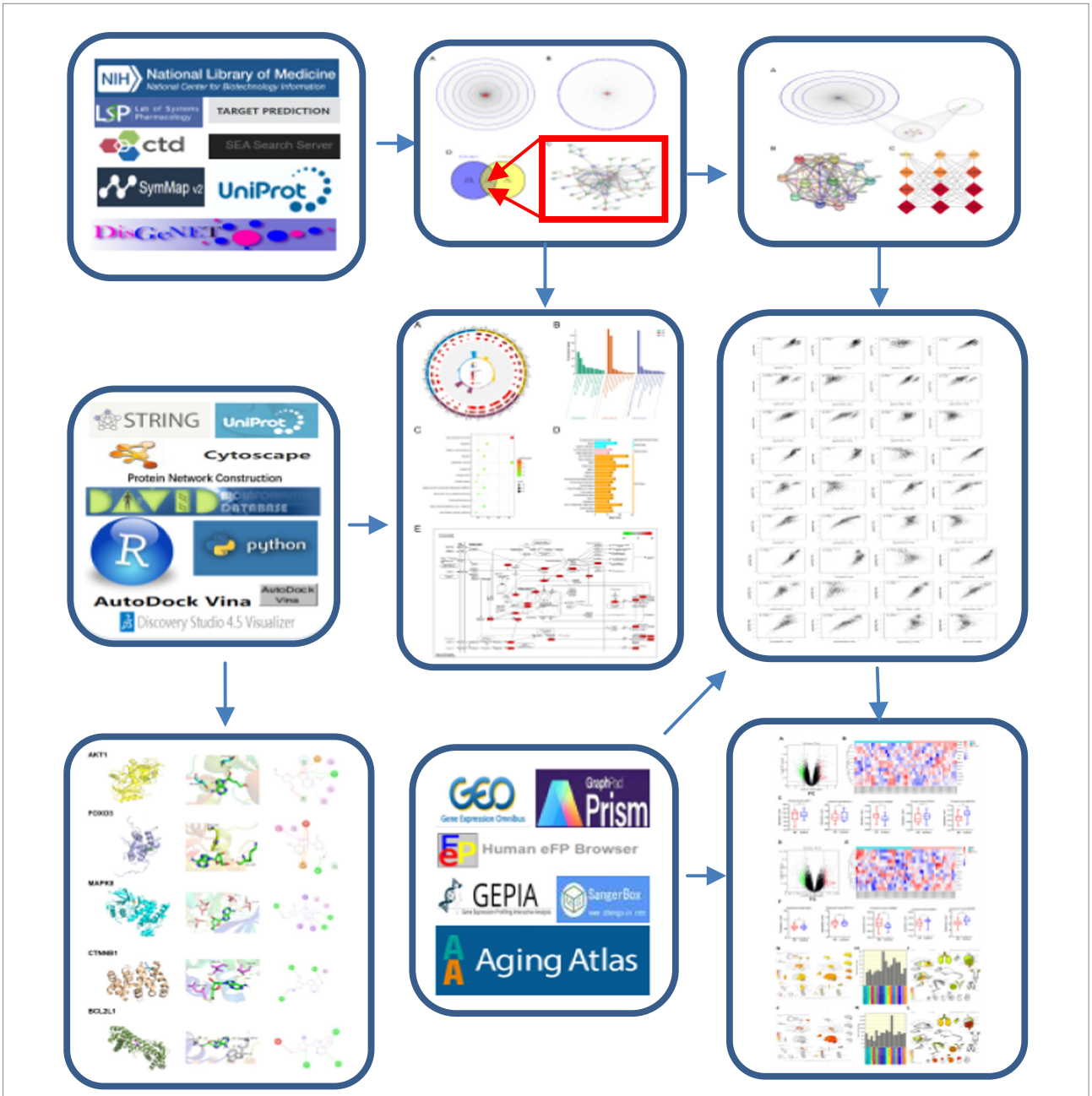

FIGURE 1
Network Pharmacology Workflow of Cordycepin in the treatment of Alzheimer's Disease.

Result

The intersected targets of Cordycepin and Alzheimer's disease

Based on TCMSP, Pubmed, SYMMAP, CTD, Super-pred and SEA, we obtained 136 putative targets of Cordycepin. After retrieval from the DisGeNet, CTD, and GeneCards databases, 2,848 AD-related targets were obtained based on an Inference Score > 30. The intersection of Cordycepin targets and the Alzheimer's disease targets was visualized in a Venn plot, yielding 74 putative targets for treating AD (Figure 2D).

Go and KEGG pathway enrichment analysis

74 intersection genes were uploaded to DAVID for GO/KEGG analyses, and the significance level was set at $p \leq 0.001$ (***). A total of 152 GO biological process (BP), 12 GO cellular component (CC), 30 GO molecular function (MF) and 96 KEGG pathways were significantly enriched. As shown in Figures 3A,B,

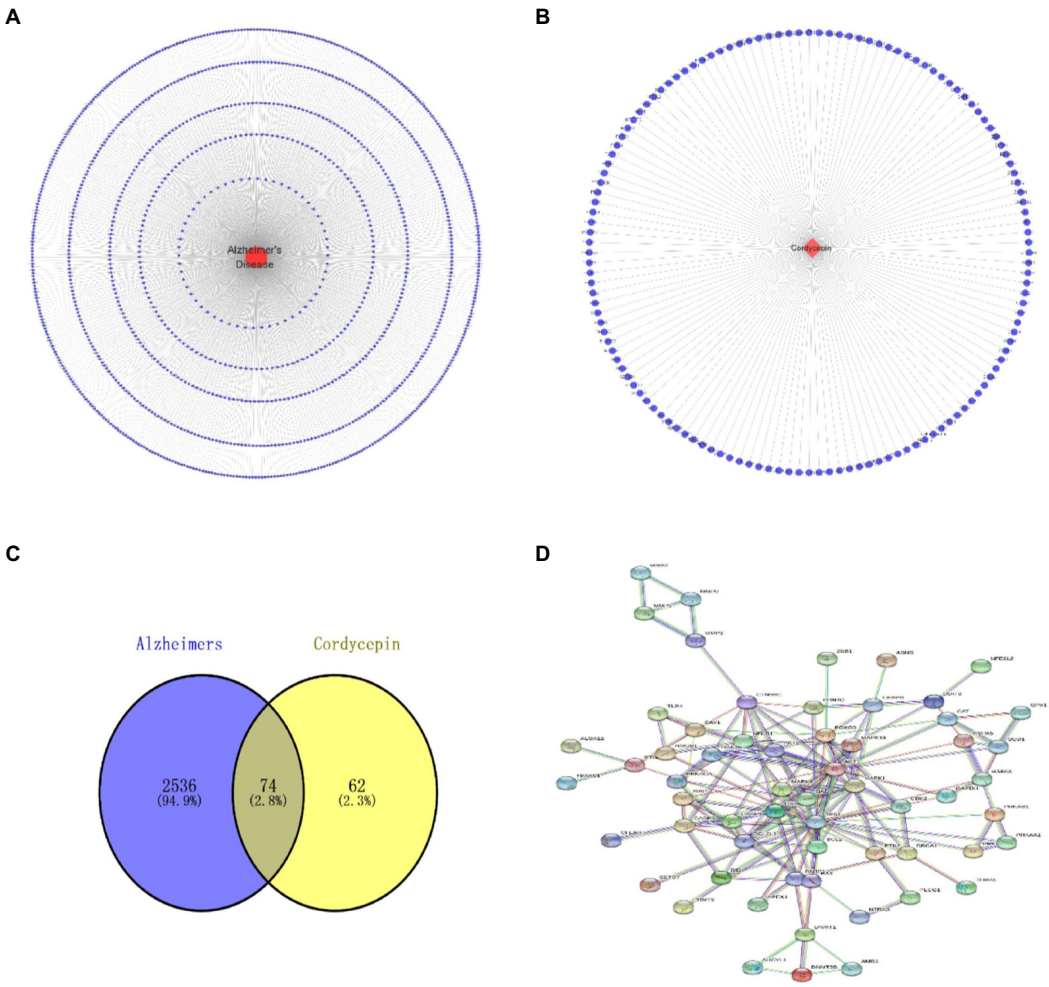

FIGURE 2
Alzheimer's disease target network diagram **(A)**; Cordycepin related target network diagram **(B)**; Cordycepin-anti-Alzheimer disease target PPI network diagram **(C)**; Cordycepin-anti-Alzheimer disease Venn plot **(D)**.

significantly enriched biological processes mainly included positive and negative regulation of apoptosis, neuron apoptosis and drug response. Significantly enriched GO terms in the molecular function category included 'enzyme activity', 'protease binding' and 'transcription factor binding'. Cellular components (CC) terms included nucleus, macromolecular complex and mitochondria. The enriched GO items were also associated with neuronal apoptosis, death-induced signal complex formation, and cysteine-type endopeptidase activity involved in the apoptotic process. Taken together, our results indicate that the effect of Cordycepin on AD is primarily associated with these biological processes.

KEGG pathway analysis

KEGG analysis yielded a total of 96 pathways, and the top 13 enriched pathways are shown in Figures 3C,D. The potential targets in Cordycepin treatment of AD disease mainly focused on lipids arteriosclerosis (hsa05417), Platinum drug resistance (hsa01524), Apoptosis (hsa04210), Pathways in Cancer (hsa05200). Taken together, these results imply that Cordycepin may exert anti-AD effects by binding to cysteine-type endopeptidase in mitochondria from the caspase family that plays an essential role in apoptosis, and then inhibiting the formation of the death-inducing signaling complex of endopeptidases *via* the death domain protein recruitment, which in turn affects the occurrence of apoptosis, slowing neuronal cell death.

Screening cordycepin-anti-Alzheimer disease key targets and target interaction network.

The names of cordycepin-target and Alzheimer's disease-target genes were converted into gene ID based on the UniProt database. Subsequently, we selected the intersected target genes between cordycepin-targets and Alzheimer's disease-related targets using Venn plots. The intersected target genes were analyzed with the

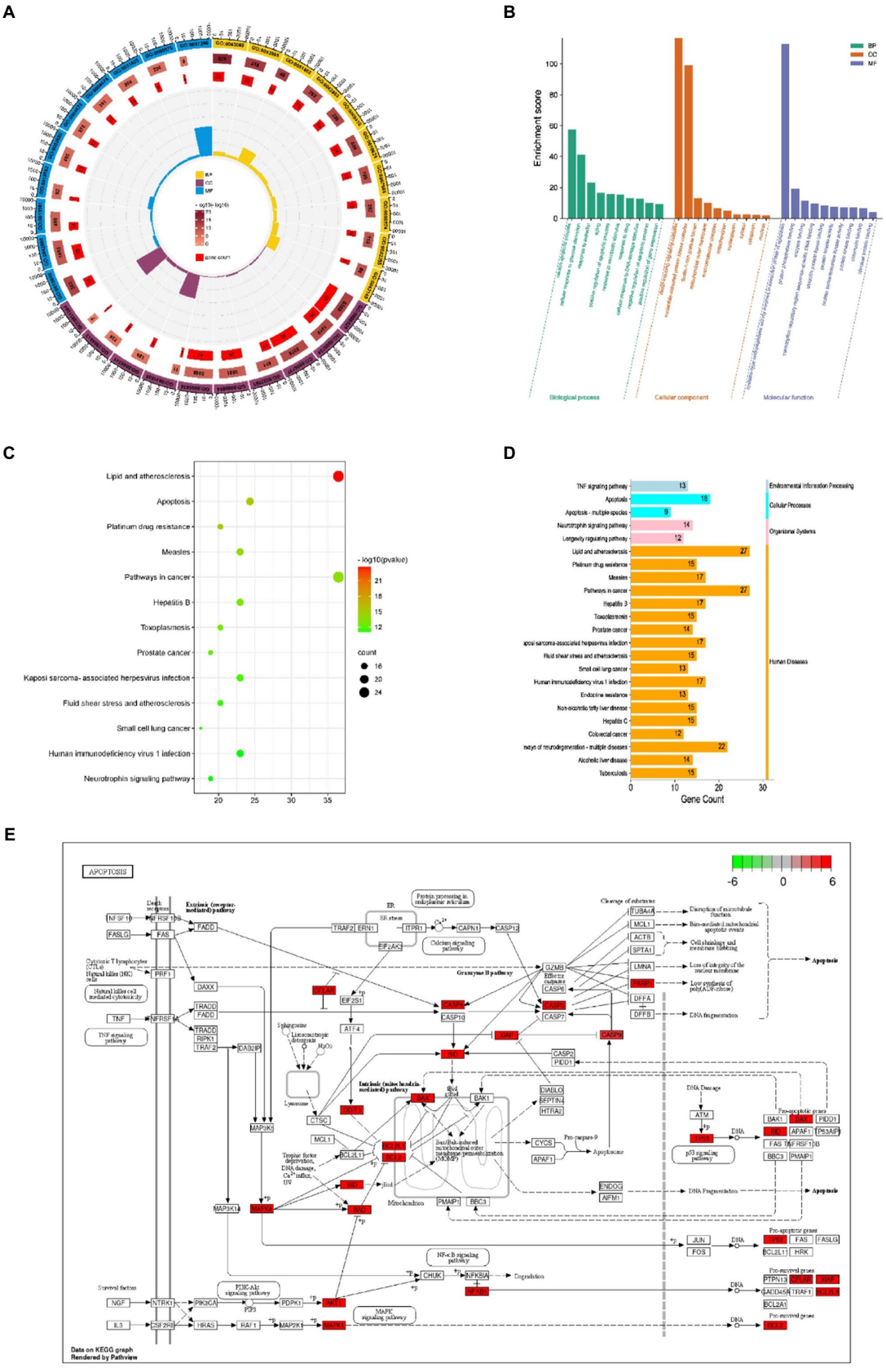

FIGURE 3
GO annotation of the Cordycepin-anti-Alzheimer disease targets **(A,B)**; KEGG pathway analysis of Cordycepin-anti-Alzheimer disease targets **(C,D)**; apoptosis pathway **(E)**. The red mark represents enrichment of the target of Cordycepin in the apoptosis pathway.

STRING database[14] and imported interactions with a confidence score ≥ 0.9 for visualization. Next, a topological analysis of gene–gene network graphs was performed; 12 genes were selected as the Cordycepin-anti-Alzheimer key targets according to the rank node degree scores. Then, a protein–protein interaction (PPI) network of the 12 enrichment genes was constructed by the STRING database, then core targets including TP53, AKT1, CASP3, BCL2L1, MAPK8, MAPK1, CASP8, CTNNB1, FOXO3, BAD, BCL2, and NFE2L2 were obtained (Figure 4).

Analysis of Core targets based on GEPIA

Missense mutation of APP gene changes A β Metabolize and regulate A β And cause A β Cognitive decline (Lan et al., 2014). To confirm the relationship between key genes and major causative gene APP, MAPT, or PSEN2, gene correlation analysis was conducted using GEPIA. Four indexes were significantly correlated with APP, 7 with PSEN2, and 8 with MAPT (Figures 5–7). It is well-established that aging accelerates and promotes cognitive disorders and is the most prominent risk factor for neurodegenerative diseases, including AD (Hou et al., 2019). We obtained 8 metrics correlated with age through analysis of the Aging Altas database (Table 1). The results showed that the five targets of AKT1, MAPK8, BCL2L1, FOXO3 and CTNNB1 were not only significantly related to APP, PSEN2 and MAPT but also related to age. Accordingly, we speculate that these five targets mediate the preventive and therapeutic effects of Cordycepin against AD (Figures 5–7).

Molecular docking

The docking energy associated with the binding of Cordycepin to the core target was calculated using the AutoDock Vina

14 https://string-db.org/

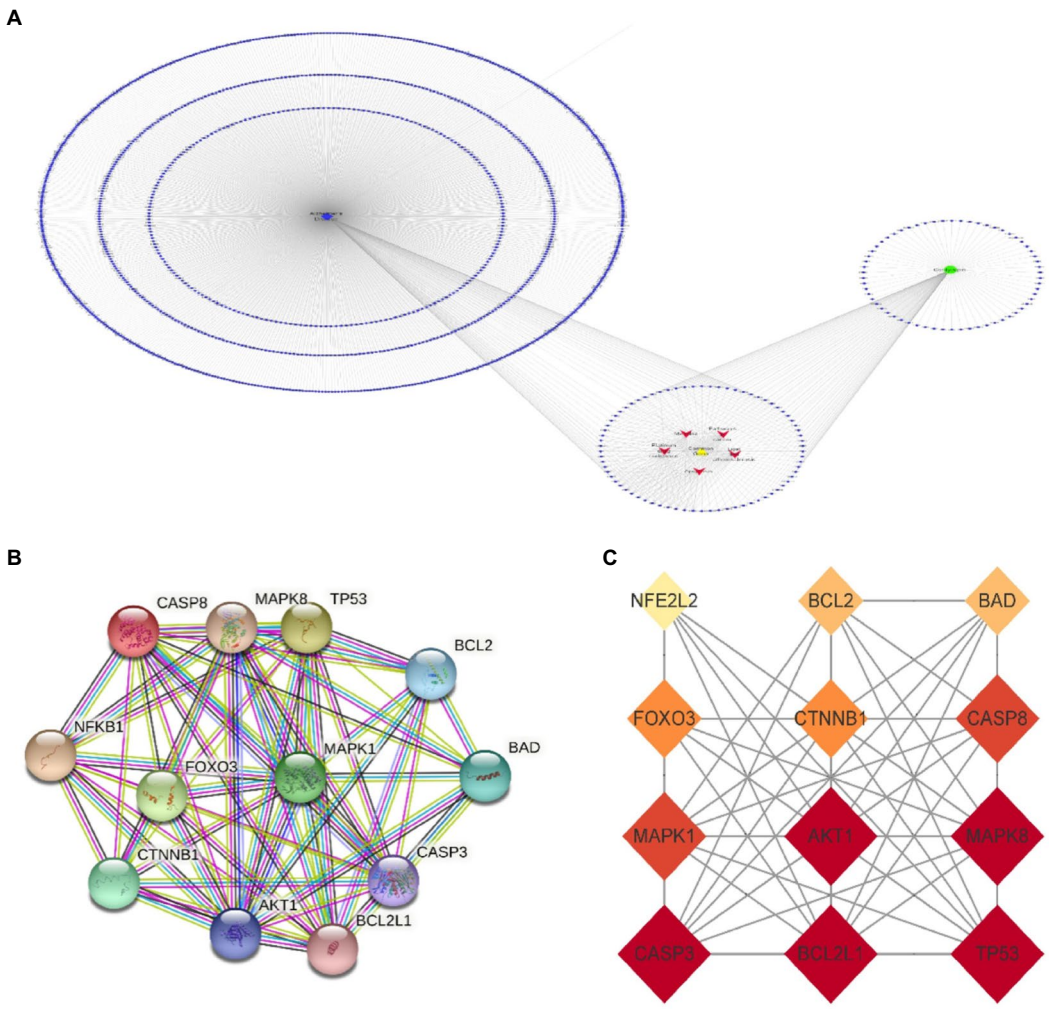

FIGURE 4
Cordycepin-Alzheimer disease-pathway target network **(A)**; 12 key targets of Cordycepin-anti-Alzheimer PPI network **(B,C)**.

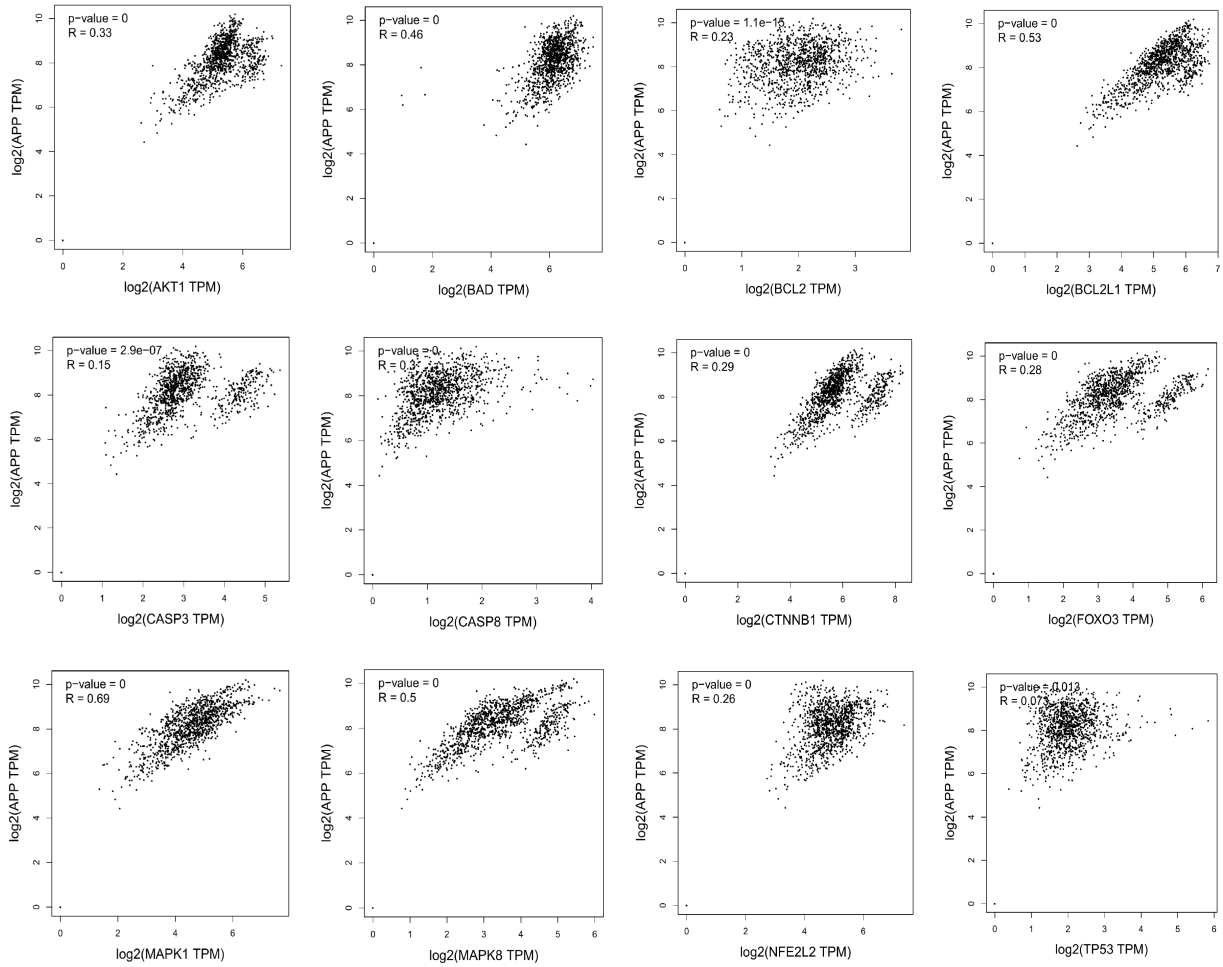

FIGURE 5
Analysis of the correlation between 12 key targets of Cordycepin and the pathogenic gene of Alzheimer's disease APP.

software. It has been established that the target possesses significant binding capacity with the compound when the docking energy is less than −1.2 kcal/mol or −5 kJ/mol. In our study, the binding energy between 5 core targets and Cordycepin were less than −5 kJ/mol, respectively (Table 2), which indicates that the ligand can spontaneously bind to the receptor molecule. These results suggested that these targets might play an important role in Cordycepin treatment of AD. The specific docking parameters are shown in Figure 8.

Analysis of core gene expression

The AD brain transcriptome GSE122063 dataset, which examined the expression of two different brain regions, frontal cortex (FC) and temporal cortex (TC) in AD ($n = 12$) and normal controls ($n = 11$), was used to evaluate the expression changes of 5 core targets in brain tissue of AD patients. Among AD patients, the mRNA expression of CTNNB1 was significantly increased in TC and FC tissues, while MAPK8 was significantly downregulated. In contrast, FOXO3 was significantly reduced only in TC tissues. There was no significant difference in BCL2L1 and AKT1 levels between TC and FC tissues (Figures 9A–F). The expression of MAPK8 and CTNNB1 in the normal nervous system was analyzed by the Human eFP Browser. As shown in Figures 9G–L, MAPK8 was expressed in the whole human nervous system in healthy subjects, with the highest expression in male testis and the colon, mandible and hindbrain of mice. The expression of CTNNB1 was the highest in the cerebellum of the nervous system and the highest in the human female ovary. It was mainly distributed in mouse colon, embryonic development and teeth.

Discussion

In this article, we analyzed the multi-level mechanism of Cordycepin in treating AD. The intersection of active component targets and disease-related targets yielded 74 common targets. Twelve targets were identified by PPI network analysis, while 5 targets AKT1, MAPK8, BCL2L1, FOXO3 and CTNNB1 were

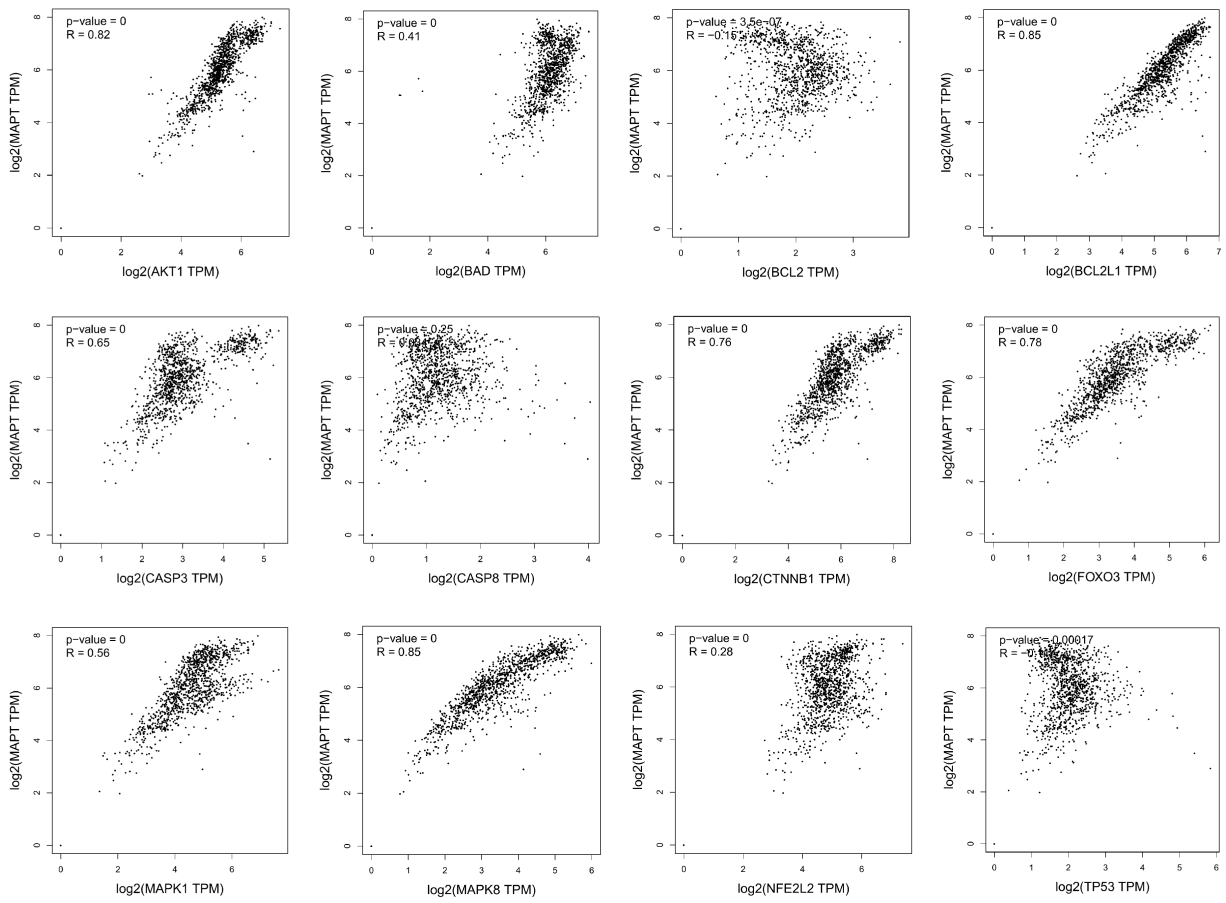

FIGURE 6
Analysis of the correlation between 12 key targets of Cordycepin and the pathogenic gene of Alzheimer's disease MAPT.

positively correlated with AD pathogenic genes APP, PSEN2 and MAPT, and associated with aging genes Our findings suggest that MAPK8, FOXO3 and CTNNB1 have clinical research value. GO annotation and KEGG pathway analysis were conducted. As shown in Figures 3A,B, significantly enriched BP terms mainly included positive and negative regulation of apoptosis, neuron apoptosis and drug response, MF terms included participation in enzyme activity, protease and transcription factor binding, and CC terms included nucleus, macromolecular complex and mitochondria. The enriched GO items were also associated with neuronal apoptosis, death-induced signal complex formation, cysteine endopeptidase activity, and so on.

AD is considered to be a continuous and gradual process, about 25 years from the onset of pathology to death. Amyloid initiates this process, which is followed by a variety of neurobiological processes, including tau pathology, brain atrophy and synaptic dysfunction, initially with a slight cognitive decline, followed by memory impairment, aphasia, visual–spatial skills impairment, executive dysfunction, personality and behavioral changes (Aisen et al., 2022). Two neuropathological features of AD are extracellular deposition ofβ-amyloid (Aβ) peptide and intracellular accumulation / deposition of hyperphosphorylated tau protein (Montine et al., 2011; Hyman et al., 2012). The study found that although amyloid protein levels were similar, people with strong resilience to AD had lower levels of hyperphosphorylated tau accumulation in synapses and neocortical regions (Van Rossum et al., 2012). There are many genetic changes in AD disease, and many genes are involved in the process of remission and aggravation of the disease (Hansen et al., 2017; Yu et al., 2020). Amyloid precursor protein (APP) is a kind of intramembrane protein expressed in various tissues, which is concentrated in the synapses of neurons. It can bind to death receptor 6 to initiate apoptosis and further induce neuronal death (Michaud et al., 2013; Xu et al., 2022).The hyperphosphorylation and accumulation of microtubule-associated protein tau (MAPT) forms the initial event before neurodegeneration (Lee et al., 2001). In humans, neuroinflammation is positively correlated with tau pathology and participates in tau hyperphosphorylation, accumulation and neurodegeneration (Zilka et al., 2009). Of the 12 core targets obtained in this study, 7 were significantly correlated with MAPT, indicating that they were more closely related to tau lesions.

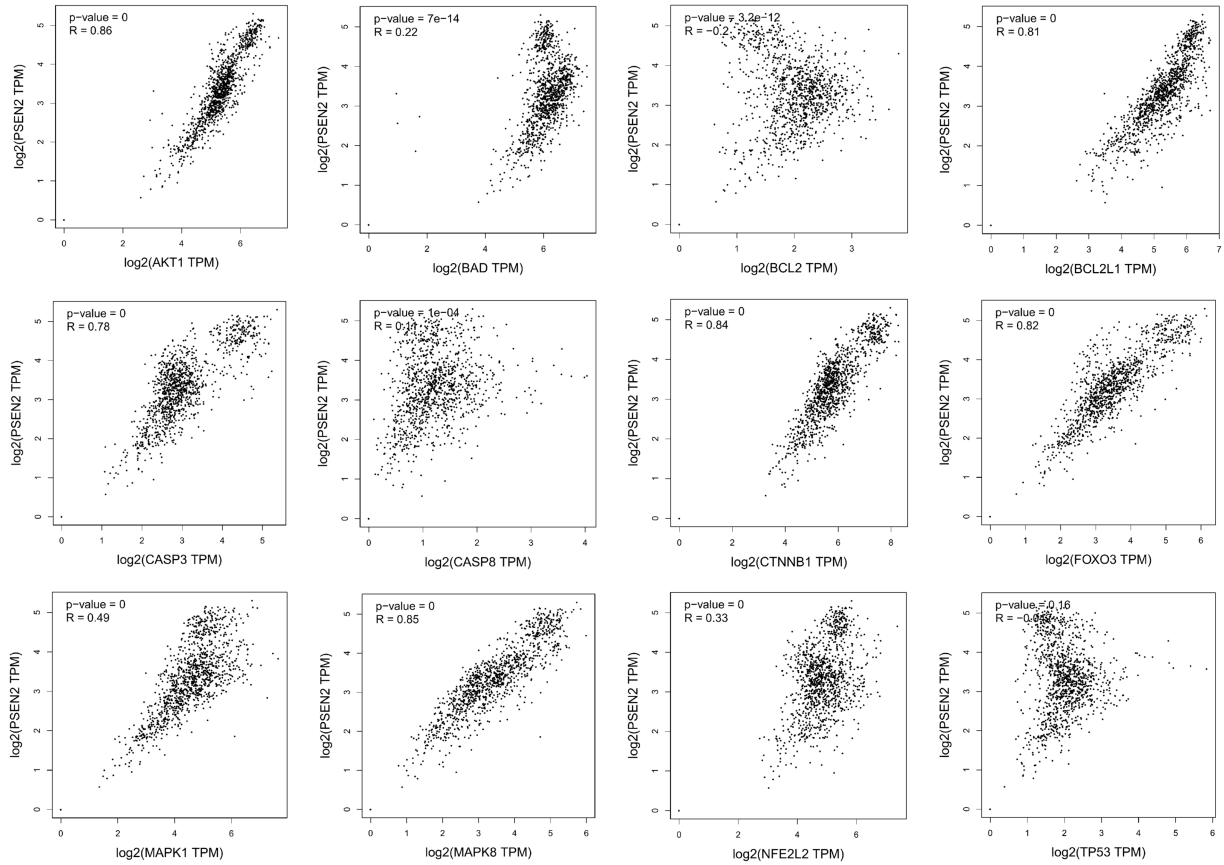

FIGURE 7
Analysis of the correlation between 12 key targets of Cordycepin and the pathogenic gene of Alzheimer's disease PSEN2.

The growing evidence that both Aβ and tau lesions are powerful causes of cell aging Senescent cells have been detected in the brains of patients with AD. (Gebicke-Haerter, 2001; Baker et al, 2018; Zhang et al, 2019; Han et al, 2020; SaezAtienzar et al, 2020). The removal of aging cells by drug and genetic methods can reduce the brain Aβ load and tau disease, and improve the memory (Bussian et al., 2018; Musi et al., 2018; Zhang et al., 2019; Tam and Ju, 2022) of these AD model mice, Not only that, the study found that people with strong resilience to AD showed a unique cytokine spectrum (McKay et al., 2019), including higher levels of anti-inflammatory cytokines and neurotrophins, as well as lower levels of chemokines (Perez-Nievas et al., 2013; Barroeta-Espar et al., 2019). Initial studies have identified neurotrophic factors including NRN1 and BDNF that may contribute to the recovery of AD pathology (Neuner et al., 2022). As neurotrophic factors, they play an important role in synaptic function and plasticity as well as in maintaining axonal morphology (Yao et al., 2018). It is worth noting that the five core targets of cordycepin in alleviating AD obtained in this study were significantly correlated with the expression of NRN1 and BDNF except AKT1 (Figure 10). This further indicates that cordycepin can increase the expression of neurotrophic factors.

We have identified five target genes which were potential core targets mediating the therapeutic effect of Cordycepin against AD in this study. There is compelling evidence that the activity of β-and γ-secretase can regulate MAPK signal pathway (Salminen et al., 2016; Sochocka et al., 2017; Benito-Cuesta et al., 2020), neuronal apoptosis and phosphorylation of APP and Tau participate in the pathogenesis of AD (Kim and Choi, 2010). The anti-apoptotic protein BCL2L1 regulates the death of β-apoptotic cells through Bcl-2 proteins. Interestingly, it has been shown that increased expression of BCL2L1 is related to the chemotherapy resistance of T-ALL (Broome et al., 2002). β-catenin signals encoded by CTNNB1 regulate a variety of different pathways in the pathogenesis of AD, such as synaptic plasticity, neuronal survival, inflammation and tau phosphorylation (Jia et al., 2019). AD is an age-related disease, and the activation of FOXO3 has been found to improve somatic cell maintenance and prolong life. As a transcription factor, FOXO3 plays a central role in cellular stress and contributes to redox regulation, autophagy, energy homeostasis, DNA repair, cell cycle arrest, telomere maintenance and stem cell homeostasis (Davy et al., 2018). Recent studies have shown that the PI3K-Akt signal pathway may be an important target for AD therapy. Moreover, the PI3K-Akt pathway regulates many biological processes such as cell proliferation, movement, growth, survival and metabolism and inhibits different neurotoxic

TABLE 1 Core targets of Cordycepin-anti-Alzheimer and pathways related to aging.

Symbol	Description	Function	Gene_Set	Literature_Name	KEGG
AKT1	v-akt murine thymoma viral oncogene homolog 1	AKT1 is one of 3 closely related serine/threonine-protein kinases (AKT1, AKT2 and AKT3) called the AKT kinase that regulates many processes, including metabolism, proliferation, cell survival, growth and angiogenesis.	cellular senescence	Akt negatively regulates the in vitro lifespan of human endothelial cells via a p53/p21-dependent pathway	Longevity regulating pathway
TP53	tumor protein p53	TP53 acts as a tumor suppressor in many tumor types; induces growth arrest or apoptosis depending on the physiological circumstances and cell type. TP53 is involved in cell cycle regulation as a trans-activator that acts to negatively regulate cell division by controlling a set of genes required for this process.	others	Variation in the human TP53 gene affects old age survival and cancer mortality	Longevity regulating pathway
MAPK8	mitogen-activated protein kinase 8	MAPK8, also known as JNK1, encodes many transcripts and is an important player in stress response. Overexpression of JNK in roundworms also increases lifespan.	deregulated nutrient sensing	JNK Extends Life Span and Limits Growth by Antagonizing Cellular and Organism-Wide Responses to Insulin Signaling	Insulin signaling pathway
BCL2L1	BCL2 like 1	Potent inhibitor of cell death. Inhibits activation of caspases. Appears to regulate cell death by blocking the voltage-dependent anion channel (VDAC) by binding to it and preventing the release of the caspase activator, CYC1, from the mitochondrial membrane.	NF-κB related gene	Human exceptional longevity: transcriptome from centenarians is distinct from septuagenarians and reveals a role of Bcl-xL in successful aging	NF-kappa B signaling pathway
FOXO3	forkhead box O3	A transcription factor of the Fox family, FOXO3, is crucial in development.	others	Fox's in Development and Disease	Longevity regulating pathway
BCL2	B-cell CLL/lymphoma 2	Suppresses apoptosis in various cell systems, including factor-dependent lymphohematopoietic and neural cells. Regulates cell death by controlling the mitochondrial membrane permeability.	others	Regulation of apoptosis resistance and ontogeny of age-dependent diseases	p53 signaling pathway
CTNNB1	catenin (cadherin-associated protein), beta 1, 88 kDa	CTNNB1, also known as beta-catenin, is a member of the adherens junctions proteins, involved in epithelial layers that mediate adhesion between cells, cell communication, growth, embryogenesis, and wound healing.	altered intercellular communication	beta-Catenin Controls Hair Follicle Morphogenesis and Stem Cell Differentiation in the Skin	Wnt signaling pathway
NFE2L2	nuclear factor, erythroid 2-like 2	NFE2L2 is a transcription factor that plays a key role in the response to oxidative stress: The NFE2L2/NRF2 pathway is also activated in response to selective autophagy: autophagy promotes interaction between KEAP1 and SQSTM1/p62 and subsequent inactivation of the BCR(KEAP1) complex, leading to NFE2L2/NRF2 nuclear accumulation and expression of cytoprotective genes.	genomic instability	p62/SQSTM1 Is a Target Gene for Transcription Factor NRF2 and Creates a Positive Feedback Loop by Inducing Antioxidant Response Element-Driven Gene Transcription	Unknown

10.3389/fnagi.2022.1058780

TABLE 2 Molecular docking parameters of cordycepin core targets.

Target	PDB ID	Coordinate	Binding energy (kJ/mol)	Cordycepin docking amino acid residues
AKT1	4ejn	x = 29.817; y = 43.243; z = 15.125	−7.8	Chain A: ASN53 ASN54 PHE55 SER56 VAL57 ALA58 GLN59 CYS60 CYS77 LEU78 GLN79 TRP80 VAL270
BCL2L1	6uvg	x = 87.133; y = −4.627; z = 136.989	−7	Chain A: GLU7 VAL10 ASP11 SER14 TYR15 SER18 TYR22 SER23 TRP24 SER25 MET83 ALA84 ALA85 LYS87 GLN88 ARG91; Chain B: ASP11 LYS87 ARG91
MAPK8	3elj	x = 21.284; y = 16.240; z = 29.260	−6.8	Chain A: ILE32 GLY33 SER34 GLY35 VAL40 ALA53 ILE86 MET108 GLU109 LEU110 MET111 ASP112 ASN114 SER155 ASN156 VAL158 LEU168
FOXO3	2uzk	x = 14.088; y = −19.100; z = 39.088	−6.6	Chain C: SER1181 TYR1184 GLU1185 VAL1188 PHE1194 LYS1195 ASP1196 LYS1197 GLY1198 ASP1199 SER1202 SER1203 ALA1204 TRP1206 LYS1207
CTNNB1	7afw	x = 65.770;y = −43.227; z = 28.298	−6.2	Chain A: LEU160 ASN161 ASP162 GLN165 VAL168 ALA197 ARG200 THR201 ASN204 THR205 ASN206 ASP207

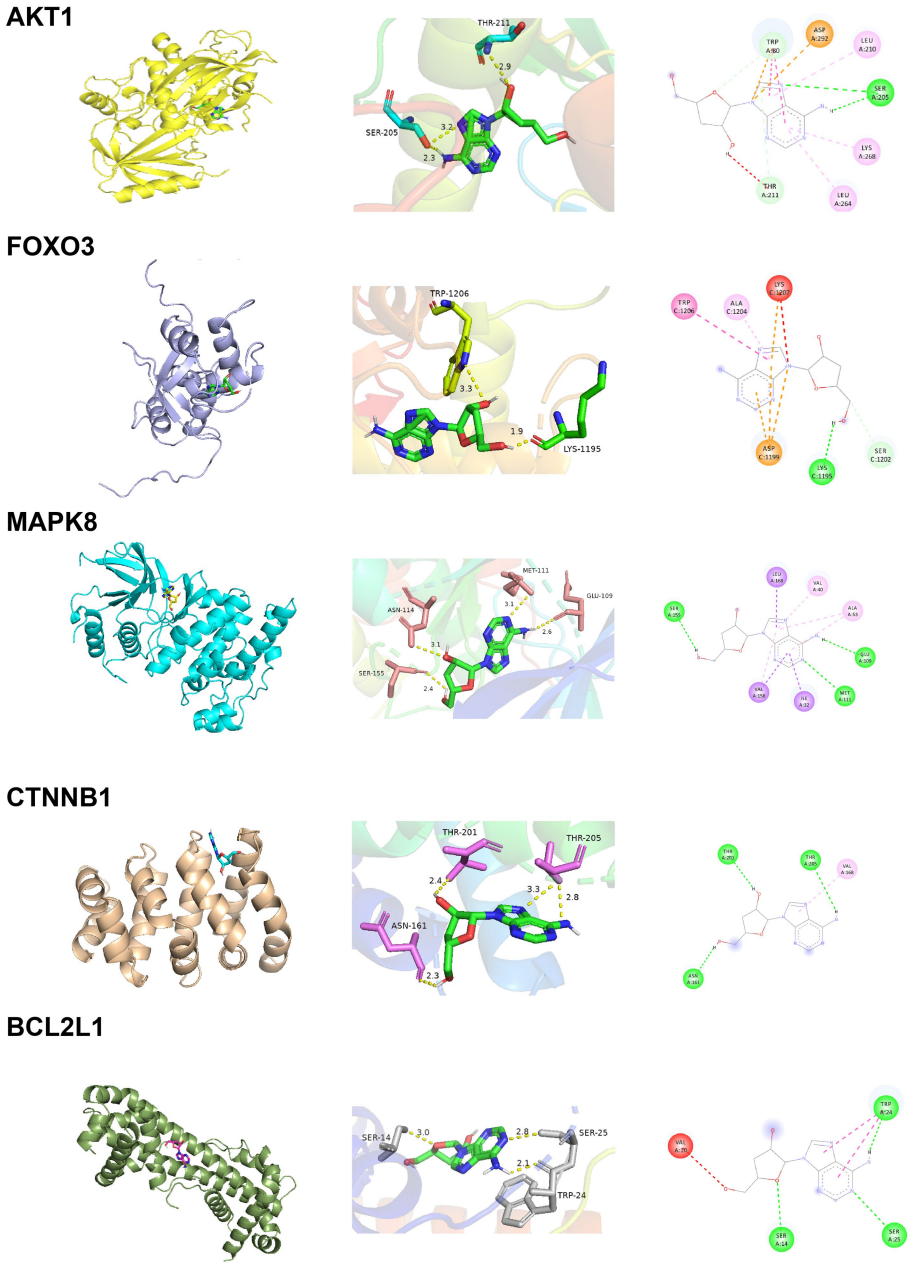

FIGURE 8
Docking results of Cordycepin with the core target.

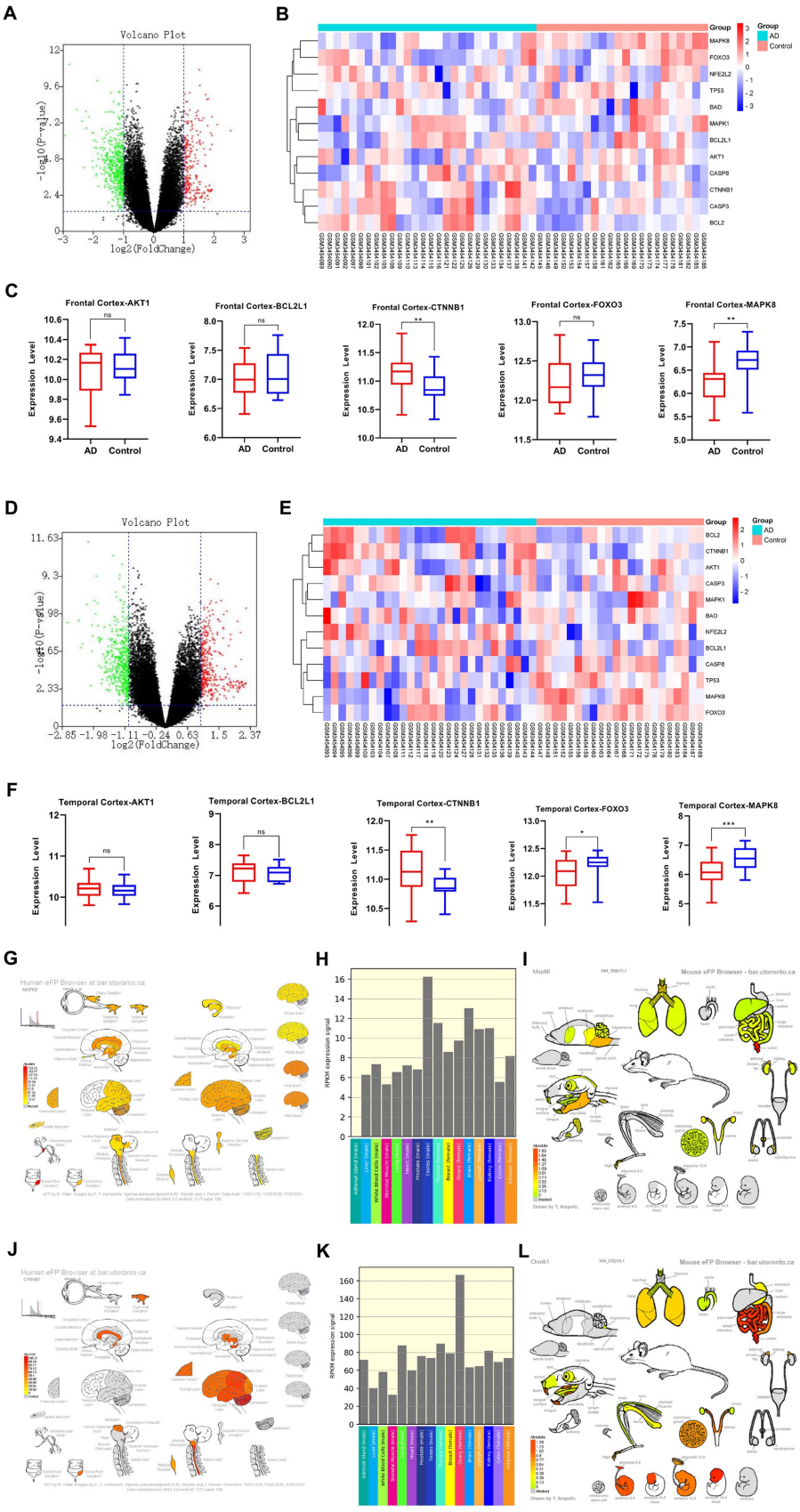

FIGURE 9
AD mRNA Expression analysis using GEO Dataset **(A,C,D,F)**. Composition-Target binding energy heat map **(B,E)**. MAPK8 expression analysis in the regular human nervous system **(G,H)**. MAPK8 expression analysis in tissues and organs of a normal mouse **(I)**. CTNNB1 expression in the normal human nervous system **(J,K)**. CTNNB1 expression analysis in tissues and organs of normal mouse **(L)**. *p<0.05, **p<0.01.

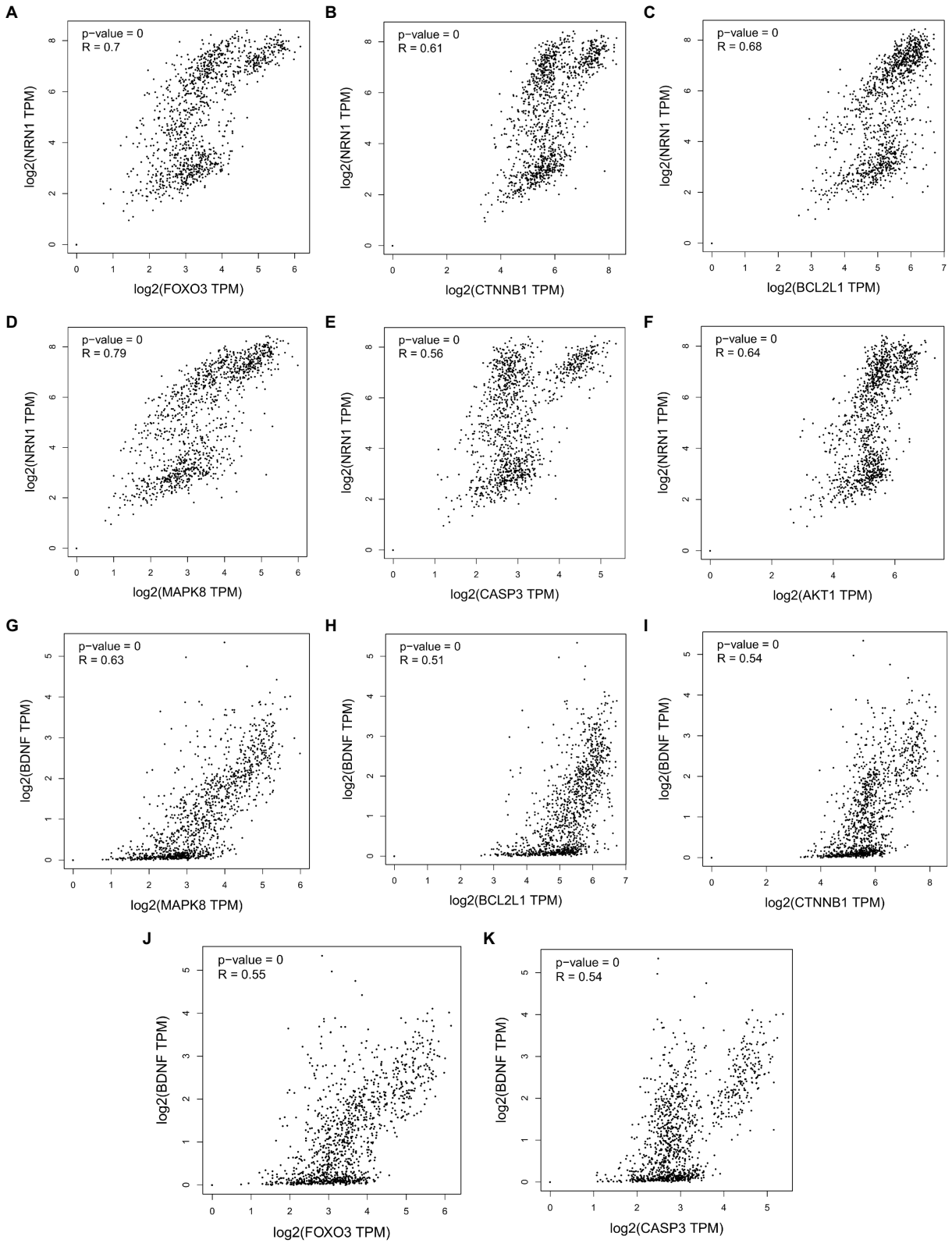

FIGURE 10
Correlation analysis between cordycepin key targets and neurotrophin NRN1 **(A–F)**; correlation analysis between cordycepin key targets and neurotrophin BDNF **(G–K)**.

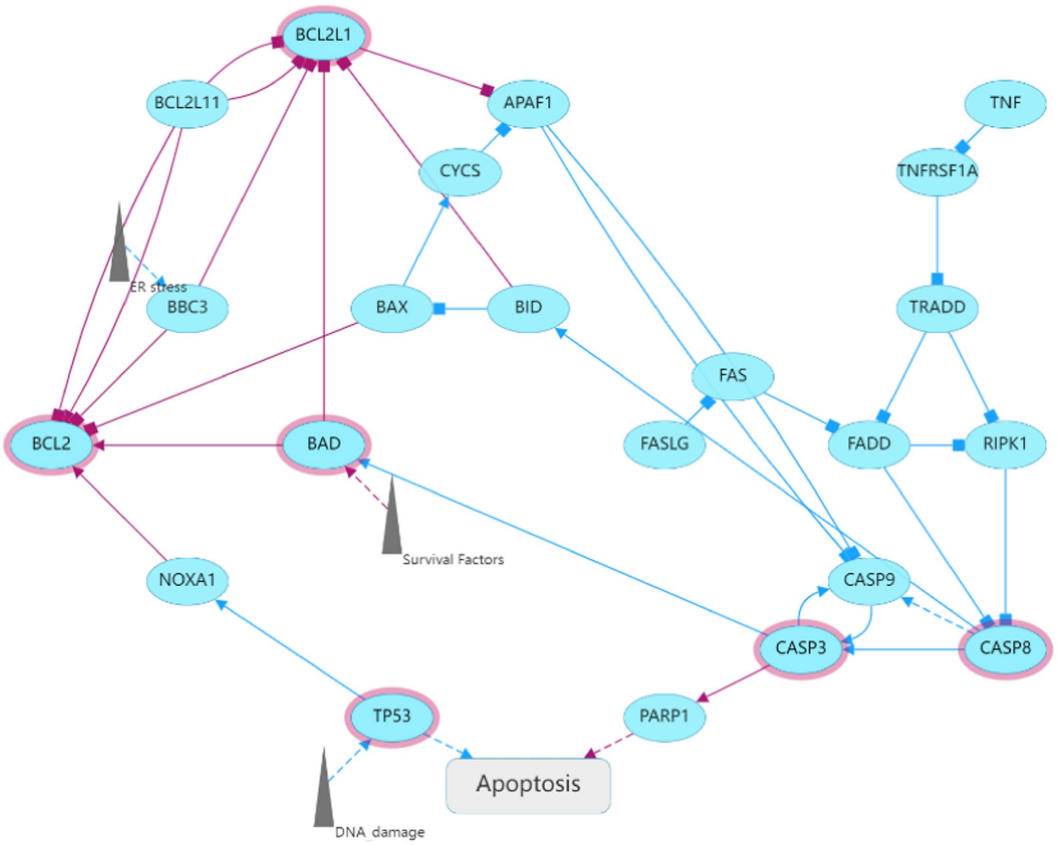

FIGURE 11
Key genes of cordycepin against AD involved in apoptosis.

mechanisms (Kumar and Bansal, 2022). In addition, PI3K/Akt facilitates the activation of neurons and neural stem cells (Razani et al., 2021).

Cordycepin is a metabolite with antiviral activity produced by fungal Cordyceps Militaris. It has a variety of pharmacological functions, including immunomodulatory, neuroprotective and anti-inflammatory activities, and even inhibits tumorigenesis and cancer development (Wang et al., 2019). Interestingly, we found that cordycepin was first extracted from fungi of Cordyceps, but not only present in Cordyceps, but some have also detected genes that synthesize pentostatin and cordycepin from Aspergillus (Xia et al., 2017). This perhaps suggests that similar mechanisms of active ingredient synthesis may exist for different fungi. In a Parkinson's disease model, Cordycepin was found to relieve motor disorders and exert a neuroprotective role (Cheng and Zhu, 2019) by reducing inflammation and oxidative stress. Overwhelming evidence substantiates that Cordycepin can weaken the inflammatory response and the production of pro-apoptotic proteins, increase the expression of anti-apoptotic proteins, and inhibit the activation of the MAPK/NF- κB signaling pathway (Ding et al., 2022), consistent with the findings of this study (Figure 11). It has been established that Cordycepin can bind to the cysteine endopeptidase of the caspase family in mitochondria to inhibit the formation of the death-induced signal complex of endopeptidases recruited in the death domain and then affect the activation of apoptosis and slow down the death of neurons. Moreover, the five core targets of Cordycepin are significantly related to MAPT. Among these, AKT1, BCL2L1, and MAPK8 exhibit a high linear correlation with the expression of MAPT. Besides, AKT1, MAPK8, BCL2L1, FOXO3, and CTNNB1 exhibited a high linear correlation with PSEN2 expression, indicating that they were more closely related to tau lesions and PSEN2 expression. Finally, correlation analysis found that the five core targets were significantly correlated with the expression of neurotrophic factors NRN1 and BDNF. The above results suggest that Cordycepin can slow down neuronal apoptosis and inhibit inflammation. Moreover, Cordycepin can affect pathological tau formation and increase the expression of neurotrophic factors and maintain synaptic function.

Conclusion

Taken together, Cordycepin exhibits multitarget characteristics during AD therapy providing novel insights for developing an optimal treatment for this patient population. Importantly, in this work, we harnessed pharmacologic strategies to investigate the therapeutic mechanisms and potential disease therapeutic mechanisms of Cordycepin for the prevention and treatment of Alzheimer's disease. Cordycepin is expected to be a potential active ingredient for treating AD. However, further studies are warranted to increase the robustness of our findings.

Data availability statement

Publicly available datasets were analyzed in this study. This data can be found here: GSE122063.

Author contributions

XM designed the paper. JX revised the paper. All authors contributed to the article and approved the submitted version.

Funding

This work was supported by the Department of Science & Technology of Liaoning Province (2021JH1/10400035) and Applied Basic Research Program of Liaoning Province 2022JH2/101300160.

Conflict of interest

The authors declare that the research was conducted in the absence of any commercial or financial relationships that could be construed as a potential conflict of interest.

Publisher's note

All claims expressed in this article are solely those of the authors and do not necessarily represent those of their affiliated organizations, or those of the publisher, the editors and the reviewers. Any product that may be evaluated in this article, or claim that may be made by its manufacturer, is not guaranteed or endorsed by the publisher.

References

Aisen, P. S., Jimenez-Maggiora, G. A., Rafii, M. S., Walter, S., and Raman, R. (2022). Early-stage Alzheimer disease: getting trial-ready. *Nat. Rev. Neurol.* 18, 389–399. doi: 10.1038/s41582-022-00645-6

Baker, D. J., and Petersen, R. C. (2018). Cellular senescence in brain aging and neurodegenerative diseases: evidence and perspectives. *J. Clin. Investig.* 128, 1208–1216. doi: 10.1172/jci95145

Barroeta-Espar, I., Weinstock, L. D., Perez-Nievas, B. G., Meltzer, A. C., Siao Tick Chong, M., Amaral, A. C., et al. (2019). Distinct cytokine profiles in human brains resilient to Alzheimer's pathology. *Neurobiol. Dis.* 121, 327–337. doi: 10.1016/j.nbd.2018.10.009

Benito-Cuesta, I., Ordóñez-Gutiérrez, L., and Wandosell, F. (2020). AMPK activation does not enhance autophagy in neurons in contrast to MTORC1 inhibition: different impact on β-amyloid clearance. *Autophagy* 17, 656–671. doi: 10.1080/15548627.2020.1728095

Broome, H. E., Yu, A. L., Diccianni, M., Camitta, B. M., Monia, B. P., and Dean, N. M. (2002). Inhibition of Bcl-XL expression sensitizes T-cell acute lymphoblastic leukemia cells to chemotherapeutic drugs. *Leuk. Res.* 26, 311–316. doi: 10.1016/s0145-2126(01)00118-7

Bussian, T. J., Aziz, A., Meyer, C. F., Swenson, B. L., van Deursen, J. M., and Baker, D. J. (2018). Clearance of senescent glial cells prevents tau-dependent pathology and cognitive decline. *Nature* 562, 578–582. doi: 10.1038/s41586-018-0543-y

Cheng, C., and Zhu, X. (2019). "Cordycepin mitigates MPTP-induced Parkinson's disease through inhibiting TLR/NF-κB signaling pathway.". *Life sciences* 223, 120–127. doi: 10.1016/j.lfs.2019.02.037

Davy, P. M. C., Allsopp, R. C., Donlon, T. A., Morris, B. J., Willcox, D. C., and Willcox, B. J. (2018). FOXO3 and exceptional longevity: insights from hydra to humans. *Curr. Top. Dev. Biol.* 127, 193–212. doi: 10.1016/bs.ctdb.2017.10.001

Ding, J., Yang, W., Jiang, Y., Ji, J., Zhang, J., Wu, L., et al. (2022). Cordycepin protects against hepatic ischemia/reperfusion injury via inhibiting MAPK/NF-KB pathway. *Mediat. Inflamm.* 2022, 1–14. doi: 10.1155/2022/5676256

Elkhateeb, W., Daba, G. M., Elnahas, M. O., and Thomas, P. W. (2019). Fomitopsis officinalis mushroom: ancient gold mine of functional components and biological activities for modern medicine. *Egyp. Pharm. J.* 18:285. doi: 10.4103/epj.epj_46_19

Gebicke-Haerter, P. J. (2001). Microglia in neurodegeneration: molecular aspects. *Microsc. Res. Tech.* 54, 47–58. doi: 10.1002/jemt.1120

Govindula, A., Pai, A., Baghel, S., and Mudgal, J. (2021). Molecular mechanisms of Cordycepin emphasizing its potential against Neuroinflammation: an update. *Eur. J. Pharmacol.* 908:174364. doi: 10.1016/j.ejphar.2021.174364

Han, X., Zhang, T., Liu, H., Mi, Y., and Gou, X. (2020). Astrocyte senescence and Alzheimer's disease: a review. *Front. Aging Neurosci.* 12:9. doi: 10.3389/fnagi.2020.00148

Hansen, D. V., Hanson, J. E., and Sheng, M. (2017). Microglia in Alzheimer's disease. *J. Cell Biol.* 217, 459–472. doi: 10.1083/jcb.201709069

Holtzman, D., and Ulrich, J. (2019). Senescent glia spell trouble in Alzheimer's disease. *Nat. Neurosci.* 22, 683–684. doi: 10.1038/s41593-019-0395-2

Hou, Y., Dan, X., Babbar, M., Wei, Y., Hasselbalch, S. G., Croteau, D. L., et al. (2019). "ageing as a risk factor for neurodegenerative disease." nature reviews. *Neurology* 15, 565–581. doi: 10.1038/s41582-019-0244-7

Hyman, B. T., Phelps, C. H., Beach, T. G., Bigio, E. H., Cairns, N. J., Carrillo, M. C., et al. (2012). National Institute on Aging–Alzheimer's Association guidelines for the Neuropathologic assessment of Alzheimer's disease. *Alzheimers Dement.* 8, 1–13. doi: 10.1016/j.jalz.2011.10.007

Jeong, J. W., Jin, C. Y., Kim, G. Y., Lee, J. D., Park, C., Kim, G. D., et al. (2010). Anti-inflammatory effects of Cordycepin via suppression of inflammatory mediators in BV2 microglial cells. *Int. Immunopharmacol.* 10, 1580–1586. doi: 10.1016/j.intimp.2010.09.011

Jia, L., Piña-Crespo, J., and Li, Y. (2019). "restoring Wnt/β-catenin signaling is a promising therapeutic strategy for Alzheimer's disease." molecular. *Brain* 12:104. doi: 10.1186/s13041-019-0525-5

Ju, Y., and Tam, K. Y. (2020). 9R, the cholinesterase and amyloid Beta aggregation dual inhibitor, as a multifunctional agent to improve cognitive deficit and neuropathology in the triple-transgenic Alzheimer's disease mouse model. *Neuropharmacology* 181:108354. doi: 10.1016/j.neuropharm.2020.108354

Ju, Y., Tam, K. Y. (2021). "Pathological mechanisms and therapeutic strategies for Alzheimer's disease.". *PNeural regeneration research* 17, 543–549. doi: 10.4103/1673-5374.320970

Kettenmann, H., Hanisch, U. K., Noda, M., and Verkhratsky, A. (2011). Physiology of microglia. *Physiol. Rev.* 91, 461–553. doi: 10.1152/physrev.00011.2010

Kim, E. K., and Choi, E. J. (2010). Pathological roles of MAPK signaling pathways in human diseases. *Biochim. Biophys. Acta (BBA) - Mol. Basis Dis.* 1802, 396–405. doi: 10.1016/j.bbadis.2009.12.009

Kumar, M., and Bansal, N. (2021). Implications of phosphoinositide 3-kinase-Akt (PI3K-Akt) pathway in the pathogenesis of Alzheimer's disease. *Mol. Neurobiol.* 59, 354–385. doi: 10.1007/s12035-021-02611-7

Lan, M. Y., Liu, J. S., Wu, Y. S., Peng, C. H., and Chang, Y. Y. (2014). A novel APP mutation (D678H) in a Taiwanese patient exhibiting dementia and cerebral microvasculopathy. *J. Clin. Neurosci.* 21, 513–515. doi: 10.1016/j.jocn.2013.03.038

Lee, V. M. Y., Goedert, M., and Trojanowski, J. Q. (2001). Neurodegenerative Tauopathies. *Annu. Rev. Neurosci.* 24, 1121–1159. doi: 10.1146/annurev.neuro.24.1.1121

Liu, G. H., Bao, Y., Qu, J., Zhang, W., Zhang, T., Kang, W., et al. (2020). Aging atlas: a multi-omics database for aging biology. *Nucleic Acids Res.* 49, D825–D830. doi: 10.1093/nar/gkaa894

McKay, E. C., Beck, J. S., Khoo, S. K., Dykema, K. J., Cottingham, S. L., Winn, M. E., et al. (2019). Peri-infarct upregulation of the oxytocin receptor in vascular dementia. *J. Neuropathol. Exp. Neurol.* 78, 436–452. doi: 10.1093/jnen/nlz023

Michaud, J. P., Hallé, M., Lampron, A., Thériault, P., Préfontaine, P., Filali, M., et al. (2013). Toll-like receptor 4 stimulation with the detoxified ligand Monophosphoryl lipid a improves Alzheimer's disease-related pathology. *Proc. Natl. Acad. Sci.* 110, 1941–1946. doi: 10.1073/pnas.1215165110

Montine, T. J., Phelps, C. H., Beach, T. G., Bigio, E. H., Cairns, N. J., Dickson, D. W., et al. (2011). National Institute on Aging–Alzheimer's Association guidelines for the Neuropathologic assessment of Alzheimer's disease: a practical approach. *Acta Neuropathol.* 123, 1–11. doi: 10.1007/s00401-011-0910-3

Musi, N., Valentine, J. M., Sickora, K. R., Baeuerle, E., Thompson, C. S., Shen, Q., et al. (2018). Tau protein aggregation is associated with cellular senescence in the brain. *Aging Cell* 17:e12840. doi: 10.1111/acel.12840

Neuner, S. M., Telpoukhovskaia, M., Menon, V., O'Connell, K. M. S., Hohman, T. J., and Kaczorowski, C. C. (2022). Translational approaches to understanding resilience to Alzheimer's disease. *Trends Neurosci.* 45, 369–383. doi: 10.1016/j.tins.2022.02.005

Patel, R. V., Hamanishi, E. T., and Provart, N. J. (2016). A human "EFP" browser for generating gene expression Anatograms. *PLoS One* 11:e0150982. doi: 10.1371/journal.pone.0150982

Peng, J., Wang, P., Ge, H., Qu, X., and Jin, X. (2015). Effects of Cordycepin on the microglia-Overactivation-induced impairments of growth and development of hippocampal cultured neurons. *PLoS One* 10:e0125902. doi: 10.1371/journal.pone.0125902

Perez-Nievas, B. G., Stein, T. D., Tai, H. C., Dols-Icardo, O., Scotton, T. C., Barroeta-Espar, I., et al. (2013). Dissecting phenotypic traits linked to human resilience to Alzheimer's pathology. *Brain* 136, 2510–2526. doi: 10.1093/brain/awt171

Qin, P., Li, X. K., Yang, H., Wang, Z. Y., and Lu, D. X. (2019). Therapeutic potential and biological applications of Cordycepin and metabolic mechanisms in Cordycepin-producing fungi. *Molecules* 24:2231. doi: 10.3390/molecules24122231

Razani, E., Pourbagheri-Sigaroodi, A., Safaroghli-Azar, A., Zoghi, A., Shanaki-Bavarsad, M., and Bashash, D. (2021). The PI3K/Akt signaling Axis in Alzheimer's disease: a valuable target to stimulate or suppress. *Cell Stress Chaperones* 26, 871–887. doi: 10.1007/s12192-021-01231-3

Saez-Atienzar, S., and Masliah, E. (2020). Cellular senescence and Alzheimer disease: the egg and the chicken scenario. *Nat. Rev. Neurosci.* 21, 433–444. doi: 10.1038/s41583-020-0325-z

Salminen, A., Kaarniranta, K., and Kauppinen, A. (2016). AMPK and HIF signaling pathways regulate both longevity and cancer growth: the good news and the bad news about survival mechanisms. *Biogerontology* 17, 655–680. doi: 10.1007/s10522-016-9655-7

Sochocka, M., Diniz, B. S., and Leszek, J. (2017). Inflammatory response in the CNS: friend or foe? *Mol. Neurobiol.* 54, 8071–8089. doi: 10.1007/s12035-016-0297-1

Tam, K. Y., and Ju, Y. (2022). Pathological mechanisms and therapeutic strategies for Alzheimer's disease. *Neural Regen. Res.* 17, 543–549. doi: 10.4103/1673-5374.320970

van Rossum, I. A., Visser, P. J., Knol, D. L., van der Flier, W. M., Teunissen, C. E., Barkhof, F., et al. (2012). Injury markers but not amyloid markers are associated with rapid progression from mild cognitive impairment to dementia in Alzheimer's disease. *J. Alzheimers Dis.* 29, 319–327. doi: 10.3233/jad-2011-111694

Wang, Y., Lv, T. S., Liu, W., Di Yan, L. Y., Chen, Z. H. (2019). "Cordycepin suppresses cell proliferation and migration by targeting CLEC2 in human gastric cancer cells via Akt signaling pathway.". *Life sciences*, 223, 110–119. doi: 10.1016/j.lfs.2019.03.025

Xia, Y. L., Luo, F., Shang, Y., Chen, P., Lu, Y., and Wang, C. (2017). Fungal Cordycepin biosynthesis is coupled with the production of the safeguard molecule Pentostatin. *Cell Chem. Biol.* 24, 1479–1489.e4. doi: 10.1016/j.chembiol.2017.09.001

Xu, W., Jiang, Y., Wang, N., Bai, H., Xu, S., Xia, T., et al. (2022). Traditional Chinese medicine as a promising strategy for the treatment of Alzheimer's disease complicated with osteoporosis. *Front. Pharmacol.* 13:842101. doi: 10.3389/fphar.2022.842101

Yang, R., Wang, X., Xi, D., Mo, J., Wang, K., Luo, S., et al. (2019). Cordycepin attenuates IFN-γ-induced macrophage IP-10 and Mig expressions by inhibiting STAT1 activity in CFA-induced inflammation mice model. *Inflammation* 43, 752–764. doi: 10.1007/s10753-019-01162-3

Yao, J. J., Zhao, Q. R., Lu, J. M., and Mei, Y. A. (2018). Functions and the related signaling pathways of the neurotrophic factor Neuritin. *Acta Pharmacol. Sin.* 39, 1414–1420. doi: 10.1038/aps.2017.197

Yu, L., Tasaki, S., Schneider, J. A., Arfanakis, K., Duong, D. M., Wingo, A. P., et al. (2020). Cortical proteins associated with cognitive resilience in community-dwelling older persons. *JAMA Psychiat.* 77, 1172–1180. doi: 10.1001/jamapsychiatry.2020.1807

Zhai, L., Ning, Z. W., Huang, T., Wen, B., Liao, C. H., Lin, C. Y., et al. (2018). Cyclocarya Paliurus leaves tea improves dyslipidemia in diabetic mice: a Lipidomics-based network pharmacology study. *Front. Pharmacol.* 9:28. doi: 10.3389/fphar.2018.00973

Zhang, P., Kishimoto, Y., Grammatikakis, I., Gottimukkala, K., Cutler, R. G., Zhang, S., et al. (2019). Senolytic therapy alleviates Aβ-associated oligodendrocyte progenitor cell senescence and cognitive deficits in an Alzheimer's disease model. *Nat. Neurosci.* 22, 719–728. doi: 10.1038/s41593-019-0372-9

Zhang, H., and Zheng, Y. (2019). β amyloid hypothesis in Alzheimer's disease:Pathogenesis,Prevention,and management. *Zhongguo Yi Xue Ke Xue Yuan Xue Bao* 41, 702–708. doi: 10.3881/j.issn.1000-503X.10875

Zilka, N., Stozicka, Z., Kovac, A., Pilipcinec, E., Bugos, O., and Novak, M. (2009). Human misfolded truncated tau protein promotes activation of microglia and leukocyte infiltration in the transgenic rat model of Tauopathy. *J. Neuroimmunol.* 209, 16–25. doi: 10.1016/j.jneuroim.2009.01.013

frontiers | Frontiers in Human Neuroscience

TYPE Original Research
PUBLISHED 01 February 2023
DOI 10.3389/fnhum.2023.1059091

OPEN ACCESS

EDITED BY
Ann-Maree Vallence,
Murdoch University, Australia

REVIEWED BY
Deokjong Lee,
Yonsei University Health System,
Republic of Korea
Rachel Anne Hill,
Monash University, Australia

*CORRESPONDENCE
Thamires N. C. Magalhães
✉ thamiresncm@tamu.edu
Tracey H. Hicks
✉ tslonim@tamu.edu

†These authors have contributed equally to this work

SPECIALTY SECTION
This article was submitted to Brain Imaging and Stimulation, a section of the journal Frontiers in Human Neuroscience

RECEIVED 30 September 2022
ACCEPTED 13 January 2023
PUBLISHED 01 February 2023

CITATION
Hicks TH, Magalhães TNC, Ballard HK, Jackson TB, Cox SJ and Bernard JA (2023) Network segregation in aging females and evaluation of the impact of sex steroid hormones.
Front. Hum. Neurosci. 17:1059091.
doi: 10.3389/fnhum.2023.1059091

Network segregation in aging females and evaluation of the impact of sex steroid hormones

Tracey H. Hicks[1*†], Thamires N. C. Magalhães[1*†], Hannah K. Ballard[1], T. Bryan Jackson[1], Sydney J. Cox[2] and Jessica A. Bernard[1,2]

[1]Department of Psychological and Brain Sciences, Texas A&M University, College Station, TX, United States, [2]Texas A&M Institute for Neuroscience, Texas A&M University, College Station, TX, United States

Males and females show differential patterns in connectivity in resting-state networks (RSNs) during normal aging, from early adulthood to late middle age. Age-related differences in network integration (effectiveness of specialized communication at the global network level) and segregation (functional specialization at the local level of specific brain regions) may also differ by sex. These differences may be due at least in part to endogenous hormonal fluctuation, such as that which occurs in females during midlife with the transition to menopause when levels of estrogens and progesterone drop markedly. A limited number of studies that have investigated sex differences in the action of steroid hormones in brain networks. Here we investigated how sex steroid hormones relate to age-network relationships in both males and females, with a focus on network segregation. Females displayed a significant quadratic relationship between age and network segregation for the cerebellar-basal ganglia and salience networks. In both cases, segregation was still increasing through adulthood, highest in midlife, and with a downturn thereafter. However, there were no significant relationships between sex steroid hormone levels and network segregation levels in females, and they did not exhibit significant associations between progesterone or 17β-estradiol and network segregation. Patterns of connectivity between the cerebellum and basal ganglia have been associated with cognitive performance and self-reported balance confidence in older adults. Together, these findings suggest that network segregation patterns with age in females vary by network, and that sex steroid hormones are not associated with this measure of connectivity in this cross-sectional analysis. Though this is a null effect, it remains critical for understanding the extent to which hormones relate to brain network architecture.

KEYWORDS

functional connectivity, aging, steroid hormones, sex differences, network segregation

1. Introduction

Advanced age is associated with an overall decrease in the effectiveness of specialized communication at the global network level (i.e., integration) and loss of functional specialization at the local level of specific brain regions (i.e., segregation). That is, neuronal networks become less distinct with advanced age (Foo et al., 2021).

Age-related differences in the reorganization of functional connectivity and cognitive abilities may also differ by sex. In adulthood, sex differences in brain structure and function

can be observed (Cosgrove et al., 2007) and, similarly, sex differences in resting state networks (RSNs) have been reported. For example, studies of age differences have observed that males show increasing connectivity between-networks when compared to females (Allen et al., 2011; Filippi et al., 2013; Goldstone et al., 2016). Males also exhibited more marked changes in default mode network (DMN) connectivity, especially in the posterior cingulate cortex (PCC), but showed smaller differences (and possibly increases) in connectivity to the lateral prefrontal regions of the fronto-parietal network (FPN) relative to females (Allen et al., 2011; Filippi et al., 2013). Females on the other hand showed smaller differences in DMN connectivity but showed greater decreases in FPN connectivity when compared to males.

Sex differences in network architecture have also been reported (Zhang et al., 2016). Zhang et al. (2016) observed that female functional networks have significantly more connected nodes than males suggest an increase in network homogeneity in female brains. They also observed that the cerebellar nodes have a higher clustering coefficient and local efficiency for females (Zhang et al., 2016). This adds evidence to their findings that the clustering coefficient and local efficiency in males are higher, while female connections are diffuse across lobes and the network is less modular. These results jointly support the notion that networks in female brains, compared to those in males, are more spatially distributed but with lower correlation strengths (Scheinost et al., 2015; Zhang et al., 2016). Overall, males and females showed differential patterns in connectivity in RSNs during normal aging, and from early adulthood to late middle age (Allen et al., 2011; Filippi et al., 2013; Scheinost et al., 2015). However, these differences vary between studies with respect to regions and networks that are impacted.

Just as there are mixed results regarding sex differences with age in brain networks, there are also disagreements in the literature regarding differences in resting-state functional connectivity in the context of hormonal differences between biological sexes. To this point, there have been a limited number of studies that have investigated sex steroid hormones on brain networks. Further, there is currently disagreement among the rapidly expanding number of studies on the possible neuroprotective effects of sex hormones on cognitive and brain function more generally (Moffat, 2005; Sundström Poromaa and Gingnell, 2014; Toffoletto et al., 2014). Given that RSNs appear to be differentially impacted in males in females in later life, further exploration of the impact of sex steroid hormone levels on network architecture across adulthood stands to improve our understanding of underlying factors contributing to these differences. Specifically, it may be that sex hormone levels are related to the integration and segregation of neuronal networks (Peper et al., 2011).

In the brain, hormone receptors can be found across several regions. Post-mortem studies have found estrogen receptors in the hippocampus, claustrum, cerebral cortex, amygdala, hypothalamus, subthalamic nucleus, and thalamus (Osterlund et al., 2000; Weiser et al., 2008; Syan et al., 2017). As for progesterone, a post-mortem study reported high concentrations of its receptors in the amygdala, hypothalamus, and cerebellum (Bixo et al., 1997; Syan et al., 2017). Testosterone exerts an early organizational effect on the development of the hypothalamus (Jacobson et al., 1981), the cerebral cortex (Diamond, 1991), and the hippocampus (Roof and Havens, 1992) in addition to other brain structures. With respect to testosterone, after conversion to estradiol, it can also interact with estrogen receptors (Moffat, 2005). The relationship between these two hormones (testosterone and estrogen) have been shown to affect vascular health directly (Aggarwal et al., 2018; Raparelli et al., 2022). The ratio of testosterone to estradiol is important for vascular function suggesting that these hormones may not act independently (van Koeverden et al., 2019; Raparelli et al., 2022). Therefore, it is also important to investigate the interactions that may occur between sex hormones and whether together they may be involved related to aging processes, as well as differences in neuronal networks (Syan et al., 2017). Testosterone, progesterone, and estrogens are present in both males and females, but their levels and production vary, mainly with respect to sex and age, though fluctuations in estrogens and progesterone occur across the female menstrual cycle as well (Sundström Poromaa and Gingnell, 2014).

The influence of sex hormones on functional networks is vital to our understanding of brain function and organization during periods of endogenous hormonal fluctuation, such as that which occurs in females during midlife with the transition to menopause when levels of estrogens and progesterone drop markedly (Toffoletto et al., 2014; Foo et al., 2021). Our study here aims to investigate how sex steroid hormones relate to age-network relationships in both males and females, with a focus on network segregation. As such, we predicted that there would be associations between network segregation and hormone levels, as well as interactions between hormones that may be affecting or enhancing the segregation of RSNs.

2. Materials and methods

2.1. Study sample

One hundred and fifty-seven participants (total n = 157) were enrolled as part of a larger study on aging. All participants underwent a battery of cognitive and motor tasks and during this assessment, the participants provided saliva samples for hormone quantification (for details about collection see Section "2.2 Hormone quantification"). After the behavioral visit the participants returned for a magnetic resonance imaging (MRI) session approximately 2 weeks later. However, due to unexpected delays related to the COVID-19 pandemic, the time between the two sessions (39.0 days ± 21.4 days) varied between participants. For our analyses here, we focused only on the hormone and brain imaging data.

Exclusion criteria were history of neurological disease, stroke, or formal diagnosis of psychiatric illness (e.g., depression or anxiety), contraindications for the brain imaging environment, and use of hormone therapy (HTh) or hormonal contraceptives [intrauterine device (IUD), possible use of continuous birth control (oral), and history of hysterectomy]. These latter exclusions were made to evaluate impacts of normative endocrine aging on healthy adult females. For our analyses here we focused only on those with available neuroimaging data and hormonal assays. Thus, our final sample included 121 participants [55 males (age 57 ± 14.76) and 66 females (age 57 ± 12.17)]. A flowchart showing the exclusions and determination of the final sample for analysis is presented below (**Figure 1**).

All study procedures were approved by the Institutional Review Board at Texas A&M University, and written informed consent was obtained from each participant prior to initiating any data collection.

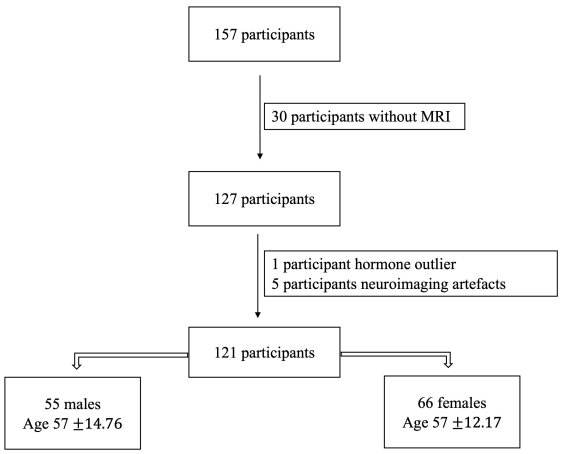

FIGURE 1
The initially collected number of participants and after following the exclusion criteria, the final number of our sample.

2.2. Hormone quantification

For hormonal analyses, we followed the methodology used in recent work from our research group (Ballard et al., 2022a). For the sake of clarity and replicability, the methods reporting here matches what was reported in our recent work (Ballard et al., 2022a). Before collecting the saliva sample, participants were asked to refrain from consuming alcohol 24 h prior and eating or drinking 3 h prior to their first study session to avoid exogenous influences on hormone levels. Participants were also screened for oral disease or injury, use of substances such as nicotine or caffeine, and prescription medications that may impact the saliva pH and compromise samples. Participants were asked to rinse their mouth with water 10 min prior to providing a saliva sample to clear out any residue.

Samples were then collected in pre-labeled cryovials provided by Salimetrics[1] using the passive drool technique. For our study, participants were asked to supply 1 mL of saliva, after which samples were immediately stored in a −80° Celsius bio-freezer for stabilization. Assays were completed by Salimetrics to quantify 17β-estradiol, progesterone, and testosterone levels for each participant. The amount of saliva collected was sufficient to detect 17β-estradiol at a high sensitivity threshold of 0.1 pg/mL (Salimetrics, 2022), along with 5.0 pg/mL and 1.0 pg/mL thresholds for progesterone and testosterone, respectively.

The protocol used by Salimetrics includes two repetitions of each assay; thus, the values used in our analyses represent an average of both repetitions. A few samples were insufficient in quantity and were unable to be properly assayed (n = 3; 2 progesterone, 1 testosterone). The intra-assay coefficient of variability for our hormone samples was 0.15 for 17β-estradiol, 0.11 for progesterone, and 0.07 for testosterone. This non-invasive method is adequate for precisely measuring reproductive hormones. Salivary measurements are strongly correlated with blood-derived measurements to index sex hormone levels (17β-estradiol: r = 0.80; progesterone: r = 0.80; testosterone: r = 0.96).[2]

2.3. Imaging acquisition

Participants underwent structural and resting-state MRI using a Siemens Magnetom Verio 3.0 Tesla scanner and a 32-channel head coil. For structural MRI, we collected a high-resolution T1-weighted 3D magnetization prepared rapid gradient multi-echo (MPRAGE) scan [repetition time (TR) = 2,400 ms; acquisition time = 7 min; voxel size = 0.8 mm^3] and a high-resolution T2-weighted scan [TR = 3,200 ms; acquisition time = 5.5 min; voxel size = 0.8 mm^3], each with a multiband acceleration factor of two. For resting-state imaging, we administered four blood-oxygen level dependent (BOLD) functional connectivity (fcMRI) scans with the following parameters: multiband factor of eight, 488 volumes, TR of 720 ms, and 2.5 mm^3 voxels. Each fcMRI scan was 6 min in length for a total of 24 min of resting-state imaging, and scans were acquired with alternating phase encoding directions (i.e., two anterior to posterior scans and two posteriors to anterior scans). During the fcMRI scans, participants were asked to lie still with their eyes open while fixating on a central cross. In total, the acquisition of images takes about 45 min, including a 1.5-min localizer.

Scanning protocols were adapted from the multiband sequences developed by the Human Connectome Project (HCP) (Harms et al., 2018) and the Center for Magnetic Resonance Research at the University of Minnesota to facilitate future data sharing and reproducibility.

2.3.1. Imaging processing

2.3.1.1. Pre-processing

Images were converted from DICOM to NIFTI and organized into a Brain Imaging Data Structure (BIDS, version 1.6.0) format *via* the latest docker container version of bidskit (version 2021.6.14).[3] Using the split tool distributed with the FMRIB Software Library (FSL) package (Jenkinson et al., 2012), a single volume was extracted from two oppositely encoded BOLD images to estimate B_0 field maps. Next, fMRIPrep (version 20.2.3)[4] was used to preprocess anatomical and functional images. The fMRIPrep preprocessing pipeline includes basic steps such as co-registration, normalization, unwarping, noise component extraction, segmentation, and skull-stripping.

While basic pre-processing was performed in the fMRI preparation, we also completed remaining steps in the Conn toolbox, version 21a (Whitfield-Gabrieli and Nieto-Castanon, 2012). We used the default preprocessing pipeline, which consists of realignment and unwarping with motion correction, centering to (0, 0, 0) coordinates, slice-timing correction, outlier detection using a 95th percentile threshold and the Artifact Rejection Toolbox (ART), segmentation of gray matter, white matter, and cerebrospinal fluid, normalization to Montreal Neurological Institute (MNI) space, and spatial smoothing with a 5 mm full width at half-maximum (FWHM) Gaussian kernel. A band-pass filter of 0.008–0.099 Hz was applied to denoise data.

1 https://salimetrics.com/saliva-collection-training-videos/

2 https://salimetrics.com/analyte/salivary-estradiol/

3 https://github.com/jmtyszka/bidskit

4 https://fmriprep.org/

The threshold for global-signal *z*-values was set at three, while the motion correction threshold was set at 0.5 mm. After being de-spiked during denoising to adhere to the global mean, 6-axis motion data and frame-wise outliers were included as first-level covariates.

2.3.1.2. Region of interest selection

In our study, we used the same Region of Interest (ROIs) selection used by Ballard et al. (2022c), in work previously completed by our group. The MNI coordinates for each cortical node retrieved from Cassady et al. (2019) [originally derived from Power et al. (2011)] were selected by our group. Further, we included 20 subcortical nodes of the [extracted from Hausman et al. (2020)] for the cerebellar-basal ganglia network (Diedrichsen, 2006; Di Martino et al., 2008; Diedrichsen et al., 2009). Cerebellar seeds were determined *via* the SUIT atlas (Power et al., 2011; Cassady et al., 2019). Our final set of ROIs contained 234 nodes across 11 networks (10 cortical, 1 subcortical, see **Table 1** for a list of included networks). MNI coordinates for each node were translated to voxel coordinates, which were subsequently used to create spherical seeds with 3.5 mm diameters in FSL (Jenkinson et al., 2012). These seeds were then treated as ROIs.

First-level ROI-to-ROI relationships were evaluated with a bivariate correlation approach; those correlations are needed to calculate the variables within and between the network for each subject which are then used in the network segregation equation. Correlation values were transformed into *z*-values *via* Fisher's r-to-z conversion (Zar Jerrold, 1996). Corrections for multiple comparisons were applied during statistical analyses.

2.3.1.3. Network segregation equation

For the analysis of network segregation, we again followed our previous work reported by Ballard et al. (2022a,c) and based off analyses initially conducted by Chan et al. (2014). Network segregation values were determined using Equation 1 below. In the formula, $\underline{z}_w$ corresponds to the mean correlation between ROIs within an individual network, and $\underline{z}_b$ represents the mean correlation between ROIs of an individual network and all remaining ROIs of other networks. Group-level analyses were performed with a voxel threshold of $p < 0.001$ and cluster threshold, FDR-corrected, of $p < 0.05$.

TABLE 1 Network abbreviation key.

Abbreviation	Network
Au	Auditory
CBBG	Cerebellar-basal ganglia
COTC	Cingulo-opercular task control
DA	Dorsal attention
DM	Default mode
FPTC	Fronto-parietal task control
Sa	Salience
SSH	Sensory somatomotor hand
SSM	Sensory somatomotor mouth
Vi	Visual
VA	Ventral attention

Equation 1. Network segregation values were determined using this formula.

$$Network\ segregation = \frac{\underline{z}_w - \underline{z}_b}{\underline{z}_w}$$

2.4. Statistical analysis

We first sought to ascertain sex differences in hormone levels within our sample. Analyses of variance (ANOVAs) were conducted to determine sex differences in hormone levels (i.e., estradiol, progesterone, and testosterone separately). ANOVAs were completed using the ANOVA function from the default "stats" package in R (v4.0.5, R Core Team, 2021) which determined beta coefficients, degrees of freedom, *F*-values, and *p*-values; the sjstats and pwr packages were used to compute η^2 and partial η^2 values (v0.18.1, (Lüdecke, 2022)).

As our primary area of interest lies within the impact of fluctuating hormones on female brain network segregation, our main analyses investigated females only. However, exploratory analyses evaluated males and all participants combined which are included in the supplement.

To explore the unique associations between hormone levels (i.e., estradiol, progesterone, and testosterone separately) and each network of interest in females, linear regressions were performed in which hormone levels served as the predictor and network segregation as the outcome. These linear regressions were also conducted in exploratory analyses with males and all participants collapsing the two sexes (**Supplementary Tables 1–6**). The lm function from the default "stats" package in R (v4.0.5, R Core Team, 2021) determined beta coefficients, degrees of freedom, *F*-values, *p*-values, R^2, and adjusted R^2. False discovery rate (FDR) correction was applied to account for multiple comparisons (i.e., number of networks examined) using the FSA package in R exclusively on results with a *p*-value ≤ 0.05 (FSA v0.9.3, Ogle et al., 2022). Linear regressions with hormone level interactions (i.e., estradiol*progesterone, estradiol*testosterone, and progesterone*testosterone) as the predictor variables explored the relationship between combined hormone levels and network segregation in females. Exploratory analyses investigated the same hormone level interactions in males and all participants together (**Supplementary Tables 12, 13**). FDR correction was applied as previously described (FSA v0.9.3, Bernard et al., 2015). Our cross-sectional hormone level data is also visualized *via* locally weighted scatterplot smoothing (**Supplementary Figure 1**) to provide comparison to normal distributions of sex hormone levels by age.

Associations between network segregation and age were evaluated *via* linear regression with age as the predictor and network connectivity as the outcome in females; males and all participants together were run as exploratory analyses (**Supplementary Tables 7, 8**). We conducted similar regressions with quadratic age [Age + I (Age^2)] as the predictor to investigate whether network segregation demonstrated better fit with a quadratic function rather than linear across middle-to advanced-age adults, given prior work suggesting non-linear relationships between brain system segregation (Chan et al., 2014) as well as brain volume (Bernard et al., 2015) and age. Quadratic regressions for males and all participants were run as exploratory analyses (**Supplementary Tables 9, 10**). Linear and quadratic regressions were performed using the lm function from the default "stats" package in R (v4.0.5,

R Core Team, 2021) which determined beta coefficients, degrees of freedom, F-values, *p*-values, R^2, and adjusted R^2. FDR correction was applied as previously described to account for multiple comparisons (i.e., number of networks examined) (FSA v0.9.3, Chan et al., 2014). Akaike's An Information Criterion (AIC) (Sakamoto et al., 1986) compared fit between linear and quadratic models with a requirement that model value must differ by 10 to be considered a superior fit (Burnham and Anderson, 2004; Bohon and Welch, 2021). AIC was calculated by the default "stats" package in R (v4.0.5, R Core Team, 2021).

The stargazer package (v5.2.2; Hlavac, 2018) was used to create **Tables 2–7**. The ggplot2 package was used to create linear and quadratic plots (Figures 1–5; v3.3.3; Wickham, 2016). All figures were created using a colorblind friendly palette *via* RColorBrewer (Neuwirth and Neuwirth, 2023).

3. Results

3.1. Hormone levels by sex

An ANOVA revealed significant sex differences in testosterone when accounting for age [$F(1,111) = 79.496$, $p < 0.001$; **Figure 1**], that is testosterone levels were significantly lower in females. ANOVAs did not reveal significant sex differences in estradiol or progesterone levels [$F(1,105) = 3.318$, $p = 0.071$, $\eta^2 = 0.031$], and [$F(1,109) = 3.270$, $p = 0.073$, $\eta^2 = 0.029$], respectively **Figure 2**.

3.2. Network segregation and hormone levels in females

When examining females alone, network segregation was not significantly associated with progesterone, estradiol, or testosterone in females after FDR correction (see **Tables 2–4**). Similar exploratory analyses were conducted with hormone levels (i.e., estradiol, progesterone, and testosterone; respectively) across participants and in males and all participants (see **Supplementary Tables 1–3**).

3.3. Interactions between hormone levels and network segregation in females

Regressions evaluating combined effects (interactions) of hormone levels (i.e., Estradiol*Progesterone, Estradiol*Testosterone, and Progesterone*Testosterone) as the predictor and network segregation as the outcome were not significant (see **Table 5**). Similar analyses were conducted in males and all participants (see **Supplementary Tables 12, 13**). Notably, though the 17β-estradiol*testosterone interaction was associated with segregation in both the sensory somatomotor hand and mouth networks, these did not survive FDR correction.

3.4. Linear and quadratic associations between age and network segregation

Network segregation was evaluated in females across the adult lifespan with respect to age. Linear regressions with age as the predictor and network segregation as the outcome revealed no significant associations after corrections for multiple comparisons (see **Table 6**).

However, in females, regressions with quadratic age as the predictor and network segregation as the outcome, demonstrated significant associations in the cerebellar-basal ganglia (CBBG) [$F(2, 63) = 10.020$, raw $p = 0.002$, FDR adjusted $p = 0.011$] and salience (Sa) [$F(2, 63) = 10.806$, raw $p < 0.001$, FDR adjusted $p = 0.011$] networks (**Figures 3**, **4** and **Table 7**). There were no additional significant associations in network segregation and quadratic age for females or males as revealed in our exploratory analyses (detailed results are presented in **Table 7**).

Comparisons of model fit between linear and quadratic regressions revealed that salience network segregation fits significantly better with a quadratic model as compared to linear in females (AIC difference = 11.11, **Figure 3**). However, all other comparisons of model fit between linear, and quadratic were not statistically significant (see **Supplementary Table 11**).

TABLE 2 This table presents results from linear regressions for estradiol and network segregation in females.

Female estradiol linear associations with network segregation						
	Estradiol β coefficient	Raw *P*-value	R^2	Adjusted R^2	Residual std. error (df = 55)	F statistic (df = 1; 55)
Au	−0.008	0.738	0.002	−0.016	0.103	0.114
CBBG	0.039	0.313	0.019	0.001	0.157	1.037
COTC	0.914	0.385	0.014	−0.004	4.27	0.769
DA	−0.023	0.392	0.013	−0.005	0.109	0.746
DM	0.018	0.625	0.004	−0.014	0.146	0.242
FPTC	0.015	0.646	0.004	−0.014	0.129	0.214
Sa	0.038	0.259	0.023	0.005	0.138	1.306
SSH	−0.008	0.761	0.002	−0.016	0.111	0.094
SSM	−0.024	0.205	0.029	0.011	0.077	1.646
Vi	−0.013	0.705	0.003	−0.015	0.137	0.146
VA	−0.022	0.731	0.002	−0.016	0.26	0.120

Raw *p*-values are listed, and FDR correction was only performed if raw *p*-value was < 0.05.

TABLE 3 This table presents results from linear regressions for progesterone and network segregation in females.

Female progesterone linear associations with network segregation							
	Progesterone β coefficient	Raw *P*-value	FDR corrected *P*-value	R^2	Adjusted R^2	Residual std. error (df = 59)	F statistic (df = 1; 59)
Au	0.0001	0.575	0.926	0.005	−0.011	0.107	0.318
CBBG	0.0003	0.176	0.484	0.031	0.014	0.166	1.880
COTC	0.015	0.010	0.110	0.109	0.094	3.873	7.247
DA	0.0001	0.674	0.926	0.003	−0.014	0.107	0.179
DM	0.0002	0.255	0.561	0.022	0.005	0.143	1.323
FPTC	0.0004	0.049	0.270	0.064	0.049	0.123	4.067
Sa	0.0003	0.102	0.374	0.045	0.029	0.134	2.764
SSH	0.0001	0.711	0.926	0.002	−0.015	0.116	0.139
SSM	0.00001	0.926	0.926	0.0002	−0.017	0.082	0.009
Vi	0.00004	0.850	0.926	0.001	−0.016	0.133	0.036
VA	−0.0001	0.881	0.926	0.0004	−0.017	0.246	0.023

Raw *p*-values and FDR corrected *p*-values are included. There were no significant findings after FDR correction.

TABLE 4 This table presents results from linear regressions for testosterone and network segregation in females.

Female testosterone linear associations with network segregation						
	Testosterone β coefficient	Raw *P*-value	R^2	Adjusted R^2	Residual std. error (df = 60)	F statistic (df = 1; 60)
Au	−0.0001	0.881	0.0004	−0.016	0.106	0.023
CBBG	0.0003	0.668	0.003	−0.014	0.167	0.187
COTC	0.009	0.561	0.006	−0.011	4.115	0.342
DA	−0.0002	0.715	0.002	−0.014	0.106	0.135
DM	0.001	0.112	0.042	0.026	0.141	2.605
FPTC	0.0001	0.900	0.0003	−0.016	0.126	0.016
Sa	0.001	0.262	0.021	0.005	0.136	1.284
SSH	−0.0001	0.872	0.0004	−0.016	0.116	0.027
SSM	−0.0003	0.283	0.019	0.003	0.08	1.175
Vi	−0.0002	0.676	0.003	−0.014	0.131	0.177
VA	−0.001	0.364	0.014	−0.003	0.245	0.837

Raw *p*-values are listed, and FDR correction was only performed if raw *p*-value was < 0.05.

4. Discussion

This study investigated network segregation in aging females in the context of sex steroid hormones. Primarily, we were interested in network segregation in adult females, as sex steroid hormone levels—which undergo dramatic changes in females during mid and later life—may impact brain network properties. Understanding differences in network segregation in females in the context of aging and hormone levels stands to provide a greater understanding around factors contributing to functional differences in aging, particularly given that older females are at greater risk for negative outcomes in later life (Gao et al., 1998; Burger, 2008; Lahousse et al., 2014; Alzheimer's Association, 2022). Somewhat surprisingly, we found no significant relationships between sex steroid hormone levels and network segregation levels in adult females. To our knowledge, this is the first study to directly investigate endogenous hormone levels with network segregation and patterns of aging.

In the context of both endogenous hormone levels and exogenous sex hormone treatments, sex hormones have displayed impacts on brain structure and function (e.g., cortical connectivity, subcortical connectivity, and within-network coherence) (Peper et al., 2011; Taylor et al., 2019; Pritschet et al., 2020). Given the notable vacillations in hormone levels during distinct reproductive stages (Diedrichsen, 2006) and cognitive inefficiencies associated with certain reproductive stages (Greendale et al., 2011; Epperson et al., 2013; Weber et al., 2014; Rentz et al., 2017; Taylor et al., 2019; Pritschet et al., 2020), we expected to find associations between network segregation and hormone levels. However, females did not exhibit significant associations between progesterone, 17β-estradiol, or testosterone and network segregation. These findings are inconsistent with a recent study of network segregation from our group (Ballard et al., 2022c) which demonstrated some differences with reproductive stage, suggesting hormones may play impact network segregation. That is, female reproductive aging is associated

TABLE 5 This table exhibits results from linear regressions for hormone interactions and network segregation in females.

Female hormone level interactions with network segregation											
	Estradiol by progesterone (E*P) β coefficient	Raw E*P *P*-value	Estradiol by testosterone (E*T) β coefficient	Raw E*T *P*-value	Progesterone by testosterone (P*T) β coefficient	Raw P*T *P*-value	FDR corrected *P*-value for estradiol by testosterone (E*T)	R^2	Adjusted R^2	Residual std. error (df = 48)	F statistic (df = 6; 48)
Au	0.0003	0.669	−0.003	0.072	0.00001	0.360	0.264	0.096	−0.017	0.103	0.851
CBBG	0.001	0.131	−0.003	0.167	0.00001	0.760	0.359	0.133	0.024	0.155	1.225
COTC	−0.029	0.245	−0.056	0.315	0.001	0.111	0.429	0.182	0.079	4.087	1.776
DA	−0.0005	0.489	−0.001	0.511	0.00001	0.507	0.511	0.05	−0.069	0.111	0.422
DM	0.0002	0.792	−0.002	0.333	0	0.856	0.429	0.085	−0.029	0.148	0.747
FPTC	−0.0002	0.786	−0.002	0.196	0.00001	0.496	0.359	0.135	0.027	0.126	1.248
Sa	0.0001	0.940	−0.002	0.359	0.00002	0.363	0.429	0.072	−0.044	0.14	0.619
SSH	0.0002	0.755	−0.003	0.035	0.00003	0.088	0.193	0.133	0.025	0.111	1.23
SSM	0.0001	0.766	−0.002	0.028	0.00002	0.137	0.193	0.157	0.051	0.076	1.485
Vi	−0.001	0.125	0.002	0.390	0.00001	0.711	0.429	0.059	−0.059	0.142	0.497
VA	0.002	0.307	−0.005	0.127	0.00001	0.691	0.349	0.072	−0.044	0.26	0.617

Raw *p*-values and FDR corrected *p*-values are included. FDR correction was only performed if raw *p*-value was < 0.05. There were no significant findings after FDR correction.

10.3389/fnhum.2023.1059091

TABLE 6 This table exhibits results from linear regressions for age and network segregation in females.

Female linear age associations with network segregation							
	Age β coefficient	Raw *P*-value	FDR corrected *P*-value	R^2	Adjusted R^2	Residual std. error (df = 64)	F statistic (df = 1; 64)
Au	−0.002	0.024	0.088	0.078	0.064	0.105	5.414
CBBG	−0.005	0.01	0.077	0.099	0.085	0.168	7.061
COTC	−0.082	0.044	0.103	0.062	0.047	3.918	4.231
DA	−0.001	0.311	0.342	0.016	0.001	0.106	1.043
DM	−0.002	0.18	0.283	0.028	0.013	0.146	1.843
FPTC	−0.003	0.047	0.103	0.06	0.046	0.126	4.114
Sa	−0.004	0.014	0.077	0.092	0.078	0.141	6.466
SSH	−0.001	0.276	0.337	0.019	0.003	0.113	1.210
SSM	−0.001	0.065	0.119	0.052	0.037	0.077	3.529
Vi	−0.001	0.357	0.357	0.013	−0.002	0.13	0.862
VA	−0.003	0.252	0.337	0.021	0.005	0.241	1.341

Raw *p*-values and FDR corrected *p*-values are included. There were no significant findings after FDR correction.

TABLE 7 This table exhibits results from quadratic regressions for age and network segregation in females.

Female quadratic age associations with network segregation							
	Quadratic β coefficient	Raw *P*-value	FDR corrected *P*-value	R^2	Adjusted R^2	Residual std. error (df = 63)	F statistic (df = 2; 63)
Au	−0.0002	0.014	0.051	0.164	0.138	0.1	6.202
CBBG	−0.0003	0.002	0.011*	0.241	0.217	0.155	10.020
COTC	−0.002	0.391	0.430	0.073	0.044	3.925	2.482
DA	−0.0001	0.071	0.112	0.066	0.036	0.104	2.23
DM	−0.0002	0.043	0.095	0.09	0.061	0.142	3.109
FPTC	−0.0002	0.058	0.106	0.113	0.085	0.124	4.011
Sa	−0.0003	0.0005	0.011*	0.255	0.232	0.129	10.806
SSH	−0.0002	0.035	0.095	0.086	0.057	0.11	2.977
SSM	−0.0001	0.16	0.210	0.082	0.053	0.077	2.808
Vi	−0.0001	0.172	0.210	0.042	0.012	0.129	1.393
VA	−0.0001	0.578	0.578	0.025	−0.006	0.242	0.820

Raw *p*-values and FDR corrected *p*-values are included. Asterisks indicate significance at $p < 0.05$* for FDR corrected values. Only FDR corrected values are interpreted as significant.

with declines in 17β-estradiol and progesterone (Burger, 2008; Harlow et al., 2012; Sundström Poromaa and Gingnell, 2014) and Ballard et al. (2022c) demonstrated significant differences between distinct reproductive stages and network segregation (i.e., COTC, DMN, DA, FPTC, and Sa) in females (Ballard et al., 2022c). Of note, Ballard et al.'s (2022c) findings may be driven by age as they also found linear relationships between age and network segregation in the aforementioned networks. Pritschet et al. (2020) demonstrated that estradiol is associated with increasing global efficiency in the DMN and DA networks, whereas progesterone was associated with reduced coherence throughout the brain (Pritschet et al., 2020). While Pritschet et al.'s (2020) findings suggested influences of estradiol and progesterone on network dynamics, it is difficult to directly compare their findings to ours as their study was based on dense sampling in a young female across a menstrual cycle and evaluated a different aspect of network function. However, it broadly demonstrates the purported relationship between brain network organization and sex steroid hormones in the female brain. Although we cannot directly compare our findings with this and other studies, network segregation is a proxy for measuring functional organization in the brain and may loosely be interpreted as such.

Lastly, the combined impact (interaction) of hormone levels (i.e., estradiol, progesterone, and testosterone) on network segregation did not reveal a relationship with network segregation in females. We found interactions between estradiol and testosterone in SSH and SSM networks for raw *p*-values, but these findings did not survive FDR correction. However, this finding agrees with the study by Moffat (2005), in which they note that testosterone can interact not only with androgen receptors, but also with estradiol receptors, and therefore, its administration can, in some cases, parallel the effects of estradiol on the entire nervous system. An important element in understanding the effects of testosterone on the nervous system is that many of its behavioral and anatomical effects occur after it has been converted to its metabolically active derivatives–estradiol or dihydrotestosterone (Moffat, 2005).

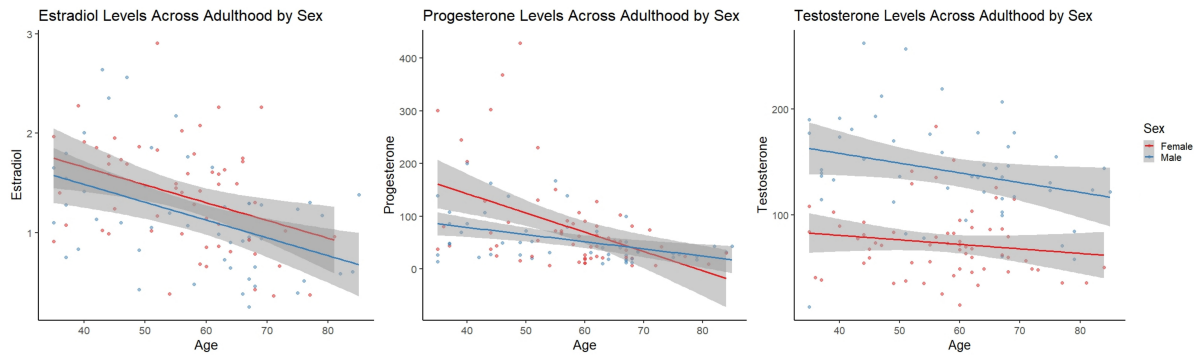

FIGURE 2
Linear scatter plots demonstrate estradiol levels in females and males across adulthood. The gray superimposed on each colored line depicts the 95% confidence interval in each sex. Estradiol levels **(left)** were not significantly different by sex when accounting for age (p = 0.071). Progesterone levels **(middle)** were not significantly different by sex when accounting for age (p = 0.073). Testosterone levels **(right)** were significantly different by sex when accounting for age ($p < 0.001$).

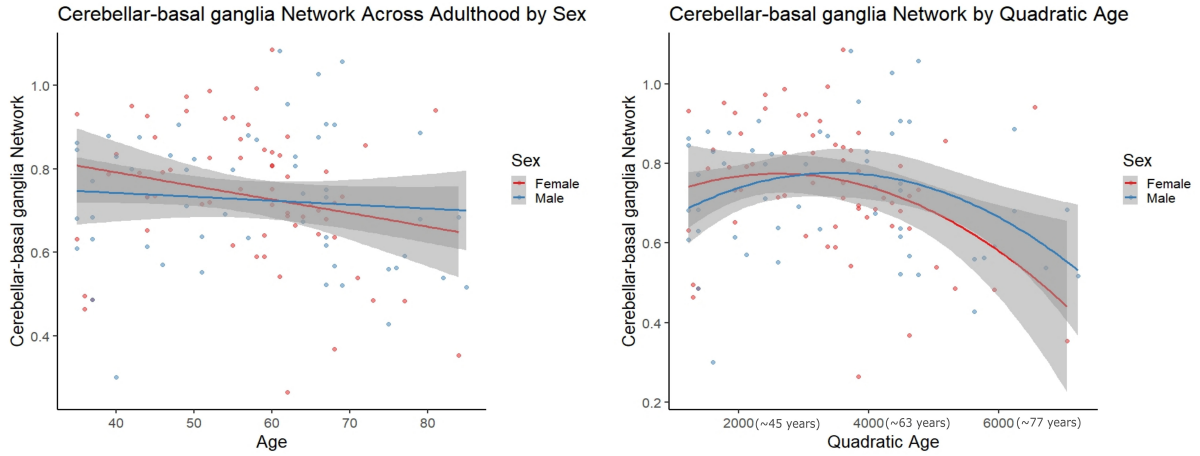

FIGURE 3
Scatter plots demonstrate the linear **(left)** and quadratic **(right)** relationship between Cerebellar-basal ganglia network connectivity and age. Parentheses next to quadratic values **(right)** indicate the approximate square root of the quadratic value for interpretative purposes. The gray superimposed on each colored line depicts the 95% confidence interval in each sex.

One consideration beyond the scope of the current study is how stages within a female menstrual cycle or menopausal stage could impact brain connectivity. Syan et al. (2017) examined endogenous estradiol, progesterone, and a neuroactive metabolite of progesterone (allopregnanolone) at different menstrual phases and demonstrated an impact of hormone levels in the late luteal phase on resting state connectivity in both cortical and subcortical regions for reproductive aged females (Syan et al., 2017). As mentioned earlier, Pritschet et al. (2020) exhibited an impact of sex hormones on network architecture in tandem with the cycle of a reproductive aged female. Thus, sex steroid hormones have shown a relationship with brain connectivity as it relates to regular menstrual cycle fluctuation. Individual variation exists both in a regular menstrual cycle and menopausal stages (Fehring et al., 2006; Harlow et al., 2012; Boker et al., 2014). Notably, hormone levels are not the sole indicator for identifying distinct reproductive stages. Seminal work in categorizing stages in reproductive aging described principal criteria for determining reproductive stage by changes in cycle regularity and days to years since last cycle (Harlow et al., 2012). Endocrine information such as follicle stimulating hormones, antimullerian hormone, and inhibin-B are used to support categorization by changes in cycle (Harlow et al., 2012). We did not examine menstrual cycle, the above specified endocrine information, menopausal stage, or within individual hormone variance in this investigation. As such, the nature of our analyses and scope of our study may not capture the complexity of female network segregation.

In the context of aging, females did display a significant quadratic relationship between age and network segregation for the CBBG and Sa networks. In both cases, segregation was still increasing through adulthood and highest in midlife with a downturn thereafter. Patterns of connectivity between the cerebellum and basal ganglia have been positively linked to cognitive performance and self-reported balance confidence in older adults (Power et al., 2011; Bernard and Seidler, 2013). Further, in their review Diedrichsen et al. (2009) (Diedrichsen, 2006) implicated the relationship between the cerebellum and basal ganglia as critical for modulating cortical functions such as cognition and relying on subcortical processes. We can see in **Figure 3**, that both females and males demonstrate an inverted "U-shaped" decline in CBBG network segregation across the span of aging adults. Functionally this pattern in females may be related to the drop in

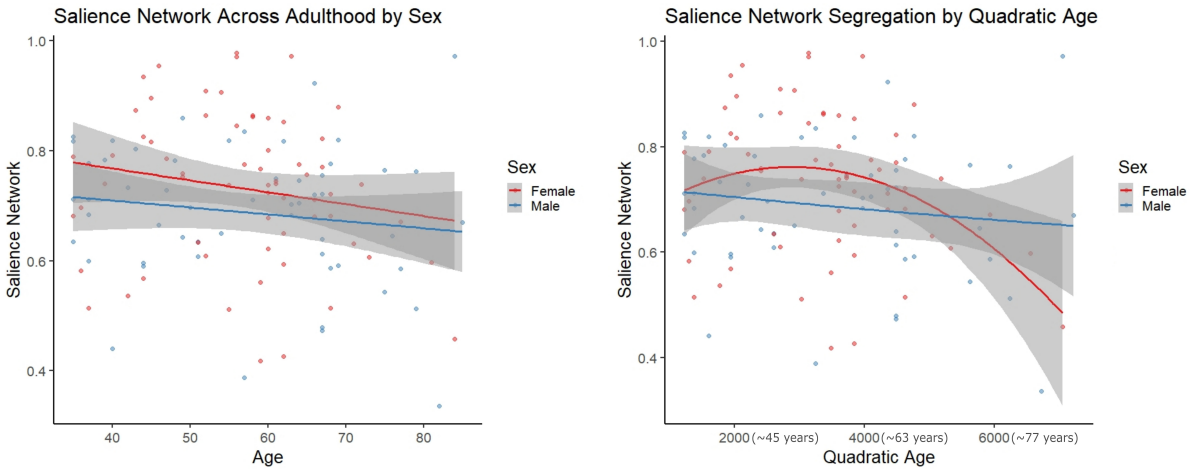

FIGURE 4
Scatter plots demonstrate the linear **(left)** and quadratic **(right)** relationship between salience network connectivity and age. Parentheses next to quadratic values **(right)** indicate the approximate square root of the quadratic value for interpretative purposes. The gray superimposed on each colored line depicts the 95% confidence interval in each sex. The quadratic model demonstrated significantly better fit than the linear model for salience network segregation across adulthood (AIC difference = 11.11).

cognition and decreased balance that females experience above and beyond males in aging (Burger, 2008; Pritschet et al., 2020), though we should note that this is speculative as we did not include any behavioral analyses here.

The quadratic age relationship with Sa network segregation in females was somewhat consistent with work from Chan et al. (2014), where they showed a significant quadratic age relationship across female and male participants in "association systems" which included the Sa network, but was aggregated with DMN, FPTC, VA, COTC, and DA (Chan et al., 2014). The Sa network has been associated with "conscious integration of autonomic feedback and responses with internal goals and environmental demands" (Weis et al., 2008). This network has also been conceptualized as an "integral hub" for facilitating communication between the DMN and central executive networks in a triple network model (Van Goozen et al., 1995). Notably, dysfunction in the Sa network has been linked to reduced cognitive performance in older adults (Dimech et al., 2019) and increased connectivity in this network has been linked to Alzheimer's disease (Morrison et al., 2006). The quadratic relationship seen in females, but not males (see **Figure 3**), could similarly be highlighting cognitive inefficiencies that have been demonstrated during advanced aging in females (Pritschet et al., 2020).

It is important to emphasize that we did not find significant quadratic age relationships in any additional networks for females, nor any networks in males in our exploratory analyses. These findings are consistent with Lee et al. (2016) study that examined rs-fMRI graph network analysis in the DMN, Sa, and Central Executive network and a quadratic age relationship in both groups of "good" and "poor" cognitive performers (Lee et al., 2016). While Lee et al. (2016) assessed components of both network segregation and network integration (i.e., global efficiency, local efficiency, betweenness centrality, connectivity strength, and nodal degree), their analyses notably varied from ours in that they controlled for gender (Lee et al., 2016). That is, the relationship between quadratic age and segregation in certain networks may be driven by inherent hormonal differences between sexes, but as gender was controlled for in their study that relationship was left unexplored (Lee et al., 2016). Thus, the methodological differences may explain the differences in outcomes relative to what we report here.

Comparisons of model fit demonstrated the quadratic model as a substantially better fit for Sa network segregation and age in females; however, no additional quadratic age models displayed a significantly better fit in our analyses. To our knowledge, associations between quadratic age and network segregation have not been otherwise evaluated or reported. We would suggest that this may be a useful area of investigation in future work. We did not, however, find linear relationships between age and network segregation when examining females or males after FDR correction. Similarly, Grady et al. (2016), did not see linear relationships with age and network segregation, although their examination was specific to the DMN, DA, and FPTC networks (Grady et al., 2016). As stated, earlier Chan et al. (2014) found a significant quadratic age relationship in association systems (Chan et al., 2014); however, these systems were also significantly linearly associated with age. The same study also revealed linear age relationships with network segregation in "sensory-motor systems" which aggregated Hand somato-motor, Visual, Mouth somato-motor, and Auditory within-network segregations (Hausmann, 2005). While we did not replicate Chan et al.' (2014) findings, we also did not aggregate networks for analysis in the same fashion. Further there are also differences in the data used for analyses with respect to both sample size and length of scans. That is, their sample size was twice as large as our study and scan length was about 5 min per participant. Of note, our approach to data collection (guided by recent scientific advancement and literature) often produces more reliable data (Pannunzi et al., 2017) as we collected 24 total minutes of resting state scans, alternating from anterior to posterior slice collection. Thus, Chan et al.' (2014) investigation of network segregation in sensory-motor systems may not be appropriate for drawing direct comparisons to our data given methodological advancements in recent years resulting in differences in data collection parameters. Additional studies evaluating linear and quadratic relationships by sex are warranted, particularly with larger samples that include longer resting state acquisition times such as that used here.

Overall, we found quadratic age relationships for females in CBBG and Sa network segregation. We did not find significant impacts of individual or combined hormone levels on within-network segregation in the networks of interest. Future research would benefit from examining inter-individual differences over time to gain more insight into subtle influences of endogenous hormones. Another relevant area of research would be examining individual differences of network segregation over time in those taking hormonal contraceptives or receiving hormone replacement therapy to better understand the dynamic interplay between sex steroid hormones and brain network organization.

4.1. Limitations

There are several limitations relevant to the present investigation. Namely, the variability and collection of hormone assays and the cross-sectional nature of these data. It is important to recognize that hormone levels can vary almost as much within a naturally cycling female as they can between naturally cycling females (Fehring et al., 2006; Bernard and Seidler, 2013). Furthermore, the hormone assay was collected on a different day than the scan as freezing the sample at a particular temperature is required immediately, and our study design incorporated a delay to allow for additional measures of activity and questionnaire completion (not related to the research questions presented here). The large variance of hormone levels within a cycle implies that levels could change in a matter of days for reproductive age females. Thus, given the age range of our female sample, the offset between the hormone sample and the scan may impact these relationships for those that still have regular menstrual cycles. While this is only a small subset of this sample, it is an important limitation, nonetheless. Hormone levels vary within and between naturally cycling females so examining sex hormone levels in the same participant over time would account for some individual variance in hormone fluctuations. Regarding menopause, our study did ask about participant start date of menopause (date of final menstrual period) with additional questions to help categorize menopausal stages. That is, all participants completed 6-month menstrual diaries after undergoing the brain imaging session. The impact of menopausal stage is a question of interest for us, and indeed we have studied this recently (Ballard et al., 2022b). However, sex hormone levels have been directly associated with menopausal stages (Burger et al., 2007) and we are interested in the variability in hormone levels more generally, as this also provides a quantitative measure, as opposed to self-report menstrual cycle information. Regarding obstetrics history, we do not have that information for this sample, although the literature suggests that parity has been positively related to brain volume in aging females (de Lange et al., 2019). Several females who had undergone hysterectomy were included in the study, but the surgeries were dated over 10 years prior to enrollment in the study. As such, it was assumed that hormones had reached a stable low. Another notable limitation is our sex hormone analyses did not account for age. This was intentional as preliminary analyses demonstrated age was significantly correlated with female estradiol and progesterone ($p < 0.01$) and testosterone maintains a relatively consistent level throughout for mid- to older-age females (Andersen et al., 2011). Thus, incorporating age into hormone-based analyses would account for very similar variance to sex hormone levels. Sleep patterns have also demonstrated a relationship with sex hormone levels (Li et al., 2015; Brown and Gervais, 2022). Indeed, we do find this aspect important to investigate and it has been explored by proxy with this sample in the context of reproductive stages (Ballard et al., 2022b). Lastly, our sample size was relatively small in relation to the number of analyses conducted. With this in mind, we were very targeted in our analyses and applied a correction for multiple comparisons (FDR correction). However, replication of this study in a larger sample is warranted.

5. Conclusion

This study demonstrated a quadratic relationship between aging and network segregation for the CBBG and Sa networks in females. In both cases, segregation was still increasing through adulthood and highest in midlife with a downturn thereafter. These networks are functionally related to cognitive performance, balance, and integrating autonomic feedback in response to environmental demands (Bernard and Seidler, 2013; Chan et al., 2014; Hausman et al., 2020).

Prior research has shown that the sex hormones can regulate neurogenesis, inflammatory processes, impact network segregation, and may also play a role in regulating cognitive and affective processes, mainly in the aging process (Syan et al., 2017; Foo et al., 2021). Furthermore, the notable variability in hormone levels in certain reproductive stages and cognitive deficits associated with specific reproductive stages did not have an impact on network segregation as was expected (Greendale et al., 2011; Epperson et al., 2013; Weber et al., 2014; Rentz et al., 2017; Taylor et al., 2019; Pritschet et al., 2020).

Future studies could focus on examining participants longitudinally and pairing these types of data with behavioral outcomes.

Data availability statement

The raw data supporting the conclusions of this article will be made available by the authors, without undue reservation.

Ethics statement

The studies involving human participants were reviewed and approved by the Texas A&M Institutional Review Board. The patients/participants provided their written informed consent to participate in this study.

Author contributions

TH, HB, TJ, and SC completed the data collection. TH, TM, HB, and TJ conducted the data analyses under the guidance and supervision of JAB. TH and TM drafted the manuscript with input from all authors and again under the guidance of JAB. All authors contributed to the conceptualization of this project.

Funding

This work was supported by R01AG065010 to JAB. This work was further supported by the Texas Virtual Data Library (ViDaL), a high-performance cluster, funded by the Texas A&M University Research Development fund. In this cluster, the imaging analyses for the current work were carried out using the resources provided by the Texas A&M High Performance Research Computing organization.

Conflict of interest

The authors declare that the research was conducted in the absence of any commercial or financial relationships that could be construed as a potential conflict of interest.

Publisher's note

All claims expressed in this article are solely those of the authors and do not necessarily represent those of their affiliated organizations, or those of the publisher, the editors and the reviewers. Any product that may be evaluated in this article, or claim that may be made by its manufacturer, is not guaranteed or endorsed by the publisher.

Supplementary material

The Supplementary Material for this article can be found online at: https://www.frontiersin.org/articles/10.3389/fnhum.2023.1059091/full#supplementary-material

References

Aggarwal, N., Patel, H., Mehta, L., Sanghani, R., Lundberg, G., Lewis, S., et al. (2018). Sex differences in ischemic heart disease: Advances, obstacles, and next steps. *Circ. Cardiovasc. Qual. Outcomes* 11:e004437. doi: 10.1161/CIRCOUTCOMES.117.004437

Allen, E., Erhardt, E., Damaraju, E., Gruner, W., Segall, J., Silva, R., et al. (2011). A baseline for the multivariate comparison of resting-state networks. *Front. Syst. Neurosci.* 5:2. doi: 10.3389/fnsys.2011.00002

Alzheimer's Association. (2022). *Alzheimer's disease facts and figures*. Chicago, IL: Alzheimer's Association.

Andersen, M., Alvarenga, T., Mazaro-Costa, R., Hachul, H., and Tufik, S. (2011). The association of testosterone, sleep, and sexual function in men and women. *Brain Res.* 1416, 80–104. doi: 10.1016/j.brainres.2011.07.060

Ballard, H., Jackson, T. B., Hicks, T., Cox, S., Miller, A., Maldonado, T., et al. (2022a). Hormone-sleep interactions predict cerebellar connectivity and behavior in aging females. *bioRxiv [Preprint]* doi: 10.1101/2022.08.30.505858

Ballard, H., Jackson, T., Miller, A., Hicks, T., and Bernard, J. (2022c). Age-related differences in functional network segregation in the context of sex and reproductive stage. *Hum. Brain Mapp.* doi: 10.1101/2022.03.28.486067 [Epub ahead of print].

Ballard, H. K., Jackson, T. B., Hicks, T. H., and Bernard, J. A. (2022b). The association of reproductive stage with lobular cerebellar network connectivity across female adulthood. *Neurobiol. Aging* 117, 139–150. doi: 10.1016/j.neurobiolaging.2022.05.014

Bernard, J., and Seidler, R. (2013). Relationships between regional cerebellar volume and sensorimotor and cognitive function in young and older adults. *Cerebellum* 12, 721–737. doi: 10.1007/s12311-013-0481-z

Bernard, J., Leopold, D., Calhoun, V., and Mittal, V. (2015). Regional cerebellar volume and cognitive function from adolescence to late middle age. *Hum. Brain Mapp.* 36, 1102–1120. doi: 10.1002/hbm.22690

Bixo, M., Andersson, A., Winblad, B., Purdy, R., and Bäckström, T. (1997). Progesterone, 5alpha-pregnane-3,20-dione and 3alpha-hydroxy-5alpha-pregnane-20-one in specific regions of the human female brain in different endocrine states. *Brain Res.* 764, 173–178. doi: 10.1016/S0006-8993(97)00455-1

Bohon, C., and Welch, H. (2021). Quadratic relations of BMI with depression and brain volume in children: Analysis of data from the ABCD study. *J. Psychiatr. Res.* 136, 421–427. doi: 10.1016/j.jpsychires.2021.02.038

Boker, S., Neale, M., and Klump, K. (2014). "A differential equations model for the ovarian hormone cycle," in *Handbook of developmental systems theory and methodology*, eds P. C. M. Molenaar, R. M. Lerner, and K. M. Newell (New York, NY: The Guilford Press), 369–394.

Brown, A., and Gervais, N. (2022). Role of ovarian hormones in the modulation of sleep in females across the adult lifespan. Endocrinology. 2020 Sep 1;161(9): bqaa128. Erratum in. *Endocrinology* 163:bqab227. doi: 10.1210/endocr/bqaa128

Burger, H. (2008). The menopausal transition–endocrinology. *J. Sex. Med.* 5, 2266–2273. doi: 10.1111/j.1743-6109.2008.00921.x

Burger, H. G., Hale, G. E., Robertson, D. M., and Dennerstein, L. (2007). A review of hormonal changes during the menopausal transition: Focus on findings from the Melbourne Women's Midlife Health Project. *Hum. Reprod. Update* 13, 559–565. doi: 10.1093/humupd/dmm020

Burnham, K., and Anderson, D. (2004). Multimodel inference: Understanding AIC and BIC in model selection. *Sociol. Methods Res.* 33, 261–304. doi: 10.1177/0049124104268644

Cassady, K., Gagnon, H., Lalwani, P., Simmonite, M., Foerster, B., Park, D., et al. (2019). Sensorimotor network segregation declines with age and is linked to GABA and to sensorimotor performance. *Neuroimage* 186, 234–244. doi: 10.1016/j.neuroimage.2018.11.008

Chan, M., Park, D., Savalia, N., Petersen, S., and Wig, G. (2014). Decreased segregation of brain systems across the healthy adult lifespan. *Proc. Natl Acad. Sci. U. S. A.* 111, E4997–E5006. doi: 10.1073/pnas.1415122111

Cosgrove, K., Mazure, C., and Staley, J. (2007). Evolving knowledge of sex differences in brain structure, function, and chemistry. *Biol. Psychiatry* 62, 847–855. doi: 10.1016/j.biopsych.2007.03.001

de Lange, A. M. G., Kaufmann, T., van der Meer, D., Maglanoc, L. A., Alnæs, D., Moberget, T., et al. (2019). Population-based neuroimaging reveals traces of childbirth in the maternal brain. *Proc. Natl. Acad. Acad. Sci. U.S.A.* 116, 22341–22346. doi: 10.1073/pnas.1910666116

Di Martino, A., Scheres, A., Margulies, D., Kelly, A., Uddin, L., Shehzad, Z., et al. (2008). Functional connectivity of human striatum: A resting state FMRI study. *Cereb. Cortex* 18, 2735–2747. doi: 10.1093/cercor/bhn041

Diamond, M. (1991). Hormonal effects on the development or cerebral lateralization. *Psychoneuroendocrinology* 16, 121–129. doi: 10.1016/0306-4530(91)90074-4

Diedrichsen, J. (2006). A spatially unbiased atlas template of the human cerebellum. *Neuroimage* 33, 127–138. doi: 10.1016/j.neuroimage.2006.05.056

Diedrichsen, J., Balsters, J., Flavell, J., Cussans, E., and Ramnani, N. (2009). A probabilistic MR atlas of the human cerebellum. *Neuroimage* 46, 39–46. doi: 10.1016/j.neuroimage.2009.01.045

Dimech, C., Anderson, J., Lockrow, A., Spreng, R., and Turner, G. (2019). Sex differences in the relationship between cardiorespiratory fitness and brain function in older adulthood. *J Appl Physiol.* 126, 1032–1041. doi: 10.1152/japplphysiol.01046.2018

Epperson, C., Sammel, M., and Freeman, E. (2013). Menopause effects on verbal memory: Findings from a longitudinal community cohort. *J. Clin. Endocrinol. Metab.* 98, 3829–3838. doi: 10.1210/jc.2013-1808

Fehring, R., Schneider, M., and Raviele, K. (2006). Variability in the phases of the menstrual cycle. *J Obstetr. Gynecol. Neonatal Nurs.* 35, 376–384. doi: 10.1111/j.1552-6909.2006.00051.x

Filippi, M., Valsasina, P., Misci, P., Falini, A., Comi, G., and Rocca, M. (2013). The organization of intrinsic brain activity differs between genders: A resting-state fMRI study in a large cohort of young healthy subjects. *Hum. Brain Mapp.* 34, 1330–1343. doi: 10.1002/hbm.21514

Foo, H., Thalamuthu, A., Jiang, J., Koch, F., Mather, K., Wen, W., et al. (2021). Age- and sex-related topological organization of human brain functional networks and their relationship to cognition. *Front. Aging Neurosci.* 13:758817. doi: 10.3389/fnagi.2021.758817

Gao, S., Hendrie, H., Hall, K., and Hui, S. (1998). The relationships between age, sex, and the incidence of dementia and Alzheimer disease: A meta-analysis. *Arch. Gen. Psychiatry* 55, 809–815. doi: 10.1001/archpsyc.55.9.809

Goldstone, A., Mayhew, S., Przezdzik, I., Wilson, R., Hale, J., and Bagshaw, A. (2016). Gender specific re-organization of resting-state networks in older age. *Front. Aging Neurosci.* 8:285. doi: 10.3389/fnagi.2016.00285

Grady, C., Sarraf, S., Saverino, C., and Campbell, K. (2016). Age differences in the functional interactions among the default, frontoparietal control, and dorsal attention networks. *Neurobiol. Aging* 41, 159–172. doi: 10.1016/j.neurobiolaging.2016.02.020

Greendale, G., Derby, C., and Maki, P. (2011). Perimenopause, and cognition. *Obstetr. Gynecol. Clin. North Am.* 38, 519–535. doi: 10.1016/j.ogc.2011.05.007

Harlow, S., Gass, M., Hall, J., Lobo, R., Maki, P., Rebar, R., et al. (2012). Executive summary of the stages of reproductive aging workshop + 10: Addressing the unfinished agenda of staging reproductive aging. *Fertil. Steril.* 97, 1159–1168. doi: 10.1016/j.fertnstert.2012.01.128

Harms, M., Somerville, L., Ances, B., Andersson, J., Barch, D., Bastiani, M., et al. (2018). Extending the human connectome project across ages: Imaging protocols for the lifespan development and aging projects. *Neuroimage.* 183, 972–984. doi: 10.1016/j.neuroimage.2018.09.060

Hausman, H., Jackson, T., Goen, J., and Bernard, J. (2020). From synchrony to asynchrony: Cerebellar-basal ganglia functional circuits in young and older adults. *Cereb. Cortex* 30, 718–729. doi: 10.1093/cercor/bhz121

Hausmann, M. (2005). Hemispheric asymmetry in spatial attention across the menstrual cycle. *Neuropsychologia* 43, 1559–1567. doi: 10.1016/j.neuropsychologia.2005.01.017

Hlavac, M. (2018). *Stargazer: Well-formatted regression and summary statistics tables. R package version, 5.2.2.*

Jacobson, C., Csernus, V., Shryne, J., and Gorski, R. (1981). The influence of gonadectomy, androgen exposure, or a gonadal graft in the neonatal rat on the volume of the sexually dimorphic nucleus of the preoptic area. *J. Neurosci.* 1, 1142–1147. doi: 10.1523/JNEUROSCI.01-10-01142.1981

Jenkinson, M., Beckmann, C., Behrens, T., Woolrich, M., and Smith, S. (2012). FSL. *Neuroimage* 62, 782–790. doi: 10.1016/j.neuroimage.2011.09.015

Lahousse, L., Maes, B., Ziere, G., Loth, D., Verlinden, V., Zillikens, M., et al. (2014). Adverse outcomes of frailty in the elderly: The Rotterdam Study. *Eur. J. Epidemiol.* 29, 419–427. doi: 10.1007/s10654-014-9924-1

Lee, A., Tan, M., and Qiu, A. (2016). Distinct aging effects on functional networks in good and poor cognitive performers. *Front. Aging Neurosci.* 8:215. doi: 10.3389/fnagi.2016.00215

Li, D., Romans, S., De Souza, M., Murray, B., and Einstein, G. (2015). Actigraphic and self-reported sleep quality in women: Associations with ovarian hormones and mood. *Sleep Med.* 16, 1217–1224. doi: 10.1016/j.sleep.2015.06.009

Lüdecke, D. (2022). *sjstats: Statistical functions for regression models*. Genève: Zenodo.

Moffat, S. (2005). Effects of testosterone on cognitive and brain aging in elderly men. *Ann. N. Y. Acad. Sci.* 1005, 80–92. doi: 10.1196/annals.1323.014

Morrison, J., Brinton, R., Schmidt, P., and Gore, A. (2006). Estrogen, menopause, and the aging brain: How basic neuroscience can inform hormone therapy in women. *J. Neurosci.* 26, 10332–10348. doi: 10.1523/JNEUROSCI.3369-06.2006

Neuwirth, E., and Neuwirth, M. (2023). *The apache software foundation, licensed under the apache license, version 2.0*. Available online at: https://www.apache.org/licenses/LICENSE-2.0 (accessed December 15, 2022).

Ogle, D., Doll, J., Wheeler, P., and Dinno, A. (2022). *FSA: Fisheries stock analysis.* Available online at: https://fishr-core-team.github.io/FSA/authors.html (accessed December 15, 2022).

Osterlund, M., Gustafsson, J., Keller, E., and Hurd, Y. (2000). Estrogen receptor beta (ERbeta) messenger ribonucleic acid (mRNA) expression within the human forebrain: Distinct distribution pattern to ERalpha mRNA. *J. Clin. Endocrinol. Metab.* 85, 3840–3846. doi: 10.1210/jc.85.10.3840

Pannunzi, M., Hindriks, R., Bettinardi, R., Wenger, E., Lisofsky, N., Martensson, J., et al. (2017). Resting-state fMRI correlations: From link-wise unreliability to whole brain stability. *Neuroimage* 157, 250–262. doi: 10.1016/j.neuroimage.2017.06.006

Peper, J., van den Heuvel, M., Mandl, R., Hulshoff Pol, H., and van Honk, J. (2011). Sex steroids and connectivity in the human brain: A review of neuroimaging studies. *Psychoneuroendocrinology* 36, 1101–1113. doi: 10.1016/j.psyneuen.2011.05.004

Power, J., Cohen, A., Nelson, S., Wig, G., Barnes, K., Church, J., et al. (2011). Functional network organization of the human brain. *Neuron* 72, 665–678. doi: 10.1016/j.neuron.2011.09.006

Pritschet, L., Santander, T., Taylor, C., Layher, E., Yu, S., Miller, M., et al. (2020). Functional reorganization of brain networks across the human menstrual cycle. *Neuroimage* 220:117091. doi: 10.1016/j.neuroimage.2020.117091

R Core Team. (2021). *The R project for statistical computing*. Vienna: R Foundation for Statistical Computing.

Raparelli, V., Nocella, C., Proietti, M., Romiti, G., Corica, B., Bartimoccia, S., et al. (2022). Testosterone-to-estradiol ratio and platelet thromboxane release in ischemic heart disease: The EVA project. *J. Endocrinol. Invest.* 45, 1367–1377. doi: 10.1007/s40618-022-01771-0

Rentz, D., Weiss, B., Jacobs, E., Cherkerzian, S., Klibanski, A., Remington, A., et al. (2017). Sex differences in episodic memory in early midlife: Impact of reproductive aging. *Menopause* 24, 400–408. doi: 10.1097/GME.0000000000000771

Roof, R., and Havens, M. (1992). Testosterone improves maze performance and induces development of a male hippocampus in females. *Brain Res.* 572, 310–313. doi: 10.1016/0006-8993(92)90491-Q

Sakamoto, Y., Ishiguro, M., and Kitagawa, G. (1986). *Akaike information criterion statistics*. Dordrecht: D. Reidel.

Salimetrics. (2022). *Salivary Estradiol –: @Salimetrics*. Carlsbad, CA: Salimetrics.

Scheinost, D., Finn, E., Tokoglu, F., Shen, X., Papademetris, X., Hampson, M., et al. (2015). Sex differences in normal age trajectories of functional brain networks. *Hum. Brain Mapp.* 36, 1524–1535. doi: 10.1002/hbm.22720

Sundström Poromaa, I., and Gingnell, M. (2014). Menstrual cycle influence on cognitive function and emotion processing-from a reproductive perspective. *Front. Neurosci.* 8:380. doi: 10.3389/fnins.2014.00380

Syan, S., Minuzzi, L., Costescu, D., Smith, M., Allega, O., Coote, M., et al. (2017). Influence of endogenous estradiol, progesterone, allopregnanolone, and dehydroepiandrosterone sulfate on brain resting state functional connectivity across the menstrual cycle. *Fertil. Steril.* 107, 1246–1255.e4. doi: 10.1016/j.fertnstert.2017.03.021

Taylor, C., Pritschet, L., Yu, S., and Jacobs, E. (2019). Applying a Women's health lens to the study of the aging brain. *Front. Hum. Neurosci.* 13:224. doi: 10.3389/fnhum.2019.00224

Toffoletto, S., Lanzenberger, R., Gingnell, M., Sundström-Poromaa, I., and Comasco, E. (2014). Emotional and cognitive functional imaging of estrogen and progesterone effects in the female human brain: A systematic review. *Psychoneuroendocrinology* 50, 28–52. doi: 10.1016/j.psyneuen.2014.07.025

Van Goozen, S., Cohen-Kettenis, P., Gooren, L., Frijda, N., and Van de Poll, N. (1995). Gender differences in behaviour: Activating effects of cross-sex hormones. *Psychoneuroendocrinology* 20, 343–363. doi: 10.1016/0306-4530(94)00076-X

van Koeverden, I., de Bakker, M., Haitjema, S., van der Laan, S., de Vries, J., Hoefer, I., et al. (2019). Testosterone to oestradiol ratio reflects systemic and plaque inflammation and predicts future cardiovascular events in men with severe atherosclerosis. *Cardiovasc. Res.* 115, 453–462. doi: 10.1093/cvr/cvy188

Weber, M., Maki, P., and McDermott, M. (2014). Cognition, and mood in perimenopause: A systematic review and meta-analysis. *J. Steroid Biochem. Mol. Biol.* 142, 90–98. doi: 10.1016/j.jsbmb.2013.06.001

Weis, S., Hausmann, M., Stoffers, B., Vohn, R., Kellermann, T., and Sturm, W. (2008). Estradiol modulates functional brain organization during the menstrual cycle: An analysis of interhemispheric inhibition. *J. Neurosci.* 28, 13401–13410. doi: 10.1523/JNEUROSCI.4392-08.2008

Weiser, M., Foradori, C., and Handa, R. (2008). Estrogen receptor beta in the brain: From form to function. *Brain Res. Rev.* 57, 309–320. doi: 10.1016/j.brainresrev.2007.05.013

Whitfield-Gabrieli, S., and Nieto-Castanon, A. (2012). Conn: A functional connectivity toolbox for correlated and anticorrelated brain networks. *Brain Connect.* 2, 125–141. doi: 10.1089/brain.2012.0073

Wickham, H. (2016). *Ggplot2: Elegant graphics for data analysis*. Midtown Manhattan, NY: Springer International Publishing. doi: 10.1007/978-3-319-24277-4

Zar Jerrold, H. (1996). *Biostatistical analysis*, 3rd Edn. Upper Saddle River: Prentice Hall, 662.

Zhang, C., Cahill, N., Arbabshirani, M., White, T., Baum, S., and Michael, A. (2016). Sex and age effects of functional connectivity in early adulthood. *Brain Connect.* 6, 700–713. doi: 10.1089/brain.2016.0429

frontiers | Frontiers in Aging Neuroscience

TYPE Systematic Review
PUBLISHED 06 February 2023
DOI 10.3389/fnagi.2023.1069439

OPEN ACCESS

EDITED BY
John Semmler,
The University of Adelaide, Australia

REVIEWED BY
Allan Bregola,
University Hospitals Bristol and Weston NHS Foundation Trust, United Kingdom
David Adamowicz,
University of California, San Diego, United States

*CORRESPONDENCE
Sofia Leonardo
✉ Sleonardo@hsph.harvard.edu

SPECIALTY SECTION
This article was submitted to Neuroinflammation and Neuropathy, a section of the journal Frontiers in Aging Neuroscience

RECEIVED 13 October 2022
ACCEPTED 05 January 2023
PUBLISHED 06 February 2023

CITATION
Leonardo S and Fregni F (2023) Association of inflammation and cognition in the elderly: A systematic review and meta-analysis. *Front. Aging Neurosci.* 15:1069439. doi: 10.3389/fnagi.2023.1069439

Association of inflammation and cognition in the elderly: A systematic review and meta-analysis

Sofia Leonardo[1]* and Felipe Fregni[2]

[1]Ph.D. Department, Universidad Francisco Marroquín, Guatemala City, Guatemala, [2]Center for Neuromodulation and Clinical Research Learning, Spaulding Rehabilitation Hospital and Massachusetts General Hospital, Boston, MA, United States

Background: The development of mild cognitive impairment (MCI) and Alzheimer's disease (AD) may be associated with an inflammatory process. Inflammatory cytokines may be a surrogate for systemic inflammation leading to worsening neurological function. We aim to investigate the association between cognitive impairment and inflammation by pooling and analyzing the data from previously published studies.

Methods: We performed a systematic literature search on MEDLINE, PubMed, Embase, Web of Science, and Scopus for prospective longitudinal and cross-sectional studies evaluating the relationship between inflammation and cognitive functions.

Results: A total of 79 articles were included in our systematic review and meta-analysis. Pooled estimates from cross-sectional studies have demonstrated an increased level of C-reactive protein (CRP) [Hedges's g 0.35, 95% CI (0.16, 0.55), $p < 0.05$], IL-1β [0.94, 95% CI (−0.04, 1.92), $p < 0.05$], interleukin-6 (IL-6) [0.46, 95% CI (0.05, 0.88), $p < 0.005$], TNF alpha [0.22, 95% CI (−0.24, 0.68), $p < 0.05$], sTNFR-1 [0.74, 95% CI (0.46, 1.02), $p < 0.05$] in AD compared to controls. Similarly, higher levels of IL-1β [0.17, 95% CI (0.05, 0.28), $p < 0.05$], IL-6 [0.13, 95% CI (0.08, 0.18), $p < 0.005$], TNF alpha [0.28, 95% CI (0.07, 0.49), $p < 0.05$], sTNFR-1 [0.21, 95% CI (0.05, 0.48), $p < 0.05$] was also observed in MCI vs. control samples. The data from longitudinal studies suggested that levels of IL-6 significantly increased the risk of cognitive decline [OR = 1.34, 95% CI (1.13, 1.56)]. However, intermediate levels of IL-6 had no significant effect on the final clinical endpoint [OR = 1.06, 95% CI (0.8, 1.32)].

Conclusion: The data from cross-sectional studies suggest a higher level of inflammatory cytokines in AD and MCI as compared to controls. Moreover, data from longitudinal studies suggest that the risk of cognitive deterioration may increase by high IL-6 levels. According to our analysis, CRP, antichymotrypsin (ACT), Albumin, and tumor necrosis factor (TNF) alpha may not be good surrogates for neurological degeneration over time.

KEYWORDS

elderly, inflammation, cytokines, CRP, IL-6, cognition

1. Introduction

A variety of cell types can produce cytokines and non-antibody proteins. Interleukins (IL-1–24), tumor necrosis factors (TNFs), and transforming growth factors (TGFs Beta 1–3) are among the approximately 30 cytokines known. Cytokines are proteins that mediate cellular communication by autocrine, paracrine, or endocrine processes. Unique cytokine cell membrane receptors dictate the specificity of the cytokine response. The total response relies on its different components' synergistic or antagonistic activities. Cytokine actions are the product of a complex network, frequently comprising feedback loops and cascades. The exact activities of different cytokines are hard to identify because of their pleiotropism (Papanicolaou et al., 1998; Wilson et al., 2002). IL-1, IL-6, and TNF are regarded as proinflammatory, but IL-4, IL-10, and IL-13 are typically considered anti-inflammatory in the periphery (Kronfol and Remick, 2000). The aging process is associated with a general decrease in immune function. Increasing age has been related to variations in blood levels of different cytokines (Wells et al., 2000). It has been extensively observed that serum IL-6 levels rise with aging in a variety of healthy groups (Wei et al., 1992; Ershler, 1993; Hager et al., 1994; Roubenoff et al., 1998). As a result, increases in IL-6 appear to be the normal outcome of aging, regardless of co-morbidity. Thymic atrophy and inhibition of thymopoiesis during aging may be linked to an increase in IL-6 with age (Sempowski et al., 2000).

It has been hypothesized that Alzheimer's disease (AD) inflammation is linked and contributes to vascular dementia (Wilson et al., 2002). Central nervous system (CNS) levels of certain cytokines appear to increase as a function of age. Neurologically intact patients show a progressive increase in brain level of IL-1 and microglial activation with age (Sheng et al., 1998). Brain IL-6 levels in the mouse brain have been observed to rise with age, most likely as a result of increasing microglial output (Ye and Johnson, 1999). Cytokines' impacts on cognition work in two ways, with systemic cytokines signaling the CNS inflammation and the behavioral effects of systemic cytokines producing systemic consequences that eventually negatively influence cognition. The cognitive manifestations of the abovementioned neural degeneration processes arise when acute and chronic excessive cytokine levels exceed a person's homeostatic threshold, which may be measured by synaptic density or plasticity, and is termed a "cognitive reserve" (Wilson et al., 2002).

Beyond the conventional paradigms of cytokine-induced neurodegeneration and consequent cognitive impairment, processes affecting cognition in its broadest meaning must be investigated. The relationship between increased inflammatory markers in the serum and the occurrence and deterioration of cognitive degenerative diseases is still ambiguous. The correlation between inflammation and cognitive decline has been poorly studied. Older persons with no signs of dementia had higher levels of the inflammatory biomarkers interleukin-6 (IL-6) and C-reactive protein (CRP), according to a cross-sectional studies from the Netherlands (Schram et al., 2007) and the US (Yaffe et al., 2003). Consistently contradictory findings may be seen in longitudinal investigations of populations without dementia. Among older Finnish women, a higher CRP level at baseline was associated with worse cognitive performance 12 years later (Komulainen et al., 2007), while a cognitive decline was observed after 2 years in white and black elderly Americans (Yaffe et al., 2003). In white and black Americans, IL-6 predicted the cognitive decline after 2 years (Yaffe et al., 2003), while in Dutch older adults after 5 years (Weaver et al., 2002). Although, there are few systematic reviews and meta-analyses where authors have reviewed the level of biomarkers in cognitive decline (Swardfager et al., 2010; Holmes, 2013) but all of them have considered cross sectional studies only and mostly focused on AD vs. normal comparison in blood samples.

As a result, we aim to systematically review studies comparing cytokine levels between AD and mild cognitive impairment (MCI) vs. healthy controls from the cross-sectional as well as longitudinal studies to test the hypothesis of increased inflammatory levels associated with cognitive decline in this population.

2. Materials and methods

To conduct this systematic review and meta-analysis: we followed the Preferred Reporting Items for Systematic Reviews and Meta-Analyses (PRISMA) statements guidelines (Page et al., 2021), as well as the standards of the Cochrane Handbook for systematic review.

2.1. Literature search strategy

We searched the published literature in two electronic databases including MEDLINE, PubMed, Embase, and Web of Science and Scopus up to December 2021. Search terms were as follows:

(1) *Cognition OR cognitive decline OR cognitive function OR cognitive impairment OR cognitive loss OR memory.*
(2) *Peripheral OR blood OR plasma OR plasm* OR serum OR sera.*
(3) *Inflammatory markers OR inflammation OR cytokine OR chemokine OR IFN OR interleukin OR TGF OR TNF OR CRP.* Boolean operators (AND/OR) were used to combine the respective searches. We also manually searched the biography of the included studies for any additional relevant references cited within retrieved articles that were not retrieved during the literature search.

2.2. Eligibility criteria and study selection

Studies were included if they met the following criteria: (i) the study had a cross sectional or longitudinal prospective cohort design; (ii) the cross sectional studies should have reported data of AD, MCI with respect to controls, while in longitudinal studies, cognition performance was used at baseline and follow-up; in (iii) levels of cytokines were measured in blood; (iv) the longitudinal study measured the association of cytokine level and cognitive decline; (v) the article was available in English. Exclusion criteria included: (i) participants with dementia or cognitive impairment were included at baseline; (ii) the association between baseline cytokine level and cognitive decline was not reported; (iii) if the concentration of cytokine markers were measured in post-mortem samples. (iv) Small sample size less than 5 was used.

2.3. Quality assessment

The quality assessment was performed by two authors independently according to the Newcastle–Ottawa Scale, and

disputes were resolved by discussion. The quality score was calculated based on three major components of cohort studies: quality of selection (zero to four stars), comparability (zero to two stars), and exposure and outcome of study participants (zero to three stars). A higher score represents better methodological quality. Studies were defined as high (greater than seven stars), medium (six to seven stars), or low quality (less than six stars).

2.4. Data extraction

Each type of dataset was extracted independently by two authors. Discrepancies were reconciled through full discussion and consensus among the reviewers. For longitudinal studies, the extracted data involved the following: (I) summary and baseline of patients included in our study including study ID (name of the author, year, and setting of the publication), study design, subjects at baseline, the proportion of females at baseline, mean age at baseline (years), mean follow up assessment of global cognition in months, and the conclusion of each study; (II) risk of bias (ROB) domains including three major components of cohort studies: quality of selection (zero to four stars), comparability (zero to two stars), and exposure and outcome of study participants (zero to three stars); and (III) the outcome measures. The outcome measures were extracted as odds ratio (OR) and 95% confidence intervals (CIs) for the adjusted model, and confounders were adjusted for in the regression analysis. For cross sectional studies, the sample sizes and mean (±SD) concentrations of markers were extracted and Hedge's g was used for effect size (ES) for meta-analysis.

2.5. Data analysis

Statistical analyses were performed using Open Meta Analyst (*AHRQ, CEBM; Brown University, Providence, RI, USA*) and STATA version 16.0 (*StataCorp LLC, College Station, TX, USA*). We ultimately employed the random-effects model with the DerSimonian and Liard method (DerSimonian and Laird, 1986). From cross sectional studies, the sample sizes and mean (±SD) concentrations of markers were extracted and Hedges's g was used for ES for meta-analysis. For longitudinal studies, all data were dichotomous (events and no events) and were pooled as weighted proportions and risk ratios (RRs) with 95% CI (Cumpston et al., 2019). Pooled rates of proportions were calculated through the Freeman–Tukey transformation meta-analysis of proportions using MedCalc (Version 15.0; MedCalc Software, Ostend, Belgium).

Heterogeneity between studies was examined visually and statistically through Chi-square and I2 tests: a Q statistic with $P < 0.1$ indicated heterogeneity, whereas I2 values of 0, 25, 50, and 75% represented no, low, moderate, and high heterogeneity, respectively (Higgins et al., 2003). When detecting considerable heterogeneity, we performed sensitivity analyses to ascertain the source of heterogeneity by excluding one study at a time in addition to and subgroup analyses. Publication bias was visually examined through funnel plot symmetry as well as mathematically through Egger's regression test, Begg's

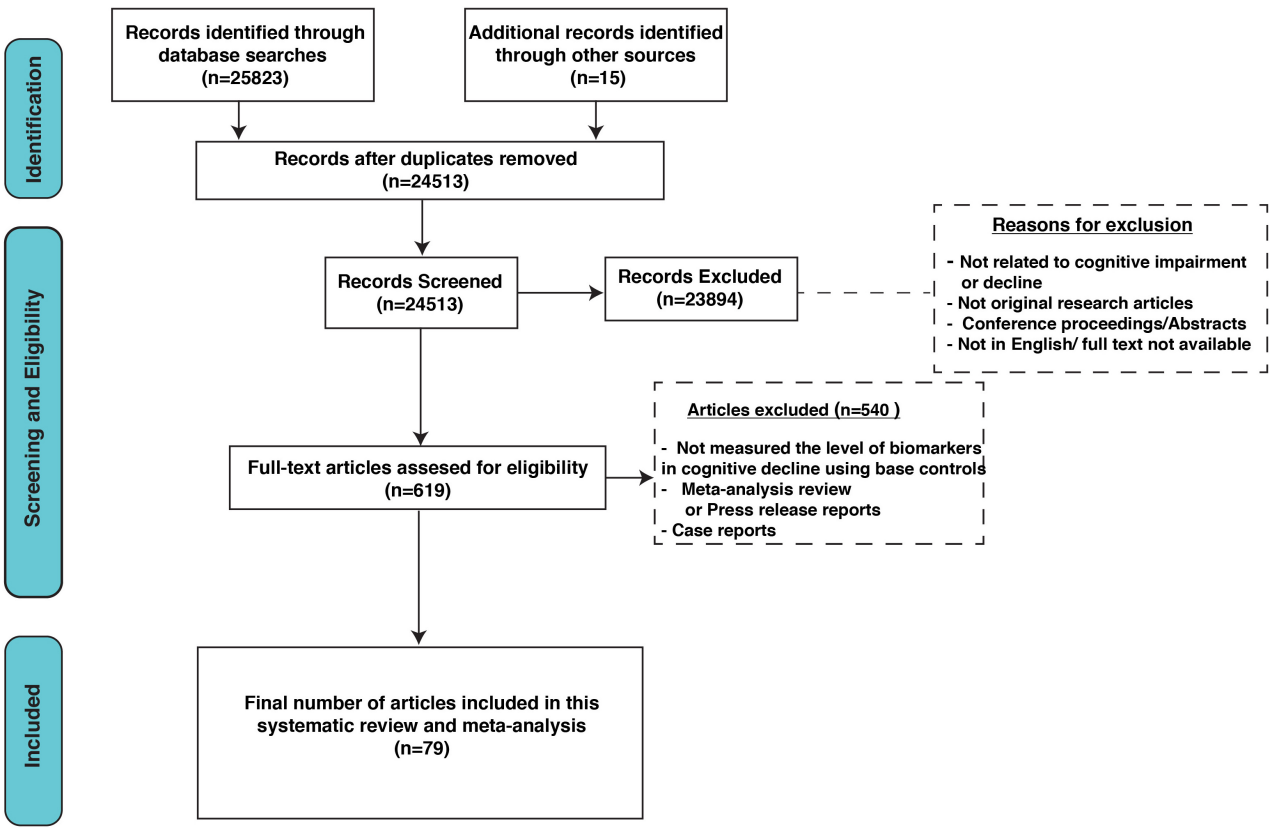

FIGURE 1
Preferred Reporting Items for Systematic Reviews and Meta-Analyses (PRISMA) flow diagram.

TABLE 1 Characteristics of included patients and cross-sectional studies.

Sr. No	References	Samples			Age (mean ± SD)			Female (%)			Diagnosis	Sample type	Assay type
		AD	MCI	CI	AD	MCI	CT	AD	MCI	CT			
1	Teunissen et al., 2003	34		61	73.0 ± 10.0		68.0 ± 6.7	59		43	DSM-IV; NINCDS-ADRDA	Serum	ELISA
2	Ciabattoni et al., 2007	44		44	73.0 ± 8.0		75.0 ± 7.0	56.8		61.4	NINCDS-ADRDA	Plasma	ELISA, Bio-Plex cytokine assay
3	Kassner et al., 2008	5		5	75.2 ± 3.5		71.0 ± 3.2	40		40	NINCDS-ADRDA	Serum	ELISA
4	Porcellini et al., 2008	195	69	830	79.2 ± 8.3	78.0 ± 8.0	73.0 ± 6.0	69.7	53.6	54.2	DSM-IV; NINCDS-ADRDA	Plasma	ELISA, Immunonephelometry
5	Davis et al., 2009	18		51	NA			NA			NINCDS-ADRDA; DSM-IVR	Serum	Immunoturbidimetric assay
6	Yarchoan et al., 2013	203	58	117	74.5 ± 7.7	71.6 ± 8.4	69.9 ± 10.1	58	52	68	NA	Plasma	ELISA
7	Bozluolcay et al., 2016	145		25	73.2 ± 10.2		73.1 ± 10.6	50		48	NINCDS-ADRDA	Serum	ELISA, Immunonephelometry
8	Villarreal et al., 2016	28	30	77	81.9 ± 9.2	81.2 ± 7.8	76.5 ± 6.7	78.6	66.7	64.9	NINCDS-ADRDA	Serum	Multiplex assay
9	Dukic et al., 2016	70	48	50	74.0 ± 7.6	72.0 ± 6.1	67.3 ± 7.6	61	65	60	NINCDS-ADRDA; the Petersen rating criteria	Serum	Complex
10	King et al., 2018	20	21	20	75.9 ± 6.7	78.5 ± 6.4	75.9 ± 7.3	25	66.7	20	NINCDS-ADRDA; NIA-AA	Plasma	Mixed
11	Choi et al., 2008	11		13	73.5 ± 4.0		68.5 ± 7.2	81.8		61.5	NINCDS-ADRDA	Serum, CSF	Immunoassay
12	Llano et al., 2012	15		7	70.2 ± 7.4		65.0 ± 5.2	20		28.6	NINCDS-ADRDA	Plasma	MSD
13	Leung et al., 2013	117	122	112	76.2 ± 6.1	73.9 ± 5.6	72.3 ± 6.7	66.7	49.2	53.6	MMSE; CDR; CERAD; ADAS-Cog	Plasma	Multiplex, ELISA
14	Rubio-Perez and Morillas-Ruiz, 2013	48		52	76.5 ± 3.5		79.0 ± 4.0	72.9		76.9	NINCDS-ADRDA	Serum	Immunoassay
15	Licastro et al., 2000	145		51	75.0 ± 12.0		78.0 ± 14.3	62.8		60.8	NINCDS-ADRDA; DSM-III R	Plasma	ELISA
16	De Luigi et al., 2002	58		47	NA			NA			NINCDS-ADRDA	Plasma	ELISA
17	Zuliani et al., 2007	60		42	78.5 ± 7.6		72.3 ± 5.8	65		46	NINCDS-ADRDA	Plasma	ELISA
18	Forlenza et al., 2009	58	74	21	76.3 ± 6.5	70.7 ± 10.3	69.9 ± 6.7	82.8	74.3	64.5	NINCDS-ADRDA	Serum	ELISA
19	Kamer et al., 2009	18		16	NA			78		94	DSM-IV; NINCDS-ADRDA	Plasma	Immunoassay
20	Richardson et al., 2013	24		35	79.0 ± 6.3		75.6 ± 7.6	63.8		61.8	NINCDS-ADRDA	Serum	ELISA
21	Bozluolcay et al., 2016	145		25	73.2 ± 10.2		73.1 ± 10.6	50		48	NINCDS-ADRDA	Serum	Immunoassay
22	Dursun et al., 2015	53	30	32	74.0 ± 3.9	74.4 ± 2.9	72.1 ± 3.4	NA			DSM-IV	Serum	ELISA
23	D'Anna et al., 2017	27		18	74.3 ± 8.0		70.7 ± 5.0	51.9		44.4	NINCDS-ADRDA	Serum	Pro human cytokine 10-Plex
24	Zhao et al., 2012	150		150	70.7 ± 4.3		69.9 ± 5.2	47.3		41.3	Peterson et al's clinical criteria	Serum	ELISA
25	Wang et al., 2014	97	54	122	73.7 ± 9.4	76.6 ± 9.1	73.7 ± 8.4	44.3	57.4	54.0	DSM-IV; NINCDS-ADRDA	Plasma	ELISA

(Continued)

10.3389/fnagi.2023.1069439

TABLE 1 (Continued)

Sr. No	References	Samples			Age (mean ± SD)			Female (%)			Diagnosis	Sample type	Assay type
		AD	MCI	CI	AD	MCI	CT	AD	MCI	CT			
26	Villarreal et al., 2016	28	30	77	81.9 ± 9.2	81.2 ± 7.8	76.5 ± 6.7	78.6	66.7	64.9	NINCDS-ADRDA	Serum	Multiplex assay
27	Kim et al., 2017	35	29	28	77.7 ± 8.1	75.0 ± 7.5	72.0 ± 7.3	71.4	61.5	57.1	NINCDS-ADRDA; IWG criteria	Serum	ELISA
28	Zhu et al., 2017	96	140	79	77.3 ± 7.3	71.2 ± 8.1	68.3 ± 6.0	62.5	47.9	51.9	NINCDS-ADRDA	Serum	Luminex assays
29	Bonotis et al., 2008	49		21	75.0 ± 6.0		71.2 ± 4.4	57.1		52.4	INCDS-ADRDA	Blood	ELISA
30	Bozluolcay et al., 2016	145		25	73.2 ± 10.2		73.1 ± 10.6	50		48	NINCDS-ADRDA	Serum	ELISA, immunoassays
31	Eriksson et al., 2011	71		205	81.6 ± 5.3		81.3 ± 5.6	73.3		62	NINCDS-ADRDA; DSM-III R, IV	Serum	Immunoassays
32	Kamer et al., 2009	18		16	NA			78		94	DSM-IV; NINCDS-ADRDA	Plasma	Immunoassays
33	Kong et al., 2002	70		52	71.8 ± 9.7		69.0 ± 4.0	51.4		51.9	DSM-IV R, MMSE, ADL	Serum	ELISA
34	O'Bryant et al., 2016	79		65	76.1 ± 8.6		71.2 ± 9.2	70		68	NINCDS-ADRDA	Serum	Multiplex biomarker assay
35	Richartz et al., 2005	20		21	72.0 (60.0–88.0)	68.0 (59.0–82.0)		80	33	3	NINCDS-ADRDA	Serum	ELISA

test, and Duval's non-parametric trim-and-fill analysis (Begg and Mazumdar, 1994; Irwig et al., 1998; Duval and Tweedie, 2000).

3. Results

3.1. Search results and characteristics of included studies

Our search extracted 25,513 unique citations after searching electronic databases. Following title and abstract screening, 619 full-text articles were retrieved and screened for eligibility. Of them, 540 articles were excluded, and 79 studies were reviewed in detail and included in this meta-analysis (PRISMA flow diagram; **Figure 1**).

The bibliography of the included randomized control trials (RCTs) was manually searched but added no further records. All studies were conducted between 2002 and 2021. **Table 1** summarizes the characteristics of included patients and cross-sectional studies, while **Table 2** represents longitudinal studies.

3.2. The potential sources of bias

Following the Newcastle Ottawa Scale, the quality of the included studies ranged from moderate to high. The main concern was absent control groups. A summary of quality assessment domains with authors' judgments is attached. Funnel plots of the inverse of the standard error vs. the ES demonstrated asymmetry. However, Egger's test ($P = 0.08$) and Begg's test ($P = 0.13$) indicated no small-study effects. Also, we employed the trim-and-fill approach to verify the robustness of the results, which exhibited no significant changes to the results when imputing three missing studies.

3.3. Comparisons between AD/control and MCI/control cross-sectional studies

A total of 46 studies were included in this analysis. Cross-sectional studies have demonstrated an increased level of CRP (Hedges's g 0.35, $p < 0.05$) (**Figure 2**), IL-1β (0.94, $p < 0.05$) (**Figure 3**), IL-6 (0.46, $p < 0.005$) (**Figure 4**), TNF alpha (0.22, $p < 0.05$) (**Figure 5**), and sTNFR-1 (0.74, $p < 0.05$) (**Figure 6**) in AD compared to controls. Similarly, higher levels of IL-1β (0.17, $p < 0.05$) (**Figure 7**), IL-6 (0.13, $p < 0.005$) (**Figure 8**), TNF alpha (0.28, $p < 0.05$) (**Figure 9**), and CRP (0.21, $p < 0.05$) (**Figure 10**) was also observed in MCI vs. control samples.

3.4. Outcomes from longitudinal studies

3.4.1. IL-6

A total of 33 studies were included in this analysis and they followed subjects for an average of 58.35 months (min. 24 months and max. 144 months). High levels (>3.1 pg/ml) of IL-6 significantly increased the risk of cognitive decline [OR = 1.34, 95% CI (1.13, 1.56)]. However, intermediate levels (1.6–3.1 pg/ml) of IL-6 had no significant effect on the final endpoint [OR = 1.06, 95% CI (0.8,

TABLE 2 Characteristics of included patients and longitudinal studies.

References	Cohort	Setting	Subjects at baseline (*n*)	Female (%)	Mean age at baseline (years)	Mean follow up (years)	Conclusion
Dik et al., 2005	Longitudinal aging study Amsterdam	The Netherlands	1,284	51	75.4 ± 6.6	3	Serum inflammatory protein _1-antichymotrypsin (ACT) is associated with cognitive decline in older persons, whereas C-reactive protein (CRP), interleukin-6 (IL-6), and albumin are not.
Jordanova et al., 2007	N/A	Britain	290	57	65.5 ± 5.5	3	Raised IL-6 but not CRP predicted cognitive decline in this population inflammatory changes associated with cognitive decline may be specific to particular causal pathways.
Rafnsson et al., 2007	Edinburgh artery study	Britain	452	50	73.1 ± 5.0	4	Systemic markers of inflammation and hemostasis are associated with a progressive decline in general and specific cognitive abilities in older people, independent of major vascular comorbidity.
Schram et al., 2007 (Rotterdam study)	Rotterdam cohort	The Netherlands	3,874	58	72.1 ± 6.9	4.6	Systemic markers of inflammation are only moderately associated with cognitive function and decline and tend to be stronger in carriers of the APOE e4 allele. Systemic markers of inflammation are not suitable for risk stratification.
Schram et al., 2007 (Leiden 85-plus Study)	Leiden 85-Plus cohort	The Netherlands	491	65	85	5	Systemic markers of inflammation are only moderately associated with cognitive function and decline and tend to be stronger in carriers of the APOE e4 allele. Systemic markers of inflammation are not suitable for risk stratification.
Singh-Manoux et al., 2014	The Whitehall II Study	Britain	5,217	28	55.7 ± 6.0	5	Elevated IL-6 but not CRP in midlife predicts cognitive decline; the combined cross sectional and longitudinal effects over the 10-year observation period corresponded to an age effect of 3.9 years.
Weaver et al., 2002	The MacArthur study of successful aging	America	1,189	55	74.3 ± 2.7	7	There is a relationship between elevated baseline plasma IL-6 and risk for subsequent decline in cognitive function. These findings are consistent with the hypothesized relationship between brain inflammation, as measured here by elevated plasma IL-6, and neuropathologic disorders.
Yaffe et al., 2003	The health ABC study	America	3,031	52	73.6 ± 2.9	2	Serum markers of inflammation, especially IL-6 and CRP, are prospectively associated with cognitive decline in well-functioning elders. These findings support the hypothesis that inflammation contributes to cognitive decline in the elderly.
Alley et al., 2008	MacArthur study of successful aging	United States	533	51.8	74.4	7	Although high levels of inflammation are associated with incident cognitive impairment, these results do not generalize to the full range of cognitive changes, where the role of inflammation appears to be marginal.
Chen et al., 2014	Prospective, observational, cohort study	China	109	NA	74.1 ± 6.0	NA	Increased CRP was associated with cognitive impairment, and additive effects of increased CRP with hypertriglyceridemia and hyperglycemia on cognitive impairment were observed among elderly individuals.
Tilvis et al., 2004	Prospective cohort	Finland	650	73	75	5	Five-year decline was predicted by the presence of atrial fibrillation [relative risk (RR) 2.8], APOE4 (RR 2.4), elevated CRP (RR 2.3), diabetes mellitus (RR 2.2), and heart failure (RR 1.8). They also tended to increase 5-year all-cause mortality.
Adriaensen et al., 2014	Prospective, observational, cohort study	Belgium	303	37.3	84.3 ± 3.4	NA	Simple serum levels of IL-6 may be very useful in short-term identification or evaluation of global functional status in the oldest old.
Ashraf-Ganjouei et al., 2020	Longitudinal study	Iran	216	36.1	39.12 ± 20.19	NA	Healthy subjects with higher levels of CRP exhibit poorer performance in verbal learning memory and general wakefulness domains of cognition.
Baierle et al., 2015	Prospective cohort	Brazil	57	64.9	75	NA	Individuals with lower antioxidant status are more vulnerable to oxidative stress, which is associated with cognitive function, leading to reduced life quality and expectancy.

(Continued)

10.3389/fnagi.2023.1069439

TABLE 2 (Continued)

References	Cohort	Setting	Subjects at baseline (*n*)	Female (%)	Mean age at baseline (years)	Mean follow up (years)	Conclusion
Beydoun et al., 2018	Prospective cohort	United States	2,574	55	46.9	4.64	Strong associations between systemic inflammation and longitudinal cognitive performance were detected, largely among older individuals (>50 y) and African-Americans. Randomized trials targeting inflammation are warranted.
Beydoun et al., 2019	Prospective cohort	United States	195	65	46.90 ± 1.00	4.64	Cytokines were shown to be associated with age-related cognitive decline among middle-aged and older urban adults in an age group and race-specific manner.
Boots et al., 2020	Longitudinal secondary analysis	United States	86	50	69.03 ± 6.65	NA	Peripheral inflammation is inversely associated with select cognitive domains and white matter integrity (but not WMHs), particularly in older Black adults. It is important to consider race when investigating inflammatory associates of brain and behavior.
Chi et al., 2017	Longitudinal study	United States	1,182	45	78.9 ± 3.4	8	Inflammation is associated with memory and psychomotor speed. In particular, systemic inflammation, vascular inflammation, and altered endothelial function may play roles in domain-specific cognitive decline of non-demented individuals.
Giudici et al., 2019	Prospective observational study	France	1,516	64.5	75.4 ± 4.5	5	Low-grade inflammation and hyperhomocysteinemia were both related with impairment on the combined IC levels among older adults after a 5-year follow-up. Identifying biomarkers that strongly associate with IC may help to settle strategies aiming to prevent the incidence and slow down the evolution of age-related functional decline and care dependency.
Goldstein et al., 2015	Longitudinal study	United States	278	63.7	57.4 ± 5.4	NA	There is strong association between IL-8 and cognitive performance in African Americans than Caucasians. This relationship should be further examined in larger samples that are followed over time.
Gunathilake et al., 2016	Longitudinal study	Australia	3,293	53	66.8 ± 7.8	NA	There is a weak positive association between obesity and cognitive performance in older persons, which is partially antagonized by inflammation and elevated fasting plasma glucose, but not hypertriglyceridemia.
Hajjar et al., 2018	Longitudinal cohort study	United States	511	68	49.1	4	Increased oxidative stress reflected by decreased glutathione was associated with a decline in executive function in a healthy population. In contrast, inflammation was not linked to cognitive decline. Oxidative stress may be an earlier biomarker that precedes the inflammatory phase of executive decline with aging.
Jung et al., 2019	Longitudinal cohort study	Republic of Korea	70	44.2	25.68 ± 3.89	NA	Cytokines, stress, and emotional and cognitive intelligence are closely connected one another related to brain structure and functions. Also, the pro-inflammatory cytokines tumor necrosis factor (TNF)-alpha and IL-6 had negative effects, whereas the anti-inflammatory cytokines [e.g., IL-10 and interferon (IFN)-gamma] showed beneficial effects, on stress levels, and multiple dimensions of emotional and cognitive intelligence.
Komulainen et al., 2007	Longitudinal cohort study	Finland	97	100	63.8	12	High serum hs-CRP concentration predicts poorer memory 12 years later in elderly women. Hs-CRP may be a useful biomarker to identify individuals at an increased risk for cognitive decline.
Marioni et al., 2009	Longitudinal cohort study	United Kingdom	3,350	72	61.9 ± 6.7	5	Increased circulating levels of CRP, fibrinogen, and elevated plasma viscosity predicted poorer subsequent cognitive ability and were associated with age-related cognitive decline in several domains, including general ability.
McHugh Power et al., 2019	Longitudinal cohort study	United Kingdom	116	66	65.81 ± 6.63	2	Inflammatory markers, cognitive function, social support, and psychosocial wellbeing were evaluated. A structural equation modelling approach was used to analyse the data. The model was a good fit (_108 2 = 256.13, $p < 0.001$).

(Continued)

10.3389/fnagi.2023.1069439

TABLE 2 (Continued)

References	Cohort	Setting	Subjects at baseline (*n*)	Female (%)	Mean age at baseline (years)	Mean follow up (years)	Conclusion
Mooijaart et al., 2011	Prospective observational study	Scotland, Ireland, and the Netherlands	5,680	52	75.3	3.2	Plasma CRP concentrations associate with cognitive performance in part through pathways independent of cardiovascular disease. However, lifelong exposure to higher CRP levels does not associate with poorer cognitive performance in old age.
Sánchez-Rodríguez et al., 2006	Longitudinal cohort study	Mexico	189	75	66.8	NA	The elderly in urban areas have more oxidative stress and a higher risk of developing confidence interval (CI) compared with elderly individuals in a rural environment.
Sasayama et al., 2012	Longitudinal cohort study	Japan	576	75	45.1 ± 15.0	NA	Elevated IL-6 and soluble IL-6R levels in Ala carriers may have negative impact on acquiring verbal cognitive ability requiring long-term memory.
Sharma et al., 2016	Longitudinal case-cohort study	United States	1,298	45	79.0 ± 3.4	6	This study did not find strong evidence of the utility of the biomarkers evaluated for identifying individuals at risk of cognitive decline.
Shi et al., 2020	Prospective observational study	China	372	31.5	60.58 ± 7.86	2	IL-35 polymorphisms were not associated with cognitive decline in CHD patients over a 2-year period yet.
Sochocka et al., 2017	Longitudinal case-cohort study	Poland	128	64.8	55–90	NA	The comorbidity of the periodontal health status may deepen the cognitive impairment and neurodegenerative lesions and advance to dementia and Alzheimer's disease (AD).
Yang et al., 2020	Longitudinal cohort study	China	122	49.18	NA	NA	T2DM patients have more cognitive impairment than T1DM patients. Changes in brain function connections and metabolites may be the structural basis of the differences in cognitive functional impairment. Inflammation is related to cognitive impairment in diabetes patients, especially in T2DM patients.
Yirmiya et al., 2020	Longitudinal cohort study	Israel	33	60.6	NA	NA	Sleep impairments in individuals with 22q11.2 deletion syndrome, which might negatively affect their cognitive functioning, and corroborate a potential role of immunological pathways in the 22q11.2 deletion syndrome neuro-phenotype.
Zheng et al., 2019	Case-control study	China	126	50	74.06	NA	Serum IL-6 and hs-CRP were associated with the risk of mild cognitive impairment (MCI) in Chinese patients with T2D. Serum folate might modify the association between serum hs-CRP and MCI in T2D patients.

10.3389/fnagi.2023.1069439

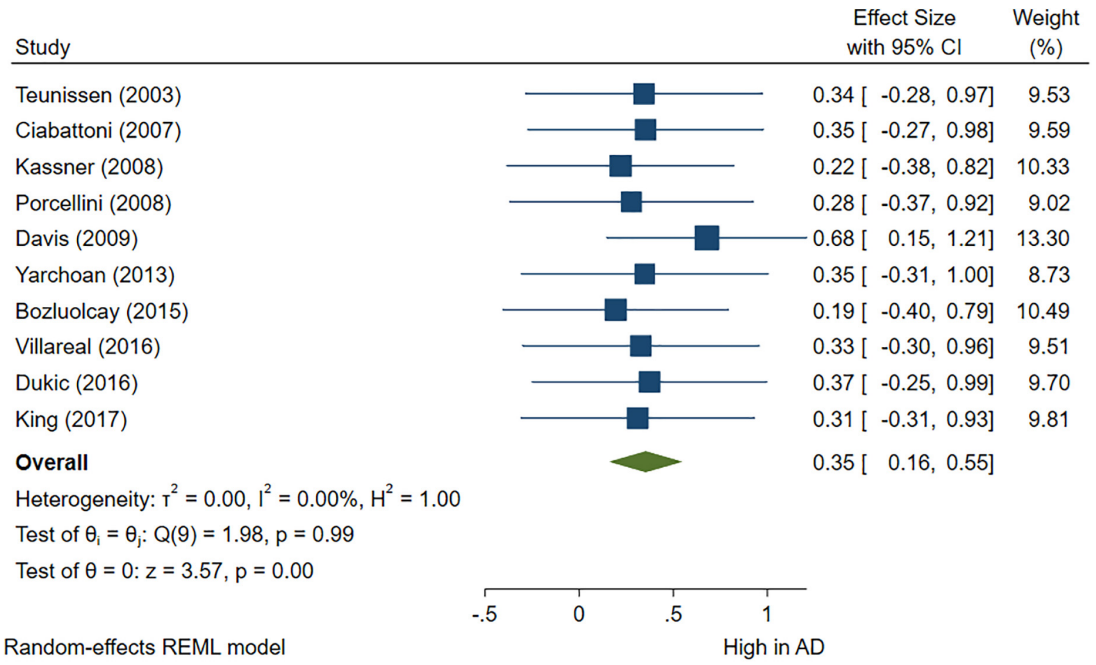

FIGURE 2
Forest plot of pooled Hedge's g depicting high C-reactive protein (CRP) concentration in Alzheimer's disease (AD) samples compared to controls.

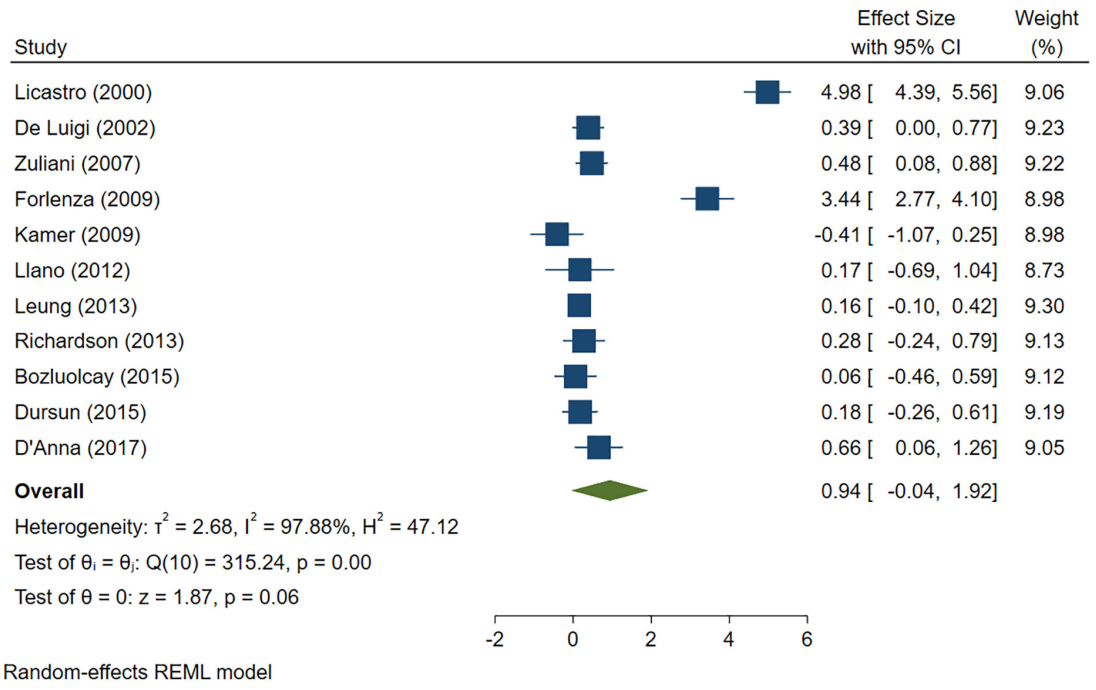

FIGURE 3
Forest plot of pooled Hedge's g depicting high IL-1β concentration in Alzheimer's disease (AD) samples compared to controls.

1.32)]. The pooled analysis was homogeneous (I2 = 0%, $p = 0.5$) (Figures 11A, B).

3.4.2. CRP

Interestingly, high and intermediate levels of CRP showed no significant impact on cognitive decline [OR = 1.08, 95% CI (0.74, 1.42)] and [OR = 1.05, 95% CI (0.64, 1.46)], respectively. The pooled analysis was moderately heterogeneous (I2 = 52.56%, $p = 0.05$), and heterogeneity did not resolve after further sensitivity analysis; thus, the random effect model was employed (Figures 11C, D).

3.4.3. ACT, Albumin, and TNF

Only two studies reported the effects of alpha1-antichymotrypsin (ACT), Albumin, and TNF alpha on cognitive outcomes. Neither

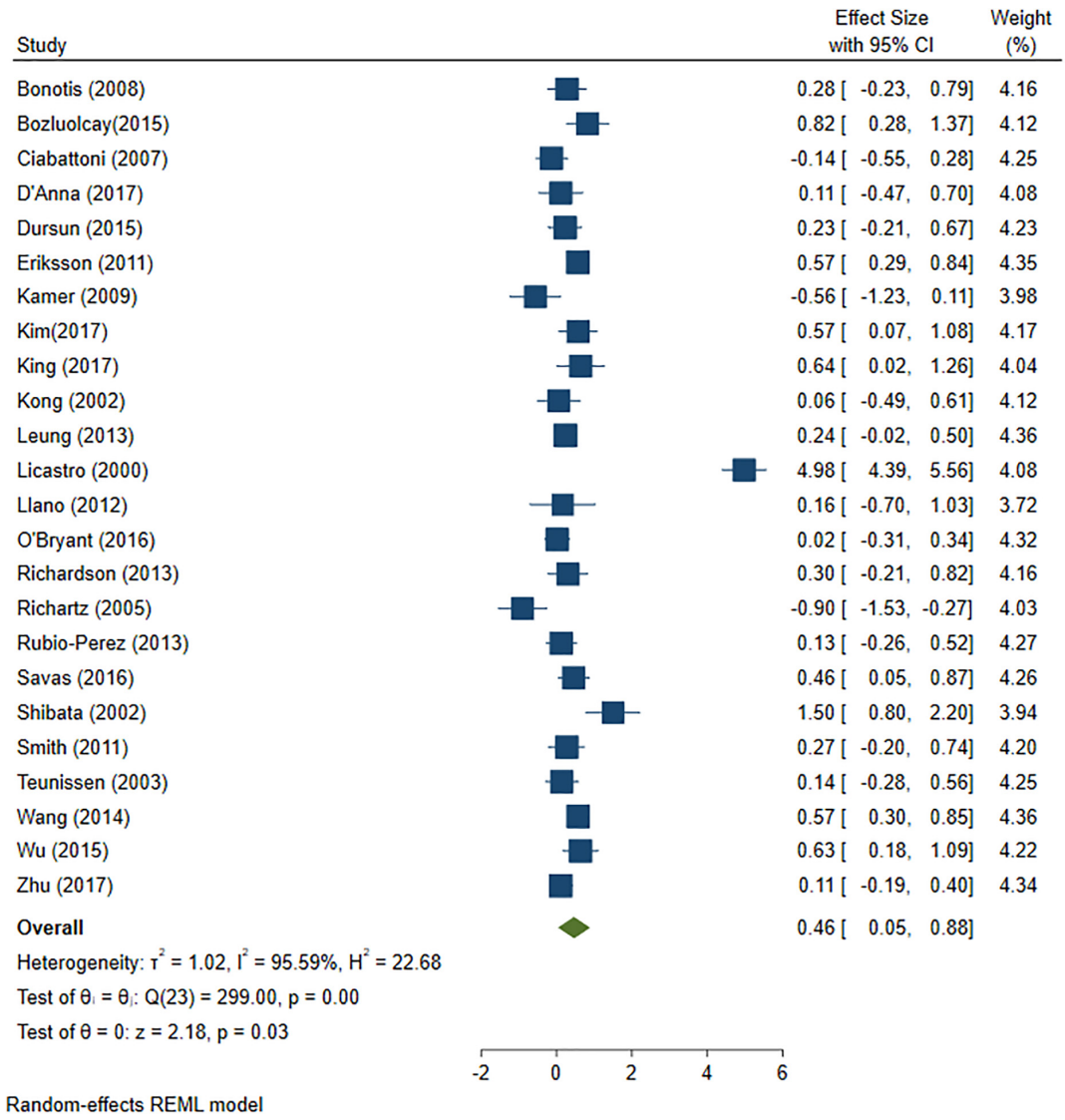

FIGURE 4
Forest plot of pooled Hedge's g depicting high IL-6 concentration in Alzheimer's disease (AD) samples compared to controls.

ACT [OR = 1.6, 95% CI (0.9, 2.29)] Albumin [OR = 1.12, 95% CI (0.61, 1.63)] nor TNF [OR = 1.23, 95% CI (0.91, 1.55)] had a statistically significant effect on cognitive impairment. The pooled analysis was homogeneous (I2 = 0%, $p = 0.5$) (**Figure 12A**). Funnel plots of the inverse of the standard error vs. the ES demonstrated asymmetry (**Figure 12B**). However, Egger's test ($P = 0.08$) and Begg's test ($P = 0.13$) indicated no small-study effects.

4. Discussion

In this meta-analysis, we have compiled and analyzed the varied results from individual studies that looked at the relationship between AD and MCI and inflammatory markers in peripheral blood or cerebrospinal fluid. Different levels of inflammatory markers were found to be significantly different across the AD, MCI, and control groups. A total of 79 articles were included in our systematic review and meta-analysis which include cross-sectional and longitudinal cohort studies and case-control. Cross-sectional studies demonstrated several changes in the inflammatory marker levels in the comparisons between AD, MCI, and control groups.

Notably, IL-6 level was found to be significantly increased in patients with AD compared with controls and MCI vs. controls. This meta-analysis confirmed the elevated levels of interleukin family molecules including as IL-1, IL-6, and IL-8 in AD patients. These cytokines and chemokines connect with the existence and breakdown of amyloid-beta (Aβ) or tau proteins, which contribute to neurodegeneration pathways in AD (Teixeira et al., 2008). Specifically, IL-6 was revealed to have a potential characteristic that identifies the extent of cognitive decline in AD patients. Deposition of Aβ has been demonstrated to stimulate IL-6 production by microglia and astrocytes, which may speed the progression of AD's degenerative cascade (Uslu et al., 2012). There are many common cytokines whose level were detected in AD and MCI conditions including CRP, IL1β, TNFα, IL6, and sTNFR1. However, their overall level was less in MCI compared to AD which suggest them as markers of neuroinflammation in AD and there may be an association between raised levels of cytokines in the blood and the development of AD.

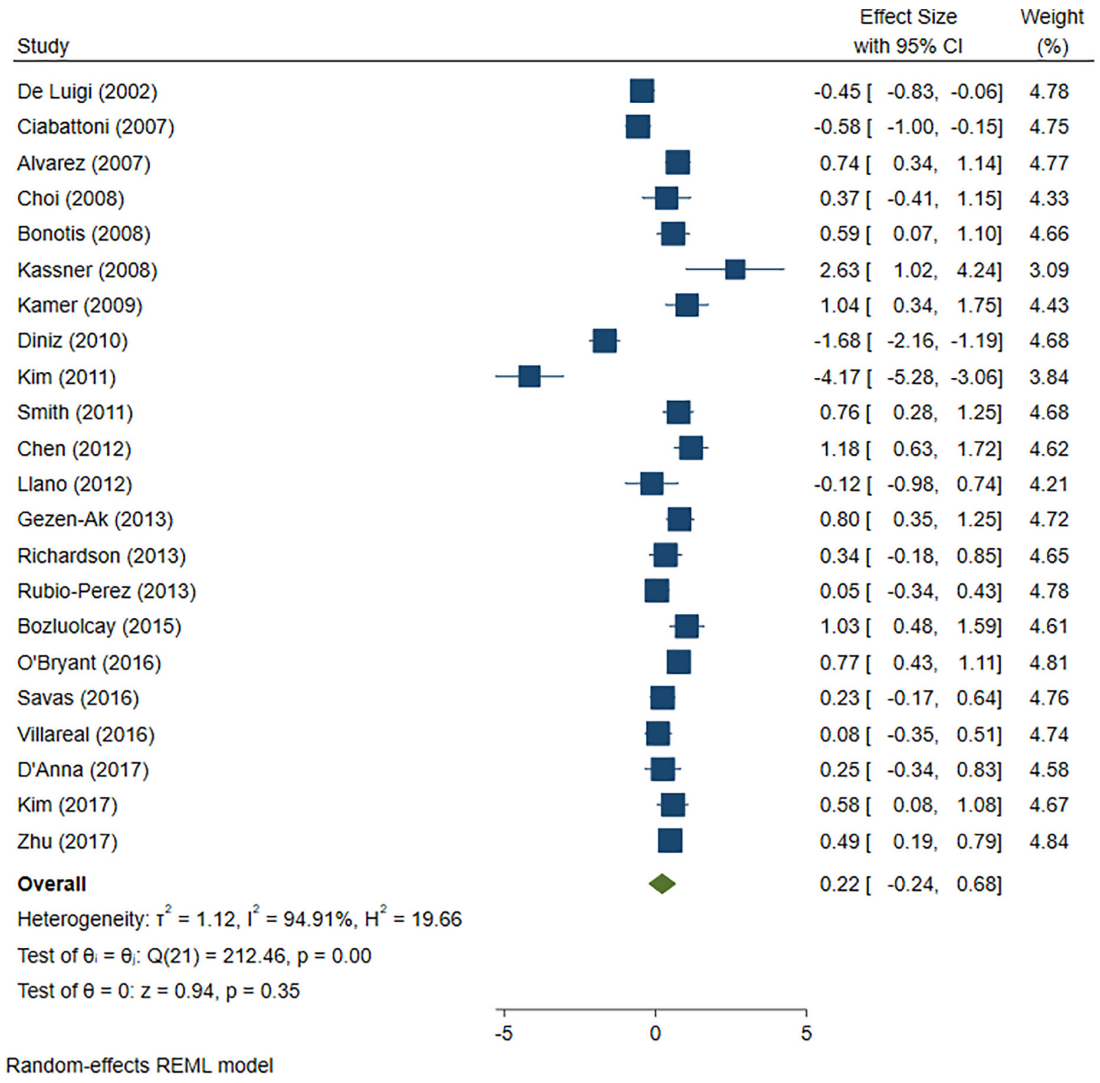

FIGURE 5
Forest plot of pooled Hedge's g depicting high tumor necrosis factor (TNF)-alpha concentration in Alzheimer's disease (AD) samples compared to controls.

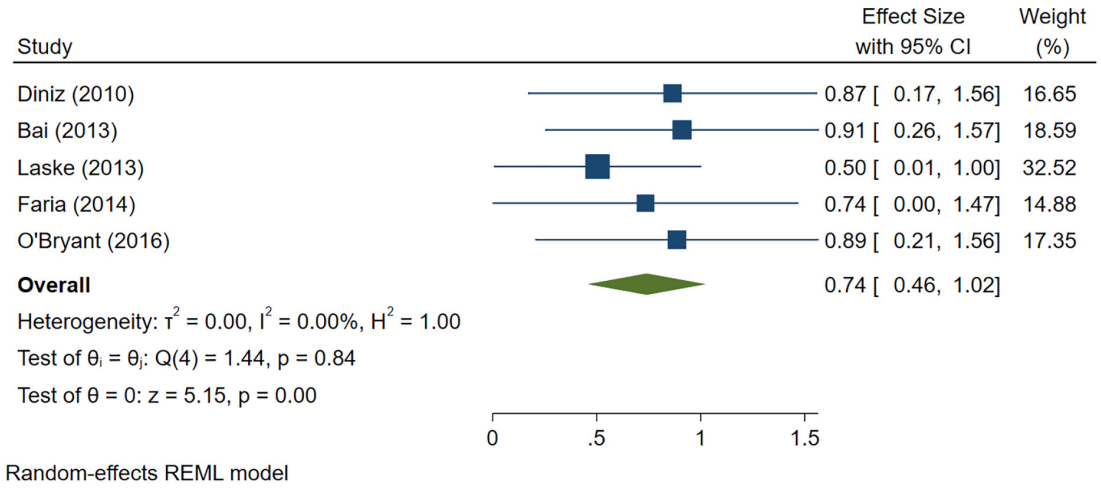

FIGURE 6
Forest plot of pooled Hedge's g depicting high sTNFR-1 concentration in Alzheimer's disease (AD) samples compared to controls.

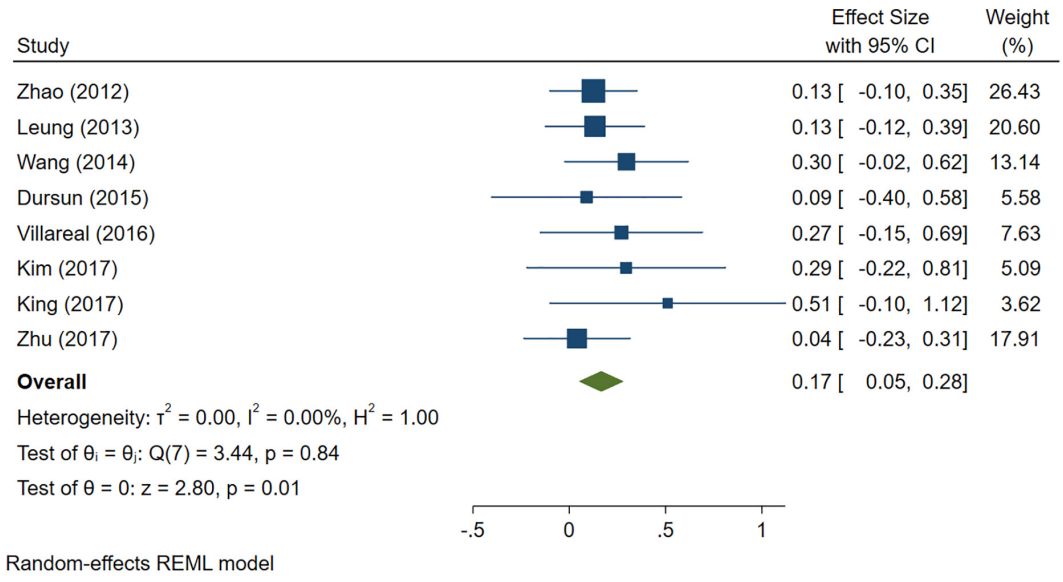

FIGURE 7
Forest plot of pooled Hedge's g depicting high IL-1β concentration in mild cognitive impairment (MCI) samples compared to controls.

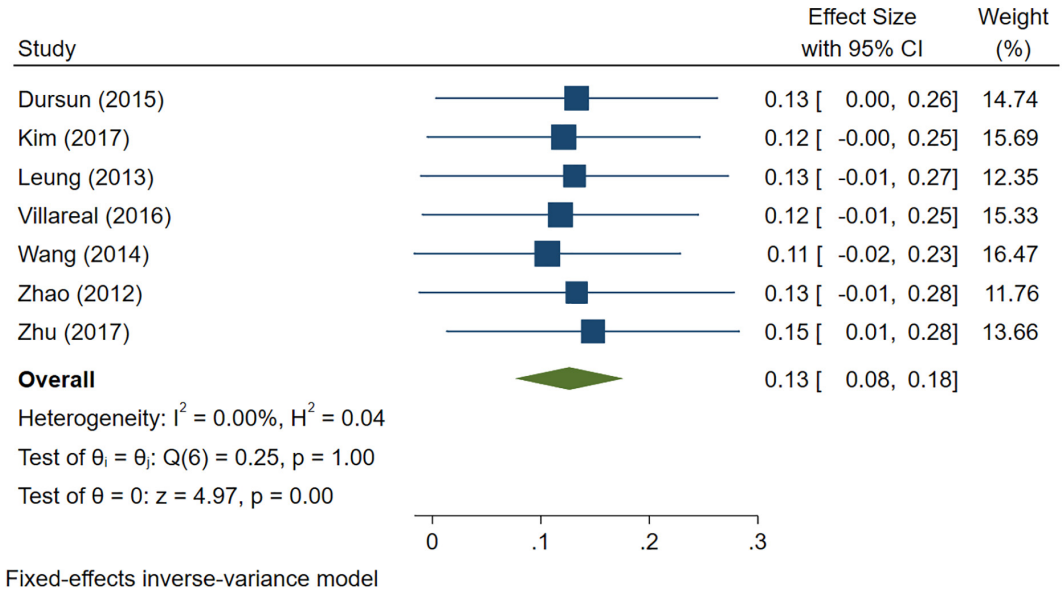

FIGURE 8
Forest plot of pooled Hedge's g depicting high IL-6 concentration in mild cognitive impairment (MCI) samples compared to controls.

4.1. Impact of systemic inflammation on cognitive performance

One hypothesis to explain the effects of increased cytokines in MCI and AD as compared to healthy controls is the impact of systemic inflammation on brain plasticity and function. Systemic inflammation raises pro-inflammatory cytokines such as IL-6, TNF-, and CRP, which may interact with the CNS in three ways: (1) pro-inflammatory cytokine transport proteins facilitate active trafficking across the blood brain barrier (BBB) for central activity (Dantzer et al., 2008; Fung et al., 2012). (2) Systemically generated cytokines may excite afferent nerves (e.g., the vagal nerve), which send inflammation to the brain stem. Vagal nerve projects to the solitary tract nucleus and higher brain areas (McCusker and Kelley, 2013). (3) Circulating cytokines reach outside-BBB organs. There, cells expressing toll-like receptors react to the increased inflammation by releasing pro-inflammatory cytokines, which may reach the brain by volume diffusion (Vitkovic et al., 2000b; McCusker and Kelley, 2013; Sankowski et al., 2015). When triggered peripherally, these three routes activate brain microglia and astrocytes to create pro-inflammatory cytokines, spreading the signal into the neuronal environment (Dantzer et al., 2008; Sankowski et al., 2015).

The blood-brain barrier, often known as the BBB, is an important component in both the preservation of the CNS's highly specialized milieu and the facilitation of communication with the systemic compartment. Alterations to the BBB may be seen in a variety of

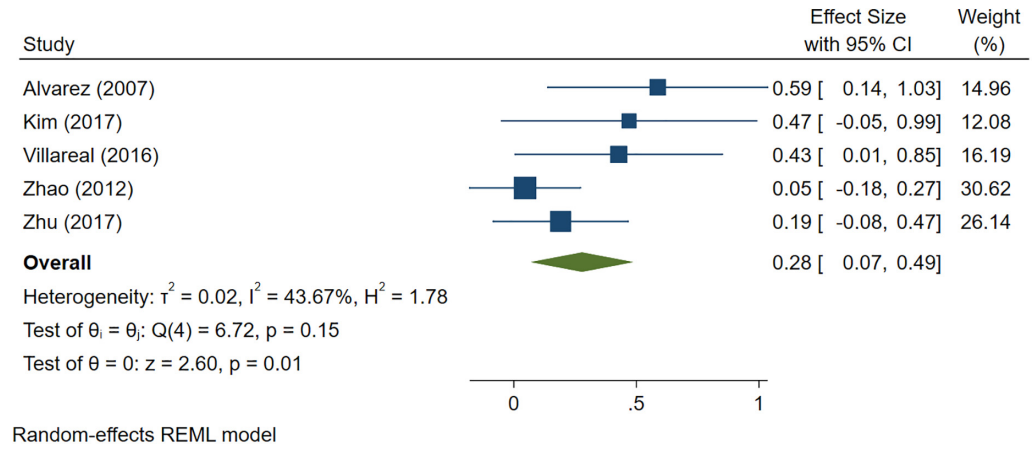

FIGURE 9
Forest plot of pooled Hedge's g depicting high tumor necrosis factor (TNF)-alpha concentration in mild cognitive impairment (MCI) samples compared to controls.

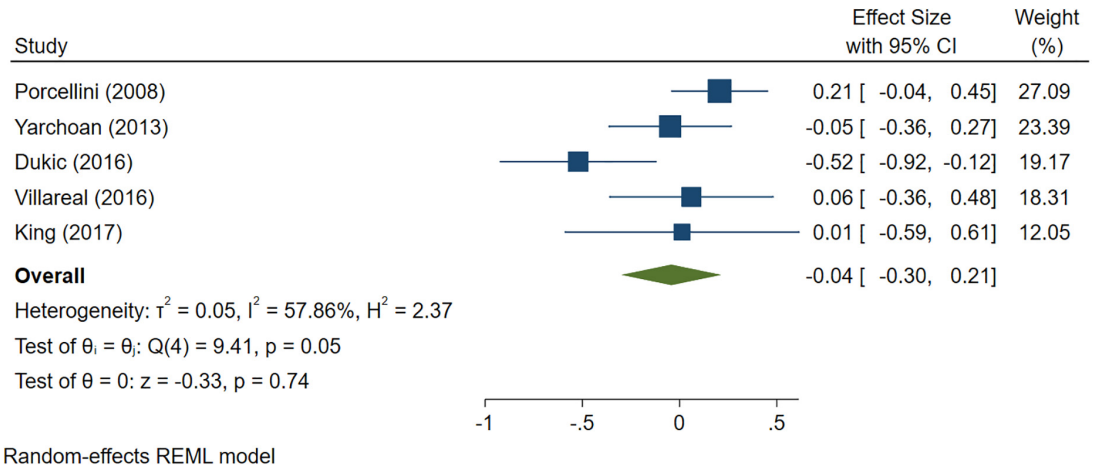

FIGURE 10
Forest plot of pooled Hedge's g depicting high C-reactive protein (CRP) concentration in mild cognitive impairment (MCI) samples compared to controls.

CNS diseases, including AD. Some non-disruptive BBB alterations are mediated directly by cytokines (Ericsson et al., 1995). The cerebral endothelium expresses several cytokines, including IL-1, IL-6, and TNF- receptors. Activation of the endothelium is caused by IL-1 before that of neighboring brain regions, which suggests that activation of the BBB is an intermediary stage (Herkenham et al., 1998). It is interesting to note that IFN- decreases the transmigration of type 1 T helper lymphocytes without having any effect on the diffusibility of albumin. This suggests that the effect is not caused by a change in the tight junctions but rather by cytokine-induced non-disruptive changes that discourage neuroinflammation (Prat et al., 2005).

Systemic inflammation is also known to play an important role in altering the hormonal levels. There are a number of cytokines, including TNF-alpha, interleukin-1 beta (IL-1 beta), and IL-6 that work as feedback loops to inhibit the immunological response when the hypothalamic-pituitary-adrenal (HPA) axis is stimulated by the stress of trauma or exercise (Brenner et al., 1997; Licinio and Wong, 1997; Teblick et al., 2019). However, persistent increase of cytokines might potentially inhibit the HPA axis, which can lead to decreased levels of glucocorticoids, growth hormone, and adrenocorticotropic hormone (Teblick et al., 2019).

4.2. Increased cytokine levels as a marker of central nervous system inflammation

Preclinical and clinical research have demonstrated that infection-related peripheral inflammation contributes to the development and progression of CNS disorders such AD, personality disorders (PD), Multiple Sclerosis (MS), and stroke. Patients with AD have increased levels of Aβ in their brains due to peripheral inflammation (Le Page et al., 2018). In amyloid precursor protein (APP) transgenic mice, peripheral lipopolysaccharide (LPS) injection enhanced BBB permeability, enabling proinflammatory factors such as IL-6 and TNF- to infiltrate the brain and promote disease development (Jaeger et al., 2009; Takeda et al., 2013). The increased level of cytokines in included studies suggests that patients might have CNS inflammation.

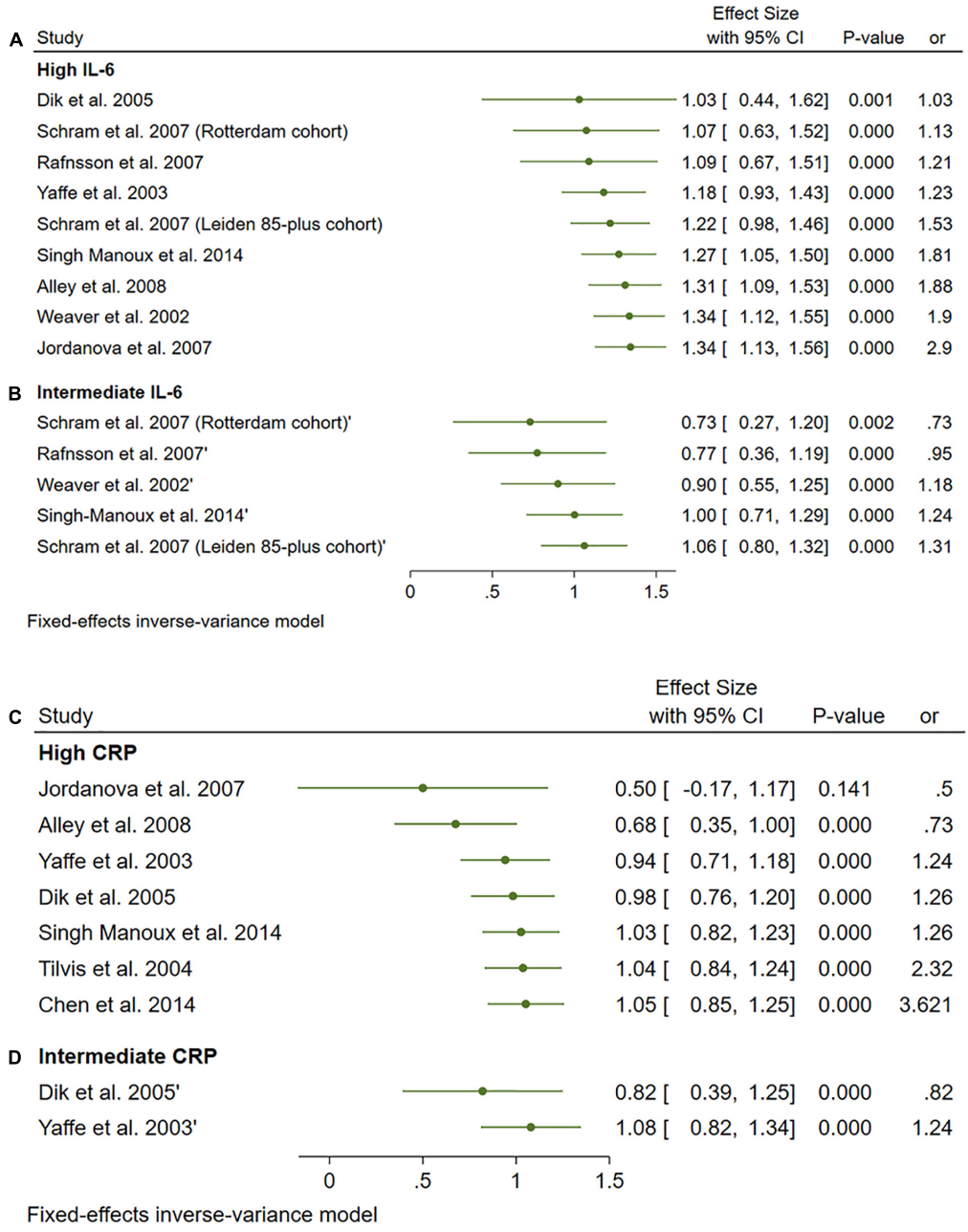

FIGURE 11
(A) Forest plot of pooled odds ratio (OR) for interleukin-6 (IL-6) high concentration and cognitive decline. **(B)** Forest plot of pooled odds ratio (OR) for IL-6 intermediate concentration and cognitive decline. **(C)** Forest plot of pooled odds ratio (OR) for C-reactive protein (CRP) high concentration and cognitive decline. **(D)** Forest plot of pooled odds ratio (OR) for CRP intermediate concentration and cognitive decline.

4.3. Longitudinal studies and risk of IL-6

Results from longitudinal studies also showed high levels of IL-6 significantly increased the risk of cognitive decline. However, intermediate levels of IL-6 had no significant effect on the final endpoint. Likewise, neither CRP, ACT, Albumin, or TNF alpha showed a significant impact on cognitive decline.

The neuronal and glial cell function is modulated by a highly controlled network of cytokines and soluble cytokine receptors (Benveniste, 1998; Vitkovic et al., 2000a). This is related to their capacity to modulate neurotransmission. Increases in noradrenergic, dopaminergic, and serotonergic metabolism in the hypothalamus, hippocampus, and nucleus accumbens can be caused by both systemic and central cytokine administration (Mohankumar et al., 1991; Shintani et al., 1993; Linthorst et al., 1995; Merali et al., 1997). IFN- stimulates neuronal differentiation, while IL-1, IL-6, and TNF- have trophic effects on developing neurons and glia (Jonakait, 1997; Zhao and Schwartz, 1998). In the developing brain, IL-1 may also play a role in regulating the synaptic plasticity that underpins learning and memory (Zhao and Schwartz, 1998).

Jordanova et al. (2007), Singh-Manoux et al. (2014) reported that raised IL-6 but not CRP predicted cognitive decline in this population. Inflammatory changes associated with cognitive decline may be specific to particular causal pathways which is consistent

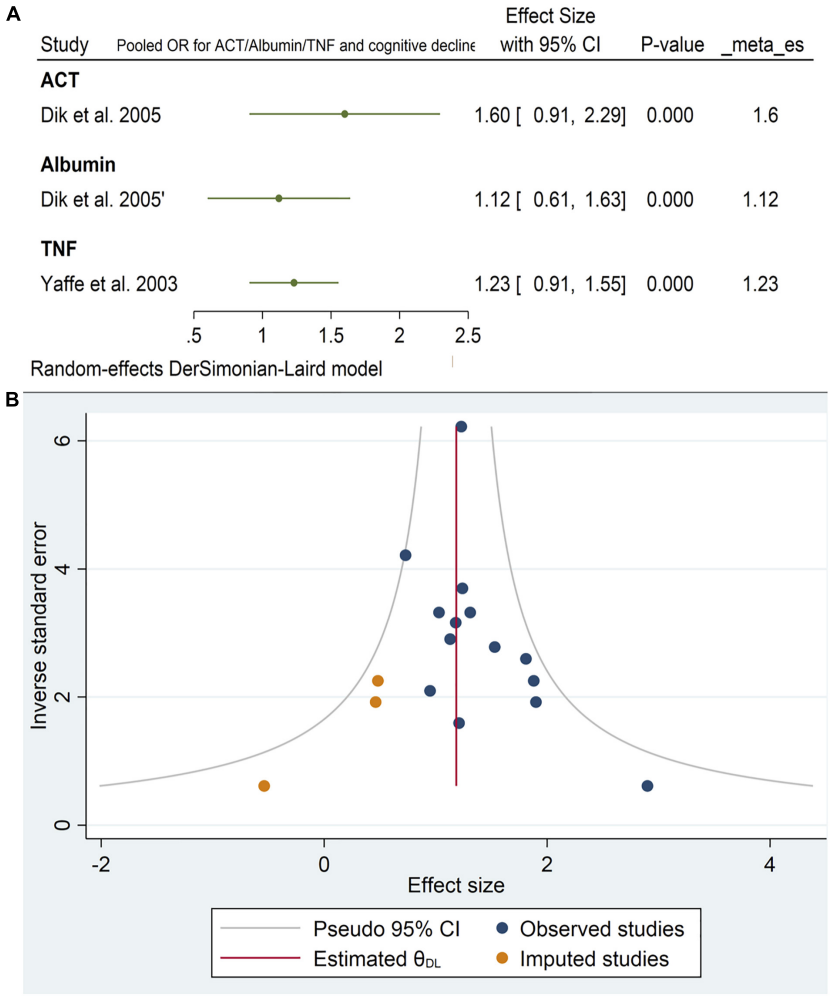

FIGURE 12
(A) Forest plot of pooled odds ratio (OR) for antichymotrypsin (ACT), albumin, tumor necrosis factor (TNF), and cognitive decline. **(B)** Funnel plot for the included longitudinal studies for interleukin-6 (IL-6) levels (intermediate and high).

with our findings. Weaver et al. (2002), Sasayama et al. (2012), Adriaensen et al. (2014) found a strong association between the level of IL-6 and short-term identification or evaluation of global functional status in the old. They reported that elevated IL-6 and soluble IL-6R levels in Ala carriers may have a negative impact on acquiring verbal cognitive ability requiring long-term memory. Mooijaart et al. (2011) found that plasma CRP concentrations associate with cognitive performance in part through pathways independent of cardiovascular disease. However, lifelong exposure to higher CRP levels does not associate with poorer cognitive performance in old age.

On the other hand, Yaffe et al. (2003), Chen et al. (2014) documented an association between CRP elevation and cognitive impairment which is inconsistent with our meta results. This may be because of the limited number of participants in these studies compared to our meta-analysis. Ashraf-Ganjouei et al. (2020) found that healthy subjects with higher levels of CRP exhibit poorer performance in verbal learning memory and general wakefulness domains of cognition.

Some other interleukins have a role in cognitive impairment other than IL-6. Goldstein et al. (2015) recorded strong relation between IL-8 and cognitive performance in African Americans than Caucasians. However, this relationship should be further examined in larger samples that are followed over time. Conversely, Shi et al. (2020) reported IL-35 polymorphisms were not associated with cognitive decline in coronary heart disease patients over 2 years.

Shen et al. (2019) reported that inflammatory marker levels were found to be significantly different in AD and control groups, supporting the idea that AD is accompanied by inflammatory responses in the peripheral and cerebro spinal fluid (CSF). In a previous review, Wilson et al. (2002) reported that cytokine-mediated inflammation in neurodegenerative disorders such as AD and vascular dementia is increasingly appreciated. Cytokines are an important part of stress activation in the hypothalamic-hypo physiologic-adrenal axis.

Our study is the first meta-analysis to our knowledge to differentiate between several inflammatory cytokines and their relation individually to cognitive impairment. In spite of the large sample size of our study and the strength of meta-analysis, these results are limited by the study design of included studies and the insufficient data about other inflammatory markers other than IL-6. Only two studies reported the effects of ACT, Albumin, and TNF

alpha on cognitive outcomes. We need more controlled studies that have the least confounders to assure the strength of results.

4.4. Future perspectives: Inflammatory markers as a novel therapeutic target for AD

Although this meta-analysis only provides additional evidence for the association between some inflammatory markers and cognitive decline, it is worthwhile to discuss the potential impact for the development of novel treatments for AD. There has been an important debate on the current therapeutic target for AD, the amyloid β-protein. However, studies have not demonstrated that anti-amyloid therapies have induced significant therapeutic effects. In this context, some inflammatory markers, especially if targeted before the onset of cognitive deterioration, may be an interesting marker to target. For instance, it has been suggested that some diets, such as the Mediterranean-DASH Intervention for Neurodegenerative Delay (MIND) diets, can improve cognition and also have an anti-inflammatory effect (van den Brink et al., 2019). Also, non-invasive brain stimulation can also improve cognition (Martins et al., 2017) and reduce inflammation in animal models (Laste et al., 2012; de Oliveira et al., 2019; Toledo et al., 2021). One of the limitations of the current review is not including studies related to comorbid vascular dementia, which is connected with AD and MCI especially in elderly patients.

5. Conclusion

This review included inflammatory biomarkers in AD and MCI conditions supported from cross sectional and longitudinal studies. Cross sectional studies included in this review and meta-analysis demonstrated remarkable alterations in the peripheral levels of CRP, IL-1β, IL-6, sTNFR1, and TNF alpha. The findings from longitudinal studies indicated that the risk of cognitive deterioration has been substantially increased by high IL-6 levels. However, intermediate IL-6 levels did not affect the outcome significantly. Neither CRP, ACT, Albumin, or TNF alpha have had a major influence on cognitive degradation. These results provided further proof that AD and MCI are accompanied by inflammatory processes originating in the CNS.

Data availability statement

The original contributions presented in this study are included in this article/supplementary material, further inquiries can be directed to the corresponding author.

Author contributions

Both authors listed have made a substantial, direct, and intellectual contribution to the work, and approved it for publication.

Conflict of interest

The authors declare that the research was conducted in the absence of any commercial or financial relationships that could be construed as a potential conflict of interest.

Publisher's note

All claims expressed in this article are solely those of the authors and do not necessarily represent those of their affiliated organizations, or those of the publisher, the editors and the reviewers. Any product that may be evaluated in this article, or claim that may be made by its manufacturer, is not guaranteed or endorsed by the publisher.

References

Adriaensen, W., Matheï, C., Vaes, B., van Pottelbergh, G., Wallemacq, P., Degryse, J., et al. (2014). Interleukin-6 predicts short-term global functional decline in the oldest old: Results from the BELFRAIL study. *Age* 36:9723. doi: 10.1007/s11357-014-9723-3

Alley, D. E., Crimmins, E., Karlamangla, A., Hu, P., and Seeman, T. (2008). Inflammation and rate of cognitive change in high-functioning older adults. *J. Gerontol. A Biol. Sci. Med. Sci.* 63, 50–55. doi: 10.1093/gerona/63.1.50

Ashraf-Ganjouei, A., Moradi, K., Bagheri, S., and Aarabi, M. (2020). The association between systemic inflammation and cognitive performance in healthy adults. *J. Neuroimmunol.* 345:577272.

Baierle, M., Nascimento, S., Moro, A., Brucker, N., Freitas, F., Gauer, B., et al. (2015). Relationship between inflammation and oxidative stress and cognitive decline in the institutionalized elderly. *Oxid. Med. Cell. Longev.* 2015:804198. doi: 10.1155/2015/804198

Begg, C. B., and Mazumdar, M. (1994). Operating characteristics of a rank correlation test for publication bias. *Biometrics* 50, 1088–1101. doi: 10.2307/2533446

Benveniste, E. N. (1998). Cytokine actions in the central nervous system. *Cytokine Growth Factor Rev.* 9, 259–275. doi: 10.1016/S1359-6101(98)00015-X

Beydoun, M. A., Dore, G., Canas, J., Liang, H., Beydoun, H., Evans, M., et al. (2018). Systemic inflammation is associated with longitudinal changes in cognitive performance among urban adults. *Front. Aging Neurosci.* 10:313. doi: 10.3389/fnagi.2018.00313

Beydoun, M. A., Weiss, J., Obhi, H., Beydoun, H., Dore, G., Liang, H., et al. (2019). Cytokines are associated with longitudinal changes in cognitive performance among urban adults. *Brain Behav. Immun.* 80, 474–487. doi: 10.1016/j.bbi.2019.04.027

Bonotis, K., Krikki, E., Holeva, V., Aggouridaki, C., Costa, V., and Baloyannis, S. (2008). Systemic immune aberrations in Alzheimer's disease patients. *J. Neuroimmunol.* 193, 183–187. doi: 10.1016/j.jneuroim.2007.10.020

Boots, E. A., Castellanos, K., Zhan, L., Barnes, L., Tussing-Humphreys, L., Deoni, S., et al. (2020). Inflammation, cognition, and white matter in older adults: An examination by race. *Front. Aging Neurosci.* 12, 553998. doi: 10.3389/fnagi.2020.553998

Bozluolcay, M., Andican, G., Fırtına, S., Erkol, G., and Konukoglu, D. (2016). Inflammatory hypothesis as a link between Alzheimer's disease and diabetes mellitus. *Geriatr. Gerontol. Int.* 16, 1161–1166. doi: 10.1111/ggi.12602

Brenner, I. K., Zamecnik, J., Shek, P., and Shephard, R. (1997). The impact of heat exposure and repeated exercise on circulating stress hormones. *Eur. J. Appl. Physiol. Occup. Physiol.* 76, 445–454. doi: 10.1007/s004210050274

Chen, J. M., Cui, G., Jiang, G., Xu, R., Tang, H., Wang, G., et al. (2014). Cognitive impairment among elderly individuals in Shanghai suburb, China: Association of C-reactive protein and its interactions with other relevant factors. *Am. J. Alzheimers Dis. Other Dement.* 29, 712–717. doi: 10.1177/1533317514534758

Chi, G. C., Fitzpatrick, A., Sharma, M., Jenny, N., Lopez, O., DeKosky, S., et al. (2017). Inflammatory biomarkers predict domain-specific cognitive decline in

older adults. *J. Gerontol. A Biol. Sci. Med. Sci.* 72, 796–803. doi: 10.1093/gerona/glw155

Choi, C., Jeong, J., Jang, J., Choi, K., Lee, J., Kwon, J., et al. (2008). Multiplex analysis of cytokines in the serum and cerebrospinal fluid of patients with Alzheimer's disease by color-coded bead technology. *J. Clin. Neurol.* 4, 84–88. doi: 10.3988/jcn.2008.4.2.84

Ciabattoni, G., Porreca, E., Di Febbo, C., Di Iorio, A., Paganelli, R., Bucciarelli, T., et al. (2007). Determinants of platelet activation in Alzheimer's disease. *Neurobiol. Aging* 28, 336–342. doi: 10.1016/j.neurobiolaging.2005.12.011

Cumpston, M., Li, T., Page, M., Chandler, J., Welch, V., Higgins, J., et al. (2019). Updated guidance for trusted systematic reviews: A new edition of the Cochrane Handbook for Systematic Reviews of Interventions. *Cochrane Database Syst. Rev.* 10:ED000142. doi: 10.1002/14651858.ED000142

D'Anna, L., Abu-Rumeileh, S., Fabris, M., Pistis, C., Baldi, A., Sanvilli, N., et al. (2017). Serum Interleukin-10 levels correlate with cerebrospinal fluid amyloid beta deposition in Alzheimer disease patients. *Neurodegener. Dis.* 17, 227–234. doi: 10.1159/000474940

Dantzer, R., O'Connor, J., Freund, G., Johnson, R., and Kelley, K. (2008). From inflammation to sickness and depression: When the immune system subjugates the brain. *Nat. Rev. Neurosci.* 9, 46–56. doi: 10.1038/nrn2297

Davis, G., Baboolal, N., Nayak, S., and McRae, A. (2009). Sialic acid, homocysteine and CRP: Potential markers for dementia. *Neurosci. Lett.* 465, 282–284. doi: 10.1016/j.neulet.2009.09.035

De Luigi, A., Pizzimenti, S., Quadri, P., Lucca, U., Tettamanti, M., Fragiacomo, C., et al. (2002). Peripheral inflammatory response in Alzheimer's disease and multiinfarct dementia. *Neurobiol. Dis.* 11, 308–314. doi: 10.1006/nbdi.2002.0556

de Oliveira, C., de Freitas, J., Macedo, I., Scarabelot, V., Ströher, R., Santos, D., et al. (2019). Transcranial direct current stimulation (tDCS) modulates biometric and inflammatory parameters and anxiety-like behavior in obese rats. *Neuropeptides* 73, 1–10. doi: 10.1016/j.npep.2018.09.006

DerSimonian, R., and Laird, N. (1986). Meta-analysis in clinical trials. *Control Clin. Trials* 7, 177–188. doi: 10.1016/0197-2456(86)90046-2

Dik, M. G., Jonker, C., Hack, C., Smit, J., Comijs, H., and Eikelenboom, P. (2005). Serum inflammatory proteins and cognitive decline in older persons. *Neurology* 64, 1371–1377.

Dukic, L., Simundic, A., Martinic-Popovic, I., Kackov, S., Diamandis, A., Begcevic, I., et al. (2016). The role of human kallikrein 6, clusterin and adiponectin as potential blood biomarkers of dementia. *Clin. Biochem.* 49, 213–218. doi: 10.1016/j.clinbiochem.2015.10.014

Dursun, E., Gezen-Ak, D., Hanağası, H., Bilgiç, B., Lohmann, E., Ertan, S., et al. (2015). The interleukin 1 alpha, interleukin 1 beta, interleukin 6 and alpha-2-macroglobulin serum levels in patients with early or late onset Alzheimer's disease, mild cognitive impairment or Parkinson's disease. *J. Neuroimmunol.* 283, 50–57.

Duval, S., and Tweedie, R. (2000). Trim and fill: A simple funnel-plot-based method of testing and adjusting for publication bias in meta-analysis. *Biometrics* 56, 455–463. doi: 10.1111/j.0006-341x.2000.00455.x

Ericsson, A., Liu, C., Hart, R., and Sawchenko, P. (1995). Type 1 interleukin-1 receptor in the rat brain: Distribution, regulation, and relationship to sites of IL-1-induced cellular activation. *J. Comp. Neurol.* 361, 681–698. doi: 10.1002/cne.903610410

Eriksson, U. K., Pedersen, N., Reynolds, C., Hong, M., Prince, J., Gatz, M., et al. (2011). Associations of gene sequence variation and serum levels of C-reactive protein and interleukin-6 with Alzheimer's disease and dementia. *J. Alzheimers Dis.* 23, 361–369. doi: 10.3233/JAD-2010-101671

Ershler, W. B. (1993). Interleukin-6: A cytokine for gerontologists. *J. Am. Geriatr. Soc.* 41, 176–181.

Forlenza, O. V., Diniz, B., Talib, L., Mendonça, V., Ojopi, E., Gattaz, W., et al. (2009). Increased serum IL-1beta level in Alzheimer's disease and mild cognitive impairment. *Dement. Geriatr. Cogn. Disord.* 28, 507–512.

Fung, A., Vizcaychipi, M., Lloyd, D., Wan, Y., and Ma, D. (2012). Central nervous system inflammation in disease related conditions: Mechanistic prospects. *Brain Res.* 1446, 144–155. doi: 10.1016/j.brainres.2012.01.061

Giudici, K. V., de Souto Barreto, P., Guerville, F., Beard, J., Araujo de Carvalho, I., Andrieu, S., et al. (2019). Associations of C-reactive protein and homocysteine concentrations with the impairment of intrinsic capacity domains over a 5-year follow-up among community-dwelling older adults at risk of cognitive decline (MAPT Study). *Exp. Gerontol.* 127:110716. doi: 10.1016/j.exger.2019.110716

Goldstein, F. C., Zhao, L., Steenland, K., and Levey, A. (2015). Inflammation and cognitive functioning in African Americans and Caucasians. *Int. J. Geriatr. Psychiatry* 30, 934–941.

Gunathilake, R., Oldmeadow, C., McEvoy, M., Inder, K., Schofield, P., Nair, B., et al. (2016). The association between obesity and cognitive function in older persons: How much is mediated by inflammation, fasting plasma glucose, and hypertriglyceridemia? *J. Gerontol. A Biol. Sci. Med. Sci.* 71, 1603–1608. doi: 10.1093/gerona/glw070

Hager, K., Machein, U., Krieger, S., Platt, D., Seefried, G., and Bauer, J. (1994). Interleukin-6 and selected plasma proteins in healthy persons of different ages. *Neurobiol. Aging* 15, 771–772.

Hajjar, I., Hayek, S., Goldstein, F., Martin, G., Jones, D., and Quyyumi, A. (2018). Oxidative stress predicts cognitive decline with aging in healthy adults: An observational study. *J. Neuroinflammation* 15:17. doi: 10.1186/s12974-017-1026-z

Herkenham, M., Lee, H. Y., and Baker, R. A. (1998). Temporal and spatial patterns of c-fos mRNA induced by intravenous interleukin-1: A cascade of non-neuronal cellular activation at the blood-brain barrier. *J. Comp. Neurol.* 400, 175–196. doi: 10.1002/(sici)1096-9861(19981019)400:2<175::aid-cne2>3.0.co;2-6

Higgins, J. P., Thompson, S., Deeks, J., and Altman, D. (2003). Measuring inconsistency in meta-analyses. *BMJ* 327, 557–560.

Holmes, C. (2013). Review: Systemic inflammation and Alzheimer's disease. *Neuropathol. Appl. Neurobiol.* 39, 51–68.

Irwig, L., Macaskill, P., Berry, G., and Glasziou, P. (1998). Bias in meta-analysis detected by a simple, graphical test. Graphical test is itself biased. *BMJ* 316, 470–471.

Jaeger, L. B., Dohgu, S., Sultana, R., Lynch, J., Owen, J., Erickson, M., et al. (2009). Lipopolysaccharide alters the blood-brain barrier transport of amyloid beta protein: A mechanism for inflammation in the progression of Alzheimer's disease. *Brain Behav. Immun.* 23, 507–517. doi: 10.1016/j.bbi.2009.01.017

Jonakait, G. M. (1997). Cytokines in neuronal development. *Adv. Pharmacol.* 37, 35–67.

Jordanova, V., Stewart, R., Davies, E., Sherwood, R., and Prince, M. (2007). Markers of inflammation and cognitive decline in an African-Caribbean population. *Int. J. Geriatr. Psychiatry* 22, 966–973. doi: 10.1002/gps.1772

Jung, Y. H., Shin, N., Jang, J., Lee, W., Lee, D., Choi, Y., et al. (2019). Relationships among stress, emotional intelligence, cognitive intelligence, and cytokines. *Medicine* 98:e15345. doi: 10.1097/MD.0000000000015345

Kamer, A. R., Craig, R., Pirraglia, E., Dasanayake, A., Norman, R., Boylan, R., et al. (2009). TNF-alpha and antibodies to periodontal bacteria discriminate between Alzheimer's disease patients and normal subjects. *J. Neuroimmunol.* 216, 92–97. doi: 10.1016/j.jneuroim.2009.08.013

Kassner, S. S., Bonaterra, G., Kaiser, E., Hildebrandt, W., Metz, J., Schröder, J., et al. (2008). Novel systemic markers for patients with Alzheimer disease? - a pilot study. *Curr. Alzheimer Res.* 5, 358–366. doi: 10.2174/156720508785132253

Kim, Y. S., Lee, K. J., and Kim, H. (2017). Serum tumour necrosis factor-alpha and interleukin-6 levels in Alzheimer's disease and mild cognitive impairment. *Psychogeriatrics* 17, 224–230.

King, E., O'Brien, J., Donaghy, P., Morris, C., Barnett, N., Olsen, K., et al. (2018). Peripheral inflammation in prodromal Alzheimer's and Lewy body dementias. *J. Neurol. Neurosurg. Psychiatry* 89, 339–345.

Komulainen, P., Lakka, T., Kivipelto, M., Hassinen, M., Penttilä, I., Helkala, E., et al. (2007). Serum high sensitivity C-reactive protein and cognitive function in elderly women. *Age Ageing* 36, 443–448. doi: 10.1093/ageing/afm051

Kong, Q. L., Zhang, J., Zhang, Z., Ge, P., Xu, Y., Mi, R., et al. (2002). [Serum levels of macrophage colony stimulating factor in the patients with Alzheimer's disease]. *Zhongguo Yi Xue Ke Xue Yuan Xue Bao* 24, 298–301.

Kronfol, Z., and Remick, D. G. (2000). Cytokines and the brain: Implications for clinical psychiatry. *Am. J. Psychiatry* 157, 683–694. doi: 10.1176/appi.ajp.157.5.683

Laste, G., Caumo, W., Adachi, L., Rozisky, J., de Macedo, I., Filho, P., et al. (2012). After-effects of consecutive sessions of transcranial direct current stimulation (tDCS) in a rat model of chronic inflammation. *Exp. Brain Res.* 221, 75–83. doi: 10.1007/s00221-012-3149-x

Le Page, A., Dupuis, G., Frost, E., Larbi, A., Pawelec, G., Witkowski, J., et al. (2018). Role of the peripheral innate immune system in the development of Alzheimer's disease. *Exp. Gerontol.* 107, 59–66.

Leung, R., Proitsi, P., Simmons, A., Lunnon, K., Güntert, A., Kronenberg, D., et al. (2013). Inflammatory proteins in plasma are associated with severity of Alzheimer's disease. *PLoS One* 8:e64971. doi: 10.1371/journal.pone.0064971

Licastro, F., Pedrini, S., Caputo, L., Annoni, G., Davis, L., Ferri, C., et al. (2000). Increased plasma levels of interleukin-1, interleukin-6 and alpha-1-antichymotrypsin in patients with Alzheimer's disease: Peripheral inflammation or signals from the brain? *J. Neuroimmunol.* 103, 97–102.

Licinio, J., and Wong, M. L. (1997). Interleukin 1 receptor antagonist gene expression in rat pituitary in the systemic inflammatory response syndrome: Pathophysiological implications. *Mol. Psychiatry* 2, 99–103.

Linthorst, A. C., Flachskamm, C., Müller-Preuss, P., Holsboer, F., and Reul, J. (1995). Effect of bacterial endotoxin and interleukin-1 beta on hippocampal serotonergic neurotransmission, behavioral activity, and free corticosterone levels: An *in vivo* microdialysis study. *J. Neurosci.* 15, 2920–2934. doi: 10.1523/JNEUROSCI.15-04-02920.1995

Llano, D. A., Li, J., Waring, J., Ellis, T., Devanarayan, V., Witte, D., et al. (2012). Cerebrospinal fluid cytokine dynamics differ between Alzheimer disease patients and elderly controls. *Alzheimer Dis. Assoc. Disord.* 26, 322–328. doi: 10.1097/WAD.0b013e31823b2728

Marioni, R. E., Stewart, M., Murray, G., Deary, I., Fowkes, F., Lowe, G., et al. (2009). Peripheral levels of fibrinogen, C-reactive protein, and plasma viscosity predict future cognitive decline in individuals without dementia. *Psychosom. Med.* 71, 901–906. doi: 10.1097/PSY.0b013e3181b1e538

Martins, A. R., Fregni, F., Simis, M., and Almeida, J. (2017). Neuromodulation as a cognitive enhancement strategy in healthy older adults: Promises and pitfalls. *Neuropsychol. Dev. Cogn. B Aging Neuropsychol. Cogn.* 24, 158–185. doi: 10.1080/13825585.2016.1176986

McCusker, R. H., and Kelley, K. W. (2013). Immune-neural connections: How the immune system's response to infectious agents influences behavior. *J. Exp. Biol.* 216(Pt 1), 84–98. doi: 10.1242/jeb.073411

McHugh Power, J., Carney, S., Hannigan, C., Brennan, S., Wolfe, H., Lynch, M., et al. (2019). Systemic inflammatory markers and sources of social support among older adults in the Memory Research Unit cohort. *J. Health Psychol.* 24, 397–406. doi: 10.1177/1359105316676331

Merali, Z., Lacosta, S., and Anisman, H. (1997). Effects of interleukin-1beta and mild stress on alterations of norepinephrine, dopamine and serotonin neurotransmission: A regional microdialysis study. *Brain Res.* 761, 225–235. doi: 10.1016/s0006-8993(97)00312-0

Mohankumar, P. S., Thyagarajan, S., and Quadri, S. K. (1991). Interleukin-1 stimulates the release of dopamine and dihydroxyphenylacetic acid from the hypothalamus *in vivo*. *Life Sci.* 48, 925–930. doi: 10.1016/0024-3205(91)90040-i

Mooijaart, S. P., Sattar, N., Trompet, S., Polisecki, E., de Craen, A., Schaefer, E., et al. (2011). C-reactive protein and genetic variants and cognitive decline in old age: The PROSPER study. *PLoS One* 6:e23890. doi: 10.1371/journal.pone.0023890

O'Bryant, S. E., Lista, S., Rissman, R., Edwards, M., Zhang, F., Hall, J., et al. (2016). Comparing biological markers of Alzheimer's disease across blood fraction and platforms: Comparing apples to oranges. *Alzheimers Dement.* 3, 27–34. doi: 10.1016/j.dadm.2015.12.003

Page, M. J., McKenzie, J., Bossuyt, P., Boutron, I., Hoffmann, T., Mulrow, C., et al. (2021). The PRISMA 2020 statement: An updated guideline for reporting systematic reviews. *BMJ* 372:n71. doi: 10.1136/bmj.n71

Papanicolaou, D. A., Wilder, R., Manolagas, S., and Chrousos, G. (1998). The pathophysiologic roles of interleukin-6 in human disease. *Ann. Intern. Med.* 128, 127–137.

Porcellini, E., Davis, E., Chiappelli, M., Ianni, E., Di Stefano, G., Forti, P., et al. (2008). Elevated plasma levels of alpha-1-anti-chymotrypsin in age-related cognitive decline and Alzheimer's disease: A potential therapeutic target. *Curr. Pharm. Des.* 14, 2659–2664. doi: 10.2174/138161208786264151

Prat, A., Biernacki, K., and Antel, J. P. (2005). Th1 and Th2 lymphocyte migration across the human BBB is specifically regulated by interferon beta and copolymer-1. *J. Autoimmun.* 24, 119–124. doi: 10.1016/j.jaut.2005.01.004

Rafnsson, S. B., Deary, I., Smith, F., Whiteman, M., Rumley, A., Lowe, G., et al. (2007). Cognitive decline and markers of inflammation and hemostasis: The Edinburgh Artery Study. *J. Am. Geriatr. Soc.* 55, 700–707. doi: 10.1111/j.1532-5415.2007.01158.x

Richardson, C., Gard, P., Klugman, A., Isaac, M., and Tabet, N. (2013). Blood pro-inflammatory cytokines in Alzheimer's disease in relation to the use of acetylcholinesterase inhibitors. *Int. J. Geriatr. Psychiatry* 28, 1312–1317. doi: 10.1002/gps.3966

Richartz, E., Stransky, E., Batra, A., Simon, P., Lewczuk, P., Buchkremer, G., et al. (2005). Decline of immune responsiveness: A pathogenetic factor in Alzheimer's disease? *J. Psychiatr. Res.* 39, 535–543. doi: 10.1016/j.jpsychires.2004.12.005

Roubenoff, R., Harris, T., Abad, L., Wilson, P., Dallal, G., and Dinarello, C. (1998). Monocyte cytokine production in an elderly population: Effect of age and inflammation. *J. Gerontol. A Biol. Sci. Med. Sci.* 53, M20–M26. doi: 10.1093/gerona/53A.1.M20

Rubio-Perez, J. M., and Morillas-Ruiz, J. M. (2013). Serum cytokine profile in Alzheimer's disease patients after ingestion of an antioxidant beverage. *CNS Neurol. Disord. Drug Targets* 12, 1233–1241. doi: 10.2174/18715273113129990075

Sánchez-Rodríguez, M. A., Santiago, E., Arronte-Rosales, A., Vargas-Guadarrama, L., and Mendoza-Núñez, V. (2006). Relationship between oxidative stress and cognitive impairment in the elderly of rural vs. urban communities. *Life Sci.* 78, 1682–1687. doi: 10.1016/j.lfs.2005.08.007

Sankowski, R., Mader, S., and Valdes-Ferrer, S. I. (2015). Systemic inflammation and the brain: Novel roles of genetic, molecular, and environmental cues as drivers of neurodegeneration. *Front. Cell. Neurosci.* 9:28. doi: 10.3389/fncel.2015.00028

Sasayama, D., Hori, H., Teraishi, T., Hattori, K., Ota, M., Matsuo, J., et al. (2012). Association of cognitive performance with interleukin-6 receptor Asp358Ala polymorphism in healthy adults. *J. Neural Transm.* 119, 313–318. doi: 10.1007/s00702-011-0709-3

Schram, M. T., Euser, S., de Craen, A., Witteman, J., Frölich, M., Hofman, A., et al. (2007). Systemic markers of inflammation and cognitive decline in old age. *J. Am. Geriatr. Soc.* 55, 708–716. doi: 10.1111/j.1532-5415.2007.01159.x

Sempowski, G. D., Hale, L., Sundy, J., Massey, J., Koup, R., Douek, D., et al. (2000). Leukemia inhibitory factor, oncostatin M, IL-6, and stem cell factor mRNA expression in human thymus increases with age and is associated with thymic atrophy. *J. Immunol.* 164, 2180–2187. doi: 10.4049/jimmunol.164.4.2180

Sharma, M., Fitzpatrick, A., Arnold, A., Chi, G., Lopez, O., Jenny, N., et al. (2016). Inflammatory biomarkers and cognitive decline: The Ginkgo evaluation of memory study. *J. Am. Geriatr. Soc.* 64, 1171–1177. doi: 10.1111/jgs.14140

Shen, X. N., Niu, L., Wang, Y., Cao, X., Liu, Q., Tan, L., et al. (2019). Inflammatory markers in Alzheimer's disease and mild cognitive impairment: A meta-analysis and systematic review of 170 studies. *J. Neurol. Neurosurg. Psychiatry* 90, 590–598. doi: 10.1136/jnnp-2018-319148

Sheng, J. G., Mrak, R. E., and Griffin, W. S. (1998). Enlarged and phagocytic, but not primed, interleukin-1 alpha-immunoreactive microglia increase with age in normal human brain. *Acta Neuropathol.* 95, 229–234.

Shi, Y., Zhang, S., Xue, Y., Yang, Z., Lin, Y., Liu, L., et al. (2020). IL-35 polymorphisms and cognitive decline did not show any association in patients with coronary heart disease over a 2-year period: A retrospective observational study (STROBE compliant). *Medicine* 99:e21390. doi: 10.1097/MD.0000000000021390

Shintani, F., Kanba, S., Nakaki, T., Nibuya, M., Kinoshita, N., Suzuki, E., et al. (1993). Interleukin-1 beta augments release of norepinephrine, dopamine, and serotonin in the rat anterior hypothalamus. *J. Neurosci.* 13, 3574–3581. doi: 10.1523/JNEUROSCI.13-08-03574.1993

Singh-Manoux, A., Dugravot, A., Brunner, E., Kumari, M., Shipley, M., Elbaz, A., et al. (2014). Interleukin-6 and C-reactive protein as predictors of cognitive decline in late midlife. *Neurology* 83, 486–493. doi: 10.1212/WNL.0000000000000665

Sochocka, M., Sobczyński, M., Sender-Janeczek, A., Zwolińska, K., Błachowicz, O., Tomczyk, T., et al. (2017). Association between periodontal health status and cognitive abilities. The role of cytokine profile and systemic inflammation. *Curr. Alzheimer Res.* 14, 978–990. doi: 10.2174/1567205014666170316163340

Swardfager, W., Lanctôt, K., Rothenburg, L., Wong, A., Cappell, J., and Herrmann, N. (2010). A meta-analysis of cytokines in Alzheimer's disease. *Biol. Psychiatry* 68, 930–941. doi: 10.1016/j.biopsych.2010.06.012

Takeda, S., Sato, N., Ikimura, K., Nishino, H., Rakugi, H., Morishita, R., et al. (2013). Increased blood-brain barrier vulnerability to systemic inflammation in an Alzheimer disease mouse model. *Neurobiol. Aging* 34, 2064–2070. doi: 10.1016/j.neurobiolaging.2013.02.010

Teblick, A., Peeters, B., Langouche, L., and Van den Berghe, G. (2019). Adrenal function and dysfunction in critically ill patients. *Nat. Rev. Endocrinol.* 15, 417–427.

Teixeira, A. L., Reis, H., Coelho, F., Carneiro, D., Teixeira, M., Vieira, L., et al. (2008). All-or-nothing type biphasic cytokine production of human lymphocytes after exposure to Alzheimer's beta-amyloid peptide. *Biol. Psychiatry* 64, 891–895. doi: 10.1016/j.biopsych.2008.07.019

Teunissen, C. E., Lütjohann, D., von Bergmann, K., Verhey, F., Vreeling, F., Wauters, A., et al. (2003). Combination of serum markers related to several mechanisms in Alzheimer's disease. *Neurobiol. Aging* 24, 893–902. doi: 10.1016/S0197-4580(03)00005-8

Tilvis, R. S., Kähönen-Väre, M., Jolkkonen, J., Valvanne, J., Pitkala, K., Strandberg, T., et al. (2004). Predictors of cognitive decline and mortality of aged people over a 10-year period. *J. Gerontol. A Biol. Sci. Med. Sci.* 59, 268–274. doi: 10.1093/gerona/59.3.m268

Toledo, R. S., Stein, D., Sanches, P., da Silva, L., Medeiros, H., Fregni, F., et al. (2021). rTMS induces analgesia and modulates neuroinflammation and neuroplasticity in neuropathic pain model rats. *Brain Res.* 1762:147427. doi: 10.1016/j.brainres.2021.147427

Uslu, S., Akarkarasu, Z., Ozbabalik, D., Ozkan, S., Colak, O., Demirkan, E., et al. (2012). Levels of amyloid beta-42, interleukin-6 and tumor necrosis factor-alpha in Alzheimer's disease and vascular dementia. *Neurochem. Res.* 37, 1554–1559. doi: 10.1007/s11064-012-0750-0

van den Brink, A. C., Brouwer-Brolsma, E., Berendsen, A., and van de Rest, O. (2019). The mediterranean, dietary approaches to stop hypertension (DASH), and mediterranean-DASH Intervention for Neurodegenerative Delay (MIND) diets are associated with less cognitive decline and a lower risk of Alzheimer's disease-a review. *Adv. Nutr.* 10, 1040–1065. doi: 10.1093/advances/nmz054

Villarreal, A. E., O'Bryant, S., Edwards, M., Grajales, S., Britton, G., and Panama Aging Research Initiative. (2016). Serum-based protein profiles of Alzheimer's disease and mild cognitive impairment in elderly Hispanics. *Neurodegener. Dis. Manag.* 6, 203–213. doi: 10.2217/nmt-2015-0009

Vitkovic, L., Konsman, J., Bockaert, J., Dantzer, R., Homburger, V., and Jacque, C. (2000b). Cytokine signals propagate through the brain. *Mol. Psychiatry* 5, 604–615. doi: 10.1038/sj.mp.4000813

Vitkovic, L., Bockaert, J., and Jacque, C. (2000a). "Inflammatory" cytokines: Neuromodulators in normal brain? *J. Neurochem.* 74, 457–471.

Wang, T., Xiao, S., Liu, Y., Lin, Z., Su, N., Li, X., et al. (2014). The efficacy of plasma biomarkers in early diagnosis of Alzheimer's disease. *Int. J. Geriatr. Psychiatry* 29, 713–719.

Weaver, J. D., Huang, M., Albert, M., Harris, T., Rowe, J., and Seeman, T. (2002). Interleukin-6 and risk of cognitive decline: MacArthur studies of successful aging. *Neurology* 59, 371–378. doi: 10.1212/wnl.59.3.371

Wei, J., Xu, H., Davies, J., and Hemmings, G. (1992). Increase of plasma IL-6 concentration with age in healthy subjects. *Life Sci.* 51, 1953–1956. doi: 10.1016/0024-3205(92)90112-3

Wells, G., Shea, B. J., O'Connell, D., Peterson, J., Welch, V., Losos, M., et al. (2000). *The Newcastle-Ottawa Scale (NOS) for assessing the quality of nonrandomised studies in meta-analyses.* Available online at: http://www.ohri.ca/programs/clinical_epidemiology/oxford.htm (accessed December, 2020).

Wilson, C. J., Finch, C. E., and Cohen, H. J. (2002). Cytokines and cognition–the case for a head-to-toe inflammatory paradigm. *J. Am. Geriatr. Soc.* 50, 2041–2056. doi: 10.1046/j.1532-5415.2002.50619.x

Yaffe, K., Lindquist, K., Penninx, B., Simonsick, E., Pahor, M., Kritchevsky, S., et al. (2003). Inflammatory markers and cognition in well-functioning African-American and white elders. *Neurology* 61, 76–80. doi: 10.1212/01.wnl.0000073620.42047.d7

Yang, X., Chen, Y., Zhang, W., Zhang, Z., Yang, X., Wang, P., et al. (2020). Association between inflammatory biomarkers and cognitive dysfunction analyzed by MRI in diabetes patients. *Diabetes Metab. Syndr. Obes.* 13, 4059–4065.

Yarchoan, M., Louneva, N., Xie, S., Swenson, F., Hu, W., Soares, H., et al. (2013). Association of plasma C-reactive protein levels with the diagnosis of Alzheimer's disease. *J. Neurol. Sci.* 333, 9–12. doi: 10.1016/j.jns.2013.05.028

Ye, S. M., and Johnson, R. W. (1999). Increased interleukin-6 expression by microglia from brain of aged mice. *J. Neuroimmunol.* 93, 139–148. doi: 10.1016/S0165-5728(98)00217-3

Yirmiya, E. T., Mekori-Domachevsky, E., Weinberger, R., Taler, M., Carmel, M., Gothelf, D., et al. (2020). Exploring the potential association among sleep disturbances, cognitive impairments, and immune activation in 22q11.2 deletion syndrome. *Am. J. Med. Genet. A* 182, 461–468. doi: 10.1002/ajmg.a.61424

Zhao, B., and Schwartz, J. P. (1998). Involvement of cytokines in normal CNS development and neurological diseases: Recent progress and perspectives. *J. Neurosci. Res.* 52, 7–16. doi: 10.1002/(SICI)1097-4547(19980401)52:1<7::AID-JNR2>3.0.CO;2-I

Zhao, S. J., Guo, C., Wang, M., Chen, W., and Zhao, Y. (2012). Serum levels of inflammation factors and cognitive performance in amnestic mild cognitive impairment: A Chinese clinical study. *Cytokine* 57, 221–225. doi: 10.1016/j.cyto.2011.11.006

Zheng, M., Chang, B., Tian, L., Shan, C., Chen, H., Gao, Y., et al. (2019). Relationship between inflammatory markers and mild cognitive impairment in Chinese patients with type 2 diabetes: A case-control study. *BMC Endocr. Disord.* 19:73. doi: 10.1186/s12902-019-0402-3

Zhu, Y., Chai, Y., Hilal, S., Ikram, M., Venketasubramanian, N., Wong, B., et al. (2017). Serum IL-8 is a marker of white-matter hyperintensities in patients with Alzheimer's disease. *Alzheimers Dement.* 7, 41–47. doi: 10.1016/j.dadm.2017.01.001

Zuliani, G., Ranzini, M., Guerra, G., Rossi, L., Munari, M., Zurlo, A., et al. (2007). Plasma cytokines profile in older subjects with late onset Alzheimer's disease or vascular dementia. *J. Psychiatr. Res.* 41, 686–693. doi: 10.1016/j.jpsychires.2006.02.008

frontiers | Frontiers in Aging Neuroscience

TYPE Original Research
PUBLISHED 07 February 2023
DOI 10.3389/fnagi.2023.1051298

OPEN ACCESS

EDITED BY
Ann-Maree Vallence,
Murdoch University,
Australia

REVIEWED BY
Richard J. Elsworthy,
University of Birmingham,
United Kingdom
Ola Osama Khalaf,
Cairo University,
Egypt

*CORRESPONDENCE
Kai Zheng
✉ diazna2002@sina.com
Cuntai Zhang
✉ ctzhang0425@163.com

SPECIALTY SECTION
This article was submitted to Neurocognitive Aging and Behavior, a section of the journal Frontiers in Aging Neuroscience

RECEIVED 22 September 2022
ACCEPTED 16 January 2023
PUBLISHED 07 February 2023

CITATION
Chen J, Chen X, Mao R, Fu Y, Chen Q, Zhang C and Zheng K (2023) Hypertension, sleep quality, depression, and cognitive function in elderly: A cross-sectional study. *Front. Aging Neurosci.* 15:1051298. doi: 10.3389/fnagi.2023.1051298

Hypertension, sleep quality, depression, and cognitive function in elderly: A cross-sectional study

Jiajie Chen, Xi Chen, Ruxue Mao, Yu Fu, Qin Chen, Cuntai Zhang* and Kai Zheng*

Department of Geriatrics, Tongji Hospital, Tongji Medical College, Huazhong University of Science and Technology, Wuhan, China

Background: Hypertension, sleep disorders, and depression are highly prevalent in the elderly population and are all associated with cognitive impairment, but the role that sleep quality and depression play in the association between hypertension and cognitive impairment is unclear. The aim of this study was to investigate whether sleep quality and depression have a mediating role in the association between hypertension and cognitive impairment.

Methods: A cross-sectional study was conducted to collect data from the Tongji Hospital Comprehensive Geriatric Assessment Database. Sleep quality, depression and cognitive function were measured by the Pittsburgh Sleep Quality Index (PSQI), the Geriatric Depression Scale (GDS-15) and the Mini-Mental State Examination (MMSE), respectively. Correlation analysis, regression analysis and Bootstrap analysis were used to examine correlations between key variables and mediating effects of sleep quality and depression. Adjustments for multiple comparisons were performed using Benjamini-Hochberg adjustment for multiple testing.

Results: A total of 827 participants were included, hypertension was present in 68.3% of the sample. After correcting for covariates, hypertensive patients aged 65years or older had worse cognitive function, poorer-sleep quality and higher levels of depression. Sleep quality was significantly negatively associated with depression and cognitive function, while depression was negatively associated with cognitive function. Mediation analysis revealed that hypertension can affect cognitive function in older adults through a single mediating effect of sleep quality and depression and a chain mediating effect of sleep quality and depression.

Conclusion: This study found that sleep quality and depression can mediate the relationship between hypertension and cognitive function in elderly. Enhanced supervision of sleep quality and depression in elderly patients with hypertension may be beneficial in maintaining cognitive function.

KEYWORDS

hypertension, sleep quality, depression, cognitive function, mediating effects

Introduction

Hypertension is a highly prevalent disease affecting two-thirds of adults over 65 years old (Mills et al., 2016). It is associated with a significantly increased risk of major adverse cardiovascular and cerebrovascular events and death, including heart disease, stroke, renal failure, and cognitive impairment (Oliveros et al., 2020; Heizhati et al., 2021). Numerous studies have found that hypertension is associated with increased incidence of cognitive decline, vascular cognitive

impairment, and Alzheimer's disease (Chudiak et al., 2018; Ungvari et al., 2021). But in a cohort study with an average age of 75 years, no association was found between hypertension and dementia (Shah et al., 2006). In addition, a protective effect of hypertension on cognitive function was found in a cohort study of participants over 90 years (Corrada et al., 2017).

In addition to increasing the incidence of cardiovascular events, hypertension is often associated with somatic symptoms, lower quality of life, and role impairment (He, 2016). The headache, chest pain, and dizziness of hypertension often cause poor sleep quality (Saccò et al., 2013; Rabner et al., 2018). A large population-based study conducted in China found that hypertensive patients had poorer sleep quality than healthy people (Liu et al., 2016). In addition to this, hypertension is also associated with psychological problems and depression (Cramer et al., 2020; Hamam et al., 2020), and the prevalence of depression in adults with hypertension was 37.8% (Asmare et al., 2022). Among them, older hypertensive patients (aged 50 years and above) have a higher chance of depression, roughly twice as much as younger hypertensive patients (aged 18–49 years; Boima et al., 2020). However, the sleep quality and emotional state of many patients with hypertension have not been paid enough attention by doctors and patients themselves.

One third of human life is spent in sleep, and too long or too short sleep duration increases the risk of cardiovascular events and death (Wang et al., 2019). The prevalence of sleep disorders increases with age, thereby affecting a variety of neurological functions including cognitive function (Bradley et al., 2020). Poor sleep quality is an important symptom of sleep disorders (Fabbri et al., 2021). Studies found that poor sleep quality would aggravate the decline of subjective cognitive ability and increase the risk of dementia (Li et al., 2021; Xu et al., 2021). There is also a relationship between sleep quality and depression, and the link may be bidirectional (Komada et al., 2011; Li et al., 2018). And the relationship between depression and cognitive impairment in the elderly has been reported in several studies (Camacho-Conde and Galán-López, 2020; Chow et al., 2022).

Therefore, we aimed to determine the relationship between hypertension and cognitive function in adults over 50 years of age, and specifically analyze different age groups, and assess whether sleep quality and depression are mediating factors. This may provide a reference for improving the cognitive dysfunction of patients with hypertension and poor sleep quality or depression.

Materials and methods

Study design and population

This cross-sectional study was conducted between October 2019 and August 2022. Data were collected from the Comprehensive Geriatric Assessment Database of Tongji Hospital, Tongji Medical College, Huazhong University of Science and Technology, in China, whose ethics committee approved the study (TJ-IBR20220731). Inclusion criteria were as follows: (1) age 50 or older, (2) complete data on sleep quality, depression and cognitive function. Exclusion criteria were as follows: (1) brain tumors or mental illnesses including schizophrenia, organic psychosis and anxiety, (2) medical records were incomplete.

Hypertension assessment

Hypertension was previously diagnosed by a physician as high blood pressure or systolic blood pressure ≥140 mm Hg or diastolic blood pressure ≥90 mm Hg (Jones et al., 2020). To measure blood pressure, participants remained seated and rested for at least 5 min, and then blood pressure was measured three times, each 2 min apart. The last measurement was recorded as the average of the second and third measurements (Lima-Costa et al., 2018).

Cognitive assessment

Cognitive function was assessed by Mini-Mental State Examination (MMSE). MMSE consists of 30 individual items in eight dimensions (time orientation, place orientation, concentration, attention and calculation, recall, naming, comprehension/executive function, visuospatial skills), with a total score ranging from 0 to 30 (Jia et al., 2021). A higher score indicates better cognitive function. The diagnosis of cognitive impairment based on MMSE are different for people with different education levels. MMSE ≤19 for illiterate individuals, ≤22 participants with primary education, and ≤26 for those with middle school education and above was considered to be mild cognition impairment (MCI; Jia et al., 2021). The diagnostic criteria for dementia are according to the Diagnostic and Statistical Manual of Mental Disorders, Fourth Edition (DSM-IV; Creavin et al., 2016).

Sleep quality

The Pittsburgh Sleep Quality Index (PSQI) was used to assess the quality of sleep during the past month. PSQI consists of 19 individual items in seven dimensions (subjective sleep quality, sleep latency, sleep duration, habitual sleep efficiency, sleep disturbances, use of sleep medication, and daytime dysfunction), each with a score of 0–3. The total score of PSQI is between 0 and 21, higher scores indicate poorer sleep quality (Xu et al., 2021). Mostly, scores >5 are considered as poor self-reported sleep quality (Buysse et al., 1989).

Depression

The Geriatric Depression Scale (GDS-15) was used to assess depression. The GDS-15 asks participants to answer 15 yes/no questions related to depressive symptoms. The total score ranges from 0 to 15, with a score of 5 or more being considered a symptom of depression, with higher scores representing more severe depressive symptoms (Chen et al., 2021).

Covariates

In the present study, we included as covariates confounding factors that may influence the relationship between hypertension and cognitive function. Among these, information on demographic and social characteristics included age, gender, and education level (primary school or below, middle school, high school, and college or above). Information on participants' cases was also reviewed to collect information on whether participants had comorbid diabetes, stroke, coronary heart disease (CHD), and hyperlipidemia. Body Mass Index (BMI) = weight (in kg)/height^2 (in m^2). Smoking was defined as current smoking of at least one cigarette per day for 6 months or more. Drinking was defined as alcohol consumption at least once per week.

Statistical analysis

We used unpaired *t*-test for continuous variables and χ^2 test for categorical variables to compare participants with and without hypertension. Given that age-specific effects of hypertension on cognitive function may differ, we stratified our analyses by two age groups (aged 50–64 years, aged 65 years or older). Pearson correlation analysis and Spearman correlation analysis were used to explore the associations between hypertension, sleep quality, depression, and cognitive function. Linear regression models were used to investigate the association between hypertension, sleep quality, depression and cognitive function. We showed the beta coefficients for three nested models: (1) unadjusted; (2) adjusted for sociodemographic factors (age, sex, and education); (3) fully adjusted, including sociodemographic factors, diabetes, stroke, CHD, hyperlipidemia, BMI, smoking, and drinking. Before analysis, PSQI, GDS-15 and MMSE were standardized (Z score). The false discovery rates were adjusted by Benjamini-Hochberg, where $p < 0.05$ was the cutoff value for significance of coefficients of independent variables. All statistical analyses were performed using IBM SPSS V24.0 software (SPSS Inc., Chicago, IL, United States), and all tests were two-sided with significance level set at 0.05 (two-tailed).

Based on the results of the correlation analysis, we specifically examined the mediating effect of sleep quality and depression on the association between hypertension and cognitive function. The bias-corrected Bootstrap method in the PROCESS 3.5 Procedure for SPSS was used to explore a multiple mediation model, which was developed by Hayes (2013).

Results

A total of 982 participants were searched in the database, and 827 participants were finally included for analysis according to the inclusion and exclusion criteria, as described in Figure 1. The sociodemographic, anthropometric, lifestyle factors, sleep quality, depression, and cognitive function of participants grouped by hypertension status were shown in Table 1. In the whole sample, the average age of the subjects was 77.18 ± 10.78 years old, and 45.0% of them were women. Hypertension was present in 68.3% of the sample. In both age groups, the prevalence of hypertension was higher in people aged 65 years or older (73.5% vs. 36.0%). The MMSE score of the total participants was 23.30 ± 7.09, PSQI score was 7.74 ± 4.50, and GDS-15 score was 5.01 ± 3.84. In these two age groups, patients with hypertension have poorer cognitive function, more smokers, higher BMI, and higher stroke prevalence. Compared with participants aged 50–64, among people aged 65 or older, patients with hypertension drank and smoked more, had higher BMI, lower education level, higher prevalence of diabetes, stroke, coronary heart disease, hyperlipidemia, poorer cognitive function, higher GDS-15 scores, and poorer sleep quality.

The correlation between key variables is shown in Table 2. Hypertension was positively associated with poor sleep quality and depression, but negatively associated with cognitive function. Depression was positively associated with poor sleep quality and significantly negatively associated with cognitive function. There was a significant negative association between poor sleep quality and cognitive function. The correlation was evident mainly among participants over 65 years or older. Table 3 shows the regression analysis of sleep quality and depression between hypertension and cognitive function. The total and direct effects of hypertension on cognitive function were significant in participants over 65 years of age. However, in people aged 50–64, there was no significant correlation between the above variables. The above conclusions were obtained after adjusting the covariates. The results of linear regression between the covariates and MMSE are in Supplementary Table 1.

Table 4 shows the mediating effect values of sleep quality and depression between hypertension and cognitive function in participants aged 65 years or older. Figure 2 shows the chain mediation model between hypertension and cognitive function in participants aged 65 years or older. Sleep quality and depression had a significant mediating effect between hypertension and

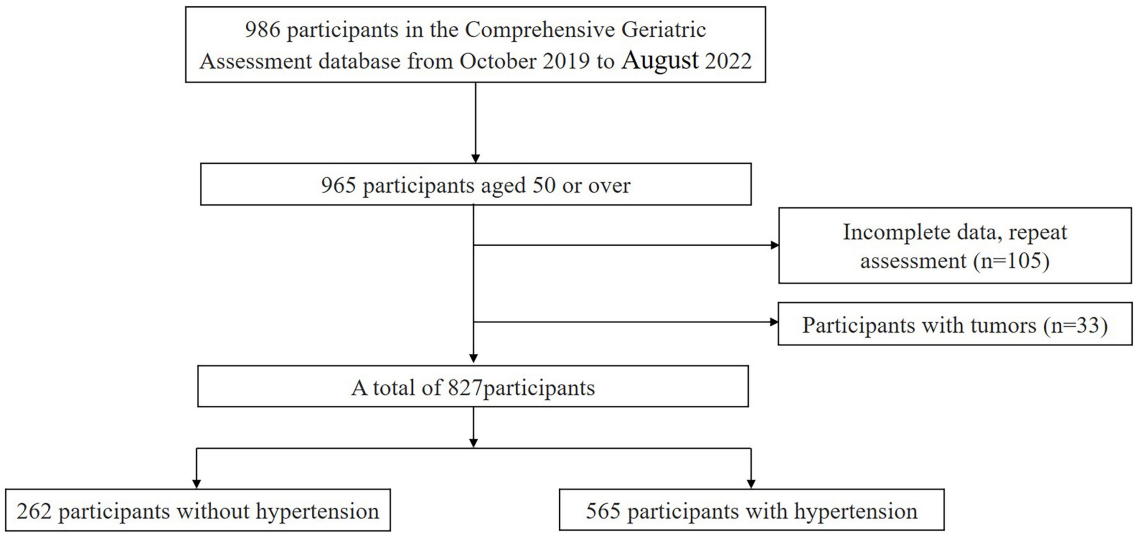

FIGURE 1
Participant inclusion flow chart.

TABLE 1 Participant characteristics according to hypertension and stratified by age groups.

	Whole sample			Adults aged 50-64years			Adults aged 65years or older		
	No (*n*=262)	Yes (*n*=565)	*p*	No (*n*=73)	Yes (*n*=41)	*p*	No (*n*=189)	Yes (*n*=524)	*p*
MMSE, mean (SD)	26.50 ± 4.35	21.82 ± 7.62	<0.001	27.38 ± 3.46	26.12 ± 4.24	0.09	26.15 ± 4.61	21.49 ± 7.72	<0.001
Age (years), mean (SD)	72.23 ± 11.04	79.47 ± 9.85	<0.001	59.00 ± 3.85	59.07 ± 4.25	0.93	77.33 ± 8.33	81.07 ± 8.25	<0.001
Women, *n* (%)	128 (48.9)	244 (43.2)	0.13	41 (56.2)	18 (43.9)	0.21	87 (46.0)	226 (43.1)	0.49
Drinking, *n* (%)	19 (7.3)	88 (15.6)	0.001	8 (11.0)	4 (9.8)	0.84	11 (5.8)	84 (16.0)	<0.001
Smoking, *n* (%)	39 (14.9)	155 (27.4)	<0.001	11 (15.1)	13 (31.7)	0.04	28 (14.8)	142 (27.1)	0.001
BMI, mean (SD)	22.08 ± 3.31	23.17 ± 3.47	<0.001	22.12 ± 3.34	24.35 ± 3.98	0.002	22.06 ± 3.31	23.08 ± 3.42	<0.001
Education, *n* (%)			0.001			0.06			0.008
Primary school or below	50 (19.0)	106 (18.8)		2 (2.7)	4 (9.8)		48 (25.4)	102 (19.5)	
Middle school	44 (16.7)	165 (29.3)		12 (16.4)	12 (29.3)		32 (16.9)	153 (29.2)	
High school	65 (24.7)	100 (17.7)		23 (31.5)	6 (14.6)		42 (22.2)	94 (17.9)	
University or over	104 (39.5)	193 (34.2)		36 (49.3)	19 (46.3)		67 (35.4)	175 (33.4)	
Diabetes, *n* (%)	32 (12.2)	125 (22.1)	0.001	8 (11.0)	7 (17.1)	0.35	24 (12.7)	118 (22.5)	0.004
Stroke, *n* (%)	30 (11.5)	164 (29.0)	<0.001	4 (5.5)	13 (31.7)	<0.001	26 (13.8)	151 (28.8)	<0.001
Coronary heart disease, *n* (%)	12 (4.6)	121 (21.4)	<0.001	3 (4.1)	3 (7.3)	0.46	9 (4.8)	118 (22.5)	<0.001
Hyperlipidemia, *n* (%)	34 (13.0)	128 (22.7)	0.001	7 (9.6)	8 (19.5)	0.13	27 (14.3)	120 (22.9)	0.01
PSQI, mean (SD)	6.78 ± 3.92	8.19 ± 4.68	<0.001	6.23 ± 3.16	7.54 ± 4.69	0.12	6.99 ± 4.16	8.24 ± 4.68	0.001
GDS-15, mean (SD)	4.22 ± 3.76	5.38 ± 3.83	<0.001	4.19 ± 3.17	5.17 ± 3.71	0.14	4.23 ± 3.97	5.40 ± 3.84	<0.001

p compare participants with and without hypertension using the independent-samples *t*-test for continuous variables and the χ^2 test for categorical variables.

cognitive function, and the total mediating effect was −0.026. Specifically, the mediating effect consisted of three indirect effects: path 1 hypertension → sleep quality → cognitive function (−0.012), path 2 hypertension → depression → cognitive function (−0.01), and path 3 hypertension → sleep quality → depression → cognitive function (−0.004). The proportion of the three indirect effects of path 1, path 2 and path 3 was 7.02, 5.85 and 2.34%, respectively, and the 95% confidence interval did not contain zero, indicating that the three indirect effects were all significant. There was no significant difference among the three indirect effects. These results suggest that hypertension affects cognitive function not only through a single mediating effect of sleep quality and depression, but also through a chain mediating effect of sleep quality and depression in the elderly aged 65 years or older.

Discussion

Hypertension, sleep disorders, depression, and cognitive impairment all have a high prevalence in older adults, and the prevalence all increases with age, and co-morbidity of these disorders is common (Ou et al., 2020; Vanek et al., 2020). Our study explored the association between hypertension and cognitive function in elderly and is the first time to analyze the role of sleep quality and depression in it. The findings suggest that hypertension was significantly negatively associated with cognitive function in participants aged 65 years or older and this association was partially mediated by sleep quality and depression.

In our study, the prevalence of hypertension in the elderly over 65 years or old was much higher than that in the middle-aged (50–64 years old), which has also been reported in previous studies (Tsimihodimos et al., 2018). We found that elderly with hypertension had worse cognitive function than those with normal blood pressure, which is consistent with previous findings. Vasilopoulos et al. (2012) reported no significant difference in cognitive function in hypertensive patients aged 51–60 years, while in the relationship between hypertension and cognitive function in the elderly, hypertension was found to have a negative effect on cognitive function in people aged 60–74 years (Qiu et al., 2005), and hypertension over 75 years patients showed a significant decrease in cognitive function (Streit et al., 2019). The possible mechanism for this is that as we age, the form of hypertension may change from systolic/diastolic hypertension to systolic hypertension and aortic atherosclerosis, which severely affects the blood supply to the brain and thus causes cognitive impairment (Boutouyrie et al., 2021).

The phenomenon of cognitive impairment in hypertensive patients can be partially explained by sleep disturbances and depressive symptoms. First, numerous studies have found a much higher prevalence of poor sleep quality in hypertensive patients than in non-hypertensive patients (Lo et al., 2018; Li et al., 2020). The prevalence of poor sleep quality in hypertensive patients was 35.5%, of which high diastolic blood pressure and lack of exercise were independent predictors of poor sleep quality (Birhanu et al., 2021). Sleep is essential for good health, and sleep benefits the consolidation of memory (Westermann et al., 2015), while sleep deprivation may cause brain dysfunction and lead to cognitive impairment (Porter et al., 2015). The formation of new memories in the hippocampus depends on undisturbed sleep, either before or after the initial encoding of potential memories (Mander et al.,

TABLE 2 The correlation among key variables.

	Whole sample				Adults aged 50–64years				Adults aged 65years or older			
	Hypertension	PSQI	GDS-15	MMSE	Hypertension	PSQI	GDS-15	MMSE	Hypertension	PSQI	GDS-15	MMSE
Hypertension	1				1				1			
PSQI	0.14**	1			0.1	1			0.12**	1		
GDS-15	0.17**	0.34**	1		0.12	0.24*	1		0.17**	0.35**	1	
MMSE	−0.36**	−0.20**	−0.22**	1	−0.18	0.04	−0.00	1	−0.33**	−0.20**	−0.23**	1

*$p < 0.05$.
**$p < 0.01$.

2017). In a large cohort study of older Chinese adults, lower habitual sleep efficiency was associated with a higher risk of memory impairment and poorer cognitive function (Ma X. Q. et al., 2019). Hypertension can not only directly impair cognitive function in the elderly, but also indirectly by reducing sleep quality.

Several studies have reported that hypertensive patients are more likely to experience depressive symptoms (Li et al., 2015; Ademola et al., 2019). Hypertensive patients often suffer from psychological distress due to antihypertensive medication side effects, decreased quality of life, and health impairment (Song et al., 2018). Recurrent depressive symptoms can lead to progressive hippocampal atrophy, which impairs memory function (Sheline et al., 2019). Due to the excessive activation of astrocytes and microglia, the level of inflammation in the hippocampus of depression model mice increased, and the cognitive function was impaired (Santos et al., 2016; Zhang et al., 2020). In population studies, depressive symptoms predict poorer memory scores and may be an early indicator of declining situational memory in older adults (Zahodne et al., 2014). A prospective study found that increased depressive symptoms at each life stage were associated with cognitive outcomes, and that depressive symptoms in later life were negatively associated with cognitive function and associated with a more rapid rate of cognitive decline (Mirza et al., 2016). Therefore, depression may play an important role in the impairment of cognitive function caused by hypertension.

The correlation between depressive symptoms and poor sleep quality in the elderly has been reported several times (Hu et al., 2020; Hsu et al., 2021). In animal experiments, chronic sleep deprivation induced depression-like behaviors in rat (Ma W. et al., 2019). Sleep deprivation in mice induces hippocampal neuroinflammation, which is a risk factor for depression (Kang et al., 2021). Sleep deprivation over-activated microglia in the mouse brain and causes a decrease in the level of anti-inflammatory factors associated with the hippocampus, which may be a possible cause of its depression (Ahmed et al., 2021). Among college students, as sleep quality deteriorates, the level of depression also increases., and the risk of depressive symptoms in students with poor sleep quality was 3.28 times (Çelik et al., 2019). Similarly, adolescent females exposed to stress such as sleep disruption are prone to hypothalamic–pituitary–adrenal sensitization which contributes to the development of mood disorders, such as depression (Murack et al., 2021). Of the 162 sleep related functional connections found in the human connectome study, 39 were also associated with depression scores (Cheng et al., 2018), which may partially explain the association between depression and poor sleep quality.

This study found the relationship between hypertension and cognitive impairment in people over 65 years or older can be partially mediated by sleep quality and depression, which suggests that attention should be paid to screening for sleep quality and depressive symptoms in elderly hypertensive patients, strengthening the diagnosis and treatment of sleep disorders and depression in the elderly, and improving the perception of mood disorders in elderly hypertensive patients, which may help to reduce the cognitive impairment and cardiovascular burden in patients.

Our study also has some limitations. This study was a cross-sectional study and could not establish a causal relationship between hypertension and cognitive function. Therefore, the

TABLE 3 Associations from multiple linear regression models of hypertension with sleep quality, depression and cognitive function.

	Result variable	Predictor variable	Unadjusted		Model 1		Model 2	
			β (95% CI)	p	β (95% CI)	p	β (95% CI)	p
Whole sample	MMSE	Hypertension	−0.31 (−0.37, −0.24)	<0.001	−0.21 (−0.27, −0.14)	<0.001	−0.14 (−0.19, −0.08)	<0.001
	PSQI	Hypertension	0.15 (0.08, 0.21)	<0.001	0.13 (0.06, 0.20)	<0.001	0.13 (0.06, 0.21)	0.001
	GDS-15	Hypertension	0.09 (0.03, 0.16)	0.005	0.09 (0.03, 0.16)	0.008	0.11 (0.04, 0.18)	0.004
		PSQI	0.32 (0.26, 0.39)	<0.001	0.32 (0.25, 0.38)	<0.001	0.31 (0.25, 0.38)	<0.001
	MMSE	Hypertension	−0.27 (−0.34, −0.21)	<0.001	−0.18 (−0.24, −0.12)	<0.001	−0.11 (−0.17, −0.06)	0.001
		PSQI	−0.11 (−0.18, −0.04)	0.002	−0.08 (−0.14, −0.02)	0.01	−0.08 (−0.13, −0.03)	0.004
		GDS-15	−0.15 (−0.21, −0.08)	<0.001	−0.13 (−0.19, −0.07)	<0.001	−0.09 (−0.15, −0.04)	0.001
Adults aged 50-64 years	MMSE	Hypertension	−0.16 (−0.18, 0.01)	0.15	−0.10 (−0.15, 0.04)	0.32	0.00 (−0.09, 0.10)	0.98
	PSQI	Hypertension	0.17 (−0.02, 0.29)	0.15	0.13 (−0.04, 0.26)	0.32	0.17 (−0.04, 0.31)	0.46
	GDS-15	Hypertension	0.10 (−0.07, 0.25)	0.38	0.11 (−0.07, 0.25)	0.32	0.14 (−0.06, 0.29)	0.46
		PSQI	0.22 (0.04, 0.42)	0.15	0.20 (0.02, 0.40)	0.2	0.16 (−0.03, 0.36)	0.46
	MMSE	Hypertension	−0.17 (−0.19, 0.01)	0.15	−0.12 (−0.16, 0.04)	0.32	−0.01 (−0.10, 0.09)	0.98
		PSQI	0.06 (−0.08, 0.16)	0.6	0.11 (−0.05, 0.19)	0.32	0.07 (−0.06, 0.15)	0.71
		GDS-15	0.01 (−0.11, 0.12)	0.95	−0.02 (−0.13, 0.11)	0.88	−0.00 (−0.11, 0.11)	0.98
Adults Aged 65 years or older	MMSE	Hypertension	−0.28 (−0.38, −0.23)	<0.001	−0.23 (−0.32, −0.18)	<0.001	−0.16 (−0.24, −0.11)	<0.001
	PSQI	Hypertension	0.12 (0.05, 0.21)	0.001	0.12 (0.04, 0.20)	0.003	0.12 (0.04, 0.21)	<0.001
	GDS-15	Hypertension	0.09 (0.02, 0.17)	0.01	0.09 (0.02, 0.17)	0.02	0.10 (0.03, 0.19)	0.006
		PSQI	0.33 (0.27, 0.40)	<0.001	0.33 (0.26, 0.40)	<0.001	0.32 (0.25, 0.39)	<0.001
	MMSE	Hypertension	−0.25 (−0.34, −0.19)	<0.001	−0.20 (−0.29, −0.15)	<0.001	−0.13 (−0.21, −0.08)	<0.001
		PSQI	−0.11 (−0.19, −0.04)	0.002	−0.10 (−0.17, −0.03)	0.005	−0.10 (−0.16, −0.04)	0.002
		GDS-15	−0.16 (−0.24, −0.09)	<0.001	−0.13 (−0.20, −0.06)	<0.001	−0.09 (−0.15, −0.03)	0.004

Estimates were calculated using linear regression analysis. Model 1 = adjusted for sociodemographic factors (age, sex and education). Model 2 = adjusted for sociodemographic factors + diabetes, stroke, coronary heart disease, hyperlipidemia, BMI, smoking and drinking. CI, credibility interval. A Benjamini-Hochberg adjustment was applied to the false discovery rate, where $p < 0.05$ was considered a statistically significant coefficient of the independent variable.

TABLE 4 Sleep quality and depression in the mediation effect analysis.

	Indirect effects	Boot SE	Boot LLCI	Boot ULCI	Relative mediation effect
Total indirect effect	−0.026	0.009	−0.044	−0.011	15.20%
Indirect effect 1	−0.012	0.006	−0.025	−0.003	7.02%
Indirect effect 2	−0.01	0.006	−0.023	−0.001	5.85%
Indirect effect 3	−0.004	0.002	−0.008	−0.001	2.34%
Compare 1	−0.002	0.008	−0.018	0.015	
Compare 2	−0.009	0.006	−0.021	0.001	
Compare 3	−0.006	0.005	−0.018	0.002	

The direct and indirect effects of hypertension on cognitive function are shown in this table. Boot SE, Boot LLCI, and Boot ULCI refer, respectively, to the standard error and the lower and upper limits of the 95% confidence interval of the indirect effects estimated by the percentile bootstrap method with deviation correction. Indirect effect1: hypertension→ sleep quality→ cognitive function; indirect effect 2: hypertension→ depression→ cognitive function; indirect effect 3: hypertension→ sleep quality→ depression→ cognitive function.

conclusion of this study is relatively less reliable than that of a cohort study. On the basis of this study, more in-depth cohort study should be conducted to further verify our conclusion after follow-up of the included patients. In terms of basic experiments, the specific mechanism of this mediating effect may be revealed by detecting depression and cognitive function in hypertensive model mice after sleep deprivation. Second, no specific classification of hypertension was made in this study, and also the small sample size may cause bias in the results.

Conclusion

In conclusion, the results of this study suggest that sleep quality and depression may partially mediate the relationship between hypertension and cognitive function in elderly over 65 years. Importantly, sleep quality and depression status can be reversed by intervention, which suggests that strengthening the supervision of sleep quality and depression in elderly hypertensive patients is of great significance for the prevention of cognitive dysfunction.

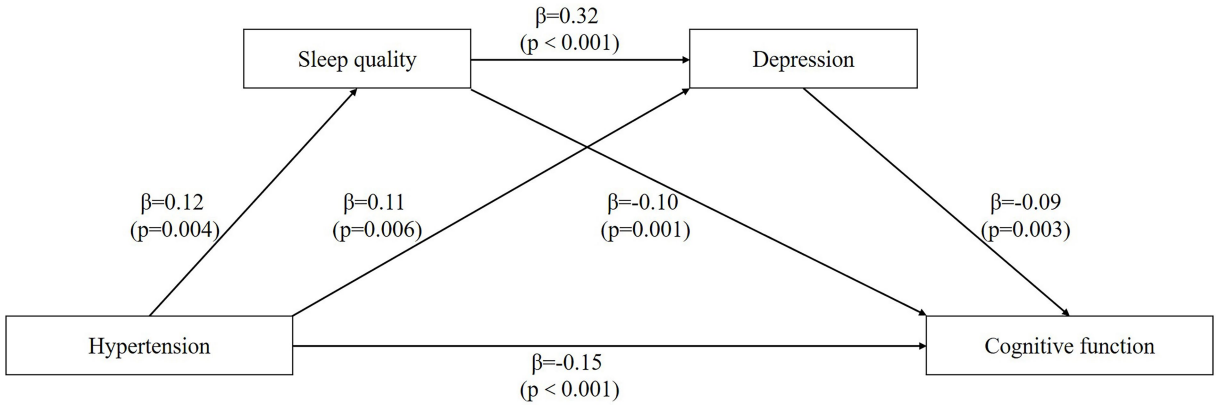

FIGURE 2
The chain mediation model. The chain mediation model shows the effects of hypertension, sleep quality, and depression on the cognitive function.

Data availability statement

The raw data supporting the conclusions of this article will be made available by the authors, without undue reservation.

Ethics statement

This study was approved by the ethics committee of the Huazhong University of Science and Technology, China (TJ-IBR20220731). Written informed consent was not required in accordance with local and institutional legislation.

Author contributions

KZ conceived and supervised the study, wrote the commentary and edited it. CZ conceptualized and supervised the study. JC analyzed the data and wrote the original draft. XC collected the data and wrote the original draft. RM and YF curated data. QC edited the manuscript. All authors contributed to the article and approved the submitted version.

Funding

This research was funded by the Fundamental Research Funds for the Central Universities (item number: 2019kfyXKJC055), and the National Key Research and Development Program of China (Project No. 2019YFC2004805 and 2020YFC2004800).

Acknowledgments

Thanks to all participants in this study and to the Department of Geriatrics, Tongji Hospital, Tongji Medical College, Huazhong University of Science and Technology, Wuhan, China for their support.

Conflict of interest

The authors declare that the research was conducted in the absence of any commercial or financial relationships that could be construed as a potential conflict of interest.

Publisher's note

All claims expressed in this article are solely those of the authors and do not necessarily represent those of their affiliated organizations, or those of the publisher, the editors and the reviewers. Any product that may be evaluated in this article, or claim that may be made by its manufacturer, is not guaranteed or endorsed by the publisher.

Supplementary material

The Supplementary material for this article can be found online at: https://www.frontiersin.org/articles/10.3389/fnagi.2023.1051298/full#supplementary-material

References

Ademola, A. D., Boima, V., Odusola, A. O., Agyekum, F., Nwafor, C. E., and Salako, B. L. (2019). Prevalence and determinants of depression among patients with hypertension: a cross-sectional comparison study in Ghana and Nigeria. *Niger. J. Clin. Pract.* 22, 558–565. doi: 10.4103/njcp.njcp_351_18

Ahmed, A., Misrani, A., Tabassum, S., Yang, L., and Long, C. (2021). Minocycline inhibits sleep deprivation-induced aberrant microglial activation and Keap1-Nrf2 expression in mouse hippocampus. *Brain Res. Bull.* 174, 41–52. doi: 10.1016/j.brainresbull.2021.05.028

Asmare, Y., Ali, A., and Belachew, A. (2022). Magnitude and associated factors of depression among people with hypertension in Addis Ababa, Ethiopia: a hospital based cross-sectional study. *BMC Psychiatry* 22:327. doi: 10.1186/s12888-022-03972-6

Birhanu, T. E., Getachew, B., Gerbi, A., and Dereje, D. (2021). Prevalence of poor sleep quality and its associated factors among hypertensive patients on follow up at Jimma University medical center. *J. Hum. Hypertens.* 35, 94–100. doi: 10.1038/s41371-020-0320-x

Boima, V., Tetteh, J., Yorke, E., Archampong, T., Mensah, G., Biritwum, R., et al. (2020). Older adults with hypertension have increased risk of depression compared to their younger counterparts: evidence from the World Health Organization study of global ageing and adult health wave 2 in Ghana. *J. Affect. Disord.* 277, 329–336. doi: 10.1016/j.jad.2020.08.033

Boutouyrie, P., Chowienczyk, P., Humphrey, J. D., and Mitchell, G. F. (2021). Arterial stiffness and cardiovascular risk in hypertension. *Circ. Res.* 128, 864–886. doi: 10.1161/CIRCRESAHA.121.318061

Bradley, A. J., Anderson, K. N., Gallagher, P., and Mcallister-Williams, R. H. (2020). The association between sleep and cognitive abnormalities in bipolar disorder. *Psychol. Med.* 50, 125–132. doi: 10.1017/S0033291718004038

Buysse, D. J., Reynolds, C. F., Monk, T. H., Berman, S. R., and Kupfer, D. J. (1989). The Pittsburgh sleep quality index: a new instrument for psychiatric practice and research. *Psychiatry Res.* 28, 193–213. doi: 10.1016/0165-1781(89)90047-4

Camacho-Conde, J. A., and Galán-López, J. M. (2020). Depression and cognitive impairment in institutionalized older adults. *Dement. Geriatr. Cogn. Disord.* 49, 107–120. doi: 10.1159/000508626

Çelik, N., Ceylan, B., Ünsal, A., and Çağan, Ö. (2019). Depression in health college students: relationship factors and sleep quality. *Psychol. Health Med.* 24, 625–630. doi: 10.1080/13548506.2018.1546881

Chen, L., Huang, J., Yang, L., Zeng, X.-A., Zhang, Y., Wang, X., et al. (2017). Sleep deprivation accelerates the progression of Alzheimer's disease by influencing Aβ-related metabolism. *Neurosci. Lett.* 650, 146–152. doi: 10.1016/j.neulet.2017.04.047

Chen, X., Zhao, L., Liu, Y., Zhou, Z., Zhang, H., Wei, D., et al. (2021). Otago exercise programme for physical function and mental health among older adults with cognitive frailty during COVID-19: a randomised controlled trial. *J. Clin. Nurs.* 1–14. doi: 10.1111/jocn.15964

Cheng, W., Rolls, E. T., Ruan, H., and Feng, J. (2018). Functional Connectivities in the brain that mediate the association between depressive problems and sleep quality. *JAMA Psychiat.* 75, 1052–1061. doi: 10.1001/jamapsychiatry.2018.1941

Chow, Y. Y., Verdonschot, M., Mcevoy, C. T., and Peeters, G. (2022). Associations between depression and cognition, mild cognitive impairment and dementia in persons with diabetes mellitus: a systematic review and meta-analysis. *Diabetes Res. Clin. Pract.* 185:109227. doi: 10.1016/j.diabres.2022.109227

Chudiak, A., Uchmanowicz, I., and Mazur, G. (2018). Relation between cognitive impairment and treatment adherence in elderly hypertensive patients. *Clin. Interv. Aging* 13, 1409–1418. doi: 10.2147/CIA.S162701

Corrada, M. M., Hayden, K. M., Paganini-Hill, A., Bullain, S. S., Demoss, J., Aguirre, C., et al. (2017). Age of onset of hypertension and risk of dementia in the oldest-old: the 90+ study. *Alzheimers Dement.* 13, 103–110. doi: 10.1016/j.jalz.2016.09.007

Cramer, H., Lauche, R., Adams, J., Frawley, J., Broom, A., and Sibbritt, D. (2020). Is depression associated with unhealthy behaviors among middle-aged and older women with hypertension or heart disease? *Womens Health Issues* 30, 35–40. doi: 10.1016/j.whi.2019.09.003

Creavin, S. T., Wisniewski, S., Noel-Storr, A. H., Trevelyan, C. M., Hampton, T., Rayment, D., et al. (2016). Mini-mental state examination (MMSE) for the detection of dementia in clinically unevaluated people aged 65 and over in community and primary care populations. *Cochrane Database Syst. Rev.* 2016:CD011145. doi: 10.1002/14651858.CD011145.pub2

Fabbri, M., Beracci, A., Martoni, M., Meneo, D., Tonetti, L., and Natale, V. (2021). Measuring subjective sleep quality: a review. *Int. J. Environ. Res. Public Health* 18, 1082–1132. doi: 10.3390/ijerph18031082

Hamam, M. S., Kunjummen, E., Hussain, M. S., Nasereldin, M., Bennett, S., and Miller, J. (2020). Anxiety, depression, and pain: considerations in the treatment of patients with uncontrolled hypertension. *Curr. Hypertens. Rep.* 22:106. doi: 10.1007/s11906-020-01117-2

Hayes, A. (2013). Introduction to Mediation, Moderation, and Conditional Process Analysis: A Regression-Based Approach.

He, J. (2016). Hypertension in China: a large and increasing public health challenge. *J. Hypertens.* 34, 29–31. doi: 10.1097/HJH.0000000000000818

Heizhati, M., Li, N., Wang, L., Hong, J., Li, M., Yang, W., et al. (2021). Association of Hypertension with mild cognitive impairment in population from less-developed areas of multiethnic Northwest China. *Neuroepidemiology* 55, 407–415. doi: 10.1159/000517956

Hsu, M.-F., Lee, K.-Y., Lin, T.-C., Liu, W.-T., and Ho, S.-C. (2021). Subjective sleep quality and association with depression syndrome, chronic diseases and health-related physical fitness in the middle-aged and elderly. *BMC Public Health* 21:164. doi: 10.1186/s12889-021-10206-z

Hu, Z., Zhu, X., Kaminga, A. C., Zhu, T., Nie, Y., and Xu, H. (2020). Association between poor sleep quality and depression symptoms among the elderly in nursing homes in Hunan province, China: a cross-sectional study. *BMJ Open* 10:e036401. doi: 10.1136/bmjopen-2019-036401

Jia, X., Wang, Z., Huang, F., Su, C., Du, W., Jiang, H., et al. (2021). A comparison of the mini-mental state examination (MMSE) with the Montreal cognitive assessment (MoCA) for mild cognitive impairment screening in Chinese middle-aged and older population: a cross-sectional study. *BMC Psychiatry* 21:485. doi: 10.1186/s12888-021-03495-6

Jones, N. R., Mccormack, T., Constanti, M., and Mcmanus, R. J. (2020). Diagnosis and management of hypertension in adults: NICE guideline update 2019. *Br. J. Gen. Pract.* 70, 90–91. doi: 10.3399/bjgp20X708053

Kang, X., Jiang, L., Lan, F., Tang, Y.-Y., Zhang, P., Zou, W., et al. (2021). Hydrogen sulfide antagonizes sleep deprivation-induced depression-and anxiety-like behaviors by inhibiting neuroinflammation in a hippocampal Sirt1-dependent manner. *Brain Res. Bull.* 177, 194–202. doi: 10.1016/j.brainresbull.2021.10.002

Komada, Y., Nomura, T., Kusumi, M., Nakashima, K., Okajima, I., Sasai, T., et al. (2011). Correlations among insomnia symptoms, sleep medication use and depressive symptoms. *Psychiatry Clin. Neurosci.* 65, 20–29. doi: 10.1111/j.1440-1819.2010.02154.x

Li, X., Ding, D., Zhao, Q., Wu, W., Xiao, Z., Luo, J., et al. (2021). Sleep timing and risk of dementia among the Chinese elderly in an Urban Community: the Shanghai aging study. *Front. Neurol.* 12:629507. doi: 10.3389/fneur.2021.629507

Li, Y., Hao, Y., Fan, F., and Zhang, B. (2018). The role of microbiome in insomnia, circadian disturbance and depression. *Front. Psychiatry* 9:669. doi: 10.3389/fpsyt.2018.00669

Li, L., Li, L., Chai, J.-X., Xiao, L., Ng, C. H., Ungvari, G. S., et al. (2020). Prevalence of poor sleep quality in patients with hypertension in China: a meta-analysis of comparative studies and epidemiological surveys. *Front. Psychiatry* 11:591. doi: 10.3389/fpsyt.2020.00591

Li, Z., Li, Y., Chen, L., Chen, P., and Hu, Y. (2015). Prevalence of depression in patients with hypertension: a systematic review and meta-analysis. *Medicine* 94:e1317. doi: 10.1097/MD.0000000000001317

Lima-Costa, M. F., De Andrade, F. B., De Souza, P. R. B., Neri, A. L., Duarte, Y. A. D. O., Castro-Costa, E., et al. (2018). The Brazilian longitudinal study of aging (ELSI-Brazil): objectives and design. *Am. J. Epidemiol.* 187, 1345–1353. doi: 10.1093/aje/kwx387

Liu, R.-Q., Qian, Z., Trevathan, E., Chang, J.-J., Zelicoff, A., Hao, Y.-T., et al. (2016). Poor sleep quality associated with high risk of hypertension and elevated blood pressure in China: results from a large population-based study. *Hypertens. Res.* 39, 54–59. doi: 10.1038/hr.2015.98

Lo, K., Woo, B., Wong, M., and Tam, W. (2018). Subjective sleep quality, blood pressure, and hypertension: a meta-analysis. *J. Clin. Hypertens. (Greenwich)* 20, 592–605. doi: 10.1111/jch.13220

Ma, X. Q., Jiang, C. Q., Xu, L., Zhang, W. S., Zhu, F., Jin, Y. L., et al. (2019). Sleep quality and cognitive impairment in older Chinese: Guangzhou biobank cohort study. *Age Ageing* 49, 119–124. doi: 10.1093/ageing/afz120

Ma, W., Song, J., Wang, H., Shi, F., Zhou, N., Jiang, J., et al. (2019). Chronic paradoxical sleep deprivation-induced depression-like behavior, energy metabolism and microbial changes in rats. *Life Sci.* 225, 88–97. doi: 10.1016/j.lfs.2019.04.006

Mander, B. A., Winer, J. R., and Walker, M. P. (2017). Sleep and human aging. *Neuron* 94, 19–36. doi: 10.1016/j.neuron.2017.02.004

Mills, K. T., Bundy, J. D., Kelly, T. N., Reed, J. E., Kearney, P. M., Reynolds, K., et al. (2016). Global disparities of hypertension prevalence and control: a systematic analysis of population-based studies from 90 countries. *Circulation* 134, 441–450. doi: 10.1161/CIRCULATIONAHA.115.018912

Mirza, S. S., Wolters, F. J., Swanson, S. A., Koudstaal, P. J., Hofman, A., Tiemeier, H., et al. (2016). 10-year trajectories of depressive symptoms and risk of dementia: a population-based study. *Lancet Psychiatry* 3, 628–635. doi: 10.1016/S2215-0366(16)00097-3

Murack, M., Chandrasegaram, R., Smith, K. B., Ah-Yen, E. G., Rheaume, É., Malette-Guyon, É., et al. (2021). Chronic sleep disruption induces depression-like behavior in adolescent male and female mice and sensitization of the hypothalamic-pituitary-adrenal axis in adolescent female mice. *Behav. Brain Res.* 399:113001. doi: 10.1016/j.bbr.2020.113001

Oliveros, E., Patel, H., Kyung, S., Fugar, S., Goldberg, A., Madan, N., et al. (2020). Hypertension in older adults: assessment, management, and challenges. *Clin. Cardiol.* 43, 99–107. doi: 10.1002/clc.23303

Ou, Y.-N., Tan, C.-C., Shen, X.-N., Xu, W., Hou, X.-H., Dong, Q., et al. (2020). Blood pressure and risks of cognitive impairment and dementia: a systematic review and meta-analysis of 209 prospective studies. *Hypertension* 76, 217–225. doi: 10.1161/HYPERTENSIONAHA.120.14993

Porter, V. R., Buxton, W. G., and Avidan, A. Y. (2015). Sleep, cognition and dementia. *Curr. Psychiatry Rep.* 17:97. doi: 10.1007/s11920-015-0631-8

Qiu, C., Winblad, B., and Fratiglioni, L. (2005). The age-dependent relation of blood pressure to cognitive function and dementia. *Lancet Neurol.* 4, 487–499. doi: 10.1016/S1474-4422(05)70141-1

Rabner, J., Kaczynski, K. J., Simons, L. E., and Lebel, A. (2018). Pediatric headache and sleep disturbance: a comparison of diagnostic groups. *Headache* 58, 217–228. doi: 10.1111/head.13207

Saccò, M., Meschi, M., Regolisti, G., Detrenis, S., Bianchi, L., Bertorelli, M., et al. (2013). The relationship between blood pressure and pain. *J. Clin. Hypertens. (Greenwich)* 15, 600–605. doi: 10.1111/jch.12145

Santos, L. E., Beckman, D., and Ferreira, S. T. (2016). Microglial dysfunction connects depression and Alzheimer's disease. *Brain Behav. Immun.* 55, 151–165. doi: 10.1016/j.bbi.2015.11.011

Shah, R. C., Wilson, R. S., Bienias, J. L., Arvanitakis, Z., Evans, D. A., and Bennett, D. A. (2006). Relation of blood pressure to risk of incident Alzheimer's disease and change in global cognitive function in older persons. *Neuroepidemiology* 26, 30–36. doi: 10.1159/000089235

Sheline, Y. I., Liston, C., and Mcewen, B. S. (2019). Parsing the hippocampus in depression: chronic stress, hippocampal volume, and major depressive disorder. *Biol. Psychiatry* 85, 436–438. doi: 10.1016/j.biopsych.2019.01.011

Song, X., Zhang, Z., Zhang, R., Wang, M., Lin, D., Li, T., et al. (2018). Predictive markers of depression in hypertension. *Medicine* 97:e11768. doi: 10.1097/MD.0000000000011768

Streit, S., Poortvliet, R. K. E., Elzen, W. P. J. D., Blom, J. W., and Gussekloo, J. (2019). Systolic blood pressure and cognitive decline in older adults with hypertension. *Ann. Fam. Med.* 17, 100–107. doi: 10.1370/afm.2367

Sun, J., Wu, J., Hua, F., Chen, Y., Zhan, F., and Xu, G. (2020). Sleep deprivation induces cognitive impairment by increasing blood-brain barrier permeability via CD44. *Front. Neurol.* 11:563916. doi: 10.3389/fneur.2020.563916

Tsimihodimos, V., Gonzalez-Villalpando, C., Meigs, J. B., and Ferrannini, E. (2018). Hypertension and diabetes mellitus: coprediction and time trajectories. *Hypertension* 71, 422–428. doi: 10.1161/HYPERTENSIONAHA.117.10546

Ungvari, Z., Toth, P., Tarantini, S., Prodan, C. I., Sorond, F., Merkely, B., et al. (2021). Hypertension-induced cognitive impairment: from pathophysiology to public health. *Nat. Rev. Nephrol.* 17, 639–654. doi: 10.1038/s41581-021-00430-6

Vanek, J., Prasko, J., Genzor, S., Ociskova, M., Kantor, K., Holubova, M., et al. (2020). Obstructive sleep apnea, depression and cognitive impairment. *Sleep Med.* 72, 50–58. doi: 10.1016/j.sleep.2020.03.017

Vasilopoulos, T., Kremen, W. S., Kim, K., Panizzon, M. S., Stein, P. K., Xian, H., et al. (2012). Untreated hypertension decreases heritability of cognition in late middle age. *Behav. Genet.* 42, 107–120. doi: 10.1007/s10519-011-9479-9

Wang, C., Bangdiwala, S. I., Rangarajan, S., Lear, S. A., Alhabib, K. F., Mohan, V., et al. (2019). Association of estimated sleep duration and naps with mortality and cardiovascular events: a study of 116632 people from 21 countries. *Eur. Heart J.* 40, 1620–1629. doi: 10.1093/eurheartj/ehy695

Westermann, J., Lange, T., Textor, J., and Born, J. (2015). System consolidation during sleep - a common principle underlying psychological and immunological memory formation. *Trends Neurosci.* 38, 585–597. doi: 10.1016/j.tins.2015.07.007

Xu, W.-Q., Lin, L.-H., Ding, K.-R., Ke, Y.-F., Huang, J.-H., Hou, C.-L., et al. (2021). The role of depression and anxiety in the relationship between poor sleep quality and subjective cognitive decline in Chinese elderly: exploring parallel, serial, and moderated mediation. *J. Affect. Disord.* 294, 464–471. doi: 10.1016/j.jad.2021.07.063

Zahodne, L. B., Stern, Y., and Manly, J. J. (2014). Depressive symptoms precede memory decline, but not vice versa, in non-demented older adults. *J. Am. Geriatr. Soc.* 62, 130–134. doi: 10.1111/jgs.12600

Zhang, H.-Y., Wang, Y., He, Y., Wang, T., Huang, X.-H., Zhao, C.-M., et al. (2020). A1 astrocytes contribute to murine depression-like behavior and cognitive dysfunction, which can be alleviated by IL-10 or fluorocitrate treatment. *J. Neuroinflammation* 17:200. doi: 10.1186/s12974-020-01871-9

frontiers | Frontiers in Aging Neuroscience

TYPE Original Research
PUBLISHED 09 March 2023
DOI 10.3389/fnagi.2023.1045263

OPEN ACCESS

EDITED BY
George M. Opie,
University of Adelaide,
Australia

REVIEWED BY
Jessica Bernard,
Texas A&M University, United States
Ruiwang Huang,
South China Normal University,
China

*CORRESPONDENCE
Hua Jin
✉ jinhua@tjnu.edu.cn

SPECIALTY SECTION
This article was submitted to Neurocognitive Aging and Behavior, a section of the journal Frontiers in Aging Neuroscience

RECEIVED 15 September 2022
ACCEPTED 20 February 2023
PUBLISHED 09 March 2023

CITATION
Yan S, Zhang Y, Yin X, Chen J, Zhu Z, Jin H, Li H, Yin J and Jiang Y (2023) Alterations in white matter integrity and network topological properties are associated with a decrease in global motion perception in older adults. *Front. Aging Neurosci.* 15:1045263. doi: 10.3389/fnagi.2023.1045263

Alterations in white matter integrity and network topological properties are associated with a decrease in global motion perception in older adults

Shizhen Yan[1], Yuping Zhang[2], Xiaojuan Yin[1], Juntao Chen[1], Ziliang Zhu[3], Hua Jin[1,4]*, Han Li[5], Jianzhong Yin[6] and Yunpeng Jiang[1,4]

[1]Faculty of Psychology, Tianjin Normal University, Tianjin, China, [2]Medicine School of Rehabilitation, Henan University of Chinese Medicine, Zhengzhou, China, [3]State Key Laboratory for Cognitive Neuroscience and Learning, Beijing Normal University, Beijing, China, [4]Key Research Base of Humanities and Social Sciences of the Ministry of Education, Academy of Psychology and Behavior, Tianjin Normal University, Tianjin, China, [5]The First Central Clinical College of Tianjin Medical University, Tianjin, China, [6]Department of Radiology, People's Hospital of Haikou, Haikou, China

Previous studies have mainly explored the effects of structural and functional aging of cortical regions on global motion sensitivity in older adults, but none have explored the structural white matter (WM) substrates underlying the age-related decrease in global motion perception (GMP). In this study, random dot kinematogram and diffusion tensor imaging were used to investigate the effects of age-related reductions in WM fiber integrity and connectivity across various regions on GMP. We recruited 106 younger adults and 94 older adults and utilized both tract-based spatial statistics analysis and graph theoretical analysis to comprehensively investigate group differences in WM microstructural and network connections between older and younger adults at the microscopic and macroscopic levels. Moreover, partial correlation analysis was used to explore the relationship between alterations in WM and the age-related decrease in GMP. The results showed that decreased GMP in older adults was related to decreased fractional anisotropy (FA) of the inferior frontal-occipital fasciculus, inferior longitudinal fasciculus, anterior thalamic radiation, superior longitudinal fasciculus, and cingulum cingulate gyrus. Decreased global efficiency of the WM structural network and increased characteristic path length were closely associated with decreased global motion sensitivity. These results suggest that the reduced GMP in older adults may stem from reduced WM integrity in specific regions of WM fiber tracts as well as decreased efficiency of information integration and communication between distant cortical regions, supporting the "disconnection hypothesis" of cognitive aging.

KEYWORDS

global motion perception, aging, white matter, structural network, TBSS

1. Introduction

Global motion perception (GMP) is a fundamental visual process that refers to the ability to combine local motion signals within a visual scene into a global percept to obtain information about motion speed and direction (Narasimhan and Giaschi, 2012). For example, in a football scene, the trajectory of each player (a local moving element) constantly changes, but the audience can obtain a global precept of the entire scene by integrating the trajectory of all players (e.g., the players on the field advancing toward a team's goal). This perceptual process plays an important role in navigation, judgment of motion speed, and avoidance of moving obstacles (Hoffman et al., 2015). One method extensively used to assess GMP is the random dot kinematogram (RDK), which consists of dots moving in various directions: signal dots move in a specific direction, while noise dots move in random directions (Pilz et al., 2017; Ward et al., 2018; Benassi et al., 2021; Joshi et al., 2021). The task is to identify the global direction of the moving dots. GMP is evaluated by measuring the individual motion coherence threshold (MCT): the minimum proportion of signal dots required to correctly identify the direction of global motion. A higher MCT indicates poorer performance and worse global motion sensitivity. Several studies have employed the RDK paradigm to study the effect of age on GMP. These studies found that older adults have reduced global motion sensitivity and significantly higher MCT than younger adults (Snowden and Kavanagh, 2006; Roudaia et al., 2010; Bower and Andersen, 2012). Several studies have shown that aging of the GMP is associated with a decreased ability to perceive hazards while driving (Wilkins et al., 2013; Lacherez et al., 2014). In addition, Yamasaki et al. (2016) reported that GMP aging may also be a predictor of cognitive decline in older adults. Thus, age-related declines in GMP are not only detrimental to the quality of life of older people, but also pose a serious threat to their safety as well.

Many studies have attempted to determine the neural mechanism underlying age-related decreases in GMP in older adults. Nevertheless, these studies have mainly focused on the effects of age-related structural and functional alterations in specific cerebral regions (Biehl et al., 2017; Ward et al., 2018; Jin et al., 2020, 2021). To date, little is known about the impact of white matter (WM) degeneration with age on GMP. WM fiber tracts are anatomical substrate underlying information transmission across various cerebral regions and are responsible for enabling information transfer between neurons and coordinating the fundamental functions of brain regions. According to the "disconnected brain" hypothesis of cognitive aging, decreases in structural and functional connectivity contribute to cognitive decline (Damoiseaux, 2017; Fjell et al., 2017; Coelho et al., 2021). More rapid higher-order cognitive functions require efficient communication across brain regions, but age-related alterations in the microstructural architecture of WM fiber tracts disrupt this communication, reducing cognitive function.

Diffusion tensor imaging (DTI) has been widely used to track alterations in WM underlying cognitive aging at a microstructural level. This method provides WM parameters that quantify and characterize the directionality and magnitude of water molecules in brain tissues and address WM integrity (Basser et al., 1994). Four parameters are commonly used to assess WM integrity: fractional anisotropy (FA), mean diffusivity (MD), axial diffusivity (AD), and radial diffusivity (RD). FA reflects the anisotropy of water molecule diffusion; MD represents the mean diffusivity of water molecules; AD reflects the diffusivity of water molecules parallel to the axon fibers; and RD indicates the diffusivity of water molecules perpendicular to the axon fibers. Higher FA values and lower MD, AD, and RD values indicate better microstructural integrity of brain tissues (Bennett and Madden, 2014). Numerous DTI studies have found a link between decreased WM integrity and cognitive impairment with age (Bennett and Madden, 2014; de Lange et al., 2016; Merenstein et al., 2021). These studies primarily concentrated on executive function, information processing speed, memory, and general cognitive ability; their findings supported the "disconnected brain" hypothesis (Sullivan and Pfefferbaum, 2007; Davis et al., 2009; Borghesani et al., 2013; Bennett and Madden, 2014; de Lange et al., 2016; Coelho et al., 2021). For example, the longitudinal study by Coelho et al. (2021) showed that FA in the corpus callosum (CC) and superior longitudinal fasciculus (SLF) significantly decreased in older adults, and this reduction in WM integrity was significantly associated with decreases in memory, executive function, and general cognitive performance.

Many researchers have investigated the neural underpinnings of GMP in WM (Csete et al., 2014; Braddick et al., 2017; Pamir et al., 2021). Using diffusion magnetic resonance imaging (dMRI), Csete et al. (2014) investigated the WM microstructure during motion detection; they observed that the local FA in specific WM regions (e.g., the left optic radiation) of adults was significantly correlated with their motion detection threshold. Advanced probabilistic tractography revealed that the SLF may be the tract that is closely associated with the GMP. Subsequently, Braddick et al. (2017) found that global motion sensitivity in children was positively correlated with FA in the right SLF and negatively correlated with FA in the left SLF. Furthermore, Pamir et al. (2021) recruited patients with impairment in the visual cortex and observed that the higher the RD in the tracts that connect the right V1 and V5 was, the worse the GMP. These studies demonstrate that GMP has neural correlates, providing indirect evidence for the hypothesis that age-related decreases in GMP may be associated with WM degradation.

In addition, researchers have not only explored changes in WM integrity but have also applied graph theoretical analysis to construct a WM structural network at a macroscopic level to quantitatively assess individual information transmission efficiency, network integration, and functional differentiation by using DTI. Graph theoretical analysis offers a global perspective that overcomes the limitations of previous research, in which each brain region was viewed as a discrete anatomical neural structure. This method provides new insights into the neural activity patterns of the brain and the connectivity mechanisms of various cognitive functions. Moreover, the quantitative topological measures of the WM structural network are sensitive to individual aging. Gong et al. (2009) applied graph theoretical analysis and that the local efficiency and overall cortical connectivity of the WM network decreased with increasing age after maturity. Moreover, older adults' cognitive function is impacted by this reduction in information integration. With 342 healthy older adults, Wen et al. (2011) explored the relationship between the WM network and multidimensional cognition and found that discrete neuroanatomical networks were highly associated with cognitive performance in specific domains, such as processing speed and visuospatial and executive function. Thus, exploration of GMP-related WM substrates can enhance understanding of neurological changes associated with age-related decreases in GMP

from the perspective of information integration and transmission efficiency.

The aim of the present study was to investigate the effects of age-related reduction in WM integrity and connectivity on GMP at WM microscopic and macroscopic levels using RDK and DTI. Previous studies have revealed that GMP mainly depends on regions of the dorsal visual stream and the parietal lobe (Biehl et al., 2017; Chaplin et al., 2017; Sousa et al., 2018; Ward et al., 2018). Our hypotheses were as follows: (1) Changes in the integrity of WM fiber tracts connecting the visual cortex to other cortical regions would be significantly correlated with changes in GMP in older adults. For example, the SLF provides bidirectional connections among the parietal, frontal, occipital, and temporal lobes and may thus play an important role in transmitting motion information from the occipital lobe to the parietal and prefrontal areas (Kamali et al., 2014); we predicted that its changes in the integrity would be correlated with changes in GMP. (2) Older adults would exhibit a reduced ability to integrate information in the WM network, as indicated by significant changes in topological properties (e.g., a significant increase in characteristic path length) that affect GMP.

2. Methods

2.1. Participants

We recruited 118 older and 113 younger adults for this study through an advertisement. The older adults were locals aged 60 years or older from Tianjin, China, and the younger adults were healthy university students. Before the formal experiment, all participants underwent screening for visual function and MRI contraindications. Vision screening was designed to assess the participants' eye health, i.e., whether there were physiological or pathological abnormalities of the visual system such as myopia, hyperopia, amblyopia, glaucoma, cataracts and age-related macular degeneration. The younger adults completed this assessment by self-reported questionnaires, while the older adults completed it with the help of two clinicians. In addition, the mental health of older adults was assessed using the Mini-Mental State Examination (MMSE), and their brain aging and pathological abnormalities were examined by two imaging clinicians.

Twenty-one older participants were excluded from the study because of the following structural abnormalities: brain tumors, atrophy, leukoaraiosis, infarcts, and cystic lesions. A total of 3 older and 7 younger participants were additionally excluded due to head movement artifacts (ring) in structural images or geometric distortions in DTI. Finally, 106 younger adults aged 18–27 years (23.04 ± 5.17 years old, 66 female) and 94 older adults aged 60–84 years (65.74 ± 4.50 years old, 55 female) were included in this study. The final participants met the following criteria: (1) normal or corrected-to-normal vision; (2) no significant history of neurological or psychiatric disease, serious physical illness, or substance abuse; (3) no contraindications to MRI or structural brain abnormalities; and (4) older adults scored more than 24 points on the MMSE (scores range: 26 ~ 30; $M \pm SD$: 28.80 ± 1.18) (Porter et al., 2017). All participants provided written informed consent and received payment for their participation. The study was approved by the Ethics Committees of Tianjin First Central Hospital and Tianjin Normal University.

2.2. RDK

The stimuli were created in MATLAB 2015a (MathWorks Inc. Natick, MA, United States), generated using a 17-inch HP Zbook17 G3 workstation, and displayed at a resolution of 1920 × 1,080 pixels (refresh rate of 60 Hz) and a mean luminance of 180 cd/m^2. A horizontally oriented RDK paradigm was used to assess individual GMP. The stimulus was presented in a circular aperture with a diameter of 11° at the center of the black screen, and it contained 1,00 white dots. The dot diameter was 2.16 arcmin, and the dot density was 0.88 dots/cm^2. All dots had a limited lifetime of 500 ms (equivalent to 10 frames). The position of each dot was randomly allocated at the beginning of each trial. Some of these dots (signal dots) moved horizontally to the left or right in a coherent manner. Once the dot moved out of the stimulus region, it was placed at a random position within the aperture, and set to move in the same direction as before. The other parts of dots (noise dots) are plotted in new locations, randomly selected within the display area, on each frame of the sequence. The global motion direction of each trial was randomly assigned, but the numbers of leftward and rightward trials were equal overall. The speed of the dots was set at 1°/s, 1.4°/s, or 1.8°/s to prevent potential anticipation or adaptation effects (Berry et al., 1999; Anton-Erxleben et al., 2013).

We employed a three-down/one-up (79.37% correct) adaptation staircase procedure to control the coherence level of moving dots. In other words, if three consecutive accurate responses were given, the coherence level was reduced by one step; if one incorrect response was given, it was increased by one step. For each session, there were eight reversals in coherence. The starting coherence level of the dots was 100%; the decrements had a step size of 10% (for the first two reversals) and 5% (for the third to eighth reversals). We calculated the average coherence level for the third to eighth reversals and regarded it as the global MCT for each participant. The MCT is the ratio of the minimum number of signal dots to the total number of dots required for an individual to identify the global motion direction of an RDK.

Participants sat in front of the center of the screen with a viewing distance of 60 cm. At the beginning of the sequence, a red fixation point was presented, followed by an RDK. Then, the participants were instructed to complete a two-alternative forced-choice task indicating whether the global direction of the RDK was to the left or to the right as quickly and accurately as possible. After participants responded, a white dot appeared, indicating the beginning of the next trial (Figure 1). The test consisted of six blocks, each block containing 60 trials, and was conducted in two sessions. Before the formal test, participants were given 20 practice trials to familiarize themselves with the procedure. The participants were able to control the rest time between blocks. The entire test took approximately 30 min to complete.

2.3. MRI data acquisition

Both older and younger adults were scanned using a 3.0 T Prisma (Siemens Healthcare, Germany) MRI scanner with a standard 64-channel head coil at the Brain Imaging Research Centers of Tianjin First Central Hospital and Tianjin Normal University, respectively. During the scan, the participants lay flat in the scanner with their heads immobilized by cushions to reduce head movement and wore earplugs to reduce noise and enhance comfort. For each participant,

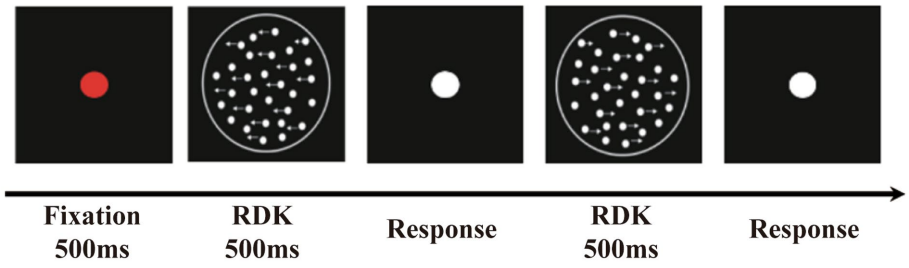

FIGURE 1
The random dot kinematogram paradigm (RDK). The stimuli contained some white luminance dots moved horizontally to the left or right coherently (signal dots) and other dots moved randomly (noise dots).

whole-brain anatomical data were collected using a T1-weighted 3-D MPRAGE sequence with the following parameters: echo Time (TE) = 2.98 ms, field of view (FOV) = 256 × 256 mm2, acquisition matrix size = 256 × 256, and voxel size = 3.5 mm, 176 layers, slice thickness = 1 mm, repetition time (TR) = 2,300 ms (older adults) or 2,530 ms (younger adults), and duration of approximately 8 min. DTI was performed using an echo planar imaging (EPI) sequence with the following parameters: TR = 8,500 ms, TE = 63 ms, FOV = 224 mm × 224 mm, acquisition matrix size = 112 × 112, 75 layers, slice thickness = 2 mm, b value = 1,000 s/mm^2, 64 diffusion gradient coding directions, and duration of 10 min and 56 s. Older adults underwent two routine scans to exclude individuals with structural brain alterations: tse2d1_15: TR = 3,500 ms, TE = 89 ms, TA = 68 s, FA = 150°, slice thickness = 5 mm, FOV = 195 mm × 240 mm, matrix = 250 × 384, slices = 22. *fl2d1: TR = 250 ms, TE = 2.43 ms, TA = 70 s, FA = 85°, slice thickness = 5 mm, FOV = 195 mm × 240 mm, matrix = 250 × 384, 22 slices.

2.4. Data analysis

2.4.1. DTI data preprocessing and tract-based spatial statistics analysis

DTI data preprocessing was performed using PANDA (Pipeline for Analyzing Brain Diffusion) software,[1] which is an automated toolbox for dMRI analysis. In brief, the preprocessing included the following steps: (1) conversion of DICON files to NIfTI images; (2) brain tissue extraction; and (3) correction for head motion artifacts and eddy current distortions. To avoid image distortion, each image was coregistered to the b0 image. Additionally, (4) gradient orientation correction was performed based on the deformation field to estimate the tensor and fiber direction more accurately, and (5) four dMRI measures (FA, MD, AD, and RD) were calculated by fitting a diffusion tensor model.

Tract-based spatial statistics (TBSS) in FSL[2] software was performed to enable voxelwise comparison between the groups. In brief, the analysis steps were as follows: (1) individual FA images were aligned to the mean FA standard template (FMRIB58_FA) in Montreal Neurological Institute (MNI) space using the nonlinear registration algorithms of FNIRT; (2) the mean of all aligned FA images was calculated and skeletonized to generate a WM FA skeleton, with analysis limited to major WM tracts using a threshold of FA > 0.2; and (3) individual FA values (obtained by finding the maximum value perpendicular to the local skeletal structure from the nearest skeletal center) were projected onto the mean FA skeleton. These steps were repeated to calculate individual MD, AD, and RD and project these maps onto the mean FA skeleton.

2.4.2. WM network construction

After preprocessing, a WM structural network, consisting of a collection of nodes connected by edges, was constructed using PANDA. In the present study, the automated anatomical labeling 90 atlas (AAL 90) was used to define the nodes of the WM network, which included a total of 90 cortical and subcortical regions (45 for each hemisphere). To transform the AAL template in MNI space to the DTI space, where the subject data were located, we first coregistered the individual T1 structural images to b0 images with transformations. Then, a nonlinear transformation to register the aligned T1 images in MNI space to the AAL template was applied. Finally, the AAL template in MNI space was transformed into the individual DTI space using the inverse transform to locate the 90 nodes for each participant.

The edges represent the WM connectivity or features of the brain between two nodes. We used the Fiber Assignment by continuous tracking algorithm (FACT) for deterministic tractography to define the connectivity between nodes. Fiber tracking was performed using each voxel with FA greater than 0.2 as a seed point, and tracking was stopped when the turning angle exceeded 35°. Each pair of nodes was considered structurally connected if there was at least one streamline whose end points were located in the pair. The mean FA of the streamline linking the two nodes was defined as the edge and used to construct an FA-weighted matrix. Finally, the FA-weighted structural network was obtained for each participant from their DTI data, which was represented as a 90 × 90 symmetric matrix.

2.4.3. Graph theoretical analysis

To characterize the topological organization of WM structural connections, topological properties were calculated by the GRETNA toolkit.[3] The following four global topological properties were used in

1 http://www.nitrc.org/projects/panda
2 http://www.fmrib.ox.ac.uk/fsl/tbss/index.html
3 http://www.nitrc.org/projects/gretna/

TABLE 1 The mathematical definitions and descriptions of global and small-world parameters.

Network parameters	Definitions	Descriptions
Global parameters	Characteristic path length $Lp = \frac{1}{N(N-1)} \sum_{i \neq j \in G} L_{ij}$	l_{ij} is the shortest absolute path length between nodes i and j. N is the total number of nodes and G is the set of all nodes. Paths are sequences of distinct nodes and links in the network to represent potential routes of information flow between pairs of brain regions.
	Clustering coefficient $Cp = \frac{1}{N} \sum_{i=1} \frac{E_i}{D_{nod}(i)(D_{nod}(i)-1)/2}$	$D_{nod}(i)$ is the degree of node i, E_i is the number of edges in the subgraph of node i and N is the number of nodes in the network.
	Global efficiency $Eg(G) = \frac{1}{N(N-1)} \sum_{i \neq j \in G} \frac{1}{L_{ij}}$	Eg is computed on disconnected networks. Paths between disconnected nodes are defined to have infinite length and correspondingly zero efficiency.
	Local efficiency $Eloc(G) = \frac{1}{N} \sum_{i \in G} Eg(G_i)$	G_i denotes the subgraph composed of the nearest neighbors of node i.
Small-world parameters	Normalized clustering coefficient $\gamma = C_p^{real} / C_p^{rand}$	C_p^{real} is the clustering coefficient of the real network and C_p^{rand} is the mean clustering coefficient of 100 matched random network.
	Normalized path length $\lambda = L_p^{real} / L_p^{rand}$	L_p^{real} is the characteristic path length of the real network and L_p^{rand} is the mean characteristic path length of 100 matched random network.
	Small-worldness $\sigma = \gamma / \lambda$	network is said to be small-world if it satisfies $\lambda \approx 1$ and $\gamma >> 1$, or $\delta = \gamma/\lambda >> 1$. Small-world organization reflects an optimal balance of functional integration and segregation.

this study: the global clustering coefficient (Cp), characteristic path length (Lp), global efficiency (Eg), and local efficiency (Eloc). Cp is mainly used to measure the extent of local clusters or cliquishness of the network. Lp indicates the length of the shortest path of information from one node to another in the network and reflects the extent of the overall routing efficiency of a network. E.g., measures the global information propagation of the network. Eloc represents the local efficiency of the network. We focused on these global network properties to examine the efficiency of global integration and segregation of information flow. We also assessed small-world properties (λ, σ, and γ). Briefly, normalized path length (λ) is a measure that reflects the global integration of the brain, while the normalized clustering coefficient (γ) represents global segregation. Detailed calculations and interpretations of the topological properties are seen in Table 1 and Rubinov and Sporns (2010). We calculated these two properties at each sparsity threshold (0.05 ~ 0.5, step 0.05) and computed the respective area under the curve (AUC) over the range of sparsity thresholds. The ratio between segregation and integration is the small-worldness (σ) of a network. In a network, $\lambda \approx 1$ and $\gamma \gg 1$ suggest an optimal balance between functional segregation and integration.

2.4.4. Data analysis

The mean MCT at the three dot speeds for each participant was calculated as the individual GMP. Independent-sample t tests were used to analyze group differences in age, body mass index (BMI), and the MCT. The chi-square test was used to analyze sex differences between the two groups.

To investigate age-related alterations in WM microstructure, a permutation-based nonparametric inference was performed in Randomise[4] to compare voxelwise differences in the FA skeleton between the younger and older groups. The number of random permutations was set to 5,000, and the threshold-free cluster enhancement (TFCE) method was used to correct for multiple comparisons. Subsequently, to explore the relationship between age-related decreases in GMP and changes in WM integrity, we applied masks to WM regions that differed significantly between groups, and partial correlation analyses between the MCT and FA in these masks were performed separately for the older and younger groups. As sex and BMI may affect individual WM integrity and the present study was not concerned with the effects of these factors, these variables were controlled as covariates (Daoust et al., 2021). The significance threshold of the partial correlation coefficient was set at $p < 0.05$, and the same TFCE method was used to correct for multiple comparisons.

We segmented the correlated regions according to the "JHU White-Matter Tractography Atlas" to visualize the location of WM fiber tracts associated with age-related decreases in GMP. We focused on only the tracts that contained at least one cluster with a voxel number greater than 100. The mean FA was extracted from the significant clusters of each tract, and a partial correlation analysis was performed between the mean FA and MCT to determine the strength of their correlation. Finally, we also extracted the AD and RD of older and younger adults in the same significant regions of tracts to investigate whether FA alterations associated with age-related decreases in GMP were impacted by changes in RD or AD. For this

4 https://fsl.fmrib.ox.ac.uk/fsl/fslwiki/Randomise

analysis, we first used independent-sample t tests to compare RD and AD between the older and younger groups and then performed partial correlation analyses of the MCT with RD and AD in the older and younger groups.

To examine the changes in the topological organization of the WM network with age, we first examined the group differences in small-world properties (λ, σ, and γ) and global topological properties (Cp, Lp, Eg, and Eloc) between older and younger groups using independent-sample *t* tests. Second, partial correlations between topological properties and the MCT were determined, with sex and BMI as covariates, in the older and younger groups to explore the relationship between alterations in network topology and age-related decreases in GMP. Multiple comparisons were corrected using the Bonferroni method.

3. Results

3.1. Behavioral results

The demographic information and GMP of the participants are shown in Table 2. The results showed statistically significant differences in age and BMI between the older and younger groups but no significant difference in the sex ratio. Since BMI may affect individual white matter integrity, this variable was controlled as a covariate in subsequent analyses (Daoust et al., 2021). Independent-sample t tests showed that the MCT of the older group was significantly higher than that of the younger group, indicating a decline in GMP and a decrease in global motion sensitivity with age.

3.2. TBSS results

The older group exhibited significantly lower FA in most regions of the WM skeleton than the younger group, suggesting that integrity in most WM regions decreases with age. In addition, a small fraction of voxels exhibited a significant increase in FA in older adults (Figure 2).

For older adults, partial correlation analysis showed that the MCT was significantly negatively correlated with FA in four main clusters (Table 3). The effects were spread over large portions of the WM skeleton, including the bilateral CC forceps major (Fmaj) and minor (Fmin), inferior frontal-occipital fasciculus (IFOF), inferior longitudinal fasciculus (ILF), anterior thalamic radiation (ATR), SLF, and cingulum cingulate gyrus (CCG). We located the significant regions using the "JHU White-Matter Tractography Atlas," and the voxel size of each fiber tract is shown in Table 4. We did not find any significant positive correlation between the MCT and FA in the WM regions that differed significantly between groups. We extracted the average FA in the regions of each WM tract that showed significant negative correlations with MCT and plotted the correlation between FA and the MCT to visualize the correlation strength. With sex and BMI included as covariates, the MCT was significantly negatively correlated with FA in the Fmin ($r = -0.32$, $p = 0.002$), Fmaj ($r = -0.21$, $p = 0.044$), left ATR ($r = -0.32$, $p = 0.002$), right ATR ($r = -0.34$, $p = 0.034$), left CCG ($r = -0.26$, $p = 0.011$), right CCG ($r = -0.31$, $p = 0.003$), left IFOF ($r = -0.23$, $p = 0.027$), right IFOF ($r = -0.22$, $p = 0.033$), and left SLF ($r = -0.27$, $p = 0.010$). The FA in the right SLF ($r = -0.20$, $p = 0.058$) and left ILF ($r = -0.20$, $p = 0.055$) was marginally significantly correlated with the MCT (Figure 3). In the young adults, there was no significant correlation between the MCT and FA in the WM regions that differed significantly between groups.

To explore the underlying causes of FA alterations leading to GMP decline, we additionally extracted the mean AD and RD in the relevant regions of each tract. The results showed that both the AD and RD in each tract in older adults were significantly greater than those in younger adults. The results of partial correlation analysis with sex and BMI as covariates showed that, except for the Fmaj and right SLF, the mean RD in most tracts was positively correlated with the MCT in older adults (Figure 4). However, the MCT was only positively correlated with the AD in the left ATR ($r = 0.30$, $p = 0.003$).

TABLE 2 Demographic information and motion coherence threshold (*M*±*SD*).

Term	Older adults (*n*=94)	Younger adults (*n*=106)	t/χ^2	*p*	Cohen's *d*
Age	65.74 ± 4.50	23.04 ± 5.17	61.94	<0.001	8.78
Sex (female/male)	55/39	66/40	0.29	0.59	
BMI	24.08 ± 2.91	21.42 ± 3.28	6.06	<0.001	0.86
MCT	34.37 ± 25.06	18.66 ± 12.19	5.74	<0.001	0.81

3.3. Results of the graph theoretical analysis

The results showed that the WM networks of both the older and younger adults exhibited "small-world" properties ($\lambda \approx 1$, $\gamma > > 1$) (Figure 5A). Small-world networks have high local and global efficiency, requiring minimal connectivity costs and resulting in a balance between local processing and global integration (Watts and Strogatz, 1998). In addition, both global efficiency and the characteristic path length were found significantly decreased in older adults compared to younger adults, as shown in Table 5 and Figure 5B. Therefore, these results confirm that significant network changes occur in older adults. The results of partial correlation analyses revealed that the MCT was significantly negatively correlated with global efficiency ($r = -0.29$, $p = 0.005$) and significantly positively correlated with characteristic path length ($r = 0.32$, $p = 0.002$) in older adults, and these results survived correction for multiple comparisons. However, we did not find any significant correlations between the MCT and topological properties in younger adults.

4. Discussion

In the present study, we attempted to explain the age-related decline in GMP according to age-related WM changes in the brain. TBSS analysis and graph theoretical analysis of dMRI data were used to assess WM integrity and construct structural networks that represented the anatomical connectivity of the cerebral cortex at the microscopic and regional levels. The behavioral findings, with the

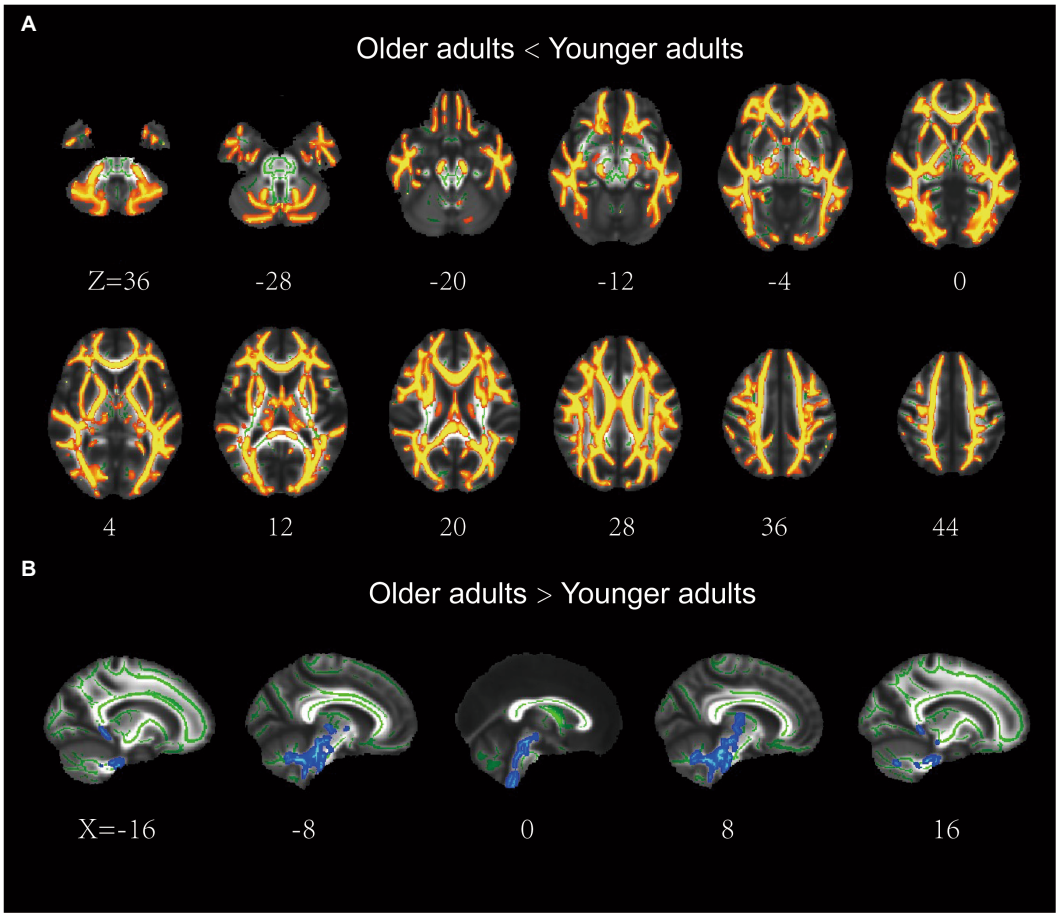

FIGURE 2
Results of the tract-based spatial statistics of fractional anisotropy between the older and younger adults. **(A)** the older adults showed lower FA than the younger adults in a large portion of the WM skeleton, including IFOF, ILF, SLF, ATR, CCG, Fmaj, and Fmin. **(B)** the older adults showed higher FA than the younger adults in a small fraction of voxels (e.g., brainstem). IFOF, inferior frontal-occipital fasciculus; ILF, inferior longitudinal fasciculus; ATR, anterior thalamic radiation; SLF, superior longitudinal fasciculus; CCG, cingulum cingulate gyrus.

TABLE 3 The regions in the WM skeleton that negatively related to motion coherence threshold in older adults.

Regions	MNI coordinates of peak			Size (voxel)
	X	Y	Z	
Cluster1	4	4	24	8,694
Cluster2	−26	−70	24	1,282
Cluster3	31	−15	50	469
Cluster4	40	25	16	260

Only significant regions thresholded at $p = 0.05$, TFCE corrected.

TABLE 4 The tracts that positively corelated to motion coherence threshold.

Tracts	MNI coordinates of peak			Size (voxel)
	X	Y	Z	
Fmin	−12	46	−15	3,356
IFOF.R	35	−54	−3	1,087
IFOF.L	−28	13	−5	840
ILF.L	−41	1	−32	588
ATR.L	−10	−3	−3	498
Fmaj	30	−69	8	368
ATR.R	11	−3	−6	357
SLF.L	−52	−2	16	324
SLF.R	35	−35	24	208
CCG.L	−4	−25	−35	197
CCG.R	22	−30	42	162

older group exhibiting significantly higher MCT values than the younger group (indicating a decrease in GMP with age), are consistent with previous literature (Biehl et al., 2017; Conlon et al., 2017; Meier et al., 2018; Mikellidou et al., 2018). According to the correlation analyses, the decreased GMP in older adults was associated with decreased WM integrity in specific tracts as well as alterations in

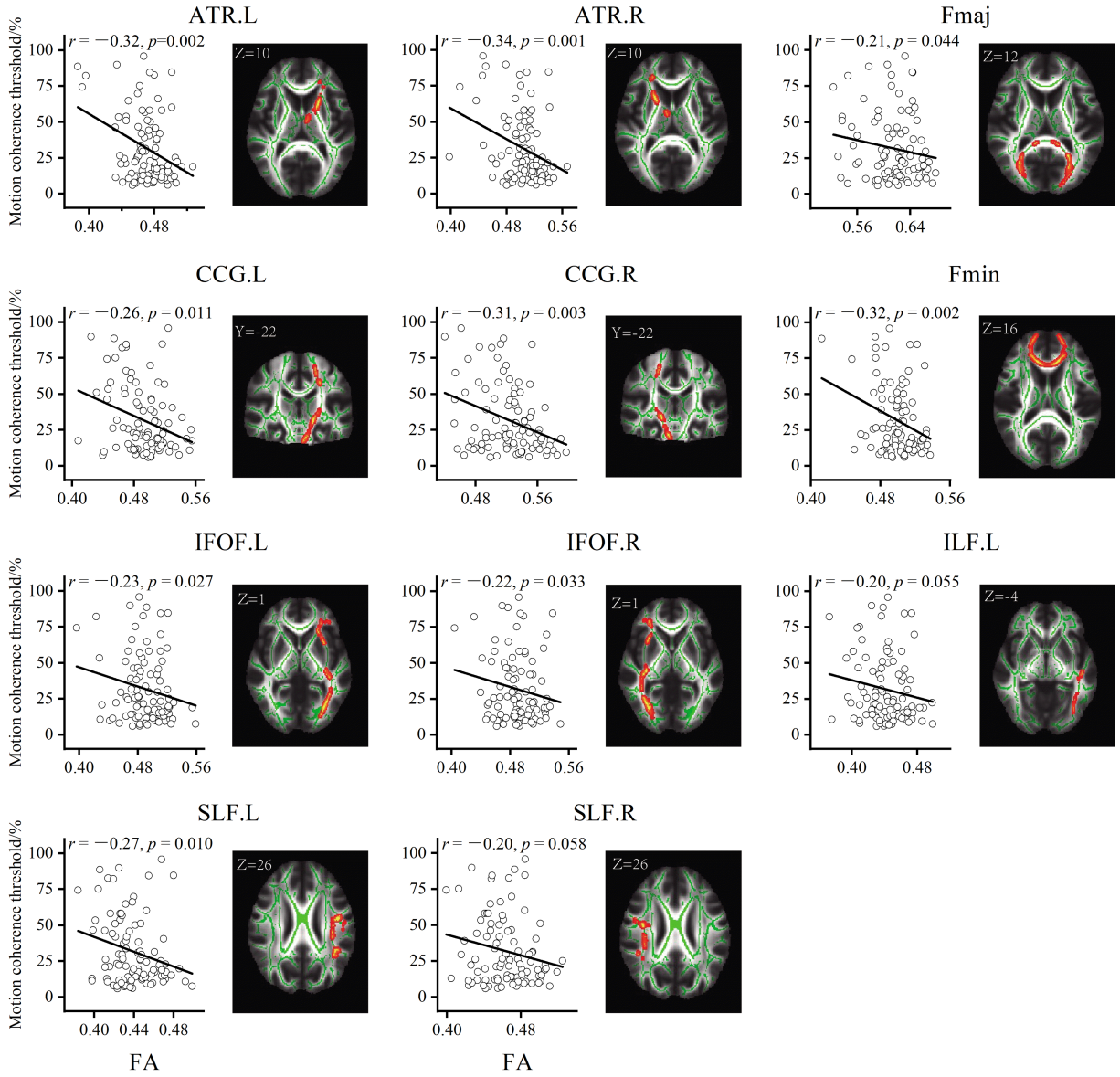

FIGURE 3
Results of the partial correlation analyses between FA and MCT in older adults. All correlations were significant at $p<0.05$ (threshold-free cluster enhancement corrected). Decreased fractional anisotropy in the bilateral SLF, IFOF, ATR, CCG, and left ILF was associated with worse GMP.

characteristic path length and global efficiency in the WM network. The findings support the "disconnection hypothesis" of the aging brain with data on the transmission efficiency of the WM network.

4.1. Microstructural changes in WM associated with age-related decreases in GMP

Older adults showed decreased FA in the majority of WM compared to younger adults, indicating that WM integrity decreased with age; this finding is consistent with the literature (Benitez et al., 2018; Molloy et al., 2021; Dhiman et al., 2022). More importantly, the results revealed correlations between the decrease in global motion sensitivity and decreased WM integrity in the IFOF, ILF, SLF, ATR, CCG, Fmaj, and Fmin. The CC is the largest commissural fiber, and the main WM tract connects the two hemispheres of the brain. This tract is crucial for the transmission of sensory, motor, and cognitive information between the brain hemispheres (Aboitiz et al., 1992; Gazzaniga, 2000). The Fmaj is the callosal tract that connects the bilateral occipital lobes through the splenium. In motion processing, the Fmaj is associated with visuomotor integration between the two hemispheres (Miller, 1991; Mordkoff and Yantis, 1991; Tamura et al., 2007). In particular, the Fmaj directly connects the right and left V5 (Strong et al., 2019), a crucial area for global motion processing that is responsible for integrating dynamic local visual information into a global percept (Newsome and Pare, 1988; Britten et al., 1993; Rust et al., 2006; Chakraborty et al., 2017). The Fmin refers to the callosal tract that passes through the rostrum and genu of the CC and bends forward to connect the right and left frontal lobes. The dorsolateral

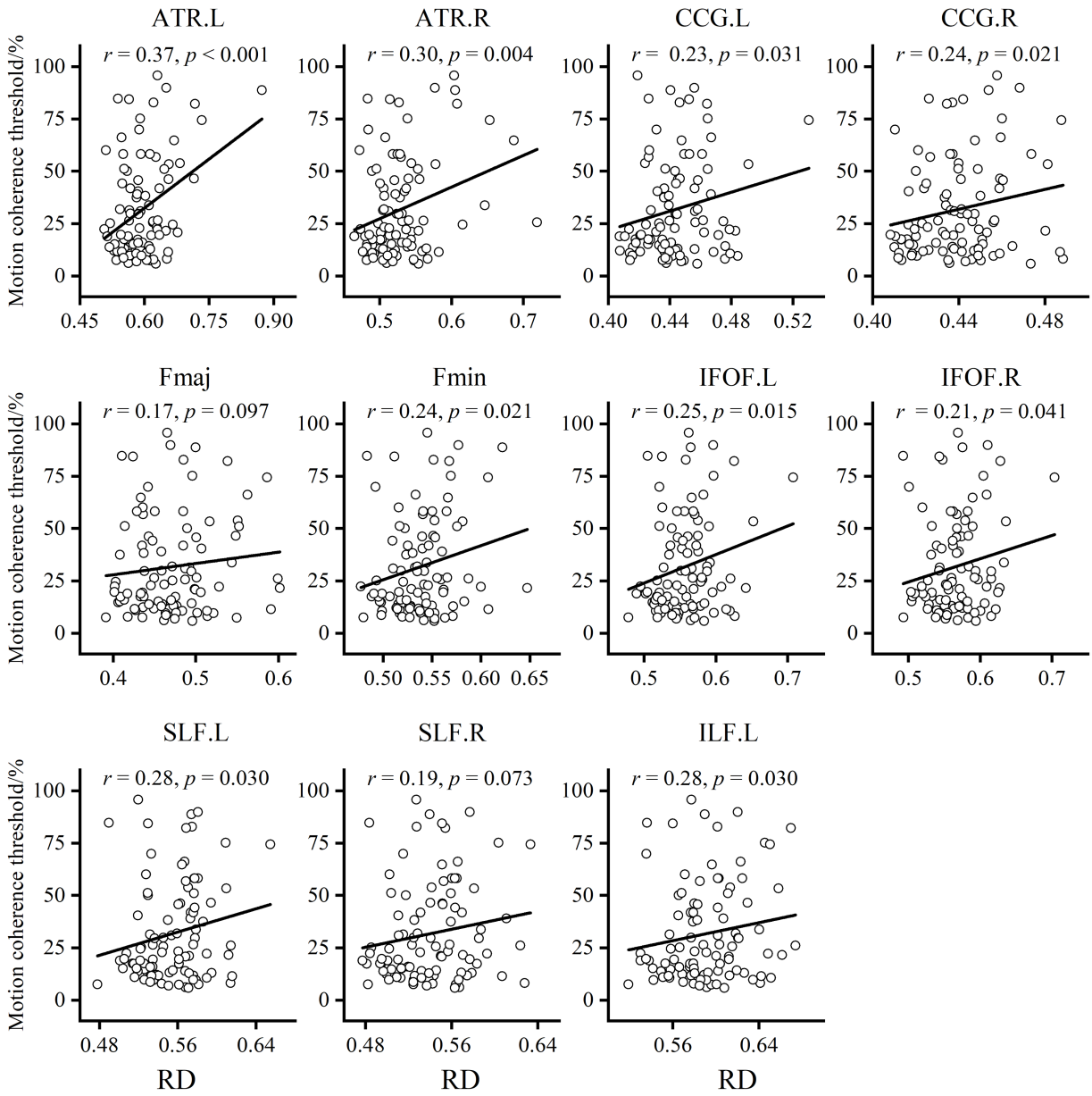

FIGURE 4
Results of the partial correlation analysis between RD and MCT in older adults. Except for Fmaj and right SLF, mean RD in most tracts showed a positive correlation with MCT of the older adults.

prefrontal cortex of the frontal lobe participates in top-down motor control (Kim and Shadlen, 1999), while the medial prefrontal cortex may be associated with spatial working memory in self-navigation (Sherrill et al., 2015). These results suggest that decreased efficiency of information transmission between the right and left frontal and occipital lobes, especially between the right and left V5, may contribute to the reduction in GMP in older adults.

The SLF, ILF, and IFOF are association fibers. The SLF is a bundle that connects the frontal, occipital, parietal, and occipital lobes on the ipsilateral side; the ILF connects the visual areas in the temporal and occipital areas to the amygdala and hippocampus; and the IFOF is the longest association fiber in the brain, linking the frontal and occipital lobes. These tracts connect the occipital lobe to ipsilateral cortical areas and are thought to be associated with spatial information processing (Vaessen et al., 2016). For example, long-term sports training (e.g., table tennis, gymnastics) can increase the structural integrity of these three tracts (Huang et al., 2015; Qi et al., 2021), while brain injuries to these tracts affect visuospatial processing (Chechlacz et al., 2012; McGrath et al., 2013; Hattori et al., 2018). In the present study, we found that decreased WM integrity in the SLF, ILF, and IFOF leads to a decline in GMP (in terms of behavioral performance) in older adults, consistent with previous findings in region of interest (ROI) analyses that GMP is strongly related to the SLF in adults and children (Csete et al., 2014; Braddick et al., 2017). We suggest that the correlation between association fiber integrity and GMP may be due to GMP requirements. The GMP involves processing of local movement across the visual field and integrating local moving elements into a global percept; these two processes depend on the

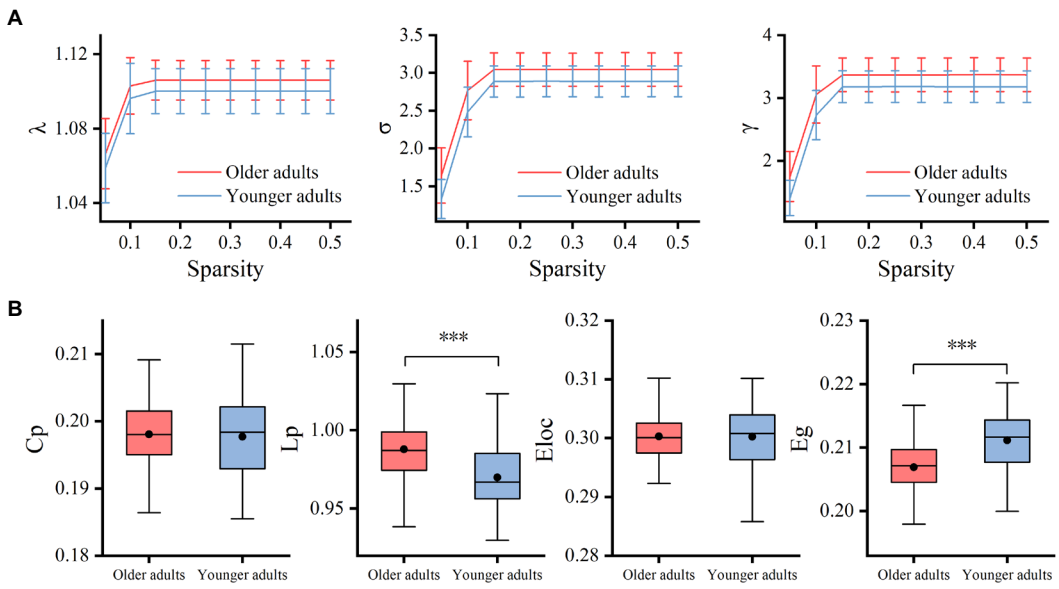

FIGURE 5
Group differences between small-world properties (λ, σ, γ) and global topological properties (Lp, Cp, Eloc, and Eg) of the WM network. $\lambda \approx 1$ and $\gamma >> 1$ indicated both the older and younger adults exhibited economic "small-world" properties **(A)**. The older adults showed increased Lp and decreased Eg compared to younger adults. There was no significant difference in Cp and Eloc between the two groups **(B)**. Cp, the global clustering coefficient; Lp, characteristic path length; Eg, global efficiency; Eloc, local efficiency; λ, normalized path length; γ, normalized clustering coefficient; σ, small-worldness, ***p < 0.001.

TABLE 5 Comparisons of global topological properties between groups (×10^{-1}).

	Older adults (*n*=94)	Younger adults (*n*=106)	*t*	*p*	Cohen's d
Eg	2.07 ± 0.05	2.11 ± 0.05	−6.34	<0.001	−0.90
Eloc	3.00 ± 0.04	3.00 ± 0.05	0.05	0.957	0.01
Cp	1.98 ± 0.05	1.98 ± 0.05	0.41	0.680	0.06
Lp	9.88 ± 0.21	9.70 ± 0.21	6.07	<0.001	0.86

primary visual cortex, located in the occipital lobe, and the middle temporal gyrus, located in the temporal lobe, respectively (Britten et al., 1993; Rust et al., 2006). In the RDK task, participants need to make decisions about the direction of motion; these decisions mainly depend on the intraparietal sulcus, located in the parietal lobe (Kayser et al., 2010). Lack of structural connections between the occipital lobe and other cortices may cause a decrease in motion sensitivity in older adults, explaining why alterations in the SLF, ILF, and IFOF lead to impaired GMP.

Decreased FA in the ATR and CCG was also associated with decreased GMP. The CCG plays a critical role in cognitive control, conflict monitoring in response selection, and spatial attentional control (Morecraft et al., 1993, 2012; Nieuwenhuis et al., 2003). The reduced WM integrity in the CCG of older adults may thus affect spatial attentional control and decision-making processes involving motion direction in GMP. Additionally, thalamic neurons receive sensory and motion information from the external environment and transmit information to the cerebral cortex through the ATR (Perani et al., 2021). The reduced WM integrity of the ATR may have a negative influence on the transmission of visuomotor information to the cerebral cortex, leading to a reduction in GMP.

In addition, we found that most RD values of GMP-related tracts were significantly correlated with the MCT, which further indicated that the decrease in WM integrity may be caused by the increased RD of tracts in older adults. Different patterns of WM changes have been examined to elucidate aging processes in different tracts and their underlying biological profiles. Molloy et al. (2021) identified five main patterns of overlap between diffusion measures in WM areas that showed age-related negative correlations with FA. Consistent with the results reported by Molly et al., we also found decreased FA and increased RD in the Fmaj, Fmin, SLF, ILF, IFOF, and CCG, consistent with the "FA and RD only" pattern. This pattern may reflect age-related demyelination of WM tracts (Sullivan and Pfefferbaum, 2007; Molloy et al., 2021).

4.2. Changes in topological properties of WM networks associated with age-related decreases in GMP

In the WM structural network, global efficiency and the characteristic path length are commonly used measures of functional integration, which refers to the ability to rapidly combine specialized information from distributed cortical regions. The shorter the path length and the higher global efficiency of a network the higher the efficiency of information transmission across network nodes (Watts and Strogatz, 1998). Local efficiency and the global clustering coefficient are considered indicators of network segregation in the brain. Network segregation is the ability of densely interconnected groups of brain regions to perform specialized processing and is

thought to reflect the local information transmission of the network (Latora and Marchiori, 2001; Rubinov and Sporns, 2010). Thus, our findings showed that the global efficiency of older adults was significantly lower than that of younger adults, while the characteristic path length of older adults was significantly higher; however, we found no significant difference in local efficiency or the global clustering coefficient between the two groups, indicating that the changes in the connectivity of older adults may reduce parallel information processing and the speed and efficiency of information transmission across brain regions (Achard et al., 2012). Moreover, the age-related decrease in global efficiency and the increase in characteristic path length were closely related to the reduction in global motion sensitivity in older adults, suggesting that the reduction in global motion sensitivity in older adults may be affected by the decrease in information integration and communication efficiency between distant cortical regions. Long-range connectivity (e.g., between the frontal and occipital lobes) is thought to play an important role in visuospatial attention, which is a prerequisite for global motion processing (Barceló et al., 2000; Ruff et al., 2006). Therefore, reduced efficiency of information integration and communication between distant cortical regions in older adults may lead to decreased GMP by affecting individual visuospatial attention.

This study has some limitations. First, aging is a lifelong process, but we selected participants with two discrete age ranges; thus, we were unable to explore the relationship of alterations in WM microstructure and network properties with perceptual changes caused by aging along a continuum. Second, this study mainly examined the alterations in WM integrity in 20 main tracts; we did not assess changes in structural connectivity along the dorsal visual stream (such as the connections between V1 and V5). In previous studies, patients with cortical visual impairments exhibited worse GMP, suggesting that structural disconnection along the dorsal visual stream may also cause a decrease in motion sensitivity in older adults (Pamir et al., 2021). In the future, we plan to explore the effects of structural disconnection along the dorsal visual stream on global motion sensitivity in older adults.

5. Conclusion

In this study, we used RDK and DTI to study the effects of age-related reductions in WM fiber integrity and connectivity on the decrease in GMP at the microscopic and macroscopic levels. We found that reduced WM integrity in specific fiber tracts, such as the Fmaj, Fmin, ILF, SLF, ATR, IFOF, and CCG, may underlie age-related decreases in GMP in older adults. Moreover, age-related decreases in GMP may also be associated with reduced information integration and communication efficiency between distant cortical areas. This study demonstrated, for the first time, that age-related reductions in WM integrity and connectivity in older adults affect the efficiency of information transfer between brain regions, leading to a decrease in global motion sensitivity. Our results thus support the "disconnection hypothesis" of cognitive aging.

Data availability statement

The raw data supporting the conclusions of this article will be made available by the authors, without undue reservation.

Ethics statement

The studies involving human participants were reviewed and approved by Ethics Committees of Tianjin First Central Hospital and Tianjin Normal University. The patients/participants provided their written informed consent to participate in this study.

Author contributions

SY, YZ, and HJ gave study conceptualization and design. SY, XY, JC, ZZ, HL, JY, and YJ were involved in data collection. SY and HJ helped with data analysis and interpretation. SY, YZ, and HJ contributed to the supervision of the study procedures. SY and HJ contributed to drafting the manuscript. All authors contributed to the article and approved the submitted version.

Funding

This work was supported by grants from the National Natural Science Foundation of China (31971021) and Tianjin Postgraduate Research Innovation Project (2019YJSB129).

Conflict of interest

The authors declare that the research was conducted in the absence of any commercial or financial relationships that could be construed as a potential conflict of interest.

Publisher's note

All claims expressed in this article are solely those of the authors and do not necessarily represent those of their affiliated organizations, or those of the publisher, the editors and the reviewers. Any product that may be evaluated in this article, or claim that may be made by its manufacturer, is not guaranteed or endorsed by the publisher.

References

Aboitiz, F., Scheibel, A. B., Fisher, R. S., and Zaidel, E. (1992). Fiber composition of the human corpus callosum. *Brain Res.* 598, 143–153. doi: 10.1016/0006-8993(92)90178-C

Achard, S., Delon-Martin, C., Vértes, P. E., Renard, F., Schenck, M., Schneider, F., et al. (2012). Hubs of brain functional networks are radically reorganized in comatose patients. *Proc. Natl. Acad. Sci.* 109, 20608–20613. doi: 10.1073/pnas.1208933109

Anton-Erxleben, K., Herrmann, K., and Carrasco, M. (2013). Independent effects of adaptation and attention on perceived speed. *Psychol. Sci.* 24, 150–159. doi: 10.1177/0956797612449178

Barceló, F., Suwazono, S., and Knight, R. T. (2000). Prefrontal modulation of visual processing in humans. *Nat. Neurosci.* 3, 399–403. doi: 10.1038/73975

Basser, P. J., Mattiello, J., and LeBihan, D. (1994). MR diffusion tensor spectroscopy and imaging. *Biophys. J.* 66, 259–267. doi: 10.1016/S0006-3495(94)80775-1

Benassi, M., Giovagnoli, S., Pansell, T., Mandolesi, L., Bolzani, R., Magri, S., et al. (2021). Developmental trajectories of global motion and global form perception from 4 years to adulthood. *J. Exp. Child Psychol.* 207:105092. doi: 10.1016/j.jecp.2021.105092

Benitez, A., Jensen, J. H., Falangola, M. F., Nietert, P. J., and Helpern, J. A. (2018). Modeling white matter tract integrity in aging with diffusional kurtosis imaging. *Neurobiol. Aging* 70, 265–275. doi: 10.1016/j.neurobiolaging.2018.07.006

Bennett, I. J., and Madden, D. J. (2014). Disconnected aging: cerebral white matter integrity and age-related differences in cognition. *Neuroscience* 276, 187–205. doi: 10.1016/j.neuroscience.2013.11.026

Berry, M. J., Brivanlou, I. H., Jordan, T. A., and Meister, M. (1999). Anticipation of moving stimuli by the retina. *Nature* 398, 334–338. doi: 10.1038/18678

Biehl, S. C., Andersen, M., Waiter, G. D., and Pilz, K. S. (2017). Neural changes related to motion processing in healthy aging. *Neurobiol. Aging* 57, 162–169. doi: 10.1016/j.neurobiolaging.2017.05.018

Borghesani, P. R., Madhyastha, T. M., Aylward, E. H., Reiter, M. A., Swarny, B. R., Schaie, K. W., et al. (2013). The association between higher order abilities, processing speed, and age are variably mediated by white matter integrity during typical aging. *Neuropsychologia* 51, 1435–1444. doi: 10.1016/j.neuropsychologia.2013.03.005

Bower, J. D., and Andersen, G. J. (2012). Aging, perceptual learning, and changes in efficiency of motion processing. *Vis. Res.* 61, 144–156. doi: 10.1016/j.visres.2011.07.016

Braddick, O., Atkinson, J., Akshoomoff, N., Newman, E., Curley, L. B., Gonzalez, M. R., et al. (2017). Individual differences in children's global motion sensitivity correlate with TBSS-based measures of the superior longitudinal fasciculus. *Vis. Res.* 141, 145–156. doi: 10.1016/j.visres.2016.09.013

Britten, K. H., Shadlen, M. N., Newsome, W. T., and Movshon, J. A. (1993). Responses of neurons in macaque MT to stochastic motion signals. *Vis. Neurosci.* 10, 1157–1169. doi: 10.1017/s0952523800010269

Chakraborty, A., Anstice, N. S., Jacobs, R. J., Paudel, N., LaGasse, L. L., Lester, B. M., et al. (2017). Global motion perception is related to motor function in 4.5-year-old children born at risk of abnormal development. *Vis. Res.* 135, 16–25. doi: 10.1016/j.visres.2017.04.005

Chaplin, T. A., Allitt, B. J., Hagan, M. A., Price, N. S. C., Rajan, R., Rosa, M. G. P., et al. (2017). Sensitivity of neurons in the middle temporal area of marmoset monkeys to random dot motion. *J. Neurophysiol.* 118, 1567–1580. doi: 10.1152/jn.00065.2017

Chechlacz, M., Rotshtein, P., Hansen, P. C., Riddoch, J. M., Deb, S., and Humphreys, G. W. (2012). The neural underpinings of simultanagnosia: disconnecting the visuospatial attention network. *J. Cogn. Neurosci.* 24, 718–735. doi: 10.1162/jocn_a_00159

Coelho, A., Fernandes, H. M., Magalhães, R., Moreira, P. S., Marques, P., Soares, J. M., et al. (2021). Signatures of white-matter microstructure degradation during aging and its association with cognitive status. *Sci. Rep.* 11:4517. doi: 10.1038/s41598-021-83983-7

Conlon, E. G., Power, G. F., Hine, T. J., and Rahaley, N. (2017). The impact of older age and sex on motion discrimination. *Exp. Aging Res.* 43, 55–79. doi: 10.1080/0361073X.2017.1258226

Csete, G., Szabó, N., Rokszin, A., Tóth, E., Braunitzer, G., Benedek, G., et al. (2014). An investigation of the white matter microstructure in motion detection using diffusion MRI. *Brain Res.* 1570, 35–42. doi: 10.1016/j.brainres.2014.05.006

Damoiseaux, J. S. (2017). Effects of aging on functional and structural brain connectivity. *NeuroImage* 160, 32–40. doi: 10.1016/j.neuroimage.2017.01.077

Daoust, J., Schaffer, J., Zeighami, Y., Dagher, A., García-García, I., and Michaud, A. (2021). White matter integrity differences in obesity: a meta-analysis of diffusion tensor imaging studies. *Neurosci. Biobehav. Rev.* 129, 133–141. doi: 10.1016/j.neubiorev.2021.07.020

Davis, S. W., Dennis, N. A., Buchler, N. G., White, L. E., Madden, D. J., and Cabeza, R. (2009). Assessing the effects of age on long white matter tracts using diffusion tensor tractography. *NeuroImage* 46, 530–541. doi: 10.1016/j.neuroimage.2009.01.068

de Lange, A. M. G., Bråthen, A. C. S., Grydeland, H., Sexton, C., Johansen-Berg, H., Andersson, J. L. R., et al. (2016). White matter integrity as a marker for cognitive plasticity in aging. *Neurobiol. Aging* 47, 74–82. doi: 10.1016/j.neurobiolaging.2016.07.007

Dhiman, S., Fountain-Zaragoza, S., Jensen, J. H., Fatima Falangola, M., McKinnon, E. T., Moss, H. G., et al. (2022). Fiber ball white matter modeling reveals microstructural alterations in healthy brain aging. *Aging Brain* 2:100037. doi: 10.1016/j.nbas.2022.100037

Fjell, A. M., Sneve, M. H., Grydeland, H., Storsve, A. B., and Walhovd, K. B. (2017). The disconnected brain and executive function decline in aging. *Cereb. Cortex* 27, bhw082–bhw2317. doi: 10.1093/cercor/bhw082

Gazzaniga, M. S. (2000). Cerebral specialization and interhemispheric communication: does the corpus callosum enable the human condition? Brain: a. *J. Neurol.* 123, 1293–1326. doi: 10.1093/brain/123.7.1293

Gong, G., Rosa-Neto, P., Carbonell, F., Chen, Z. J., He, Y., and Evans, A. C. (2009). Age-and gender-related differences in the cortical anatomical network. *J. Neurosci.* 29, 15684–15693. doi: 10.1523/JNEUROSCI.2308-09.2009

Hattori, T., Ito, K., Nakazawa, C., Numasawa, Y., Watanabe, M., Aoki, S., et al. (2018). Structural connectivity in spatial attention network: reconstruction from left hemispatial neglect. *Brain Imaging Behav.* 12, 309–323. doi: 10.1007/s11682-017-9698-7

Hoffman, D. D., Singh, M., and Prakash, C. (2015). The interface theory of perception. *Psychon. Bull. Rev.* 22, 1480–1506. doi: 10.3758/s13423-015-0890-8

Huang, R., Lu, M., Song, Z., and Wang, J. (2015). Long-term intensive training induced brain structural changes in world class gymnasts. *Brain Struct. Funct.* 220, 625–644. doi: 10.1007/s00429-013-0677-5

Jin, H., Liang, Z. P., Zhu, Z. L., Yan, S. Z., Lin, L., Aisikaer, A., et al. (2021). Aging of global motion perception is accompanied by the changes of resting-state functional activity in the middle temporal gyrus. *Acta Psychol. Sin.* 53, 38–54. doi: 10.3724/SP.J.1041.2021.00038

Jin, H., Zhu, Z. L., Yan, S. Z., Liang, Z. P., Aikedan, A., Yin, J. Z., et al. (2020). The brain gray matter basis of the decline of global motion sensitivity in elderly adults. *Stud. Psychol. Behav.* 18, 603–610.

Joshi, M. R., Simmers, A. J., and Jeon, S. T. (2021). The interaction of global motion and global form processing on the perception of implied motion: an equivalent noise approach. *Vis. Res.* 186, 34–40. doi: 10.1016/j.visres.2021.04.006

Kamali, A., Flanders, A. E., Brody, J., Hunter, J. V., and Hasan, K. M. (2014). Tracing superior longitudinal fasciculus connectivity in the human brain using high resolution diffusion tensor tractography. *Brain Struct. Funct.* 219, 269–281. doi: 10.1007/s00429-012-0498-y

Kayser, A. S., Buchsbaum, B. R., Erickson, D. T., and D'Esposito, M. (2010). The functional anatomy of a perceptual decision in the human brain. *J. Neurophysiol.* 103, 1179–1194. doi: 10.1152/jn.00364.2009

Kim, J. N., and Shadlen, M. N. (1999). Neural correlates of a decision in the dorsolateral prefrontal cortex of the macaque. *Nat. Neurosci.* 2, 176–185. doi: 10.1038/5739

Lacherez, P., Turner, L., Lester, R., Burns, Z., and Wood, J. M. (2014). Age-related changes in perception of movement in driving scenes. *Ophthalmic Physiol Opt* 34, 445–451. doi: 10.1111/opo.12140

Latora, V., and Marchiori, M. (2001). Efficient behavior of small-world networks. *Phys. Rev. Lett.* 87:198701. doi: 10.1103/PhysRevLett.87.198701

McGrath, J., Johnson, K., O'Hanlon, E., Garavan, H., Gallagher, L., and Leemans, A. (2013). White matter and visuospatial processing in autism: a constrained spherical Deconvolution Tractography study. *Autism Res.* 6, 307–319. doi: 10.1002/aur.1290

Meier, K., Partanen, M., and Giaschi, D. (2018). Neural correlates of speed-tuned motion perception in healthy adults. *Perception* 47, 660–683. doi: 10.1177/0301006618771463

Merenstein, J. L., Corrada, M. M., Kawas, C. H., and Bennett, I. J. (2021). Age affects white matter microstructure and episodic memory across the older adult lifespan. *Neurobiol. Aging* 106, 282–291. doi: 10.1016/j.neurobiolaging.2021.06.021

Mikellidou, K., Frijia, F., Montanaro, D., Greco, V., Burr, D. C., and Morrone, M. C. (2018). Cortical BOLD responses to moderate-and high-speed motion in the human visual cortex. *Sci. Rep.* 8:8357. doi: 10.1038/s41598-018-26507-0

Miller, J. (1991). Channel interaction and the redundant-targets effect in bimodal divided attention. *J. Exp. Psychol. Hum. Percept. Perform.* 17, 160–169. doi: 10.1037//0096-1523.17.1.160

Molloy, C. J., Nugent, S., and Bokde, A. L. W. (2021). Alterations in diffusion measures of white matter integrity associated with healthy aging. *J. Gerontol. A* 76, 945–954. doi: 10.1093/gerona/glz289

Mordkoff, J. T., and Yantis, S. (1991). An interactive race model of divided attention. *J. Exp. Psychol. Hum. Percept. Perform.* 17, 520–538. doi: 10.1037/0096-1523.17.2.520

Morecraft, R. J., Geula, C., and Mesulam, M.-M. (1993). Architecture of connectivity within a cingulo-fronto-parietal neurocognitive network for directed attention. *Arch. Neurol.* 50, 279–284. doi: 10.1001/archneur.1993.00540030045013

Morecraft, R. J., Stilwell-Morecraft, K. S., Cipolloni, P. B., Ge, J., McNeal, D. W., and Pandya, D. N. (2012). Cytoarchitecture and cortical connections of the anterior cingulate and adjacent somatomotor fields in the rhesus monkey. *Brain Res. Bull.* 87, 457–497. doi: 10.1016/j.brainresbull.2011.12.005

Narasimhan, S., and Giaschi, D. (2012). The effect of dot speed and density on the development of global motion perception. *Vis. Res.* 62, 102–107. doi: 10.1016/j.visres.2012.02.016

Newsome, W. T., and Pare, E. B. (1988). A selective impairment of motion perception following lesions of the middle temporal visual area (MT). *J. Neurosci.* 8, 2201–2211. doi: 10.1523/JNEUROSCI.08-06-02201.1988

Nieuwenhuis, S., Yeung, N., van den Wildenberg, W., and Ridderinkhof, K. R. (2003). Electrophysiological correlates of anterior cingulate function in a go/no-go task: effects of response conflict and trial type frequency. *Cogn. Affect. Behav. Neurosci.* 3, 17–26. doi: 10.3758/cabn.3.1.17

Pamir, Z., Bauer, C. M., Bailin, E. S., Bex, P. J., Somers, D. C., and Merabet, L. B. (2021). Neural correlates associated with impaired global motion perception in cerebral visual impairment (CVI). *NeuroImage Clin* 32:102821. doi: 10.1016/j.nicl.2021.102821

Perani, D., Scifo, P., Cicchini, G. M., Rosa, P. D., Banfi, C., Mascheretti, S., et al. (2021). White matter deficits correlate with visual motion perception impairments in dyslexic carriers of the DCDC2 genetic risk variant. *Exp. Brain Res.* 239, 2725–2740. doi: 10.1007/s00221-021-06137-1

Pilz, K. S., Miller, L., and Agnew, H. C. (2017). Motion coherence and direction discrimination in healthy aging. *J. Vis.* 17:31. doi: 10.1167/17.1.31

Porter, G., Wattam-Bell, J., Bayer, A., Haworth, J., Braddick, O., Atkinson, J., et al. (2017). Different trajectories of decline for global form and global motion processing in aging, mild cognitive impairment and Alzheimer's disease. *Neurobiol. Aging* 56, 17–24. doi: 10.1016/j.neurobiolaging.2017.03.004

Qi, Y. P., Wang, Y. X., Zhu, H., Zhou, C. L., and Wang, Y. Y. (2021). Effects associated with long-term training in sports requiring high levels of strategy on brain white matter structure in expert players: a DTI study. *Acta Psychol. Sin.* 53, 798–806. doi: 10.3724/SP.J.1041.2021.00798

Roudaia, E., Bennett, P. J., Sekuler, A. B., and Pilz, K. S. (2010). Spatiotemporal properties of apparent motion perception and aging. *J. Vis.* 10, 1–5. doi: 10.1167/10.14.5

Rubinov, M., and Sporns, O. (2010). Complex network measures of brain connectivity: uses and interpretations. *NeuroImage* 52, 1059–1069. doi: 10.1016/j.neuroimage.2009.10.003

Ruff, C. C., Blankenburg, F., Bjoertomt, O., Bestmann, S., Freeman, E., Haynes, J.-D., et al. (2006). Concurrent TMS-fMRI and psychophysics reveal frontal influences on human retinotopic visual cortex. *Curr. Biol.* 16, 1479–1488. doi: 10.1016/j.cub.2006.06.057

Rust, N. C., Mante, V., Simoncelli, E. P., and Movshon, J. A. (2006). How MT cells analyze the motion of visual patterns. *Nat. Neurosci.* 9, 1421–1431. doi: 10.1038/nn1786

Sherrill, K. R., Chrastil, E. R., Ross, R. S., Erdem, U. M., Hasselmo, M. E., and Stern, C. E. (2015). Functional connections between optic flow areas and navigationally responsive brain regions during goal-directed navigation. *NeuroImage* 118, 386–396. doi: 10.1016/j.neuroimage.2015.06.009

Snowden, R. J., and Kavanagh, E. (2006). Motion perception in the ageing visual system: minimum motion, motion coherence, and speed discrimination thresholds. *Perception* 35, 9–24. doi: 10.1068/p5399

Sousa, T., Sayal, A., Duarte, J. V., Costa, G. N., Martins, R., and Castelo-Branco, M. (2018). Evidence for distinct levels of neural adaptation to both coherent and incoherently moving visual surfaces in visual area hMT+. *NeuroImage* 179, 540–547. doi: 10.1016/j.neuroimage.2018.06.075

Strong, S. L., Silson, E. H., Gouws, A. D., Morland, A. B., and McKeefry, D. J. (2019). An enhanced role for right hV5/MT+ in the analysis of motion in the contra-and ipsi-lateral visual hemi-fields. *Behav. Brain Res.* 372:112060. doi: 10.1016/j.bbr.2019.112060

Sullivan, E. V., and Pfefferbaum, A. (2007). Neuroradiological characterization of normal adult ageing. *Br. J. Radiol.* 80, S99–S108. doi: 10.1259/bjr/22893432

Tamura, I., Kitagawa, M., Otsuki, M., Kikuchi, S., Tashiro, K., and Dubois, B. (2007). Pure topographical disorientation following a right forceps major of the splenium lesion: a case study. *Neurocase* 13, 178–184. doi: 10.1080/13554790701448812

Vaessen, M. J., Saj, A., Lovblad, K. O., Gschwind, M., and Vuilleumier, P. (2016). Structural white-matter connections mediating distinct behavioral components of spatial neglect in right brain-damaged patients. *Cortex* 77, 54–68. doi: 10.1016/j.cortex.2015.12.008

Ward, L. M., Morison, G., Simmers, A. J., and Shahani, U. (2018). Age-related changes in global motion coherence: conflicting haemodynamic and perceptual responses. *Sci. Rep.* 8:10013. doi: 10.1038/s41598-018-27803-5

Watts, D. J., and Strogatz, S. H. (1998). Collective dynamics of 'small-world' networks. *Nature* 393, 440–442. doi: 10.1038/30918

Wen, W., Zhu, W., He, Y., Kochan, N. A., Reppermund, S., Slavin, M. J., et al. (2011). Discrete neuroanatomical networks are associated with specific cognitive abilities in old age. *J. Neurosci.* 31, 1204–1212. doi: 10.1523/JNEUROSCI.4085-10.2011

Wilkins, L., Gray, R., Gaska, J., and Winterbottom, M. (2013). Motion perception and driving: predicting performance through testing and shortening braking reaction times through training. *Invest. Ophthalmol. Vis. Sci.* 54, 8364–8374. doi: 10.1167/iovs.13-12774

Yamasaki, T., Horie, S., Ohyagi, Y., Tanaka, E., Nakamura, N., Goto, Y., et al. (2016). A potential VEP biomarker for mild cognitive impairment: evidence from selective visual deficit of higher-level dorsal pathway. *J. Alzheimer's Dis* 53, 661–676. doi: 10.3233/JAD-150939

Frontiers in
Aging Neuroscience

Explores the mechanisms of central nervous system aging and age-related neural disease

The third most-cited journal in the field of geriatrics and gerontology, with a focus on understanding the mechanistic processes associated with central nervous system aging.

Discover the latest Research Topics

See more →

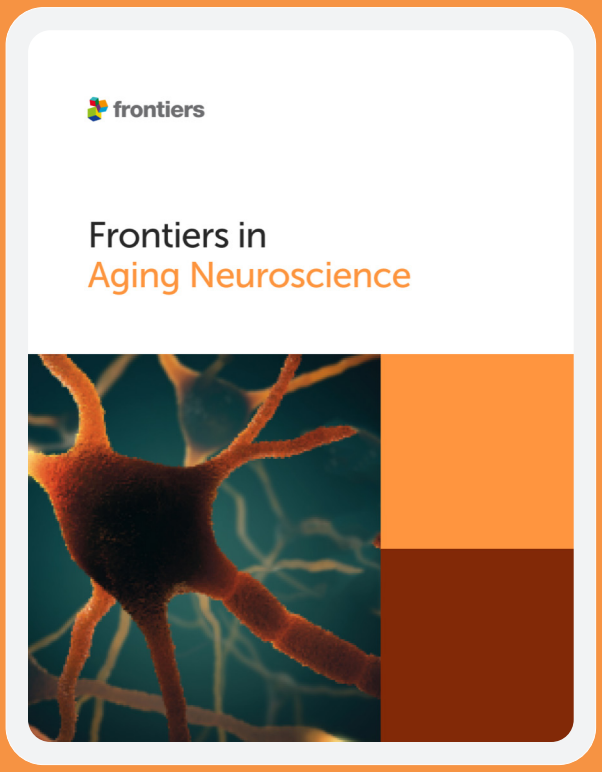

Frontiers

Avenue du Tribunal-Fédéral 34
1005 Lausanne, Switzerland
frontiersin.org

Contact us

+41 (0)21 510 17 00
frontiersin.org/about/contact